VOLUME 9
NUMBER 1–2
1974

Acta biochimica et biophysica

ACADEMIAE SCIENTIARUM HUNGARICAE

AKADÉMIAI KIADÓ, BUDAPEST

ABBPAP 9 (1–2) 1–158 (1974)

Acta Biochimica et Biophysica

Academiae Scientiarum Hungaricae

Szerkeszti:

STRAUB F. BRUNÓ és ERNST JENŐ

Technikai szerkesztők:

SAJGÓ MIHÁLY és NIEDETZKY ANTAL

Szerkesztőség postai címe: 1502 Budapest, Pf. 7 (biokémia)
7643 Pécs, Pf. 99. (biofizika)

Az *Acta Biochimica et Biophysica* a Magyar Tudományos Akadémia idegen nyelvű folyóirata, amely angol nyelven (esetleg német, francia vagy orosz nyelven is) eredeti tanulmányokat közöl a biokémia és a biofizika — fehérjék (struktúra és szintézis), enzimek, nukleinsavak, szabályozó és transzport-folyamatok, bioenergetika, izom-összehúzódás, radiobiológia, biokibernetika, funkcionális és ultrastruktúra stb. — tárgyköréből.

A folyóirat negyedévenként jelenik meg, a négy füzet évente egy kb. 400 oldalas kötetet alkot. Kiadja az Akadémiai Kiadó.

Megrendelhető az Akadémiai Kiadónál (1363 Bp. Pf. 24.), a külföld részére pedig a Kultúra Könyv és Hírlap Külkereskedelmi Vállalatnál (1389 Budapest 62, P.O.B. 149).

The *Acta Biochimica et Biophysica*, a periodical of the Hungarian Academy of Sciences, publishes original papers, in English, on biochemistry and biophysics. Its main topics are: proteins (structure and synthesis), enzymes, nucleic acids, regulatory and transport processes, bioenergetics, excitation, muscular contraction, radiobiology, biocybernetics, functional structure and ultrastructure.

The Acta Biochimica et Biophysica is a quarterly, the four issues make up a volume of some 400 pages per annum. Manuscripts and correspondence with the editors and publishers should be sent to

Akadémiai Kiadó, Budapest 24, P.O.B. 502.

The subscription rate is $ 32.00 per volume. Orders may be placed with *Kultúra* Trading Co. for Books and Newspapers (1389 Budapest 62, P.O.B. 149) or with its representatives abroad, listed on p. 3 of the cover.

Acta Biochimica et Biophysica — журнал Академии Наук Венгрии, публикующий на английском языке (возможно и на немецком, французском и русском языках) оригинальные статьи по проблемам биохимии и биофизики — белков (структура и синтез), энзимов, нуклеиновых кислот, процессов регуляции и транспорта, биоэнергетики, мышечного сокращения, радиобиологии, биокибернетики, функциональной структуры и ультраструктуры и т. д.

Журнал выходит ежеквартально, выпуски каждого года составляют том объемом около 400 страниц. Журнал выпускает Издательство Академии Наук Венгрии.

Рукописи и корреспонденцию просим направлять по следующему адресу:

Akadémiai Kiadó, Budapest 24, P.O.B. 502.

Подписная цена — $ 32.00 за том. Заказы принимает:

Предприятие по внешней торговле книгами и газетами «Kultúra» (1389 Budapest 62, P.O.B. 149) или его заграничные агентства.

Acta Biochimica et Biophysica

Academiae Scientiarum Hungaricae

Volume 9

Akadémiai Kiadó, Budapest

1974

Contents

Author Index

Subject Index

Acta Biochim. et Biophys. Acad. Sci. Hung. Vol. 9 (1—2), pp. 1—13 (1974)

Freezing-induced Alkylation of SH Groups and Inactivation of Rabbit Muscle Aldolase

P. FRIEDRICH, J. FÖLDI, KATALIN VÁRADI*

Enzymology Department, Institute of Biochemistry, Hungarian Academy of Sciences, Budapest, Hungary

(Received January 8, 1974)

Rabbit muscle aldolase is rapidly inactivated by alkylating agents if subjected to freeze-thaw treatment in sodium or potassium phosphate buffer at −21.5°C. Without freezing, at 0°C, enzyme activity is not impaired by alkylating agents even during several hours of incubation. Freezing-induced inactivation is complete after the alkylation of 3 SH-groups per aldolase tetramer. The radioactive label from (^{14}C)-bromoacetate is distributed between two peptides containing residues Cys-231 and Cys-341, respectively. The transient apparent high reactivity of SH-groups acquired during freeze-thawing can partly be attributed to a conformational change of the protein induced by freezing. The low number of covalently attached carboxymethyl groups suggests that the inactivating effect brought about by chemical modification propagates from one subunit to the other within the metastable tetrameric enzyme.

Introduction

Rabbit muscle aldolase (Fructose 1,6-diphosphate : D-glyceraldehyde-3-phosphate lyase, EC 4.1.2.13) consists of four nearly identical subunits (Lai, 1968; Sajgó, 1971; Midelfort, Mehler, 1972), which are catalytically independent and equivalent within the tetramer (Meighen, Schachman, 1970; Penhoet, Rutter, 1971). The quaternary structure of the enzyme is very stable, inasmuch as tetrameric aldolase does not dissociate into lower aggregational forms either *in vivo* (Midelfort, Mehler, 1972) or *in vitro* without drastic influence (Masters, Winzor, 1971; Lebherz, 1972; Friedrich et al., 1972).

Aldolase contains 8 SH-groups per subunit (Anderson, Perham, 1970; Hajós, Sajgó, 1972; Lai et al., 1971), two of which (Cys-231, Cys-341 (Szajáni et al., 1970; Biszku et al., 1973)) are accessible in the native state. As shown in this laboratory (Szajáni et al., 1969) and elsewhere (Anderson, Perham, 1970) even these SH-groups react sluggishly with alkylating agents: at 37°C they are carboxymethylated in a parallel manner and modification of the less reactive residue (Cys-341)

* Present address: National Institute of Haematology and Blood Transfusion, Budapest.

inactivates the enzyme (Szajáni et al., 1969, 1970). It was concluded that both SH-groups are on the surface of the protein and their low reactivity is due to steric hindrance or to interaction with another functional group.

Since it has been shown that freezing may alter the state of aggregation and side chain reactivity of an oligomeric enzyme (Markert, 1963; Chilson et al., 1965; Gold, Segal, 1965; Südi, Khan, 1970) we undertook to study the behaviour of rabbit muscle aldolase under freeze-thaw conditions. We found that during such a treatment some SH-groups of aldolase acquire a high apparent reactivity towards alkylating agents and the enzyme is inactivated. In the present paper the detailed analysis of this phenomenon will be described.

Materials and methods

Rabbit muscle aldolase (aldolase A) was isolated and three times recrystallized according to Taylor et al. (1948). Succinylated rabbit muscle aldolase and aldolase **B** from hog kidney were prepared as described by Meighen and Schachman (1970) and Alarçon et al. (1971), respectively.

Protein concentration was determined spectrophotometrically by using the coefficients, $A_{280}^{0,1\%} = 0.74$ for aldolase A (Biszku et al., 1964) and 0.85 for aldolase B (Rutter et al., 1966). Calculations were based on a molecular weight of 158 000 for aldolase A (Kawahara, Tanford, 1966; Závodszky, Biszku, 1967).

Aldolase activity was assayed by the hydrazine test of Jagannathan et al. (1956) with fructose 1,6-diphosphate as substrate as described earlier (Friedrich et al., 1972).

Standard freeze-thaw procedure. Enzyme samples (0.5 ml) in 0.1 M sodium phosphate buffer, pH 7.0, made up in Wassermann test tubes at 0°C, were transferred into a thermos bottle containing eutectic NaCl (32 g of NaCl mixed with 100 g of snow), which had a temperature of -21.5 ± 0.3°C. Freezing was completed in about 45 sec. After 2 hours of incubation the samples were removed from the eutectic bath and immediately thawed in a water bath of 22–23°C, during vigorous shaking. Before complete thawing (about 40 sec) the tubes were placed into ice-water (0°C) and kept there until activity assay.

The time of freezing-down was determined by monitoring the solidification of the central upper part of the solution.

In the determination of the number of carboxymethyl groups bound upon freeze-thawing and in the localization of alkyl residues in the primary structure of aldolase (^{14}C)-bromoacetate (specific radioactivity 1.2 mCi per mmole) was used as reagent. Immediately after thawing trichloroacetic acid was added to the samples to 6.6% final concentration. The precipitated protein was washed several times with 3 to 1% trichloroacetic acid to remove excess reagent. Radioactivity was assayed in a Packard Tri-Carb type 2420 liquid scintillation counter. The samples for peptide mapping were fully carboxymethylated in 8 M urea with unlabelled iodoacetate, subjected to tryptic hydrolysis followed by two-dimensional

paper electrophoresis at pH 6.5 and 1.9 and paper chromatography as carried out by Sajgó (1969). The electrochromatograms were stained with ninhydrin and radioautographed. The intensity of spots was compared visually only.

Polyacrylamide-gel electrophoresis was performed according to the method of Hjertén et al. (1965).

Results and discussion

1. *Effect of alkylating agents on aldolase activity during freeze-thaw treatment*

Fig. 1 shows the inactivation of aldolase frozen for different times in the presence of iodoacetamide or iodoacetate. With samples containing iodoacetamide the decrease in activity levels off after 15 min and below 10 mM reagent con-

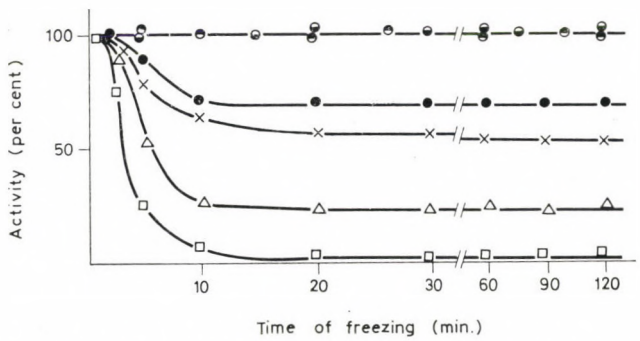

Fig. 1. Dependence of freezing-induced inactivation in the presence of alkylating agents on the time of freezing. Aldolase concentration in all samples: 6.3×10^{-3} mM (= 1m g/ml). Final volume: 0.1 ml. Time of freezing down: 15 sec. ◓: control sample subjected to freezing in the absence of reagent; ◒: control samples containing 10 mM iodoacetamide or 6 mM iodoacetate kept at 0°C; ●, △, □: frozen samples containing 3.5, 5.0 and 10 mM iodoacetamide, respectively, and ×: sample containing 6 mM iodoacetate

centration only partial inactivation occurs. The effect of iodoacetate develops somewhat slower and reaches its final value after about 90 min of freezing. The inactivated enzyme was unstable and precipitated from solution. On the other hand, samples incubated at 0°C with reagent or subjected to freezing without reagent remained fully active. If the enzyme was frozen for 2 hours without reagent, the earliest possible measurement after the beginning of thawing (1 min) showed the enzyme to be 100% active. The residual activities after thawing did not change for at least one hour at 0°C.

It is also seen in Fig. 1 that small changes in iodoacetamide concentration resulted in markedly different levels of inactivation, although even at the lowest concentration applied iodoacetamide was in a large molar excess to the 8 accessible SH-groups of aldolase.

In order to get comparable results, in the routinely applied standard freeze-thaw procedure the time of freezing was kept constant: 2 hours.

In Fig. 2 the dependence of inactivation of aldolase on the concentration of three alkylating agents during standard freeze-thaw treatment is presented. There

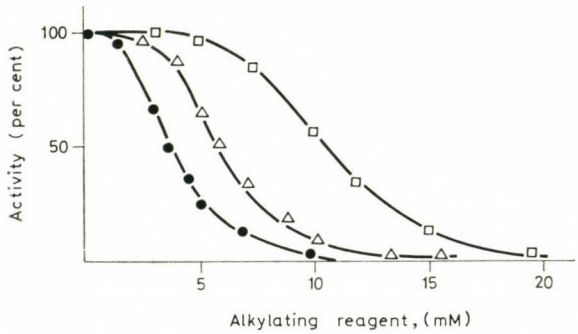

Fig. 2. Effect of concentration of alkylating agents on the inactivation of aldolase during standard freeze-thaw treatment. Aldolase concentration: 6.3×10^{-3} mM. ●: iodoacetamide; △: iodoacetate; □: bromoacetate

is a definite order of efficiency among the reagents to inactivate aldolase, i.e. iodoacetamide > iodoacetate > bromoacetate, which is the pattern excepted from an SH-group as reactant (Webb, 1966). The plots are markedly sigmoidal, which cannot be interpreted in term of a simple bimolecular reaction.

2. *Carboxymethylation of aldolase during freeze-thaw treatment with (^{14}C)-bromoacetate*

In order to test whether alkyl groups are really bound to aldolase during freezing-induced inactivation, the enzyme was subjected to the standard freeze-thaw procedure at different (^{14}C)-bromoacetate concentrations. As shown in Fig. 3A, aldolase is indeed carboxymethylated in the process and the extent of modification is not more than 4 carboxymethyl groups bound per aldolase tetramer even at the highest bromoacetate concentration tested. Furthermore, the relationship between residual activity and the number of carboxymethyl groups bound is not linear (Fig. 3B). The first alkyl group causes little inactivation whereas enzymatic activity is practically completely lost when 3 groups are bound per tetramer.

In order to localize the covalently bound alkyl groups in the primary structure of aldolase, enzyme samples (1 mg/ml) were subjected to the standard freeze-thaw procedure at various (^{14}C)-bromoacetate concentrations. From the partly or completely inactivated enzyme samples tryptic peptide maps were prepared. It was found on radioautography that the isotopic label (maximally 4 carboxymethyl groups per tetramer) was only attached to two peptides: a basic

and a neutral one, which contain Cys-231 and Cys-341, respectively (Sajgó, 1969; Biszku et al., 1973). The proportion of radioactivity was roughly the same in the two peptides at different stages of inactivation.

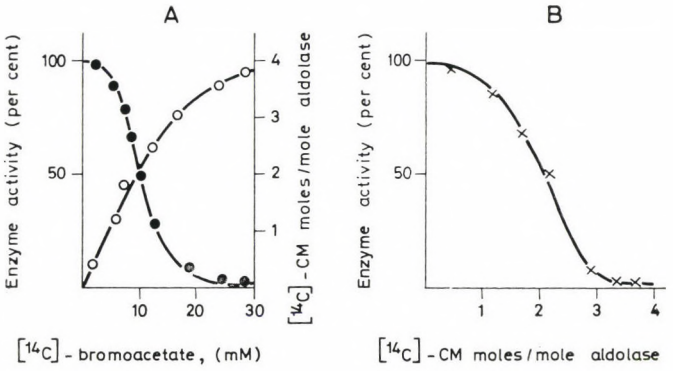

Fig. 3. Carboxymethylation and inactivation of aldolase during freeze-thawing. Aldolase samples (6.3×10^{-3} mM) were subjected to the standard freeze-thaw procedure at various (^{14}C)-bromoacetate concentrations. *A*: ●, enzyme activity; ○, carboxymethylation. Plot *B* was derived from the data of *A*

3. *Effect of repeated freeze-thaw cycles on inactivation*

It appears from the above results that during a freeze-thaw cycle there is a limited period of time when certain SH-groups of aldolase acquire a high apparent reactivity, which leads to their alkylation and to the inactivation of the enzyme. If this is so, then repeated freeze-thaw cycles at a reagent concentration that causes partial inactivation in a single cycle must result in the progressive loss of activity. Furthermore, as each freeze-thaw cycle offers the same time period for a pseudo first order reaction to proceed, one would expect a linear relationship of log residual activity *vs* time, in case of a simple one-by-one mechanism of inactivation. Fig. 4 shows that there is indeed progressive inactivation on repeated freeze-thaw treatments. However, the "progress curve" is of the autocatalytic-type, which suggests a more complex mechanism.

4. *Effect of electrolyte composition on freezing-induced inactivation of aldolase*

The inactivation of 1 mg/ml aldolase samples by 10 mM iodoacetamide or iodoacetate in the standard procedure was completely prevented by 80mM alanine or 1 M NaCl. On the other hand, 10^{-3} M fructose-1,6-diphosphate exerted no protective effect at all. The addition of 0.1 M Tris-HCl, pH 7.5, resulted in the preservation of 60% activity.

Sodium phosphate could be replaced by potassium phosphate without any appreciable change in the basic effect. On the other hand, iodoacetamide in the 5

to 50 mM concentration range failed to cause any inactivation if aldolase was frozen in 0.002 M sodium acetate, pH 6.8, or 0.2 M $(NH_4)_2SO_4$ or 0.2 M sucrose solutions.

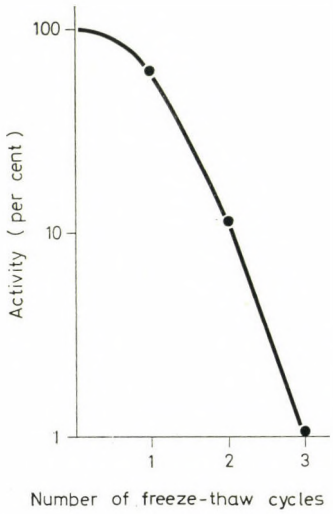

Fig. 4. Effect of repeated freeze-thaw treatment in the presence of iodoacetamide on aldolase activity. Aldolase concentration: 6.3×10^{-3} mM; iodoacetamide concentration: 3 mM. One and the same sample was carried through three cycles, each performed as described for the standard procedure except that time of freezing was 15 min instead of 2 hours (cf. Fig. 1). After complete thawing the next freezing cycle was immediately started

5. *Effect of "simulated" eutectic conditions on aldolase activity*

When a 0.1 M sodium phosphate buffer, pH 7.0, is being frozen marked changes occur both in the composition and in the pH of the solution (Van den Berg, Rose, 1959). At the eutectic point (−9.9°C) the pH is 3.6 and phosphate concentration is 3.5 M. The dissociation of tetrameric lactate dehydrogenase, which occurs on freezing only in sodium phosphate, has been attributed by Chilson et al. (1965) to a compound effect of low pH, low temperature and high ionic strength. In contrast freezing-induced alkylation of aldolase worked just as well in potassium phosphate buffer, the eutectic parameters of which are: −16.7°C, 4.0 M phosphate, pH 7.5 (Van den Berg, Rose, 1959). Apparently, the eutectic pH has no influence on the reaction.

We studied the behaviour of aldolase in phosphate buffer media resembling eutectic conditions (for sodium phosphate: 3.5 M phosphate pH 3.6, for potassium phosphate: 4.0 M phosphate pH 7.5). In either of these media at 0°C or at the eutectic temperatures (−9.9°C and −16.7°C, respectively) or even below in super-cooled solutions without freezing, 1 mg/ml aldolase was stable for hours, inasmuch as it displayed full enzymic activity immediately after dilution. The

addition of 20 mM iodoacetamide to the above mixtures did not affect the enzyme either, even on prolonged incubation. However, if the super-cooled solutions containing iodoacetamide were seeded with an ice crystal so that freezing took place, after thawing the enzyme was completely inactive. The formation of ice lattice seemed to be indispensable for inactivation.

6. *Effect of aldolase concentration on freezing-induced inactivation by alkylating agents*

Figs. 5 and 6 show freezing-induced inactivation as a function of iodoacetate and iodoacetamide concentration, respectively, at different aldolase concentrations. It is seen that on increasing protein concentration the same extent of inactivation could be observed at about proportionally greater reagent concentrations.

In addition, at high iodoacetamide concentrations the inactivating effect was reversed: increasing amounts of the reagent caused less inactivation. Although

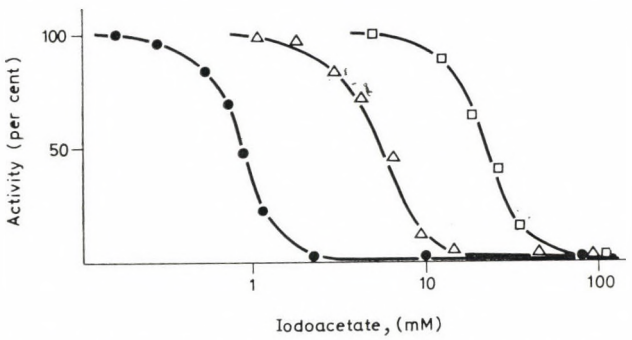

Fig. 5. Inactivation by iodoacetate during standard freeze-thaw treatment at different aldolase concentrations. Aldolase concentrations: ●: 0.1 mg/ml (0.63 μM); ▲: 1.0 mg/ml (6.3 μM); □: 5.0 mg/ml (32 μM)

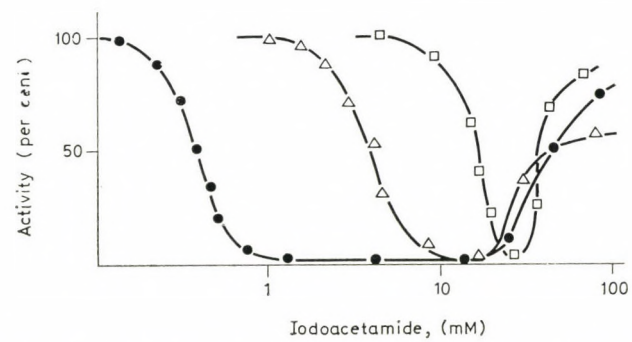

Fig. 6. Inactivation by iodoacetamide during standard freeze-thaw treatment at different aldolase concentrations. Symbols the same as in Fig. 5

the mechanism underlying this paradoxical phenomenon is not clear, this finding suggests that the concentration of reagent during freezing cannot alone account for the high apparent reactivity of aldolase SH-groups. There must be an additional effect of freezing, most probably a conformational change of the enzyme, which by exposing the SH-groups promotes alkylation. We may then assume that in high concentration iodoacetamide markedly alters the solvent medium, the structure of ice formed and therefore the structural change of the protein required for inactivation does not take place. This assumption is supported by the fact that the paradoxical reversion of the inactivating effect of iodoacetamide did not depend on protein concentration; it became pronounced when the concentration of reagent approached that of the buffer anion.

For the interpretation of protein concentration dependence shown in Figs. 5 and 6 (disregarding now the anomalous behavior at high iodoacetamide concentration) we must consider the process of freezing-induced alkylation. The most plausible hypothesis is that during the course of freezing aldolase undergoes a structural change, the SH-groups located on or near the surface become more exposed, and during thawing the concentrated reagent alkylates some of these SH-groups. In this case one would expect that during thawing the reversal of structural change and the alkylation of SH-groups are parallel, mutually exclusive reactions, the former of first order and the latter of second order kinetics. Were this true, however, then all three curves in Figs. 5 and 6 should coincide. The experimental data unequivocally disprove such a simple explanation.

Another interpretation would be a mechanism analogous to that described by Südi and Khan (1970) for lactate dehydrogenase. This tetrameric enzyme transiently dissociates after freeze-thawing and the subunits are susceptible to inactivation by iodoacetamide. Since the recombination and alkylation of subunits are parallel, mutually exclusive reactions, and the rate of the former is proportional to a higher power of protein concentration than that of the latter, an increase in protein concentration at unchanged reagent concentration enhances recombination (and reactivation) at the expense of alkylation (and inactivation). In other words a protein concentration dependence resembling those of Figs. 5 and 6 was observed.

In order to test this mechanism for aldolase, we examined by means of the hybridization technique whether aldolase dissociated on freeze-thaw treatment. Namely, if the tetramer transiently falls apart into subunits then with a suitable partner, which behaves similarly, aldolase should give hybrid tetramers. We chose aldolase B from hog kidney (Alarçon et al., 1971) and succinyl aldolase, an artificial "isoenzyme" of aldolase A (Meighen, Schachman, 1970) as such partners, both of which are able to form hybrids with rabbit muscle aldolase on acid or urea treatment. All our attempts to produce hybrids from these species by freeze-thawing proved negative as detected by polyacrylamide-gel electrophoresis. It might be worth mentioning in addition to standard freezing at various protein concentrations, we also tried 0.1 M potassium phosphate, pH 7.0, as medium, sodium or potassium phosphate containing 1 M NaCl, and also changed the mode

of freezing and thawing in these media by allowing the sample tubes to stand in a deep-freeze at $-26°$ (freezing time about 30 min) and to thaw at room temperature in air (thawing time about 20 min). This slow freezing and/or thawing did not significantly alter the inactivation pattern with alkylating agents. These findings are in accord with recent data (Lebherz, 1972) on the failure to hybridize aldolase by freeze-thaw treatment.

Of course, the lack of detectable hybrids in our systems does not conclusively disprove the dissociation-recombination model. However, it suggests that if the subunits separate at all, this must be very limited both in time and space. Accordingly, it renders the above explanation for the data of Figs. 5 a nd 6 rather unlikely.

7. *Time of attack of alkylating reagents during freeze-thaw treatment*

To be able to interpret our observations described in the previous sections, it was necessary to examine more closely when, during the course of a freeze-thaw cycle, alkylation occurs. Obviously, there are three different stages to be considered, A) the process of freezing down, B) the frozen state and C) the period during and/or after thawing.

A) *Freezing down*

As shown in Fig. 1 above, to reach the final stage of inactivation needs much longer time than freezing down proper. After 1 min of freezing activity was 100%. This can only mean that during freezing down either no alkylation occurs or only Cys-231 is alkylated, which was shown not to impair enzyme activity (Szajáni et al., 1970). Our data could be reconciled with the latter alternative by assuming that the enzyme thus modified must undergo a structural change in the frozen state to become inactive after thawing.

In order to test this assumption we performed the following experiment. An aldolase sample (1 mg/ml) containing 10 mM iodoacetamide was frozen for 1 min. Within this time the solution completely froze. The sample was then rapidly thawed as in the standard procedure. The enzyme remained fully active and was stable on further incubation at 0°C. The same sample was then gel-filtered on a small Sephadex G-50 column equilibrated with 0.1 M sodium phosphate buffer, pH 7.0, to remove unbound iodoacetamide. The gel-filtered aldolase solution was then subjected to the standard freeze-thaw procedure, after which the enzyme was still 100% active.

This experiment seems to exclude that any alkylation takes place during freezing down, since in that case we should have observed activity loss after the second freeze-thaw procedure.

B) *The frozen state*

It has been reported that there are always unfrozen cores in polycrystalline ice (Paren, Walker, 1971). As shown by PMR studies, in a macroscopically frozen protein solution an appreciable amount of water, that bound to protein, remains

liquid around −20°C (Kuntz et al., 1969). This bound, super-cooled water amounts to about 0.5 g per g of protein. Although according to these data a protein molecule in a frozen solution is surrounded by quasi-mobile water molecules, it seems unlikely that in this thin aqueous envelope a reagent molecule would have the translational freedom to collide and to react (Kuntz, Brassfield, 1971).

C) *Thawing*

The curves in Fig. 1 can be readily interpreted by assuming that the reagents react with aldolase on thawing if a slow structural alteration of the protein had taken place in the frozen state. Our attempts to seize aldolase in its reactive state after thawing are summarized in Table 1. It is seen, however, that iodoacetamide was only effective if added before freezing.

Table 1

Effect of reagents added before or after freezing on aldolase activity

The standard freeze-thaw procedure was applied

Aldolase conc. mM	Iodoacetamide		Cysteine		Residual activity, per cent
	mM	time of addition	mM	time of addition	
6.2×10^{-3} (= 1 mg/ml)	—	—	—	—	100
6.2×10^{-3}	10	before freezing	—	—	2
6.2×10^{-3}	10	before thawing*	—	—	100
6.2×10^{-3}	10	before freezing	50	before freezing	99
6.2×10^{-3}	10	before freezing	50	before thawing*	1
6.2×10^{-4}	10	before thawing*	—	—	95

* Pipetted on top of the ice just before thawing.

Similarly, cysteine added before freezing could ward off the inactivating effect of iodoacetamide, obviously by using up the reagent, but had no protective effect at all if applied at thawing. Essentially the same results were obtained with iodoacetate. The above data suggest that if there is a freezing-induced structural change in the protein, it is very rapidly reverted after thawing; at any rate faster than any additives given at the time of thawing could gain access to the reactive side chains.

8. *Interpretation of freezing-induced alkylation and inactivation of aldolase*

In light of the experimental data presented the events taking place during a freeze-thaw cycle might be explained as follows. At the start of the freezing water is being frozen out. The ice lattice excludes solute molecules, which become con-

centrated in unfrozen water. As a result more and more reagent molecules will be "dissolved" in the bound water of the protein, which means that they displace H_2O molecules. In the extremes all the reagent molecules would accumulate around the enzyme molecules forming a "shell", and the extent of alkylation and consequential inactivation during thawing may depend upon the continuity or density of this shell. At a certain stage the enzyme molecules surrounded by the shell will be left behind as huge "mistakes" in the ice lattice. The distorting force of ice crystals brings about a structural change in the enzyme, which results in the ready accessibility of certain SH-groups. On thawing, the reagent molecules included in the shell will have a ready access to these SH-groups, before the structural change would be reversed or any other substance, for example cysteine, added before thawing could reach the enzyme surface by mixing and diffusion.

At all protein concentrations tested 50% inactivation was observed when the iodoacetamide/aldolase molar ratio was about 5×10^2. Since the amount of bound water, in a given volume, is proportional to protein concentration as shown by PMR studies (Kuntz et al., 1969), it may well be that this constant "stoichiometry" at different enzyme concentrations, i.e. the displacement of curves in Figs. 5 and 6 along the abscissa, reflects the reagent requirement to form shells of equal density. More sophisticated techniques, such as NMR spectroscopy, would be needed to test whether the reagent molecules replace, or intercalate between, molecules of bound water.

Three lines of evidence suggest that the freezing-induced inactivation of rabbit muscle aldolase by alkylating agents proceeds in a co-operative manner: 1) the sigmoidicity of curves activity loss *vs* reagent concentration (Fig. 2), 2) the autocatalytic-type progress curve of inactivation on repeated freeze-thaw treatments (Fig. 4), and 3) the sigmoidicity of the curve inactivation *vs* bound carboxymethyl groups (Fig. 3B). Co-operativity can be exercised here at two levels: a) alkylation of one residue facilitates the reaction of the other, and b) binding of the first alkyl group potentiates the inactivating effect of the next one(s). The latter mechanism seems to be supported by point 3) above, whereas points 1) and 2) can be interpreted in terms of either mechanism. Although such co-operative effects are probably, but need not be, mediated through subunits interactions, in the present case there is evidence that, at least in part, this is the case. The fact that inactivation is complete upon the binding of three carboxy-methyl groups per aldolase tetramer, and even these few groups are distributed over Cys-231 and Cys-341, indicates that certain subunits must be inactivated just because their neighbours are alkylated.

Fig. 7 gives a simplified scheme of the postulated events. On freezing the enzyme undergoes a reversible structural change, and some SH-groups become more exposed than in the native state. The covalent attachment of a single alkyl group to the tetramer has no deleterious effect on the enzyme, it will regain its native structure with little, if any, loss of activity. However carboxy-methylation of further cysteinyl residues brings about the collapse of the whole molecule.

In our earlier studies on the carboxymethylation of aldolase at 37°C, the

enzyme was inactive but fairly stable after the alkylation of both Cys-231 and Cys-341 residues in all four subunits. Our present experiments thus reflect another feature of protein architecture in the aldolase molecule. Namely, at 37°C the alkyl

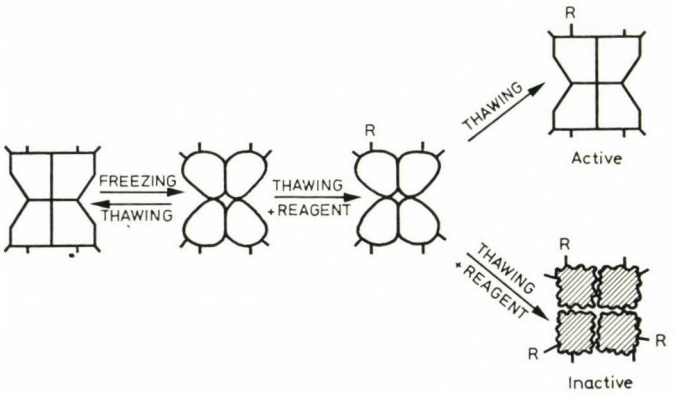

Fig. 7. Proposed scheme of freezing induced inactivation of aldolase by alkylating agent. *Reagent* means that freezing-thawing is performed in the presence of alkylating reagent. The short and long stems on the subunits designate SH-groups exposed to different extents. *R* denotes alkyl groups bound to aldolase. The arrangement of *R* in the right-hand scheme is arbitrary. The hatched species with wavy contours is inactivated, denatured aldolase

groups were bound to an enzyme with intact quaternary structure, where the mutual saturation of contact surfaces endowed the protein with a considerable structural stability (Chan, Mawer, 1972; Deal et al., 1963). On the other hand, in the freeze-thaw experiment the alkylating agent attacks the enzyme in a metastable state, where the intersubunit bonds are probably weakened, and therefore is able to induce a profound and irreversible structural disorganization.

Thanks are due to Professor F. B. Straub for his continued interest in the present work and to Dr Gertrud Szabolcsi for valuable discussions and thorough criticism.

References

Anderson, P. J., Perham, R. N. (1970) Biochem. J. *117* 291–298
Alarçon, O., Gonsales, F., Marcus, F., Flores, H. (1971) Biochim. Biophys. Acta *227* 460–463
Van den Berg, L., Rose, D. (1959) Arch. Biochem. Biophys. *81* 319–329
Biszku, E., Boross, L., Szabolcsi, G. (1964) Acta Physiol. Acad. Sci. Hung. *25* 161–167
Biszku, E., Sajgó, M., Solti, M., Szabolcsi, G. (1973) Eur. J. Biochem. *38* 283–292
Chan, W. W. C., Mawer, H. M. (1972) Arch. Biochem. Biophys. *149* 136–145
Chilson, O. P., Costello, C. A., Kaplan, N. O. (1965) Biochemistry *4* 271–281
Deal, W. C., Ritter, W. J., Van Holde, K. E. (1963) Biochemistry *2* 246–251
Friedrich, P., Arányi, P., Nagy, I. (1972) Acta Biochim. Biophys. Acad. Sci. Hung. *7* 11–19

Gold, A. H., Segal, H. L. (1965) Biochemistry *4* 1506—1511
Hajós, Gy., Sajgó M. (1972) Acta Biochim. Biophys. Acad. Sci. Hung. *7* 315—318
Hjertén, S., Jerstedt, S., Tiselius, A. (1965) Anal. Biochem. *11* 219—223
Jagannathan, V., Singh, K., Damodaran, M. (1956) Biochem. J. *63* 94—105
Kawahara, K., Tanford, C. (1966) Biochemistry *5* 1578—1584
Kuntz, I. D. Jr., Brassfield, T. S., Law, G. D., Purcell, G. V. (1969) Science *163* 1329—1331
Kuntz, I. D. Jr., Brassfield, T. S. (1971) Arch. Biochem. Biophys. *142* 660—664
Lai, C. Y. (1968) Arch. Biochem. Biophys. *128* 202—211
Lai, C. Y., Chen, C., Smith, J. D., Horecker, B. L. (1971) Biochem. Biophys. Res. Comm. *45* 1497—1505
Lebherz, H. G. (1972) Biochemistry *11* 2243—2250
Markert, C. L. (1963) Science *140* 1329—1330
Masters, C. J., Winzor, D. J. (1971) Biochem. J. *121* 735—736
Meighen, E. A., Schachman, H. K. (1970) Biochemistry *9* 1163—1176
Midelfort, C. F., Mehler, A. H. (1972) Proc. Nat. Acad. Sci. US. *69* 1816—1819
Paren, J. G., Walker, J. C. F. (1971) Nature Phys. Sciences *230* 77—79
Penhoet, E., Rutter, W. J. (1971) J. Biol. Chem. *246* 318—323
Rutter, W. J., Henley, J. R., Groves, W. E. Calder, J., Rajkumar, T. V., Woodfin, B. M. (1966) in "Methods in Enzymology" (Colowick, S. P., Kaplan, N. O. Eds.) Vol. IX. pp. 479—498. Acad. Press, N. Y., London
Sajgó, M. (1969) Acta Biochim. Biophys. Acad. Sci. Hung. *4* 385—389
Sajgó, M. (1971) FEBS Letters *12* 349—351
Südi, J., Khan, M. G. (1970) FEBS Letters *6* 245—256
Szajáni, B., Friedrich, P., Szabolcsi, G. (1969) Acta Biochim. Biophys. Acad. Sci. Hung. *4* 265—272
Szajáni, B., Sajgó, M., Biszku, E., Friedrich, P., Szabolcsi, G. (1970) Eur. J. Biochem. *15* 171—178
Taylor, J. F., Green, A. A., Cori, G. T. (1948) J. Biol. Chem. *173* 591—604
Webb, J. L. (1966) in Enzyme and Metabolic Inhibitors. Vol. III. pp. 9—13, Acad. Press, N. Y., London
Závodszky, P., Biszku, E. (1967) Acta Biochim. Biophys. Acad. Sci. Hung. *2* 109—112

Acta Biochim. et Biophys. Acad. Sci. Hung. Vol. 9 (1–2), pp. 15–32 (1974)

Study of the Oxygen Effect Mediated by Janus Green B

G. ELEK,* B. TURCSÁNYI,** R. HOLLAND***, L. LADÁNYI****

* 1st Department of Pathology, Semmelweis University Medical School, ** Central Research Institute for Chemistry of the Hungarian Academy of Sciences, *** Department of Pathology Péterfy Sándor Street Hospital, *** Institute of Inorganic and Analytical Chemistry, Eötvös Loránd University Budapest, Hungary

(Received September 3, 1973)

Janus Green B at concentrations 5×10^{-5} to 5×10^{-4} M kills mouse ascites tumour cells in oxygen atmosphere, whereas in nitrogen atmosphere the tumour remains transplantable. The dye is reduced in the cells. Among the other phenazine derivatives tested only N-methyl-phenazinium methylsulfate exhibited similar effect in the same concentration. JgB gives two cathodic waves on dropping mercury electrode. It was shown by cyclic voltammetry that the first step is chemically reversible (JgB → Leuco JgB II). The cleavage of the azo-bond can be excluded at this potential. In the first reduction step a free radical intermediate is also formed; the electron spin resonance signal of which is a singlet of 2.003 g value and of 14.69 gauss width. It has been shown by line narrowing that the ESR signal consists of at least nine lines. The same singlet was obtained when the dye was reduced chemically in the cell suspension. In the second cathodic step of JgB reduction the formation of free radicals could not be detected. Here the four-electron reduction of leuco JgB II takes place which gives N,N diethyl-amino 5,10-dihydrophenazine and N,N-dimethyl-1,4-phenylenediamine. The reduction decreases the biological "oxygen effect" of JgB. The dye after reduction by six electrons does not inhibit the growth of mouse ascites tumours in oxygen atmosphere.

Introduction

Janus green B, a dye usually applied to vital staining, induces a so-called "oxygen effect" in amytal and other mouse ascites tumours. The phenomenon is as follows. At a certain dye concentration the cells incubated at 37°C in oxygen athmosphere perish, whereas if maintained in nitrogen atmosphere the cells prove viable when inoculated into animals. Cells kept in oxygen atmosphere at 0°C also remain viable (Braun et al., 1967). We could elicit the same phenomenon with

Abbreviations: DES, diethylsafranine; DEHS, N,N'-diethylamino 5,10-dihydrophenazine; DME, dropping mercury electrode; DPD, N,N-dimethyl-1,4-phenylenediamine; ESR, electron spin resonance; *g*, gyromagnetic factor; JgB, Janus green B; C^+, phenazinium cation; L, leuco form; MFM, N-methyl-phenazinium methylsulfate; $R^\cdot$, neutral radical form.

N-methyl-phenazinium methylsulfate (MFM) applied in similar concentrations. We also observed that on the effect of JgB the free radical concentration of the cell suspension increased (Holland, Elek, in preparation). It has already been stated that MFM is reduced in the cells with the concomitant formation of free radicals (Ishizu et al., 1968) and in the presence of oxygen it may damage the biological systems. On this basis we assumed that the effects of the two substances could be traced back to some common mechanism.

MFM and certain other compounds of similar effect known from the literature (White, White, 1968) are compounds that can reversibly reduced and re-oxidized and exhibit marked similarity to the quinone-semiquinone-hydroquinone system. Although it had not been demonstrated earlier that JgB can be reduced reversibly, it was assumed that it incorporated into the mitochondrial electron transport chain and formed a "pathological shunt" (Braun et al., 1967; Stein et al., 1969). Therefore we made an attempt to elucidate the mechanism of reduction of the dye both in vitro and in vivo. First of all we wanted to clarify whether the reduction is reversible or not. Furthermore we examined whether during this reduction the same products are formed as during the reduction of MFM. Further, the possibility of producing radicals having the same ESR spectrum as observed in the tumour cells, was studied.

Materials and methods

Materials

JgB, diethylsafranine (Michrome), N-methyl-phenazinium methyl and ethylsulfate (British Drug Houses), brillant cresyl blue and Nileblue sulfate (Bayer), neutral violet, neutral red, coelestin blue (Merck), ascorbic acid (Reanal),tetraethyl ammonium bromide, potassium borohydride, N,N-dimethyl-1,4-phenylene diamine (Fluka) were of reagent grade. Acetonitrile for the electrochemical experiments was pre-treated according to the method of Forcier and Olver (1965). The nitrogen gas (99.95%) for the electrolytic experiments to remove oxygen from the solutions to be tested was freed from oxygen by bubbling it through solutions of copper (I) amine complex and 5% alkaline pyrogallol. The gas was dried by letting it through concentrated sulfuric acid, a Klinosorb molecular sieve, and granular KOH. Tetraethyl ammonium bromide (0.1 M) was used as base electrolyte.

A) *Chemical methods*

The polarographic measurements were carried out with a Radelkis OH-102 type polarograph, dropping mercury and saturated calomel electrodes. The accuracy of the determination of half wave potentials was ± 5 mV. The cyclic

voltammetric measurements (cf. Adams, 1969) were made with a Radiometer PO-4 G polarograph, a Methrohm E 446-IR compensator using impregnated graphite indicator and saturated calomel reference electrode, in Britton Robinson and phosphate buffers in the usual three-electrode system. The data of electrodes are shown in Table 1. Macro-electrolysis was performed in aqueous medium with a

Table 1

Polarographic data of JgB in aqueous medium

pH 6.6; temperature 25.0°C; $m^{2/3} \cdot t^{1/6} = 2.951$ $mg^{2/3}sec^{1/2}$; $h = 70$ cm.
Accuracy of half wave potential measurements: ± 5 mV

JgB	$E_{1/2}$ (Volt)	Logarithmic analysis $C = 5 \cdot 10^{-4}$ M/L $\lg \frac{i_d - i}{i} = f(E)$ (Volt/lg. unit)	$i_d = f(C)$ function
Wave 1	−0.287	0.075	linear
Wave 2	−0.477	0.038	linear
JgB reduced by six electrons	−0.463	—	—

mercury pool electrode. The reference electrode was a Radiometer K 401 type saturated calomel electrode. The anode was a platinum spiral that merged into the separated cathode compartment, which was connected to the solution by an agar/KNO_3 bridge. Radelkis type OH-404 potentiostat and coulometer were used. The determination of the number of electrons involved (n) was based on Faraday's 1st and 2nd laws. The pH values were measured by a Radelkis OP-205 type precision pH-meter, using Methrohm EA-120-X type combined glass electrode. The ESR spectrum was registered with a JES-P-10 or JES-ME-3X spectrometer. The electrolysis cell placed into the cylindrical resonance cavity was constructed after Geske and Maki (1960) applying mercury cathode and an Ag/AgCl electrode as anode. The cell was checked by reduction of nitrobenzene (Geske, Maki, 1960), 1,4-dinitrobenzene (Maki, Geske, 1960), 4-nitrobenzaldehyde (Maki, Geske, 1961) and terephtal-aldehyde (Maki, 1961). Before registering the ESR spectrum, the polarographic reduction of the compound investigated was also carried out in the cell, and the potential of the working electrode was adjusted 0.1 to 0.5 V more negative than the half wave potential of the compound to be reduced (Clark, 1960; Berg, 1955). The measurement of magnetic fields corresponding to the spectrum lines was performed by JES-FC-1 proton field calibrator unit. The value of g was determined relative to the 3rd line of Mn^{2+}MgO control. The ESR spectrum of the tumour cell suspension was determined at the temperature of liquid nitrogen (Kovalenko et al., 1971; cf. Fig. 1). The resolution of the singlet

ESR spectrum of JgB was made by line narrowing technique (Mohos, Tüdős, 1970; Mohos, 1971). In field calibration and spectrum analysis IRA-5 and CDC-3300 computers were used.

B) *Biological methods*

The "oxygen effect" was studied in Swiss white mice weighing 30–35 g. The amytal ascites tumour (Juhász et al., 1955) was also maintained such random bred mice. The ascites cell suspension used was 8 to 10 days old. Cell count was determined after staining with Schrek's solution in a Bürker chamber. The compound

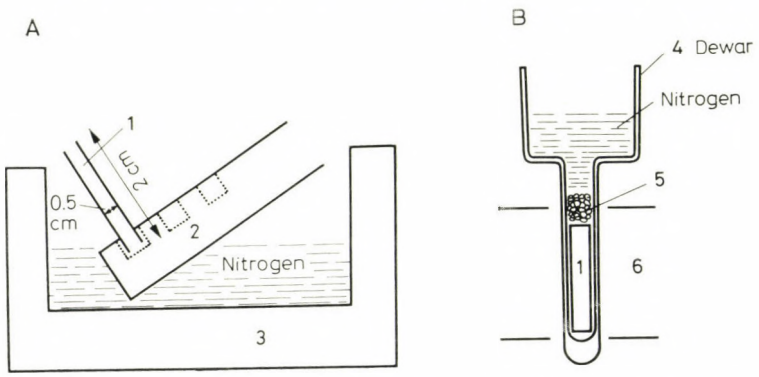

Fig. 1. Preparation of specimens at the temperature of liquid nitrogen for ESR measurement. The sample was either pressed into a teflon form (Kovalenko et al., 1971) or poured into a plastic tube fixed in a teflon board. *A)* The form or teflon board is placed into liquid nitrogen. 1. Plastic tube containing the sample. 2. Teflon board into which the plastic tube is fixed before pouring the sample. 3. Plastic basin made of porous plastic material containing the liquid nitrogen for freezing. *B)* The measurement is carried out in a Dewar flask (4) made of quartz. The sample is removed from the teflon form and is placed into the Dewar flask. In the case of the plastic tube the removal is unnecessary, the tube is placed into the Dewar flask together with the sample. A loose plug of cotton wool is placed on top of the sample (5) and then liquid nitrogen is poured on the cotton wool. Thus nitrogen only cools from above, and one can register the spectrum for a long time undisturbed even at the highest sensitivity of the instrument. It is advisable to wrap the upper wider cylinder of the Dewar flask with cotton wool, not to let the condensed vapour leak into the resonance cavity. Finally the Dewar flask is placed into the resonance cavity (6)

to be tested, in concentrations 0.5 to 5×10^{-4} M, was incubated in the dark for 30 minutes with a suspension of 10^7 tumour cells per ml in oxygen or nitrogen atmosphere. Gas perfusion was performed in mildly shaken glass flasks merged into a 37°C water bath. Then 0.5 ml samples were inoculated into mice intraperitoneally. The growth of tumours was observed for 100 days. The died animals were dissected and if they had no tumour, they were classified into the category "died for other reason".

Results

I. *Cyclic voltammetric studies*

1. The reduction of JgB was studied at pH 6.6 on carbon paste electrode (Fig. 2A, B and C). As shown in Fig. 2A, both cathodic waves of JgB are to a first approximation reversible, i.e. the cathodic peaks (waves a and b) have their anodic counterparts (waves c and d, respectively).

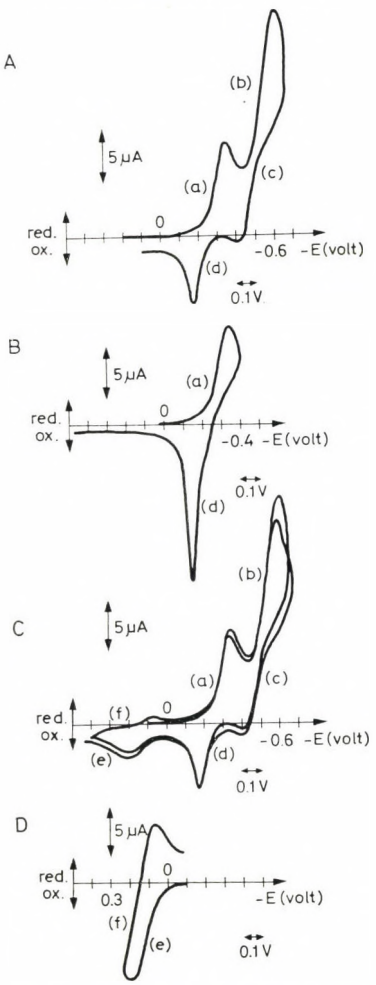

Fig. 2. Reduction of JgB by cyclic voltammetry on a carbon paste electrode at pH 6.6. *A.* Anodic reversal of the direction of polarization after the second cathodic peak *(b)*. *B.* Anodic reversal of the direction of polarization after the first cathodic peak *(a)*. *C.* Further anodic polarization after the second anodic peak *(d)*. *D.* Cyclic voltammogram of N,N-dimethyl-1,4-phenylene diamine at a carbon paste electrode at pH 6.6

2. The reversibility of wave (a) can also be observed if the direction of the scan is reversed before reaching wave (b). In such cases no further waves can be found after the peak (d) on further anodic polarization (Fig. 2B). If 25 sec are allowed to elapse after registering wave (a) and then the direction of polarization is reversed, wave (d) appears as a sharp, "stripping" peak.

3. Proceeding as described in I/1, but scan is continued after registrating wave (d), a new quasi-reversible redox system appears (Fig. 2C, waves (e) and (f)).

4. The two waves of this new redox system appeared if DPD was subjected to cyclic voltammetric oxidation under identical conditions (Fig. 2D).

II. *Polarography, potentiostatic macroreduction and coulometry*

JgB gives two consecutive cathodic waves in aqeuous solution on DME at pH 6.6 ($E^a_{1/2} = -0.287$ V; $E^b_{1/2} = -0.477$ V; Fig. 3, curve A). The ratio of wave heights ($i^a_d : i^b_d$) is 1 : 2 within the limits of experimental error. The concentration dependence of both waves is linear in the 5×10^{-5} to 10^{-3} M interval (Table 1).

Potentiostatic macro-reduction (mercury pool cathode, $C = 10^{-3}$ M, nitrogen atmosphere) on the second wave ($E = -0.700$ V) yielded $n = 6$ as number of electrons involved ($n = 6.0 \pm 1.1$). At the end of electrolysis the solution is pale yellow and gives a single anodic wave ($E^c_{1/2} = -0.463$ V; Fig. 3, curve C wave (c)). If the mercury pool electrode was used as anode ($E = -0.500$ V), JgB reduced with six electrons could be oxidized into a dark purple product. This latter gives a cathodic wave ($E^r_{1/2} = E^c_{1/2}$) at the DME. If this oxidation is only partial, a redox wave is obtained (Fig. 3, curve B, wave (r)). The dark purple product is also formed on the effect of air or oxygen.

The chloroform extract of the solution of the dark purple product was evaporated and we could demonstrate three compounds from the residue of mass number 342, 343 and 344 by means of mass spectrometry.

As seen in Fig. 3 and in Table 1, $E^a_{1/2}$ and $E^r_{1/2}$ are half wave potentials differing from each other only slightly, but still beyond the limits of experimental error. It should be mentioned that the height of the anodic or redox waves $(i^c_d = i^r_d)_b$ is just one-half of that of the second cathodic wave (i^b_d), i.e. $i^b_d/i^c_d = 2$.

III. *ESR studies*

1. *Chemical reduction*

JgB was reduced by an excess of ascorbic acid in the presence of air, in alkaline aqueous medium. The mixture turned violet only on heating and in contrast to the strongly reducing alkali borohydride, ascorbic acid did not bleach the solution. In this case the first polarographic wave of JgB did not completely disappear. In aliquots taken before, during and after heating ESR absorption was not observed.

Most free radicals have very short half-lives in aqueous media. We assumed that if neutral radicals are formed as intermediates, these could be extracted with benzene. Therefore we continued the reduction experiment by layering benzene

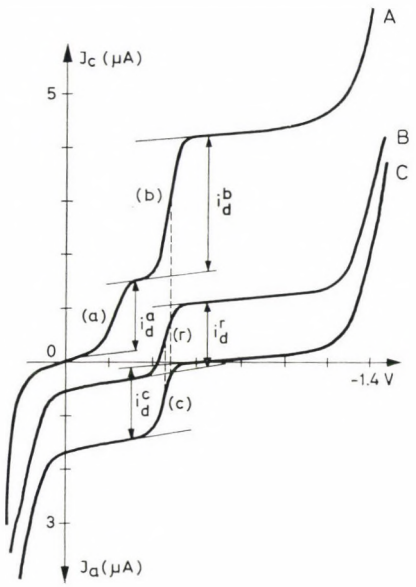

Fig. 3. Potentiostatic macro-electrolysis of JgB. *A*. Polarogram of JgB before macro-reduction. *B*. Polarogram after complete macro-reduction. *C*. Polarogram recorded after partial macro-oxidation following the six-electron macro-reduction

over the alkaline (pH 8 to 9) ascorbic acid-JgB reaction mixture, and the two phases were mixed by vigorous shaking. Already at the beginning of reduction free radicals could be detected by means of ESR. In the aqueous phase a narrow singlet (about 1.9 gauss), whereas in the benzene phase a 14.6 gauss wide intensive signal could be recorded. The most intensive signal was detected at the beginning of reduction in the blue-coloured mixture. The signal of the aqueous phase vanishes within minutes, but that of the benzene phase is more stable, it can be detected even after several days. We also observed free radicals in the benzene extract of the reaction mixture of other phenazine dyes when reduced with ascorbic acid (Table 2, Fig. 4).

The half-line width and g value of ESR signal observed in the benzene phase were the same as those of the singlet found in tumour cells treated with the dye (Fig. 5). Only some hydrophobic part of the cell structure could ensure the environment required for the maintenance of the radical. Presumably lipids play the role that was fulfilled by benzene in the above experiment. To test this hypothesis, we performed the reduction also by substituting living or dead tumour

Table 2

The "oxygen effect" of some phenazine and phenoxazine compounds and the ESR absorption after reduction in vitro

The "oxygen effect" was measured with 5×10^{-5} M dye and the ESR spectra were registered as described in Methods. While incubating in the tumour cell suspension the colour of dye changes: +; it does not change: −. Hyperfine structure: ++, singlet spectrum: +; lack of paramagnetic resonance: 0. The number of animals died for other reasons is indicated in brackets

Compound tested				Nitrogen atmosphere	Oxygen atmosphere	ESR signal
No.	Group	Name	Colour change	Ratio of the number of animals inoculated with the tumour incubated in the indicated atmosphere *and* the number of tumours that have taken		
1.	Phen-azines	N-methyl-phenazinium methyl sulfate (MFM)	+	15/14	15/2	++
2.		N-ethyl-phenazinium ethyl sulfate	+	10/10	$10/9_{(1)}$	++
3.		Neutral violet	+	10/9	$10/8_{(1)}$	+
4.		Neutral red	−	10/9	$10/9_{(1)}$	0
5.		Safranin T extra	+	10/10	10/10	+
6.		Diethylsafranine (DES)	+	$20/18_{(2)}$	$20/19_{(1)}$	+
7.		Janus green B(JgB)	+	20/20	20/0	+
8.	Phenox-azines	Brilliant cresyl blue	+	10/10	10/10	++
9.		Nile blue sulfate	+	10/10	10/10	++
10.		N,N-dimethyl-1,4-phenylene diamine (DPD)	−	10/10	10/10	+

cells for benzene. The mixture contained 20 to 50 million cells per ml in physiological NaCl and JgB. On the effect of the reducing agent (ascorbic acid, KCN) then a singlet appeared in the aqueous cell suspension, similar to that observed in the benzene phase. The intensity of this signal was 10 to 50 times as high as the intensity of the signal found in normal tissues at the $g = 2$ position. The reducing agents failed to evoke this effect if applied alone, without the dye. By centrifuging the cell suspension we could make it sure that the paramagnetic centres are localized in the cells.

2. *Electrolytic reduction in the resonance cavity of the spectrometer*

The spectrum of JgB did not exhibit any hyperfine structure after reduction either in solution or in the cell suspension. As the reduction was not performed in the absence of oxygen, it could be assumed that the lines were broadened by oxygen (cf. Hedvig–Zentai, 1969). Therefore we also reduced the compound in

another way, which can be better standardized, namely by electrolysis in nitrogen atmosphere. In addition to JgB we also reduced the other phenazine dyes at our disposal (Table 2). These phenoxazine dyes had also been applied to the staining of mitochondria (Tanaka, 1968).

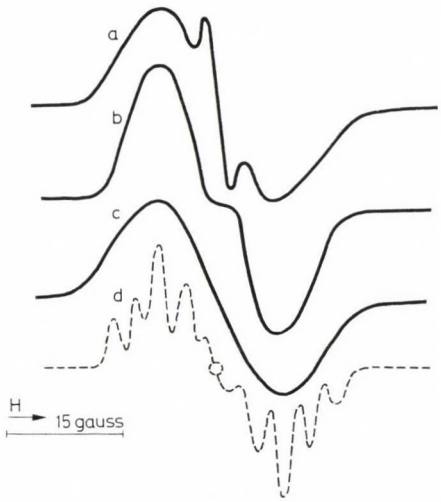

Fig. 4. ESR spectra of radicals obtained by the reduction of certain dyes. *A*. Brilliant cresyl blue. *B*. Neutral violet. *C*. JgB. *D*. Spectrum obtained for JgB after line-narrowing transformation. Modulation: 0.8 gauss; $\tau = 0.3$, amplification 2000-fold, $t = 5$ minutes

JgB exhibited the same ESR signals in nitrogen atmosphere in acetonitrile, as in the benzene phase after reduction with ascorbic acid. With the exception of neutral red, all other dyes were reduced *via* the formation of free radicals.

With the exception of Nile blue sulfate, low intensity paramagnetic absorption in aqueous solution was only observed under extreme conditions (10 to 12 gauss modulation, 3000-fold amplification). The signal of JgB was a singlet of 2.003 ± 0.001 g, 14.69 ± 0.14 gauss wide, in both acetonitrile and water. In electrolysis the 1.97 gauss wide, 2.004 ± 0.001 g signal found in the aqueous phase of the ascorbic acid reduction mixture, was never observed. Apparently, this signal might be related to the oxidation of ascorbic acid (cf. the review of Wyard, 1969).

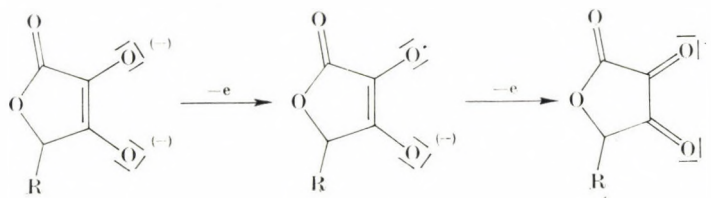

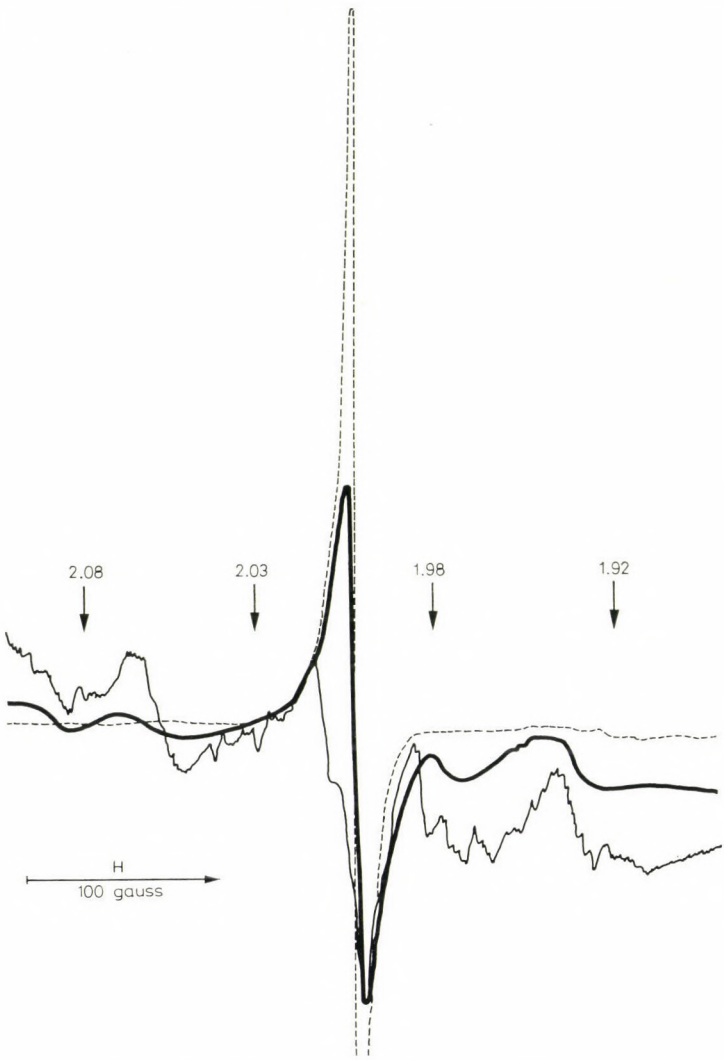

Fig. 5. ESR spectrum of JgB reduced in the presence of tumour cells. As starting material 30 ml ascites cell suspension (6×10^7 cells per ml) was used. To 20 ml suspension 2 ml 3×10^{-3} M JgB solution was added, then the suspension was divided into two equal portions and in one of them 2 mg KCN was dissolved. After centrifugation at 0°C the ESR spectra were recorded as described in Methods. Microwave power: 2.5 mW; modulation: 6.3 gauss. Thin line: control cells, 600-fold amplification; heavy line: cells containing JgB, amplification: 400-fold; dotted line: tumour cell pellet + JgB + KCN, amplification 200-fold. The figures at the arrows indicate the g values

If the electrolyzing potential was above the half-wave potential value of the second cathodic step, the formation of free radicals could not be observed. At this potential the ESR spectrum of JgB, formed previously at lower potentials gradually disappeared.

The DPD formed as a result of the six-electron reduction of JgB can be oxidized into a cation radical (Wurster red, cf. Forrester et al., 1968).

Wurster

The 10^{-3} M DPD solution turned red after flushing with oxygen for 30 minutes and a 2.003 ± 0.001 *g*, 24.05 gauss wide singlet ESR spectrum was obtained. The spectrum is much broader than the signal observed in tissues on the effect of JgB, therefore they cannot be identical.

Some characterization of the structure of the radical that appears during reduction of JgB might be possible by a mathematical transformation of the registered spectrum, which narrows the component lines (Mohos, Tüdős, 1970; Mohos, 1971). The line number of the JgB spectrum thus transformed (Fig. 4D) is 9, i.e. odd.

IV. *Induction of the oxygen effect by the reduced dye in vitro and in vivo*

The majority of dyes studied (Table 2) changed their colours when incubated with tumour cell suspension. With the exception of JgB and MFM, 10^{-4} M solution of the dyes did not affect the growth of 10^7 tumour cells per ml incubated either in oxygen or in nitrogen. Thus at this concentration only JgB and MFM exhibited an "oxygen effect".

The oxygen effect of JgB was consistently decreased by reduction (Table 3). With the yellow product obtained by six-electron macro-reduction in nitrogen atmosphere, the oxygen effect could not be elicited. The two end products of reduction, DES and DPD, failed to induce the oxygen effect when applied separately. The toxicity of dye reduced to pale yellow with potassium borohydride in oxygen atmosphere only decreased but was not cancelled. A similar change was observed in the toxicity of JgB degraded in vivo or heated with excess of ascorbic acid. The in vivo reduction of the dye was carried out by the tumour cells. The dye solution and the tumour suspension were shaken in nitrogen atmosphere until the colour of the dye changed faint pink (100 minutes). The oxygen bubbling was applied only after the reduction of the dye.

As a control, a similar cell suspension was incubated in nitrogen atmosphere for the same period of time.

Table 3

Effect of reduced JgB on the growth of amytal ascites tumour

The dye solution was reduced in an aqueous medium as indicated in the first column. Electrolytic and biological reductions were carried out in nitrogen atmosphere. Reduction with ascorbic acid and potassium borohydride was performed with heating in air atmosphere. The chemically reduced samples were mixed with the cell suspension after adjusting the pH to neutrality. The mixture contained the reducing agent and the dye at the concentrations indicated, and 10^7 tumour cells per ml. The gas was bubbled through the suspension for 30 minutes, then 0.5 ml aliquots were inoculated into Swiss mice intraperitoneally. Numerator: total number of animals inoculated; denominator: animals died from ascites tumour up to the 6th week

Reduction by	10^{-2} M reducing agent	10^{-4} M JgB	Flushing gas-phase	
			oxygen	nitrogen
Electrolysis	−	+	20/20	10/10
Ascorbic acid	+	+	25/8	25/24
Ascorbic acid	+	−	10/10	10/10
Potassium borohydride	+	+	30/7	35/34
Potassium borohydride	+	−	10/9	10/10
Biological	−	+	30/9	30/29
−	−	+	30/0	30/30

Discussion

The data in the literature concerning the mechanism of reduction of JgB in vitro are contradictory. According to earlier studies the reduction of most azo-dyes, thus also that of JgB, appeared to be irreversible (Michaelis, 1933; Hoppe-Seyler, 1953). It was first assumed by Brenner (1953) and Lazarow and Cooperstein (1953) on the basis of biological data that in the first reductive step the formation of an intermediate is reversible. This was thought to be a hydrazo-derivative ("leuco JgB I"). According to these authors the first cathodic wave obtained by polarography would correspond to the irreversible four-electron reduction of the azo-bond, whereas the second wave would represent the two-electron reduction of DES to DEHS (Cooperstein et al., 1953). As the ratio of the appropriate wave-heights measured by us was $i_d^a : i_d^b = 1 : 2$, whereas the postulated process could only be reconciled with a 2 : 1 ratio, the above assumption seems rather improbable.

Havemann et al. (1960) studied the reduction of JgB by potentiometric titration with $TiCl_3$ at pH 3. They came to the conclusion that the first step of reduction was irreversible and involved four electrons ($JgB + 4e + 4H^+ \rightarrow \rightarrow DPD + DES$), whereas the second step was a reversible two-electron process ($DES + 2e + 2H^+ \rightleftarrows DEHS$). The formation of a hydrazo-derivative was also excluded. However the stoichiometry of the reaction and the number of steps are not unambiguously defined by the data reported.

In the present experiments we applied several independent procedures (polarography, cyclic voltammetry, potentiostatic macro-electrolysis and coulometry, ESR, etc.) and the mechanism derived is a synthesis of all results, with the necessary condition that it is also in agreement with each type of measurement separately.

There appear to be two mechanisms we may suggest for the reduction of JgB on the basis of our experiments.

1. In the first step the phenazinium cation is reversibly reduced (JgB $\rightleftarrows$ leuco

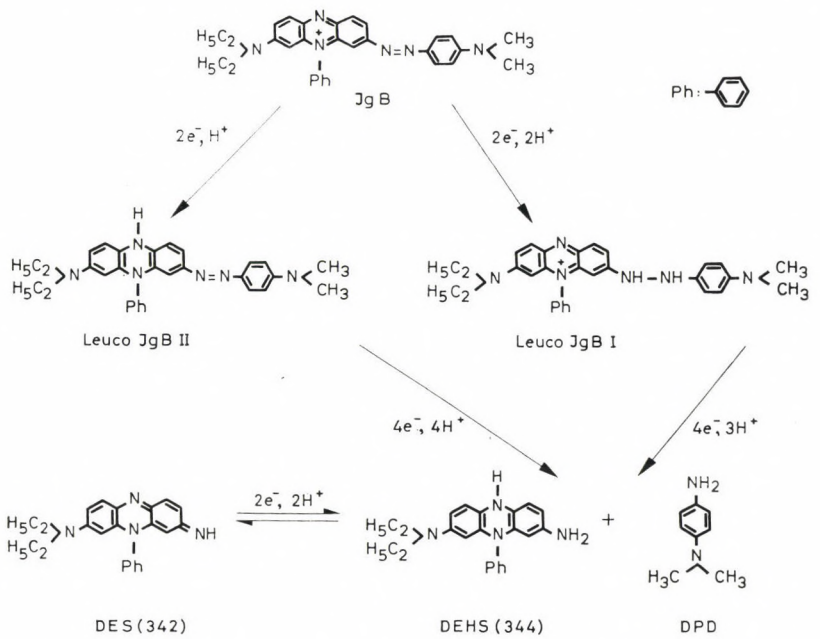

Fig. 6. Reduction of JgB in aqueous medium. Two mechanisms can possibly account for the occurrence of two- and four-electron polarographic waves. Our data support (cf. the text) reduction *via* Leuco JgB II. The figures in brackets are mass numbers

JgB II), followed by a four-electron, chemically irreversible reduction of leuco JgB II with the complete splitting of azo-bond (leuco JgB II → DPD + DEHS).

2. In the first step a hydrazo-derivative is produced (JgB $\rightleftarrows$ leuco JgB I); in the second one the hydrazo-derivative and the phenazinium cation are reduced in a concerted manner (leuco JgB I → DEHS + DPD, cf. Fig. 6).

The second alternative seems improbable for several reasons.

a) Aromatic hydrazo-compounds containing nucleophilic groups ($-NH_2$, $-OCH_3$, $-N(CH_3)_2$, etc.) very rapidly disproportionate in aqueous solutions according to the following scheme (Lukashevich, 1959, 1960, 1964; Florence, 1965; Ladányi et al., 1971; Hazard, Tallec, 1971):

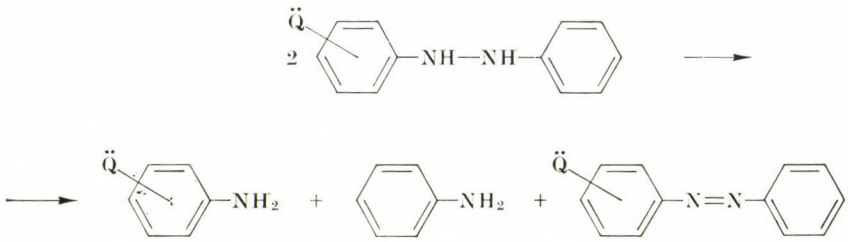

In our case both the safranin skeleton and the diethylamino group are nucleophilic, which would cause the rapid disproportionation of the "Leuco JgB I" hydrazo-derivative and would render wave (a) completely irreversible.

b) *The direct electrochemical reduction* of aromatic hydrazo-compounds yelding amines has not been described so-far. In other words, the hydrazo-derivatives formed during the electrochemical reduction of azo and azoxy compounds cannot be further reduced electrochemically (cf. azobenzene + 2e + $2H^+$ $\rightleftarrows$ hydrazobenzene), but disproportionation of the hydrazo forms can proceed if they contain nucleophilic groups.

c) DPD is only formed in the second step as shown above (Fig. 2, curves B and C), whereas it ought to have been produced already in the first step because of the disproportionation of leuco JgB I, if this compound were formed at all.

On the basis of the foregoing the first alternative for the interpretation of JgB reduction seems probable. Accordingly, first the phenazinium system is reduced. This process can be paralleled with the reduction of MFM.

In the mechanism outlined the reversibility of wave (b) is only apparent (Fig. 2A), which is also proved by the formation of the redox wave shown in Fig. 3 (curve 3, wave (r)). The height of this latter (i_d^r) should only be one-half of the limiting current i_d^b of the four-electron reduction in the second cathodic step of JgB (Fig. 3, wave (b)), as indicated in the number of electrons involved (n = 2). The apparent reversibility of waves (b) and (c) (Fig. 2) is due to the fact that the half-wave potentials of these waves differ from each other only slightly (Table 1). There is a transient violet discoloration during the reduction because the unreduced JgB oxidizes the 5,10-dihydro-phenazine derivative formed. Our electrochemical measurements are well complemented by the mass spectrometric studies described above. The mechanism proposed on the basis of electrochemical evidence postulates the existence of two species, of mass number 342 and 344, which was proved by mass spectrometry.

The reduction of phenazinium cation in the first cathodic step is itself a complex process. From the dye cation (C^+) a radical ($R^\cdot$) is produced by the uptake of one electron, which in the next step is protonated ($R^\cdot$ H^+), and eventually is transformed into the leuco compound (L) by the uptake of another electron (Hausser et al., 1961; Gordienko, 1965; Brodski et al., 1967). The concentration of radical intermediates in aqueous media is, among others, the function of pH (Chaylet et al., 1963; Zaugg, 1964). The reduction potential of protonated

radicals ($R^{\cdot}$ H^{+}) may be lower than that of the cation (C^{+}), therefore free radical intermediates can only be detected directly during reduction in aprotic solvents. Although in aqueous solutions at pH near the physiological free radical concentration is below the limit of detectability, the formation of radicals can still be proven by the extraction of the ($R^{\cdot}$) radical from the aqueous medium by some apolar solvent, e.g. benzene. If reduction and extraction are carried out simultaneously, free radical concentration in the benzene phase may exceed even 10^{-4} M. This was the case in our experiments not only with JgB, but also with the other phenazine dyes and N-alkyl phenazinium salts (Fig. 7).

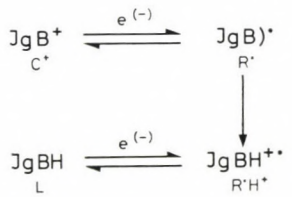

Fig. 7. Reduction of the phenazinium cation. The phenazinium cation (C^{+}) is transformed into a neutral radical ($R^{\cdot}$) by electron uptake. After protonation it becomes a radical cation ($R^{\cdot}H^{+}$), then after the uptake of another electron it is converted into the leuco-compound (L)

Several data have been published during the last few years which suggest that a number of compounds are reduced in a biochemical system, or even in a living tissue, with the formation of free radicals (Ishizu et al., 1968; Nakamura, Yamazaki, 1969). Instead of the appropriate pH or aprotic medium the microheterogeneous biological tissue stabilizes the $R^{\cdot}$ free radical intermediate. The apolar phase of tissues (the lipids) extract the uncharged, relatively weakly polar $R^{\cdot}$ radicals. This is the case with JgB, too. This dye has already been applied to the selective vital staining of mitochondria by Michaelis, who was the first to postulate the existence of free radical intermediates in the mechanism of action of redox enzymes (cf. Chance, 1961). JgB is bound to the co-enzyme Q-lipoprotein fraction and can be extracted from the cell only by lipophilic solvents (Udvardy, Holland, 1969). It is probable that the N,N-dimethylamino-phenylazo structure is located in a hydrophobic environment (lipoids), whereas the hydrated phenazinium moiety is accommodated in the aqueous phase. The cancellation of charge on the phenazinium group, i.e. the one-electron reduction, results in the disorganization of hydrate shell and then the whole ($R^{\cdot}$) radical is displaced into the lipoid phase owing to hydrophobic interactions.

As shown by the results of mild reduction with ascorbic acid or of reduction electrolytically in the ESR cavity, the free radicals are formed in the initial phase of the reaction, which is required for the triggering of "oxygen effect". Free radicals may also be produced on the reduction of azo-bond in aprotic media (Aylward et al., 1967; Sadler, Bard, 1968). As we have demonstrated the "oxygen effect" also with phenazine methylsulfate and our data suggest that in aqueous

medium first the phenazine skeleton of JgB is reduced, we assume that the paramagnetic absorption is due to a phenazine-type free radical. This is supported by the fact that electrolysis in an aprotic medium failed to produce free radicals at the second cathodic step.

The ESR signal observed in amytal ascites cells treated with the dye was singlet without hyperfine structure. We thought that the singlet character was due to the overlapping of lines of the hyperfine structure. This assumption was proven to be correct by the method of line narrowing. The origin of the observed line broadening may be caused by the hindrance of the free motion of the radicals bound to some cellular components (cf. Hedvig, Zentai, 1969; pp. 65–66). (It is known about JgB that it electively stains mitochondria, i.e. it binds to them.) In solution, however, where adsorption cannot take place we observed the same singlet. But the presence of the singlet signal in the reduced solution *does not exclude* the conclusion that this free radical is formed in the tumour cells, too. The line number (9) of the spectrum obtained after line narrowing suggests that the hyperfine structure is produced by the nuclear spin of two non-equivalent nitrogen atoms, but the intensity of lines is not completely identical (cf. Hedvig–Zentai, 1969). Therefore we also assume further proton induced splittings in the spectrum. With coupling constant of $N_1 = 6$, $N_2 = 3$, and $H = 6$ gauss the following nine-line spectrum could be obtained:

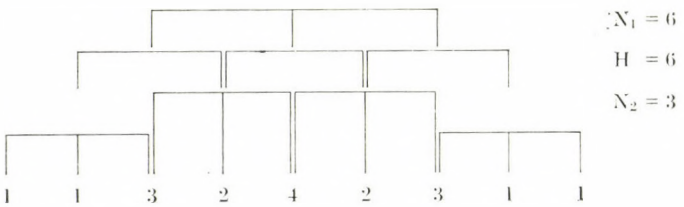

N_1 and H have the same values in the ESR spectrum of phenazine radical cation (Hausser et al., 1961), whereas the coupling constant of N_2 may be decreased by the electron-attracting effect of the phenyl group. The figures assigned to the elementary component lines indicate relative intensities.

The reversibility of the first cathodic step of JgB suggests that its "oxygen effect" is similar to that of the group of compounds to which streptonigrin and some quinoidal substances belong (White, White, 1968). The reduction of phenazine-compounds displays great similarity to the quinone-semiquinone-hydroquinone system (see review, Clark 1960). It has been assumed for the interpretation of "oxygen effect" that some peroxide-like compound is produced in the tissues, which effectuates the oxidation of functional groups, mainly of SH-groups, and the breakage of molecules (Swartz, 1973). During the reduction of phenazine derivatives in vitro, free radicals occur, which on the effect of oxygen are indeed transformed into short-lived secondary radicals (Sawyer, Komai, 1972).

However, one cannot explain the oxygen effect of JgB by the damaging effect of radicals alone. The majority of the phenazine dyes tested are reduced

reversibly, and in the course of reduction free radicals are also formed. In spite of this, "oxygen effect" could only be elicited with JgB and phenazine methylsulfate (at 10^{-4} to 10^{-5} M concentration). However, intracellular location may contribute to understanding the phenomenon. Vital dyes do not stain the cellular structures in a uniform manner, therefore their location cannot be identical either. One has to assume that certain structures of the cell are more sensitive to toxic effects, and the highly effective dyes, or their degradation products (e.g. free radicals), are localized just here. Both JgB and MFM are adsorbed to mitochondria in the lipid-rich environment of succinate dehydrogenase (Zaugg, 1964; Udvardy, Holland, 1969).

It is known already from the studies of Cowdry in 1918 (cf. Lazarow, Cooperstein, 1953) that, for example, diethylsafranine stains mitochondria only at a concentration 15 times as high as that of JgB used for staining. Radiation biology also provided data concerning the intracellular localization of free radicals. After irradiation peroxide-like compounds accumulated in lipids (Romancev, 1966; Gelicki, 1971) and the concentration of free radicals increase at just the same site (Kolomeytzeva, 1963). The question can be raised: is there any parallelism between the oxygen effects caused by JgB and by ionizing radiation? Namely the "oxygen effect" of JgB is an interesting model, in which the effect of reactions involving the formation of free radical can be studied in the cell or in one of its organelles, the mitochondrion.

One of the authors (G. E.) wishes to express his thanks for the helpful advises of Drs F. Tüdős and K. Lapis. Thanks are due for the helpful discussions to Mr S. Szakács, Mr B. Mohos and to Mrs J. Erő.

References

Adams, R. N. (1969) Electrochemistry at Solid Electrodes. M. Dekker, Inc. New York
Aylward, G. H., Garnett, I. L., Sharp, I. H. (1967) Anal. Chem. *39* 457
Berg, H. (1955) Chem. Tech. (Berlin) *6* 585. Cit.: Chem. Abst. *49* 9400 d, e, f
Braun, S., Erdélyi, M., Udvardy, A. (1967) Cancer Res. *27* 660
Brenner, S. (1953) Biochim. Biophys. Acta (Amsterdam) *11* 480
Brodski, A. I., Gordienko, L. L., Krugljak, Ju. A. (1967) Teor. Eksp. Him. *3* 98
Chance, B. (1961) in: Free Radicals in Biologic Systems. Academic Press, New York, London. In Russian (1963) Inlit, Moscow pp. 11—29
Chaylet, C., Steele, R. H., Breckinridge, B. S. (1963) Biochem. Biophys. Res. Comm. *10* 390
Clark, W. (1960) Oxidation-Reduction Potentials of Organic Systems. Williams and Wilkins Co., Baltimore
Cooperstein, S. J., Lazarow, A., Patterson, I. W. (1953) Exp. Cell. Res. *5* 69
Florence, T. M. (1965) Austr. J. Chem. *18* 609
Forcier, G. A., Olver, I. W. (1965) Anal. Chem. *37* 1447
Forrester, A. R., Hay, I. M., Thomson, R. H. (1968) Organic Chemistry of Stable Free Radicals. Academic Press London. N.Y. p. 226
Gelicki, J. M. (1971) in: Biophysical Aspects of Radiation Quality. Proceedings of a Symposium held by the International Atomic Energy Agency in Lucas Heights, Australia 12 March. 1971. Int. At. Energy Agency, Vienna p. 229

Geske, D. H., Maki, A. H. (1960) J. Am. Chem. Soc. *82* 2671
Gordienko, L. L. (1965) Elektrohimija *1* 1497
Hausser, K. H., Häbich, A., Franzen, V. (1961) Z. Naturforsch. *16a* 836
Havemann, P., Pietsch, H., Wielgosch, H. (1960) Z. Wiss. Photogr. *54* 91
Hazard, R., Tallec, A. (1971) Bull. Soc. Chim. No. 8 p. 2917
Hedvig, P., Zentai, G. (1969) Microwave Study of Chemical Structures and Reactions. Akadémiai Kiadó, Budapest
Hoppe-Seyler/Thierfelder: Handbuch der physiologisch und pathologisch-chemischen Analyse. 10. Auflage. Springer, Berlin—Göttingen—Heidelberg—N.Y. Vol. I (1953) p. 654; Vol. VI (1964) Teil A. pp, 171—173, 240
Ishizu, K., Dearman H. H., Huang. M. T., White, J. R. (1968) Biochim. Biophys. Acta *165* 283
Juhász J., Baló, Kendrey, G. (1955) Acta morph. Hung. *5* 243
Kolomeytzeva, I. K. (1963: Radiobiologiya Moscow *3* 359
Kovalenko, O. A., Anfalova, T. V., Sokolov, V. S., Chibrikin, V. M. (1971) Biofizika *16* 663
Ladányi, L., Vajda, M., Vámos, Gy. (1971) Acta Chim. Acad. Sci. Hung. *68* 47
Lazarow, A., Cooperstein, S. I. (1953) Exp. Cell. Res. *5* 56
Lukashevich, V. O. (1959) Dokl. Akad. Nauk S.S.S.R. *129* 117
Lukashevich, V. O. (1960) Dokl. Akad. Nauk S.S.S.R. *133* 115
Lukashevich, V. O. (1964) Dokl. Akad. Nauk S.S.S.R. *159* 5
Lukashevich, V. O. (1964) Dokl. Akad. Nauk S.S.S.R. *159* 1095
Maki, A. H., Geske, D. H. (1960) J. Chem. Phys. *33* 825
Maki, A. H. (1961) J. Chem. Phys. *35* 761
Maki, A. H., Geske, D. H. (1961) J. Am. Chem. Soc. *83* 1852
Michaelis, L. (1933) Oxidation-Reduktionspotentiale. II. Auflage. Springer, Berlin. In Russian (1936) Him. Lit.
Mohos, B. (1971) Ph. D. Thesis
Mohos, B., Tüdős, F. (1970) Phys. Letters *31a* 78
Nakumara, S., Yamazaki, I. (1969) Biochim. Biophys. Acta (Amsterdam) *189* 29
Romancev, E. F. (1966) Rannie radiacionno biochimicheskie reakcii. Atomizdat, Moscow
Sadler, I. L., Bard, A. J. (1968) J. Am. Chem. Soc. *90* 1979
Sawyer, D. I., Komai, R. Y. (1972) Anal. Chem. *44* 715
Stein, E., Iditoiu, C., Deleanu, M. (1969) Experientia *25* 916
Swartz, H. M. (1973) Toxic Oxigen Effects. In: International Review of Cytology. Academic Press, New York, London, vol. *35*. 321
Tanaka, I. (1968) Exp. Cell. Res. *52* 338
Udvardy, A., Holland, R. (1969) Cancer Res. *29* 1550
White, H. L., White, J. R. (1968) Mol. Pharmacol. *4* 549
Wyard, S. J. (1969) Some Medical Applications of ESR Spectroscopy. In: Solid State Biophysics (Ed.: Wyard) McGraw-Hill, New York
Zaugg, W. S. (1964) J. Biol. Chem. *239* 3964

Acta Biochim. et Biophys. Acad. Sci. Hung. Vol. 9 (1—2), pp. 33—41 (1974)

Adenosine 3':5'-Monophosphate Dependent Protein Kinase Isolated from Rat Harderian Gland

A. TAKÁTS, ANNA FARAGÓ, F. ANTONI, F. FÁBIÁN

Institute of Medical Chemistry, Semmelweis University of Medicine, Budapest, and Department of Biochemistry, Eötvös Loránd University, Budapest, Hungary

(Received August 29, 1973 and in revised form December 10, 1973)

A relatively high, cyclic AMP-dependent histone kinase activity was found in rat Harderian gland. Some properties of this enzyme were studied after purification.

The maximal activation of the enzyme was attained at 10^{-6} M cAMP. At higher concentrations cAMP inhibited the reaction. Half-maximal activation was brought about by 1.1×10^{-8} M cAMP, and also by 2.5×10^{-8} M N^6-butyryl-cAMP or about 10^{-6} M cGMP. In the presence of cAMP the apparent K_m values of the different histone fractions (f1, f2a, f2b and f3) were markedly decreased. The f2b fraction was preferentially phosphorylated by this enzyme.

After tryptic digestion of the phosphorylated f2b histone a single [^{32}P]-phosphopeptide fragment was detectable in the two dimensional paper electrophoretic map.

Introduction

The presence of cyclic AMP-dependent protein kinases has been demonstrated in several animal tissues (Krebs et al., 1964; Langan, 1968; Kuo et al., 1970) and in some cases the exact role of these enzymes in regulation has also been clarified (Soderling, Hickenbottom, 1970). In eukaryotic cells most of the wide variety of effects elicited by cAMP may be mediated through stimulation of protein kinases (Kuo, Greengard, 1969). The cyclic AMP-activated phosphorylation of histones may also be a part of an important regulatory process (Langan, 1968), although the function of histone-phosphorylation is yet unclear. The common properties of cAMP-dependent histone kinases isolated from different tissues may give some information for the better understanding of their function.

In the present work the cAMP-dependent histone kinase of rat Harderian gland has been investigated.

Abbreviations used: cAMP, adenosine 3':5'-monophosphate; cGMP, guanosine 3':5'-monophosphate; TCA, trichloroacetic acid.

Materials and methods

[^{32}P]-ATP (250 mCi/mmole) was prepared according to the method of Avron (1961). The histone fractions and whole histone were obtained from Worthington Biochemical Corporation, or were prepared from calf thymus by Johns' method I (Johns, 1964).

The Harderian glands were removed immediately after decapitation of albino rats and put in ice. The glands were minced and homogenized in 5 volumes of 4 mM EDTA with a teflon pestle. This and all subsequent steps were carried out at 0°C. The homogenate was filtered through four layers of gauze and centrifuged at 27,000 g for 30 min. The supernatant was called the crude extract.

The crude extract was acidified to pH 4.85 and centrifuged (Kuo, Greengard, 1970). The supernatant was neutralized to pH 6.5 and ammonium sulfate was added (32.5 g/100 ml). After centrifugation the precipitate was dissolved in potassium phosphate buffer (5 mM, pH 7.0) and the solution was dialyzed against the same buffer. This solution was used as the partially purified preparation of cAMP-dependent protein kinase.

Kinase activity was measured as described previously (Takáts et al., 1972). The standard assay mixture contained: 0.05 M sodium glycerophosphate (pH 6.5) 0.01 M $MgCl_2$, 0.01 M NaF, 0.002 M theophylline, 0.002 M EDTA, 0.6 nmoles of γ-[^{32}P]-ATP and 0.2 ml of enzyme solution (containing about 350 μg protein) in a final volume of 1.6 ml. The incubation time was 10 minutes. The reaction was stopped by the addition of trichloroacetic acid. The precipitate was washed twice with TCA. Generally, 5% TCA (final concentration) was used, but when f1 histone was the substrate, 20% TCA was applied.

The two-dimensional paper electrophoresis of trypsin-digested f2b histone was carried out as described in our previous work (Faragó et al., 1973).

ATPase activity was measured by determining the $^{32}P_i$ radioactivity liberated from γ-[^{32}P]-ATP. The amount of protein was determined by the method of Lowry et al. (1951).

The radioactivity of ^{32}P was measured on the basis of Cerenkov effect in a Packard liquid scintillation spectrometer.

Results and discussion

The cyclic AMP-dependent histone kinase activity (total activity) was found to be significantly higher in the partially purified enzyme preparation than in the crude extract of rat Harderian gland. This was due to two factors. First, strong ATPase activity was demonstrated in the crude extract, which interfered with histone kinase activity assay. Second, the crude extract also contained a histone kinase inhibitor factor. During the purification process both the ATPase and the inhibitor were precipitated at pH 4.85 and removed by centrifugation from the enzyme solution.

Dissolving this acidic precipitate in potassium phosphate buffer (5 mM pH 7.5), the ATPase activity could be abolished by heating the solution (98°C, 5 min.) but the supernatant of the heated preparation (obtained by centrifugation at 27,000 *g* for 10 min) still inhibited the activity of purified histone kinase. The heat stable inhibitor factor was not dialyzable, but it probably was not identical with the one described by Walsh et al. (1971), because its inhibitory effect on the kinase was observed in both the presence and absence of cAMP.

The activity of the partially purified preparation, measured in the presence of 10^{-6} M cAMP, 1 mg/ml f2b and at approximately saturating ATP concentration (2×10^{-4} M) was 2.9 nmole of phosphate/min/mg "enzyme" protein. It is difficult to compare enzyme activities found in different tissues and measured at different substrate saturating conditions, but the cyclic AMP-dependent histone kinase activity of rat Harderian gland proved to be relatively high (43 nmoles of phosphate/min/g wet weight of tissue as estimated on the basis of the activity found in the partially purified preparation).

When the partially purified Harderian protein kinase was incubated with different histone fractions as substrates, the f2b histone proved to be the best phosphate acceptor, in both the presence and absence of cyclic AMP, similarly to our previous results obtained with the cAMP-dependent histone kinases from other tissues (Faragó et al., 1973; Takáts et al., 1972). A significant phosphorylation was also found in the f1 fraction. In contrast, lysozyme, also a basic protein of molecular weight nearly equaling that of the histones, was not phosphorylated at all (Table 1).

The effect of the different cyclic nucleotides on the activity of Harderian protein kinase was measured (Fig. 1). N^6-Butyryl cAMP and cGMP also activated this histone kinase but their concentration that caused 50% of the maximal activation was higher than that of cAMP (10^{-8} and 2.5×10^{-8} M for cAMP and

Table 1

Phosphorylation of different basic proteins by partially purified cAMP-dependent histone kinase of rat Harderian gland

The reaction was carried out in the standard reaction mixture in the presence of 1.0 mg/ml protein substrate and 10^{-6} M cAMP

Substrate added to the enzyme preparation	Phosphate incorporated, nmoles $\times 10^2$	
	in the absence of cAMP	in the presence of cAMP
—	0.375	0.631
Whole histone	1.05	3.1
f1 fraction	1.05	3.23
f2a fraction	0.815	2.48
f2b fraction	2.22	11.65
f3 fraction	0.720	1.68
Lysozyme	0.406	0.545

N^6-butyryl cAMP, respectively, cGMP in the range of 10^{-6} M). The maximal activations caused by the different cyclic nucleotides seem to be equal (as extrapolated from the data of Fig. 1).

It is, however, important to note that the maximal activation of histone kinase was attained at 10^{-6} M cAMP. At higher concentrations cAMP inhibited the reaction (Fig. 2). A similar effect has been reported by Murray et al. (1972). In the presence of 10^{-4} M cAMP the reaction velocity was about 60% of the maxi-

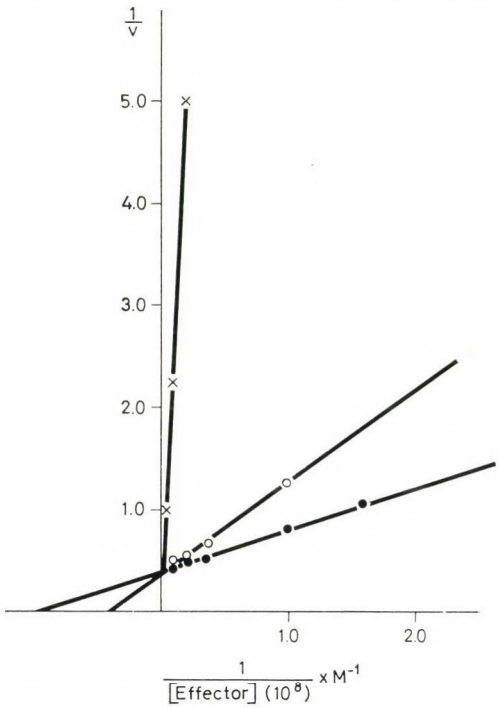

Fig. 1. Double reciprocal plots of cAMP, N^6-butyryl-cAMP and cGMP saturation of rat Harderian histone kinase. v is the difference in the reaction velocity measured in the presence and in the absence of the cyclic nucleotide, and it is expressed as 10^{-2} nmoles of phosphate incorporated during incubation time. The reaction was carried out in the basal reaction mixture containing 5.8×10^{-5} M f2b histone. ·—·—· cAMP; o—o—o—o N^6-butyryl-cAMP; ×—×—× cGMP. These and all data in other figures are the means of duplicate measurements

mum. This inhibition may give some explanation for the contradictory physiological effects of cAMP at different concentrations.

The effect of cyclic AMP on the substrate saturation of the enzyme with the four different histone fractions was then studied. Cyclic AMP decreased markedly the apparent K_m of the histone substrate in all the cases, whereas the maximal activity was unaffected by cAMP (Fig. 3). This "K" type activation differs from

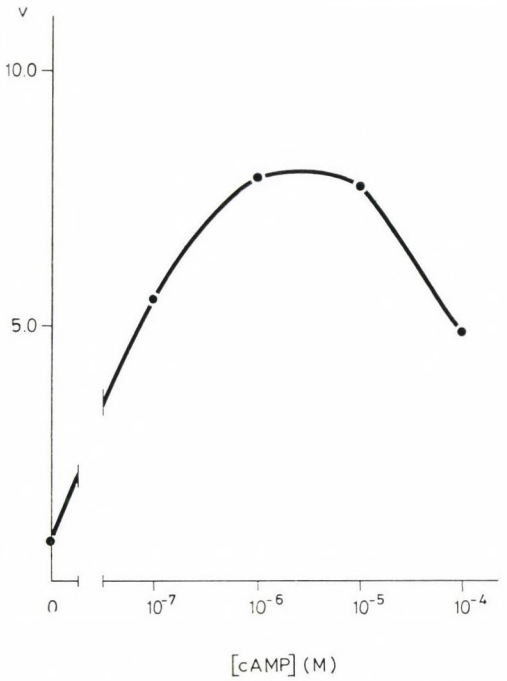

Fig. 2. Inhibition of histone kinase activity by high cAMP concentration. The reaction was carried out in the basal reaction mixture containing 5.8×10^{-5} M f2b histone. v is expressed as 10^{-2} nmoles of phosphate incorporated during the incubation time

the behaviour of skeletal muscle protein kinase reported by Reimann et al. (1971). The apparent K_m measured in the presence of 10^{-6} M cAMP was in the range of 10^{-5} M for each histone fraction. Whereas this value was in the range of 10^{-4} M without cAMP (Table 2), 4×10^{-5} M ATP ensured the half-maximal activity in the presence of 10^{-6} M cAMP and 5.8×10^{-5} M f2b (Fig. 4).

Table 2

The apparent K_m values of the different histone fractions

The values were obtained from the data of Fig. 3

Histone fraction	Apparent K_m (M)	
	in the absence of cAMP	in the presence of 10^{-6} M cAMP
f1	5×10^{-4}	5×10^{-5}
f2a	1.1×10^{-4}	2.4×10^{-5}
f2b	5×10^{-4}	3.6×10^{-5}
f3	2×10^{-4}	2×10^{-5}

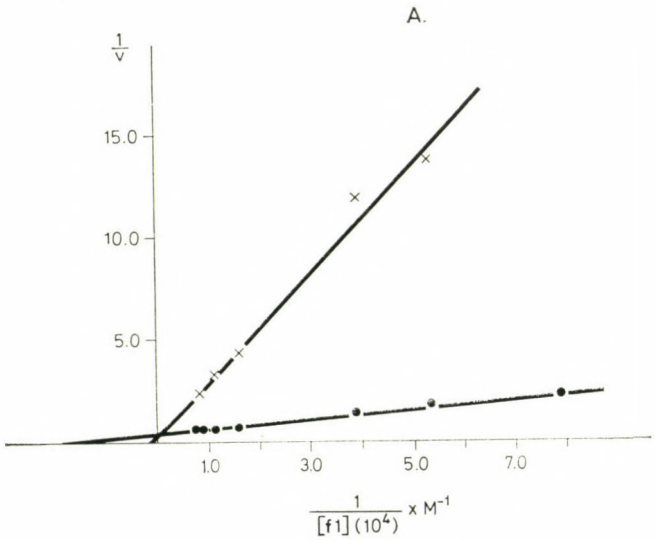

Fig. 3

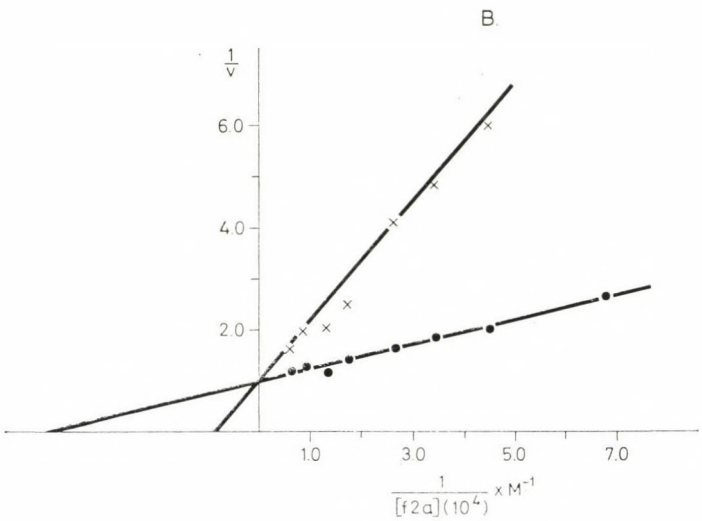

Fig. 3

Since the maximal activity of the enzyme was the highest with f2b as substrate, an attempt was made to pinpoint the phosphate acceptor site of this histone fraction. 32 mg f2b was phosphorylated (in 32 ml of the standard assay mixture containing 60 nmoles γ-[^{32}P]-ATP) in the absence and in the presence of 10^{-6} M cAMP. The reaction velocity was constant in both cases for 40 minutes, therefore

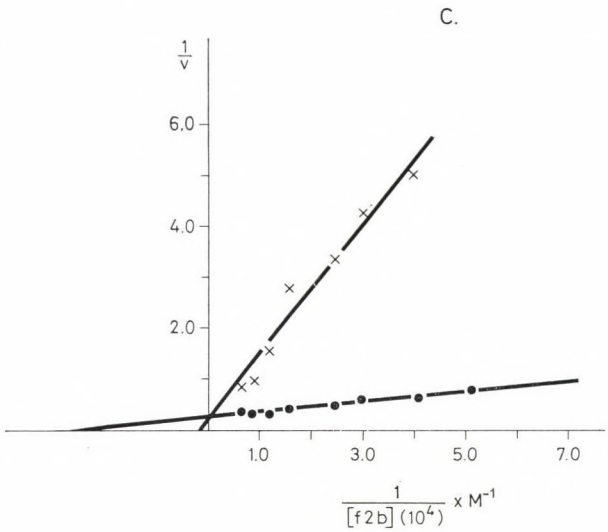

Fig. 3

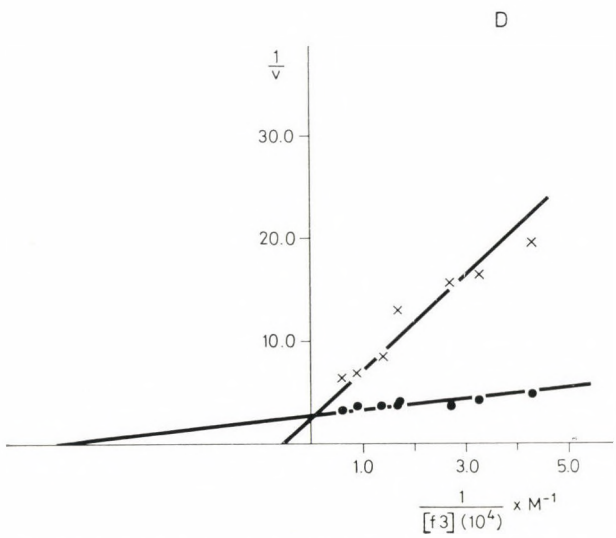

Fig. 3. Double reciprocal plots of the substrate saturation of rat Harderian histone kinase. Parts A, B, C and D represent the results with histone fractions f1, f2a, f2b and f3, respectively. v is expressed as 10^{-2} nmoles of phosphate incorporated during the incubation time. The reaction was carried out in the basal reaction mixture in the absence $\times - \times - \times$, or in the presence of 10^{-6} M cAMP $\cdot - \cdot - \cdot$

the incubation time, with or without cAMP, could be predetermined to get finally equal amounts of histone-bound phosphate in both samples. (The incubation time

was about seven times as long in the absence as in the presence of cAMP). The recovery after the washing procedure (Faragó et al., 1973) was about 1.5×10^{-6} mole of histone labelled with 1.2×10^{-9} mole of phosphate.

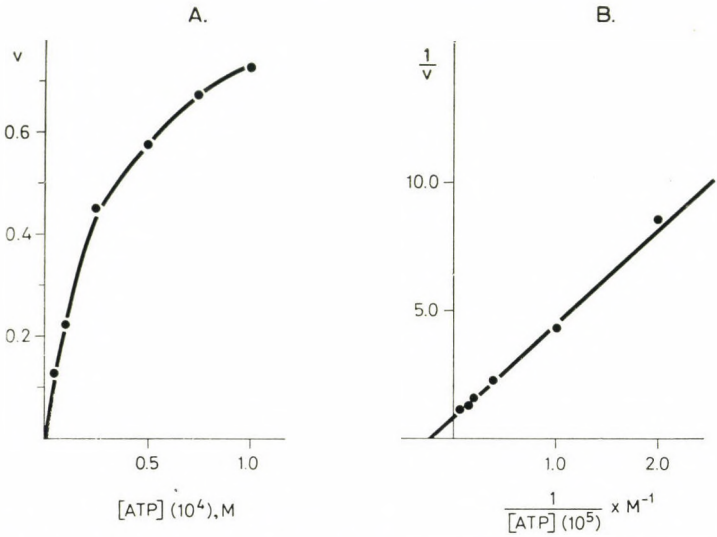

Fig. 4. Saturation of rat Harderian histone kinase with ATP. The reaction was carried out in the standard assay mixture containing 10^{-6} M cAMP and 5.8×10^{-5} M f2b histone. Each sample contained the same amount of radioactivity (approximately 300 000 dpm). v is expressed as nmoles of phosphate incorporated during the incubation time

Fingerprints were produced from two trypsin digested samples by two-dimensional paper electrophoresis as previously described (Faragó et al., 1973). The radioautography of the fingerprints of the two samples showed the same single radioactive peptide fraction (a slightly acidic one), which indicates that the same site is phosphorylated in the presence or absence of cAMP. In addition the peptide fraction of f2b phosphorylated by this enzyme was found to be the same peptide (on the basis of the fingerprints) as the one phosphorylated preferentially by cAMP-dependent histone kinase of human tonsillar lymphocytes (Faragó et al., 1973).

Similarly, the phosphorylation of one distinct site of f1 histone by a cAMP-dependent kinase of rat liver has been reported by Langan (1969). Since both the f2b and the f1 histone fractions also have other phosphate acceptor sites, different from that phosphorylated by the cAMP-dependent enzyme (Faragó et al., 1973; Langan, 1969), these data suggest that the cAMP-dependent histone kinase has some particular role and cannot be responsible for the phosphorylation of histones in general.

We are grateful to Miss Zita Solti for her excellent technical assistance.

References

Avron, M. (1961) Anal. Biochem. *2* 535
Faragó, A., Antoni, F., Takáts, A., Fábián, F. (1973) Biochim. Biophys. Acta *297* 517
Johns, E. W. (1964) Biochem. J. *92* 55
Krebs, E. G., Love, D. I., Bratvold, Gloria, E., Trayser, K. A., Meyer, W. L., Fisher, E. H. (1964) Biochemistry *3* 1022
Kuo, J. F., Greengard, P. (1969) J. Biol. Chem. *244* 3417
Kuo, J. F., Krueger, B., Sames, J. R., Greengard, P. (1970) Biochim. Biophys. Acta *212* 79
Langan, T. A. (1968) Science *162* 579
Langan, T. A. (1969) J. Biol. Chem. *244* 5763
Lowry, O. H., Rosebrough, N. J., Farr, A. L., Randall, R. J. (1951) J. Biol. Chem. *193* 265
Murray, A. W., Francis, M., Kemp, B. E. (1972) Biochem. J. *129* 995
Reimann, E. M., Walsh, D. A., Krebs, E. G. (1971) J. Biol. Chem. *246* 1986
Soderling, T. R., Hickenbottom, J. P. (1970) Fed. Proc. *29* 601
Takáts, A., Faragó, A., Antoni, F. (1972) Biochim. Biophys. Acta *268* 77
Walsh, D. A., Ashby, C. D., Gonzalez, C., Calkins, D., Fischer, E. H., Krebs, E. G. (1971) J. Biol. Chem. *246* 1977

Acta Biochim. et Biophys. Acad. Sci. Hung. Vol. 9 (1–2), pp. 43–52 (1974)

On the Mechanism of Uptake of Iron by Reticulocytes

A. EGYED

Department of Cell Metabolism, National Institute of Haematology and Blood Transfusion, Budapest, Hungary

(Received December 3, 1973)

The uptake of iron by reticulocytes can be inhibited by certain oxidizing agents capable of altering the state of redox co-enzyme pool of the cells, such as nitrite and methylene blue. Cells treated with oxidizing agents are incapable of detaching anion and iron from transferrin, while their transferrin-binding ability seems to be unaltered. Reticulocytes inactivated in this way can be reactivated by substrates the metabolism of which involves the NAD → NADH conversion (e.g., lactate, inosine, glucose).

Experiments with cyanide indicate that no direct connection exists between respiration and the iron detaching ability of reticulocytes.

In view of these results, the following hypothesis concerning the mechanism of this process is proposed: cells detach the anion and iron from the transferrin-iron-carbonate complex enzymatically. In this enzymatic process NADH + H^+ is used by the enzyme for the conversion of carbonate ion into bicarbonate and for the reduction of iron in a simultaneous or subsequent step. The bicarbonate ion is released into the medium, while the bivalent iron is taken over by a cellular iron acceptor.

Introduction

The mechanism of iron uptake by reticulocytes has been interpreted on the basis of two concepts fundamentally different from each other in principle. In the first hypothesis, the uptake of iron by reticulocytes takes place by endocytosis in a transferrin-bound form (Morgan, Appleton, 1969; Martinez-Medellin, Schulman, 1972), whereas in the other, transferrin is assumed not to enter the cell, but after its binding to the membrane receptors iron is detached from the complex by the cell, then transferred to the site of haem synthesis (Jandl, Katz, 1963; Verhoef et al., 1973).

In connection with the latter concept of the iron uptake process, the importance of the anion present in the transferrin-iron-anion complex has been recognized. Recent reports indicate that cells detaching iron attack the complex at its anion component (Aisen, Leibman, 1973; Egyed, 1973; Martinez-Medellin, Schulman, 1973). After the binding of the transferrin-iron-anion complex to the cell, the anion is eliminated from it, iron is reduced in a subsequent or simultaneous step, then taken over by a cellular iron acceptor molecule. The anion-

detaching process is assumed to be enzymatic in its nature (Egyed, 1973; Martinez-Medellin, Schulman, 1973).

In the present work we endeavoured to elucidate further characteristics of the mechanism by which cells detach iron and the anion molecule from the transferrin-iron-anion complex.

Materials and methods

Chemicals

Reagents of analytical grade were used: 2,2-bipyridine, 2,4-dinitrophenol (DNP) – Fluka AG Buchs, Switzerland, $^{59}FeCl_3$ (16–20 Ci/g Fe^{3+}) – Central Institute of Nuclear Research, Berlin, GDR; other inhibitors, substrates and chemicals, of analytical grade, were purchased from Reanal, Budapest, Hungary.

Reticulocytes and transferrin were prepared as described previously (Egyed, 1973).

Inactivation of the iron uptake of reticulocytes with nitrite and methylene blue

Reticulocytes were incubated with 10 mM $NaNO_2$ or 0.5 mM methylene blue for 30 minutes at 37°C and washed three times with 50 volumes of ice-cold physiological saline. Cells treated in this way were used in the experiments as nitrite- or methylene blue-inactivated reticulocytes.

Estimation of iron uptake

The reaction mixture was as follows: 0.05 ml reticulocytes, 1 mM sodium phosphate (pH 7.4), 0.16 M NaCl, 0.5 mg ^{59}Fe-labelled transferrin. This amount of transferrin contained 0.15 μg of iron, which represented 2×10^5 cpm. Final volume of the reaction mixture was 0.5 ml. Substrates were preincubated with the cells before the addition of transferrin, where indicated. The reaction was initiated by adding ^{59}Fe-labelled transferrin. After a 10-minute incubation at 37°C, the cells were washed three times with 50 volumes of ice-cold physiological saline. After washing, the radioactivity of the sample was counted, and this value was considered as total iron uptake. Subsequently, the percentage of iron incorporated into haem was determined by a method elaborated in our laboratory (Egyed, 1972). The difference between the two values represents the amount of iron incorporated into the non-haem fraction. The non-haem iron fraction includes the transferrin-bound iron on the cell surface and the intermediary iron detached from transferrin, but not yet incorporated into haem. The amount of iron in the haem and non-haem fractions provides valuable information on the iron metabolism of the cell. If iron uptake is undisturbed, but haem synthesis is inhibited, the total iron uptake changes only slightly if at all, while the amount of iron in the non-haem fraction increases. If iron uptake is inhibited but the attachment of the transferrin-iron-anion complex is not, the amount of non-haem iron is practically unaltered,

while the amount of total iron taken up and the amount of iron incorporated into haem decreases proportionally. Under normal conditions, 50–70% of the total iron taken up becomes incorporated into the haem molecule, whereas only a low percentage of iron is in the intermediary state.

Determination of iron detachment

Based on the principle of Morgan's dialysis technique (Morgan, 1971) we elaborated a procedure to measure iron detachment within a short interval and to eliminate the main possible sources of error in the dialysis method. The principle of the Morgan-procedure is that iron cannot be detached from transferrin by certain permeable iron-chelators. If, however, iron is removed from transferrin by the cell and it enters the membrane or the cytoplasm it is immediately chelated and at the same time becomes unavailable for haem synthesis.

In our modified procedure we made use of the fact that the bipyridine-iron complex dissolves in acetone, but the transferrin-iron-anion complex does not, thus we could separate the chelate-bound iron from the transferrin-bound iron.

Reaction mixture: 0.05 ml reticulocytes, 0.16 M NaCl, 1 mM 2,2'-bipyridine, 1 mM sodium phosphate (pH 7.4), 0.5 mg ^{59}Fe-labelled transferrin. The final volume of the mixture was 0.5 ml. After incubation at 37°C, the reaction mixture was cooled and 0.01 ml 1% saponin was added. It was kept in the cold for 30 minutes. Proteins were precipitated with 5 ml of acetone. After another 30-minute the precipitate was centrifuged and the radioactivity of the aliquot of the supernatant was measured. The rate of appearance of chelated radioactive iron was proportional to the rate of iron transport.

^{59}Fe radioactivity was determined with a Frieseke – Hoepfner well-type scintillation counter.

The ATP content of the cells was determined by the luciferin-luciferase method (Stanley, Williams, 1969).

Results

The integrity of the cell membrane is a prerequisite of the detachment of anion and iron from transferrin (Jandl et al., 1959; Egyed, 1973), hence only intact cells could be used in the experiments. The connection between the redox state of coenzymes and iron uptake was studied by varying the extent of reduction of the intracellular coenzyme pool. The intracellular coenzymes of intact cells can be reversibly oxidized by various oxidizing agents (Mányai, Székely, 1954). In our experiments, sodium nitrite and methylene blue were used for this purpose.

Reticulocytes were preincubated in the presence of 10 mM sodium nitrite, then nitrite was washed out of the system and its effect on iron uptake was tested. As it is shown in Fig. 1, the amount of iron incorporated into the haem and non-

haem fractions varied with the duration of preincubation with nitrite in different manners. The amount of iron incorporated into haem fell rapidly to about 4% of the initial value, while the ^{59}Fe content of the non-haem fraction first increased, then reached a constant level at about 80% of the initial value. In this period, the total amount of iron is in the non-haem fraction. Since under the conditions applied the cells were incapable of detaching either the iron or the anion from the complex (unpublished results), it is very probable that the radioactivity-measured represents iron being in the transferrin-iron-anion complex bound to the membrane receptors.

Reactivation of reticulocytes that lost their iron-detaching ability due to a 30-minute sodium nitrite pretreatment was attempted by the addition of the following substrates: lactate, inosine, glucose, which all generate reduced co-enzymes (e.g., NADH) when metabolized (Jaffé, 1959). Preincubation of the cells with any of these substrates for 10 minutes resulted in the reactivation expected (Fig. 2). The total iron uptake approached the value obtained with untreated reticulocytes, whereas, the ratio of the amounts of haem and non-haem iron varied with the substrate; the extent of haem synthesis did not reach the control value.

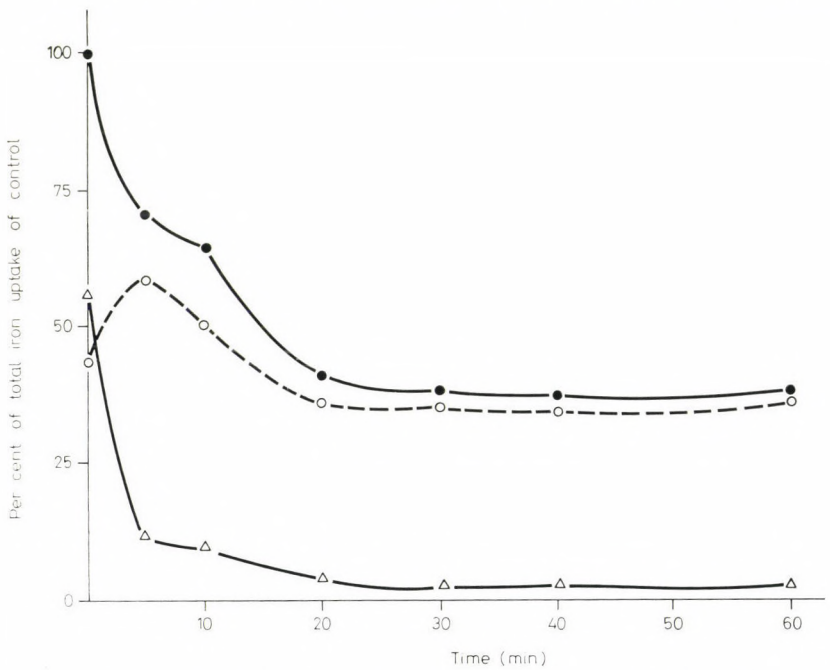

Fig. 1. Effect of nitrite treatment on the uptake of iron by reticulocytes. Reaction mixtures: 1. for nitrite pretreatment: 0.15 M NaCl; 1 mM sodium phosphate (pH 7.4); 10 mM $NaNO_2$; 0.05 ml reticulocytes. Final volume: 0.5 ml. Incubation temperature: 37°C; 2. for iron uptake: 0.16 M NaCl; 1 mM sodium phosphate (pH 7.4); 0.5 mg ^{59}Fe-labelled transferrin; 0.05 ml nitrite treated and washed reticulocytes. Final volume: 0.5 ml. Incubation at 37°C for 10 minutes. The abscissa shows the time of nitrite pretreatment. ●———● total iron uptake, ○———○ non-haem iron, △———△ haem iron, 100% = 1.4 μg Fe^{3+}/ml cell

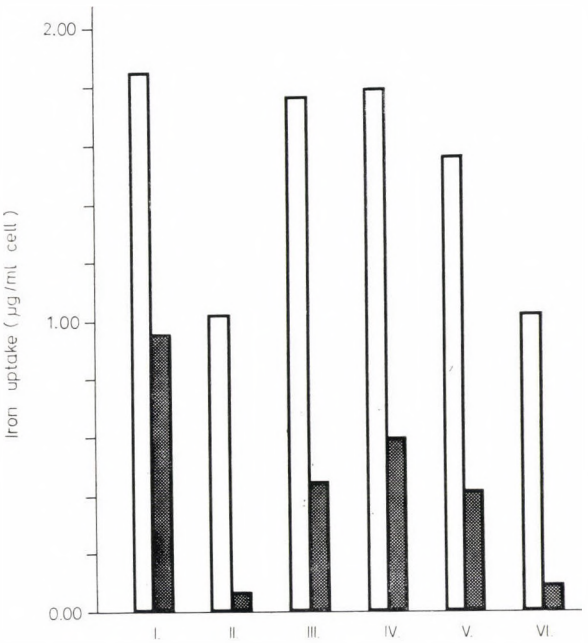

Fig. 2. Effect of various substrates on the uptake of iron by reticulocytes inactivated with nitrite. Time of nitrite-treatment: 30 minutes. Conditions of pretreatment and iron uptake as in Fig. 1. Cells were preincubated with substrates for 10 minutes at 37°C before adding ^{59}Fe-labelled transferrin. White columns: total iron uptake; black columns: iron incorporated into haem. I, control; II, nitrite-inactivated reticulocytes (iR); III, iR + 10 mM lactate, IV, iR + 10 mM inosine; V, iR + 10 mM glucose; VI, iR + 10 mM pyruvate

The fact that the first product of lactate metabolism, i.e. pyruvate, was ineffective in the rapid reactivation of iron uptake indicates the role of NADH in the process (Fig. 2).

Reactivation of reticulocytes could not be achieved by the addition of SH-protective agents, such as mercapto-ethanol and glutathione (3 mM).

In the next step, the effect of various metabolic inhibitors on reactivation was investigated. After a 10-minute preincubation both the substrate and inhibitor were removed by washing the cells. Lactate reactivation could not be inhibited with 4 mM NaF or 1 mM NaCN, but it could be abolished by 0.5 mM DNP. This can be explained by the inhibition of lactate-dehydrogenase by DNP. (Stockdale, Selwyn, 1971). Reactivation with inosine could not be inhibited with NaCN or DNP in the above concentrations, but was sensitive to NaF (Table 1). The question might arise, whether these substrates really reactivate iron uptake through the generation of reduced coenzymes or eventually act by increasing the ATP level of reticulocytes, which decreased by about 50% during the 30-minute treatment with nitrite. Therefore, the ATP level was measured at

Table 1

Effect of various inhibitors on the reactivation of nitrite-treated reticulocytes with lactate and inosine

For conditions see Fig. 1. Both the substrate and inhibitor were washed out of the system after preincubation for 10 minutes at 37°C. Following this procedure iron uptake was measured. The amount of iron taken up by the control reticulocytes was 0.9 μg Fe^{3+}/ml cell

Substrate	Inhibitor	Total iron uptake (% of the control)
—	—	42
10 mM lactate	—	85
10 mM lactate	4 mM NaF	89
10 mM lactate	1 mM NaCN	86
10 mM lactate	0.5 mM DNP	33
10 mM inosine	—	92
10 mM inosine	4 mM NaF	53
10 mM inosine	1 mM NaCN	96
10 mM inosine	0.5 mM DNP	80

both the beginning and at the end of 10-minute preincubation. Although the same extent of reactivation was achieved with lactate and inosine, the ATP level decreased slightly further in the presence of lactate, whereas it increased when the reactivating substrate was inosine. Hence, reactivation of iron uptake by the substrates added cannot be attributed to an increase in the ATP level (Table 2).

Identical results were obtained when 0.1 mM methylene blue was used during preincubation instead of nitrite. The iron uptake of reticulocytes inactivated in this way could also be reactivated by the above substrates. The majority of iron taken up in amounts approaching or exceeding the control value was found, however, in the non-haem fraction. The incorporation into haem increased only slightly (Table 3).

Table 2

Effect of preincubation with lactate and inosine on the uptake of iron by nitrite-inactivated reticulocytes and on the ATP content of the cells
For conditions see Fig. 1. 100% Iron uptake = 1.9 μg Fe^{3+}/ml cell; 100% ATP content = 5.5 μM/ml cell

Substrate	Total iron uptake (per cent of the control)	ATP content of the cells	
		at the beginning of preincubation (per cent of the control)	at the end of preincubation (per cent of the control)
—	55	60	52
10 mM lactate	98	56	49
10 mM inosine	102	59	69

Table 3

Effect of various substrates on the uptake of iron by reticulocytes inactivated with methylene blue

Time of methylene blue-treatment: 30 minutes at 37°C. Reaction mixture for estimating iron uptake: 0.16 M NaCl; 1 mM sodium phosphate (pH 7.4); 0.5 mg ^{59}Fe-labelled transferrin; 0.05 ml methylene blue-treated and washed reticulocytes. Incubation at 37°C for 10 minutes. Final volume: 0.5 ml. Cells were preincubated with substrates for 10 minutes at 37°C before adding ^{59}Fe-labelled transferrin. Total iron uptake 100% = 1.1 μg Fe^{3+}/ml cell

Substrate	Uptake of iron by methylene-blue-treated reticulocytes (per cent of the values obtained with untreated reticulocytes)		
	total	haem	non-haem
—	52	17	98
10 mM lactate	94	26	180
10 mM inosine	105	36	190
10 mM glucose	80	24	150
10 mM pyruvate	63	18	125

In our further experiments, the effect of cyanide on iron uptake was studied. In the presence of 10 mM cyanide the uptake of iron by the cells was strongly inhibited and this finding is in agreement with the literature data (Morgan, Baker, 1969). It was found, however, that the addition of inosine to cells inhibited in this way resulted in an increase in the amount of iron taken up, while incorporation of iron into haem remained inhibited (Fig. 3a). The same phenomenon was examined by the modified Morgan method, too. In the presence of 10 mM cyanide, the iron detachment by cells fell to 32% of the control value, whereas it increased to 62% on the addition of inosine (Fig. 3b). Cyanide at such a concentration completely inhibits respiration of reticulocytes, as also checked by Warburgs manometric method. Consequently, the partial reactivating action of inosine on the iron-detaching ability of cells with blocked respiration indicates that there is no direct link between the iron-detaching ability and respiration of cells.

Cyanide presumably affects the iron-detaching process directly, and inosine can partially eliminate this effect. Deeper understanding of this phenomenon requires further studies.

Discussion

In the present work the mechanism of the detachment of anion and iron from transferrin by reticulocytes was studied.

In the transferrin-iron-anion complex, according to recent results of Bates (Bates, 1972; Bates and Schlabach, 1973), the anion component is not bicarbonate,

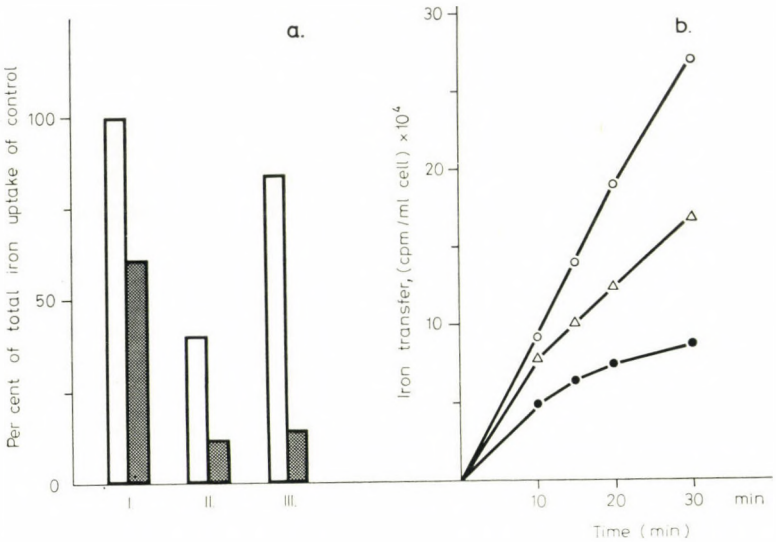

Fig. 3. Effect of NaCN on iron uptake *(a)* and iron detachment *(b)*. *a)* Reaction mixture: 0.16 M NaCl; 1 mM sodium phosphate (pH 7.4); 0.05 ml reticulocytes; 0.5 mg ^{59}Fe-labelled transferrin. Final volume 0.5 ml. Incubation at 37°C for 10 minutes. White columns: total iron uptake; black columns: iron incorporated into haem; 100% = 1.6 μg Fe^{3+}/ml cell. I, control; II, 10 mM NaCN; III, 10 mM NaCN + 10 mM inosine. *b)* Reaction mixture: 0.16 M NaCl; 1 mM sodium phosphate (pH 7.4); 1 mM 2,2'-bipyridine; 0.05 ml reticulocytes; 0.5 mg ^{59}-Fe-labelled transferrin. Final volume 0.5 ml. Incubation at 37°C. The ordinate shows the amount of radioactive iron transferred to chelator. ○———○ control, ●———● in the presence of 10 mM NaCN, △———△ in the presence of 10 mM NaCN + 10 mM inosine

but the carbonate ion. In this complex iron is in the trivalent form. Since iron is used in its divalent form for haem synthesis, it has to be reduced in the course of iron uptake. Therefore, the role of redox coenzymes in the process of iron uptake was investigated.

The reduced coenzymes of the cells can be oxidized by certain oxidizing agents, such as nitrite and methylene blue. Preincubating reticulocytes with nitrite or methylene blue, and washing off the agent, the iron and anion detaching ability of the cells is lost. Reactivation of reticulocytes cannot be effected by the addition of SH-protective agents. We supposed this inactivation to be the consequence of the oxidation of redox coenzymes.

Reticulocytes inactivated in this way could be reactivated by a short preincubation with substrates generating reduced coenzymes: e.g., lactate, inosine, and glucose. A common characteristic of the metabolism of these substrates is that the reduction of NAD is always involved. The assumption that the reactivation can be attributed to the reduction of NAD is justified by the results obtained with lactate. Using lactate as substrate, the rapid oxidizing step is the lactate pyruvate trans-

formation accompanied only by the reduction of NAD. With the product of this reaction, pyruvate, reticulocytes could not be reactivated during such a short pre-incubation period. The reactivation with lactate could be inhibited by DNP which inhibits lactate-dehydrogenase, but could not be abolished with NaF and NaCN, which inhibit other metabolic steps. It should be noted that these results do not conclusively prove the direct role of NADH, since other reduced coenzymes might also be involved through transhydrogenation reactions.

Since in the course of a 30-minute nitrite treatment the ATP content of the cell decreases by about 50%, we considered it necessary to check the alternative, namely that the substrates reactivate reticulocytes by augmenting the ATP content of the cell. Measuring the ATP level at the beginning and at the end of the reactivation process we could establish that while reactivation was the same, the ATP level decreased further in the presence of one substrate and increased in the presence of the other. Thus the possibility that the reactivation was the consequence of an elevated ATP content could be excluded.

Two alternative explanations can be given for the role of NADH in the uptake of iron by reticulocytes. Morgan has assumed a direct connection between NADH-linked respiration and iron uptake (Morgan, Baker, 1969). On the basis of our experiments carried out with cells of blocked respiration, however, we would favour the following hypothesis on the mechanism of anion and iron detachment by reticulocytes, supposing a direct involvement of NADH in this process:

1. The transferrin-iron-carbonate complex becomes bound to the membrane receptors.

2. An enzyme functioning with a $NADH + H^+$ coenzyme detaches anion and iron from the transferrin-iron-carbonate complex sequentially or simultaneously. NADH reduces trivalent iron to the divalent state and the accompanying proton induces a carbonate → bicarbonate transformation:

$$\text{Transferrin-}Fe^{3+}\text{-carbonate} + NADH + H^+ \rightarrow \text{transferrin} + Fe^{2+} + HCO_3^- + NAD$$

The bicarbonate ion is released into the medium. Divalent iron cannot be bound by transferrin and is taken over by the cellular iron acceptor.

3. Iron is subjected to another transport process through the mitochondrial membrane and becomes incorporated into the haem molecule.

Thanks are due to Prof. S. R. Hollán and Prof. G. Gárdos for their valuable help. The author is grateful to Dr I. Szász for the useful discussions of results and problems. The excellent technical assistance of Miss A. Thaly is gratefully acknowledged.

References

Aisen, P., Leibman, A. (1973) Biochim. Biophys. Acta *304* 797–804
Bates, G. W. (1972) XIV. Int'l Confr. Coord. Chem. 1972. Toronto (Abstract)
Bates, G. W., Schlabach, M. R. (1973) FEBS Lett. *33* 289–292

Egyed, A. (1972) Experientia *28* 1396
Egyed, A. (1973) Biochim. Biophys. Acta *304* 805—813
Jaffé, E. R. (1959) J. Clin. Invest. *38* 1555—1563
Jandl, J. H., Inman, I. K., Simmons, R. L., Allen, D. W. (1959) J. Clin. Invest. *38* 161—185
Jandl, J. H., Katz, J. H. (1963) J. Clin. Invest. *42* 314—326
Mányai, S., Székely, M. (1954) Acta Physiol. Acad. Sci. Hung. *5* 7—18
Martinez-Medellin, J., Schulman, H. M. (1972) Biochim. Biophys. Acta *264* 272—284
Martinez-Medellin, J., Schulman, H. M. (1973) Biochem. Biophys. Res. Commun. *53* 32—38
Morgan, E. H., Appleton, T. C. (1969) Nature *223* 1371—1372
Morgan, E. H., Baker, E. (1969) Biochim. Biophys. Acta *184* 442—454
Morgan, E. H. (1971) Biochim. Biophys. Acta *244* 103—116
Stanley, P. E., Williams, S. G. (1969) Anal. Biochem. *29* 381—392
Stockdale, M. J., Selwyn, M. J. (1971) Eur. J. Biochem. *21* 416—423
Verhoef, N. J., Kremers, J. H. W., Leijnse, B. (1973) Biochim. Biophys. Acta *304* 114—122

Acta Biochim. et Biophys. Acad. Sci. Hung. Vol. 9 (1—2), pp. 53—61 (1974)

Glucosamine Incorporation during the Mitotic Cycle of Primary Chicken Fibroblast Cells

TAMARA KUBASOVA, L. VARGA, G. J. KÖTELES

"Frédéric Joliot-Curie" National Research Institute for Radiobiology and Radiohygiene, Budapest, Hungary

(Received July 28, 1973)

The uptake of radioactive glucosamine by primary chicken fibroblast cells in the interphase and in the various phases of mitosis has been studied by continuous labelling in radioautographic experiments. The interphase cells incorporated the precursor to the greatest extent. Two phases could be differentiated in the incorporation rate of the interphase cells: an initial, rapid one, when the precursor was located above the Golgi complex, and a later slow phase during the course of which the labelled molecules were located diffusely above the cell and then appeared also in the intercellular region. The investigation of the cells in mitosis suggest that glycoprotein synthesis either stops or decreases 20 to 30 minutes before the cells enter mitosis and restarts in the late anaphase or rather in the telophase. Since the labelling of cells leaving the G_2 phase and entering the M-phase was always lower than that of the intermitotic cells, a premitotic degradation of glycoproteins might be assumed.

Introduction

Over the last few years an ever increasing number of papers have been devoted to the importance of glycoproteins and their carbohydrate components in the biological membranes (Froger, Louisot, 1972; Nowakowski et al., 1972; Rambourg, 1971). Indeed, the carbohydrates on the cell surface are thought to be involved also in "recognition", "association" and "motility" phenomena (Buck et al., 1970; Cook, 1968; Hamaguchi, Cleve, 1972; Ito, 1969; Kalckar, 1965; Martinez-Palomo, 1972; Rambourg, Leblond, 1967; Rambourg et al., 1969; Weiss, 1969). There are hypotheses according to which the information capacity concealed in the protein structure can be augmented by the addition of special carbohydrate chains. Further, it may be supposed that the carbohydrate substances deriving from the cell have some special "information" capacity exerting an effect of wide spectrum on the activity of the cell (Spiro, 1970; Whaley et al., 1972). Among the various membrane systems the Golgi complex appears to have an important function in glycoprotein metabolism (Evans, Gurd, 1971; Favard, 1969; Neutra, Leblond, 1970; Wakowiak et al., 1972). As suggested both by biochemical analyses (Cheetman et al., 1970; Fleischer et al., 1969; Molnár et al., 1969) and radioautographic studies (Barland et al., 1968; Bennett, 1970; Bennett, Leblond, 1970; Halbhuber et al., 1972; Ito, 1969; Moscarello et al., 1972; Neutra,

Leblond, 1966), this cell organelle appears to be one of the central sites of glycoprotein "assembly" and synthesis, whereas owing to its secretory function, it is closely connected with the plasma membrane, too.

In spite of the extensive studies devoted to the biochemistry and cellular physiology of the various phases of cell cycle, the rate of glycoprotein synthesis has not been assessed for the whole life cycle. Data are available for the intermitosis only (Bosmann, Winston, 1970).

The present paper reports on our investigations connected with glucosamine incorporation by interphase cells and by cells in mitosis.

Materials and methods

Cell culture

Eleven-days-old chicken embryos were used for preparing the primary chicken fibroblast culture (PCFB). The cells were cultured on cover-slips at 37°C in Parker 199 medium containing 10% calf serum, 100 I.U./ml penicillin and 100 μg/ml streptomycin. Monolayer cultures of 48 to 72 hours growing asynchronously were used.

Determination of cell cycle parameters

The mitotic cycle of exponentially growing PCFB was determined by continuous labelling according to Cleaver (1967). The cells were made to incorporate ^{3}H-TdR for various times (0.1 μCi/ml, specific radioactivity 1.9 Ci/mM, The Radiochemical Centre, Amersham, England). The evaluation of the radioautographs gave the following parameters: $t_1 = 8.8$ hours; $t_s = 9.0$ hours; $t_2 = 3.1$ hours. For the accomplished cell cycle time $T = 22.0$ hours. Substituting these values into the equation

$$LI = (\exp. \ln 2/T - 1) \exp. t_2 \ln 2/T$$

the theoretical labelling index, LI (Dendy, Cleaver, 1964), was calculated. For the growth fraction (GF) 0.75 was obtained as the ratio of the experimental labelling index (T_x) and LI. The experimental mitotic index (MI = 2.36%) was corrected for the GF value. As a result, 3.24% was obtained for the corrected mitotic index (cMI).

Substituting this value into the equation

$$t_m = cMI \times T/\ln 2$$

The value 1.03 hours was obtained for the time of mitosis (t_m).

Labelling of glycoproteins

The cells on the cover-slips were labelled continuously with D-glucosamine-6-H-3.HCl (1 μCi/ml; specific radioactivity 16 Ci/mM; code number TRK 398; The Radiochemical Centre, Amersham, England).

Radioautography

The cover-slip cultures incubated with the radioactive precursor for various times were fixed in Carnoy's solution for 2×20 minutes, then in 96% cold ethanol for another 2×20 minutes. After rinsing with distilled water and drying, the cover-slips were mounted on slides and coated with liquid emulsion according to the dipping method (Ilford Nuclear Research Emulsion, Type G-5, Ilford Ltd. England). The slides were exposed at +4°C for 6 days. After photographic development (ORWO A 49; WEB Filmfabrik, Wolfen, GDR) and acidic fixation the slides were thoroughly washed with distilled water and stained with 5% Giemsa solution.

Evaluation of radioautographs

For the interphase cells our data represent the grains counted over 5×25 cells and the average of 5 cells was represented. For the dividing cells the grain count over at least 10 cells was taken as a single value and the results were plotted accordingly.

Results

^{3}H-glucosamine incorporation by interphase cells

The grain counts found over the interphase cells of the continuously labelled PCFB culture, as a function of incubation time, are shown on Fig. 1. The cells kept incorporating the precursor over the whole incubation period. However, on the basis of incorporation rate two phases could be distinguished; the curve rises steeply in the first 30 minutes after that the slope decreases. The two different phases also distinguished by the intracellular location of the labelled amino-sugar. During the first 30 minutes of incubation the grains appear mainly over the area

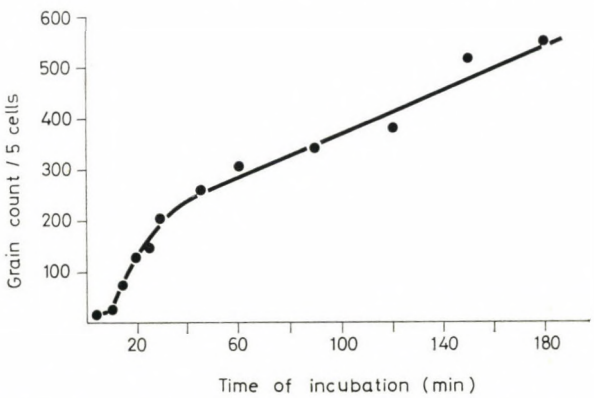

Fig. 1. Incorporation of radioactive glucosamine by interphase cells. Abscissa: incubation time with the radioactive precursor in minutes. Ordinate: mean grain-count of 5 cells

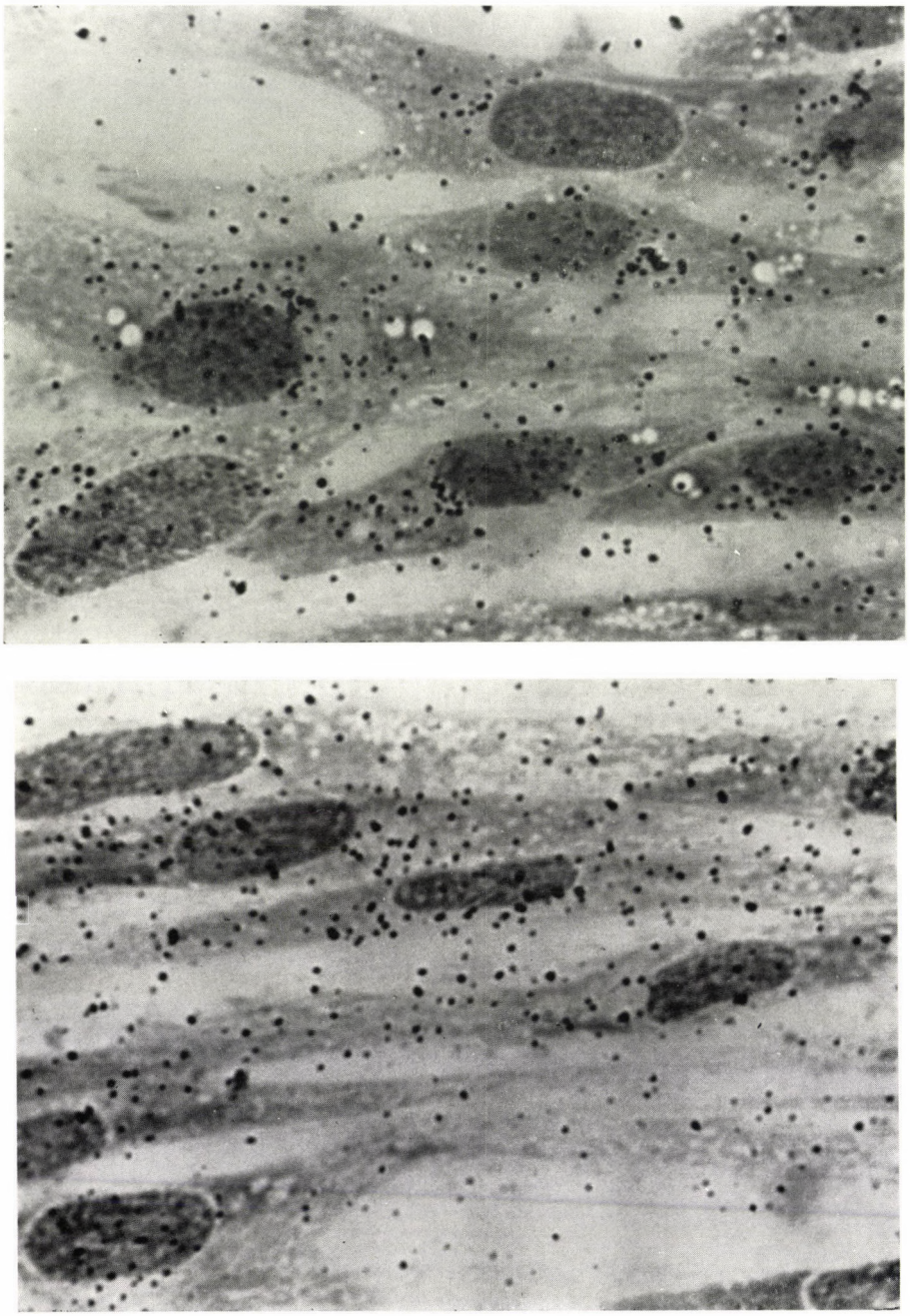

Fig. 2. Chicken fibroblasts after incubation with the radioactive precursor for 45 *(a)* and 75 *(b)* minutes, resp. (Magnification about 1300×)

of the Golgi complex. Later beside the labelling of the Golgi complex, the whole cytoplasm becomes labelled gradually and diffusely (Fig. 2a). On further incubation the radioactively labelled macromolecules appear also in the intercellular region (Fig. 2b).

^{3}H-glucosamine incorporation by dividing cells

Under the above experimental conditions, the grain counts over the dividing cells also gradually increased with the duration of incubation. For these cells too, about 15 to 20 minutes represent the earliest time when the grain number could be quantitatively evaluated. However, at all times appreciable differences were found between the grain counts of interphase and dividing forms, as well as between the grain counts of cells in the various mitotic phases (Fig. 3).

At the beginning of incubation (10–45′), the grain count over the dividing cells was generally lower than that over the interphase cells. The comparison of grain counts among the dividing forms indicated that the grain count of the early mitotic forms (pro- and metaphase) was always lower than the grain count of later mitotic forms (ana- and telophase). After prolonged incubation, the anaphase cells reached, and the telephase cells even exceeded, the interphase cells in respect of grain count.

Accordingly, intensive glucosamine incorporation could be observed for the late mitotic forms. As to the localization of the grains, in the cytoplasms of the arising two new cells of telophase, one could already distinguish lighter areas, the Golgi complex referred to earlier, which contain the majority of grains (Fig. 4) and are located near to the chromosome groups just being transformed into nuclei

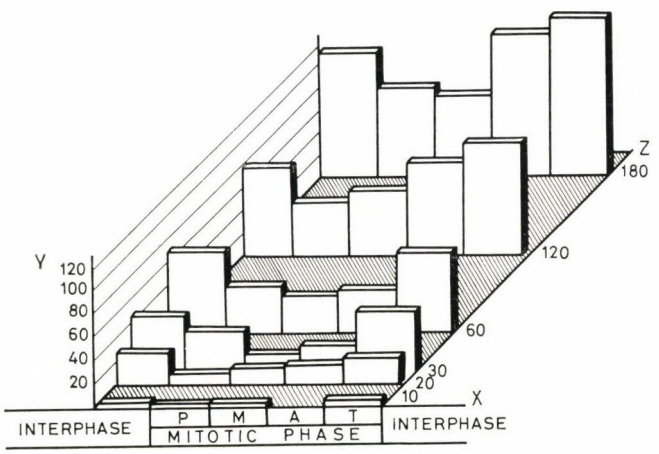

Fig. 3. Incorporation of radioactive glucosamine by interphase and mitotic cells (P = prophase, M = metaphase, A = anaphase, T = telophase) are indicated at the *X*-axis; the mean grain count per cell is given on the *Y*-axis and incubation time with the radioactive precursor in minutes is shown on the *Z*-axis

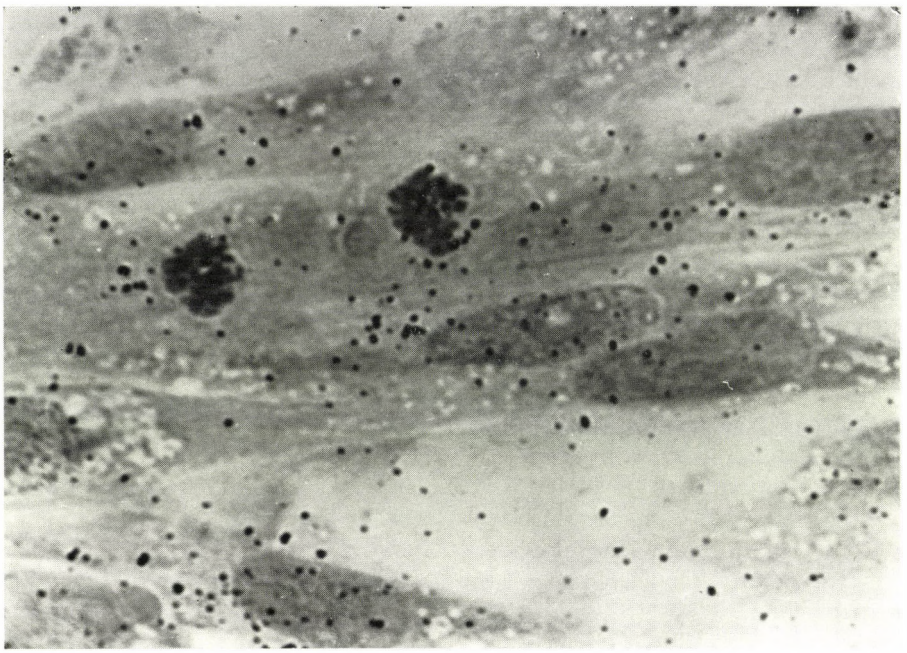

Fig. 4. Chicken fibroblasts after incubation with radioactive glucosamine for 30 minutes. The arising two new cells from telophase contain besides the chromosome groups transforming into nuclei, a lighter area, the Golgi complex, covered by most of the grains. (Magnification about 1300×)

Discussion

By monitoring the incorporation of radioactive glucosamine we were able to study glycoprotein synthesis. This precursor is metabolized into some other sugars but to negligible extent. Furthermore, its acetylated derivatives are preferentially taken up into the glycoproteins in contrast to galactosamine, which is known to accumulate mainly in the glycolipids (Bosmann, Winston, 1970; Evans, Gurd, 1971; Macbeth et al., 1965; Molnár et al., 1965; Roberts et al., 1971). Experiments with mouse lymphoma cells clearly showed that about 90% of glucosamine was incorporated into the intracellular glycoproteins and only 10% was bound to lipids (Bosmann, Winston, 1970). In previous experiments we examined to what extent the tissue-fixing agents of various compositions affected grain counts. It was found, after parallel fixing with 40% formaldehyde or with Carnoy's solution, that the grain counts did not change significantly. We consider this finding as a further evidence for the suggestion that glucosamine is mainly incorporated into glycoproteins. The fact that glucosamine incorporates at several sites of the oligosaccharide side chain of glycoproteins offers a further methodological

advantage; it is easier to detect than, for example, fucose which only occupies terminal positions (Sturgess et al., 1972).

Analysing the above glucosamine incorporation kinetics of *interphase cells* (with the radioautographs) three phases of glycoprotein synthesis and distribution become evident: 1. the accumulation of glycoprotein in the Golgi complex, 2. its segregation from this complex into the plasma, and other cellular membranes, and finally 3. its secretion from the cell as a biopolymer. Under continuous labelling, as in the present experiments, these three processes occur simultaneously.

The efflux of part of labelled glycoprotein from the cell (Spiro, 1970), evidenced in our experiments by the increasing radioactivity of the intercellular region with the progress of time, may account for the sudden change in the rate (Fig. 1). A similar glycoprotein transfer from the Golgi complex of the liver to the serum has also been demonstrated *in vivo* (Sturgess et al., 1972).

The different phases of glycoprotein synthesis in the interphase deserve some comment. As it appears from these data, though glycoprotein synthesis is going on during the whole cell cycle, its rate begins to rise in G_1, reaches the maximum during S and G_2, and decreases in the M phase (Bosmann, Winston, 1970). The changes over the intramitotic stages have not yet been studied in detail. Therefore our attention was focused on them.

Three features were particularly striking in the glucosamine incorporation pattern of *dividing cells*: 1. the grain count over the prophase, metaphase and early anaphase cells was smaller than that over the interphase cells; 2. at 25 to 30 minutes of incubation an intense increase in the grain count could be observed over the prophase cells. This phenomenon might mean that those cells which in the intermitotic phase synthesized an appreciable amount of glycoprotein leave the G_2 phase and enter the prophase just at this point of time – about 25 to 35 minutes after the beginning of labelling. This increased grain count of the prophase will always raise the grain count of the least labelled metaphase. After the first 30 minutes the grain count over the anaphase cells began to increase at such a rate that they approached the grain level of prophase, and exceeded the grain level of metaphase cells. Furthermore similar to the telophase cells, at 120 minutes the grain count reached, and at 180 minutes exceeded, that of the interphase cells, too. 3. The grain count over the telophase cells was already at early points of time at about the same level as, and later even higher than, that over the interphase cells.

Our results lead us to the conclusion that 20 to 30 minutes prior to the M phase the glycoprotein synthesis either stops or decreases. Later, the grain count over the prophase forms approaches the labelling level of interphase cells but never reaches it. Labelling in the metaphase cells proved to be the lowest at almost every evaluation point. This phenomenon may be due to the fact that glycoprotein synthesis not only stops but a part of glycoprotein synthesized earlier is also degraded. Glick et al. (1971) observed a similar phenomenon: concomitant to the beginning of the M-phase they observed the decrease of mannose, galactose and fucose content, and then, with some delay, the loss of sialic acid in a synchronized KB culture. It may be assumed that both the decrease of monosaccharide content

found by Glick et al. (1971) and the reduced incorporation of labelled glucosamine as shown in our radioautographic experiments are the consequences either of the inhibition of synthesis owing to the relative lack of precursor (e.g. increased permeability) or of the degradation of glycoproteins.

On the other hand, the rise of grain-counts in the anaphase and particularly in the telophase suggests a renewed glycoprotein synthesis. The reorganization of the Golgi complex and its glucosamine incorporation at the late ana- and early telophases are in good agreement with the above findings and are assumedly appreciably contributing to the reorganization of the nuclear membrane, which proceeds in the late telophase.

The authors express their best thanks to Miss Sarolta Győr and Miss Mária Tihanyi for their excellent technical assistance.

References

Barland, P., Smith, C., Hamerman, D. (1968) J. Cell. Biol. *37* 13
Bennett, G. (1970) J. Cell. Biol. *45* 668
Bennett, G., Leblond, C. P. (1970) J. Cell. Biol. *46* 409
Bosmann, H. B., Winston, R. A. (1970) J. Cell. Biol. *45* 23
Buck, C. A., Glick, M. C., Warren, L. (1970) Biochem. J. *9* 4567
Cheetman, R. D., Morré, D. J., Junghans, W. N. (1970) J. Cell. Biol. *44* 402
Cleaver, J. E. (1967) Thymidine metabolism and cell kinetics. North-Holland Publishing Co. Amsterdam
Cook, G. M. (1968) Biol. Rev. *43* 363
Dendy, P. P., Cleaver, J. E. (1964) Intern. J. Radiat. Biol. *8* 301
Evans, W. H., Gurd, J. W. (1971) Biochem. J. *125* 615
Favard, P. (1969) in Handbook of Molecular Cytology, Lima-de Faria, A. (editor) p. 1131
Fleischer, B., Fleischer, S., Ozawa, H. (1969) J. Cell. Biol. *43* 59
Froger, C., Louisot, P. (1972) Comp. Biochem. Physiol. *43B* 223
Glick, M. C., Gerner, E. W., Warren, L. (1971) J. Cell. Physiol. *77* 1
Halbhuber, K. J., Cristner, A., Schirrmeister, W. (1972) Acta histochem. *42* 157
Hamaguchi, H., Cleve, H. (1972) Biochem. Biophys. Res. Comm. *47* 459
Ito, S. (1969) Fed. Proc. *28* 12
Kalckar, H. M. (1965) Science *150* 305
Macbeth, R. A., Békési, J. G., Sugden, E., Bice, S. (1965) J. Biol. Chem. *240* 3707
Martinez-Palomo, A. (1972) Int. Rev. Cytol. *29* 29
Molnár, J., Tetas, M., Chao, H. (1969) Biochem. Biophys. Res. Comm. *37* 684
Molnár, J., Robinson, G. B., Winzler, R. J. (1965) J. Biol. Chem. *240* 182
Moscarello, M. A., Kashuba, L., Sturgess, J. M. (1972) FEBS Letters *26* 87
Neutra, M., Leblond, C. P. (1966) J. Cell. Biol. *30* 119, 137
Neutra, M., Leblond, C. P. (1970) Molekuli i kletki, vip. *5* p. 93
Nowakowski, M., Atkinson, P. H., Summers, D. F. (1972) Biochim. Biophys. Acta *266* 154
Rambourg, A., Leblond, C. P. (1967) J. Cell. Biol. *32* 27
Rambourg, A., Hernandez, W., Leblond, C. P. (1969) J. Cell. Biol. *40* 395
Rambourg, A. (1971) Intern. Rev. Cytol. *31* 57
Roberts, R. M., Connor, A. B., Cetorelli, J. J. (1971) Biochem. J. *125* 99
Spiro, R. G. (1970) Ann. Rev. Biochem. *39* 599

Sturgess, J. M., Mitranic, M., Moscarello, M. A. (1972) Biochem. Biophys. Res. Comm. *46* 1270

Wakowiak, H., Sarzala, M. G., Zybrzycka, E., 1st Conf. of experts from sccialist countries: Physical, Chemical and Biochemical Aspects of Ion Transport across Membranes, Reinhardsbrunn, GDR (1972)

Whaley, W. R., Dauwalder, M., Kephart, J. E. (1972) Science *175* 596

Weiss, L. (1969) Int. Rev. Cytol. *26* 63

Acta Biochim. et Biophys. Acad. Sci. Hung. Vol. 9 (1—2), pp. 63—72 (1974)

Emetine and Macromolecular Biosynthesis in Mammalian Cells

GYÖNGYI FARKAS, F. ANTONI, MÁRIA STAUB, P. PIFFKÓ

Institute of Medical Chemistry, Semmelweis University of Medicine, and National Institute for Neurosurgery, Budapest, Hungary

(Received June 11, 1973)

The effect of emetine on protein and RNA synthesis has been examined in human tonsillar lymphocytes and in *Ehrlich ascites* cells. 10^{-7} M of emetine inhibited protein synthesis by 50% in lymphocytes and by 30% in ascites cells. The inhibition was observed already in the first 10 minutes and it could not be reversed by washing the cells.

The incorporation of (^{14}C)-D-glucosamine into ascites cells was also inhibited but to a lesser extent than the protein synthesis.

At higher concentrations the incorporation of (^{3}H)-uridine was also inhibited. 10^{-3} M emetine exerted 90% inhibition in human tonsillar lymphocytes, whereas in ascites cells the inhibition was 50%. The effect of emetine on RNA synthesis seemed to be reversible in the first 30 min of treatment.

Introduction

The alkaloids of *Ipecacuanha* have widely been used for medical purposes. Emetine is the principal component of these alkaloids and it is used for the treatment of amoebic diseases (Janot, 1953). The mode of action remained obscure until the recent years. Attention has been directed to conformational and functional similarities between the ipecac alkaloids and cycloheximide, the well-known antibiotic (Grollman, 1966). Cycloheximide is extensively used as a potent inhibitor of protein synthesis. Grollman (1966, 1968) demonstrated that emetine inhibited protein and DNA synthesis in HeLa cells and in cell-free extracts. Gilead and Becker (1971) have studied the inhibition of emetine on RNA synthesis in HeLa cells and the reversibility of the inhibitory effect of the drug has been examined. Perry and Kelley (1968, 1970) have also demonstrated the inhibitory effect of emetine on the synthesis of RNA and compared it with the effect of actinomycin D.

The present paper describes the effect of emetine on the synthesis of protein and RNA in human tonsillar lymphocytes and in *Ehrlich ascites* cells. The experiments provide a biochemical basis for most of the known toxic properties of emetine in human cells.

Materials and methods

Preparation of cell suspension

Cells were prepared from freshly removed tonsils of children (4–7 years old) by the method of Piffkó et al. (1970). Cells obtained from 1 g tissue were suspended in 1.5 ml Hanks' solution and the counting was performed in a Buerker-hemocytometer.

Ehrlich ascites cells were obtained from the ascites fluid of mice. After washing, the cells were suspended in Hanks' solution. The suspension contained usually 10^7 cells per ml.

Incorporation of (^{14}C)-leucine

The specific radioactivity of (^{14}C)-L-leucine (U.V.V.R. Praha) was 88.2 mCi/ /mmole. The incorporation was carried out in 1.0 ml of Hanks' solution. The reaction mixture contained 0.2 μCi (^{14}C)-leucine, 5×10^6 ascites cells or 10^7 lymphocytes and various inhibitors at the concentrations indicated. At the end of incubation at 37°C 0.02 M leucine was added and the mixture was cooled. The cells were centrifuged and washed with Hanks' solution, then suspended in 1.0 ml distilled water and frozen at −20°C. After thawing 1.0 ml 10% TCA was added. The acid precipitable material was treated according to the modified method of Siekevitz (1952). The samples were hydrolysed at 90°C for 15 min. Then the precipitate was filtered through a Whatman filter paper and washed with 5% TCA and finally with ethanol. The filter paper discs were dried and the radioactivities were measured in 5.0 ml toluene-based cocktail in a Packard Liquid Scintillation Spectrometer.

Incorporation of (^{3}H)-uridine

The specific radioactivity of (^{3}H)-uridine was 1.52 Ci/mmole (U.V.V.R., Praha). The reaction mixture (1.0 ml) contained 0.2 μCi (^{3}H)-uridine, 10^7 cells and the inhibitors. The reaction was stopped by addition of 1.0 ml cold 10% TCA. The precipitate was washed four times with cold 5% TCA and dissolved in 1.0 ml concentrated formic acid. Aliquots (0.5 ml) were added to 5.0 ml of toluene-based cocktail containing 2.0 ml absolute ethanol and the radioactivity was measured.

Incorporation of (^{14}C)-D-glucosamine

The specific radioactivity of (^{14}C)-D-glucosamine hydrochloride was 3.0 mCi/mmole (Radiochemical Centre, Amersham). 1.0 μCi (^{14}C)-glucosamine was used in the reaction mixture containing 10^7 cells in 1.0 ml of Hanks' solution. The reaction was stopped by addition of 1.0 ml 10% TCA. The acid-precipitable material was treated in the same way as in the case of (^{14}C)-leucine incorporation.

Results

Effect of emetine on protein synthesis

In the first part of our experiments the effect of emetine on (^{14}C)-leucine incorporation into human tonsillar lymphocytes and into ascites cells was studied. The effect on freshly prepared cells is shown in Fig. 1. The dose-dependence of the inhibition indicated that during the course of 10 min incubation 10^{-6} M emetine

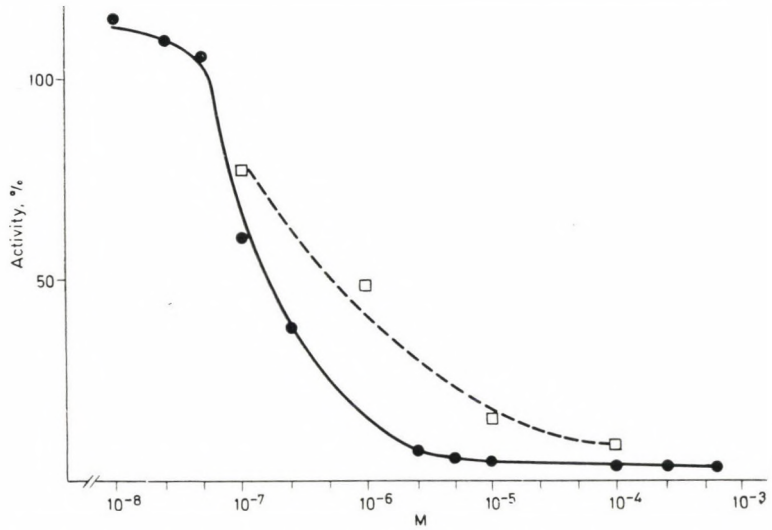

Fig. 1. (^{14}C)-leucine incorporation of human tonsillar lymphocytes and ascites cells at various concentrations of emetine. The reaction mixture contained 10^7 cells in 1.0 ml Hanks' solution and varying concentrations of emetine. The cells were incubated for 120 min at 37°C and the incorporation was measured as described in Methods and expressed as the per cent activity of the control; ●——● in lymphocytes; □- - - -□ in ascites cells

exerted 90% inhibition in lymphocytes, and 50% in ascites cells. Protein synthesis was inhibited by 50% at 10^{-7} M of emetine concentration. Emetine was used in 10^{-6} M concentration to determine the time of exposure to the drug necessary for the development of inhibition. As shown in Fig. 2, the effect was observed already after 30 min incubation at 37°C. The inhibitory effect of emetine on protein synthesis was compared with that of cycloheximide and puromycin. Fig. 3 demonstrates the incubation of ascites cells in the presence of 10^{-6} M emetine, 10^{-5} M puromycin and 10^{-5} M cycloheximide, respectively. Puromycin at this concentration has only a slight effect on protein synthesis of eukaryotic cells. As can be seen, 10^{-6} M emetine had the same effect on protein synthesis as 10^{-5} M of cycloheximide.

It was attempted to elucidate whether the mode of inhibitory action of

emetine was similar to that of cycloheximide. Grollman (1968) has shown that the effect of emetine on protein synthesis in HeLa cells was irreversible.

The reversibility of the inhibition on protein synthesis in lymphocytes and in ascites cells is presented in Fig. 4. Lymphocytes were treated for 15 min at 37°C with 10^{-6} M emetine, and ascites cells for the same time with 10^{-5} M emetine. The

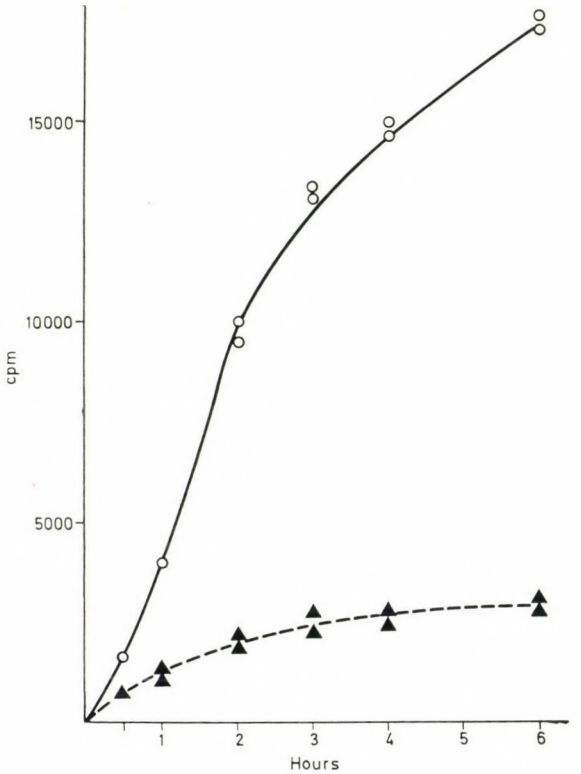

Fig. 2. (^{14}C)-leucine incorporation of human tonsillar lymphocytes as a function of time in the presence of emetine. 5×10^6 cells were incubated for the indicated times in the presence of (^{14}C)-leucine. The content of acid-insoluble radioactivity was expressed as cpm/5×10^6 cells; ○——○ control; ▲–·–·–▲ in the presence of 10^{-6} M emetine

drug was removed by centrifuging and washing, the cells were resuspended in the reaction mixture and labelled with (^{14}C)-leucine. The samples were incubated for 120 min at 37°C in the presence or absence of inhibitors. As indicated in Fig. 4 after washing, the protein synthesis of cycloheximide-treated cells reached the control values both in lymphocytes and in ascites cells. In contrast to the reversible effect of cycloheximide, in cells treated with emetine the protein synthesis was restored only to 20%. Our results are in good agreement with those found in the case of HeLa cells (Grollman, 1968).

Effect of emetine on RNA synthesis

Grollman (1968) has shown that in HeLa cells 10^{-6} M emetine, while inhibiting promptly protein synthesis, has no effect on RNA synthesis. In Fig. 5 RNA synthesis of lymphocytes is demonstrated in the presence of 10^{-6} M emetine and 2×10^{-6} M actinomycin D. It can be seen that the concentration of emetine

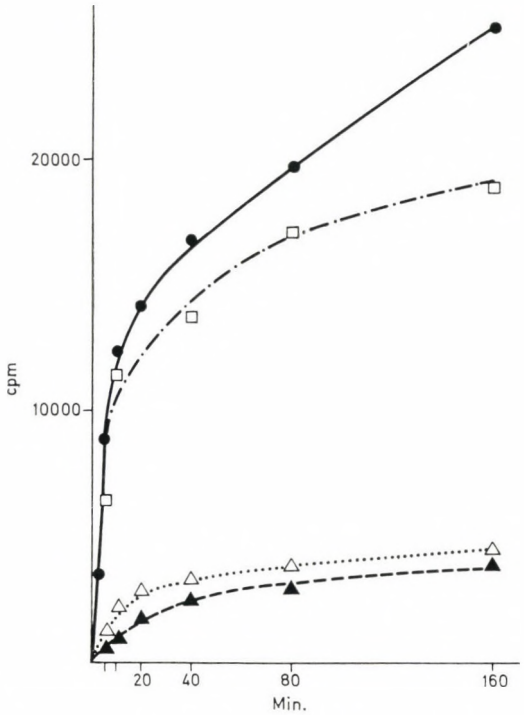

Fig. 3. Effect of puromycin, cycloheximide and emetine on the protein synthesis of ascites cells as a function of time. 10^6 cells were incubated in the presence of (^{14}C)-leucine for the indicated times at 37°C. Radioactivity was expressed as cpm/10^6 cells; ●——● control; □- - - -□ in the presence of 10^{-5} M puromycin; △- - - - △ 10^{-5} cycloheximide;▲- - - -▲ 10^{-5} M emetine

inhibiting protein synthesis fails to influence (^{3}H)-uridine incorporation, in contrast to the effect of 2×10^{-6} M actinomycin D.

The effect of higher concentrations of emetine is shown in Fig. 6. The results indicate that the RNA synthesis of human tonsillar lymphocytes is sensitive to the drug provided that concentrations are higher than 5×10^{-6} M. In ascites cells the inhibiting concentration of emetine is 10^{-5} M.

Gilead and Becker (1971) has observed that various RNA species synthesized in HeLa cells differed in their sensitivity to the inhibitory effect of emetine.

The reversibility of the inhibitory effect of emetine in lymphocytes was investigated. Lymphocytes were treated for 30 min with 10^{-3} M emetine. The drug was then removed, the cells were washed and labelled with (^{3}H)-uridine. It was found that synthesis of RNA was practically restored after the removal of emetine (Fig. 7).

The rapid and marked inhibition of protein synthesis raised the question, to what extent the glycosidation of proteins was influenced by emetine. Glycosidation was measured by following the incorporation of (^{14}C)-D-glucosamine into the acid precipitable material.

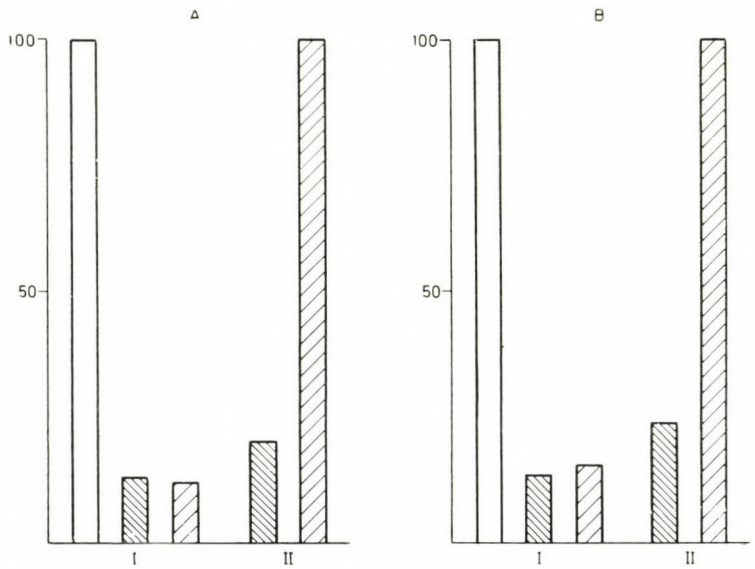

Fig. 4. Reversibility of the inhibition of protein synthesis in emetine- and cycloheximide-treated lymphocytes (A) and ascites cells (B). 5×10^{6} cells per ml were preincubated for 15 min at 37°C in the absence (I) and in the presence (II) of inhibitors. In the case of lymphocytes (A) 10^{-6} M cycloheximide ▽ and 10^{-6} M emetine ▨ was present. In ascites cells (B) 10^{-5} M cycloheximide ▨, and 10^{-5} M emetine ▧. After preincubation the cells were washed twice with Hanks' solution and resuspended in a fresh medium. The incorporation of (^{14}C)-leucine was measured for 120 min in the absence (I) and in the presence (II) of the inhibitors (at the same concentrations as in the preincubation). □ represents the control activity. The activity of treated cells was expressed as the per cent of the control

The incorporation of (^{14}C)-D-glucosamine into ascites cells is demonstrated in Fig. 8. The glycosidation of proteins does not seem to be markedly influenced by emetine in the course of 80 min of incubation.

Discussion

The studies reported in this paper show that emetine rapidly inhibits protein biosynthesis both in human tonsillar lymphocytes and in ascites cells.

The concentration of emetine required to inhibit protein synthesis by 50% in intact cells is approximately 10^{-7} M (Fig. 1). In the case of HeLa cells Grollman

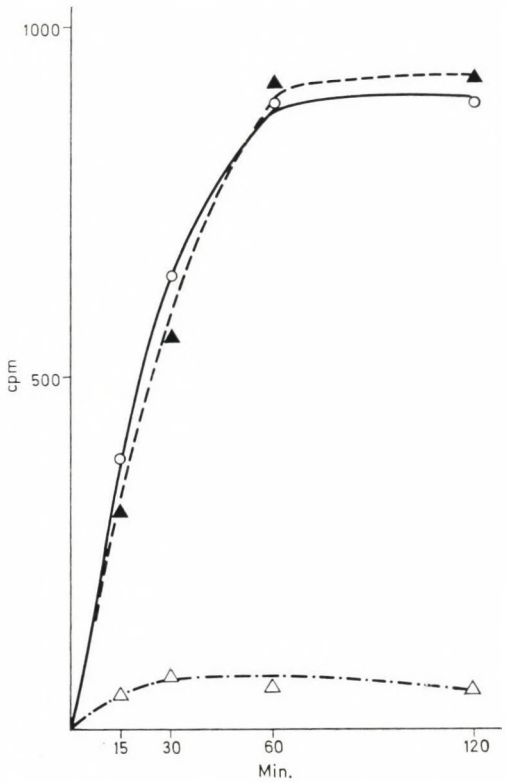

Fig. 5. Effect of emetine and actinomycin D on (^{3}H)-uridine incorporation of lymphocytes. 8×10^6 lymphocytes were incubated in the presence of 10^{-6} M emetine and 2×10^{-6} M actinomycin D for the indicated times. The radioactivity in acid-insoluble material was determined as described in Methods; ○——○ control; ▲– – –▲ 10^{-6} M emetine; △ -.-.-.- △ 2×10^{-6} M actinomycin D

(1968) has found 4×10^{-8} M to inhibit protein synthesis to the same extent. A virtually complete inhibition of protein synthesis could be achieved by 10^{-6} M emetine in lymphocytes. As shown in Fig. 4, in contrast to cycloheximide, treatment with emetine causes an irreversible damage of protein synthesis.

Relatively low concentrations of the drug are sufficient to inhibit almost completely protein synthesis in HeLa cells (Grollman, 1968), the same holds for

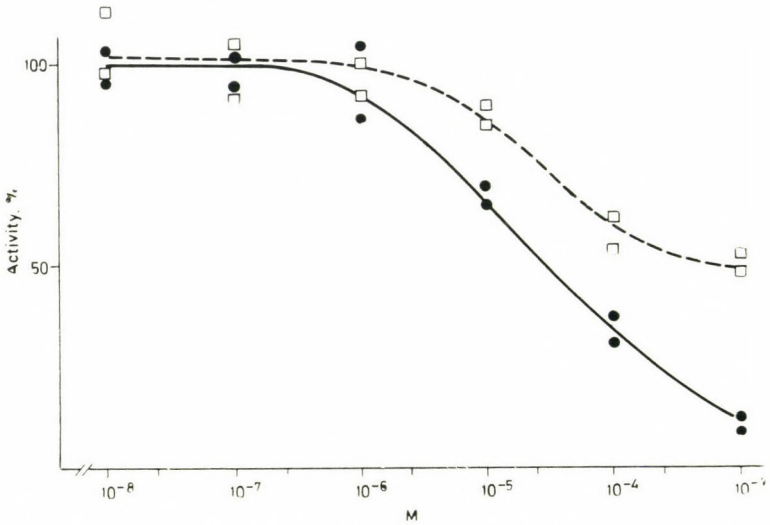

Fig. 6. (^{3}H)-uridine incorporation of human tonsillar lymphocytes and ascites cells at various emetine concentrations. 5×10^6 lymphocytes and 10^6 ascites cells were incubated to 120 min. The incorporated radioactivity was measured as described in Methods; ●——● lymphocytes; □– – –□ ascites cells

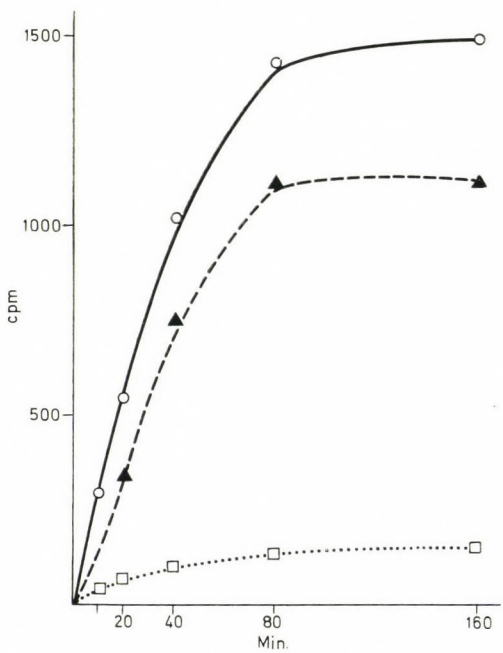

Fig. 7. Reversibility of the inhibition of RNA synthesis in emetine-treated lymphocytes. 10^7 lymphocytes were treated with 10^{-3} M emetine for 30 min at 37°C in Hanks' solution. The cells were washed twice and resuspended in the reaction mixture. (^{3}H)-uridine incorporation was measured for the indicated times; ○——○ control cells; ▲– – –▲ cells treated with 10^{-3} M and washed; □------□ incorporation in the presence of 10^{-3} M emetine

human lymphocytes, too. On the other hand, the same range of drug concentration ($10^{-7}-10^{-5}$ M) exerts only a slight inhibitory effect on RNA synthesis. At higher concentrations (10^{-3} M) RNA synthesis is also inhibited. This effect is dose-dependent (Fig. 6) and reversible (Fig. 7).

Gilead and Becker (1971) claimed that low concentrations of emetine inhibited only the synthesis of precursors of rRNA, whereas 1 mM of emetine completely abolished the synthesis of all RNA species.

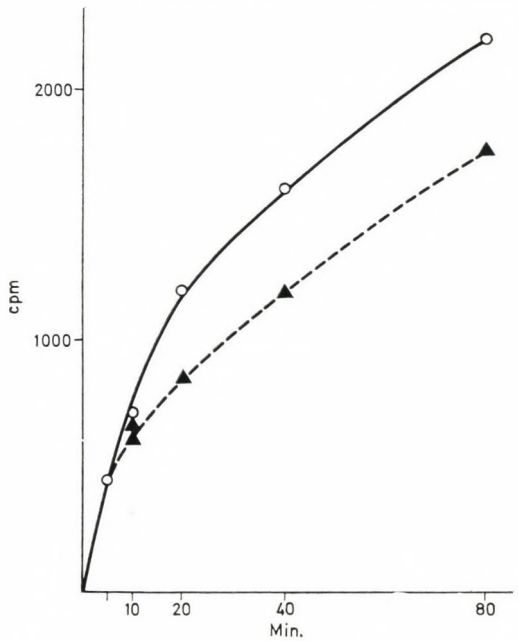

Fig. 8. (^{14}C) D-glucosamine incorporation into ascites cells. 5×10^{6} cells were incubated for the indicated times. The incorporated radioactivity was measured in the acid-precipitable material; ○——○ control; ▲- - -▲ in the presence of 10^{-5} M emetine

It has to be emphasized that 10^{-6} emetine, which almost completely inhibits the synthesis of protein, allows a prolonged RNA synthesis in HeLa cells as well as in lymphocytes.

Emetine is widely used as a medical agent and its toxic effects in man are established. There is good reason to believe that the toxic effect of emetine – at least part of it – may be attributed to the inhibition on macromolecular synthesis of human cells.

Emetine possesses several properties that might be put to use in the work with eukaryotic cells. Due to its rapid uptake by cells (Grollman, 1968), at low concentrations emetine exerts an immediate inhibitory effect on the synthesis of protein without affecting the synthesis of RNA. The most important advantage in the use of this drug comes of its specific effect on eukaryotic cells.

References

Gilead, Z., Becker, Y. (1971) Europ. J. Biochem. *23* 143
Grollman, A. P. (1966) Proc. Nat. Acad. Sci. U.S.A. *56* 1867
Grollman, A. P. (1968) J. Biol. Chem. *243* 4089
Janot, M. in The Alkaloids (ed. by R. H. Manske and H. L. Homes). Academic Press, New York, 1953. Vol. III. p. 363
Perry, R. P., Kelley, D. E. (1968) J. Cell. Physiol. *72* 235
Perry, R. P., Kelley, D. E. (1970) J. Cell. Physiol. *76* 127
Piffkó, P., Köteles, Gy. J., Antoni, F. (1970) Pract. otorhinolaryng. *32* 305
Siekevitz, P. (1952) J. Biol. Chem. *195* 549

Acta Biochim. et Biophys. Acad. Sci. Hung. Vol. 9 (1—2), pp. 73—86 (1974)

Effect of Ribonuclease Treatment on Nuclear, dRNA-containing 30 *S* Ribonucleoprotein Particles

J. MOLNÁR, L. KOMÁROMY

Institute of Biology, University Medical School of Pécs, Pécs, Hungary

(Received June 6, 1973)

Our earlier experiments have shown that from the cell nucleus such a dRNA-containing ribonucleoprotein fraction can be extracted with 0.3 M NaCl which differs in several respects from the fraction extractable with 0.1 M NaCl. Thus differences were revealed in protein composition, in the sensitivity towards higher salt concentration, in the kinetics of degradation, and in submicroscopic morphology. In the present work the susceptibility of "0.1 M" and "0.3 M 30 *S* particles" to pancreatic ribonuclease I was examined. If the particles were extracted in the absence of ribonuclease inhibitor, their RNA content decreased and this could be readily followed by the CsCl equilibrium density gradient centrifugation of the particles. Under such conditions always the buoyant density of "0.3 M particles" was lower. If the particles were incubated at room temperature, their endogenous ribonuclease content, and this effect could not be markedly enhanced by the addition of exogenous ribonuclease. It is an interesting phenomenon that the buoyant densities of particles obtained after ribonuclease treatment were identical, although they were consistently different before the treatment. On the effect of ribonuclease there was an apparent increase in the sedimentation coefficient of the particles. Electron microscopic studies showed that this phenomenon was due to the aggregation of damaged particles.

Introduction

It has been shown in our previous experiments that the dRNA-containing ribonucleoprotein components of the cell nucleus exist under physiological conditions as polysome-like complexes, and these complexes can also be isolated if the extracting solutions contain RNase inhibitor. The ribonuclease sensitivity of polysome-like complexes is so pronounced that they are decomposed into 30 *S* components already if RNase inhibitor is not applied during extraction (Samarina et al., 1968). It has also been demonstrated that treatment with RNase alters the sedimentation coefficient of 30 *S* particles: the treated particles sediment faster in sucrose density gradient centrifugation (Samarina et al., 1967).

In other experiments we also observed that the informofer that effects the intranuclear transport of dRNA is heterogeneous and if the conditions of extraction are varied particles differing in several respects can be obtained (Molnár, Ju-

hász, 1972; Molnár et al., 1972; Komáromy et al., 1973; Juhász, Molnár, 1973; Molnár, 1973).

The aim of our present work was, first, to examine what causes the increase of sedimentation coefficient of 30 *S* particles after treatment with RNase, and second, to decide whether any differences occur in biochemical and ultrastructural properties between particles obtained with 0.1 M and 0.3 M NaCl, if they are subjected to RNase treatment.

We found that the buoyant density of 30 *S* particles decreased as a result of RNase treatment because of the loss in their RNA content, and a marked aggregation occurred. The difference between the buoyant densities of "0.1 M" and "0.3 M 30 *S* particles", which was always observable, disappeared after treatment with ribonuclease.

Materials and methods

All chemicals were purchased from Reanal (Budapest) and were of reagent grade, with the exception of sucrose of pure quality. The sucrose-containing solutions were treated with diethylpyrocarbonate (Fluka) before use, to remove ribonuclease contaminations. The 1 mg/ml aqueous solution of crystalline bovine pancreatic ribonuclease was incubated before use in a 90°C water bath for 20 minutes. The 2-(^{14}C)-orotic acid (10.35 mCi per mmole) and carrier-free $NaH_2{}^{32}PO_4$ were procured from the Institute of Isotope Hungary.

Male CFY rats weighing about 200 g, from our own breed, were used for the experiments. The animals were starved for 24 hours prior to the experiment, then they were given either 15 μCi sodium (^{14}C)-orotate 20 minutes before killing or 1 mCi $Na_2H^{32}PO_4$ two hours before killing, both intraperitoneally. The animals were killed in ether anaesthesia, the livers were perfused with ice-cold physiological salt solution then they were homogenized in a glass-teflon Potter–Elvehjem type homogenizer in 5 volumes of 2.2 M sucrose containing 0.5% sodium β-glycerophosphate. From the homogenate the nuclear fraction was prepared as described earlier (Samarina et al., 1967). All operations were carried out at 0 to +4°C.

The nuclear fraction was washed with STM I buffer (0.1 M NaCl, 0.01 M Tris.HCl, 0.001 M $MgCl_2$, pH 7.2), extracted twice with STM II buffer (the same as STM I, but the pH is 7.9), then twice with STM III buffer (the same as STM II, but NaCl concentration is 0.3 M). The extracts will be referred to as "0.1 M" and "0.3 M extracts" and the particles they contain will be designated accordingly as "0.1 M" and "0.3 M particles" Molnár, Juhász, 1972.

The extracts were centrifuged in sucrose gradient, the composition of which was somewhat modified relative to our earlier protocol. A 30 ml 15–30% (w/v) linear sucrose gradient was prepared on the top of which 2 ml 15% sucrose was layered. The sucrose solutions were made up in 0.01 M triethanolamine buffer, pH 7.5. The 15–30% sucrose gradient also contained 2% formaldehyde. The 2 ml formaldehyde-free 15% sucrose solution was applied because the nuclear extracts

were prepared with Tris buffer. The nuclear extracts were then layered on top of the gradients thus prepared and were centrifuged for 13 to 15 hours in the SW 27 rotor of a Beckman Model L2-65B preparative ultracentrifuge at 24 000 r.p.m. at 3°C. When the analysis of particles already once purified by gradient centrifugation was to be performed, the appropriate fractions of the gradient were pooled and dialyzed for 4–5 hours against STM II buffer (pH 7.5) containing triethanolamine, to remove the excess of sucrose. In this case, of course, the first centrifugation was made in a sucrose gradient not containing formaldehyde.

The nuclear extract and the 30 *S* nuclear particles were treated with RNase at 25°C for 20 minutes.

For the CsCl isopycnic density gradient centrifugation the sample to be analyzed was dialyzed against 0.005 M phosphate buffer, pH 7.2, containing 1% formaldehyde (because the material had already been fixed in the sucrose gradient centrifugation) for 20 hours. After that the sample was centrifugated in a 5 ml preformed CsCl gradient in the 3 × 5 ml rotor of a Janetzki Vac 60 ultracentrifuge at 36 000 r.p.m. for 20 hours at 10°C (Molnár, 1973).

From each fraction of the gradient, or from its aliquot, the absorbancy at 260 nm was determined, then after the addition of an appropriate amount of rRNA as carrier, the acid-insoluble material was washed into a cellulose nitrate filter (Synpor 2), dried with ethanol and the radioactivity was measured in a GAMMA liquid scintillation spectrometer (Molnár et al., 1973). The scintillation cocktail contained 100 mg POPOP and 4 mg PPO in 1000 ml toluene.

The "0.1 M" and "0.3 M 30 *S* particles" extracted with STM II and III buffers, and separated in the sucrose gradient, as well as the material sedimented in other zones of the gradient, were also used for electron microscopic studies.

To remove sucrose the samples taken from each fraction were dialyzed against STM I buffer (0.1 M NaCl) through a 2% parlodium membrane for 12 hours at 4°C. The dialyzed samples were prepared partly by negative contrasting procedure, partly by shadowing with platinum-palladium vapour. In the former case the specimens were mounted on parlodium carrier membrane electron microscopic grids, then these were stained with a 2% aqueous uranylacetate (Merck) solution. For the shadowing the gradient samples were prepared according to the basic protein-film technique (Lang, Mitani, 1970). The protein-film layer which also contained the sample was taken up on grids also containing carbon-fortified fromvar membrane, then at an angle of 6°20′ they were shadowed with platinum-palladium vapour in a Zeiss Jena HBA 120/2 type apparatus. On the platinum-palladium alloy 20 mg was used up, the ratio of platinum/palladium was 3 : 2. The preparations thus prepared were analyzed with TESLA BS 513 A and 613 type electron microscopes (accelerating voltage 80 kV). The electron micrographs of shadowed preparations were made at 10 000-fold magnification, and were further magnified by photographic methods.

Results and discussion

Since one of the goals of our experiments was to establish whether the "0.1 M" and "0.3 M 30 *S* particles" behaved in a similar or different manner towards RNase, in the major part of our experiments we used preparations in which the RNA's of the individual particle types contained radioactivities of different origins. Accordingly, either the "0.1 M 30 *S* particles" comprised radioactivity from (^{14}C)-orotate (time of exposure 20 minutes) and the "0.3 M particles" were labelled with ^{32}P (exposure: 2 hours), or *vice versa*. This method we have earlier successfully applied in the study of NaCl-sensitivity of 30 *S* particles (Molnár, 1973), and it considerably facilitated the evaluation of results.

In the experiment demonstrated in Fig. 1 nuclear extracts were mixed. The "01. M extract" contained 30 *S* particles that incorporated ^{32}P, whereas the particles of "0.3 M extract" comprised radioactivity derived from (^{14}C)-orotate. The mixture of extracts was divided into three equal portions. One aliquot was allowed to stand in an ice-water bath (a), the second aliquot was incubated at 25°C for 20 minutes (b), whereas to the third aliquot pancreatic RNase was added to 1 μg/ml final concentration and the mixture was incubated at 25°C for 20 minutes (c). Samples b and c were cooled in an ice-bath at the end of incubation, and then all three preparations were layered on top of an ice-cold sucrose density gradient containing formaldehyde (cf. Methods) and were centrifuged and analyzed as usual.

It is seen that about one-third of radioactivity of the particles has already

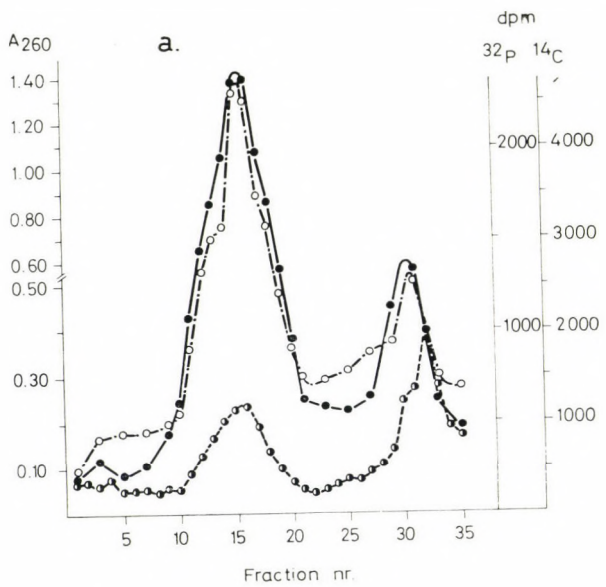

Fig. 1

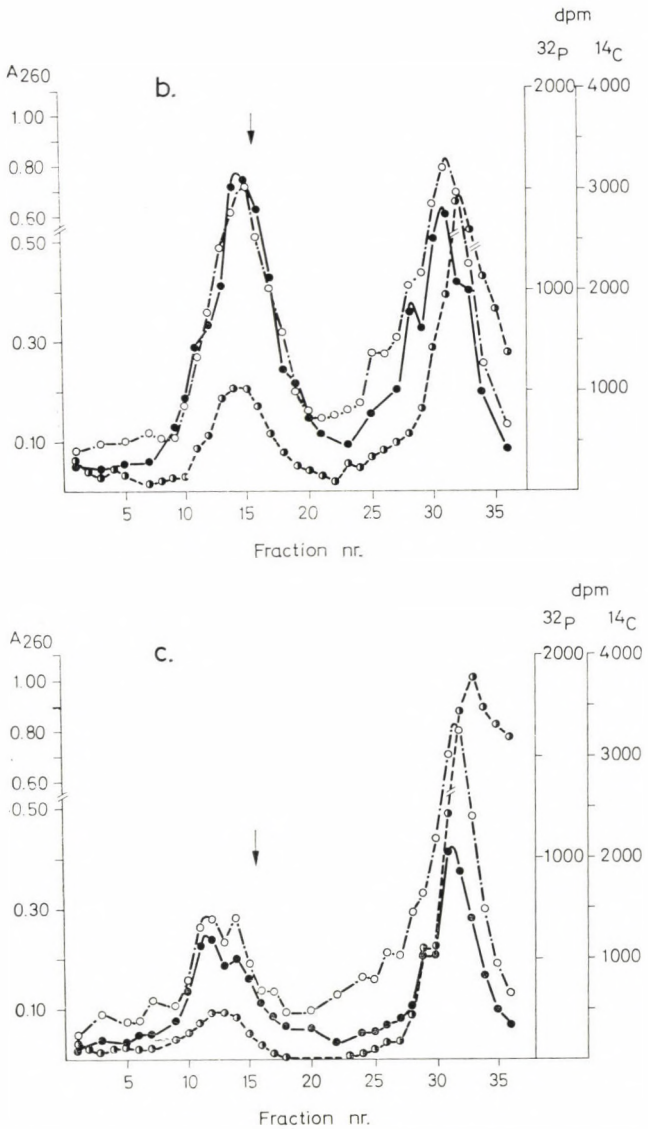

Fig. 1. Effect of ribonuclease treatment on nuclear 30 *S* particles. Five ml "0.1 M" and 3 ml "0.3 M" nuclear extracts (both prepared in the absence of RNase inhibitor) were mixed and then divided into three equal portions. One aliquct was allowed to stand in an ice-bath (a), the second aliquot was incubated at 25°C for 20 min (b), and to the third aliquot 1 μg/ml RNase was added and incubated at 25° for 20 min (c). All samples were then cooled in an ice-bath and were layered on top of a 15—30% (w/v) sucrose gradient (for the details cf. Method) containing 2% formaldehyde. The gradients were centrifuged in the SW 27 rotor of a Beckman Model L2-65B preparative ultracentrifuge at 25 000 r.p.m. and 3°C. Sedimentation from right to left. ◑--◑-- : A_{260}; ●——● : ^{14}C radioactivity ("0.3 M particles"), dpm; ○·····○ : ^{32}P radioactivity ("0.1 M particles"), dpm. The arrow indicates the position of the 30 *S* zone

been degraded during incubation at room temperature, presumably as a result of endogenous RNase activity, and could not be found in the 30 *S* zone. Treatment with RNase at the given concentration further decreased the radioactivity of 30 *S* zone, which by now represented only one-third of the original value.

It could also be observed in this process that the sedimentation coefficient of damaged 30 *S* particles gradually increased (cf. the arrows in Figs 1b and c). This might be due to two different reasons. Either the particles occupy a smaller volume, which can be tested by measuring their density, or aggregation occurs, for the further analysis of which we resorted to the methods of submicroscopic morphology.

We have already reported that there is a difference between the buoyant densities of "0.1 M" and "0.3 M 30 *S* particles", which is consistently observed if the extracting solutions do not contain RNase inhibitor, and this difference is at least 0.01 gcm^{-3}. The buoyant density of "0.1 M" particles was found to be greater, and its value was unaffected by the increase of ionic strength to 0.3 (Molnár, Juhász, 1972; Molnár, 1973). When the nuclear extract containing the 30 *S* particles was incubated at room temperature, the buoyant density of 30 *S* particles decreased relative to the control, as measured in a CsCl equilibrium density gradient (Figs 2a and b), but there was no substantial further decrease on treatment with exogenous RNase. No difference was ever found between the buoyant densities of "0.1 M" and "0.3 M particles" damaged by RNase. As the difference between the buoyant densities of particles incubated at room temperature or treated with RNase did not exceed 0.005 gcm^{-3}, we refrain from demonstrating the sedimentation patterns.

For the electron microscopic studies we only exceptionally used preparations which contained both "0.1 M" and "0.3 M 30 *S* particles", because the latter are markedly heterogeneous (Komáromy et al., 1973). The electron micrographs presented were taken of preparation that contained only one type of particles.Treatment with RNase, sucrose density centrifugation and the analysis of the gradient were carried out as described above.

On the electron micrographs of shadowed preparation of 30 *S* particles treated with RNase the pronounced aggregation of particles could be observed, in the case of both "0.1 M" and "0.3 M 30 *S* particles". In each aggregate about 5 to 10 particles are clustered, but even larger aggregates could often be discerned (Figs 3b and 4b). Such a form and extent of aggregation could never be found with control preparations, not even as artefacts. In the control preparations both "0.1 M" and "0.3 M particles" appear individually, without aggregation (Figs 3a and 4a). The aggregates formed after RNase treatment also differ from the electron micrographic formations displayed by the polysome-like chains of "0.1 M" and "0.3 M particles" if extraction is carried out in the presence of RNase inhibitor (Samarina et al., 1968; Molnár, Juhász, 1973; Lukanidin et al., 1972).

A morphologically interesting type of aggregation was observed with "0.3 M particles" after RNase treatment. During the analysis under the electron microscope of fractions containing material with 50 to 60 *S* sedimentation constant, we

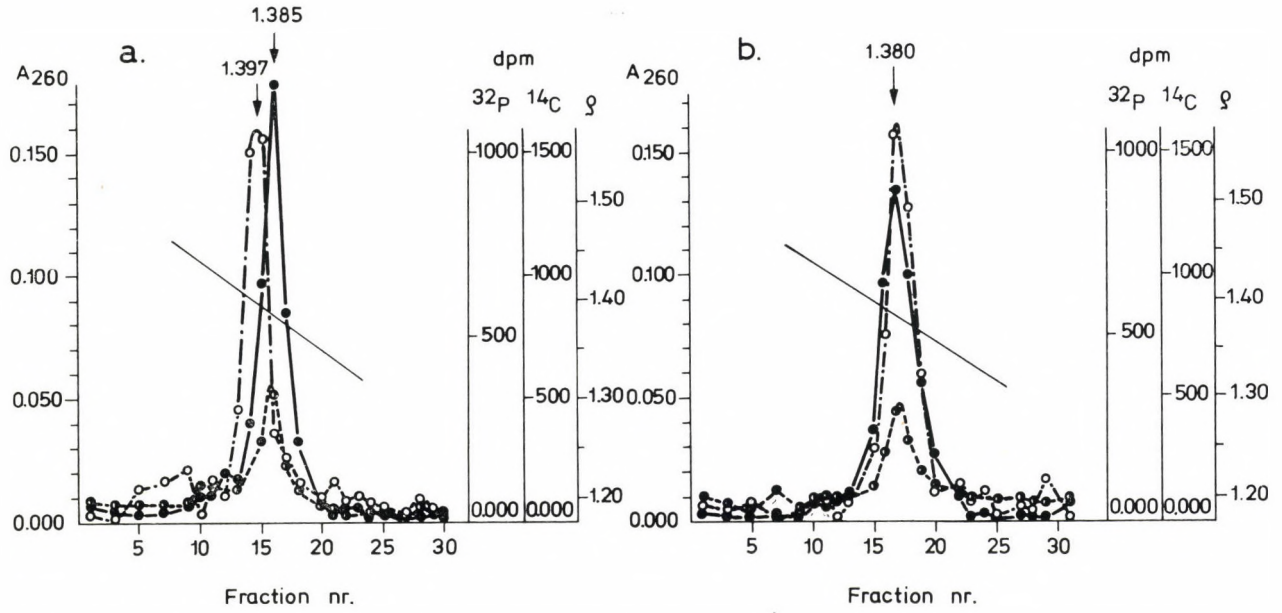

Fig. 2. Equilibrium CsCl density gradient centrifugation of nuclear 30 *S* particles after incubation at room temperature. The material derived from fractions 15 and 16 of the gradient shown in Fig. 1 (Fig. 2a) and the material from fractions 14 and 15 of the gradient shown in Fig. 1b (Fig. 2b) were dialyzed against 5 mM phosphate buffer, pH 7.2, containing 1% formaldehyde, then a performed CsCl gradient was prepared (ϱ = 1.26 to 1.49 gcm^{-3}). The gradients were centrifuged in the 3×5 ml rotor of a Janetzki VAC 60 ultracentrifuge for 20 hours at 10°, when the equilibrium was reached. Three-drop fractions were collected. Symbols are the same as in Fig. 1

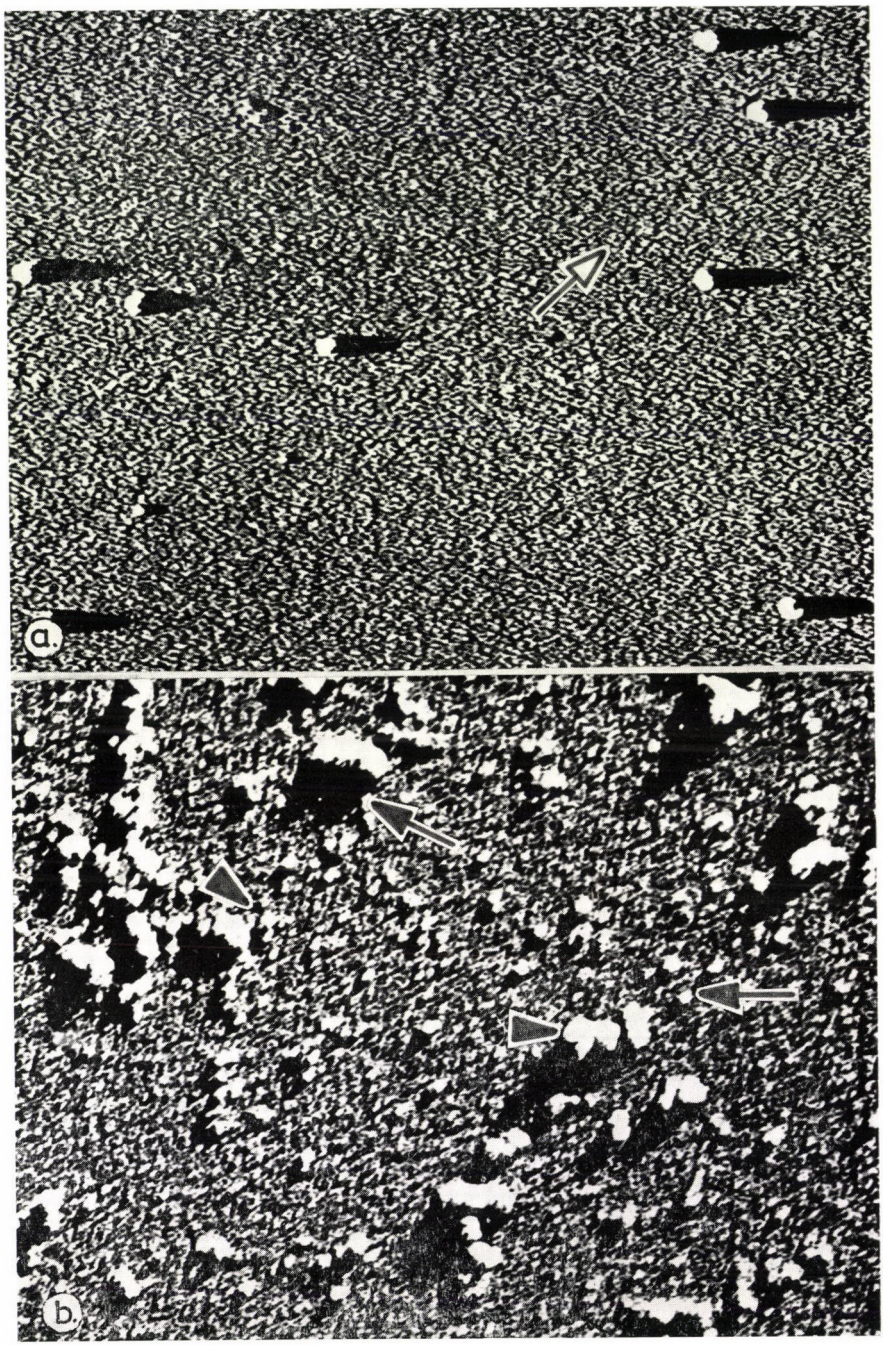
a.
b.

found forms resembling the above mentioned polysome-like complexes that could be extracted in the presence of RNase inhibitor (Fig. 4c).

In the experiments described so far always the nuclear extract was treated with RNase, which contains not only 30 *S* ribonucleoprotein particles, but also proteins and other ribonucleoproteins in large amount. Therefore we repeated the experiments with 30 *S* particles previously purified by sucrose density gradient ultracentrifugation. In this case the "0.3 M 30 *S* particles" contained radioactivity incorporated from ^{32}P. In this pure preparation of particles already 0.05 μg/ml RNase reduced the radioactive RNA content of particles to about 25% (Fig. 5b), during the time period and at the temperature used in the previous experiment, and a fourfold increase in the amount of RNase (i.e. 0.2 μg/ml) did not cause any further appreciable decrease (Fig. 5c).

The buoyant density of 30 *S* particles purified by repeated centrifugation was somewhat lower than the value obtained in the previous experiment, but the "0.1 M" and "0.3 M 30 *S* particles" could even now be readily distinguished (Fig. 6a). After treatment with RNase this difference between the two particle types was no longer detectable (Fig. 6b), but the decrease in density was again not proportional to the great loss in RNA content which would have been expected on the basis of decrease in radioactivity after RNase treatment.

The demonstrated experiments convinced us that the increased sedimentation coefficient of 30 *S* particles after treatment with RNase is due to the marked aggregation of the particles. Why the 30 *S* particles acquire this strong tendency to aggregate after RNase treatment, and what forces play a role in the process, cannot be decided from the present experiments. The answer to these questions obviously requires further investigations.

Even at low concentrations of RNase a greater proportion of the RNA content of 30 *S* particles is removed if the treatment is carried out on preparation previously purified by sucrose density gradient centrifugation. The lower sensitivity of particles in the nuclear extract is not due to the presence of RNase inhibitors, since such substances could not be detected in the nuclear extract even by very thorough analysis (Roth, Juster, 1972). A much more conceivable explanation is if we assume that part of the RNase added to the extract forms complexes with the proteins that are abundantly present in the extract, and furthermore, the protective effect of RNA content of the extract not comprised in the 30 *S* particles might also be significant.

As a result of RNase treatment the RNA in the 30 *S* particles is degraded to

Fig. 3. Electron micrographs of "0.1 M 30 *S* particles" containing nuclear dRNA in the native state and after RNase treatment. a) Micrograph of "0.1 M 30 *S* particles" isolated and prepared for electron microscopy as described in Methods. Platinum-palladium shadowing. Magnification: 65 000×. b) Micrograph of "0.1 M 30 *S* particles" isolated and treated with 1 μg/ml RNase as described in Methods. Platinum-palladium shadowing. Magnification: 50 000×. ▲ extensively aggregated particles, —▷ dimeric and trimeric particles, —▶ solitary particles

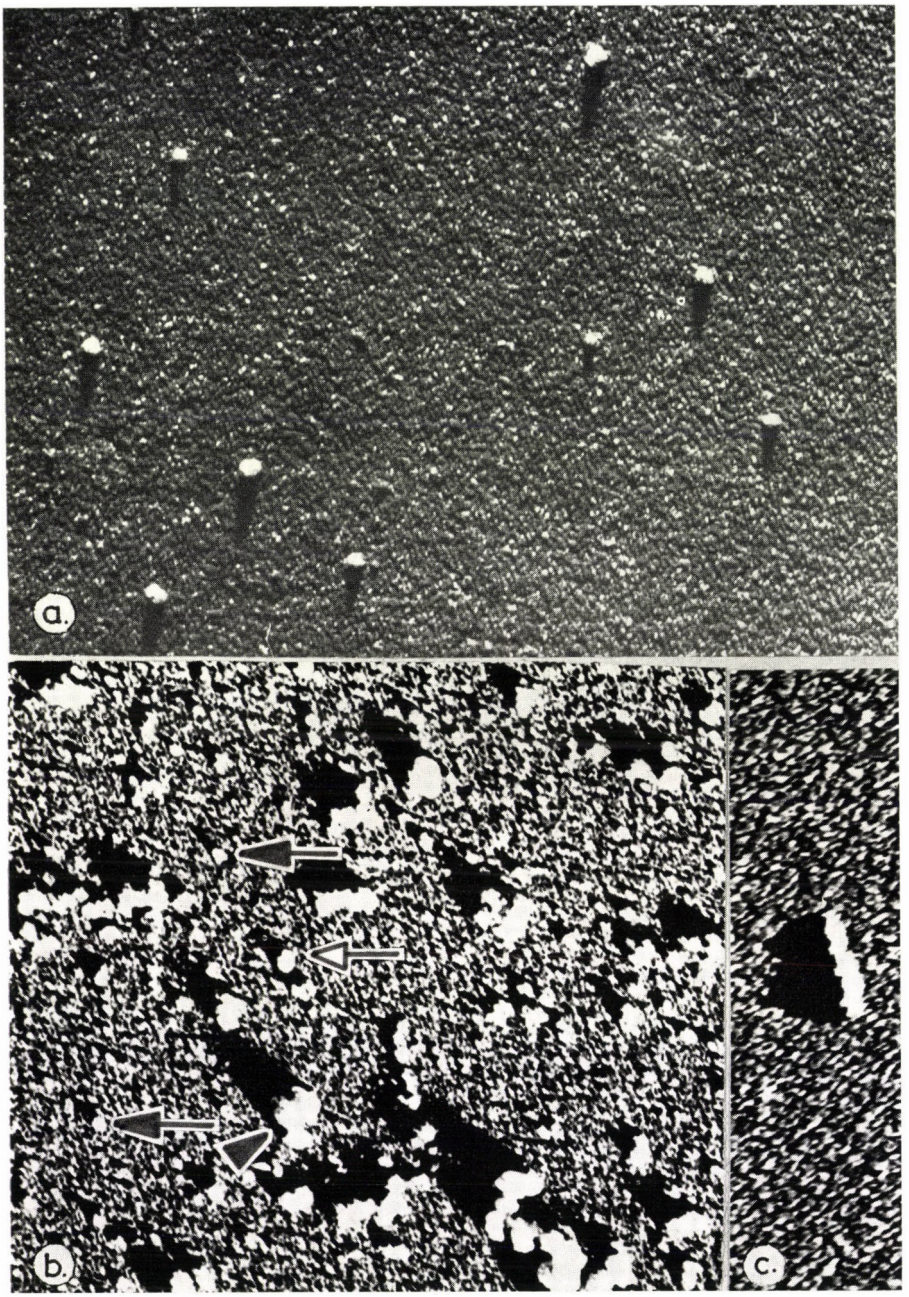
a.
b.
c.

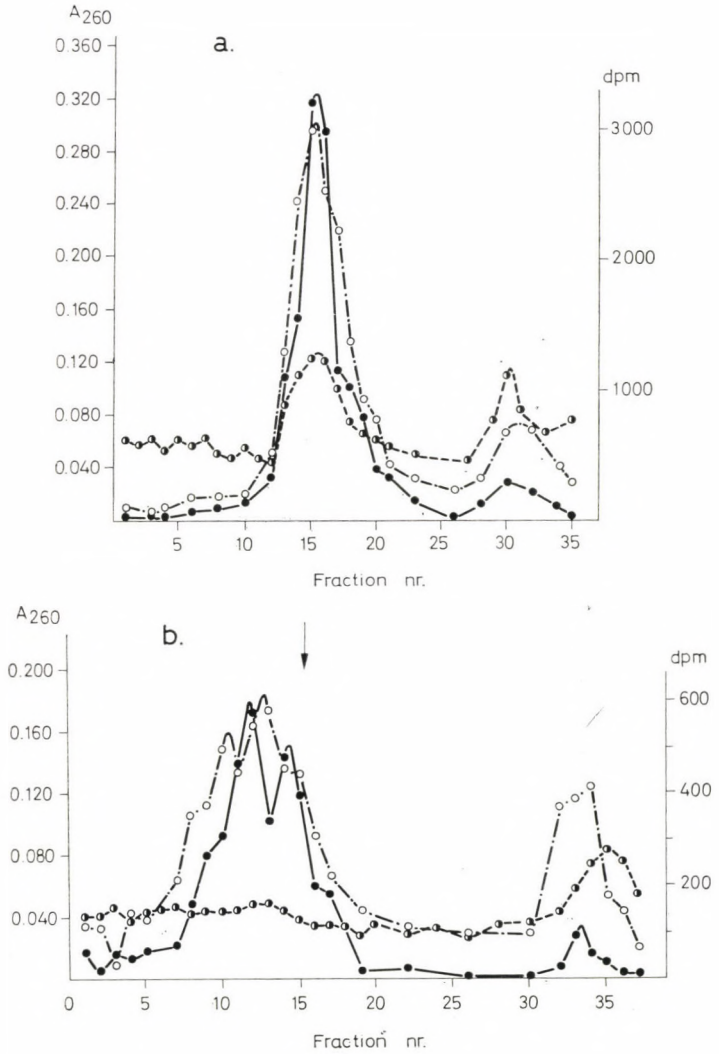

Fig. 5.

Fig. 4. Electron micrographs of "0.3 M 30 *S* particles" containing nuclear dRNA, in the native state and after RNase treatment. a) Micrograph of "0.3 M 30 *S* particles" isolated and prepared for electron microscopy as described in Methods. Platinum-palladium shadowing. Magnification 65 000×. b) Micrograph of "0.3 M 30 *S* particles" isolated and treated with 1 μg/ml RNase as described in Methods. Platinum-palladium shadowing. Magnification: 50 000×. ▲ extensively aggregated particles, —▷ dimeric and trimeric particles, —▶ solitary particles. c) Micrograph of 50 to 60 *S* material from sucrose gradient centrifugation of "0.3 M *S* particles" treated with 1 μg/ml RNase as described in Methods. Polysome-like particle associations. Magnification: 50 000×

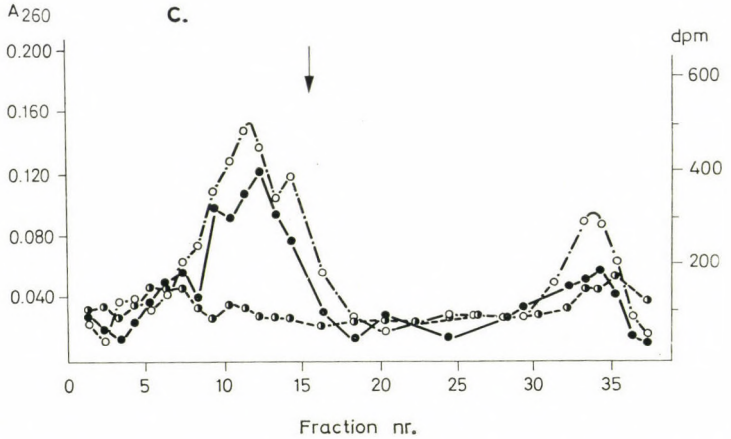

Fig. 5. Effect of ribonuclease treatment on nuclear 30 *S* particles purified by sucrose gradient centrifugation. The fractions of the sucrose gradient containing "0.1 M" and "0.3 M 30 *S* particles" were collected and mixed in a proportion that the levels of ^{14}C- and ^{32}P-radioactivities be the same. ^{14}C-radioactivity was used for the labelling of "0.1 M particles", whereas ^{32}P-radioactivity labelled the "0.3 M particles". The mixture thus obtained was dialyzed against STM II buffer (pH 7.5) for 4 hours at 3°C, and the dialyzate was divided into three equal portions. The first aliquot was kept in ice-water (a), whereas to the second (b) and third (c) 0.05 and 0.2 μg/ml pancreatic RNase was added, respectively, and incubated at 25°C for 20 min. After cooling the preparations were layered over sucrose gradients (cf. Methods) and were centrifuged in the SW 27 rotor of a Beckman Model L2-65B ultracentrifuge at 26 000 r.p.m. and 3°C for 13.5 hours. Fractions of 15 drops were collected. Sedimentation from right to left. The arrow indicates the position of 30 *S* zone. -◑--◑-: A_{260}; -●--◑- : ^{14}C-radioactivity ("0.1 M particles"), dpm; -○---○- : ^{32}P-radioactivity ("0.3 M particles"), dpm

a considerable extent and part of it also leaves the particles. There is no direct relationship between RNase concentration and the loss of radioactivity from the particles, and both the decrease in radioactivity and the decrease in the buoyant density of particles tend towards a limit. If RNA is located on the surface of 30 *S* particles (Samarina et al., 1968; Lukanidin et al., 1972) then small RNase concentrations may also effect considerable degradation, but the majority of fragments presumably remain bound to the surface of the informofer. The structure of the informofer is not influenced by the degradation and partial removal of RNA, but its tendency to aggregate is increased. This is not surprising, since the integrity of informofer is preserved even after the complete removal of RNA (Lukanidin et al., 1972).

If the nuclear 30 *S* particles are extracted in the absence of RNase inhibitor, the buoyant density of "0.1 M particles" is always greater than that of "0.3 M particles". This difference disappears already if the "0.1 M particles" are incubated at room temperature, but the same result is achieved if RNase treatment is applied. This phenomenon provides further support to our earlier assumption (Molnár,

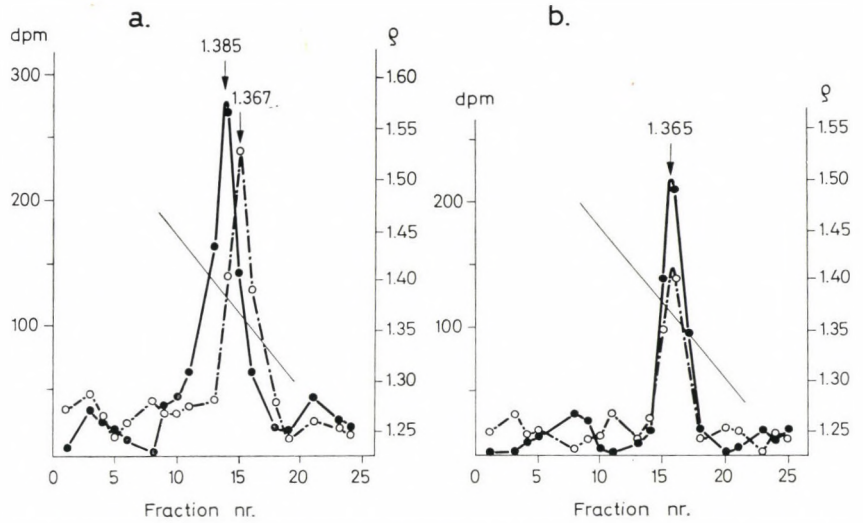

Fig. 6. Effect of ribonuclease treatment on the buoyant density of nuclear 30 *S* particles. Fractions 13 to 18 of the gradient shown in Fig. 5a (a), and fractions 11 to 15 of gradient in Fig. 5b (b) were collected, and a performed CsCl gradient was prepared ($\varrho = 1.25$ to 1.55), as described in Fig. 2. The conditions of centrifugation and the symbols are the same as above. Four-drop fractions were collected

Juhász, 1972) that the dRNA of "0.3 M particles" is more sensitive to RNase attack than that of "0.1 M particles".

As we presented earlier, the biochemical heterogeneity of "0.1 M" and "0.3 M 30 *S* particles" is accompanied by considerable ultrastructural heterogeneity (Komáromy et al., 1973). This heterogeneity is markedly diminished by treatment with RNase and the electron microscopic appearance of the two types of particles will be the same.

The authors express their thanks to Professor A. Tigyi for his continuous support and helpful criticism, and to Mrs Mária Báldy and Mrs Erzsébet Studinger for their devoted technical assistance. For the financial support of the experimental work we are indebted to the Scientific Council of Health.

References

Juhász, P. P., Molnár, J. (1973) Acta Biochim. Biophys. Acad. Sci. Hung. *8* 231

Komáromy, L., Molnár, J., Tigyi, A. (1973) Acta Biochim. Biophys. Acad. Sci. Hung. *8* 135

Lang. D., Mitani, M. (1970) Biopolymers *9* 373

Lukanidin, E. M., Zalmanzon, E. S., Komáromy, L., Samarina, O. P., Georgiev, G. P. (1972) Nature New Biology *238* 193

Molnár, J. (1973) Acta Biochim. Biophys. Acad. Sci. Hung. *8* 237
Molnár, J., Juhász, P. P. (1972) Acta Biochim. Biophys. Acad. Sci. Hung. *7* 195
Molnár, J., Komáromy, L., Tigyi, A. (1972) Acta Biochim. Biophys. Acad. Sci. Hung. *7* 299
Roth, J. S., Juster, H. (1972) Biochim. Biophys. Acta *287* 474
Samarina, O. P., Krichevskaya, A. A., Molnár, J., Bruskov, V. I., Georgiev, G. P. (1967) Mol. Biol. USSR *1* 129
Samarina, O. P., Lukanidin, E. M., Molnár, J., Georgiev, G. P. (1968) J. Mol. Biol. *33* 251

Acta Biochim. et Biophys. Acad. Sci. Hung. Vol. 9 (1–2), pp. 87–88 (1974)

Application of Dowex 50-type Resin-Coated Chromatoplates for the Base Analysis of Ribo-Oligonucleotides and RNA

(Short Communication)

J. TOMASZ

Institute of Biochemistry, Biological Research Center,
Hungarian Academy of Sciences, Szeged, Hungary

(Received Septemper 10, 1973)

One of the usual methods of base analysis of RNA is based upon acid hydrolysis (1 N HCl, 100°C, 1 hour) (Markham, Smith, 1950; Smith, Markham, 1950). This procedure converts RNA into a mixture of purine bases and pyrimidine nucleoside 2'(3')-monophosphates. Small amounts of pyrimidine nucleosides can also be found in the hydrolysate, which originate either from the 3'-termini or from a slight dephosphorylation. The base ratios are determined spectrophotometrically after partition paper chromatography and elution (0.1 N HCl).

Earlier we described the application of the commercially available Dowex 50-type resin-coated chromatoplates (Fixion* 50×8 (H^+), Chinoin, Nagytétény, Hungary) in the base analysis of DNA's from different sources with 1.0 N HCl as developing solvent (Tomasz, 1973). We found that the same thin-layer chromatographic system was equally suitable for the determination of base composition of ribo-oligonucleotides and of RNA, since it was capable of separating the six compounds in question (Fig. 1). Practically complete recoveries (94.5–102.5%) were achieved in the case of nucleosides and nucleotides, by exactly the same elution technique as described for bases (0.1 N HCl + 10% NaCl, 85°C, 15 min).

The base composition of some commercial dinucleoside monophosphates and that of *E. coli* rRNA** was determined by the method outlined. The relative proportion of acid breakdown products of dinucleoside monophosphates was as follows: UpA, adenine: 2'(3') UMP = 1.00 : 1.06; CpG, guanine: 2'(3') CMP = = 1.00 : 0.97; UpU, uridine : 2'(3') UMP = 1.00 : 0.94; CpC, cytidine : 2'(3') CMP = 1.00 : 0.98. The base composition of *E. coli* rRNA was the following: adenine 24.5% (25.1%),*** cytosine 22.1% (21.4%), guanine 31.6% (32.4%) and uracil 21.8% (21.1%). Each figure is the average of three determinations. Deviations between parallels were within 4%.

Abbreviations: 2'(3') CMP, cytidine 2'(3')-monophosphate; 2'(3') UMP, uridine 2'(3')-monophosphate; UpA = uridylyl-(3' → 5')-adenosine, etc.

* Produced under the name Ionex 25 SA, by Macherey et Nagel, Düren, W. Germany.

** This was generously supplied by Dr F. Solymosy (Institute of Plant Physiology, Biological Research Center, Hungarian Academy of Sciences, Szeged).

*** The values in parentheses are those of Stanley and Bock (1965).

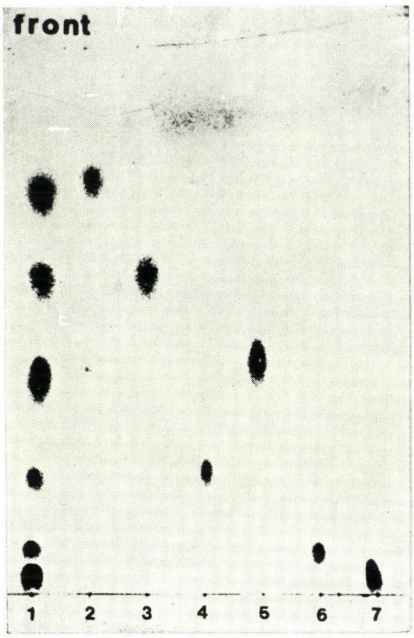

Fig. 1. Separation of an artificial mixture corresponding to the acid breakdown products of RNA on Fixion 50×8 (H^+) chromatoplates after two developments in 1.0 N HCl. First run: 90 min, 15 cm; second run: 90 min, 16 cm. Points shown the location of samples (10 μg/spot). 1 = 2 + 3 + 4 + 5 + 6 + 7; 2 = 2'(3') UMP; 3 = Uridine; 4 = Cytidine; 5 = 2'(3') CMP; 6 = Guanine; 7 = Adenine

The present method employing ion-exchange thin-layer chromatography instead of paper chromatography has the advantages of improved separation and shorter developing time compared to the original procedure (Markham, Smith, 1950; Smith, Markham, 1950).

The valuable technical assistence of Miss E. Rádi is gratefully acknowledged.

References

Markham, R., Smith, J. D. (1950) Biochem. J. *46* 513—516
Smith, J. D., Markham, R. (1950) Biochem. J. *46* 509—512
Stanley, V. M., Bock, R. M. (1965) Biochemistry *4* 1302—1308
Tomasz, J. (1973) J. Chromatogr. *84* 208—213

Acta Biochim. et Biophys. Acad. Sci. Hung. Vol. 9 (1–2), pp. 89–91 (1974)

The Effect of Ro 20-1724 upon Induced β-Galactosidase Synthesis in *Escherichia coli*

(Short Communication)

J. SCHLAMMADINGER, G. SZABÓ

Institute of Biology, University School of Medicine, Debrecen, Hungary

(Received August 2, 1973)

Ro 20-1724 (Hoffmann–La Roche), 4-(3-butoxy-4-methoxybenzyl-)2 imidazolidinon exerts a considerable inhibitory effect upon cyclic adenosine-3',5'-monophosphate (cAMP) phosphodiesterase activity in eukaryotic organisms (Sheppard et al., 1972). In mouse neuroblastoma cell culture it stimulates axon formation just as cAMP itself does (Sheppard, Prasad, 1973). Another well-known cAMP phosphodiesterase inhibitor, theophylline, has been found to affect induced β-galactosidase synthesis in *Escherichia coli* cells (Schlammadinger, Szabó, 1971; Aboud, Burger, 1971; Schlammadinger et al., 1972). Here we wish to report our first findings with Ro 20-1724 in *E. coli* K 12.

E. coli K 12 wild type cells were used. All the methods and procedures applied have earlier been described (Schlammadinger, Szabó, 1971, 1973). Log phase cells were induced with 5×10^{-4} M TMG (methyl-β-D-thiogalactoside, SIGMA) at 0 minute. All the substances tested were added after 20 minutes at a concentration of 10^{-3} M (Fig. 1).

Glucose evoked the typical picture of transient and catabolite repression. When added together with cAMP, the transient repression almost completely disappeared and the extent of permanent repression was considerably diminished.

If glucose and Ro 20-1724 were added together, this latter compound did not decrease, whereas later (after about 40 minutes) somewhat enhanced, the extent of repression caused by glucose.

When glucose, cAMP and Ro 20-1724 were added at the same time, the transient repression practically completely disappeared and after a short period of a rather slight catabolite repression the synthesis of β-galactosidase reached the same rate as that of the control. In spite of this, if we added Ro 20-1724 alone, it decreased the rate of induced β-galactosidase synthesis. The cells escaped from this permanent-type repression about 60 minutes after the addition of the compound and the rate of the enzyme synthesis became the same as in the control. (This latter part of the curve is not shown in the figure.)

cAMP alone also decreased β-galactosidase production for a while, but this repression was shorter and it was followed by a higher rate of enzyme synthesis than that of the control (not shown in the figure). To explain our findings we

suppose that Ro 20-1724 being a cAMP phosphodiesterase inhibitor, is able to prevent the degradation of added cAMP, similar to the mode of action of theophylline, as suggested by Aboud and Burger (1971), but it cannot maintain the physiological cAMP level in the *E. coli* cells alone, if added together with glucose. (This may also mean that glucose does not act through increasing phosphodiesterase activity.)

cAMP alone decreased β-galactosidase synthesis under our circumstances. This was accompanied by the diminution of growth rate as measured by following the optical density of the cultures at 570 nm. This phenomenon, therefore, is not transient repression. Our finding is in good agreement with that of Judewicz et al.

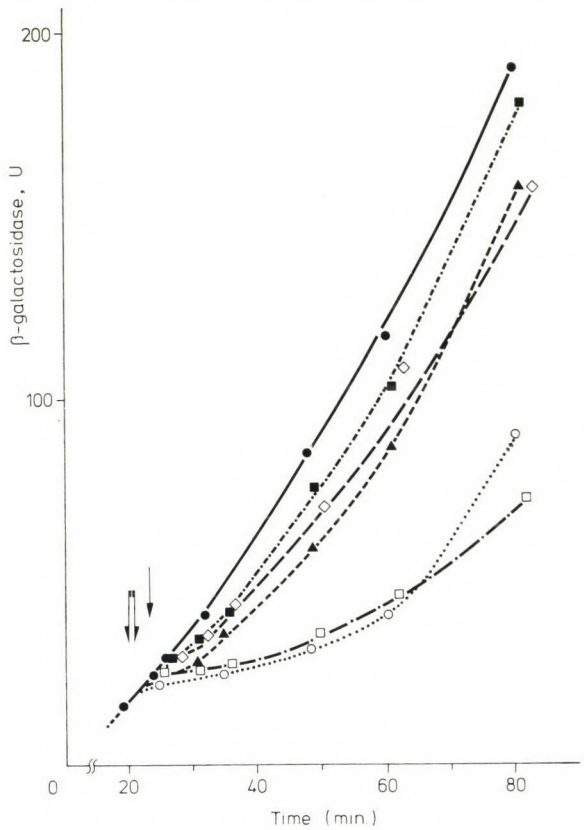

Fig. 1. Effect of glucose, cAMP and Ro 20-1724 on β-galactosidase synthesis. Induction at 0 minute. Addition of 10^{-3} M glucose (○· · · ·○), 10^{-3} M glucose + 10^{-3} M cAMP (▲ - - ▲), 10^{-3} M glucose + 10^{-3} M cAMP + 10^{-3} M Ro 20-1724 (■ ·–·–· ■), 10^{-3} M glucose + 10^{-3} M Ro 20-1724 (□ — · — □) between the 20th and 21st minutes (double arrow) and 10^{-3} M Ro 20-1724 (◇ — — — ◇) at 23.5th minute (single arrow). Control: ●– – – –●. 0.2 ml samples. 1 β-galactosidase unit = 1 μmole of o-nitrophenyl-β-D-galactopyranoside hydrolyzed in 10 minutes at 37°C

(1973), who have shown that cAMP decreases the growth rate of *E. coli* Hfr 3000 and other strains.

In contrast to this we could not observe any reduction of growth rate after adding Ro 20-1724 to our K 12 strain. Therefore we raise the hypothesis that the repression of induced β-galactosidase synthesis by this compound may be a specific effect. Similarly to the interpretation of our previous results with theophylline (Schlammadinger et al., 1972), we suppose that this molecule too, is able to compete with cAMP in the system in which this cyclic nucleotide promotes the transcription of the *lac* operon.

The authors are indebted to the F. Hoffmann-La Roche and Co., Ltd. (Basle, Switzerland) for a gift of 100 mg of Ro 20-1724 and to Mrs Ibolya Szekeres for the skilled technical assistance.

References

Aboud, M., Burger, M. (1971) Biochem. Biophys. Res. Commun. *43* 174
Judewicz, N. D., De Robertis, E. M., Jr., Torres, H. N. (1973) Biochem. Biophys. Res. Commun. *52* 1257
Schlammadinger, J., Szabó, G. (1971) Acta Microbiol. Acad. Sci. Hung. *18* 55
Schlammadinger, J., Szabó, G., Pólya, L. (1972) Acta Microbiol. Acad. Sci. Hung. *19* 43
Schlammadinger, J., Szabó, G. (1973) Acta Biochim. Biophys. Acad. Sci. Hung. *8* 257
Sheppard, H., Wiggan, G., Tsien, W. H. (1972) in Advances in Cyclic Nucleotide Research (ed. by P. Greengard and G. A. Robinson), Raven Press, New York. Vol. I, p. 103
Sheppard, J. R., Prasad, K. N. (1973) Life Sci. Part II *12* 431

Acta Biochim. et Biophys. Acad. Sci. Hung. Vol. 9 (1–2), pp. 93–96 (1974)

Electron Microscopic Study of the Nuclear Ribonucleoprotein Components Containing dRNA

(Preliminary Communication)

L. KOMÁROMY, A. TIGYI, J. MOLNÁR

Institute of Biology, University Medical School of Pécs, Pécs, Hungary

(Received August 13, 1973)

Georgiev, Samarina and their co-workers have shown that in eukaryotes the dRNA synthesized on the chromatin forms globular complexes with a specific protein, the informofer (Georgiev et al., 1972; Samarina et al., 1967, 1968). Under physiological conditions the complexes appear polysome-like, whereas if isolated in the absence of RNase inhibitor they fall apart to give 30 *S* monomers ("30 *S* nuclear particles"). The complex structures are formed by the dRNA filament, which link several 30 *S* particles. On the effect of treatment with ribonuclease the polyparticles give rise to 30 *S* components in vitro. As revealed by electron microscopy the isolated 30 *S* particles are discoidal in shape with a diameter of 180–200 Å.

The question arises wether the 30 *S* particles or the polyparticles obtained by extraction could be identified inside the cell nucleus by the aid of the electron microscope. One should consider first two, morphologically well-known but functionally entirely ill-characterized, ribonucleoprotein-containing components: the interchromatic and perichromatic granules (Monneron, Bernhard, 1969). The interchromatic granules are formations 200–250 Å in diameter, which are either located solitarily in the nucleoplasm or are arranged in small clusters or bunches. The perichromatic granules are spherical formations 400–450 Å in diameter, located on the peripheral parts of chromatin or in the interchromatic areas, mostly solitarily. They are much less in number than are interchromatic granules (Swift, 1963).

In our experiments we used CFY rats of both sexes weighing 150–180 g. After the administration of actinomycin-D intraperitoneally, we examined the electron microscopic structure of the nucleus of liver cells, focusing on the quantitative changes of the two types of granules, and further, we studied the synthesis of 30 *S* particles that can be extracted from the nucleus, by means of labelling with (^{14}C)-orotate.

In the electron microscopic experiments prefixation was made with 2.5% glutaraldehyde (for 2.5 hours), whereas fixation was accomplished with 2% osmium tetroxide, pH 7.4 (for 1 hour). Contrasting was performed with uranyl acetate and lead nitrate (Reynolds, 1963). Electron micrographs were taken with

a TESLA BS 513 A type electron microscope. The 30 *S* particles were extracted by the method of Samarina et al. (1967).

Actinomycin-D was applied in a large dose (2 μg per g body weight), to arrest the synthesis of dRNA. It the 14th hour after the treatment the amount of interchromatic granules markedly decreased, whereas the perichromatic granules were present in a large number relative to the control (Tigyi et al., 1970).

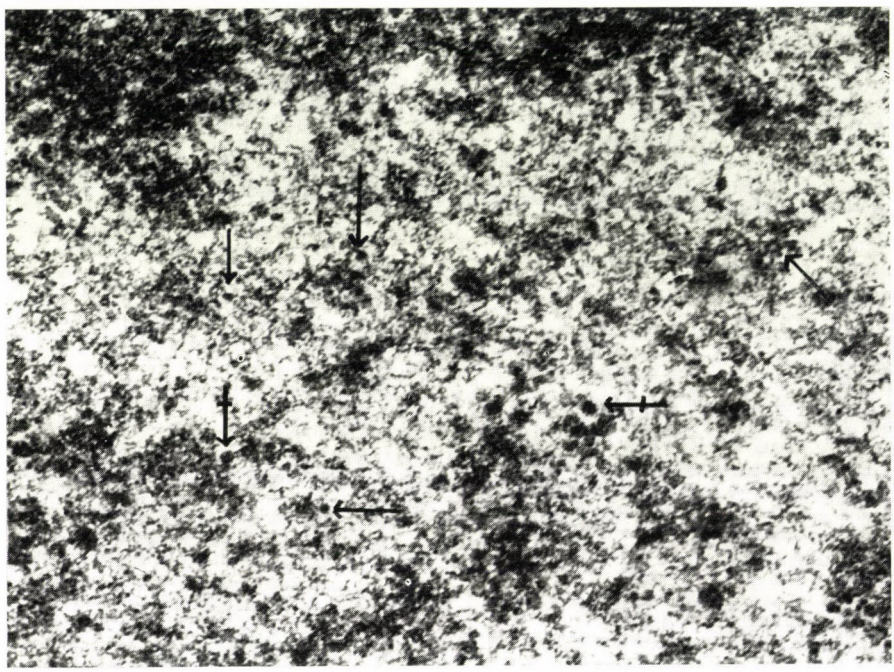

Fig. 1. Electron micrograph of part of a liver cell nucleus from a rats treated with actinomycin-D (2 μg per g body weight). In the nucleoplasm the clustered and individual interchromatic granules (→), as well as perichromatic granules (↔), can be seen. Magnification: 87 000×

The determination of the number of interchromatic and perichromatic granules was carried out on electron micrographs on which the cross-section of cell nuclei corresponded to an area of $24 \pm 0.5\ \mu^2$. In this way we wanted to eliminate the differences between the different planes of section. The determination of surface area of nuclear section was performed on electron micrographs of 100 000-fold magnification (the exact electron-optical magnification was known). Calculations were based on 50 micrographs each for the treated and control series.

In the control nuclei the number of interchromatic granules was 123 ± 14,* that of perichromatic granules 24 ± 4. After actinomycin administration (2 μg

* Standard deviation.

per g body weight) the following changes were observed: the number of interchromatic granules decreased to 81 ± 8, that of perichromatic granules increased to 31 ± 3. That is, the amount of interchromatic granules decreased by 34.1%, whereas that of perichromatic granules increased by 29% (Fig. 1).

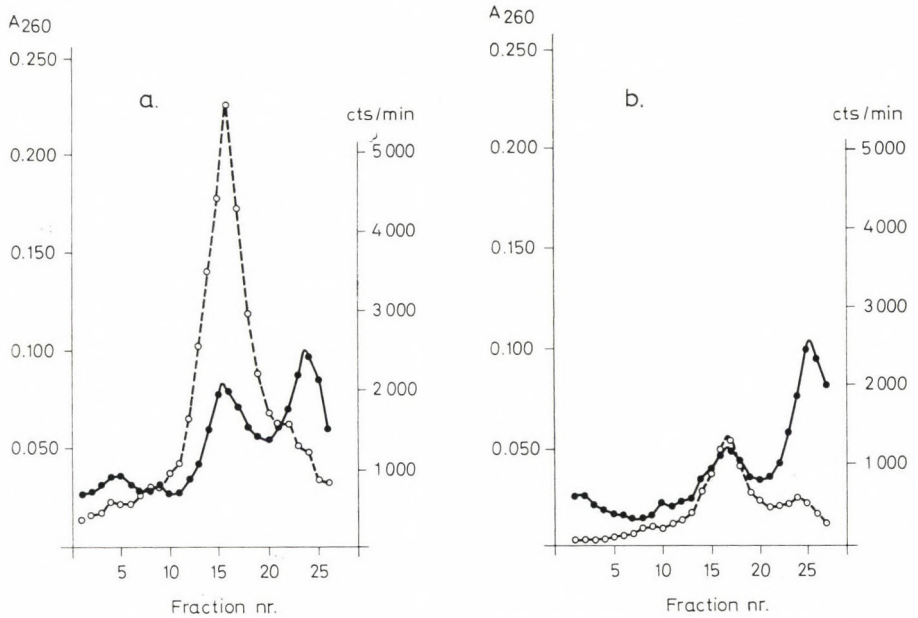

Fig. 2. Effect of actinomycin-D on the amount of dRNA-containing informofers extracted from rat liver cell nucleus. (a) (^{14}C)-orotate was administered intraperitoneally (15 μCi per 100 g) to animals, fasted for 24 hours, 35 minutes before killing. For each experiment two animals were used. 16% of the nuclear extract was layered over a 4.8 ml 15—30% (w/v) sucrose gradient and was centrifuged in the 3×5 ml rotor of a Janetzki VAC 60 ultracentrifuge for 4 hours at 3°C. Fractions of 3 drops were collected. Further details of the centrifugation were the same as described previously (Molnár et al., 1972). (b) In each experiment two starved animals were given 2 μg/g body weight actinomycin-D 14 hours before and 15 μCi/100 g (^{14}C)-orotate 35 minutes before, killing. Of the nuclear extract 14% was layered over the gradient and centrifuged as described under (a)–●–●–●–: A_{260}; ---○---○---: ^{14}C radioactivity, c.p.m. Sedimentation: from right to left

Parallel with the morphological analysis we examined the effect of actinomycin-D on the 30 *S* particles obtained from the cell nuclei. Actinomycin-D was administered intraperitoneally (2 μg per g body weight) and 14 hours later the 30 *S* particles were extracted by the method of Samarina et al. (1967) from animals which were given (^{14}C)-orotate for the labelling of dRNA 35 minutes before killing. As demonstrated in Fig. 2, actinomycin-D decreased the amount of 30 *S* particles extractable from the nucleus by 30%, and decreased the incorporation of (^{14}C)-orotate by 80% relative to the normal values.

Our results indicate that after the inhibition of dRNA synthesis by actinomycin-D, the amount of interchromatic granules of the nucleoplasm and the amount of 30 *S* particles extracted from the nucleus diminish to about the same extent. This finding, along with the morphological similarity of the two structures, allows one to assume that the interchromatic granules and the dRNA-containing ribonucleoproteins (30 *S* particles), characterized by biochemical and morphological methods in the nuclear extract, are identical. A similar suggestion has already been made by Monneron and Bernhard (1969) and by Smetana et al. (1971). Some data seem to indicate (Clever, 1963; Beermann, 1966; Stevens, Swift, 1966) that the perichromatic granules play a role in the nucleocytoplasmatic transport processes, probably in the transport of mRNA. Since in our present experiments the amount of these increased on the effect of actinomycin-D, we deem their morphological or functional relationship with mRNA rather improbable.

References

Beermann, W. (1966) Jahrbuch Max Planck Ges. p. 69
Bernhard, W. (1969) J. Ultrastr. Res. *27* 250
Clever, U. (1963) Develop. Biol. *6* 73
Georgiev, G. P., Ryskov, A. P., Coutelle, C., Mantieva, V. L., Avakyan, E. R. (1972) Biochim. Biophys. Acta *259* 259
Molnár, J., Komáromy, L., Tigyi, A. (1972) Acta Biochim. Biophys. Acad. Sci. Hung. *7* 299
Monneron, A., Bernhard, W. (1969) J. Ultrastr. Res. *27* 266
Reynolds, E. S. (1963) J. Cell. Biol. *17* 208
Samarina, O. P., Kritshevskaya, A. A., Molnár, J., Brusoszkov, V. I., Georgiev, G. P. (1967) Mol. Biol. S.S.S.R. *1* 129
Samarina, O. P., Lukanidin, E. M., Molnár, J., Georgiev, G. P. (1969) J. Mol. Biol. *33* 251
Smetana, K., Lejnar, J., Vlastivoroba, A., Busch, H. (1971) Exptl. Cell. Res. *64* 105
Stevens, B. J., Swift, H. (1966) J. Cell. Biol. *31* 55
Swift, H. (1963) Exptl. Cell. Res., Suppl. *9* 54
Tigyi, A., Komáromy, L., Molnár, J. (1970) Publications of the Demographic Research Institute of the Hungarian Academy of Sciences *32* 70

Acta Biochim. et Biophys. Acad. Sci. Hung. Vol. 9 (1—2), pp. 97—105 (1974)

Examination of the Competitive Effect of Alkali Ions in the K^+, Rb^+ and Cs^+ Transport of Rat Erythrocytes

S. GYÖRGYI, K. BLASKÓ

Biophysical Institute, Semmelweis Medical University, Budapest

(Received April 16, 1973)

The competitive effect of alkali ions was examined in the K^+, Rb^+ and Cs^+ transport of rat erythrocytes by applying ^{42}K, ^{86}Rb and ^{137}Cs isotopes. The rate of influx was characterized with the aid of the amount of ions taken up by the erythrocytes during an incubation for 15 minutes. For the quantification of the degree of competition the method of reaction kinetics used for processes of similar type was applied. On the basis of the data obtained the affinity of ions to the binding sites of the membrane decreases as follows: $Rb^+ > K^+ > Cs^+$. A similar order was obtained for the inhibitory effect of the ions as well as for the inhibitability of their transport. The strongest inhibitory effect is exerted by Rb^+, and it is the transport of this ion, which can be inhibited at the least. The inhibitory effect of Cs^+ ion is slight, and, at the same time due to its low transport rate, it is far from saturation in the concentration ranges examined. Therefore it seems to be inhibited only slightly because many free transfer sites are available for the inhibitory ions. This fact was taken into account in the quantitative characterization of the inhibitability.

Introduction

The comparison of the characteristic transport parameters of K^+, Rb^+ and Cs^+ ions having similar physical characteristics offers a good opportunity to study the mechanism of ion transport in biological membranes (Maizels, 1960; Györgyi, 1972; Györgyi, Kanyár, 1972a; 1972b). In the present investigation the competitive effect of K^+, Rb^+, Cs^+ as well as Na^+ ions was examined on each other's transport in rat erythrocytes by the application of ^{42}K, ^{86}Rb, ^{137}Cs isotopes.

The systems transporting by chemical interaction are usually able to transport several kinds of molecules or ions, and these substances of similar structure and function hinder the transport of each other. This statement is also valid for the K^+, Rb^+ and Cs^+ transport of the erythrocytes (Sachs, 1967; Sachs, Welt, 1967; Bernstein, Israel, 1970).

The reaction kinetic description applied in processes of similar type was used for the quantitative characterization of the degree of competition. It is known that in every case when the transport process is bound to a specific chemical process, the flux is a non-linear (usually hyperbolic) function of the concentration

of the transported substance. (Snell et al., 1965; Stein, 1967; Varga, 1968). In the transport processes investigated by us the chemical interaction is a specific reaction of the ion and the place of translocation. The process is demonstrated by the following scheme.

$$\begin{array}{cc|c|c} & 1. & & 2. \\ A + & X \rightleftharpoons AX \rightleftharpoons XA \rightleftharpoons X & & + A, \\ & \longleftarrow \text{membrane} \longrightarrow & & \end{array}$$

where A means the transported substance (ion), X – the "transfer site" of the membrane, and AX – some complex of the ion formed with the membrane binding site. The constants of dissociation on both sides of the membrane are:

$$K_1 = \frac{[A]_1 \cdot [X]_1}{[AX]_1} \qquad K_2 = \frac{[A]_2 \cdot [X]_2}{[AX]_2} .$$

The transport of A ion is only possible through the AX intermediate state. We do not know any detail about X, but this is not important for the formal treatment. The unidirectional flow from side 1 to side 2 is caused by the fact that the equilibrium constant is remarkably smaller on side 1. ($K_1 \ll K_2$), and it is different for the three ions within the one and the same side.

The flux of AX in the membrane is:

$$I_{AX} = p_{AX} ([AX]_1 - [AX]_2),$$

where p_{AX} is a permeability constant depending on the mobility of AX complex and on the thickness of the membrane. Using the above connection, and considering that the whole quantity of X is

$$[X_T] = [X] + [AX],$$

the equation is modified to:

$$I_{AX} = p_{AX} \left(\frac{[A]_1[X_T]_1}{[A]_1 + K_1} - \frac{[A]_2[X_T]_2}{[A]_2 + K_2} \right) .$$

In isotope experiments the activity is added to the side 1 at the beginning of the experiment and, after an incubation of 10 to 15 min, the isotope uptake of erythrocytes is measured.

In this case, considering the inequalities $A_2 \ll A_1$ and $K_2 \gg K_1$ mentioned formerly, the second part of the equation can be neglected, i.e.:

$$I_{AX} = p_{AX} \frac{[A]_1[X_T]_1}{[A]_1 + K_1} .$$

This means in other words that no radioactive ion leaks from the side 2 to 1 through our transporting system $[X]$. However, a part of the radioactive isotope which got into intracellular space gets back with a passive efflux, this fact was considered in the calculation (see later).

The above equation is a typical connection of saturation kinetics which, though contains neglections, can be well used for describing the competitive effects. With the aid of the reciprocal representation of Lineweaver-Burk the intercepts give the value of K characterizing the interaction of ion and membrane, as well as the p_{AX}. $[X_T]$ product characterizing the membrane. With the aid of the values obtained for different ions their transport can be characterized quantitatively and compared.

We should like to emphasize that the kinetic model treated here has been used for the quantitative characterization of the interaction of the membrane and ions, as well as of the effect of ions on each other's transport, without telling anything about the nature of the X "transfer site".

Experimental

Freshly drawn, heparinized (30 IU/ml) blood of albinos rato weighing about 200 g were used in the experiments. After warming up it to 37°C in a water bath the alkali ion used as substrate was added to the whole blood – taking the haematocrit value of the collected blood into consideration – in an amount increasing the ion concentration of the plasma 5 to 30 meq/l over the physiological concentration. The plasma concentration of the alkali ion acting as an inhibitor was similarly adjusted to 10 meq/l in every case. The radioactive isotope of the substrate was used as an indicator. In the calculation of the concentration of ions added to the plasma the amount of the carrier of the isotope was also taken into account. The values of the substrate concentration adjusted in this way were 30, 20, 15, 10, 5 and (depending on the carrier) 0.1 – 0.3 meq/l plasma respectively. Because of the small volume of the solution containing the substrate and the isotope (<0.01 ml/ml blood) the osmotic concentration of blood samples only changed upon the effect of the ion quantity added.

After addition of ions the blood was incubated at 37 °C for 15 min with careful stirring, and then centrifuged at room temperature. The erythrocytes were washed three times with physiological saline at 3 to 4 °C, and their activity was determined with a well-type scintillation counter. Three parallel samples were measured at each substrate concentration.

The amount of the alkali ion entered the intracellular space during the 15 minute incubation was calculated from the measured activity of the erythrocytes. Our data were corrected with the meanwhile leaked isotope quantity on the basis of the efflux values obtained in our previous measurements (Györgyi, Kanyár, 1972). The influx rate was characterized by the decrease of the plasma substrate concentration during the time of incubation.

In order to be able to compare the characteristics of K^+, Rb^+ and Cs^+ ion transport, respectively, in a direct way the K^+ flux was considered as a background value. Without this consideration, the physiological K^+ content of the plasma would have acted as an inhibitor in the case of Rb^+ and Cs^+ as substrate.

Straight lines were fitted to our experimental data with the method of least squares. The F-test was significant ($p < 0.001$) in every case (i.e. in Lineweaver-Burk's reciprocal representation a straight line could be fitted to the points), which proved that saturation kinetics could be applied to these transport processes. The straight lines obtained with and without inhibitor intersect each other in a common ordinate point within the parameter error (p_{AX} $[X_T]$), proving an identical transport mechanism of the three ions. The fitting was done with a Hewlett Packard computer, and with the aid of a suitable program the intercepts of the straight lines fitted to the points were obtained directly from the data of measurements. These values were used in the further calculations, and the straight lines of Fig. 1 to 4 were drawn with their aid.

Results and Discussion

Fig. 1 shows the rate of the transport of K^+, Rb^+, Cs^+ ions from the plasma to the erythrocytes. The reciprocals of the constants of equilibrium (K) which characterize the affinity to the binding sites of the membrane are as follows:

for K^+: 0.043 ± 0.006
for Rb^+: 0.066 ± 0.005
for Cs^+: 0.016 ± 0.002.

The order of the affinity to the binding sites of the membrane for the three ions are: $Rb^+ > K^+ > Cs^+$. If the constant of equilibrium of K^+ is taken for unit: $Rb^+ : K^+ : Cs^+ = 1.54 : 1 : 0.37$.

The inhibitory effect of an ion, as inhibitor, on the transport of another ion is well characterized by the difference in the slopes of the $1/[S] - 1/V$ straight lines obtained with or without inhibitor in the case of the ion used as a substrate (Figs 2 to 4). Table 1 shows the slopes of these curves. For the sake of a better comparison of the inhibitory effect of different ions the slope was calculated from our data even when the substrate and the inhibitor was the same ion.

For the calculation, influx values obtained in the case of 15 to 30 meq/l substrate concentrations were used, which were considered as if they had been brought about by an "inhibitor" of a concentration of 10 meq/l and substrate of 5 to 20 meq/l. Accordingly e.g. 3/5 part of the influx measured in the case of a whole concentration of 25 meq/l meant the substrate influx measured in the presence of inhibitor.

The influx of K^+ ion is inhibited by Rb^+ and Cs^+ ions as inhibitors to different degree. (Fig. 2). Rb^+, having a great affinity to the membrane, changed the

slope of the curve of K^+ influx from 9.3 to 20 (a change to a more than doubled value), while Cs^+, having extraordinarily small affinity, hardly showed any inhibitory effect (the slope changes from 9.3 to 10.8). The strength of the effect of K^+ as an inhibitor is between that of Rb^+ and Cs^+, and the slope increases to 13.3.

The influx of Rb^+ ion is less influenced by inhibitory substances (K^+, Cs^+) (Fig. 3) than that of K^+. The slope of Rb^+ uptake curve changes from a value of 6.1 to 7.7 in the case of K^+ inhibition and to 6.7 in the case of Cs^+ inhibition. The explanation of this fact is that K^+ and Cs^+ ions having smaller affinity

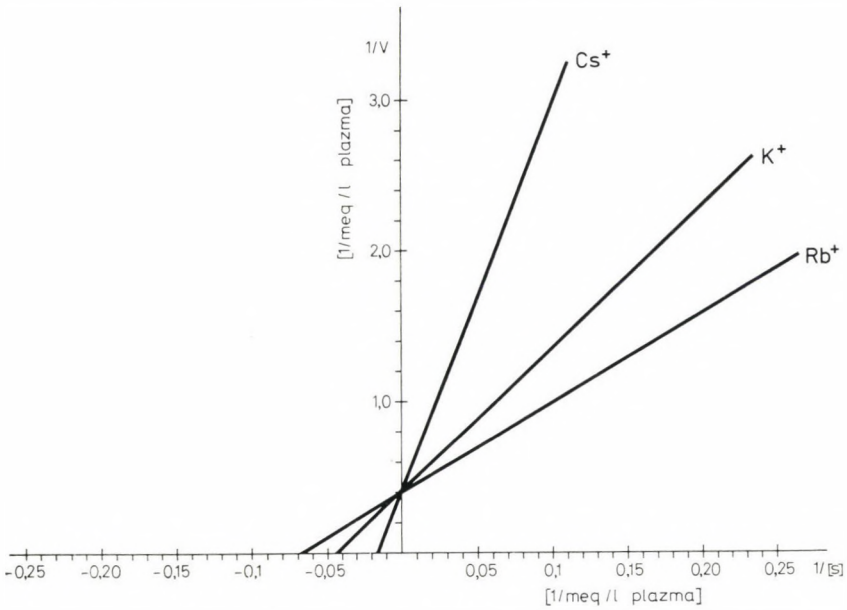

Fig. 1. Potassium- (K^+), rubidium- (Rb^+) and caesium ion (Cs^+) uptake of rat erythrocytes plotted against the ion concentration after 15-min incubation. (In Lineweaver-Burk's reciprocal representation)

Table 1

Slope values characterizing the inhibitory effect of alkali ions on each other's transport

Inhibitor / Substrate	tg α				
	without inhibitor	K^+	Rb^+	Cs^+	Na^+
K^+	9.3	13.3	20.0	10.8	5.9
Rb^+	6.1	7.7	9.5	6.7	5.3
Cs^+	25.0	33.3	36.4	30.8	22.2

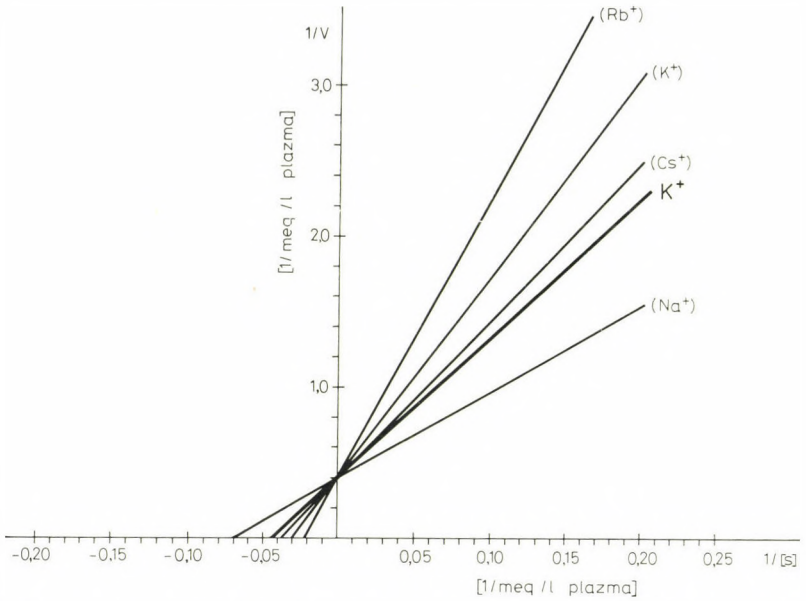

Fig. 2. Potassium ion uptake of rat erythrocytes plotted against the potassium ion concentration of the plasma without inhibitor (K^+) and in the presence of potassium [(K^+)], rubidium [(Rb^+)] caesium [(Cs^+)] as well as sodium ion [(Na^+)] as inhibitor in 10 meq/l plasma concentration

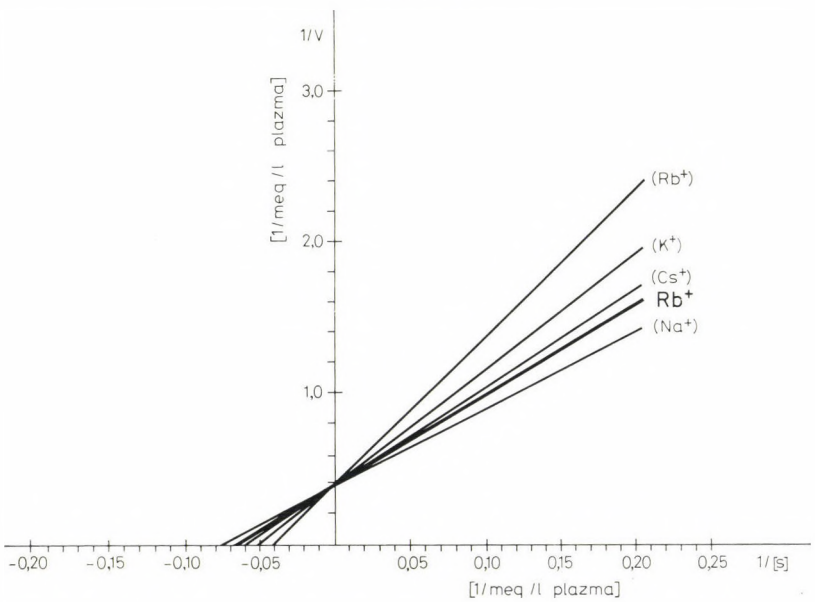

Fig. 3. Rubidium ion uptake of rat erythrocytes plotted against the rubidium ion concentration of the plasma without inhibitor (Rb^+), and in the presence of potassium [(K^+)], rubidium [(Rb^+)], caesium [(Cs^+)] and sodium ion [(Na^+)] inhibitors at a plasma concentration of 10 meq/l

can scarcely push off the Rb^+ of great affinity from the binding sites of the membrane. The intensive effect of Rb^+ ion on Rb^+ flux fits into this picture well. It can also be well seen here that the order of the strength of inhibition is $Rb^+ > K^+ > Cs^+$.

The inhibition in the case of Cs^+ ion is also of smaller degree than in the case of K^+ (Fig. 4). Cs^+ ion has a small affinity to the binding sites of the membrane (the equilibrium constant of Cs^+ is large), there are lots of free binding places on the membrane, and so the inhibitory ions need not push off Cs^+ ions from there.

As to the effect of Na^+, it was experienced for each of the three ions that the 10 meq/l Na^+ given extracellularly increased the influx of the substrate ion, which manifested itself in a decrease of the slopes (see: Table 1). In this case the higher extracellular Na^+ concentration presumably increased the passive Na^+ influx to a slight extent, this caused an increase of Na^+ on the inner surface of the membrane, which accelerated the active Na^+ efflux and, consequently, the active K^+ (Rb^+, Cs^+) influx too.

Further on we will try to compare the inhibitory effect of the three ions on each other. The slopes given in Table 1 do not unambiguously characterize the relative effect; even though they clearly show that the order of ions is the

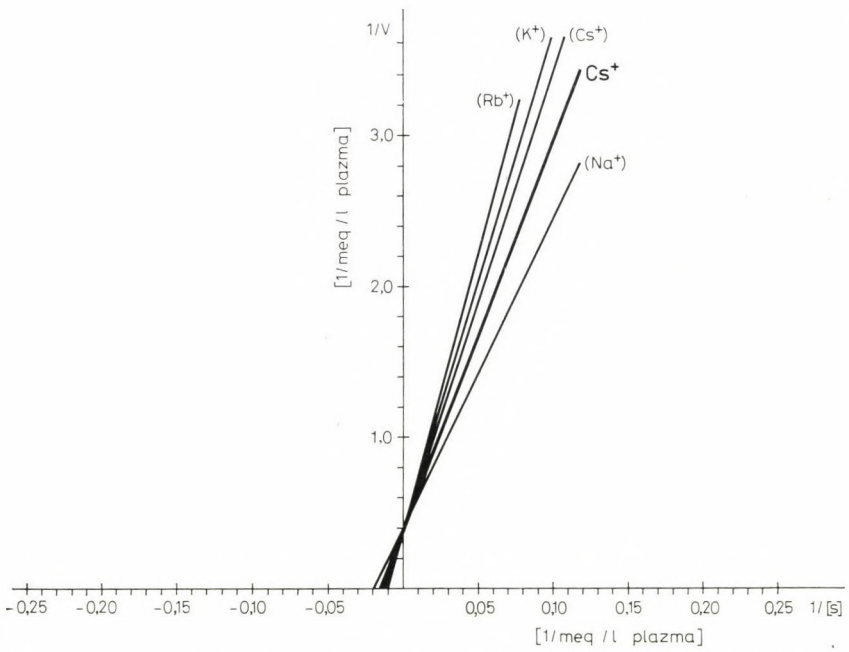

Fig. 4. Caesium ion uptake of rat erythrocytes plotted against the caesium ion concentration of the plasma without inhibitor (Cs^+) and in the presence of potassium [(K^+)], rubidium [(Rb^+)] caesium [(Cs^+)] and sodium [(Na^+)] at a plasma concentration of 10 meq/l

same in the inhibitory effect as in transport. In the case of a given ion the degree of the inhibition caused by an another ion depends on the magnitude of the ion flux examined as a substrate and on the distance from the saturation value. It is obvious that we obtained a relatively small value for the degree of the inhibition caused by K^+ and Rb^+ in the case of Cs^+ having a relatively low flux because, being far from saturation, there are relatively many free transfer places. In order to take into consideration the distance of the flux of substrate ion from the saturation value, the difference of the tangents was multiplied with the constant of equilibrium of the substrate, and the inhibitory effect was characterized with the

$$f = \frac{K_i - K_s}{V_{max}} K_s$$

value considering that $\operatorname{tg} \alpha_i = \frac{K_i}{V_{max}}$, $\operatorname{tg} \alpha_s = \frac{K_s}{V_{max}}$, where $\operatorname{tg} \alpha_s$ and K_s are the slope and the equilibrium constant, respectively, obtained without inhibitor, and $\operatorname{tg} \alpha_i$ and K_i are those obtained in the presence of an inhibitor,

$$f = (\operatorname{tg} \alpha_i - \operatorname{tg} \alpha_s) \cdot K_s = \frac{K_i - K_s}{V_{max}} K_s .$$

Table 2 shows the f value calculated in this way.

Table 2

f values characterizing the relative effect of alkali ions on each other's transport [$f = (\operatorname{tg} \alpha_i - \operatorname{tg} \alpha_s) K_s$, where $\operatorname{tg} \alpha_s$ and K_s are the slope and the constant of equilibrium obtained without inhibitor, respectively, $\operatorname{tg} \alpha_i$ is the slope obtained in the presence of an inhibitor]

Substrate \ Inhibitor	K^+	Rb^+	Cs^+	Na^+
K^+	93.2	24.9	34.8	− 79.6
Rb^+	24.6	52.4	9.2	− 18.6
Cs^+	520	713	360	−173.8

The data of the Table can be compared from two directions. The numbers under each other show the inhibitability of the three ions in the case of a given inhibitor. From the first column it can be read that with K^+ as inhibitor the inhibitability of ions is: $K^+ : Rb^+ : Cs^+ = 1 : 0.26 : 5.6$; in the case of Rb^+ as inhibitor: $K^+ : Rb^+ : Cs^+ = 4.75 : 1 : 13.6$, and in the case of Cs^+ ion: $K^+ : Rb^+ : Cs^+ = 0.1 : 0.03 : 1$. (The average inhibitability of each of the ions is: $K^+ : Rb^+ : Cs^+ = 1.95 : 0.43 : 6.7$.)

The horizontal lines give us information on the ratio of the inhibitory effect exerted on a given ion. For example in the case of K^+ transport the ratio of

inhibition is $K^+ : Rb^+ : Cs^+ = 1 : 2.7 : 0.37$, i.e. Rb^+ ion inhibits the K^+ transport 2.7 times stronger than K^+, while Cs^+ by 37 per cent only. It is also interesting to compare the average of the values obtained for the inhibitory effect of the three ions: $K^+ : Rb^+ : Cs^+ = 1 : 1.9 : 0.5$.

From the above data it can be concluded, that the order of the examined ions considering their inhibitor effect is $Rb^+ > K^+ > Cs^+$, just like in the case of the affinity to the membrane. The different behaviour of the three ions can be explained by the different ion-membrane molecular interaction. Further examinations will be done in order to clarify this question. The results obtained are also interesting from a practical point of view inasmuch as they clearly show that on the one hand, Rb^+ is not an unambiguous analogue of K^+ in isotope-label examinations (e.g. Kahn, 1962; Bakkeren, Bonting, 1968) and, on the other, the Cs^+ transport can be influenced by K^+, which also has radiation protection connection (Györgyi, Kanyár, 1972a).

References

Bakkeren, J. A. J. M., Bonting, S. L. (1968) Biochim. Biophys. Acta *150* 467
Bernstein, J. C., Israel, Y. (1970) J. Pharmacol. Exp. Ther. *174* 323
Györgyi, S. (1972) MTA Biol. Oszt. Közl. *15* 169
Györgyi, S., Kanyár, B. (1972a) Izotóptechnika (Budapest) *15* 298
Györgyi, S., Kanyár, B. (1972b) Acta Biochim. Biophys. Acad. Sci. Hung. *7* 359
Kahn, J. B. J. (1962) J. Pharm. Exp. Therap. *136* 197
Maizels, M. (1960) In: A. Kleinzeller and A. Kotyk. (Eds.) Symp. Membrane Transport and Metabolism. Academic Press, New York, p. 256
Sachs, J. R. (1967) J. Clin. Invest. *46* 1433
Sachs, J. R., Welt, L. G. (1967) J. Clin. Invest. *46* 65
Snell, F. M., Shulman, S., Spencer, R. P., Moos, C. (1965) Biophysical Principles of Structure and Function. Addison–Wesley Publ. Co. Reading, 325
Stein, W. D. (1967) The Movement of Molecules Across Cell Membranes. Acad. Press, New York, London
Varga, F. (1968) MTA Biol. Oszt. Közl. *11* 199

Acta Biochim. et Biophys. Acad. Sci. Hung. Vol. 9 (1—2), pp. 107—113 (1974)

Effect of Various Metal Ions on the Streptomycin Uptake of *E. coli* B Cells

GY. TAMÁS, M. SZŐGYI, I. TARJÁN

Biophysical Institute, Semmelweis University of Medicine, Budapest

(Received July 16, 1973)

The effect of monovalent and divalent metal ions (Li^+, Na^+, Cs^+, Mg^{++}, Zn^{++}) was examined on the binding of streptomycin molecules to the surface of *E. coli* B cells. The quantity of streptomycin taken up by the bacteria was determined when the majority of the drug was yet only on the surface of bacteria. According to our results a dynamic equilibrium is reached between the ions bound on surface of the bacterium and the ions in the medium not only concerning the streptomycin molecules but also concerning metal ions. The equilibrium states developed for streptomycin and metal ions are related to each other, since an exchange reaction takes place between the metal ions and the streptomycin molecules bound by cell receptors.

The process of binding and the equilibrium states were characterized quantitatively as well the probability of binding for the streptomycin molecules and for metal ions was determined. The monovalent ions are more weakly bound than streptomycin, the binding of Mg^{++} is about the same, that of Zn^{++} is stronger than streptomycin.

Introduction

The streptomycin uptake of the bacteria under different experimental conditions has been investigated by several authors (Engelberg, Artman, 1961; Hancock, 1962; Hurwith, Rosano, 1962; Kavanagh, 1963; Venis, 1969). It was stated that bacteriostatic effect of streptomycin remarkably decreases in the presence of inorganic ions. Other authors observed a competition between antibiotic molecules (streptomycin, neomycin, polymyxin etc.) and inorganic ions for the receptor sites on the nerve-endings (Pittinger, Adamson, 1972). Our observations obtained in previous examinations also prove that bacteria lose a great part of the streptomycin adsorbed on their surface when washed with solution containing ions.

Starting from these experiences we studied in detail the effect of mono- and divalent ions (Na^+, Cs^+, Li^+, Mg^{++}, Zn^{++}) on the binding of streptomycin molecules on the surface of *E. coli* B cells.

Methods

A streptomycin-sensitive *E. coli* B strain was used in the experiments. The exponentially growing bacteria were centrifuged and then incubated for 15 minutes in nutrient broth containing streptomycin, meat extract and nothing else. At the end of incubation the bacteria were centrifuged and then samples were taken for the determination of the viable cell count using a plate dilution method. The bacteria were washed with growth medium, then suspended in distilled water. This suspension contained 10^8 bacteria per ml on the average. The quantity of antibiotics taken up by the bacteria was determined with an agar diffusion method (Szőgyi, Tamás, 1969).

The metal ions influencing streptomycin uptake were added to the medium simultaneously with streptomycin. The appropriate ion concentration was achieved by using metal chlorides in every case. During the experiments the pH value of the solutions was 7.0 and the temperature 37°C.

We had shown previously (Szőgyi et al., 1969) that plotting the quantity of streptomycin taken up by bacteria against the time gives an initially rising curve, followed by a "plateau", indicating an equilibrium state. Later the curve is rising again. From the analysis of the curves we concluded that the antibiotic molecules were first bound on the cell surface (plateau period) and they penetrated into the interior of the bacteria only later. The first process can be described by the Langmuir's adsorption law. In the present examinations the amount of streptomycin bound by the bacteria was determined in the plateau phase in every case.

Results

Fig. 1 shows the quantity of streptomycin taken up from media containing 0.17 mM of streptomycin and various concentrations of Na^+ (0–300 mM) at 37°C. The concentration of Na^+ in mM is shown on the horizontal axis and the number of streptomycin molecules taken up by one bacterium on the vertical axis. The uptake decreases with increasing Na^+ concentration, the maximal value can be obtained in case of a salt free medium. The decrease is 50 per cent at Na^+ concentration of about 200 mM.

Fig. 2 shows the quantity of streptomycin taken up from media of various concentrations of Mg^{++} (0–10 mM) at 37°C.

The decrease of antibiotic uptake is greater in this case, the 50 per cent being reached at Mg^{++} concentration of about 6 mM.

Similar curves are obtained also in those cases when the release (desorption) of streptomycin bound on the surface of cells is examined in media of various Na^+ and Mg^{++} concentrations respectively.

The ion concentrations necessary to the 50 per cent decrease of streptomycin uptake are for Li^+ at 250 mM, for Cs^+ at 125 mM and for Zn^{++} at about 0.7 mM (Figs 3–5). All the data refer to a temperature of 37°C.

Discussion

According to the experiments performed with ^{14}C-labelled streptomycin (Engelberg, Artman, 1961) the streptomycin bound by bacteria is exchanged with the streptomycin in the medium. A dynamical equilibrium develops between bound streptomycin molecules and those in the medium. According to the data in the

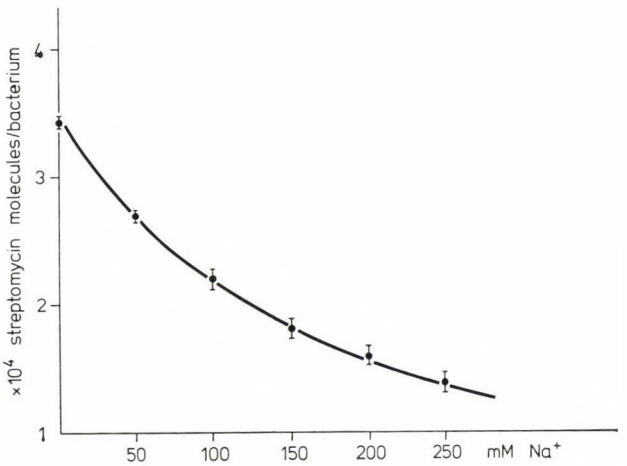

Fig. 1. Streptomycin uptake from media of various sodium ion concentrations. Each point represents an average value from 6—10 measurements. The vertical lines show the standard error of average

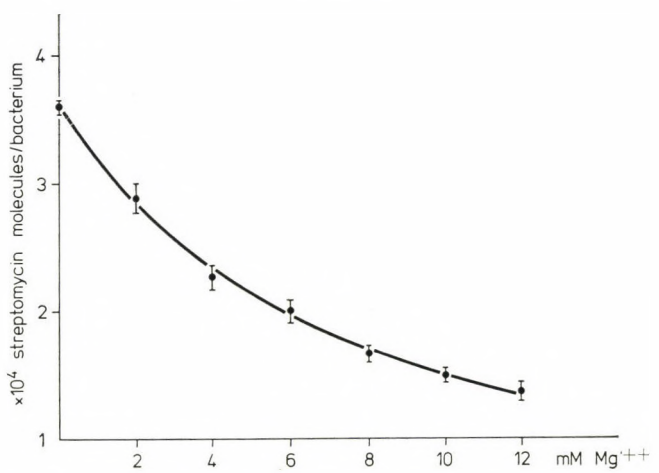

Fig. 2. Streptomycin uptake from media of various magnesium ion concentrations. Each point indicates the average value and standard error of 6 to 8 measurements

literature and our experiments it seems that an equilibrium state develops also in the case of metal ions. It also seems to be proved that the equilibrium states developed for streptomycin and metal ions are related to each other. If the concentration of metal ions increases, the quantity of the bound streptomycin decreases and *vice versa*. An exchange reaction takes place between streptomycin and metal ions bound by cell receptors.

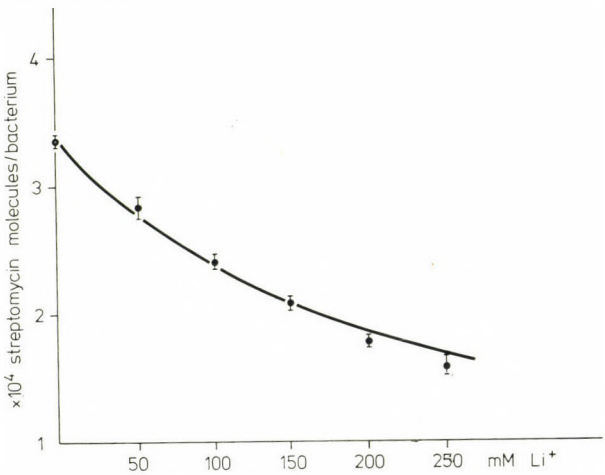

Fig. 3. Streptomycin uptake from media of various lithium ion concentrations. (For further notes see the text under Fig. 1)

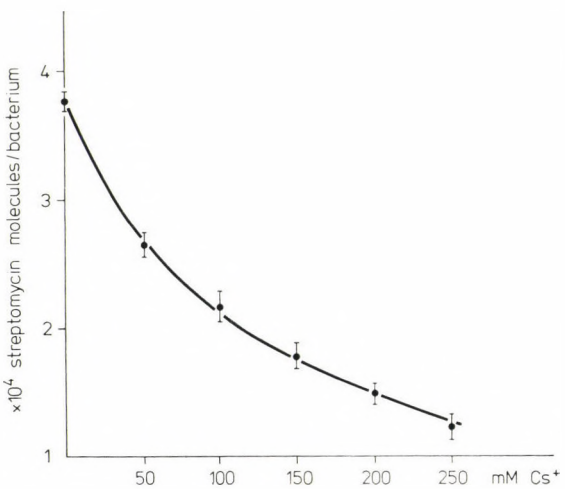

Fig. 4. Streptomycin uptake from media of various caesium ion concentrations. (For further notes see the text under Fig. 1)

In the following an attempt will be made to characterize the processes and the equilibrium states as well. The considerations are taken for the case when the solution contains sodium ions beside streptomycin. The method used for the other ions is similar, to the one described.

Let N denote the average number of possible binding sites on the surface of one bacterium for streptomycin and sodium ions respectively – the so-called active sites –. Let N_S denote the average number of the sites occupied by streptomycin molecules on the surface of one bacterium in a given case, N_N the ones occupied by sodium ions and N_A the number of free active sites.

It is evident that

$$N = N_A + N_S + N_N . \tag{1}$$

According to the law of mass action in the case of equilibrium:

$$N_S = k_S C_S N_A \tag{2}$$

and

$$N_N = k_N C_N N_A \tag{3}$$

where C_S and C_N denote the streptomycin and Na^+ concentration of the medium and k_S and k_N are the equilibrium constants for streptomycin and sodium respectively. In relation (2) and (3), the quantity of streptomycin and sodium taken up by the bacteria was neglected as compared with the quantity of streptomycin and sodium in the medium. The following relation is obtained from equations (1)–(3):

$$N_S = \frac{N k_S C_S}{1 + k_S C_S + k_N C_N} . \tag{4}$$

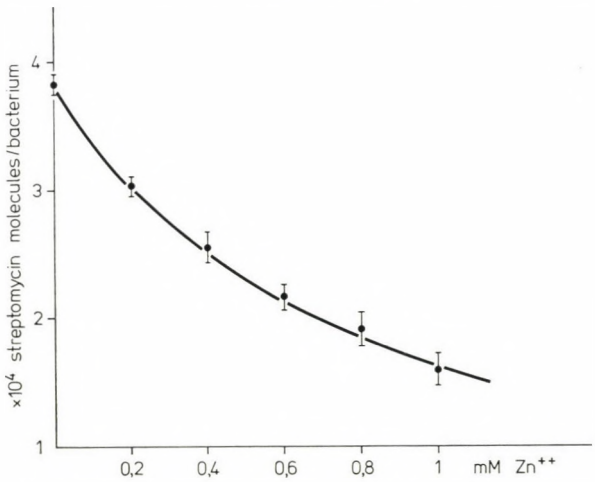

Fig. 5. Streptomycin uptake from media of various zinc ion concentrations. (For further notes see the text under Fig. 1)

Supposing that one streptomycin molecule occupies 3 active sites (Schmidt et al., 1968), the average number of streptomycin molecules present on the surface of one bacterium (N_{SS}) can also be determined:

$$N_{SS} = \frac{N_S}{3} . \tag{5}$$

According to our conception the curve of Fig. 1 can be described with relation (4) taking (5) into consideration. For N we used in the calculation our previously determined value (Szőgyi et al., 1969).[1]

$$N = 1.8 \times 10^6 .$$

The agreement with the experimental results is sufficient, if

$$k_S \approx 2 \times 10^{-19} \text{ cm}^3/\text{molecule} \tag{6}$$

$$k_N \approx 3.7 \times 10^{-21} \text{ cm}^3/\text{molecule}. \tag{7}$$

This agreement can be seen in Fig. 1, where the curve was drawn using relation (4), with the above values.

Equations (2) and (3) give:

$$\frac{k_S}{k_N} = \frac{\dfrac{N_S}{C_S}}{\dfrac{N_N}{C_N}} \tag{8}$$

and

$$\frac{k_S}{k_N} = \frac{\dfrac{N_S n}{C_S}}{\dfrac{N_N n}{C_N}} \tag{9}$$

respectively, where n denotes bacterium concentration. The left side of (9) can be interpreted as a ratio of probabilities, for one third of the numerator is equal to the probability that a streptomycin molecule can be found not in the medium, but on the surface of a bacterium. The denominator gives the similarly interpreted probability in the case of sodium ions.

[1] In the paper cited above it was not yet considered that the number of active sites occupied by streptomycin molecules on the surface of one bacterium is three times greater than the number of molecules. This is, why the presently used value of N, is also three times greater than the value in the quoted paper. $\varkappa$ occurring in the quoted paper is equal to the reciprocal value of k_S here.

According to our examinations

$$\frac{k_S}{k_N} \approx 54, \tag{10}$$

it means that the probability of staying on the surface of bacteria is 18 times greater for streptomycin molecules than that of sodium ions. This data also indicates that the energy of binding is greater in the case of streptomycin molecules than in the case of sodium ions. With the aid of our model, similar calculations were performed for the other ions, the results were summarized in Table 1. The agreement between experimental and calculated values can be regarded as sufficient also in the case of Figs 2 to 5. The continuous curves were obtained with calculation in each case, using the data of Table 1.

Table 1

Metal ions	k_S $\frac{cm^3}{molecule}$	k_{metal} $\frac{cm^3}{molecule}$	$\frac{k_S}{k_{metal}}$
Li^+	1.9×10^{-19}	2.3×10^{-21}	84
Na^+	2.0×10^{-19}	3.7×10^{-21}	54
Cs^+	2.1×10^{-19}	4.4×10^{-21}	48
Mg^{++}	2.1×10^{-19}	7.9×10^{-29}	2.6
Zn^{++}	2.2×10^{-19}	7.8×10^{-19}	0.3

Table 1 shows also that among the studied metal ions, the monovalent ions are more weakly bound than streptomycin, the binding of Mg^{++} is about the same, that of Zn^{++} is stronger than streptomycin. The binding probabilities of metal ions follow the sequence:

$$Li^+ < Na^+ < Cs^+ < Mg^{++} < Zn^{++}.$$

This sequence corresponds to Hofmeister's lyotropic series i.e. the probability of binding increases with the decrease of the hydrated ionic radius.

References

Engelberg, H., Artman, M. (1961) Biochim. Biophys. Acta *54* 533
Hancock, R. (1962) J. gen. Microbiology *28* 503
Hurwith, Ch., Rosano, C. L. (1962) J. of Bacteriol. *83* 1193
Kavanagh, F. (1963) Analytical Microbiology, New York, Acad. Press.
Pittinger, Ch., Adamson, R. (1972) Ann. Rev. Pharmacology *12* 169
Schmidt, H., Sych, F. I., Gorda, W. (1968) Pharmazie *23* 161
Szőgyi, M., Tamás, Gy., Tarján, I. (1969) Acta Biochim. Biophys. Acad. Sci. Hung. *4* 415
Szőgyi, M., Tamás, Gy. (1969) Gyógyszerészet *12* 452
Venis, M. A. (1969) Nature *221* 1147

Acta Biochim. et Biophys. Acad. Sci. Hung. Vol. 9 (1–2), pp. 115–120 (1974)

Multi-compartment Model for the Interpretation of the Radiation Injury of MS2 Phages*

JUDIT FIDY, ADRIENNE KARCZAG

Institute of Biophysics, Semmelweis University of Medicine, Budapest

(Received November 6, 1973)

The authors apply a three-compartment model for the interpretation of the UV radiation injury of MS2 phages. The mathematical description of the model contains — beside experimentally determinable quantities — only one parameter, the number of injurable places per phage. It is shown from a new aspect that the injurable places may be connected to the uracil and cytosine bases of the phage-RNA. The authors' previous experimental results and the radiobiochemical studies of others are interpreted with the aid of the model. Though the compartment model contains fewer approximations than the former stochastic radiation kinetic model of the research group the differences between the two models are well within the experimental error.

Introduction

In the last few years the use of multi-compartment models for the interpretation of biological processes has become more and more frequent. The classical field of application of the model is the description of transport phenomena between given volumes, in order to determine the quantities characterizing the transport processes (e.g. transition probabilities). Sheppard (1962) and Berman et al. (1962) have studied these models theoretically, in a fully general way, showing the limits of possibilities as well. However, beside this type of works, several other data exist on the concrete applications (Györgyi, Kanyár, 1972; G. Bartha, 1973). There are also examples for the enzyme kinetic application of the model by the generalization of the originally volume-connected compartment concept.

In the present work the multi-compartment method was used to interpret the UV radiation injury of the MS2 phage. The results obtained will be compared with our stochastic radiation kinetic model and also with the radiobiochemical measurements of others (Cerutti et al., 1969).

* Delivered at the 7th Congress of the Hungarian Biophysical Society.

The description of the model

Upon the effect of UV radiation the bases of the MS2 phage may suffer partly reversible and partly irreversible injuries, and the reversion of the latter ones is also possible (Shugar, McLaren, 1964; De Boer et al., 1967; Rontó et al., 1967). In the present case the total number of injurable places of phages in the population corresponds to the particles of the compartment model and the possible states of these places are the compartments of the model. Since the undamaged injurable places may be injured in two ways, the number of compartments is three.

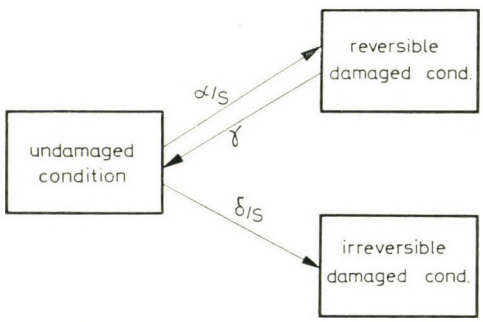

Fig. 1. Block diagram of the three-compartment model

The transitions between the compartments represent the transitions between the different states. The α, δ and γ transition probabilities between the states of MS2 phages were already previously determined, independently of the model (Karczag et al., 1972a), from the experimental dose-effect curve for inactivation. γ can be used invariably in the compartment model since it was defined as the transition probability for the reversion of one single injurable place. The further two transition probabilities of the model may be easily derived from the known α and δ probabilities dividing them by s where s denotes the number of injurable places within one phage. As these probabilities were originally defined for the case when one single photon ($\lambda = 254$ nm) was absorbed per phage in unit time, these quantities must be multiplied here by m, the number of photons absorbed by one phage in unit time. Thus the change of the number of places in different states may be given as the functions of the irradiation time by the following relations:

$$\frac{dn_0(t)}{dt} = -\frac{\alpha m}{s} n_0(t) + \gamma m n_{rev}(t) - \frac{\delta m}{s} n_0(t), \tag{1a}$$

$$\frac{dn_{rev}(t)}{dt} = \frac{\alpha m}{s} n_0(t) - \gamma m n_{rev}(t), \tag{1b}$$

$$\frac{dn_{irr}(t)}{dt} = \frac{\delta m}{s} n_0(t) \tag{1c}$$

where $n_0(t)$ is the number of undamaged, $n_{rev}(t)$ the reversibly and $n_{irr}(t)$ the irreversibly injured places after an irradiation time of t.

For the solution of the 1a–c system of linear differential equations we assumed that every injurable place was in an undamaged state at the beginning of irradiation ($t = 0$). Further on, we assumed that each injurable place might be injured at the same time only in one way: either reversibly or irreversibly. With these conditions the solutions are as follows:

$$\frac{n_0(E)}{N} = A_1 e^{-r_1 E} + A_2 e^{-r_2 E}, \tag{2a}$$

$$\frac{n_{rev}(E)}{N} = -B_1 e^{-r_1 E} + B_1 e^{-r_2 E}, \tag{2b}$$

$$\frac{n_{irr}(E)}{N} = -C_1 e^{-r_1 E} - C_2 e^{-r_2 E} + C_3, \tag{2c}$$

where $E = mt$ and $N = n_0(0)$, i.e. the total number of injurable places at $t = 0$. A_k, B_k and C_k are positive constants containing beside s only the values α, δ, γ. These latter parameters – as it was already mentioned – had been determined from the experimental dose-effect curves, thus in relations 2a–c there is only one unknown parameter value: s. The values of the constants in the solutions for the case of $s = 800$ are given in Table 1.

Table 1

A_1	A_2	B_1	C_1	C_2	C_3	r_2	r_1
$\sim 3\times 10^{-3}$	~ 1	$\sim 3\times 10^{-3}$	$\sim 10^{-5}$	~ 1	~ 1	$\sim 6\times 10^{-5}$	$\sim 2\times 10^{-7}$

Since the solutions of the equations are given as the functions of the E energy absorbed by one phage our theoretical results can be directly compared with experimental data.

Results and discussion

1. In Fig. 2 the 2a–c functions are plotted at parameter values of $\alpha = 1.3\times 10^{-4}$, $\delta = 1.7\times 10^{-4}$, $\gamma = 6\times 10^{-5}$. The calculations and plotting were carried out with a Hewlett–Packard 9100B computer at three different s values ($s = 500$, 800 and 1000). From Fig. 2 the following conclusions can be drawn. The relative number of irreversible injuries increases steadily with increasing doses (curves A), but that of reversible injuries (curves B) becomes stabilized after reaching a certain dose. The fraction of undamaged injurable places hardly falls

below 90 per cent even at very high doses, thus the curve giving the variation of the number of such places would only slightly deviate from the horizontal axis. Therefore this curve is not plotted.

The possible places of the MS2 RNA phage for reversible injury may be the uracil and cytosine bases situated above each other in the nucleotide chain. For irreversible injuries practically the uracil bases should be considered. According to the data of Strauss and Sinsheimer (1963) the pyrimidine bases are evenly dis-

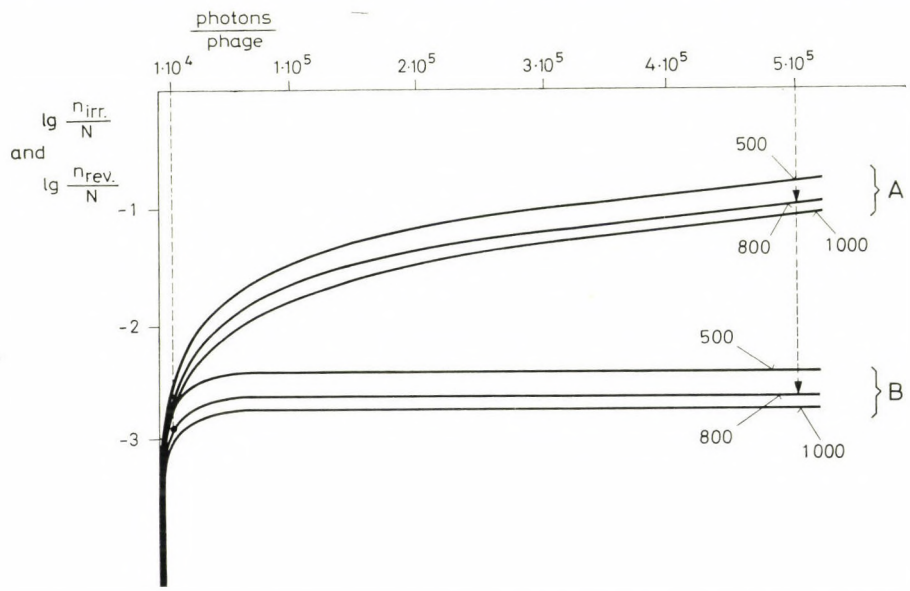

Fig. 2. Changes in the relative number of injured places as a function of the UV dose (the average number of photons absorbed by one phage). Curves A refer to irreversible, curves B to reversible injuries. Numbers at the curves give the values of s

tributed in the MS2 RNA phage and give half of the total number (3300) of bases, the number of uracil bases is about one quarter of the total number and the value of s might be estimated to be between 800 and 900.

It can be seen from Fig. 2 that the curves are only slightly sensitive to the value of s within the given range. For this reason, also considering the experimental error, one cannot give any more accurate estimate for s with the aid of concrete experimental data. Because of this we chose the value of $s = 800$ for Table 1 and will use this value later on as well.

2. With the aid of our model the radiobiochemical results of other authors can be compared with our experimental data. On the curves for $s = 800$ in Fig. 2 the fraction of reversible and irreversible injuries is denoted at the dose (5×10^5 absorbed photons/phage) for which Cerutti and his co-workers (1969) gave the

radiobiochemical data obtained on irradiation of the R17 RNA phage. The figure shows that, at this dose, the ratio of irreversible injuries is 9.5 per cent while that of reversible ones is equal to 0.27 per cent. This result agrees with the experiences of Cerutti, who found hydrated photoproducts in about 10 per cent of the uracils and no dimers at all. It is quite obvious that the reversible injuries present in 0.27 per cent cannot be detected by the usual chemical methods.

Fig. 2 gives information also on the development of biological injury in the phage. At the maximal dose applied (10^4 photons/phage) the ratio of reversible injuries is 0.12 per cent, i.e. an average of $0.96 \sim 1$ reversible injury occurs per phage. In this case the number of irreversible injuries is $1.76 \sim 2$ per phage, i.e. not considerably greater than the number of reversible injuries. Thus the two types of injury play an approximately equal part in the inactivation of the phages. It can be also seen from the Fig. 2 that the fractions of reversible and irreversible injuries differ considerably with increasing doses. While the number of reversible injuries is stabilized at a value of 2.16 injuries/phage on the average, the number of irreversible injuries increases steadily reaching at the dose applied by Cerutti et al. (1969), an average value of 76 injuries/phage.

3. The comparison of the compartment model with our former stochastic radiation kinetic model (Karczag et al., 1973) is of particular interest, because the comparison gives information on the effect of approximations applied in the former model. Namely, the stochastic model treats the reversible and irreversible injuries during irradiation independently of each other. The three-compartment model does not contain this approximation.

Both models apply a simplification considering the transition probabilities to be independent of the dose, though according to the data of Pearson and his co-workers (De Boer et al., 1967) the probability of irreversible injuries increases in the case of high doses (in the vicinity of dimers).

Our stochastic model was applied mainly to interpret the one-hit type of UV inactivation of phages. Thus, for the comparison, we have to establish a connection between the damage of the population of injurable places in our compartment model and that of the phage population containing $s = 800$ injurable places/phage. It can easily be shown that the relative number of both reversibly and irreversibly injured places (n_{rev}/N and n_{irr}/N) depends on the expectable value of injuries per phage ($\langle k_{rev} \rangle$ and $\langle k_{irr} \rangle$, respectively):

$$\frac{n_{rev}}{N} s = \langle k_{rev} \rangle \quad \text{and} \quad \frac{n_{irr}}{N} s = \langle k_{irr} \rangle$$

where $\langle k_{rev} \rangle$ and $\langle k_{irr} \rangle$ can be given by the aid of the stochastic model, n_{rev}/N and n_{irr}/N is obtained from the compartment model. This enables us to compare the two models.

Fig. 3 shows both curves obtained with the two models. It can be seen that, in the case of low doses, the curves do not deviate from each other at all. Even at

the high doses applied by Cerutti they differ only so slightly that they cannot be distinguished experimentally. Comparing the curves we may state that the simplifications applied in the stochastic model are permissible for MS2 and also for other RNA-phages.

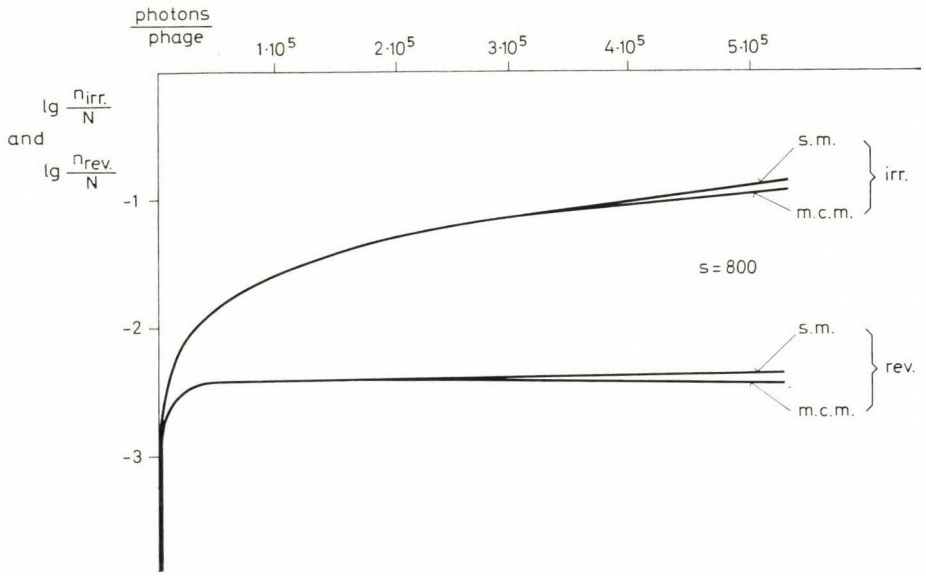

Fig. 3. Changes in the relative number of injured places as a function of the UV dose calcu lated from the multi-compartment (m. c. m.) and the stochastic model (s. m.)

References

Berman, M., Weiss, M. F., Shan, E. (1962) Biophys. J. *2* 289
De Boer, G., Pearson, M., Johns, H. E. (1967) J. Mol. Biol. *27* 131
Cerutti, P. E., Miller, N., Pleiss, M. G., Remsen, J. F. (1969) Proc. Natl. Acad. Sci. *64* 731
Garfinkel, D. (1966) J. Biol. Chem. *241* 286
G. Bartha, K. (1973) Acta Pharm. Acad. Sci. Hung. (in press)
Györgyi, S., Kanyár, B. (1972) Acta Biochim. Biophys. Acad. Sci. Hung. *7* 359
Hoy, T. G., Goldberg, D. M. (1971) Int. J. Biomed. Comput. *2* 71
Karczag, A., Rontó, Gy., Tarján, I. (1972a) Abstr. IV. Int. Biophys. Congr. Moscow *1* 122
Karczag, A., Rontó, Gy., Tarján, I. (1972b) Acta Biochim. Biophys. Acad. Sci. Hung. *7* 173
Karczag, A., Rontó, Gy., Tarján, I. (1973) Acta Biochim. Biophys. Acad. Sci. Hung. *8* 281
Rontó, Gy., Sarkadi, K., Tarján, I. (1967) Strahlenther. *134* 151
Sheppard, C. W. (1962) Basic Principles of the Tracer Method, Wiley, New York
Shugar, D., McLaren, A. D. (1964) Photochemistry of Proteins and Nucleic Acids, Pergamon Press, Oxford
Strauss, J. H., Sinsheimer, Jr. R. L. (1963) J. Mol. Biol. *7* 43

Acta Biochim. et Biophys. Acad. Sci. Hung. Vol. 9 (1–2), pp. 121–129 (1974)

The Effect of Chloroform Traces on Sonicated Liposome Systems

L. ERDEI, F. JOÓ, I. CSORBA, CS. FAJSZI

Institute of Biophysics, Biological Research Centre,
Hungarian Academy of Sciences, Szeged

(Received November 23, 1973)

Some geometrical parameters of an acidic and a neutral liposome preparation were studied by electron microscopy. The presence of chloroform traces was shown to cause a change in the pH of the medium and thus the chemical degradation of lecithin. The consequences of this effect concerning the size distribution of the liposome systems were also investigated electron microscopically. The size distribution of both preparations proved to be logarithmic normal, and the mean values of the equivalent radii were 245 and 124 Å for the acidic and neutral liposome preparation, respectively. Some observations concerning the distortion of liposomes during the preparation for electron microscopy are also presented. Liposomes in neutral preparation are geometrically very similar to some microvesicles appearing in biological systems (e.g. to synaptic vesicles), and thus, they offer an excellent model for studying biological transport processes.

Introduction

The aqueous dispersion of lipids, the so-called liposome systems, have been frequently used for modelling biomembranes. Although the preparative method, originally described by Bangham and Horne (1964), has been modified and the statistic and numerous geometric characteristics of the model system have already been given (Attwood, Saunders, 1965; Huang, 1969; Seufert, 1970; Miyamoto, Stoeckenius, 1971) the main disadvantage of liposome systems is that their geometry is generally unknown (Miyamoto, Stoeckenius, 1971). In addition, the main geometric characteristics of liposomes also depend on the chemical constitution of the dispersion (Papahadjopoulos, Miller, 1967). Recent observations call attention to the danger of changes in chemical constitution of lipids stored under chloroform. Namely, the chloroform yields protons even under nitrogenous atmosphere, which may lead to the decomposition of lipids (Schmid et al., 1973). Although the effect of sonication on lecithin molecules has been studied by Hauser (1971), relatively little attention have been paid to the effect of solvent traces remained in the dispersion.

In an electron microscopical analysis we took into account how the shape, the size and the structure of liposomes changed during the preparative work.

In the present paper the effect of chloroform on the liposome system is studied and a few geometric parameters, characteristic of an acidic and a neutral liposome system, are given.

Methods

Preparation of the liposome system

Egg yolk lecithin (Merck, "extra pure") was further purified by dissolving in chloroform, precipitating by cold acetone and was stored under nitrogen atmosphere in chloroform at $-20°C$. The purity of the lipid was checked by thin-layer chromatography (TLC) (Kieselgel G, chloroform : methanol : water 65 : 25 : 4). The liposome systems were prepared by sonication of 1 w/v per cent lecithin in aqueous medium containing 100 mM KCl + 50 mM Tris-HCl (MSE Type 150 W, 21 Kc/sec, 6.5 μ amplitude). The oxygen was expelled by bubbling pure nitrogen through the dispersion medium before sonication.

Sample A was formed by 120 min sonication in a medium of low buffer capacity (starting value pH = 7.5) while in the case of sample B the sonication time was shortened to 45 min and the initial pH of the medium (of high buffer capacity) was 8.5.

After sonication the dispersions were centrifuged to remove lipid aggregates and the titanium dust originated from the probe.

In order to controll the effect of sonication on chemical constitution of lecithin, samples were taken for TLC analysis from the liposome preparations after sonication for 25, 45 and 100 min. The transmission spectra were taken on a spectrophotometer Type Spectromom 203.

Electron microscopy

One drop of the sample was placed on a 150 mesh copper grid covered by formwar film. One part of the grids was negatively stained with 2 per cent ammonium-molibdenate neutralized by ammonium hydroxide and, when dried, covered by carbon film. The other part of the grids was shadowed with palladium metal beam of 11.3° angle of incidence in a vacuum evaporator Type Zeiss HBA I. Electron micrographs were taken on a JEOL 100B electron microscope.

Result and discussion

Acidification of the medium

To determine the appropriate sonication time, the transmission of light in the samples was measured at 550 nm during sonication. The optical transmission of the samples A and B (Fig. 1) gives a saturation curve, i.e. no change in the

degree of dispersity can be detected spectrophotometrically after 30 min sonication. This is very similar to Seufert's result (1970) obtained after 45 min minimum sonication time.

During the sonication, the pH of the samples falls (curves pH-A, pH-B, Fig. 1) particularly in the case of the slightly buffered preparation A (acidic preparation). The final pH of the system A was about 2.5, while that of the system B remained neutral. The fall of pH can be observed under both air and nitrogen

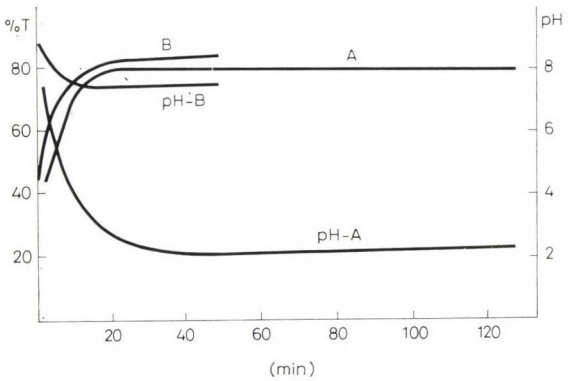

Fig. 1. Percentage transmittance and pH of preparations as function of sonication time. **A**: for sample type A. One per cent dispersion of lecithin in 100 mM KCl + 50 mM Tris-HCl buffer, initial pH 7.5
B: for sample type B. The same medium, with an initial pH of 8.6. Curves signed pH-A and pH-B mean the change of pH of preparations A and B, respectively, during sonication

atmospheres. No significant changes in the pH of the dispersion media could be observed during sonication under similar conditions.

Hauser (1971) pointed out that, during sonication, the chemical structure of lecithin changed and acidic degradation products appeared in the medium. Contrasting with this no chemical degradation of lecithin was observed in neutral medium even after 2.5 hour disintegration (Huang, Charlton, 1972). As the acidification of sample A appeared in the first minutes of sonication it could be suspected that the origin of pH drop was not a rapid destruction of lecithin. We observed, using TLC analysis, that lecithin was decomposed chemically in acidic medium during 25, 45 and 100 min sonication (Fig. 2a – c), while no decomposition occurred either in neutral or chloroform-free media (Fig. 2d – f).

It was demonstrated by radioactive tracer technique (Galzigna, Méry, 1971) that chloroform forms a strong complex with lecithin which complex remains stable even after long-term evaporation. This complexed chloroform, when interacting with oxygen, methanol and water, produces, especially during intensive sonication, protons which lead to an acidification of the medium. Even under N_2 atmosphere a considerable amount of HCl is present in chloroform as proved by

Schmid et al. (1973). It also should be noted that chloroform traces, owing to its interaction with lecithin, may influence some physical properties of the planar bimolecular lipid membranes as well (dc resistance, permeability, stability) when the membrane forming material contains chloroform (Simons, 1968; Mehard et al., 1970).

Fig. 2. The effect of sonication on lecithin dispersion
a, b, c: effect of 25, 45 and 100 min sonication, respectively, on chemical constitution of lecithin in the presence of chloroform traces (acidic medium); d, e, f: 25, 45 and 100 min sonication in neutral medium

Size and distribution

Electron micrographs of the samples A and B are shown in Fig. 3. For quantitative characterization of the liposome systems several, but at least two, independent preparations were formed and equally enlarged micrographs were taken. The area bound by the lipid layers on the photographs was measured by a planimeter and the radius of an equivalent circle was calculated, which was considered as the radius of the equivalent sphere. This equivalent radius was taken as characteristics of the size of liposomes. To obtain histograms for size distribution of the liposome systems relative frequencies have been calculated and plotted at every 20 Å. A logarithmic normal distribution (Fig. 4) could be fitted to the histograms, the parameters of which were obtained by the "maximum likelihood" method (Aitchison, Brown, 1957; Diamond, Dolch, 1972). The average equivalent radius of liposomes in sample A has been found to be $R = 245 \pm 2.3$ Å (standard deviation 124 Å), while in the case of preparation B $R = 124 \pm 1.3$ Å (standard deviation 51 Å). Although both radii are in agreement with the data of other investigators ($120 < R < 300$ Å) (Huang, 1969; Seufert, 1970; Johnson et al., 1971; Miyamoto, Stoeckenius, 1971) there is a considerable difference in the size distribution of systems A and B. The TLC analysis of both types of preparations suggests that this difference between the two types of liposome systems may be attributed to the difference in the chemical constitution; e.g. to the acidification of the sample.

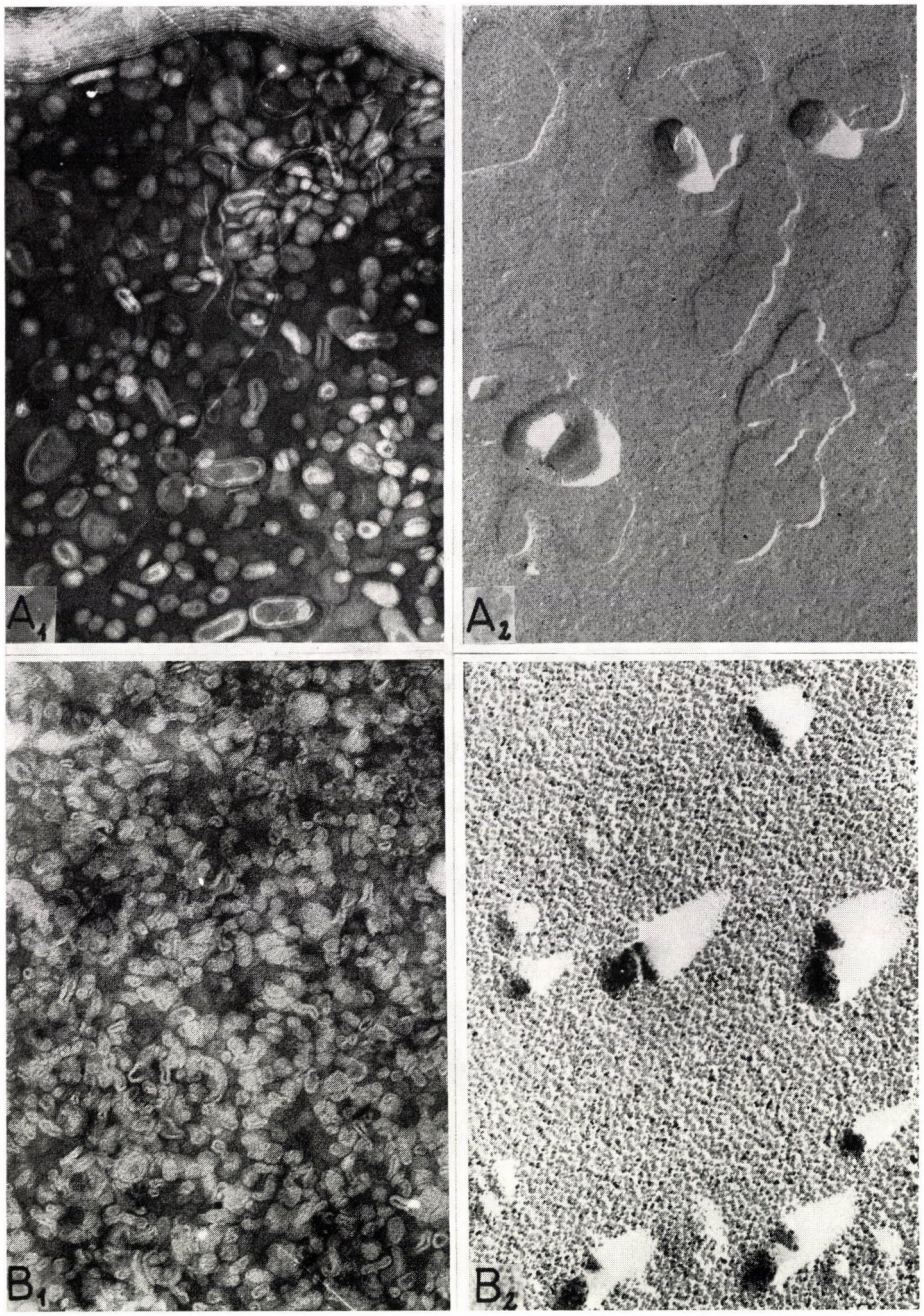

Fig. 3. Electron micrographs of negatively stained and metal-shadowed preparations A and B. A_1 = sample from the negatively stained liposome system A. Magnification: 75 000×. A_2 = sample from the metal-shadowed liposome system A. Magnification: 34 000×. B_1: sample from the system B. Magnification: 90,000×. B_2 = sample from the metal-shadowed system B. Magnification: 75 000×

Shape, volume, surface

Although it has been shown in viscosimetric (Attwood, Saunders, 1965; Saunders, 1966), light scattering (Attwood, Saunders, 1965) and electron microscopic studies (Johnson et al., 1971) that liposomes are of an ellipsoid shape, they are usually regarded as spherical vesicles (Seufert, 1970; Miyamoto, Stoeckenius, 1971).

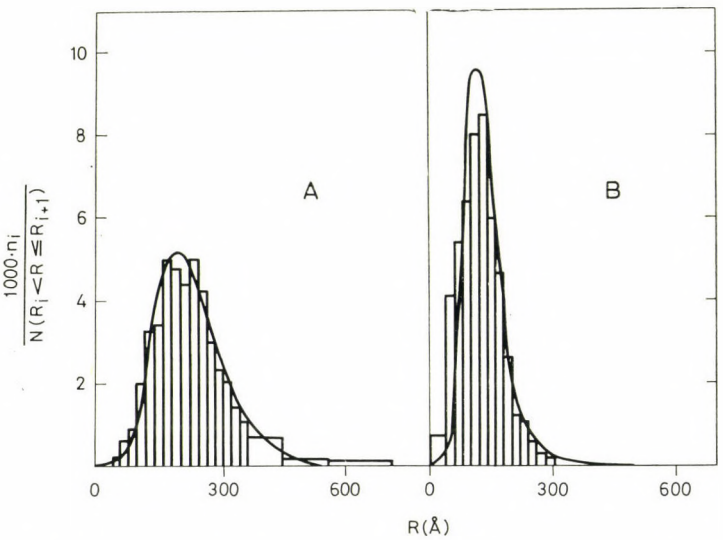

Fig. 4. Size distribution of preparations A and B. The frequency was calculated in every 20 Å range, shown by the histograms. R = equivalent radius of vesicles (Å), n_i is the number of liposomes in the $R_i < R \leq R_{i+1}$ range, N = total number of the measured vesicles. N = 3000 and 1800 for the preparations A and B, respectively. The solid lines represent the theoretical function of size distribution which is logarithmic normal in both preparations. The parameters of the distributions are presented in the text

The question arises, how reliable are the conclusions drawn from the results of successive calculations. In the following, some approximations will be made concerning the role of shape factor in relation to the specific volume and surface of lipid vesicles.

In our case the ratio of the major and the minor axes of the negatively stained liposomes is 1.73 ± 0.58. This value is in good agreement with the 1.8 axial ratio which has been obtained from viscosimetric measurements by Attwood and Saunders (1965). We wonder whether we can use an equivalent radius for calculating the specific inner volume and specific surface of ellipsoid particles?

In the case of spherical vesicles

$$V_{sph} + 1 = \frac{\langle R^3 \rangle}{d(3\langle R^2 \rangle - 3d\langle R \rangle + d^2)} \tag{1}$$

where V_{sph} is the specific inner volume of the spherical vesicles, R is the radius, $\langle R^n \rangle$ the averaged mean of R^n, d the thickness of the lipid bilayer.

Similarly, for a set of ellipsoids of equal axial ratio

$$V_e + 1 = \frac{\langle R^3 \rangle}{d\left[\left(2\sqrt{x} + \frac{1}{\sqrt{x}}\right)\langle R^2 \rangle - d(2+x)\langle R \rangle + d^2\sqrt{x}\right]} \tag{2}$$

where V_e is the specific inner volume of the ellipsoid vesicles, R is the equivalent radius and x the axial ratio.

In the same way we can obtain equation also for the specific surface referred to the lipid volume in the case of the spherical vesicles:

$$S_{sph} = \frac{3\langle R^2 \rangle}{d(3\langle R^2 \rangle - 3d\langle R \rangle + d^2)} \tag{3}$$

while for ellipsoid liposomes

$$S_e = \frac{3\langle R^2 \rangle \left(1 + \frac{x^2}{\sqrt{x^2-1}} \arcsin \frac{\sqrt{x^2-1}}{x}\right)}{2d[(2x+1)\langle R^2 \rangle - (2+x)\sqrt{x}d\langle R \rangle + d^2 x]} . \tag{4}$$

Calculation of the specific inner volume and specific outer surface of the liposome systems reveals that the specific inner volume of the vesicle strongly depends on its shape. On the contrary, the specific outer surface does not depend on the shape of the vesicle, if the thickness d of the bilayer does not change (Table 1). The data of Table 1 suggest that, in the case of single bilayer liposomes, information can be obtained concerning the real shape of liposomes in aqueous media by determining the specific inner volume of the vesicles.

Table 1

Specific inner volume and specific outer surface of a set of spherical and ellipsoid liposomes
V_{sph} and V_e are the specific inner volume of spherical and ellipsoid liposomes, respectively. S_{sph} and S_e are specific outer surface of spherical and ellipsoid liposomes, respectively. The inner volumes and outer surfaces are referred to the volume of the constituent lipid material in the case of preparations A and B
V is dimensionless and S has a dimension of (1/Å)

	V_{sph}	V_e	S_{sph}	S_e
A	2.3	2.0	0.022	0.023
B	0.51	0.39	0.027	0.029

On the deformation of vesicles during preparation for electron microscopical work

From the length of the shadow casted by the vesicles (Fig. 3 A_2, B_2) their height can be estimated. It was found to be about $1/2-1/9$ part of the minor axis. Generally, the larger the liposome, the larger the collapse (Fig. 5). As a consequence of the collapse, the size of liposomes observed after negative staining

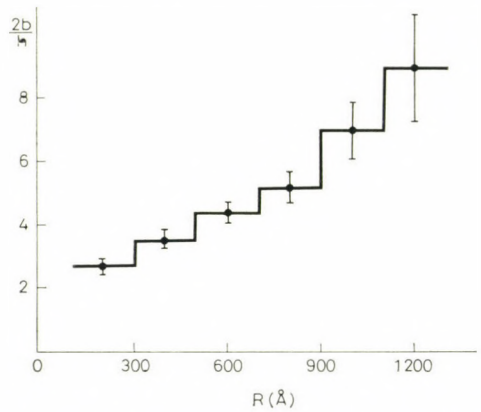

Fig. 5. Collapse of liposomes during preparation for electron microscopic examinations as function of their size. The ratio of $2b/h$ is taken for the measure of collapse, i.e. without any deformation of a prolate ellipsoid vesicle the ratio of $2b/h$ would be 1 (where b = minor axis of the ellipsoid and h = height of liposomes as estimated from their shadow, see Fig. 3 A_2 and B_2); R = equivalent radius. The ratio of collapse was calculated for every 200Å ranges. The vertical bars mean the standard deviation

was probably larger than in the reality. According to Huang's comparative studies (1969) the size of liposomes, as revealed by freeze-etching technique, is usually smaller than that obtained by negative staining (250 ± 20 Å and 300 ± 30 Å, respectively). Our results are in agreement with these data, therefore it can be said that the values of vesicle size obtained by negative staining can be regarded only as approximate ones.

Conclusion

The data in the literature, as well as our investigations, call attention to the serious limitations and consequences of chloroform traces present in lecithin. According to the TLC analysis of an acidic and a neutral liposome system, the acidic environment may lead to a significant decomposition of lecithin, which is accompanied by the alterations of some geometrical parameters of lipid vesicles.

In the liposome system B, prepared under neutral environments, the average size of liposomes is similar to that of the micro-vesicles of biological systems, for

instance, to synaptic vesicles. The liposomes are bound by one 53 Å thick lipid bilayer only. Their shape seems to be a prolate ellipsoid with an axial ratio of 1.73. Liposomes of the acidic system A are often bound by more than one lipid bilayer, i.e. they possess more compartments.

Exact evaluation of the data obtained for transport fluxes across model membranes is possible if a) the model is comparable even in its structure with biomembranes, b) it possesses only one compartment (bound by single bilayer and c) the geometric parameters of the system are known. According to the abovementioned reasons, the liposome system B seems to be preferred for studying transport and storage phenomena in microvesicle systems of living cells.

We thank Dr B. Karvaly for his helpful discussions, Prof. F. Guba for the use of the electron microscope, Mrs Éva Izsó and Mrs Krisztina Mohácsi for their technical assistance.

References

Aitchison, J., Brown, J. A. C. (1957) The Lognormal Distribution. University Press, Cambridge, p. 39
Attwood, D., Saunders, L. (1965) Biochim. Biophys. Acta *98* 344
Bangham, A. D., Horne, R. W. (1964) J. Mol. Biol. *8* 660
Diamond, S., Dolch, W. L. (1972) J. Coll. Interface Sci. *38* 234
Galzigna, L., Méry, J. (1971) Experimentia *27* 626
Hauser, H. O. (1971) Biochem. Biophys. Res. Comm. *45* 1049
Huang, C. (1969) Biochemistry *8* 344
Huang, C., Charlton, J. P. (1972) Biochem. Biophys. Res. Comm. *46* 1660
Johnson, S. M., Bangham, A. D., Hill, M. W., Korn, E. D. (1971) Biochim. Biophys. Acta *233* 820
Mehard, C. W., Lyons, J. M., Kumamoto, J. (1970) J. Membrane Biol. *3* 173
Miyamoto, V. K., Stoeckenius, W. (1971) J. Membrane Biol. *4* 252
Papahadjopoulos, D., Miller, N. (1967) Biochim. Biophys. Acta *135* 624
Saunders, L. (1966) Biochim. Biophys. Acta *125* 70
Schmid, P., Hunter, E., Calvert, J. (1973) Physiol. Chem. Physics *5* 151
Seufert, W. D. (1970) Biophysik *7* 60
Simons, R. (1968) J. Mol. Biol. *36* 287

Acta Biochim. et Biophys. Acad. Sci. Hung. Vol. 9 (1—2), pp. 131—140 (1974)

The Phylogenetic and Ontogenetic Development of the Mammalian Heart: Some Theoretical Considerations

C. E. CHALLICE,* SZ. VIRÁGH

Postgraduate Medical School, Department of Pathology, Budapest

(Received October 12, 1973)

The object of this paper is to consider the biophysical implications of morphological studies on the developing mammalian embryonic heart (reported elsewhere) along with the available information on the heart of more primitive animals. In both ontogenetic and phylogenetic development the heart begins as a tube, then becomes a series of near-spherical chambers with muscular trabeculae, finally becoming the double two-stage pump of the adult mammal, with a muscular myocardial wall.

Simple mathematical analysis shows that there is an increase in pumping efficiency as pumping force becomes three-dimensional, but (ignoring the effect of streamlining) no increase in efficiency is obtained as it proceeds from primarily trabecular to primarily myocardial wall contraction. The suggested reasons for the observed development are that the trabecular development is mechanically and nutritionally simpler, and the myocardial wall develops in response to the need for faster blood flow, and more efficient oxygenation required for higher pressures in the four-chambered closed circuit mammalian heart.

Introduction

In primitive animals such as annelida, a tubular vessel "pumps" blood around the body by slow peristaltic contractions passing along the wall of the tube (Federighi, 1928). In the more advanced vertebrates (e.g. fish and amphibians), chambers develop, in which the musculature consists of (approximately) diametrically disposed trabeculae which cause a more-or-less coherent contraction sequentially in each of the respective chambers. In the most advanced vertebrate hearts, namely those of birds and mammals, the trabeculae have almost disappeared, and the musculature consists of a compact myocardial wall in four chambers, which contract sequentially, producing a two-stage pump for both pulmonary and peripheral circulations respectively (for complete review, see Robb, 1965). The same sequence is reproduced ontogenetically in the avian and mammalian hearts (Manasek, 1968; Virágh, Challice, 1973; Challice, Virágh, 1974).

One would expect this development to be accompanied by an increase in

* Permanent address: Department of Physics, University of Calgary, Canada.

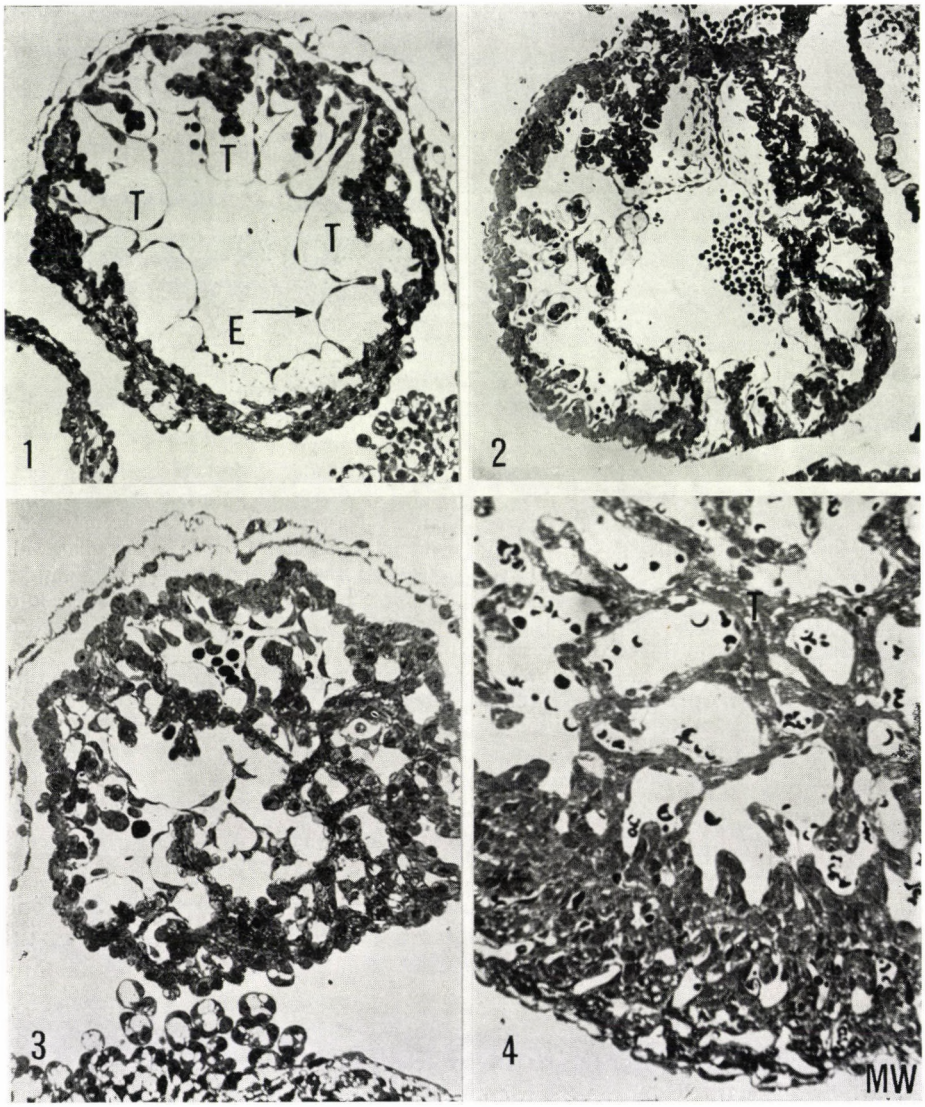

Fig. 1. Cross-section of developing ventricle of mouse heart 9 days after fertilization. The ventricle is nearly spherical in shape, but trabeculae (T) have begun to develop, growing inwards into the lumen, within the cardiac jelly which is enclosed by the endocardial lining (E). ×130

Fig. 2. As Fig. 1, but 10 days post-fertilization. The trabeculae have grown significantly further into the lumen and demonstrate a greater degree of interconnection than one day earlier. The A—V canal (top) is closed by the endocardial cushion which at this stage serves as a primitive valve. ×83

efficiency of the system, and, with this in mind, it was decided to analyze these pumps, using simple mathematics, to ascertain to what extent the efficiency was improved by moving through the sequence from tubular heart to spherical heart chambers.

Experimental procedures

The experimental procedures and experimental results obtained have been described in detail (Virágh, Challice, 1973; Challice, Virágh, 1974). The ontogenetic development of the heart of the mouse has been followed, using hearts from mouse embryos 8 days post fertilization onward. In the earliest stages the whole embryos were removed, fixed in 4 per cent glutaraldehyde, diluted in phosphate buffer (pH 7.2–7.4) postfixed in 1 per cent OsO_4, and embedded in Araldite. Older embryos were dissected in fixative and only the relevant parts fixed and embedded. The structures were studied by dissecting microscope, light microscopy of 1 μ sections stained with toluidine blue, and electron microscopy of thin sections cut on Reichert or LKB ultramicrotome.

Results

More complete documentation of the experimental results is provided in the publications devoted to the description of the sequence of cytological and architectural changes as they occur in the embryo of the mouse (Virágh, Challice, 1973; Challice, Virágh, 1974). The straight tube of the primitive embryonic heart, which demonstrates slow peristaltic contractions (Patten, Kramer, 1933) twists to form primitive chambers. In the developing chambers a trabecular system forms (Figs 1, 3) and at the same time a marked increase in pressure is developed (Faber, 1968). Then these trabeculae develop (Figs 2, 4) and later become engulfed in developing myocardial wall (Fig. 4). Ultimately this leaves a largely unencumbered lumen.

Fig. 3. Section through ventricle of 9-day mouse embryo, cut near the surface of the heart so that it passes through the layer of trabeculae (c.f. Fig. 1). Interconnections between the trabeculae form a meshwork of contractile elements. ×181

Fig. 4. Section through ventricle of 17-day mouse embryo. This shows a further development of trabeculae which now have a closely applied endocardium, and blood cells are present within the meshwork. The myocardial wall is also becoming consolidated. ×207

Theory

(1) *To find the pressure in a cylinder and sphere as a function of the force per unit area in the walls:*

(a) Consider the forces of tension applied circumferentially in the walls of a cylinder.

Consider the cylinder to be cut in two, lengthways and the forces to be pulling the two halves together.

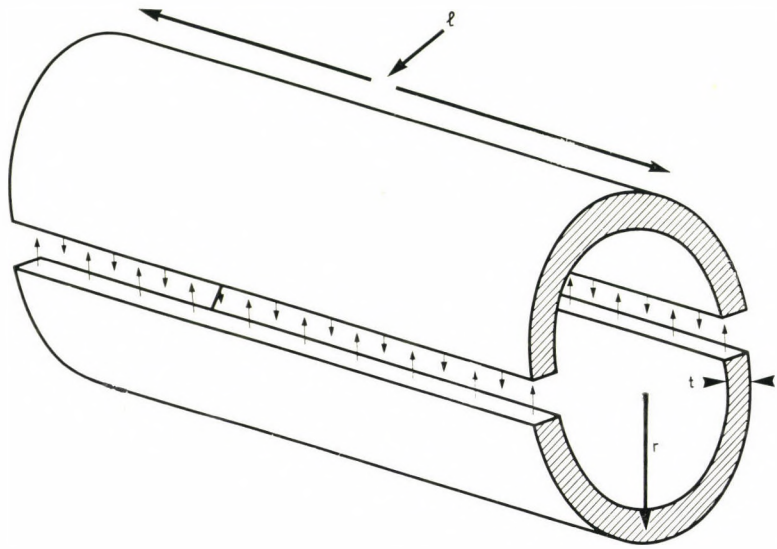

Fig. 5. Schematic drawing indicating forces pulling the two halves of a tube together (see text)

Let F be the force per unit cross-sectional area of the wall of the cylinder. The force pulling the two halves together is then given by:

$$F \cdot 2l \cdot t,$$

where t is the thickness of the wall and l is the length of the cylinder.

This force is balanced by the pressure in the cylinder, which is distributed all over the surface of each half cylinder. The force tending to push them apart is the force at right angles to the plane at which the cylinder is sectioned, i.e., is equal to the pressure multiplied by the area of the plane of section.

Area of plane of section of half cylinder is $2rl$, where r is the radius of the cylinder.

Then the pressure in the cylinder (i.e., the force per unit area of container) is given by

$$p = \frac{2Flt}{2rl} = \frac{Ft}{r}.$$

(b) Consider the forces of tension applied in the walls of a sphere (Fig. 6). Consider the sphere cut into two hemispheres, and the forces to be pulling the hemispheres together.

The force pulling the two hemispheres together is then given by

$$F \cdot 2\pi r \cdot t.$$

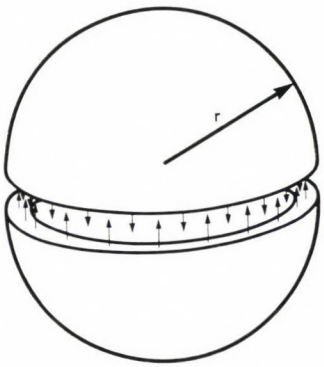

Fig. 6. As Fig. 5, but for sphere (see text)

This is counterbalanced by the pressure inside pushing the hemisphere apart. The pressure is distributed over the area of cross-section of the hemisphere.

$$\text{Pressure } p = \frac{2\pi rtF}{\pi r^2} = \frac{2Ft}{r}.$$

However, the forces in a myocardial wall are produced by fibrils which provide a linear force tension. In the mature adult, these fibrils are constituted in the form of layers (Robb, Robb, 1942) of parallel fibers which together form a two-dimensional tension. If the forces provided by these layers [or the random distribution of fibrils in the less-developed heart (Manasek, 1968; Challice, Virágh, 1973)] are resolved parallel, and at right angles, to the direction of bi-section (Fig. 2), on average, only one-half of the fibrils will be providing their force at right angles to the split. Thus, the pressure p derived above must be halved if the value of the thickness is not to be doubled.

$$p = \frac{Ft}{r}.$$

(2) *To find the pressure produced by a given volume of contractile musculature:*

Let the total available muscular material be of volume V, and find the force that it can produce in a cylinder, in a sphere with the force applied circumferentially.

(a) Consider the cylindrical tube.

The total volume of muscular material is given by

$$V = 2\pi rlt.$$

Pressure produced (from 1/a) is given by

$$p = \frac{Ft}{r} \cdot \frac{Ft}{r} = \frac{FV}{2\pi rlr} = \frac{FV}{2\pi r^2 l} .$$

(b) Consider the sphere with forces supplied by trabeculae, approximately diametrically disposed, with the total cross-sectional area of the trabeculae small compared with the internal area of the sphere.

Length of each trabecula $= 2r$
Total volume of trabeculae $= 2rA$
Total volume of trabeculae $= V$

where A is the total cross-sectional area of the trabeculae.

Total force produced $= F \cdot A$
Total force produced $= \frac{FV}{2r}$

Here the forces are applied at right-angles to the wall of the vessel, and thus all contribute directly and totally to the pressure inside the sphere. However, the force of tension in each trabecula can be considered only once, but takes up its area of cross-section on the wall of the sphere at each of its ends. Thus, we have to consider the forces applied over a hemisphere, rather than a sphere, as contributing to the pressure inside the sphere.

$$p = \frac{FV}{2r \cdot 2\pi r^2} = \frac{FV}{4\pi r^3} .$$

(c) Consider the same volume V of muscle fibers in a compact myocardial wall.

$$V = 4\pi r^2 t$$

$$t = \frac{V}{4\pi r^2}$$

from 1 (b), we have

$$p = \frac{Ft}{r} = \frac{FV}{4\pi r^2 \cdot r} = \frac{FV}{4\pi r^3} .$$

(3) *Consider the volume flow produced by contractions in the respective cases:*

(a) Volume of cylinder $= x = \pi r^2 l$.

Rate of change of volume with respect to radius (or circumference) is given by

$$\frac{dx}{dr} = 2\pi rl$$

However, r (or the circumference) does not change linearly, but rather in proportion to its length. Hence, volume flow produced by a given contraction is given by

$$r\frac{dx}{dr} = 2\pi r^2 l.$$

(b) For sphere,

$$\text{Volume} = x = \frac{4}{3}\pi r^3.$$

Rate of change of volume with respect to radius is given by

$$\frac{dx}{dr} = 4\pi r^2.$$

Again, r changes in proportion to its length. Hence, volume flow for a given contraction is given by

$$r\frac{dx}{dr} = 4\pi r^3.$$

This is the same whether the contraction is considered in the trabeculae or the circumference. The difference in volume delivery for a given contraction in these two cases is illustrated in Fig. 7.

The above calculations involve approximations, and, in particular:

(1) the thicknesses of the walls of the vessels are small compared with the diameters;

(2) the volume of the lumen occupied by the trabeculae is small compared with the volume enclosed by the myocardial wall.

To take into account the errors introduced by these assumptions makes the mathematics progressively more complex. However, it is clear that assumption 2 is not justified as development of the heart proceeds (in the case of the mouse, 10–12 days post-fertilization).

Taking into account the volume occupied by the trabeculae, and assuming their cross-section remains constant during contraction, the actual change in volume of the lumen is diminished by virtue of the presence of the trabeculae by an amount equal to their volume.

If the radius of the lumen before contraction is r_1 and after contraction is r_2, then,

Volume change without trabeculae present:

$$\Delta V_1 = \frac{4}{3}(r_2^3 - r_1^3).$$

Volume change with trabeculae present:

$$\Delta V_2 = \frac{4}{3}(r_2^3 - r_1^3) \text{ minus volume occupied by trabeculae.}$$

However, this diminution of the volume change would be the same if the same volume of muscular tissue were lining the walls of a chamber without trabeculae.

If, however, the trabeculae tended to become fatter as they contracted to a greater extent than the fibers of a compact myocardial wall, then the change in volume when a trabecular heart contracted would be greater than if the same volume of fibers were incorporated onto the myocardial wall.

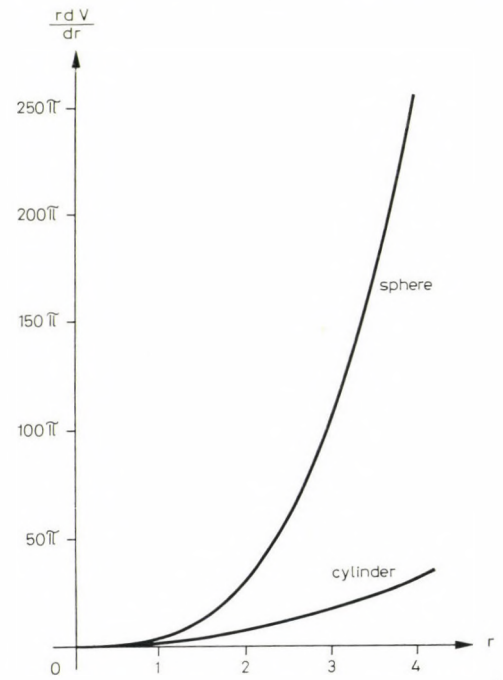

Fig. 7. Graph of volume flow for given contraction (proportional to length of contractile material) against radius of vessel

Discussion

The slow peristaltic contractions of the primitive heart, without valves, is dependent in large measure on the viscosity of the blood to provide a constraint against a back-flow in the axial part of the lumen. It may be compared with a paddling action, such as would be provided by a rowboat held still while the oars were used to paddle the water past. The development of primitive valves, however, provides a system in which a pressure may be built up by contraction of the heart wall. The mathematical analysis shows that the static pressure is less than that of a sphere when the length of the cylinder is greater than its diameter, and the volume delivery of such a system is poorer than that for the spherical chamber. However, this means that, in the cylinder, only a comparatively weak contraction is needed to produce the flow, because a higher mechanical advantage is available in the long tubular heart than in the spherical. This is consistent with the comparative weakness of the musculature found in the cylindrical heart, both phylogenetically (Edwards, Challice, 1960) and ontogenetically (Patten, 1956; Manasek, 1968; Virágh, Challice, 1973) and with the smaller blood flow required of such a heart. Thus, as the musculature becomes stronger, and the need for volume flow of blood greater, it is logical that the development should be accompanied by the formation of near-spherical heart chambers, in which strong muscle is required, but which needs to contract less for a given blood flow (i.e. lower velocity ratio).

Neglecting for the moment the volume occupied by trabeculae, the efficiency of blood delivery for a given contraction is the same for a trabecular heart as for a compact myocardial wall. Furthermore, the trabecular heart and the compact myocardial wall produce the same pressure with the same volume of contractile apparatus. One is thus led to speculate as to why the trabecular heart develops at all, since it seems to have no advantage (in the mechanical sense) over the compact myocardial wall. The most logical explanation seems to be the simple one, the growth conditions are most favorable for such a development. Strings of muscle cells (i.e. trabeculae) grow inward into the nutrient (i.e. the cardiac jelly) since under these conditions the cells have a much greater proportion of their surfaces in contact with the nutrient than if they were on the surface of the myocardial wall. This appears to be the governing factor at the stage where the speed of development of contractile material has to be fastest. However, this type of development clearly cannot proceed indefinitely, since the conclusion would be the elimination of the lumen altogether, and, well before this situation were reached, the trabecular network would be limiting the speed of blood flow through the chambers. Also, as the heart evolves, a progressively more efficient oxygenation system within the myocardial musculature becomes necessary as increased mechanical efficiency is demanded of it, involving an independent vascular system, as distinct from diffusion from the lumen which suffices in more primitive hearts. An arborized arterial system within consolidated tissue is more efficient than in long thin trabeculae, indicating a further reason for

consolidation of the musculature into a myocardial wall. All these factors combine to allow the development of the fast blood flow and higher blood pressures of the mammalian and avian circulatory systems.

There is some evidence to suggest that of the embryonic trabeculae in the heart, which establish the most direct conduction links to the myocardial wall, some retain this conduction role in the mature heart in the false tendons and subendocardial Purkinje fibers.

It is believed that this simple mathematical analysis demonstrates a logical point. The phylogenetic development of the heart and also its ontogenetic development in mammals and birds follows a sequence which is quite logical in the light of this analysis. However, the simplifications and approximations must not be overlooked, particularly as they affect the mature heart of the mammal. Here there is a sequence of contraction in response to sequential electrical stimuli, such that the blood is most effectively moved through the chambers and into the arterial system (Durrer et al., 1965). Also the chambers deviate in shape from that of a sphere, although the muscular wall completely encloses it. A detailed mathematical analysis of the forces produced in such a heart is beyond the scope of the present paper, which seeks only to compare the three systems described, namely, tube, trabecular chambers, and chambers enclosed with compact myocardial walls.

One of the authors (C. E. C.) is indebted to the National Research Council of Canada for a grant which assisted in the support of this work.

References

Challice, C. E., Virágh, Sz. (1974) Tissue and Cell (in press)
Durrer, D., Roos, J. P., Büller, J. (1965) In "International Symposium on the Electrophysiology of the Heart" (B. Taccardi and G. Marchetti, Eds.), pp. 203—214. Pergamon Press, London
Edwards, G. A., Challice, C. E. (1960) Ann. Ent. Soc. Amer. *53* 369
Faber, J. J. (1968) Amer. J. Physiol. *214* 475
Federighi, H. (1928) J. Exp. Zool. *50* 257
Manasek, F. J. (1968) J. Morph. *125* 329
Patten, B. M. (1956) Univ. Mich. Med. Bull. *22* 1
Patten, B. R., Kramer, T. C. (1933) Am. J. Anat. *53* 349
Robb, J. S. (1965) Comparative Basic Cardiology. Grune and Stratton, New York, N. Y.
Robb, J. S., Robb, R. C. (1942) Am. Heart J. *23* 455
Virágh, Sz., Challice, C. E. (1973) J. Ultrastruct. Res. *42* 1

Acta Biochim. et Biophys. Acad. Sci. Hung. Vol. 9 (1–2), pp. 141–149 (1974)

Osmosis; Facts and Theories
I. Osmosis of Water into Heavy Water

F. VETŐ

Biophysical Institute, Medical University, Pécs

(Received November 14, 1973)

The osmosis of H_2O, its volume flow into D_2O, even against a pressure of 1.6 atm without crystalloids or colloids solved corresponding with the difference of vapour pressure and without other forces was demonstrated across $Cu_2Fe(CN)_6$ membrane in a H_2O-D_2O osmometer system. The size of the measured pressure effect is approximately proportional to the "factor of merit" of the membrane. The theories of osmosis are discussed in the light of the data obtained.

Introduction

The knowledge of quantitative connections and molecular mechanism of the simplest model experiments is indispensable for the exact knowledge of biological transport processes. With the examination of more and more complex systems, both the gradual approximation of the complexity of biological processes, and the exact evaluation of increasingly interactions will become possible in possession of this knowledge (Vető, 1972).

Though the phenomenon of osmosis is known for more than 200 years and is the subject of intense investigations and debates for about a century and a half (e.g. Findlay, 1914; Thiel, 1940; Metcalf, 1940; Ray, 1960; Boyer, 1969), its interpretation is not uniform even today, and certain experimental facts can be reconciled with the too much simplified theories with difficulty, even if we consider the recent progress achieved by the thermodynamics of irreversible processes (Kedem, Katchalsky, 1958; Dainty, 1965; Katchalsky, Curran, 1965). The analysis of the causes of concrete, real "anomalies"* can give an opportunity for recognizing new and perhaps significant connections. The aim of the present work is to call attention to certain problems in the application of the simplified theories on the basis of experimental data and, as far as possible, to take into account the factors really determining osmotic transport processes.

First of all we wished to obtain an answer to the question (Ernst, 1972)

* Really, there is no "anomaly" in the phenomena of the nature, perhaps only our knowledge is insufficient.

whether osmotic volume flow and difference of osmotic pressure respectively, could be pointed out without the presence of solutes (s), by opposing pure solvents which are chemically identical, and have equal molecular size but different vapour pressure – normal water (H_2O) and heavy water (D_2O) – e.g. on $Cu_2Fe(CN)_6$ membrane. For this is what can be expected on the basis of vapour pressure theory as opposed to van't Hoff's opinion assuming the gaslike pressure of the molecules of dissolved substances, since $c_s = 0$ and so $\pi = RTc_s = 0$ should be true. The vapour pressure of normal water is 17.53 mmHg at 20°C and that of heavy water is 14.97 mmHg (Kohn, 1965). Certain pertaining data can be found in the literature (e.g. Durbin, 1960; Rastogi, Shukla, 1971), but they are insufficient and the raising of the problem is not the same either.

Methods*

Ernst's osmometer (Ernst, Homola, 1952; Vető, 1967) was used in the experiments (Fig. 1). In addition, a 3-G-4 glass filter was applied in some cases. The length of the clay cylinders was about 16 cm, with an external diameter of 3.8 cm and wall thickness of 4 mm. So the transport took place on a surface of about 180 cm^2. The inside and outside volume varied between 80 and 130 cm^3. The dry weight of the cylinders was about 140 g, the weight of wet cylinders soaked with water was about 170 g. A certain amount of water could pass through the wall at a pressure of one meter water. This values showed great variations, changing between 5 and 150 cm^3 in 1/2 hour. Usually 0.5 osm/l of $K_4Fe(CN)_6$ and 0.5 osm/l of $CuSO_4$ solutions were used for forming the membrane. They were poured on the two sides of the cylinder (or glass filter), and so the $Cu_2Fe(CN)_6$ precipitation membrane was formed about in the middle of the cylinder wall in 1 to 2 weeks. The procedure was repeated whenever necessary. We judged the "merit" of the membrane by changing the concentration of one of the membrane-forming solutions (e.g. to 2 osm/l) and observing normal osmosis. Thereafter, a soaking in distilled water being changed several times followed** and this lasted several days. Then the cylinder was subjected to the pressure of a water column, and the quantity of transmitted water measured. After that – with distilled water on both sides of the cylinder – we watched for several days whether the system was in equilibrium. Then a membrane-test was made again by applying pressure. Only 1/3 of the cylinders prepared proved to be of satisfactory quality. Concentrate heavy water of 99.75 per cent was used in the experiments (deuterium oxide, D_2O made for spectroscopy, obtained from Merck, Darmstadt and the Soviet Union). The normal water used was twice distilled from glass. The apparatus was mostly filled with D_2O inside and H_2O outside and the volume change, or the counterpressure stopping it, was measured

* With the technical assistence of Gabriella Bod.

** In order to remove even the traces of the membrane-forming solutions.

with water-, Hg-, or aneroid manometer. At the end of the experiments (or from time to time also meanwhile) the concentration of D_2O was determined with density measurement with pycnometer and Zeiss's refractometer, respectively, in both chambers, from which the quantities of transmigrated liquids could be calculated. Some inaccuracy was caused by the fact that the quantity of D_2O retained in the wet wall of the cylinder was not directly determined but obtained by calculation only. The measurements were performed at room temperature without using thermostate.

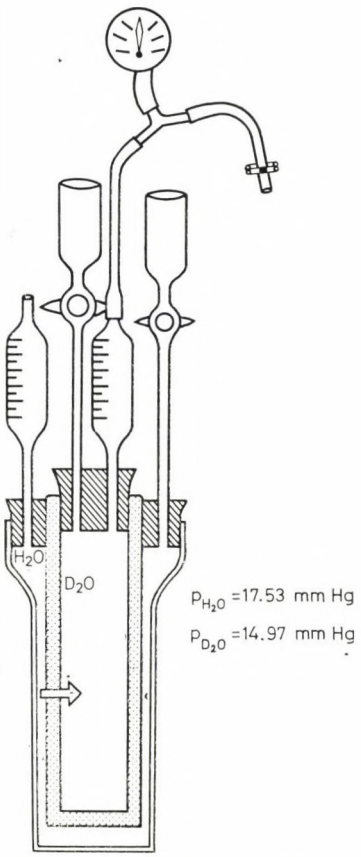

Fig. 1. The osmometer applied in the experiments

In some cases heat-coagulated egg-white gel was used as a membrane, instead of $Cu_2Fe(CN)_6$. The fresh egg-white was whisked, put in a refrigerator to be settled. Then the sediment was drawn up into the wall of the cylinder, and boiled in hot water. In the following the procedure was similar as before except that normal osmosis was brought about with sucrose solution for testing the "merit" of the membrane.

It should be noted that our osmometer is not suitable for producing pressure differences higher than 2 atm; but this was not necessary during the experiments.

Results

As summarized in Table 1 *we were able to observe a net water stream (volume-flow) towards heavy water in each* of the 33 experiments performed in 16 apparatuses. This volume flow towards heavy water could be stopped by pressures applied on D_2O. *The pressure-values stopping the process varied between* 5 *water cm and* 1.6 *atm.*

Table 1

Summary of the results

	Quality of the membrane			
	$Cu_2Fe(CN)_6$		egg white in clay cylinder	total
	in clay cylinder	in G4 glass filter		
Number of apparatuses	13	1	2	16
Number of D_2O-H_2O experiments	27	4	2	33
Measured max. pressure: ΔP_C^D atm	1.6	1.4	0.15	—
Direction of volume flow	in every case from H_2O to D_2O			

In order to find the cause of these significant differences the rate of osmotic volume flow was measured by applying different concentrations of membrane-forming solutions on the two sides, without the simultaneous presence of hydrostatical difference of pressure; moreover, the rate of volume flow caused by hydrostatical difference of pressure was also measured, applying H_2O on both sides. The values measured are shown by Table 2. By forming the quotient of the osmotic volume flow falling to one unit of concentration difference $\left(L_c^s, \frac{\text{cm}^3}{\text{hour osm/l}}\right)$ and the hydraulic volume flow falling to one unit of difference of pressure $\left(L_p, \frac{\text{cm}^3}{\text{hour} \cdot \text{atm}}\right)$, we obtain the so-called "factor of merit" (η^s):

$$\eta^s = L_c^s / L_p \left(\frac{\text{atm}}{\text{osm/l}}\right),$$

the numerical value of which means the difference of pressure expressed in atm, which would bring about the same volume flow as a difference of concentration

Table 2

Data measured in various apparatuses

No.	Sign of apparatus	Quality of membrane	Volume flow caused by membrane-forming Δc L_c^s $\frac{cm^3}{hour \cdot osm/l}$	Volume flow caused by ΔP with H_2O: L_p $\frac{cm^3}{hour \cdot atm}$	"Factor of merit" $L_c^s/L_p = \eta$ $\frac{atm}{osm/l}$	Measured stopping pressure difference: ΔP_c^D atm
1.	3.	$Cu_2Fe(CN)_6$	$\frac{0.80}{2\times 1.5}$	$\frac{0.30}{2\times 1.45}$	2.585	1.60
2.	56.	,,	$\frac{1.20}{4\times 1.5}$	$\frac{0.08}{0.67\times 0.6}$	1.000	0.60
3.	66.	,,	$\frac{0.10}{1\times 1}$	$\frac{0.02}{0.5\times 0.2}$	0.500	0.25
4.	47.	,,	$\frac{0.14}{1.5\times 1}$	$\frac{0.10}{0.5\times 0.2}$	0.093	0.20
5.	55.	,,	$\frac{0.60}{2\times 1.5}$	$\frac{1.40}{0.5\times 0.28}$	0.020	0.14
6.	46.	,,	$\frac{1.00}{4\times 1.5}$	$\frac{0.60}{1\times 0.3}$	0.083	0.10
7.	1.	,,	$\frac{0.80}{2\times 1.5}$	$\frac{0.80}{8\times 0.003}$	0.008	0.05
8.	30.	,,	$\frac{0.80}{6\times 1.5}$	$\frac{0.30}{25\times 0.004}$	0.030	0.036
9.	12.	,,	$\frac{0.80}{3\times 1.5}$	$\frac{0.20}{3\times 0.005}$	0.013	0.026
10.	*F.*	,,	$\frac{1.00}{90\times 1.5}$	—	?	0.013
11.	2.	,,	—	$\frac{1.00}{16\times 0.004}$	?	0.009
12.	23.	,,	—	$\frac{2.10}{24\times 0.003}$	?	0.006
13.	38.	,,	$\frac{0.40}{5\times 1.5}$	$\frac{1.00}{21\times 0.005}$	0.006	0.005
14.	3G4.	,,	$\frac{1.8}{20\times 4}$	$\frac{0.022}{3\times 0.5}$	1.535	1.40
15.	93.	Egg white	—	$\frac{0.30}{0.25\times 0.2}$	?	0.15
16.	85.	,,	$\frac{0.50}{7\times 1}$	$\frac{0.60}{0.083\times 0.3}$	0.003	0.007

of 1 osm/l between membrane-forming solutions (s). This value is an extrapolation calculated on the basis of one pair of measurements each, for the sake of comparability. Its value in an ideal case would be 24.0 $\frac{\text{atm}}{\text{osm/l}}$ at 20°C. Table 2 contains the η^s obtained in this way and also the stopping pressure ($\Delta P_c^{\ominus}$, atm) values measured in each apparatus. If the pairs of value belonging to each other are represented in a co-ordinate system, we obtain Fig. 2. According to this *a close correlation exists between the stopping pressure values measured and the "factors of merit"*: $r = +0.97$; ($n = 12$, $P = 0.001$); further on, the equation of linear regression is: $\Delta P_c^D = 0.66\,\eta^s + 0.05$. From this, neglecting the value

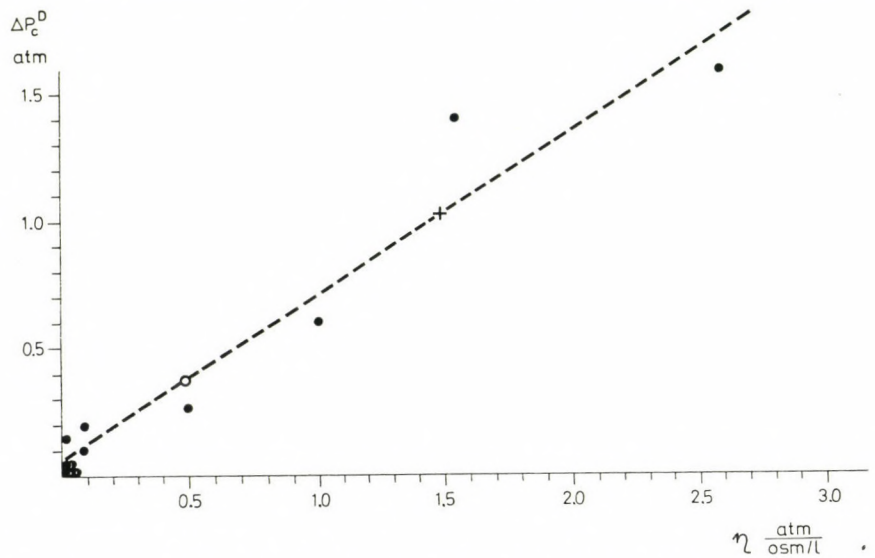

Fig. 2. Pressure values stopping the volume flow from H_2O to D_2O plotted against the "factor of merit" (η) of the membrane

of 0.05, the connection between the "factor of merit" (η^s) as well as the difference of pressure (ΔP_c^D) stopping the $H_2O \rightarrow D_2O$ volume flow is approximately

$$\Delta P_c^D = (0.66 \pm 0.05) \cdot \eta^s$$

in the case of $P < 0.001$, when expressed with the regression coefficient ($\pm$ S.E. osm/l).

The process of an experiment – e.g. on cylinder 3 – was as follows. The wet wall of the cylinder is capable of keeping 31 g, i.e. about 31 cm^3 of water imbibed. From the preceding experiment about 31 cm^3 of D_2O, of about 42 per cent, remained in the wall of the cylinder. The apparatus was filled with 84 cm^3 of D_2O of 99.75 per cent inside and with 126 cm^3 of bisdistilled water outside. A closed pressure-measuring air space of a length of 20 mm and a volume

Table 3

Changes of D_2O-H_2O concentration and volume in one experiment

	outside	in the wall	inside	whole cm^3
At the beginning of the experiment				
Volume cm^3	126	31	84	241
D_2O per cent	0	42	100	—
H_2O cm^3	126	18.7	0	144.7
D_2O cm^3	0	12.3	84	96.3
At the end of the experiment				
Volume cm^3	126	31	84	241
D_2O per cent	18	48	75	—
H_2O cm^3	105.2	16.9	22.6	144.7
D_2O cm^3	20.8	14.1	61.4	96.3
Change				
H_2O cm^3	−20.8	−1.8	+22.6	0
D_2O cm^3	+20.8	+1.8	−22.6	0

of 0.50 cm^3 was left inside, over D_2O in a thin glass tube. Two hours after starting the level of D_2O already rose 7 mm, which meant a plus pressure of 0.5 atm at this time (20/13 = 1.5). Five hours after starting the air space, 20 mm originally, already decreased to 8 mm, so the overpressure (20/8 = 2.5) was 1.5 atm over the heavy water. At that time, in order to controll the system, an artificial pressure of 1.6 atm was applied inside by means of an aneroid manometer. After that no noticeable change occurred, the system became balanced. 24 hours after the start (the pressure had somewhat decreased) the water was poured out and the D_2O concentration measured on both sides. Only a neglectable volume-change occurred during the above pressure measurement; therefore the volumes can be considered practically unaltered. The changes are summarized in Table 3. From this it can be seen that *an exchange of even about* $21-23$ *cm^3 of D_2O-H_2O occurred in the system during one day.*

For the volume flows caused by the D_2O concentration difference (in the case of $\Delta P = 0$) — similarly on cylinder 3 — we obtained the data summarized in Table 4. The coefficient of correlation is: +0.997; the coefficient of regression is:

$$b = (0.022 \pm 0.001) \frac{\text{cm}^3}{\text{hour. 10 per cent}},$$

and $P < 0.01$. *Accordingly, volume flow is approximately proportional to the difference of heavy water concentration between the two sides of the membrane.*

Table 4

Volume flow plotted against D_2O concentration difference

Inside the cylinder	Outside the cylinder	$J_{V,c}^{D}$ $\frac{cm^3}{hour}$
85 per cent D_2O	H_2O	+0.22
70 per cent D_2O	H_2O	+0.17
60 per cent D_2O	H_2O	+0.14
H_2O	H_2O	0
H_2O	43 per cent D_2O	−0.07
H_2O	87 per cent D_2O	−0.18

Discussion

The experiments have given the result expected, i.e. a net water flow towards heavy water, in some cases even against remarkable pressure without the presence of dissolved crystalloids or colloids. This experience can be interpreted qualitatively, as first approximation, with the aid of the vapour pressure theory meaning the 2nd stage of development of theories of osmosis (the first one was van't Hoff's conception). In this interpretation water flows from the pure H_2O of higher vapour pressure (from outside) to the pure D_2O of lower vapour pressure (inward), in accordance with the vapour pressure difference. On this basis the osmotic pressure might be $\pi = \frac{RT}{v} \ln \frac{p_{H_2O}}{p_{D_2O}} \cong 200$ atm at the maximum. However, values 2 orders of magnitude smaller than this were measured, and these, too, strongly differed with various apparatuses. All these events point to the *role of the given structure* ("factor of merit"). Though the size of molecules is formally equal (Kohn, 1965), the appropriate structure makes a slight distinction. It depends on this structure as to what proportion of the working ability of the given chemical potential difference would perform effective osmotic work, and what proportion dissipates without performing any work. So it is that the application of non-equilibrium thermodynamics becomes indispensable for these processes (3rd stage of development), which – though only with phenomenological coefficients and in linear approximation – considers also the concrete structural-dynamical characteristics. The "factor of merit" used by us (η^s) essentially corresponds to Staverman's (Staverman, 1951) reflection coefficient (σ^s, for the ions of membrane-forming substances), and does not differ from it but in the conversion factor ($\eta^s = \sigma^s RT$), only η^s being somewhat more concrete.

The calculation of the osmotic pressure of 200 atm in the above way raises further problems. That is to say if we calculate in this way, we implicitly suppose that there is the same substance on both sides of the membrane, i.e. water. If it were so – as no other thermodynamical force can be taken into account –

there would be no difference in activity and vapour pressure. Therefore, for the correct calculation, D_2O must be considered as a solute and in this case (if only H_2O would penetrate and D_2O not) the difference in the maximum osmotic pressure would be theoretically:

$$\pi = \frac{RT}{v} \ln \frac{a_{H_2O,\,o}}{a_{H_2O,\,i}} = \frac{RT}{v} \ln \frac{p_{H_2O,\,o}}{p_{H_2O,\,i}} = \frac{82 \cdot 293}{18} \ln \frac{17.53}{0.0487} = 7846 \text{ atm};$$

since the vapour pressure of H_2O in the D_2O of 99.75 per cent is 0.0487 mmHg. The value measured was about 4 orders of magnitude smaller, because the structure hardly makes any difference between H_2O and D_2O. For the sake of comparison it should be mentioned that, in the opinion of Durbin (1960), in a membrane dialyzing against D_2O $\sigma^D = 0.002$, and that also in the opinion of Kedem, Katchalsky (1958) ". . . heavy water behaves as an ordinary solute . . .".

For demonstrating that on the basis of the simplified vapour pressure conception we contradict the facts, further experiments were performed in systems of D_2O and normal watery solution. Their results will be reported in a forthcoming paper.

The author expresses his thanks to Prof. Ernst for raising the starting problem.

References

Boyer, J. S. (1969) Ann. Rev. Plant Physiol. *20* 345
Dainty, J. (1965) in: State and Movement of Water in Living Organisms. Cambridge, Univ. Press, p. 75
Durbin, R. P. (1960) J. Gen. Physiol. *44* 315
Ernst, E. (1972) Acta Biochim. Biophys. Acad. Sci. Hung. *7* 377
Ernst, E., Homola, L. (1952) Acta Physiol. Acad. Sci. Hung. *3* 487
Findlay, A. (1914) Der osmotische Druck. Steinkopff, Dresden
Katchalsky, A., Curran, P. F. (1965) Nonequilibrium Thermodynamics in Biophysics. Harvard Univ. Press, Cambridge, Mass.
Kedem, O., Katchalsky, A. (1958) Biochim. Biophys. Acta *27* 229
Kohn, P. G. (1965) in: State and Movement of Water in Living Organisms. Cambridge, Univ. Press, p. 3
Metcalf, W. V. (1940) Kolloid Z. *90* 11
Rastogi, R. P., Shukla, P. C. (1971) Biochim. Biophys. Acta *249* 454
Ray, M. (1960) Plant Physiol. *35* 783
Staverman, A. J. (1951) Rec. trav. chim. *70* 344
Thiel, A. (1940) Kolloid Z. *91* 316
Vető, F. (1967) Acta Biochim. Biophys. Acad. Sci. Hung. *2* 441
Vető, F. (1972) Abstracts — Ion Transport across Membranes — First Res. Conference of Experts from Socialistic Countries. Reinhardsbrunn Castle, GDR p. 62

Acta Biochim. et Biophys. Acad. Sci. Hung. Vol. 9 (1–2), pp. 151–158 (1974)

Mechanical Characteristics of Resting and Contracting Muscle

S. JURICSKAY

Biophysical Institute, Medical University, Pécs

(Received August 9, 1973)

A dynamic method of examination based on the phenomenon of resonance has been developed for measuring the mechanical (rheological) characteristics of the muscle. The quantitative data of the frequency of free oscillations, attenuation constant and factor of merit of the frog sartorius muscle loaded with a constant mass in the state of rest and in the state of contraction significantly differ from each other. The difference between the two states is brought into connection with the molecular rearrangement, crystallization, occurring during the stretch of the muscle.

Introduction

Ernst and Koczkás (1935) were the first to report that muscle performs an elastic, damped oscillatory motion just as do other elastic bodies (e.g. rubber) in the state of rest following stretching and sudden release. On the other hand, in the response of the muscle in tetanic state to stretching and quick relase there is a damping of such degree that vibration cannot be experienced at all, the muscle does not accumulate elastic energy. These facts are supported by Niedetzky's (1959, 1965) experiments performed on other muscles. The thermoelectric measurements of Hill (1950) showed that the input mechanical work in a muscle did not manifest itself during contraction even in the form of heat production. From the above experiments Ernst (1950, 1963) drew the conclusion that a qualitative transformation, crystallization of the substance of the muscle ensues during stretch.

In linear approximation, the equation of motion: $m\ddot{x} + S\dot{x} + kx = 0$ serves for the description of a damped elastic system. The equation $\ddot{x} + 2\delta\dot{x} + \omega_0^2 x = 0$ is obtained by dividing by the accelarated mass m and by introducing new constants (see e.g. Budó, 1964). It was the aim of the present experiments to determine the free oscillation frequency ω_0 characterizing elasticity and the damping factor δ connected with the internal friction in the resting (passive) and contracting (active) state of the muscle.

For the determination of the above parameters – because of the difficulties in the mathematical analysis of the vibration pattern – the phenomenon of

forced oscillation offers itself because the factor of merit Q characteristic of the energy conditions, can also be simply determined beside the above-mentioned data, on the basis of the characteristic curves of resonance.

Methods

For the measurements a new displacement measuring system, a mechano-electric transducer was constructed, which must suit the requirements as follows:

a) It should have negligibly small mass and friction during motion in order not to load the system to be measured.

b) It should have a high sensitivity in order to be able to measure even slight shifts reliably.

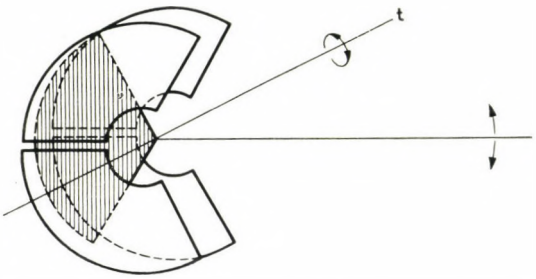

Fig. 1. Scheme of mechanics of the differential condenser transducer

c) Its characteristic curve should be linear within a wide range in order that no distortion occur because of the relatively large shifts in contraction.

Considering the above requirements a differential condenser arrangement was chosen (Fig. 1) the essentials of which were two couples of parallel-connected fixed condenser armatures which surrounded the moving armature. The three armatures are isolated by two narrow air gaps in a sandwich-like manner. Each armature is a sector of an angular aperture of 120° and a radius of 3.5 cm, made of steel plates of 0.1 mm. The moving armature is fitted up on a watch-axle with ruby bearing, perpendicular to the plate, the swing of which is ensured by a steel lever compensated to have a symmetrical moment of inertia. The small capacities of strayfield change opposite to the angular displacement of the lever, and so the mechanical shift is transformed into an electric change. Fig. 2 shows the circuit diagram of the electronic detector.

The capacity of the elements of the differential condenser is 17 pF in a symmetrical state, the change in final amplitude is ± 5 pF. The basic frequency of the oscillator of the detector is 994 kHz, the D. C. voltage of proper sign appear-

ing on the filtered output is proportional to the angular displacement from the resting state of the lever and – as we are talking about small angles – it is proportional to the shift of the end of the lever. The output voltage-shift characteristic (Fig. 3) was determined with the aid of a micrometer screw and digital voltmeter under static conditions. The sensitivity determined from the characteristic is 59.4 mV/mm, linearity and reproducability in the indicated range of 25 mm is better than 0.3 per cent. The effective mass of the transducer measured under dynamic conditions is 77 mg, the effective spring-constant of the back-moving hair-spring serving also as an electric connection is 1.27 dyn/cm, the coefficient of friction is smaller than 0.1 g/s. The technical parameters of the transducer suit the above-mentioned requirements.

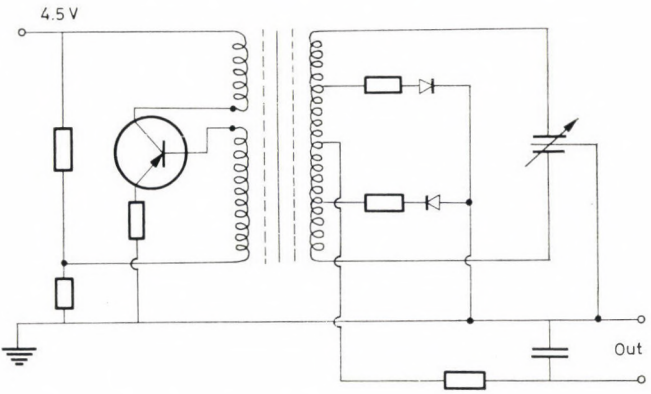

Fig. 2. Electronic circuit diagram of the detector of capacity change

Sartorius muscles of the frog *Rana esculenta* prepared in pair together with the hip-bone stumpf were used in the experiments. It is the advantage of this preparation that its fibres run parallel and the quantity of connective tissue elements can be neglected. The bone was bored and steadily fixed to a stand of large mass in vertical arrangement (Fig. 4). The lever of transducer was linked to the interconnected distal tendons by means of a steel hook and a thin chain.

The advantage of the use of the chain is that it is strong enough not to be elongated during loading, but still not rigid, so it can be used conveniently (Ernst, Koczkás, 1935; Ernst, 1963). A copper weight was hanging at the end of the chain. The soft iron core connected with the loading was placed in a vertically sliding coil which could be fixed at any position. The total load application to the muscle was chosen as the result of a compromise. In case of a small mass the frequencies of the vibrations to be measured would be too close to the eigenfrequency of the transducer, which would give false results; in case of a too large loading the muscle would stretch so much that a great deviation from the physiological

basic length (resting length) would occur. Considering these factors we have chosen the total loading to be 19 g in each experiment, and large frogs were used.

Conduction of current impulses of adjustable amplitude, time and frequency continuously into the coil, with the aid of a transistor electric swith causes the

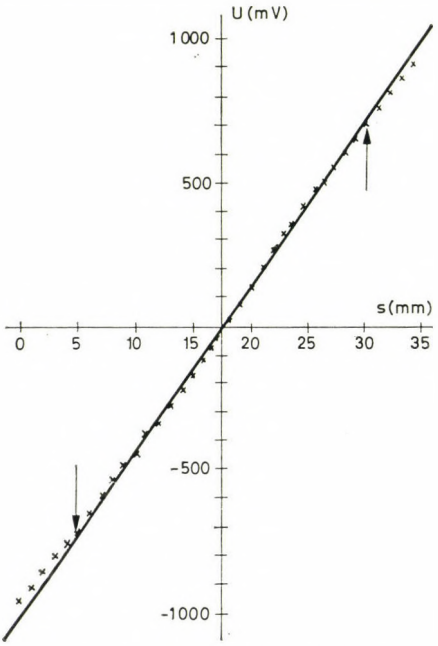

Fig. 3. Characteristics of displacement measuring transducer

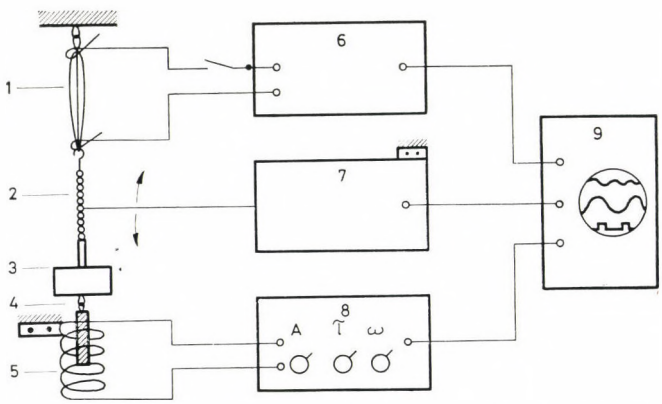

Fig. 4. Scheme of arrangement of forced oscillation experiments: (1) muscle, (2) chain, (3) loading, (4) iron-core, (5) coil (6) mains transformer, (7) shift transducer, (8) current impulse generator, (9) oscilloscope

occurring periodic power to excite the muscle to longitudinal vibration. The time of the pulling current impulses was chosen between 15 – 20 ms (and left unchanged in all experiments) so that it should not be too small for avoiding the appearance of excitations of higher order (e.g. the natural vibration of the steel lever), and it should not be too long either, since the sinusoidal character of the change of length becomes strongly distorted under such conditions, and we cannot obtain evaluable information on phase relations. In choosing the amplitude of periodic stretching the main point of view was that the amplitude of the vibration developed be well measurable noiselessly, and do not reach 0.5 mm even near the resonance.

The signals produced by the transducer and other signals proportional to the pulling current impulses were recorded on a multi-beam oscilloscope operated in triggered running, A. C. signals of 50 Hz were used as time marks. After the short transient phenomena photographs were taken of the screen. The amplitudes, phase and time (frequency) relations of quasi-sinusoidal change of length were measured by projecting them on millimeter-scale paper.

On some occasions, the muscle was brought into a state of short (3 – 5 s) tetanus by direct stimulation with the aid of the 6 V output of a mains transformer, on loops of platinum wires fixed at both ends. Shortening of the muscle in tetanus was 30 per cent of the resting length. The pulling coil and the displacement meter were adjusted during a pilot experiment higher than in tetanic experiments, in order to ensure circumstances similar to the resting condition (strength of pulling, sensitivity of detection, etc.). The muscle was left rested for 1 to 2 min between excitations of different frequency and the respective tetani and rinsed with Ringer solution of normal composition.

Results

Keeping all parameters at a constant value, only changing the time of period of pulling, we plotted the standardized data of shift amplitude and of phase delay against the frequency in a co-ordinate system in case of each experiment. The typical resonance curves obtained in the resting (passive) and tetanic (active) state of a muscle can be seen in Fig. 5. Reading the frequencies ω_r belonging to the maximum amplitude, and ω_1 and ω_2 belonging to the $A_{max}/\sqrt{2}$ value, respectively, from the curves of resonance we determined the values of ω_0 and δ with the aid of the following connections:

$$\delta = \frac{\omega_2 - \omega_1}{2}, \quad \text{and} \quad \omega_0 = \sqrt{\omega_r^2 + 2\delta^2}.$$

The equality $Q = \frac{\omega_0}{2\delta}$ was used for calculating the factor of merit. Table 1 shows the average values and mean errors of ω_0, δ and Q parameters determined

as described above in experiments performed on 11 muscles in passive and active state. The *t*-test shows a significant difference to exist between the data obtained in the two states, at a level of probability of $P = 0.001$ for each value. The frequency of free oscillation (ω_0), characteristic of the elasticity of the muscle, is

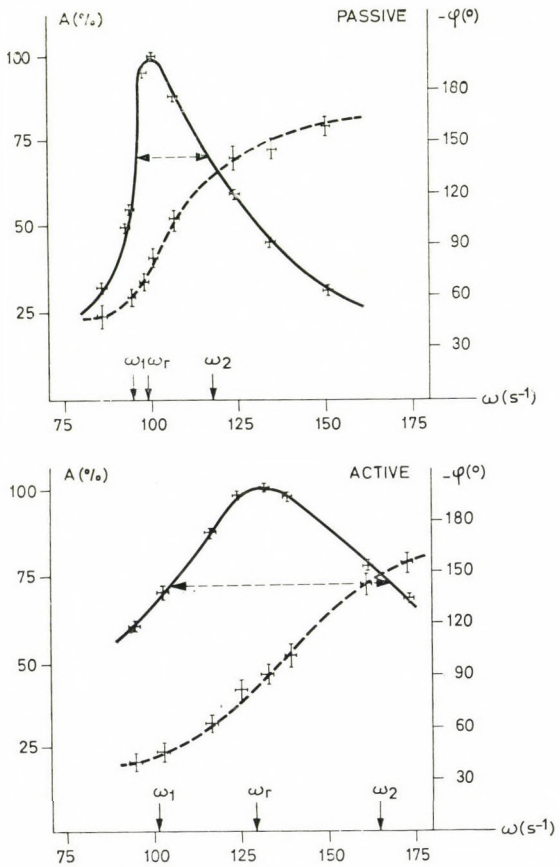

Fig. 5 Typical amplitude and phase-delay resonance curves of a muscle in passive and active state

Table 1

Mechanical characteristics of sartorius muscle

	Frequency of free oscillation (ω_0)	Damping factor (δ)	Factor of merit (Q)
Passive	112 ± 2 c/s	11.5 ± 1.0 s^{-1}	5.3 ± 0.4
Active	138 ± 4 c/s	28.0 ± 3.0 s^{-1}	2.7 ± 0.2

shifted towards higher values in the active state, and the damping factor (δ) increases over the twofold of its original value. The factor of merit (Q) which is proportional to the quotient of the average energy of the oscillating system and the energy periodically fed in, necessary for the maintenance of the vibration, decreases significantly.

Discussion

The method of examination developed in the present work proved to be appropriate for obtaining quantitative data on the mechanical characterization of the resting and contracted muscle. The result concerning the frequency of free vibration characteristic of elasticity is in accordance with the change expected on the basis of change in length – stretch diagrams measured in static circumstances (Tigyi, 1955). The dynamically measurable elastic constant of the muscle in a given steady state of loading can be determined with the rise of the static curve at this point and our result can be well interpreted on the basis of its greater values measured in contracted state.

The increase of the value of damping constant in the active state can be explained by several microphysical changes not excluding each other.

One of the explanations can be the process of settlement similar to crystallization or phase transformation of the oriented macromolecules of muscle-substance (perhaps going on in certain ranges only), which is responsible for the increased internal friction. This hypothesis is supported by the decreased water-binding under the effect of stretching of the muscle, the change of birefringence, volume decrease and other effects (Ernst, 1950, 1963). The relaxation process increased due to the delayed recovery of crystallization can be responsible for the flattening of the incomplete tetanus ensued from the effect of stretch (Ernst et al., 1951). This phenomenon can give a new explanation of the catch-mechanism experienced in the smooth muscle of shells not considered up to now, where the maintenance of stretch was attributed to an independently working rigid tropomyosin-paramyosin system (Lowy et al., 1964; Rüegg, 1964), the stiffness of which – increased during closing – should cause the great stretch resistance and the extreme increase of relaxation time. Millman and Elliott (1972) published also X-ray diffraction data in connection with this.

The change of the factor of merit and, at the same time, the change of dissipation of mechanical energy can be an essential factor (comparing it with reliable thermodynamical experimental results) in throwing light on the mechanism of contraction. In any case it is obvious that theoretical considerations describing the activity of muscle (Huxley, 1953; Garamvölgyi, Belágyi, 1968), the so-called muscle models, must take into consideration also what was said above, just as all the other data of macroscopic measurement.

The author wishes to express his thanks to Prof. Ernst for inspiration to the present work.

References

Budó, A. (1964) Mechanika. Tankönyvkiadó, Budapest (Hungarian)
Ernst, E. (1950) XVIII. Int. Physiol. Congr. Copenhagen p. 189
Ernst, E. (1963) Biophysics of Striated Muscle. Akadémiai Kiadó, Budapest
Ernst, E., Koczkás, J. (1935) Z. Biol. *96* 206
Ernst, E., Tigyi, J., Ladányi, G. (1951) Acta Physiol. Acad. Sci. Hung. *2* 261
Garamvölgyi, N., Belágyi, J. (1968) Acta Biochim. Biophys. Acad. Sci. Hung. *3* 293
Hill, A. V. (1950) Proc. Roy. Soc. B. London *137* 273
Huxley, H. E. (1953) Biochim. Biophys. Acta *12* 387
Lowy, J., Millman, B. M., Hanson, J. (1964) Proc. Roy. Soc. B. London *160* 525
Millman, B. M., Elliott, G. F. (1972) Biophys. J. *12* 1405
Niedetzky, A. (1959) Acta Physiol. Acad. Sci. Hung. *9* Suppl. 2
Niedetzky, A. (1965) Kísérletes Orvostudomány *11* 429 (Hungarian)
Rüegg, J. C. (1964) Proc. Roy. Soc. B. London *160* 536
Tigyi, J. (1955) Candidate's dissertation. Budapest (Hungarian)

Hoppe-Seyler's Zeitschrift für Physiologische Chemie

Editors in chief

A. BUTENANDT · F. LYEN · G. WEITZEL

Subscription Rate

For one volume (12 parts) DM 480,—

Vol. 354 No. 9 September 1973

CONTENTS

Indexed in Current Contents

W DE G

Walter de Gruyter · Berlin · New York

Hoppe-Seyler's Zeitschrift für Physiologische Chemie

Editors in Chief

A. BUTENANDT · F. LYNEN · G. WEITZEL

Subscription Rate

For one volume (12 parts) DM 480,–

Vol. 354 No. 10/11 Okt./Nov. 1973 10/11

CONTENTS

Indexed in Current Contents

W DE G

Walter de Gruyter · Berlin · New York

Hoppe-Seyler's Zeitschrift für Physiologische Chemie

Editors in Chief

A. BUTENANDT · F. LYNEN · G. WEITZEL

Subscription Rate

For one volume (12 parts) DM 480,—

Vol. 354 No. 17. Dezember 1973

CONTENTS

Walter de Gruyter · Berlin · New York

W DE G

Walter de Gruyter
Berlin · New York

R. C. Allen — H. R. Maurer
(Editors)

Electrophoresis and Isoelectric Focusing in Polyacrylamide Gel

Advances of Methods and Theories, Biochemical and Clinical Applications

1974. Large-octavo. 316 pages. With 115 illustrations and 19 charts.
Bound DM 105,– ISBN 3 11 004344 0

This book presents the most recent advances of the methods of electrophoresis (PAGE) and isoelectric focusing (PAGIF) in polyacrylamide gel which have gained wide use in fields of biology and medicine. Described in detail are new findings on the physico-chemical properties of the gel itself (Morris, Richards), theory and practice of optimization, standardization and evaluation of polyacrylamide gel electrophoresis (Maurer, Robard, Chrambach, Allen), isoelectric focusing and isotachophoresis in polyacrylamide gel (Vesterberg, Pogacar, Griffith, Catsimpoolas), quantification methods (Allen, Kling, Catsimpoolas), preparative methods (Nees, Grässlin), micro methods (Grossbach, Neuhoff, Ruchel, Dames, Maurer, Giebel), biochemical applications for isozymes and nucleic acids (Uriel, Richards, Staynov, Phillips), clinical applications (Hunter, Hoffmeister, Abraham, Felgenhaurer, Allen, Utterman). The various chapters in this volume are comprised of papers presented at a conference held at Tübingen, Germany October 6-7, 1972. This conference was arranged to bring together a group of specialists in the field in order to assess the state of the art, to discuss problems of standardization and optimization of separations, to relate theoretical considerations to practical application, as well as to discuss the limitations and future potential of these techniques in biology and medicine. This volume should serve as a usefull reference to investigators and students who wish to, or who are already employing PAGE and PAGIF in their work.

MATHEMATICAL MODELS OF METABOLIC REGULATION

Post-Congress FEBS Advanced Course No. 27

will be held in Hungary from 1 to 5 September, 1974.

The 9th FEBS Meeting (Budapest, August 25 – 30, 1974) will be correlated with the Advanced Course. Part of the Course will constitute of seminars on lectures given in Symposium 2 (Mechanism of Action and Regulation of Enzymes) and Colloquium III (Analysis and Simulation of Biochemical Systems) of the Meeting. Students are recommended to attend these lectures. Second part of the Course will include lectures on selected chapters of enzyme kinetics and analysis of metabolic systems not discussed at the Meeting.

The fee for scholars will be 170 dollars or equivalent, which includes the registration fee for the 9th FEBS Meeting and accommodation and meals during the Advanced Course (but *not* during the Meeting!). The papers presented at the FEBS Advanced Course No. 24 on Mathematical Models of Metabolic Regulation (Oberhof, GDR, 1972) are available at a modest price from Prof. Dr. H. Frunder (Physiol.-Chem. Inst. der Friedrich Schiller Univ. 69 Jena. Zentraler Platz. GDR).

The number of students is limited. Correspondence should be sent as soon as possible to FEBS Advanced Course, c/o Dr. T. Keleti, Enzymol. Dept., Inst. Biochem. Hung. Acad. Sci. H-1502 Budapest, Pf. 7. Hungary.

Lehrbuch der anorganischen Chemie

Begründet von **A. F. Holleman**

Von Dr. Dr. h. c. Dr. h. c. **Egon Wiberg,** Professor an der Universität München

71. — 80., völlig umgearbeitete und stark erweiterte Auflage
mit einem Anhang Chemiegeschichte, Raumbilder-Erläuterungen, einem Tabellen-Anhang, sowie 216 Figuren und einer Beilage von 37 Struktur-Bildern in stereoskopischer Darstellung.
Groß-Oktav. XXXII, 1209 Seiten. 1971. Balacron DM 58,—

Der Text der 71. — 80. Auflage des Lehrbuches wurde völlig umgestalltet und stark erweitert, so daß ein neues Werk entstanden ist, das sie jetzt nicht mehr — wie bisher — nur an den Anfänger, sondern auch an die Fortgeschrittenen der Chemie wendet.

Das Buch gliedert sich in vier große Hauptteile:

A: Atom und Molekül
B: Hauptgruppen des Periodensystems
C: Nebengruppen des Periodensystems
D: Lanthaniden und Actiniden

Den Abschluß des Buches bilden: ein chemiegeschichtlicher Anhang, ein Anhang mit Erläuterungen zur angefügten Raumbilder-Beilage und ein Tabellen-Anhang. Die Atomgewichte, Elementhäufigkeiten, physikalische Daten und atomaren Konstanten entsprechen dem neusten Stand.

Die Anzahl der Abbildungen, Tabellen und tabellarischen Überblicke wurde beträchtlich erhöht. Die Raumbilder-Beilage wurde um 6 Atomstrukturen vermehrt.

Walter de Gruyter & Co · Berlin 30

Printed in Hungary

A kiadásért felel az Akadémiai Kiadó igazgatója Műszaki szerkesztő: Zacsik Annamária

A kézirat nyomdába érkezett: 1974. II. 7. — Terjedelem: 14,70 A/5 ív, 75 ábra

74.00008 Akadémiai Nyomda, Budapest — Felelős vezető: Bernát György

Reviews of the Hungarian Academy of Sciences are obtainable at the following addresses:

ALBANIA

Drejtorija Qändrone e Pärhapjes
dhe Propagandimit tä Librit
Kruga Konferenca e Päzes
Tirana

AUSTRALIA

A. Keesing
Box 4886, GPO
Sydney

AUSTRIA

Globus
Höchstädtplatz 3
A-1200 Wien XX

BELGIUM

Office International de Librairie
30, Avenue Marnix
Bruxelles 5
Du Monde Entier
5, Place St.-Jean
Bruxelles

BULGARIA

Hemus
11 pl Slaveikov
Sofia

CANADA

Pannonia Books
2 Spadina Road
Toronto 4, Ont.

CHINA

Waiwen Shudian
Peking
P. O. B. 88

CZECHOSLOVAKIA

Artia
Ve Směčkách 30
Praha 2
Poštovní Novinová Služba
Dovoz tisku
Vinohradská 46
Praha 2
Mad'arska Kultura
Václavské nám. 2
Praha 1
Slovart A. G.
Gorkého
Bratislava

DENMARK

Ejnar Munksgaard
Nörregade 6
Copenhagen

FINLAND

Akateeminen Kirjakauppa
Keskuskatu 2
Helsinki

FRANCE

Office International de Documentation
et Librairie
48, rue Gay-Lussac
Paris 5

GERMAN DEMOCRATIC REPUBLIC

Deutscher Buch-Export und Import
Leninstraße 16
Leipzig 701
Zeitungsvertriebsamt
Fruchtstraße 3—4
1004 Berlin

GERMAN FEDERAL REPUBLIC

Kunst und Wissen
Erich Bieber
Postfach 46
7 Stuttgart S.

GREAT BRITAIN

Blackwell's Periodicals
Oxenford House
Magdalen Street
Oxford
Collet's Subscription Import
Department
Dennington Estate
Wellingsborough, Northants.
Robert Maxwell and Co. Ltd.
4—5 Fitzroy Square
London W. 1

HOLLAND

Swetz and Zeitlinger
Keizersgracht 471—487
Amsterdam C.
Martinus Nijhof
Lange Voorhout 9
The Hague

INDIA

Hind Book House
66 Babar Road
New Delhi 1

ITALY

Santo Vanasia
Via M. Macchi 71
Milano
Libreria Commissionaria Sansoni
Via La Marmora 45
Firenze
Techna
Via Cesi 16
40135 Bologna

JAPAN

Kinokuniya Book-Store Co. Ltd.
826 Tsunohazu 1-chome
Shinjuku-ku
Tokyo
Maruzen and Co. Lt
P. O. Box 605
Tokyo-Central

KOREA

Chulpanmul
Phenjan

NORWAY

Tanum-Cammermeyer
Karl Johansgt 41—43
Oslo 1

POLAND

Ruch
ul. Wronia 23
Warszawa

ROUMANIA

Cartimex
Str. Aristide Briand 14—18
Bucureşti

SOVIET UNION

Mezhdunarodnaya Kniga
Moscow G—200

SWEDEN

Almquist and Wiksell
Gamla Brogatan 26
S—101 20 Stockholm

USA

F. W. Faxon Co. Inc.
15 Southwest Park
Westwood Mass. 02090
Stechert Hafner Inc.
31 East 10th Street
New York, N. Y. 10003
Dr. Alan Bergelson
Corning Scientific Instruments
Medfield, Massachusetts 02052

VIETNAM

Xunhasaba
19, Tran Quoc Toan
Hanoi

YUGOSLAVIA

Forum
Vojvode Mišića broj 1
Novi Sad
Jugoslovenska Knjiga
Terazije 27
Beograd

Contents

4. VII. 1974 Index: 26.030

VOLUME 9
NUMBER 3
1974

Acta biochimica et biophysica

ACADEMIAE SCIENTIARUM HUNGARICAE

AKADÉMIAI KIADÓ, BUDAPEST

ABBPAP 9 (3) 159–276 (1974)

Acta Biochimica et Biophysica

Academiae Scientiarum Hungaricae

Szerkeszti:

STRAUB F. BRUNÓ és ERNST JENŐ

Technikai szerkesztők:

SAJGÓ MIHÁLY és NIEDETZKY ANTAL

Szerkesztőség postai címe: 1502 Budapest, Pf. 7 (biokémia)
7643 Pécs, Pf. 99. (biofizika)

Az *Acta Biochimica et Biophysica* a Magyar Tudományos Akadémia idegen nyelvű folyóirata, amely angol nyelven (esetleg német, francia vagy orosz nyelven is) eredeti tanulmányokat közöl a biokémia és a biofizika — fehérjék (struktúra és szintézis), enzimek, nukleinsavak, szabályozó és transzport-folyamatok, bioenergetika, izom-összehúzódás, radiobiológia, biokibernetika, funkcionális és ultrastruktúra stb. — tárgyköréből.

A folyóirat negyedévenként jelenik meg, a négy füzet évente egy kb. 400 oldalas kötetet alkot. Kiadja az Akadémiai Kiadó.

Megrendelhető az Akadémiai Kiadónál (1363 Bp. Pf. 24.), a külföld részére pedig a Kultúra Könyv és Hírlap Külkereskedelmi Vállalatnál (1389 Budapest 62, P.O.B. 149).

The *Acta Biochimica et Biophysica*, a periodical of the Hungarian Academy of Sciences, publishes original papers, in English, on biochemistry and biophysics. Its main topics are: proteins (structure and synthesis), enzymes, nucleic acids, regulatory and transport processes, bioenergetics, excitation, muscular contraction, radiobiology, biocybernetics, functional structure and ultrastructure.

The Acta Biochimica et Biophysica is a quarterly, the four issues make up a volume of some 400 pages per annum. Manuscripts and correspondence with the editors and publishers should be sent to

Akadémiai Kiadó, Budapest 24, P.O.B. 502.

The subscription rate is $ 32.00 per volume. Orders may be placed with *Kultúra* Trading Co. for Books and Newspapers (1389 Budapest 62, P.O.B. 149) or with its representatives abroad, listed on p. 3 of the cover.

Acta Biochimica et Biophysica — журнал Академии Наук Венгрии, публикующий на английском языке (возможно и на немецком, французском и русском языках) оригинальные статьи по проблемам биохимии и биофизики — белков (структура и синтез), энзимов, нуклеиновых кислот, процессов регуляции и транспорта, биоэнергетики, мышечного сокращения, радиобиологии, биокибернетики, функциональной структуры и ультраструктуры и т. д.

Журнал выходит ежеквартально, выпуски каждого года составляют том объемом около 400 страниц. Журнал выпускает Издательство Академии Наук Венгрии.

Рукописи и корреспонденцию просим направлять по следующему адресу:

Akadémiai Kiadó, Budapest 24, P.O.B. 502.

Подписная цена — $ 32.00 за том. Заказы принимает:

Предприятие по внешней торговле книгами и газетами «Kultúra» (1389 Budapest 62, P.O.B. 149) или его заграничные агентства.

Acta Biochim. et Biophys. Acad. Sci. Hung. Vol. 9 (3), pp. 159–173 (1974)

Dynamic Compartmentation in Soluble Enzyme Systems

P. FRIEDRICH

Enzymology Department, Institute of Biochemistry, Hungarian Academy of Sciences, Budapest, Hungary

(Received March 12, 1974)

A model is described that may account for compartmentation effects in soluble enzyme systems, a phenomenon frequently observed in metabolic pathways. The principal features of the model are as follows: a) functionally adjacent enzymes display affinity towards each other, which leads to the transient formation of heterologous enzyme–enzyme complexes; b) metabolites are transferred directly from one enzyme to the other in the enzyme complexes; c) the binding sets for the two functionally adjacent enzymes are created alternatively as a conformative response of the enzyme protein. The model is discussed in light of the current knowledge on protein structure and enzyme function.

Introduction

Compartmentation is one of the basic devices that enable living systems to maintain their integrity. The spatial separation of the various metabolic processes at the intracellular level ensures that undue equilibration of metabolites, as well as of macromolecules, should not take place.

The major compartments of a cell can be assigned to definite morphological entities. These are enclosures limited by well-defined boundaries, membranes, the function of which is to decide what to let into, or let out from, the compartment.

The content of a compartment is highly characteristic. As far as macromolecules, in particular enzymes, are concerned DeDuve (1964) has formulated the "*postulate of single location*", which in brief means that each enzyme in the cell has its unique site of occurrence. In respect of small molecules, the compartments accommodate the various metabolite "*pools*". This operational term denotes a certain amount of a compound, or a family of compounds, that can be distinguished from the rest of cellular material (including often the same compound(s)) on the basis of some criterion, such as extractability or isotopic labelling.

However, for not all cases of compartmentation, and thus for not all pools, can a structural counterpart be found. Several examples are known where more than one pool of a metabolite occurs in a single compartment (*e.g.* London, 1966; Macnab et al., 1973; Tokumitsu, Ui, 1973; Balusubramanian et al., 1973; Till et al., 1973) or different metabolites, and probably pathways, are segregated within one compartment (Bearden, Moses, 1972). Furthermore, certain enzyme reactions in the cell are out of equilibrium, although kinetic reason for that, based on the

study of isolated enzymes, cannot be readily visualized (Rose et al., 1962). To account for such puzzling facts, usually some *ad hoc* assumptions are made, which often involve complex formation between enzymes, thereby providing a channelling device for metabolites. In fact, the segregation of pathways, or critical points of a pathway, through protein–protein interactions has already become a familiar property in the realm of multienzyme complexes (Reed, Cox, 1970; Ginsburg, Stadtman, 1970). It is difficult, however, to conceive such a mechanism for soluble enzymes, like the glycolytic system, where the assembly of a rigid multienzyme aggregate does not seem probable, at least on the basis of data available so far.

In the present paper a molecular model is described which may account for compartmentation effects in soluble enzyme systems. It is based on prevailing ideas of protein design and enzyme function. The model will be expanded stepwise, in the order of increasing sophistication, so that it might cover simple or more complex real systems as well.

The model

1. *Direct metabolite transfer through the "complementary cage" effect*

Let us consider in a metabolic pathway catalyzed by a soluble enzyme system a step that should be segregated for some reason. In the simplest case this step is a one substrate-one-product enzyme reaction, *i.e.* the net reaction is $S \rightleftharpoons P$. The substrate, S, of the enzyme in question is at the same time the product of the preceding enzyme of the pathway, whereas the product, P, is the substrate of the subsequent enzyme. Consequently, in the compartmentation of S and P three enzymes must be involved, which will be denoted in the order they occur in the pathway as E_1, E_2 and E_3.

The following postulates are made:

i) E_2 exhibits affinity towards E_1 and E_3, the functionally adjacent enzymes. This affinity is due to specific complementary binding sets on the respective enzymes. These will be referred to as "*foreign recognition sites*".

ii) The affinities between the enzymes are low, hence the enzyme complexes formed are of marginal stability ($K_{D'S}$ are high). Nevertheless, the affinity between adjacent enzymes is significantly higher than that between functionally unrelated enzymes.

iii) The foreign recognition sites on the enzymes are located around the active centres. On the formation of an heterologous enzyme–enzyme complex, the two different active centres become juxtaposed.

iv) The time elapsed between the productive (*i.e.* complex-forming) collisions of E_2 with E_1 and E_3 is about the same as the time required for a catalytic cycle of the enzyme.

The above postulates are illustrated and expanded in more detail in Figs 1 and 2. It is seen in Fig. 1 that an enzyme by combining with another enzyme can form a "cage" accommodating the two active centres. As this enclosure is produced by

the heterologous association of complementary parts of the foreign recognition sites on the two enzymes, it will be called "*complementary cage*". Further, as shown in Fig. 2, by the proper timing of collisions and the catalytic reactions the metabolite can be transferred from one enzyme to the other rather directly, *i.e.* within the geometric confines of the complementary cage. This would result in the ideal case in a perfect compartmentation of the relevant steps of a metabolic pathway,

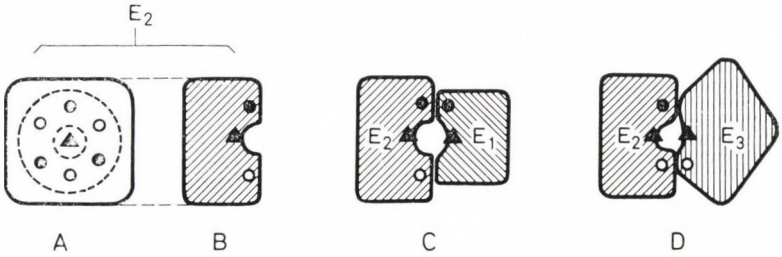

Fig. 1. Formation of "complementary cage" by the association of enzymes through the foreign recognition sites. A) A monomeric enzyme (or a subunit of an oligomeric enzyme) designated E_2, viewed from the side that accommodates in a groove the active centre (▲). The foreign recognition sites for the functionally adjacent two enzymes, E_1 and E_3, are indicated as three contact points each (denoted by o and ●, respectively), which surround the active centre groove in a ringlike fashion. B) Cross-section of E_2 perpendicular to the plane shown in A), through the centre of the groove. The designation of sites is the same as in A). C) Formation of complementary cage between E_1 and E_2. Cross-section through the middle of the cage. On E_1 the active centre is also denoted by (▲), whereas (●) means the part of foreign recognition site of E_1 falling in the plane of section and complementary to the corresponding region of E_2. D) Formation of complementary cage between E_2 and E_3. Active centres are denoted by (▲), whereas (o) designates complementary parts of the foreign recognition sites

without actually being separated by membraneous septa or the components built into a rigid multienzyme complex. Naturally, as the time constants are statistical terms, even if they precisely agreed some of the metabolites would go "astray", that is diffuse out into the liquid phase surrounding the enzyme molecules. It should be noted that this "imperfectness" may also serve biological aims: a minor proportion of a metabolite that becomes mixed in the medium may fulfill the role of allosteric effector at distant places or enter other pathways, while the main flux proceeds through the dynamic channelling device described above.

2. *Conformational changes in enzymes: the concept of alternating complementarity*

In the previous section enzymes were treated as rigid structures, as far as preformed, stable and partly overlapping binding sites were assumed to exist on their surface. However, enzymes are known to possess structural motility, which

can be altered by the binding of specific ligands. We may further develop the model if these features of protein structure are also called into play.

Three postulates are made:

i) The key enzyme, E_2, can exist in, at least, three different conformations: E^0, the state of unliganded enzyme, and E^s and E^p, the states characteristic of the enzyme-substrate and enzyme-product complexes, respectively.

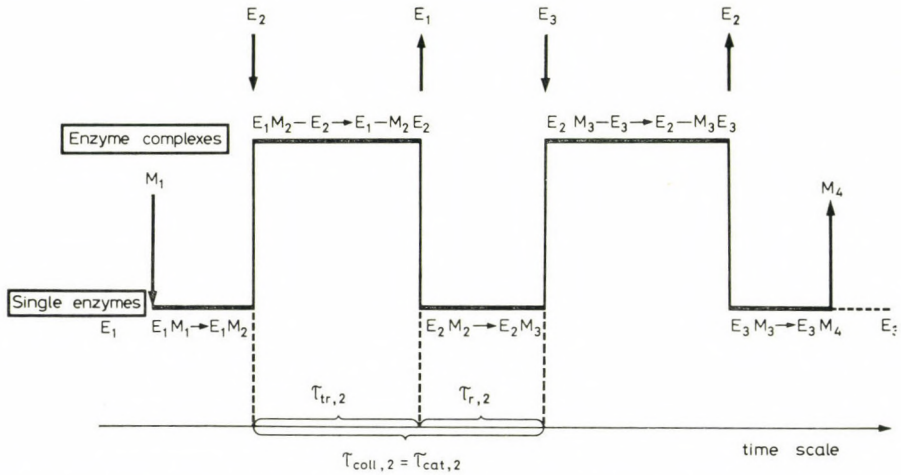

Fig. 2. Interpretation of time constants of productive collision and catalytic cycle. The diagram illustrates the events, as a function of time, that take place during the transformation of metabolite M_1 to M_4 by a soluble enzyme system that works on the basis of "complementary cage" effect. The events run on two levels: single enzymes and enzyme complexes. The transitions between the two levels (*i.e.* complex formation or breakage) are regarded as infinitely fast. Non-productive collisions are not indicated. It is assumed that the enzymatic reaction proper takes place on the level of single enzymes, whereas the life-time of enzyme complexes is required for the transfer of metabolite from one enzyme to the other. The distribution of time between the two levels, which would also reflect the degree of association, is entirely arbitrary. The time constant of productive collision ($\tau_{\mathrm{coll},n}$) for an enzyme is defined as the time period between complex formation with two functionally adjacent enzymes. The time constant of catalytic cycle ($\tau_{\mathrm{cat},n}$) for E_n is defined as the time required for the transfer of metabolite from the preceding enzyme to E_n ($\tau_{\mathrm{tr},n}$) and the time required for the catalytic reaction *per se* ($\tau_{\mathrm{r},n}$)

ii) The foreign recognition sites for the functionally preceding and subsequent enzymes are created when the enzyme assumes the E^s and E^p conformational states, respectively.

iii) The transition into one or the other conformation is promoted by both the appropriate metabolite and enzyme partner.

These postulates are illustrated in Fig. 3. Enzyme E_2 can assume three conformational states and two of these are complementary to the respective enzymes, E_1 and E_3. Accordingly, during the course of catalysis the enzyme oscil-

lates between the two forms carrying one or the other foreign recognition site. In other words E_2 exhibits *alternating complementarity* towards E_1 and E_3.

This alternating complementarity may result in the compartmentation of the substrate and product of an enzyme, as visualized in Fig. 4. For the sake of simplicity the flow of metabolites from M_1 towards M_4 is only indicated although the postulates allow the same mechanism to operate in the opposite direction.

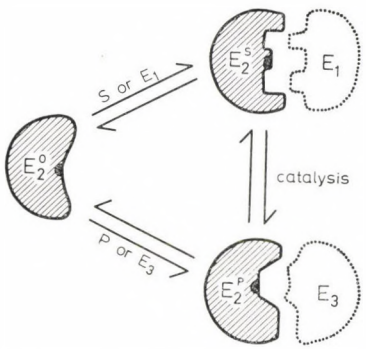

Fig. 3. Conformational transitions and alternating complementarity of enzyme E_2. S and P are the substrate and product of E_2, respectively, whereas E_1 and E_3 are the functionally adjacent enzymes of E_2. For further details see the text

Further, the model can be amplified by assigning such properties also to E_1 and E_3 (or to any number of enzymes in a pathway), or restricted if the complementary cage is only formed unilaterally with respect to E_2, *i.e.* either with E_1 or with E_3. In the latter case only one metabolite would be segregated from the rest of the compartment accommodating the enzyme system.

The simple schemes of Figs 3 and 4 need some comment. E^0 denotes the conformational state in the absence of specific ligands. Of course a host of closely related conformations are being united under E^0 (Linderstrøm-Lang, Schellman, 1959; Weber, 1972). Furthermore, it is not strictly defined whether conformations E^s and E^p are available to the unliganded enzyme, however small proportion they would mean (*i.e.* the three forms represent a pre-equilibrium) or they are produced on the effect of the corresponding metabolite, in an induced-fit manner. In fact reality might be somewhere between the two extremes: as a result of conformational fluctuation the molecule, in "conformation E^0", may well approach either E^s or E^p, but the final adjustment, as a constraint, can only be effected by ligand binding. At any rate, if we only regard this final step, then the transition is of the induced-fit type, brought about either by the appropriate metabolite or by the appropriate enzyme (or both).

In the light of the foregoing one can visualize the situation when the completion of a catalytic cycle of E_2 is promoted by the collision and complex formation

with E_3. If there is a structural change in the enzyme during catalysis, then the energy required for this may partly be covered by the interaction with the counter-enzyme. In other words, by aiding to adjust the enzyme's conformation to the state characteristic of enzyme-product complex, the counter-enzyme may speed up the catalytic reaction. This means that the termination of a cycle and the subsequent release of product are triggered by the counter-enzyme. Such a mechanism

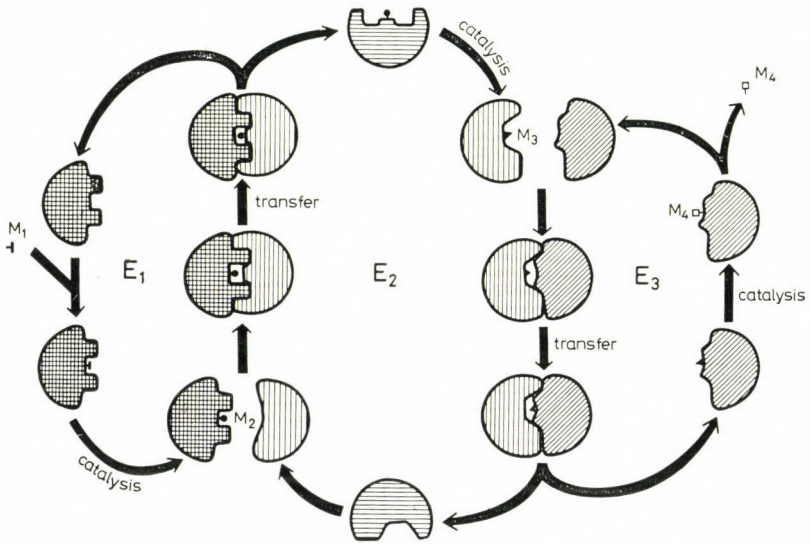

Fig. 4. Dynamic compartmentation of substrate and product of an enzyme through the "cage effect" ensured by alternating complementarity. Of the three consecutive enzymes (E_1, E_2 and E_3) of a pathway one, E_2, is assumed to undergo the conformational transitions required for alternating complementarity, whereas E_1 and E_3 are taken as fairly rigid. M_1, M_2, M_3 and M_4 are the metabolites transformed by the three enzymes. The substrate and product of E_2, *i.e.* M_2 and M_3, are compartmented

would greatly increase the degree of compartmentation that would otherwise be allowed by the statistical nature of even identical catalytic and collision time constants.

Another refinement the model might be endowed with is if we assume that the foreign recognition site is perfectly shaped only if the active site binds the appropriate metabolite. Accordingly, only "loaded" enzyme molecules, or subunits, would be able to form a heterologous complex, thereby minimizing the number of empty complementary cages.

3. *Non-random intracompartmental distribution of soluble enzymes: development of self-maintaining enzyme gradients*

Direct metabolite transfer between functionally adjacent enzymes is obviously facilitated if these enzymes preferentially collide, *i.e.* if collisions with irrelevant enzymes are scarce. This can only be achieved if these enzyme species occur in the neighbourhood of each other. However, with a genuinely "soluble" enzyme system inhomogeneous distribution within a closed space would contradict to thermodynamics.

Nevertheless, under specific conditions certain degree of polarization of soluble enzymes might still be achieved. Let us consider the above model consisting of three enzymes E_1, E_2 and E_3, where E_2 displays affinity towards E_1 and E_3.

Two futher postulates are made:

i) E_1 and E_3 are bound loosely but specifically to different structural elements of the cell, which will be referred to as *A*-wall and *Z*-wall, respectively.

ii) E_2 also exhibits affinity towards itself, *i.e.* the enzyme tends to self-associate. This is due to the existence of a specific *self-recognition site* on the enzyme surface.

In such a system the distribution of enzymes will be non-random, as far as E_1 and E_2 will have the highest concentration at the *A*-wall and *Z*-wall, respectively, whereas E_2 in the middle. Consequently, a gradient of enzymes develops owing to the specific affinities of the components. The distance over which such a gradient can be maintained is probably short, not exceeding several layers of enzyme molecules, and the actual shape of the gradient depends on all the parameters involved (association constants, concentrations, etc.). In considering the distribution of enzymes the tight intracellular packing of macromolecules should also be borne in mind, as a result of which the mean separation between enzymes is well below the diameter of an average tetrameric protein molecule (mol. wt. about 150,000) (Ling, 1969; Hess, Boiteux, 1972). In other words the enzyme molecules mutually exclude each other.

The possibility thus exists for a dynamic structuralization in "soluble" enzyme systems. It is obvious, however, that this type of organization can only exist in the living cell or in its fairly intact fragments. Disruption of the cell and the dilution of its content may weaken the interactions beyond recognition. This would be most conspicuous if for the formation of foreign recognition site the bound metabolite would be essential (cf. Section 2 above). Then the enzyme gradient is actually maintained by the metabolic flux. Switching on of the pathway would reshuffle the randomly distributed enzymes, would polarize them according to vicinal affinity, whereas the cessation of metabolite flow would cancel this orientation. The metabolic state might thus be reflected in the organization pattern of enzymes.

Discussion

In discussing the model our postulates will be examined in light of the current knowledge of protein structure and enzyme function, whether they can be accepted as reasonable working hypotheses.

A. *General features of enzyme architecture and function*

1. *Oligomeric nature of intracellular enzymes*

The overwhelming majority of enzymes catalyzing such main metabolic pathways as glycolysis, hexose monophosphate shunt and Krebs cycle are oligomeric, *i.e.* consist of at least two subunits. The biological significance of quaternary structure has been much discussed (cf. Klotz et al., 1970). In our context we should add the following. If enzymes are to collide with each other to ensure direct metabolite transfer, it is favourable if they have no "back", *i.e.* have active centers in several directions. This would increase the probability of productive collisions.

One may object that in case of direct metabolite transfer the overall rate of a pathway would depend on the diffusion rate of enzymes rather than of substrates, which might not ensure the desired metabolic flux. However, the available data do not support this objection. Gutfreund (1971) emphasized that reactions between proteins can be quite rapid, corresponding to second order rate constants of about 10^5 M^{-1} sec^{-1}. At the intracellular enzyme concentrations ($10^{-5} - 10^{-4}$ M cf. below) this would allow fluxes, operating exclusively through direct metabolite transfer, of $10^{-5} - 10^{-3}$ M sec^{-1}, which is the range observed in metabolic pathways. Furthermore the "recognition volume" for a substrate (Pollard, 1961), which roughly equals the volume of the substrate molecule (Somogyi, Damjanovich, 1971), is increased manyfold if the enzyme-substrate complex, instead of free substrate, is the reactant.

2. *Topology of enzyme active centers*

Most active centers are located in a cleft, groove or the like. For enzymes acting on macromolecules it is conceivable that the depression is needed to accommodate the substrate. Further, if several sequentially remote amino acid residues are to be juxtaposed to form an active center, the best way this can be done is to line a cleft with them. However, even if these considerations are perfectly right, it is by no means excluded that active center clefts can also be used to form "complementary cages". Here we should note that the "cage" must not be regarded invariably as a rather large hole relative to the substrate. In fact, the cavity may be virtual, in which case the bound metabolite may form an integral part of the foreign recognition site.

3. *Self-association of enzymes*

Several enzymes tend to polymerize in vitro (cf. Frieden, 1971). The physiological role of self-association is usually not clear, although mechanistic and regulatory aspects have often been implicated. In our model self-association may promote the development of short-range enzyme gradients, which in turn would facilitate direct metabolite transfer.

4. *Conformational changes in enzymes*

It has already become a solid fact that proteins possess some degree of structural motility, as originally suggested by Linderstrøm-Lang and Schellman (1959). A comprehensive survey of conformative responses in enzymes was recently given by Citri (1973). In brief, conformational alterations have been invoked in the interpretation of both enzyme catalysis and regulation.

The first major departure from the rigid template model of E. Fischer was the *induced-fit theory* of Koshland (1958), which claimed that the proper alignment of catalytic groups on the enzyme was induced by the binding of substrate. Eyring and Lumry's dynamic rack-model (cf. Lumry, 1959) as well as Hammes' (1964) model, postulates a continuous structural change during catalysis, which would be a prerequisite of enzyme action. In contrast to Koshland's *instructive* mechanism, Straub and Szabolcsi (1964) proposed a *selective* one. According to their *fluctuation-fit theory* the enzyme fluctuates between different conformational states and the substrate can bind to, and thus stabilizes, the catalytically active form.

In the regulation of enzyme activity the two principal theories were formulated in the *concerted or symmetry model* by Monod et al. (1965) and in the *sequential model* by Koshland et al. (1966). Both models are based on conformational changes mediated through subunit interactions in oligomeric enzymes. However, whereas the symmetry model postulates a selective mechanism, the sequential model adopts an instructive role for the ligand and therefore is an extention of the induced-fit theory. More recent cogitations point out that regulation through structural changes is also possible in monomeric enzymes and the conformational transitions should be described in terms of the free energies of the variously liganded states (Weber, 1972).

The model depicted in this paper attributes functional significance to the conformational response not only at the level of individual enzymes, but also in the intracellular organization of soluble enzyme systems. Although the postulate of the creation of foreign recognition sites in an alternating manner during catalysis is hypothetical, there is ample evidence that the substrate and product bring about different conformational changes in enzymes. For reference the excellent rewiew of Citri (1973) might suffice. As for the rate of these conformational transitions, Morawetz (1972) emphasized that they are fast enough not to limit the catalytic efficiency of enzymes.

Further, our assumption that functionally adjacent enzymes may induce conformational changes in each other through heterologous associations eventually boils down to the problem of protein–protein interactions, for which clear-cut examples are already available in tryptophan synthetase (Yanofsky, Crawford, 1959) lactose synthetase (Brew, 1970) and protein kinases (Reimann et al., 1971), just to mention a few. Thus our postulate basically relies on well-established features of enzyme structure and function.

B. *Enzymes in the intracellular environment*

Now we will briefly discuss our model in the light of how enzymes occur and function in the intracellular milieu. It is this area where experimental data are rather ambiguous or in some aspects are still lacking. This is not surprising at all if one compares the complexity of a crystalline enzyme solution and that of a living cell.

1. *High intracellular concentration of enzymes*

Srere (1967) provided data on the intracellular concentration of enzymes. In general, the nominal enzyme concentrations in the cell are very high, many orders of magnitude greater than those used in classical enzyme kinetics. Hess and Boiteux (1972) state that in yeast the concentration of catalytic sites of most glycolytic enzymes is about $10^{-5}-10^{-4}$ M. Moreover, the consideration of Sols and Marco (1970) is pertinent here, who question the reliability of calculating "concentrations" in subcellular compartments. Indeed, one can only get lowest estimates since, apart from the experimental pitfalls of extraction, the enzyme content is regarded as homogeneously distributed in one or another cellular compartment. This is done because of our ignorance of the existence, and possible mode, of supramolecular organization of a considerable portion of cellular material, although there are hints that, for example, in the cytoplasm free macromolecules do not occur (Kempner, Miller, 1968). At any rate the tight packing of enzymes makes frequent collisions between enzymes possible and may render even very low association constants functionally significant.

Some rough calculations can be made for a much investigated soluble system, the glycolytic enzymes of yeast. According to Hess et al. (1969) the glycolytic enzymes constitute about 65% of total soluble protein of Saccharomyces carlsbergensis. The computed time between two collisions of any glycolytic enzyme molecule is 30 nsec (Hess, Boiteux, 1972). This gives a collision frequency of about 3×10 sec^{-1}, thus the collision frequency with the functionally adjacent enzyme is approximately 2×10^6 sec^{-1}, if we count with an equimolar mixture of the ten odd glycolytic enzymes. As the turnover number of yeast glyceraldehyde-3-phosphate dehydrogenase is 90 sec^{-1} (Kirschner, Voigt, 1968), about 2×10^4 collisions take place during a catalytic cycle. However, enzymes operate in the cell far below their maximal capacity. For example, in human erythrocytes glycer-

aldehyde-3-phosphate dehydrogenase is claimed to utilize less than 1% of its catalytic potential (Mills, Hill, 1971). Thus in the living cell the number of collisions per one catalytic cycle could well be in the range $10^5 - 10^6$. In other words, to ensure the desired glycolytic flux about every 10^5th collision need to be a productive one.

It may be of interest to compare this value to that one can derive from the observed rates of interprotein reactions. If two proteins associate reversibly according to $A + B \rightleftharpoons AB$, with a second order rate constant of $10^5\ M^{-1}\ sec^{-1}$ (Gutfreund, 1971), the rate of the reaction at steady state concentrations $[A] = [B] = 10^{-4}\ M$ will be $10^{-3}\ M\ sec^{-1}$. If we accept that the collision frequency of the two proteins is $2 \times 10^6\ sec^{-1}$ under these conditions, then by simple calculation we obtain for the number of collisions per litre per sec the value 1.2×10^{20}, whereas the number of associates (AB) formed per litre per sec is 6×10^{20}. Consequently, one associate is produced in every 2×10^5 collisions. Thus the efficiency of collisions required to ensure dynamic compartmentation *via* heterologous enzyme complexes at least does not seem unrealistic in the light of existing data on protein reactivities.

2. *Interactions between soluble enzymes*

There are sporadic but quite a number of observations which suggest that soluble enzymes, such as the glycolytic ones, may interact with each other. The early experiences with enzyme purification might be illuminating in this respect. Thus aldolase and α-glycerophosphate dehydrogenase were originally co-crystallized by Baranowski and Niederland (1949) in myogen *A* and were found to migrate together on electrophoresis and sedimentation. Other studies were mainly concerned with influencing the activity of one enzyme by another (Guliy et al., 1962; Sereda, 1963; Kwon, Olcott, 1965). Hess and his co-workers (cf. Hess, Boiteux, 1972) have looked for possible interactions between various sets of glycolytic enzymes by measuring transit times and enzyme activities over a wide range of enzyme concentration. Among the several coupled systems examined they only found "anomalies", indicating some kind of interaction, between yeast pyruvate decarboxylase and alcohol dehydrogenase. However, as noted by the authors, the highest enzyme concentration they could test was about one order of magnitude lower than the intracellular protein concentration.

Most recently data have been provided which suggest that in concentrated muscle extracts there may be interactions between glycolytic enzymes, as judged from the high apparent molecular weight of certain enzymes on sedimentation and frontal analysis gel chromatography (Clarke, Masters, 1973; Földi et al., 1973).

3. *The role of subcellular structures*

The main intracellular compartment that comprises soluble enzyme systems is the cytoplasm (or cytoplasmic ground substance, matrix, cytosol). Although itself apparently devoid of structure, it accommodates a number of subcellular

organelles and structural elements. In mammalian cells the most common of these are the endoplasmic (sarcoplasmic) reticulum, mitochondria, glycogen granules and in muscle also the proteins of the contractile apparatus. The notion is generally upheld that these subcellular structures might play some role in the organization of soluble enzymes, though only few relevant data are available as yet. It has been shown for several, if not for all, glycolytic and related enzymes from a variety of sources ranging from protozoa to mammalian tissues that they are reversibly bound to one or another subcellular structure (Eichel et al., 1964; Green et al., 1965; Hernandez, Crane, 1966; Arnold, Pette, 1968, 1970; Karpatkin, 1967; Srivastava et al., 1968; Moore, 1968; Mayer, Hübscher, 1971; Risse, Blum, 1972; Carraway, Shin, 1972; Clarke, Masters, 1972; Foemmel, Bernstein, 1972). The association of the phosphorylase-glycogen synthetase system with glycogen is already well documented (Fischer et al., 1971). Recently O'Brien and Matlib (1973) provided data suggesting that some enzymes of the mitochondrial matrix are bound to the inner membrane whereas others form a "core" impermeable to certain metabolites.

In our model the putative *A*-wall and *Z*-wall may well be any of these organelles. One might visualize that the sandwiching of a metabolic pathway, or a certain "stretch" of a pathway, between definite structural elements would functionally make sense. Thus, *e.g.* glycolysis could be reasonably run between glycogen granules and mitochondria, and the spatial arrangement of enzymes could further be specified by the endoplasmic reticulum and, in muscle, by the contractile system.

It should be noted that according to our model the existence of enzyme gradients is not a necessary condition for direct metabolite transfer through the complementary cage effect. But it may serve as an additional factor in the accomplishment of dynamic compartmentation at crucial points of metabolic pathways.

4. *Non-equilibrium enzymes*

Intracellular enzyme reactions can be classified according to whether or not they are at equilibrium in the cell. To the so-called non-equilibrium enzymes belong in glycolysis hexokinase, phosphofructokinase and pyruvate kinase, whereas in the tricarboxylic acid cycle among others citrate synthetase, succinic dehydrogenase and pyruvate dehydrogenase (cf. Krebs, 1969). The failure of these enzymes to establish equilibrium is usually attributed to kinetic reasons. However, in certain instances the great molecular activity and high intracellular concentration of the enzyme do not explain the experimental findings. This seems to be the case with triosephosphate isomerase. It has been postulated, and also taken into account in the computer simulation of glycolysis (Garfinkel, Hess, 1964), that triosephosphate isomerase is complexed to aldolase and only "sees" the DHAP-site of the aldolase active center. Obviously, in this and possibly in other cases some kind of static or dynamic compartmentation of metabolites would bring the explanation of non-equilibrium behaviour within reach.

5. *Compartmentation phenomena in soluble enzyme systems*

As stated at the outset, our model is aimed at the interpretation of apparently puzzling compartmentation effects in "soluble" enzyme systems. Now an illustrative but far from complete list of references on such observations will be given. The methodical approach applied was usually the isotope tracer technique in incorporation studies.

Multiple pools for certain metabolites, sometimes two complete pathways, have been observed in the glycolysis of a wide variety of organisms and tissues such as bacteria (McBrien, Moses, 1968; Macnab et al., 1973; Moses et al., 1959), yeast (Rothstein et al., 1963), mammalian muscle (Kalant, Beitner, 1971; Dully et al., 1969), and liver (London, 1966; Threlfall, Heath, 1968).

Many compartmentation effects have been detected in various other metabolic pathways and in several cases the relevant enzymes have not been demonstrated to form a rigid multienzyme complex. Thus such phenomena were found in the amino acid and protein synthesis (Cowie, McClure, 1959; Bearden, Moses, 1972), as well as nucleic acid base synthesis (Cowie, Bolton, 1957), of yeast, in the phosphate metabolism of rat liver mitochondrial matrix (Tokumitsu, Ui, 1973) and of human erythrocytes (Till et al., 1973), and in the fate of cholesterol in rat liver microsomes (Balusubramanian et al., 1973).

6. *The possibility of metabolic regulation through dynamic compartmentation in enzyme systems*

Hess and Boiteux (1972) have lucidly pointed out that if glycolytic enzymes were to be organized in the form of complexes, this would make biological sense only if it served the regulation of the pathway. We should like to emphasize that dynamic compartmentation may be an important device in cellular regulation. In addition to the obvious benefits of segregating certain metabolic steps, which is in fact done by any kind of structuralization, a dynamic system offers an unparallelled property: versatility. One might visualize that the actual pattern of dynamic compartmentation could be altered by metabolic effectors, thereby facilitating a different flow of metabolites. The oppositely directed routes of glycolysis and gluconeogenesis spring to one's mind. Of course, if the alternating complementarity of an enzyme is to be manyfold, this would impose immensely on evolutionary protein design. However, there is no reason to reject *a priori* that such highly sophisticated systems, if biologically useful, could have evolved.

Epilogue

None of the above considerations lends strong support to the model, as none of the enumerated facts can only be interpreted in terms of the model. It is the task of future work to prove or eventually invalidate our postulates. The purpose of this paper is to focus attention to the circumstance that such mechanisms might be operative in the living cell.

The author thanks Prof. F. B. Straub and Dr. Gertrud Szabolcsi for their continued interest and criticism, and Mr P. Arányi the helpful discussions.

References

Arnold, H., Pette, D. (1968) Eur. J. Biochem. *6* 163—171
Arnold, H., Pette, D. (1970) Eur. J. Biochem. *15* 360—366
Balusubramanian, S., Mitropoulos, K. A., Myant, N. B. (1973) Eur. J. Biochem. *34* 77—83
Baranowski, T., Niederland, T. R. (1949) J. Biol. Chem. *180* 543—551
Bearden, L. Moses, V. (1972) Biochim. Biophys. Acta *279* 513—526
Brew, K. (1970) In: Essays in Biochemistry (eds P. N. Campbell, F. Dickens) Acad. Press, London, New York, Vol. *6* 93—118
Carraway, K. L., Shin, B. C. (1972) J. Biol. Chem. *247* 2102—2108
Citri, N. (1973) Adv. in Enzymol. *37* 397—648
Clarke, F. M., Masters, C. J. (1972) Arch. Biochem. Biophys. *153* 258—265
Clarke, F. M., Masters, C. J. (1973) Biochim. Biophys. Acta. *327* 223—226
Cowie, D. B., Bolton, E. T. (1957) Biochim. Biophys. Acta *25* 292—298
Cowie, D. B., McClure, F. T. (1959) Biochim. Biophys. Acta *31* 236—245
DeDuve, C. (1964) J. Theoret. Biol. *6* 33—59
Dully, C. C., Brocek, R. M., Beatty, C. H. (1969) Endocrinology *84* 855—860
Eichel, H. J., Goldenberg, E. K., Rem, L. T. (1964) Biochim. Biophys. Acta *81* 172—175
Fischer, E. H., Heilmeyer, L. M. G., Jr., Haschke, R. H. (1971) In: Current Topics in Cellular Regulation (eds. B. L. Horecker, E. R. Stadtman), Acad. Press, New York, Vol. *4* 211—251
Foemmel, R. S., Bernstein, I. A. (1972) Fed. Proc. *31* 857 Abstract No. 3638
Földi, J., Szabolcsi, G., Friedrich, P. (1973) Acta Biochim. Biophys. Acad. Sci. Hung. *8* 263—265
Frieden, C. (1971) Ann. Rev. Biochem. *40* 653—696
Garfinkel, D., Hess, B. (1964) J. Biol. Chem. *239* 971—983
Ginsburg, A., Stadtman, E. R. (1970) Ann. Rev. Biochem. *39* 429—472
Green, D. E., Murer, E., Hultin, H. O., Richardson, S. H., Salmon, B., Brierly, G. P., Baum, H. (1965) Arch. Biochem. Biophys. *112* 635—647
Guliy, M. F., Dvornikova, P. D., Fedorchenko, O. Y., Pechenova, T. M. (1962) Ukr. Biokhim. Zh. *34* 187—198
Gutfreund, H. (1971) Ann. Rev. Biochem. *40* 315—344
Hammes, G. G. (1964) Nature *204* 342—343
Hernandez, A., Crane, R. K. (1966) Arch. Biochem. Biophys. *113* 223—229
Hess, B., Boiteux, A. (1972) In: Protein-protein Interaction. Proceedings of 23rd Mosbach Colloquium, Springer V., Berlin, Heidelberg, New York 271—297
Hess, B., Boiteux, A., Krüger, J. (1969) Adv. in Enzyme Regulation *7* 149—167
Kalant, N., Beitner, R. (1971) J. Biol. Chem. *246* 504—507
Karpatkin, S. (1967) J. Biol. Chem. *242* 3525—3530
Kempner, E. S., Miller, J. H. (1968) Exp. Cell Research *51* 141—149
Kirschner, K., Voigt, B. (1968) Z. Physiol. Chem. *349* 632—644
Klotz, I. M., Langerman, N. R., Darnall, D. W. (1970) Ann. Rev. Biochem. *39* 25—62
Koshland, D. E. Jr. (1958) Proc. Natl. Acad. Sci. US *44* 98—104
Koshland, D. E. Jr., Nemethy, G., Filmer, D. (1966) Biochemistry *5* 365—385
Krebs, H. A. (1969) In: Current Topics in Cellular Regulation (eds. B. L. Horecker, E. R. Stadtman), Acad. Press, New York, Vol. *1* 45—55
Kwon, T. W., Olcott, H. S. (1965) Biochem. Biophys. Res. Comm. *19* 300—305
Latzkovits, L., Szentistványi, I. Fajszi, Cs. (1972) Acta Biochim. Biophys. Acad. Sci. Hung. *7* 55—66

Linderstrøm-Lang, K. U., Schellman, J. A. (1959) In: The Enzymes, 2nd ed. (eds P. D. Boyer, H. Lardy, K. Myrbäck), Acad. Press, New York, Vol. *1* 443—510
Ling, G. N. (1969) Int. Rev. Cytol. *26* 1—61
London, W. P. (1966) J. Biol. Chem. *241* 3008—3022
Lumry, R. (1959) In: The Enzymes (eds P. D. Boyer, H. Lardy, K. Myrbäck) 2nd ed., Acad. Press, New York, Vol. *1* 157—231
Macnab, R., Moses, V., Mowbray, J. (1973) Eur. J. Biochem. *34* 15—19
Mayer, R. J., Hübscher, G. (1971) Biochem. J. *124* 491—500
McBrien, D. C. H., Moses, V. (1968) J. Gen. Microbiol. *51* 159—172
Mills, G. C., Hill. F. L. (1971) Arch. Biochem. Biophys. *146* 306—311
Monod, J., Wyman, J., Changeux, J. P. (1965) J. Mol. Biol. *12* 88—118
Moore, C. C. (1968) Arch. Biochem. Biophys. *128* 734—744
Morawetz, H. (1972) Adv. Prot. Chem. *26* 243—277
Moses, V., Holm-Hansen, O., Calvin, M. (1959) J. Bacteriol. *77* 70—78
O'Brien, P., Matlib, A. (1973) Abstracts of 9th Int. Congr. Biochem., Stockholm, p. 378
Pollard, E. C. (1961) J. Theoret, Biol. *1* 328—341
Reed, L. J., Cox. D. J. (1970) In: The Enzymes (ed. P. D. Boyer), 3rd ed. Acad., Press, New York, Vol. *1* 213—240
Reimann, E. M., Brostrom, C. O., Corbin, J. D., King, C. A., Krebs, E. G. (1971) Biochem. Biophys. Res. Comm. *42* 187—194.
Risse, H. J., Blum, J. J. (1972) Arch. Biochem. Biophys. *149* 329—335
Rose, I. A., Kellermeyer, R., Stjernholm, R., Wood, H. G. (1962) J. Biol. Chem. *237* 3325—3331
Rothstein, A., Jennings, D. H., Demis, C., Bruce, M. (1959) Biochem. J. *71* 99—106
Sereda, A. G. (1963) Ukr. Biokhim. Zh. *35* 410—417
Sols, A., Marco, R. (1970) In: Current Topics in Cellular Regulation (eds B. L., Horecker, E. R. Stadtman) Acad. Press. New York, Vol. *2* 227—273
Somogyi, B., Damjanovich, S. (1971) Acta Biochim. Biophys. Acad. Sci. Hung. *6* 353—364
Srere, P. A. (1967) Science *158* 936—937
Srivastava, L. M., Shakespeare, P., Hübscher, G. (1968) Biochem. J. *109* 35—42
Straub, F. B., Szabolcsi, G. (1964) Molekularnaya Biologiya, Problemi i Perspektivi, Moscow, Izdatelstvo Nauka, 182—187
Threlfall, C. J., Heath, O. F. (1968) Biochem. J. *110* 303—312
Till, U., Köhler, W., Ruschke, I., Köhler, A., Lösche, W. (1973) Eur. J. Biochem. *35* 167—178
Tokumitsu, Y., Ui, M., (1973) Biochim. Biophys. Acta *292* 325—337
Weber, G. (1972) Biochemistry *11* 864—878
Yanofsky, C., Crawford, I. P. (1959) Proc. Natl. Acad. Sci. US *45* 1016—1026

Acta Biochim. et Biophys. Acad. Sci. Hung. Vol. 9 (3), pp. 175–184 (1974)

A Theoretical Model for Calculation of the Rate Constant of Enzyme–Substrate Complex Formation

II. Effect of Intermolecular Forces on the Parameters Describing the Translational Diffusion Motion of a Particle

B. SOMOGYI

Department of Biophysics, University Medical School, Debrecen

(Received November 18, 1973 and in revised form February 26, 1974)

A liquid model is presented that describes the translational diffusion motion of a particle considering the effect of intermolecular and/or external forces. It is shown that the solution of diffusion problems by the aid of this model and in Terms of Fick's laws results in compatible expressions.

Introduction

In a previous paper a liquid model was presented wich described the translational diffusion motion of a particle in a symmetrical potential field around the diffusing particle (Somogyi, 1971).

On the basis of this model, supplemented with some further assumptions, one can theoretically determine the rate constant of the formation of an enzyme–substrate complex (Somogyi, Damjanovich, 1973). However, this derivation can only be regarded as a first approximation, because the effect of nonspecific intermolecular forces has been neglected. In this paper we present a liquid model which describes the translational diffusion motion of a particle moving in the anisotropic potential field of the intermolecular forces.

Effect of anisotropic potential field on the parameter describing the translational diffusion motion.

Here we list some important symbols used below:

λ – distance between two neighbouring lattice points;

τ_0 – mean period time of vibrating liquid molecule;

τ – average lifetime of a liquid molecule in a lattice point in case of $U(x_1; x_2; x_3) = 0$;

${}_u\tau_k$ – average lifetime of a liquid molecule in the k-th lattice point when $U(x_1; x_2; x_3) \neq 0$;

E – height of potential barrier between two neighbouring lattice points when $U(x_1; x_2; x_3) = 0$;

U_k – value of $U(x_1; x_2; x_3)$ at the k-th lattice point;

U_{ki} – value of $U(x_1; x_2; x_3)$ in the middle of the distance between the k-th and i-th lattice points;

$E_{ki} = E - (U_k - U_{ki})$ – height of potential barrier belonging to the transition of the molecule from the k-th lattice point to the i-th one (in case of $U(x_1; x_2; x_3) = 0$ the $E_{ki} = E$);

P_{ki} – probability that the molecule present in the k-th lattice point enters the i-th one.

This new liquid model is built on our previous model (Somogyi, 1971).

Let us take a three dimensional $(x_1; x_2; x_3)$ Cartesian co-ordinate system in a rectangular lattice network. Two neighbouring lattice points have only one different co-ordinate and for these $\Delta x_i = \pm\lambda$ where Δx_i is the difference of the i-th co-ordinates of the two neighbouring lattice points and λ is a constant characteristic of the liquid model.

The molecules in the lattice points of the liquid model make accomplish rotational and vibrational motion. After a τ mean lifetime in a lattice point they jump to a neighbouring lattice point in a very short time that is nearly zero compared to τ.

Let us use a $U(x_1; x_2; x_3)$ external potential field. For the sake of simplicity we assume that it is constant in time, *i.e.*

$$\frac{\partial U(x_1; x_2; x_3)}{\partial t} = 0.$$

for any t.

Regarding the lattice points as equilibrium positions of liquid molecules we can say that a molecule is able to enter a neighbouring lattice point when it goes towards this lattice point during its vibrational motion and its kinetic energy is higher than or equal with, a threshold energy, the activation energy of this transition. In case of $U(x_1; x_2; x_3) = 0$, the activation energy is the same for every neighbouring lattice point. This symmetry can be deformed by the $U(x_1; x_2; x_3) \neq 0$ potential field.

First we consider the case of $U(x_1; x_2; x_3) = 0$. We can express the probability that the molecule enters a neighbouring lattice point, having the appropriate direction of its vibrational motion, according to the Maxwell–Boltzmann distribution as follows:

$$p = e^{-E/kT} \tag{1}$$

Each molecule which has an appropriate kinetic energy is able to enter a neighbouring lattice point in every $1/2\ \tau_0$ time, therefore one can write for τ (Erdey-Gruz, 1971):

$$\tau = \frac{1}{2}\tau_0 e^{E/kT}, \tag{2}$$

For water

$\tau = 1.7 \times 10^{-9}$ sec and $\tau_0 = 1.4 \times 10^{-12}$ sec. (Erdey-Gruz, 1971).

It seems that a water molecule makes about 10^3 vibrations in a lattice point before leaving it. Accordingly we regard the transitions of the liquid molecule from a lattice point to the different neighbouring lattice points as independent events.

The mean lifetime, τ_{ki} of a molecule in the k-th lattice point when the of $U(x_1; x_2; x_3) \neq 0$ and the molecule enters the i-th lattice point (the k-th and the i-th lattice points are neighbours) is:

$$\tau_{ki} = 3\tau_0 e^{E_{ki}/kT} \tag{3}$$

since the molecule goes through its equilibrium position when approaching the i-th lattice point in every $3\tau_0$ time. In other words, $3\tau_0$ is the average time elapsing between the molecule's two successive reaching such a position that the entering the i-th of the six neighbouring lattice points is possible.

According to the definition of E_{ki}, using Eq. (2) we can transform Eq. (3) as follows:

$$\tau_{ki} = 6\tau e^{-(U_k - U_{ki})/kT}. \tag{4}$$

We should note that Eq. (4) is valid only if the condition

$$|E - E_{ki}| < E$$

is fulfilled.

As the vibrational motion of the molecule in a lattice point can only approximately be regarded as a harmonic oscillation, we can assume that the probability of transition of the molecule from the k-th to the i-th lattice point is exponential. Accordingly the probability that the molecule, having entered the k-th lattice point at $t = 0$, enters the i-th (neighbouring) lattice point in the time interval $(t, t + dt)$ is:

$$p_{ki}(t)dt = \frac{1}{\tau_{ki}} e^{-t/\tau_{ki}} dt \tag{5}$$

where τ_{ki} is the same as in Eq. (4).

As there are six neighbouring lattice points ($i = 1, 2, \ldots, 6$) we obtain six $p_{ki}(t)$ functions.

With the aid of the $p_{ki}(t)$ functions one can determine the value of probability P_{ki} that a molecule leaves the k-th lattice point entering the i-th one ($i = 1, 2, \ldots, 6$). The $q_{ki}(t)$ probability that a molecule, having entered the k-th lattice point at $t = 0$, does not go over to the i-th one before time t_1, can be determined as follows:

$$q_{ki}(t_1) = 1 - \int_0^{t_1} p_{ki}(t)dt\,. \tag{6}$$

Substituting the value of $p_{ki}(t)$ into Eq. (6) after integration we get:

$$p_{ki}(t_1) = e^{-\frac{t_1}{\tau_{ki}}}. \tag{7}$$

With the help of Eqs (5) and (7) one can express the probability that the molecule, having entered the k-th lattice point at $t = 0$, does not leave this lattice point until time t_1 but it enters the i-th one in the time interval $(t_1, t_1 + dt)$:

$$p_{ki}(t_1) \prod_{j=1}^{5} q_{kj}(t_1)\, dt = \frac{1}{\tau_{ki}} e^{-t_1 \sum_{j=1}^{6} \frac{1}{\tau_{kj}}} dt. \tag{8}$$

Changing t_1 of Eq. (8) to t and integrating it between the limits 0 and ∞, we can obtain the value of P_{ki}:

$$P_{ki} = \int_0^\infty \frac{1}{\tau_{ki}} e^{-t \sum_{j=1}^{6} \frac{1}{\tau_{kj}}} dt\,.$$

After integration we have:

$$P_{ki} = \frac{\frac{1}{\tau_{ki}}}{\sum_{j=1}^{6} \frac{1}{\tau_{kj}}}. \tag{9}$$

By the aid of Eq. (4), Eq. (9) can be written in the following form:

$$P_{ki} = \frac{e^{(U_k - U_{ki})/kT}}{\sum_{j=1}^{6} e^{(U_k - U_{kj})/kT}}. \tag{10}$$

It can be seen from Eq. (10) that when $U(x_1; x_2; x_3) = 0$, the value of P_{ki} equals 1/6 for every i.

Now we turn our attention to the determination of the average life time of a molecule in the k-th lattice point in the case of $U(x_1; x_2; x_3) \neq 0$. At first we define $r_k(t)dt$ as the probability that the molecule, having entered the k-th lattice point at $t = 0$, leaves its position in the time interval $(t, t + dt)$. With this $r_k(t)dt$ function one can write the value of ${}_u\tau_k$ as follows (Frank, Mises, 1967):

$${}_u\tau_k = \int_0^\infty t r_k(t)\, dt\,. \tag{11}$$

The value of $r_k(t)dt$ can be determined on the basis of Eq. (8). The function described by Eq. (8) gives the probability that the molecule, having entered the k-th lattice point at $t = 0$, does not leave its lattice point until time $(t_1, t_1 + dt)$.

Then the value of $r_k(t)dt$ can be described, according to its definition given above, by the summation of functions as determined by Eq. (8) with regard to all neighbouring lattice points (t_1 of Eq. (8) is of course changed to t):

$$r_k(t)\,dt = \sum_{i=1}^{6} p_{ki}(t) \prod_{j=1}^{5} q_{kj}(t)\,dt\,. \tag{12}$$

Writing Eq. (12) into Eq. (11) by the aid of Eq. (8) we get:

$${}_u\tau_k = \int_0^\infty \sum_{i=1}^{6} \frac{t}{\tau_{ki}} e^{-t\sum_{j=1}^{6}\frac{1}{\tau_{ki}}}\,dt\,.$$

Changing the integration and the summing:

$${}_u\tau_k = \sum_{i=1}^{6} \int_0^\infty \frac{t}{\tau_{ki}} e^{-t\sum_{j=1}^{6}\frac{1}{\tau_{ki}}}\,dt\,. \tag{13}$$

Introducing a new parameter $x = t\sum_{j=1}^{6}\frac{1}{\tau_{kj}}$, Eq. (13) looks as:

$${}_u\tau_k = \sum_{i=1}^{6} \frac{1}{\tau_{ki}} \frac{1}{\left(\sum_{j=1}^{6}\frac{1}{\tau_{kj}}\right)^2} \int_0^\infty x e^{-x}\,dx$$

where

$$\int_0^\infty x e^{-x}\,dx = 1\,.$$

Then for the ${}_u\tau_k$ we get:

$${}_u\tau_k = \frac{1}{\sum_{j=1}^{6}\frac{1}{\tau_{kj}}}\,. \tag{14}$$

From Eq. (4) one can obtain another form for ${}_u\tau_k$

$${}_u\tau_k = \tau \frac{1}{\sum_{j=1}^{6} e^{(U_k - U_{ki})/kT}}\,. \tag{15}$$

A third form of ${}_u\tau_k$ can be obtained from the connection between the λ liquid parameter and the D diffusion constant of the diffusing molecule and τ (Somogyi, 1971):

$$\tau = \frac{\lambda^2}{6D}. \tag{16}$$

After substitution of Eq. (16) into Eq. (15) we get:

$${}_u\tau_k = \frac{\lambda^2}{D} \frac{1}{\sum_{j=1}^{6} e^{(U_k - U_{kj})/kT}}. \tag{17}$$

Relation of the model to Fick's laws

The presented liquid model is a more complex version of a simple one which is in trivial keeping with Fick's laws.

According to the additional assumptions used here there is no trivial accord between this model and Fick's laws. No we analyse the relationship between the solutions, given by our model and by Fick's laws, to the problems of diffusion.

Owing to the connection between the two Fick's laws, only the second will be considered (Jost, 1960). For the consideration we define an $U(x_1; x_2; x_3)$ potential function and $c(x_1; x_2; x_3)$ concentration function in the liquid. Both functions are continuous in every point and for the sake of simplicity let them fulfill the following identity:

$$\frac{\partial U(x_1; x_2; x_3)}{\partial t} = \frac{\partial c(x_1; x_2; x_3)}{\partial t} = 0. \tag{18}$$

This liquid can be described with our model as well. First we define the c_i concentration function as

$$c_i = \frac{1}{\lambda^3} \iiint_i c(x_1; x_2; x_3)\, dx_1\, dx_2\, dx_3 \tag{19}$$

where we integrate over the λ^3 volume around the i-th lattice point. Of course, $0 \leq c_i \leq 1$ is valid for c_i and it can be regarded as a probability function over the lattice points. Then we can write for the derivative of c_k concentration of molecules in the k-th lattice point with respect to time:

$$\frac{\partial c_k}{\partial t} = \frac{1}{\lambda^3} \sum_{i=1}^{6} (j_{ik} - j_{ki}) \tag{20}$$

where j_{ik} and j_{ki} denote the diffusion current of molecules from the i-th lattice point to the k-th one and from the k-th lattice point to the i-th one, respectively.

On the basis of Eq. (19) it can be seen that the value of $c_i\lambda^3$ gives the average number of molecules which can be found at the i-th lattice point. Consequently, the $P_{ik}c_i\lambda^3$ gives that portion of $c_i\lambda^3$ which will enter the k-th lattice point. Then using ${}_u\tau_i$ according to its definition, one can obtain the number of molecules entering the k-th lattice point from the i-th one in unit time, *i.e.* the j_{ik} diffusion current, as:

$$j_{ik} = P_{ik}\frac{c_i\lambda^3}{{}_u\tau_i}. \tag{21}$$

In a similar way one can get the value of j_{ki}:

$$j_{ki} = P_{ki}\frac{c_k\lambda^3}{{}_u\tau_k}. \tag{22}$$

Substituting Eqs (21) and (22) into Eq. (20):

$$\frac{\partial c_k}{\partial t} = \sum_{i=1}^{6}\left(\frac{P_{ik}\,c_i}{{}_u\tau_i} - \frac{P_{ki}\,c_k}{{}_u\tau_k}\right). \tag{23}$$

Taking Eqs (10) and (17) into consideration, the above form can be written as follows:

$$\frac{\partial c_k}{\partial t} = \frac{D}{\lambda^3}\sum_{i=1}^{6}\left(c_i e^{(U_i - U_{ik})/kT} - c_k e^{(U_k - U_{ki})/kT}\right) \tag{24}$$

Re-writing the right-hand side of Eq. (24):

$$\frac{\partial c_k}{dt} = \sum_{i=1}^{6}\left\{\frac{D}{\lambda^2}(c_i - c_k) + \frac{D}{\lambda^2}\left[c_i(e^{(U_i-U_{ik})/kT} - 1) + c_k(1 - e^{(U_k-U_{ki})/kT})\right]\right\}. \tag{25}$$

It is known that in case $x \ll 1$, the value of $1 + x$ gives a good approximation for e^x, so one can approximate the right side of Eq. (25) by the following form:

$$\frac{\partial c_k}{\partial t} = \sum_{i=1}^{6}\left\{\frac{D}{\lambda^2}(c_i - c_k) + \frac{D}{\lambda^2}\left[c_i\frac{U_i - U_{ik}}{kT} - c_k\frac{U_k - U_{ki}}{kT}\right]\right\}. \tag{26}$$

For the sake of simplicity the following symbolism will be used. The index of lattice points next to the-k-th will be designed by j if the neighbours are in directions x_j and by $(j + 3)$ if they are in directions $(-x_j)$ $(j = 1, 2, 3)$. In another way, the following transformation of i into j will be used: $i = 1, 2, \ldots, 6$ will be changed to $j = 1, 2, 3$ and $j + 3 = 4, 5, 6$.

Accordingly Eq. (26) becomes

$$\frac{\partial c_k}{\partial t} = \sum_{j=1}^{3}\frac{D}{\lambda^2}(c_j - c_k + c_{j+3} - c_k) + \tag{27}$$

$$+ \sum_{j=1}^{3}\frac{D}{\lambda^2}\left(c_j\frac{U_j - U_{jk}}{kT} - c_k\frac{U_k - U_{kj}}{kT} + c_{j+3}\frac{U_{j+3} - U_{kj+3}}{kT} - c_k\frac{U_k - U_{kj+3}}{kT}\right).$$

Moreover, we can re-write the first part of Eq. (27) as

$$\sum_{j=1}^{3} \frac{D}{\lambda^2}(c_j - c_k + c_{j+3} - c_k) = D \sum_{j=1}^{3} \frac{\dfrac{c_j - c_k}{\lambda} - \dfrac{c_k - c_{j+3}}{\lambda}}{\lambda}. \tag{28}$$

Now we use for the lattice points the operation of $\lim (\lambda \to 0)$, *i.e.* we approach the neighbouring lattice points to one another, while the position of the k-th lattice point is fixed in the unchanged co-ordinate system and the values of functions $U(x_1; x_2; x_3)$ and $c(x_1; x_2; x_3)$ do not change.* Then according to Eq. (19)

$$\lim_{\lambda \to 0} c_k = \lim_{\lambda \to 0} \frac{1}{\lambda^3} \iiint_k c(x_1; x_2; x_3)\, dx_1\, dx_2\, dx_3 = c({}_kx_1; {}_kx_2; {}_kx_3) \tag{29}$$

where $c({}_kx_1; {}_kx_2; {}_kx_3)$ is the value of $c(x_1; x_2; x_3)$ at the k-th lattice point.

By the aid of Eq. (29), for the Eq. (28) we get:

$$\lim_{\lambda \to 0} \sum_{j=1}^{3} \frac{D}{\lambda^2}(c_j - c_k + c_{j+3} - c_k) = D \sum_{j=1}^{3} \frac{\partial^2 c(x_1; x_2; x_3)}{\partial x_j^2}. \tag{30}$$

After this we modify the second part of Eq. (27) in the following way:

$$\sum_{j=1}^{3} \frac{D}{\lambda^2}\left(c_j \frac{U_j - U_{jk}}{kT} - c_k \frac{U_k - U_{kj}}{kT} + c_{j+3} \frac{U_{j+3} - U_{j+3,k}}{kT} - c_k \frac{U_k - U_{kj+3}}{kT} =\right.$$

$$= \frac{D}{kT\lambda^2} \sum_{j=1}^{3} \Big[c_j(U_j - U_{jk}) + c_k(U_k - U_{jk}) - c_k(U_k - U_{jk}) - c_k(U_k - U_{kj+3}) -$$

$$\left. - c_k(U_k - U_{kj}) + c_{j+3}(U_k - U_{kj}) - c_{j+3}(U_k - U_{kj}) - c_{j+3}(U_{kj+3} - U_{j+3}) \Big] = f(c;U). \right.$$

Re-writing this last expression as

$$f(c;U) = \frac{D}{2kT} \sum_{j=1}^{3} \left[\frac{c_j - c_k}{\lambda} \frac{U_j - U_{kj}}{\lambda/2} + \frac{c_k - c_{j+3}}{\lambda} \frac{U_{kj} - U_k}{\lambda/2} + \right.$$

$$\left. + c_k \frac{\dfrac{U_j - U_{kj}}{\lambda/2} - \dfrac{U_k - U_{kj+3}}{\lambda/2}}{\lambda} + c_{j+3} \frac{\dfrac{U_{kj} - U_k}{\lambda/2} - \dfrac{U_{kj+3} - U_{j+3}}{\lambda/2}}{\lambda} \right].$$

* Because of the operation $\lambda \to 0$, the $\tau \to 0$ condition is also fulfilled, while the value of diffusion constant D remains unchanged according to Eq. (16).

Furthermore, by using again the operation of $\lim (\lambda \to 0)$ we get:

$$\lim_{\lambda \to 0} f(c; U) = \frac{D}{kT} \sum_{j=1}^{3} \frac{\partial}{\partial x_j} \left(c(x_1; x_2; x_3) \operatorname{grad} U_{x_j} \right) \tag{31}$$

where grad U_{x_j} is the component of grad U falling into the x_j direction.

Now we write the final form of Eq. (21) according to Eqs (29), (30) and (31):

$$\frac{\partial c({}_k x_1; {}_k x_2; {}_k x_3)}{\partial t} = D \left[\frac{\partial^2 c(x_1; x_2; x_3)}{\partial x_1^2} + \frac{\partial^2 c(x_1; x_2; x_3)}{\partial x_2^2} + \frac{\partial^2 c(x_1; x_2; x_3)}{\partial x_3^2} \right] +$$

$$+ \frac{D}{kT} \left[\frac{\partial}{\partial x_1} \left(c(x_1; x_2; x_3) \operatorname{grad} U_{x_1} \right) + \frac{\partial}{\partial x_2} \left(c(x_1; x_2; x_3) \operatorname{grad} U_{x_2} \right) + \right.$$

$$\left. + \frac{\partial}{\partial x_3} \left(c(x_1; x_2; x_3) \operatorname{grad} U_{x_3} \right) \right] \tag{32}$$

This equation is an equivalent of Fick's second law, where D/kT is the mechanical mobility.

Discussion

It has been shown in the above treatment that by using the operation $\lim (\lambda \to 0)$ the presented liquid model is transformed into the continuous liquid model described by Fick's laws. This is true in the case of finite $U(x_1; x_2; x_3)$ potential field when Eq. (26) is identical with Eq. (25) because of operation $\lim (\lambda \to 0)$.

It is the result of the above consideration that the difference between the solutions of diffusion problems yielded by our model and by Fick's laws, depend upon the values of lattice distance λ and on the $U(x_1; x_2; x_3)$ potential field.

On the basis of the presented liquid model, making some additional assumptions one can calculate the value of association rate constant that belongs to the formation of an enzyme–substrate complex. For the calculation of the above mentioned rate constant one can take the effect of non-specific intermolecular forces into account and for this one can of course use the physical, chemical and biochemical data which have already been obtained for the enzyme and substrate molecules. This calculation will give a better approximation for the value of association rate constant than those published previously (Somogyi, Damjanovich, 1973).

Thanks are due to Prof. S. Damjanovich for valuable advice and discussion.

References

Erdey-Grúz, T. (1971) Transzportfolyamatok vizes oldatokban. Akadémiai Kiadó, Budapest, p. 40

Frank, Ph., Mises, R. v. (1967) A mechanika és fizika differenciál- és integrálegyenletei. Műszaki Könyvkiadó Budapest, Vol. II. p. 690

Jost, W. (1960) Diffusion in Solids, Liquids, Gases, Acad. Press. N. Y. p. 3

Somogyi, B. (1971) Acta Biochim. Biophys. Acad. Sci. Hung. *6* 289

Somogyi, B., Damjanovich, S. (1973) Acta Biochim. Biophys. Acad. Sci. Hung. *8* 153

Acta Biochim. et Biophys. Acad. Sci. Hung. Vol. 9 (3), pp. 185–196 (1974)

A Theoretical Model for Calculation of the Rate Constant of Enzyme–Substrate Complex Formation

III. Effect of Intermolecular Forces and Diffusion Motion of the Enzyme Molecule on the Rate Constant

B. SOMOGYI

Department of Biophysics University Medical School, Debrecen

(Received November 18, 1973, and in revised form February 26, 1974)

Two approximations for the theoretical calculation of the rate constant of enzyme–substrate complex formation are presented, based upon an enzyme and liquid model published earlier (Somogyi, Damjanovich, 1973; Somogyi, 1974).

In one approximation of the effect of non-specific intermolecular forces acting between the enzyme and substrate molecules on the rate constant, the enzyme molecule is regarded motionless during the association process.

In the other approximation the effect of non-specific intermolecular forces is disregarded, whereas the effects of translational and rotational diffusion motions of the enzyme molecule are discussed.

Introduction

In two previous papers we have discussed a theoretical model describing the association process of an enzyme with its substrate and a liquid model dealing with the effect of intermolecular (or external) forces on the translational diffusion motion (Somogyi, Damjanovich, 1973; Somogyi, 1974). According to our earlier model the formation rate constant (k_1) of an enzyme–substrate complex (ES complex) can be determined in a theoretical way (Somogyi, Damjanovich, 1973). This calculation can be, however, a first approximation only because of its limitation by two essential assumptions:

a) The effect of nonspecific forces acting between the enzyme and substrate molecules on the association rate constant can be neglected.

b) The enzyme molecule does not perform any diffusion motion during the association process.

In the first part of this study an approximation of the rate constant of the formation of an ES complex will be discussed with respect to the effect of non-specific forces acting between the enzyme and substrate molecules but neglecting the diffusion motion of the enzyme molecules during the formation of ES complex. Obviously, these non-specific forces are characteristic of the enzyme and substrate, therefore these forces appear in many different forms according to the actual ES complex. On account of this we should like to show the effect of non-

specific forces on the above rate constant only in the case of forces having a spherically symmetric potential field.

In the second part of the paper another approximation of the rate constant of ES complex formation will be considered, where the diffusion motion of enzyme molecule will be taken into account and the effect of non-specific intermolecular forces disregarded.

The form of expression determining the value of the formation rate constant, according to our earlier model is:

$$k_1 = \frac{V}{4\rho_s^2}\left(\sqrt{\frac{3D_s}{2}} + \frac{r_0}{\sqrt{\bar{t}}}\right)^2 e^{-{}^qE/kT} e^{-c_s V} \tag{1}$$

where the symbols are as follows: V – recognition volume; ρ_s – radius of the substrate molecule; D_s – translational diffusion constant of the substrate; c_s – concentration of the substrate in moles/volume; $\bar{t}$ – recognition time; r_0 – is a constant characteristic of the specific intermolecular forces which are responsible for the formation of the ES complex; ${}^qE$ – threshold energy for the formation of an ES complex; k – Boltzmann constant; T – absolute temperature (Somogyi, Damjanovich, 1973).*

The effect of nonspecific intermolecular forces on the rate constant

First the effect of the above forces on recognition volume V will be discussed.

It is assumed that these forces do not alter the structure of recognition volume, *i.e.* the number and geometric order of lattice points building up the recognition volume. But it is conceivable that a force acting between the enzyme and substrate molecules alters the substrate concentration around the enzyme molecule. In the following a single enzyme molecule will be examined.

Discussing the distribution of substrate molecules around the enzyme molecule we will describe the diffusion current density of substrate molecules in an $(x_1; x_2; x_3)$ rectangular co-ordinate system having its centre in the enzyme molecule. This current density, according to the phenomenological theory of diffusion, is (Jost, 1960):

$$J = -D_s \operatorname{grad} c_s(x_1; x_2; x_3) + c_s(x_1; x_2; x_3) F(x_1; x_2; x_3) u_s \tag{2}$$

where $c_s(x_1; x_2; x_3)$ and $F(x_1; x_2; x_3)$ refer to the concentration function of substrate molecules and the force acting between the enzyme and substrate molecules, respectively, while u_s is the mechanical mobility of the substrate. We can introduce the potential function of the forces as:

$$F(x_1; x_2; x_3) = -\operatorname{grad} U(x_1; x_2; x_3)\,.$$

* The detailed definitions of these parameters can be found in the paper cited.

It is well-known that the mechanical mobility can be expressed as (Schurr, 1970):

$$u_s = \frac{D_s}{kT} . \tag{3}$$

Substituting Eq. (3) into Eq. (2) one can write for the stationary equilibrium state of the system

$$-kT \operatorname{grad} c_s(x_1; x_2; x_3) = c_s(x_1; x_2; x_3) \operatorname{grad} U(x_1; x_2; x_3) . \tag{4}$$

In the case of inhomogeneous distribution of substrate molecules we use the Poisson distribution for the determination of the probability that a substrate molecule is found in a unit volume. Then we must define different volume units with sizes depending on the actual substrate concentration in a way that allows the expectation values of the number of substrates in different unit volumes be equal to one another. In another way:

$$\underset{\substack{\text{unit volume} \\ i-th}}{\int\int\int} c_s(x_1; x_2; x_3)dV = \underset{\substack{\text{unit volume} \\ j-th}}{\int\int\int} c_s(x_1; x_2; x_3)dV \qquad \text{for every } i \text{ and } j$$

i.e. the integrals of substrate concentrations in the unit volume give a constant value for every unit volume of the space. Thus a problem arises, since the probability that a substrate molecule can be found in the recognition volume had been used for the determination of the value of k_1 in the case of homogeneous distribution of substrate molecule (Somogyi, Damjanovich, 1973). Therefore, we define the "modified recognition volume" (V^x) as the volume in which the expectation value of the number of substrate molecules when $U(x_1; x_2; x_3) = 0$ is the same as that in the recognition volume when $U(x_1; x_2; x_3) \neq 0$.

According to the definition of modified recognition volume we can write:

$$cV^x = \int\int\int_V c_s(x_1; x_2; x_3)\, dx_1\, dx_2\, dx_3 \tag{5}$$

where $c_s(x_1; x_2; x_3)$ and c are the values of substrate concentration with and without the action of $U(x_1; x_2; x_3)$ potential field respectively and integration is performed over the recognition volume.

In the following we examine what the connection between c, $U(x_1; x_2; x_3)$ and $c_s(x_1; x_2; x_3)$ is. For the sake of simplicity we only consider the case when the value of $U(x_1; x_2; x_3)$ potential field depends only the radius measured from the origin of the potential field. By using such a potential field, the case of spherical symmetric potential field around the center of the enzyme molecule, as well as the case when the single origin of the potential field is on the surface of the enzyme, can de described.

With the aid of the solution of Eq. (4) for the spherical symmetric case the concentration function of substrate $c(r)$ can be described for $U(r)$ spherical sym-

metric potential field. The form of Eq. (4) in such a case is:

$$-kT\frac{dc(r)}{dr} = c(r)\frac{dU(r)}{dr}\,. \tag{6}$$

Denoting the enzyme concentration as c_E, we assume that the value of $U(r)$ can be taken as zero at the boundary of the volume (c_E^{-1}).

Hence Eq. (6) is:

$$c(r) = c(R)\,e^{-U(r)/kT} \tag{7}$$

where $c(R)$ is the value of $c(r)$ at the boundary of the spherelike volume c_E^{-1}.

The value of $c(R)$ can be determined on the basis of the following expression:

$$\frac{c}{c_E} = 4\pi\int_{\rho_E}^{R} r^2 c(r)\,dr \tag{8}$$

where E is the radius of the spherelike enzyme molecule. Using Eqs (7) and (8) we get for $c(r)$:

$$c(r) = \frac{c}{c_E}\,\frac{e^{-U(r)/kT}}{4\pi\int_{\rho_E}^{R} r^2 e^{-U(r)/kT}\,dr}\,. \tag{9}$$

Applying Eq. (5) into a spherical polar co-ordinate system and substituting Eq. (9) into the equation thus obtained the value of the modified recognition volume can be expressed:

$$V^x = \frac{1}{c_E}\,\frac{1}{4\pi\int_{\rho_E}^{R} r^2\,e^{-U(r)/kT}\,dr}\int_{\rho_E}^{\rho_E+r_0}\int_{\vartheta_1(r)}^{\vartheta_2(r)}\int_{\phi_1(r,\vartheta)}^{\phi_2(r,\vartheta)} r^2\sin\vartheta\, e^{-U(r)/kT}\,d\phi\,d\vartheta\,dr. \tag{10}$$

In case of a relatively small enzyme concentration *i.e.*

$$\frac{1}{c_E} \approx 4\pi\int_{\varrho_E}^{R} r^2 e^{-U(r)/kT}\,dr\,.$$

Eq. (10) becomes simpler:

$$V^x = \int_V\int\int r^2\sin\vartheta\, e^{-U(r)/kT}\,d\phi\,d\vartheta\,dr\,.$$

It can be seen from the above equation that the size of recognition volume V is modified by the $U(r)$ potential field as described by Eq. (10). Thus the rate of ES complex formation can be increased or decreased by the above potential field according to Eq. (1).

However, the recognition volume is not the only parameter which describes the rate of ES complex formation. The process is also influenced by the potential

field caused by non-specific intermolecular forces acting between the enzyme and substrate molecules. The recognition time, $\bar{t}$, is also altered by this potential field. This alteration will be discussed as follows.

According to our earlier work, the recognition time can be described as

$$\bar{t} = \frac{\sum_{i=1}^{\infty} {}'P_i \tau_i}{\sum_{i=1}^{\infty} {}'P_i} \tag{11}$$

where τ_i is the mean time during which a substrate molecule makes exactly i jumps in the recognition volume before leaving it; ${}'P_i$ is the probability that the substrate molecule makes exactly i jumps in the recognition volume (Somogyi, Damjanovich, 1973).

The value of ${}'P_n$ can be expressed as

$${}'P_n = \sum_{i_1=1}^{m} P_{i_1 b} \left(\sum_{i_2=1}^{r_{n-1}} P_{i_1 i_2} \left(\sum_{i_3=1}^{r_{n-2}} P_{i_2 i_3} \left(\ldots \sum_{i_{n-1}=1}^{r_2} P_{i_{n-2} i_{n-1}} \left(\sum_{i_n=1}^{m} P_{i_{n-1} i_n} P_{i_n o} \right) \ldots \right) \right) \right) \tag{12}$$

where P_{ib} and P_{io} are the probabilities that the substrate molecule enters the recognition volume as it reaches lattice point i of the recognition volume and leaves it when it leaves lattice point i; $P_{i_1 i_2}$ is the probability that the substrate molecule being in the i_1-st lattice point enters the i_2-nd when it leaves the i_1-st lattice point (its original position) and $m, r_1, r_2, \ldots, r_{n-1}$ are the numbers of the specific lattice points of the recognition volume (Somogyi, Damjanovich, 1973).

One can write for τ_i that

$$\begin{aligned}
\tau_1 &= \frac{\sum_{i_1=1}^{r_1} P_{i_1 b}\, {}_u\tau_{i_1}}{\sum_{i_1=1}^{r_1} P_{i_1 b}} \\
\tau_2 &= \frac{1}{\sum_{i_1=1}^{r_2} P_{i_1 b}} \sum_{i_1=1}^{r_2} P_{i_1 b} \left({}_u\tau_{i_1} + \frac{1}{\sum_{i_2=1}^{r_1} P_{i_1 i_2}} \sum_{i_2=1}^{r_1} P_{i_1 i_2}\, {}_u\tau_{i_2} \right) \\
&\vdots \\
\tau_n &= \frac{1}{\sum_{i_1=1}^{r_n} P_{i_1 b}} \sum_{i_1=1}^{r_n} P_{i_1 b} \left({}_u\tau_{i_1} + \frac{1}{\sum_{i_1=1}^{r_{n-1}} P_{i_1 i_2}} \sum_{i_2=1}^{r_{n-1}} P_{i_1 i_2} \left({}_u\tau_{i_2} + \ldots + \right. \right. \\
&\quad \left. \left. + \frac{1}{\sum_{i_{n-1}=1}^{r_2} P_{i_{n-2} i_{n-1}}} \sum_{i_{n-1}=1}^{r_2} P_{i_{n-2} i_{n-1}} \left({}_u\tau_{i_{n-1}} \frac{1}{\sum_{i_n=1}^{r_1} P_{i_{n-2} i_n}} \sum_{i_n=1}^{r_1} P_{i_{n-1} i_n}\, {}_u\tau_{i_n} \right) \ldots \right) \right)
\end{aligned} \tag{13}$$

where ${}_u\tau_i$ denotes the mean time while the substrate is found in lattice point i in the case of $U(r)$ potential fields. As it was shown, both P_{ki} and ${}_u\tau_i$ depend on the $U(r)$ potential field as follows:*

$$P_{ki} = \frac{e^{(U_k - U_{ki})/kT}}{\sum_{j=1}^{6} e^{(U_k - U_{kj})/kT}} \tag{14}$$

$${}_u\tau_k = \tau \frac{6}{\sum_{j=1}^{b} e^{(U_k - U_{kj})/kT}} \tag{15}$$

where U_k and U_{ki} are the values of $U(r)$ potential at lattice point k and at the middle point of the distance between the k-th and i-th lattice points, respectively, τ is the mean time of a substrate in a lattice point when the $U(r)$ potential field does not act, and kT is the Boltzman constant multiplied by the absolute temperature (Somogyi, 1974). Eqs (14) and (15) mean that both P_{ki} and ${}_u\tau_k$ depend on the U potential field and the places of lattice points i and k in the co-ordinate system fixed to the enzyme molecule. With the aid of Eq. (15), Eq. (13) can be written as:

$$\tau_n = \left[\frac{1}{\sum_{i_1=1}^{r_n} P_{i_1 b}} \sum_{i_1=1}^{r_n} P_{i_1 b} \left(\frac{6}{\sum_{j=1}^{6} e^{(U_{i_1} - U_{i_1 j})/kT}} + \ldots + \right. \right.$$

$$\left. \left. + \frac{1}{\sum_{i_n=1}^{r_1} P_{i_{n-1} i_n}} \sum_{i_n=1}^{r_1} P_{i_{n-1} i_n} \frac{6}{\sum_{j=1}^{6} e^{(U_{i_n} - U_{i_n j})/kT}} \right) \right]. \tag{16}$$

Using the Eqs (11) and (16) for $\bar{t}$ recognition time we have:

$$\bar{t} = \tau v$$

where v is the average number of jumps made by the substrate molecule in the recognition volume.

On the basis of Eqs (11), (14) and (16) it can be seen that the value of v only depends on the character of the U potential field and the structure of the recognition volume. For the determination of rate constant k_1 an additional expression has to be used (Setlow, Pollard, 1962):

$$\Theta = \frac{kT}{8\pi \eta \rho^3} \tag{17}$$

* The values of P_{ib} and P_{io} also depend on the $U(r)$ potential field since they are specific functions of P_{ki}-s (Somogyi, Damjanovich, 1973).

where Θ is the rotational diffusion constant, ρ and η are the radius of the diffusing molecule and the viscosity of the surrounding medium, respectively, k is the Boltzmann constant, and T is the absolute temperature. Then according to the foregoing on the basis of Eq. (1) one can write for rate constant k_1:

$$k_1 = 2V^x \Theta_s \left(\frac{1}{2} + \frac{r_0}{\lambda\sqrt{v}}\right)^2 e^{-qE/kT} e^{-c_3 V^x} \tag{18}$$

where Θ_s is the rotational diffusion constant of the substrate. The size of V^x and v are influenced by the potential field of the non-specific intermolecular forces acting between the enzyme and substrate molecules.

Effect of the diffusion motion of enzyme molecule on the rate constant of enzyme–substrate complex formation

In this part of the paper another approximation is presented for the rate constant of ES complex formation, which considers the translational and rotational diffusion motion of the enzyme molecule but neglects the non-specific intermolecular forces.

We consider the effect of the translational diffusion of the enzyme molecule on the above rate constant in a way that we regard the relative diffusion motion of the two molecules (*i.e.* the enzyme and substrate molecules) in a co-ordinate system fixed to the enzyme molecule. In this co-ordinate system the D translational diffusion constant of the substrate molecule, *i.e.* the diffusion constant of the relative diffusion motion, becomes $D = D_E + D_s$, where D_E and D_s are the translational diffusion constants of the enzyme and substrate molecules, respectively (Chandrasekhar, 1943).

As far as the effect of the translational diffusion motion of the enzyme molecule on this rate constant is concerned the question, what an expression describes the motion of the substrate molecule caused by rotational diffusion motion of the enzyme molecule with respect to a co-ordinate system fixed to the binding site of the enzyme, will be discussed on the basis of a liquid model published earlier (Somogyi, 1971).

According to this liquid model the diffusion motion is regarded as a series of transitions from one equilibrium state of the diffusing molecule to the other. It is known that in the case of rotational diffusion motion of a spherelike molecule, of radius ρ_E, the mean square rotary angle $(\bar{\alpha}^2)$ during time t is (Setlow, Pollard, 1962):

$$\bar{\alpha}^2 = \frac{kT}{4\pi\eta\rho_E^3} t \tag{19}$$

where η, k and T are the viscosity of the surrounding medium, the Boltzmann constant and the absolute temperature, respectively. Assuming that the distance

between two lattice points of the liquid is λ, we can write time τ_{11}, while a surface point of the spherelike enzyme molecule covers a distance of λ in average, because of its rotational diffusion motion, *i.e.* $\rho_E \alpha = \lambda$, on the basis of the Eq. (19) as

$$\tau_{11} = \frac{4\pi \eta \rho_E}{kT} \lambda^2 \tag{20}$$

Using the Einstein–Stokes equation

$$D = \frac{kT}{6\pi \eta \rho}$$

for Eq. (20), we have:

$$\tau_{11} = \frac{2\lambda^2}{3D_E} \tag{21}$$

where D_E denotes the translational diffusion constant of the enzyme. With regard to the fact that the size of the binding site is a small part of the whole surface of the enzyme we fix an $(x_1; x_2; x_3)$ three dimensional rectangular co-ordinate system to the binding site of the enzyme molecule in the following way: Let the x_1 axis fall in the direction of the radius of the enzyme molecule pointing to the centre of the binding site. It is obvious that the substrate molecule surrounded by six neighbouring lattice points, can enter any of the six lattice points because of its, or the enzymes, translational diffusion motion, but it can only enter any of four lattice points because of the rotational diffusion motion of the enzyme molecule (in the latter case the substrate molecule can move parallel with axis x_2 or x_3). Then using an "ordinary" co-ordinate system we can write the probability that a molecule, having entered the i-th lattice point at $t = 0$, will enter the k-th (neighbouring) lattice point in the time interval $(t, t + dt)$ if it is able to enter only the k-th lattice point (Somogyi, 1973):

$$p_{ik}(t)\, dt = \frac{1}{\tau_{ik}} e^{-t/\tau_{ik}}\, dt \tag{22}$$

where τ_{ik} is the mean lifetime of the molecule in the i-th lattice point before it enters the k-th neighbouring one. According to our earlier work we can write (Somogyi, 1973):

$$\tau_{ik} = 6\tau \tag{23}$$

where τ is the mean lifetime of a molecule in a lattice point surrounded by six equivalent lattice points (*i.e.* in the case when $U(x_1; x_2; x_3) = 0$).

In a similar manner we can write for both substrate and enzyme molecules as follows:

$$\tau'_s = 6\tau_s \tag{24}$$

$$\tau'_E = 6\tau_E \tag{25}$$

where τ'_s and τ'_E are characteristic of the substrate and enzyme molecules, respectively, similar in this respect to τ_{ik}, whereas τ_s and τ_E are parameters similar to τ. According to the foregoing to characterize the motion of the substrate molecule caused by the rotational diffusion motion of the enzyme molecule we can write (the motion of the substrate molecule is viewed here in the co-ordinate system fixed to the binding site of the enzyme molecule):

$$\tau'_{11} = 4\tau_{11}. \tag{26}$$

The definition of τ_{11} is given by Eq. (20) and τ'_{11} is a parameter similar to τ_{ik} in Eq. (23). Then changing τ_{ik} of Eq. (22) with either of the parameters τ'_s, τ'_E, or τ'_{11}, one can get three types of the probability functions similar to the probability determined by Eq. (22). These probability functions are characteristic of the motion (from one lattice point to the other) of the substrate molecule in the above co-ordinate system, caused by the translational diffusion motion of the substrate and enzyme molecules and the rotational diffusion motion of the enzyme molecule, respectively.

With the aid of one of the above three probability functions

$$\frac{1}{\tau'_s} e^{-t/\tau'_s} dt$$

we can write probability Q_s, *i.e.* that the substrate molecule, having entered a lattice point at $t = 0$, will not be able to enter one of the six neighbouring lattice points because of its translational diffusion motion during time t_0, as follows:

$$Q_s = 1 - \int_0^{t_0} \frac{1}{\tau'_s} e^{-t/\tau'_s} dt .$$

After integration we get:

$$Q_s = e^{-t_0/\tau'_s}$$

On the basis of the former equation, we can write probability p_{x_1}, *i.e.* that the substrate molecule, having entered a lattice point at $t = 0$, will enter the neighbouring lattice point falling into the $+x_1$ direction as

$$p_{x_1} = \int_0^{\infty} \left[\frac{1}{\tau'_s} e^{-\left(\frac{4}{\tau'_{11}} + \frac{6}{\tau'_s} + \frac{6}{\tau'_E}\right)t} + \frac{1}{\tau'_E} e^{-\left(\frac{4}{\tau'_{11}} + \frac{6}{\tau'_s} + \frac{6}{\tau'_E}\right)t} \right] dt . \tag{27}$$

The sum of the two terms in brackets comes from the fact that the substrate molecule can enter the above lattice point as a result of the translational diffusion motion of both the enzyme and substrate molecules. It is obvious, that

$$p_{x_1} = p_{-x_1}$$

The other probabilities ($p_{x_2}; p_{-x_2}; p_{x_3}; p_{-x_3}$) can be obtained in an analogous way:

$$p_{x_2} = p_{-x_2} = p_{x_3} = p_{-x_3} = \int_0^\infty \left[\frac{1}{\tau'_s} e^{-\left(\frac{4}{\tau'_{11}} + \frac{6}{\tau'_s} + \frac{6}{\tau'_E}\right)t} + \frac{1}{\tau'_E} e^{-\left(\frac{4}{\tau'_{11}} + \frac{6}{\tau'_s} + \frac{6}{\tau'_E}\right)t} + \right.$$

$$\left. + \frac{1}{\tau'_{11}} e^{-\left(\frac{4}{\tau'_{11}} + \frac{6}{\tau'_s} + \frac{6}{\tau'_E}\right)t} \right] dt . \tag{28}$$

After integration of Eqs (27) and (28), using Eqs (24), (25) and (26) we get:

$$p_{x_1} = p_{-x_1} = \frac{\frac{1}{\tau'_s} + \frac{1}{\tau'_E}}{\frac{1}{\tau_{11}} + \frac{1}{\tau_s} + \frac{1}{\tau_E}}$$

$$p_{x_2} = p_{-x_2} = p_{x_3} = p_{-x_3} = \frac{\frac{1}{\tau'_{11}} + \frac{1}{\tau'_s} + \frac{1}{\tau'_E}}{\frac{1}{\tau_{11}} + \frac{1}{\tau_s} + \frac{1}{\tau_E}}$$

From Eq. (21) and the following relation found for the translational diffusion motion in liquid (Somogyi, 1971):

$$\tau = \frac{\lambda^2}{6D} \tag{29}$$

one can get other forms for the above probabilities:

$$p_{x_1} = p_{-x_3} = \frac{1}{6} \frac{D_s + D_E}{D_s + \frac{5}{4} D_E} \tag{30}$$

$$p_{x_2} = p_{-x_2} = p_{x_3} = p_{-x_3} = \frac{1}{6} \frac{D_s + \frac{11}{8} D_E}{D_s + \frac{5}{4} D_E} \tag{31}$$

where D_s and D_E denote the translational diffusion constant of the substrate and enzyme molecules, respectively.

The mean lifetime ($\bar{\tau}$) of the substrate molecule in a lattice point can be obtained by averaging over the time (Somogyi, 1974).

$$\bar{\tau} = \int_0^\infty t \left[\frac{1}{\tau_s} e^{-\left(\frac{1}{\tau_{11}} + \frac{1}{\tau_s} + \frac{1}{\tau_E}\right)t} + \frac{1}{\tau_E} e^{-\left(\frac{1}{\tau_{11}} + \frac{1}{\tau_s} + \frac{1}{\tau_E}\right)t} + \frac{1}{\tau_{11}} e^{-\left(\frac{1}{\tau_{11}} + \frac{1}{\tau_s} + \frac{1}{\tau_E}\right)t} \right] dt . \tag{32}$$

After integration Eq. (32) turns into the following form:

$$\bar{\tau} = \left(\frac{1}{\tau_s} + \frac{1}{\tau_E} + \frac{1}{\tau_{11}} \right)^{-1}$$

Using Eqs (20) and (28) we get:

$$\bar{\tau} = \frac{2}{3} \frac{\lambda^2}{4D_s + 5D_E} \tag{33}$$

Now the recognition time, $\bar{t}$, can be written as

$$\bar{t} = \bar{\tau} \frac{\sum_{i=1}^{\infty} {}'P_i i}{\sum_{i=1}^{\infty} {}'P_i} \tag{34}$$

where ${}'P_i$ is the same as defined in the first part of this paper and it can be calculated on the basis of Eq. (12), by replacing P_{ki}-s in Eq. (12) by the appropriate probabilities determined from Eq.'s (30) and (31). Then using Eqs (33), (34) and (17), on the basis of Eq. (1) we can get for the value of rate constant k_1:

$$k_1 = 2V\Theta_s \left(\frac{1}{2} + \frac{r_0}{\lambda\sqrt{v}} \sqrt{\frac{4D_s + 5D_E}{4D_s}} \right) e^{-qE/kT} e^{-c_s V}$$

Discussion

The two methods presented here give a better approximation for the rate constant k_1 than our previous one (Somogyi, Damjanovich, 1973). However it is not decided yet whether the first or the second of the presented two approximations yields a better value for this constant. This depends on the actual circumstances of the association step. We can expect a better value for k_1 with the approximation considering the effect of intermolecular forces in the sole case when the enzyme molecule is much larger than the substrate. In this case the rotational and translational diffusion motions of the enzyme molecule probably play a minor role in the association step of the enzymic reaction.

As far as the limits of the approximations are concerned we note the following. We considered here the case when the formation of a single bond between the enzyme and substrate molecules is responsible for the formation of an enzyme–substrate complex. Furthermore, we remark that all the approximations presented here neglect the effect of collision of the substrate and enzyme molecules during the recognition process. This effect alters the value of recognition time ($\bar{t}$) in a specific way which is characteristic of the geometric structure of the recognition volume. This problem will be discussed in another paper.

Finally, it should be emphasized that all the above approximations are valid if the rate of enzyme-substrate complex formation is not diffusion-controlled. This follows from the fact that in a diffusion-controlled case the distribution of substrate molecules around the enzyme is perturbed by the reaction.

I am indebted to Prof. Dr. S. Damjanovich for his valuable advice and discussion.

References

Chandrasekhar, S. (1943) Rev. Mod. Phys. *15* 1
Jost, W. (1960) Diffusion in Solids, Liquids, Gases. Third Printing, Acad. Press, N. Y., p. 47
Schurr, M. (1970) Biophys. J. *10* 700
Setlow, R. B., Pollard, E. C. (1962) "Molecular Biophysics", Pergamon Press, London, Paris
Somogyi, B. (1971) Acta Biochim. Biophys. Acad. Sci. Hung. *6* 289
Somogyi, B. (1974) Acta Biochim. Biophys. Acad. Sci. Hung. *9* 175
Somogyi, B., Damjanovich, S. (1973) Acta Biochim. Biophys. Acad. Sci. Hung. *8* 153

Acta Biochim. et Biophys. Acad. Sci. Hung. Vol. 9 (3), pp. 197–207 (1974)

Chromate Uptake by Human Red Blood Cells: Comparison of Permeability for Different Divalent Anions

G. ORMOS, S. MÁNYAI

State Institute of Occupational Health, Budapest, Hungary

(Received October 3, 1973 and in revised form January 14, 1974)

Equilibrium exchange and net anion movement in washed human red blood cells were studied with sulphate ions. Both methods resulted in the same permeability constant when net movement was measured at 10^{-4} M sulphate concentration.

The permeability constant of chromate was $1.28\ (\pm 0.14) \times 10^{-1} \times \text{min}^{-1}$ as derived from uptake velocity measurements at chromate concentrations below 0.1 mM in isotonic saline at 37°, pH 7.4. The apparent activation energy of chromate uptake was about 10 kcal/mole, in contrast to 23 kcal/mole for phosphate transport.

At increasing total divalent anion concentration the permeability constant of sulphate and phosphate showed a sharp increase. The permeability constant of chromate increased only slightly at increasing sulphate and phosphate concentration and no change was observed when chloride was replaced by nitrate in the medium.

The influence of pH on chromate uptake was compatible with the relationships based on the fixed charge theory (Passow, 1969). The effect of different chloride concentrations, however, showed some divergence from the pure electrostatic competition of anions for fixed charges.

Introduction

It seems now well established that permselectivity of the red blood cell membrane is effected by fixed positive charges. A number of permeation characteristics of sulphate and phosphate ions are consistent with the regulatory role of the fixed charge region. Passow (1969) suggested that the positive charges are amino groups having a total concentration of 2.5 moles/litre membrane water and a pK value of 9.

There are, however, some features of the anion transport of red blood cells that cannot be explained on the basis of the fixed charge concept. The apparent activation energy of the transport should be approximatively 8–12 kcal/mole on the analogy of anion exchange resins. In contrast to this figure for sulphate uptake Schnell (1972) reported 33 kcal/mole, Wieth (1970) 32 kcal/mole and for sulphate release Glader and Omachi (1968) 27 kcal/mole. The activation energy of phosphate transport was found to be 16.7 kcal/mole (Gourley, Gemill, 1950), 25 kcal/mole (Gerlach et al., 1964) and for the phosphate release by iodoacetate-poisoned cells 32 kcal/mole was measured by Glader and Omachi (1968). In addition

Przestalski et al. (1971) found a decrease in the activation energy of phosphate transport from 20 to 14.2 kcal/mole with decreasing ionic strength of the medium and claimed that even this decrease is inconsistent with the fixed charge concept. With stored erythrocytes a sharp break in the Arrhenius-plot at 37° was observed by Peterson (1972). The activation energy below and above this temperature was estimated to be 20 and 7 kcal/mole, respectively.

The effect of monovalent anions on sulphate permeability was studied by Wieth (1970). The order of permeability decrease was $Cl^- = Br^- < I^- < < NO_3^- < SCN^- <$ salicylate. A similar pattern of anion effect on phosphate permeation was reported by Deuticke (1967).

Phosphate flux showed exponential dependence on extracellular phosphate concentration in chloride medium. In sulphate medium the relationship between phosphate flux and concentration was linear (Deuticke, 1967).

These findings raise a limitation to the applicability of the theory, which only considers the electrostatic nature of ions, and suggest that the barrier, limiting the rate of anion movement, is not identical with the fixed charge region.

Gray and Sterling (1950) measured chromate uptake by human red blood cells. They found that uptake kinetics could be described by a single exponential and that the intracellular chromium was completely bound to hemoglobin in the form of Cr(III) cation. Latzkovits and Szentistványi (1972) observed that at low chromate concentration the chromate bound in the membrane changed with the pH according to the formation of fixed charges.

To get more information on the transmembrane movement of anions the characteristics of chromate uptake were examined and compared with the transport of sulphate and phosphate. Because chromate is reduced and successively bound to hemoglobin, equilibrium exchange measurements cannot be performed with this anion. We followed the net chromate uptake into human red blood cells. To avoid gross changes in membrane potential and solvent movement, equilibrium was established for all other anions and the changes caused by the small quantity of chromate applied were neglected.

Methods

Freshly drawn heparinized human blood and blood stored in ACD* solution were obtained from the National Institute of Haematology and Blood Transfusion. If not otherwise stated heparinized blood was centrifuged for 10 minutes at $1200 \times g$ and the upper layer was removed by aspiration. The erythrocyte pellet was washed three times with the medium containing all components except those to be measured for net movement. The washed cells were resuspended in the medium to give a 5% suspension. This suspension was kept at the temperature of the transport

* To 400 ml blood 110 ml ACD solution was added. ACD solution: Na-citrate, 20 g/l; dextrose, 30 g/l; citric acid, 5.1 g/l.

experiment for two hours. During this time pH was adjusted with 1 N NaOH or 1 N HCl and was checked several times with a glass electrode. Equilibrium establishment for sulphate and phosphate was tested in some cases by radioactive tracer technique or by chemical analysis. Pre-incubated cells were centrifuged and the pellet was brought to a hematocrit of 50% (v/v) and dry weight was measured.

Equilibrium exchange experiments were started by mixing pre-warmed erythrocytes and medium containing $1-5$ μCi $H^{32}PO_4^{2-}$ or $5-10$ μCi $^{35}SO_4^{2-}$ per ml of final suspension. When net movement was measured extracellular sulphate concentration amounted to 0.3 mM at the start of the experiment. Chromate was applied below 0.1 mM concentration. At appropriate times samples were taken and were put on the top of Sephadex G-75 (Pharmacia, Sweden) columns (2×6.5 cm). Gel filtration was performed according to Till et al. (1972) with the exception that the columns were not thermostated. After the appearance of the cells in the effluent three fractions of 1 ml were collected and radioactivity and hemoglobin content of the cells were determined. Oxyhemoglobin was measured photometrically at 540 nm. Phosphate was determined as described by Bartlett (1959).

The experimental results were fitted to equations according to the different types of transport measurements. The following symbols are used: v_e, extracellular volume; v_i, cell water; v_{cell}, packed cell volume of 35% dry weight; C_{e0}, C_{et}, $C_{e\infty}$, extracellular permeant concentrations at time 0, t or ∞; k, rate constant (min^{-1}); P_v, permeability constant (min^{-1}). Net uptake of chromate was calculated on the basis of equations

$$\ln \frac{C_{et}}{C_{e0}} = -kt \quad \text{and} \quad P_v = \frac{v_e}{v_{cell}} \cdot k \ (\text{min}^{-1}).$$

Net movement of sulphate was related to

$$\ln \frac{C_{et} - C_{e\infty}}{C_{e0} - C_{e\infty}} = -kt \quad \text{and} \quad P_v = \frac{k}{v_{cell}} \cdot \frac{v_i \cdot v_e}{v_i + v_e} \ (\text{min}^{-1}).$$

The data of sulphate and phosphate transport measured by equilibrium exchange were treated as described by Gárdos et al. (1969) except that the permeability constant referred to packed cell volume.

Results

The time course of the change in chromate concentration outside the cells is shown in Fig. 1. After a rapid initial period $CrO_{4,e}^{2-}$ gave a straight line against time in the semilogarithmic plot. The rate constant and permeability constant were calculated from this linear phase of the plot. From measurements on six different blood samples $P_v = 1.28 \ (\pm 0.14 \text{ s.d.}) \times 10^{-1} \times \text{min}^{-1}$ under the circum-

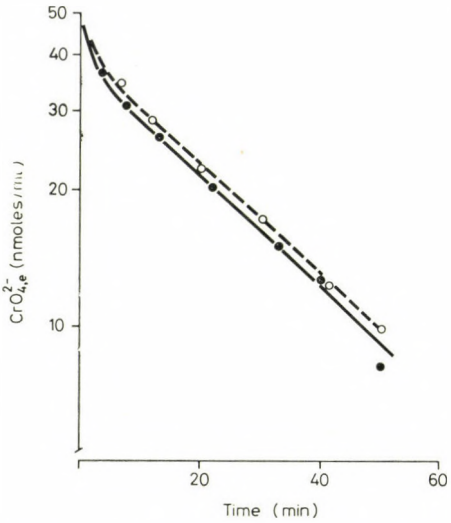

Fig. 1. Time course of the change of extracellular chromate concentration at 37°C; pH 7.4. Hematocrit: 25%; initial chromate concentration, 0.05 mM; media: ●——●, isotonic saline; ○— — ○, isotonic sodium nitrate

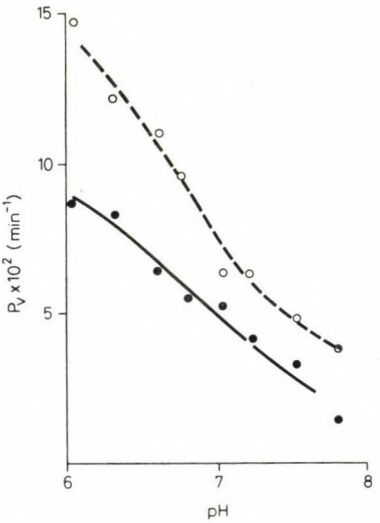

Fig. 2. Changes of the permeability constant of chromate at different pH and Cl^- concentrations at 20°C. Initial CrO_4^{2-} concentration, 0.05 mM; media: ●——●, 155 mM chloride; ○— — —○, 60 mM chloride and sucrose to ensure isotonicity

stances indicated in Fig. 1. No difference in the uptake velocity was found when Cl^- was replaced by NO_3^- in the medium.

Extracellular Cl^- concentration and pH strongly influenced the uptake of chromate (Fig. 2). The permeability constants obtained were replotted against the calculated intramembrane chromate accumulation as shown in Fig. 3. The accumulation ($CrO_{4,m}^{2-}/CrO_{4,e}^{2-}$) was calculated according to Passow (1969). At both

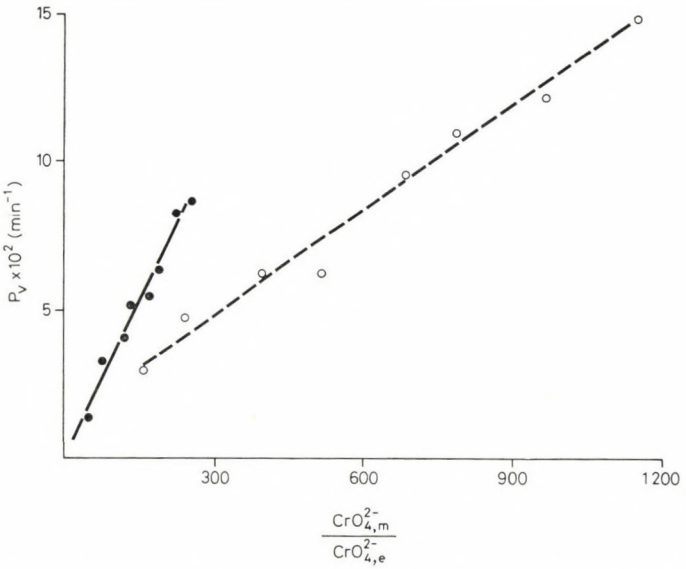

Fig. 3. Results of Fig. 2 replotted against intramembrane chromate accumulation. Symbols as in Fig. 2. Calculation of chromate accumulation was based on 2.5 M concentration and pK 8.5 for the fixed charges

60 mM and 155 mM chloride concentrations linear relationship was achieved when 2.5 moles/litre concentration and pK 8.5 were assumed for the fixed charges.

The temperature dependence of chromate uptake was measured between 22 and 42 °C. Results were plotted according to the Arrhenius-diagram in Fig. 4. The apparent activation energy of chromate uptake was calculated from the slope of the plot. The values obtained are listed in Table 1. For comparison E_{act} of the transport of 20 mM phosphate was determined on the same heparinized blood samples and on outdated blood bank bloods.

The effects of co-partner divalent anions were determined in isotonic media containing chloride and sulphate in different concentrations and the changes of the permeability constants of phosphate and chromate were measured. The results and the calculated changes in the intramembrane phosphate accumulation are illustrated in Fig. 5.

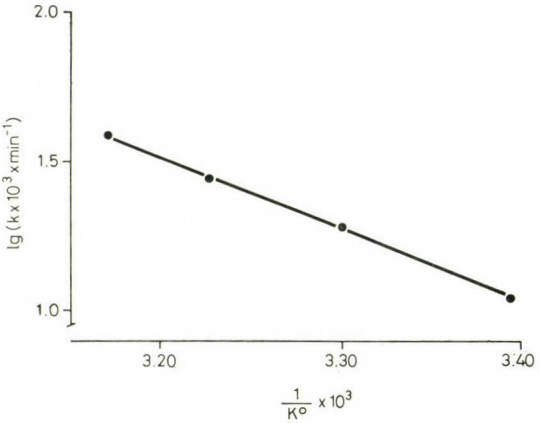

Fig. 4. Arrhenius-diagram of the rate constants of chromate uptake by human erythrocytes. Hematocrit: 27.5%; pH 7.4; medium: isotonic saline; initial CrO_4^{2-} concentration, 0.09 mM

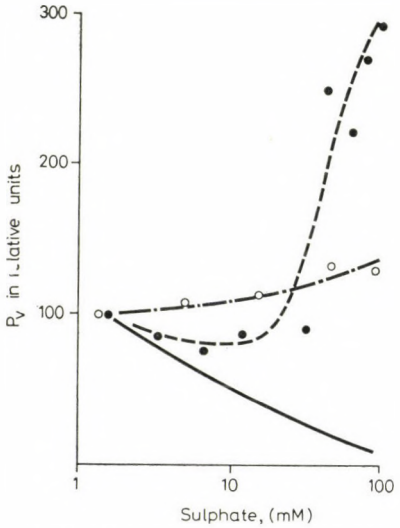

Fig. 5. Effect of the replacement of chloride by sulphate in the medium on the permability constant of phosphate and chromate. Temperature 37°C; pH 7.5; phosphate concentration: 1.65 mM; chromate concentration: 0.05 mM. For the permeability measurement of phosphate heparinized blood was washed twice with isotonic saline and was adjusted to pH 6.9. Washed erythrocytes were kept at 37° in a 10% suspension for 15 hours in the presence of 5 μg/ml streptomycin sulphate. This procedure was followed by washing and equilibration as described in Methods for fresh blood. Before transport measurement inorganic, acid-labile and total phosphorus were determined. Acid-labile phosphate could not be detected and acid-resistant phosphate (supposed to mainly consist of 2,3-DPG) decreased to 0.73 μmoles/ml cells. ——, calculated intramembrane phosphate accumulation in relative units; for the fixed charges 2.5 M total concentration and pK 9 were assumed; ●— —●, P_v of phosphate in realtive units, $100 = 4.13 \times 10^{-3} \times \text{min}^{-1}$; ○—.—.—○, P_v of chromate in relative units, $100 = 0.89 \times 10^{-1} \times \text{min}^{-1}$

Table 1

Activation energy of chromate and phosphate transport

Donor	E_{act} (kcal/mole)		Temperature range °C	Notes
	CrO_4^{2-}	HPO_4^{2-}		
A	10.0*	23.0	22–42	freshly drawn heparinized blood
B	10.9**	25.0		
C	—	22.8	37–44	4 weeks storage in ACD solution
D	—	22.0		7 weeks storage in ACD solution

* Chromate concentration: 1.0 mM
** Chromate concentration: 0.09 mM

In another series of experiments, at the expense of chloride, the extracellular phosphate concentration was increased and the effect of anion composition on sulphate and chromate movement was measured. The permeability constant of sulphate was determined by both net movement and equilibrium exchange experiments. The time course of net sulphate uptake is illustrated in Fig. 6. The changes of the permeability constants of sulphate and chromate at increasing phosphate concentration are shown in Fig. 7. The different effects of large phosphate concentration on the P_v value of chromate and sulphate might be explained by assuming that in the case of net exchange of chromate the counter anion is no longer chloride but phosphate and this would markedly slow down the movement of

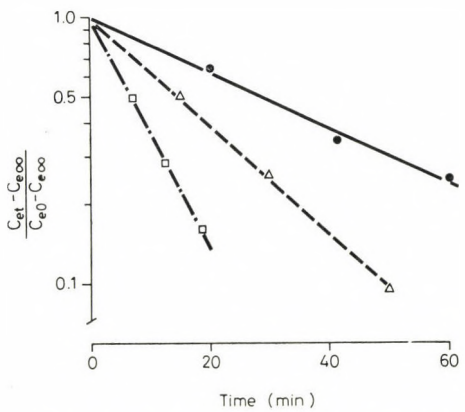

Fig. 6. Time course of net sulphate exchange in human erythrocytes. Temperature 37°C; pH 7.25; hematocrit: 33%; initial sulphate concentration 0.3 mM. Media: ●——●, 17 mM phosphate and 130 mM chloride; △ — — △, 34 mM phosphate and 105 mM chloride; □-.-.-□, 110 mM phosphate

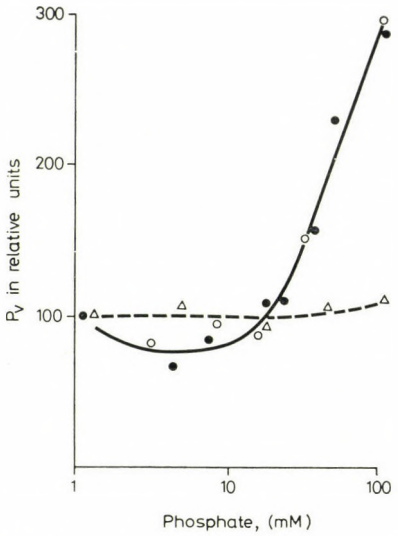

Fig. 7. Effect of replacement of chloride by phosphate in the medium on the permeability constant of sulphate and chromate. Temperature 37°C; pH 7.25; ●, ○—, P_v of sulphate determined from equilibrium exchange and net exchange, respectively; relative units, 100 = $= 1.60 \times 10^{-2} \times \min^{-1}$; △ — — △, P_v of chromate in relative units, $100 = 1.12 \times 10^{-1} \times \min^{-1}$

chromate ion. This effect is, however, excluded as chloride concentration in all experiments was much higher than that of chromate. This is further supported by the fact that no difference could be observed in the permeability constant of sulphate determined by net exchange and equilibrium exchange experiments.

Discussion

(i) *Comparison of net anion movement and equilibrium exchange measurements*

It was concluded by Passow (1969) that the permeant concentration in the fixed charge region rather than in the extracellular space is determining the transport speed of anions through red blood cell membrane. The concentration of a divalent anion in this region (Y_m^{--}) may exceed its extracellular concentration (Y_e^{--}) by several orders of magnitude. This accumulation can lead to a nonlinear relationship between Y_m^{--} and Y_e^{--}. Calculations were performed for Y_m^{--} on the basis of Passow's equations, with pK 9 for the formation and 2.5 moles/l for the total concentration of the fixed charges. In this case small concentrations of a divalent permeant in chloride medium at pH 7.25 were supposed. For the intramembrane accumulation (Y_m^{--}/Y_e^{--} ratios) 185, 182, 176, and 157 were obtained at 10^{-5}, 10^{-4}, 3×10^{-4}, and 5×10^{-4} moles/l of Y_e^{--}, respectively. These figures show that already at 0.5 mM concentration the intramembrane accumulation diverges noticeably from linearity. In the kinetic

measurement of net movement of divalent anions it is regarded a basic criterion to work below this concentration. The calculations refer to equilibrium conditions. This is not the case when net ion movement is measured therefore the assumption should be made that there is a rapid equilibrium between the fixed charge region and extracellular medium as compared to the speed of the transport process itself. This assumption seems plausible because fixed charges are supposed to be arranged in front of the barrier that is rate-limiting for anions.

For net exchange of sulphate in beef erythrocytes Schwietzer and Passow (1953) found second order kinetics at large sulphate concentration. Passow (1964) observed that flux and extracellular concentration of sulphate were related by the $J = a/1 + b\,SO_4^{2-}/SO_4^{2-}$ expression. At 10^{-4} M permeant concentration, as used in this work, the second power term seems negligible and therefore the permeability constant should be independent of concentration.

To prove our assumptions permeability constants were determined for sulphate from both net movement and equilibrium exchange experiments. The time course of net sulphate uptake could be reconciled with the expected first order kinetics (Fig. 6). The changes in the Cl^-/HPO_4^{2-} ratio of the medium showed the same effect on the P_v values determined by the two ways and the figures agreed reasonably well (Fig. 7). It is therefore concluded that at low permeant concentration net movement measurements can yield reliable permeability constant values.

The uptake kinetics of chromate is further simplified by the fact that its intracellular concentration is negligible as shown by the time course of the uptake process.

(ii) *Effect of pH, chloride concentration and temperature on chromate uptake*

The permeability constant of chromate could be linearly fitted to the calculated intramembrane chromate accumulation at different pH values (Fig. 3). This finding is compatible with the fixed charge hypothesis. Best fit was achieved when pK 8.5 was assigned to the fixed charges, a value close to pK 9 obtained by Passow (1969) from sulphate transport measurements. At different chloride concentrations of the medium, however, the permeability constant – intramembrane accumulation relationship of chromate gave separate straight lines, instead falling on a common curve as expected according to the theory. Therefore this result cannot be explained by pure electrostatic competition between Cl^- and CrO_4^{2-} for the fixed charges.

The 10 kcal/mole apparent activation energy of chromate uptake greatly differed from the known values for sulphate and phosphate transport. On the other hand, the E_{act} of chromate uptake is close to the value expected if only the fixed charge region is rate-limiting in penetrating through the membrane.

The activation energy of phosphate movement (23 kcal/mole) is in good aggreement with the values given by Gerlach et al. (1964) and Przestalski et al. (1971), but in contrast to Peterson (1972) no appreciable decrease of E_{act} could be observed between 37° and 44° even with 7-week-old blood samples.

(iii) *Effects of the anion milieu on the permeability of red blood cells to different divalent anions*

The fixed charge theory is based on the electrostatic nature of ions. Accordingly, intramembrane accumulation and hence the penetration of a divalent anion should not be altered by replacing one monovalent anion for another in the medium. The observations on phosphate and sulphate transfer contradict this supposition. Deuticke (1967) reported a decrease of phosphate flux in NO_3^- medium down to 47% of the value obtained in Cl^- medium. In this work for chromate uptake no detectable rate differences could be observed in Cl^- and NO_3^- media.

For the quantitative description of anion effects it seemed reasonable to measure the permeation of a divalent anion in a compound medium containing other mono- and divalent anions. The distribution of anions between membrane and extracellular space is given by the Donnan-equilibrium:

$$\frac{\sqrt{Y_m^{--}}}{\sqrt{Y_e^{--}}} = \frac{Cl_m^-}{Cl_e^-}.$$

An additional divalent anion should follow the same distribution as does Y^{--}. When the concentration of the divalent anion to be used for permeability measurement is kept low and the concentration of the co-partner anion Y^{--} is increased, the permeability constant should decrease according to the fixed charge hypothesis.

The changes of the permeability constants of phosphate and sulphate do not fit into this picture. The sharp increase of the permeability constants over some 10^{-2} M co-partner divalent anion concentration (Figs 5 and 7) cannot be explained on the basis of the theory. However it may be that membrane parts other than the fixed charge region are also influenced by these anions. This effect seems unspecific as it could be observed when either phosphate or sulphate was chosen as co-partner anion in bulk concentration.

The movement of chromate was only slightly accelerated by increasing sulphate and phosphate concentrations and the gap between the predicted and found changes is smaller than in sulphate or phosphate transport. In the calculation of intramembrane permeant accumulation, changes in the activity coefficient of ions were neglected as the relevant intramembrane conditions are unknown. More realistic calculations may therefore lead to a closer agreement between calculated and found changes of chromate uptake at increasing bivalent anion content of the medium.

Preliminary experiments have shown that the chromate uptake kinetics strongly depends on chromate concentrations higher than that used in this work.

The authors are grateful to Mrs Sára Végh for discussions and to Mr M. Herczegh for phosphorus analyses. The skilful technical assistance of Mr J. Dalmady is acknowledged.

References

Bartlett, G. R. (1959) J. Biol. Chem. *234* 466
Deuticke, B. (1967) Pflügers Arch. ges. Physiol. *296* 21
Gárdos, G., Hoffman, J. F., Passow, H. (1969) In: "Laboratory Techniques in Membrane Biophysics" (eds: Passow, H. and Stämfli, R.), Springer, Berlin, p. 141
Gerlach, E., Deuticke, B., Duhm, J. (1964) Pflügers Arch. ges. Physiol. *280* 243
Glader, B. E., Omachi, A. (1968) Biochim. Biophys. Acta *163* 30
Gourley, R. H., Gemill, C. L. (1950) J. Cell. Comp. Physiol. *35* 341
Gray, S. J., Sterling, K. (1950) J. Clin. Invest. *29* 1604
Latzkovits, L., Szentistványi, I. (1972) Acta Physiol. Acad. Sci. Hung. *41* 385
Passow, H. (1964) In: "The Red Blood Cell" (eds: Bishop, C. and Surgenor, D. M.), Academic Press, New York, p. 74
Peterson, S. C. (1972) Biochim. Biophys. Acta *155* 844
Przestalski, S., Gomulkiewicz, J., Bielinski, E. (1971) Proc. First Eur. Biophys. Congress, Wien, Vol. III. p. 395
Schnell, K. F. (1972) Biochim. Biophys. Acta *282* 265
Schwietzer, C. H., Passow, H. (1953) Pflügers Arch. ges. Physiol. *256* 419
Till, U., Koehler, W., Loeschke, W. (1972) Acta biol. med. germ. *28* 51
Wieth, J. O. (1970) J. Physiol. *207* 581

Acta Biochim. et Biophys. Acad. Sci. Hung. Vol. 9 (3), pp. 209–212 (1974)

Separation of Serum Cholinesterase Isozymes by Polyacrylamide Gradient Gel Electrophoresis

(Short Communication)

I. NAGY, J. SASHEGYI, *M. KURCZ, P. BARANYAI

Central Laboratory, Heim Pál Hospital for Children; *Department of Biochemistry, National Institute of Public Health, Budapest, Hungary

(Received December 5, 1973 and in revised form January 14, 1974)

For the one-step fractionation of mixtures of proteins or nucleic acids of a broad range of molecular weights continuous (Slater, 1968; Margolis, Kendrick, 1968) and discontinuous gradient gels (Wright, Mallmann, 1966; Clark, Weis, 1968; Grossbach, Weinstein, 1968) are equally suitable.

The cholinesterase ((ChE) Acylcholine acyl hydrolase, E. C. 3.1.1.8). activity of human blood serum has been found to be attached to protein fractions of different sizes and electrophoretic mobilities (La Motta, Woronick, 1971). Concerning the number of active fractions opinions are not uniform, which is mainly due to the fact that electrophoresis has been carried out in supporting media of different sieving capacities and qualities, but of a homogeneous pore size in the case of a given system (Juul, 1968; Scott, Weaver, 1970; Saeed et al., 1971).

Though the conditions of electrophoresis may be mild in the cases mentioned above, the prolonged time of fraction renders the evaluation of the enzyme activities questionable. Scott and Weaver (1970) and Saeed et al. (1971) carried out electrophoresis for 18 hours in 12% starch gel and 7.5% polyacrilamide gel, respectively. Juul (1968) could separate the more cathodic isozymes only after 3 hours of electrophoresis. By this time, however, the isozyme spectrum was no longer complete in the system applied, as the ChE active fraction which had a mobility similar to that of albumin had already migrated out from the gel into the buffer tank.

Studies in this field point to the fact that the serum components of extreme molecular size which display ChE activity, cannot be satisfactorily separated in a gel of homogeneous pore size. On this ground, we have attempted to apply heterogeneous discontinuous polyacrylamide gels instead of the homogeneous systems.

Electrophoresis was carried out according to Davis (1968). Volumes of 0.7 ml of monomer solutions containing 9%, 7% and 5% (w/v) acrylamide were polymerized on top of each other in the above order in 90 × 6 mm glass tubes; the concentrations of N,N'-methylene-bisacrylamide were 0.16%, 0.20% and 0.24% (w/v), respectively. In addition, the gel solutions contained 6.3 ml of 1 N

HCl, 3.75 g of tris(hydroxymehtly)aminomethane, 0.03 ml of N,N,N',N'-tetramethyl-ethylenediamine, 10.0 g of sucrose and 0.075 g of ammonium persulphate in final volumes of 100 ml. On top of the small pore gradient gel 0.2 ml of stacking gel solution and 0.2 ml of sample gel solution containing 20 μl of serum were polymerized.

Anode and cathode buffers (pH = 8.4) contained 0.0041 M tris(hydroxymethyl)aminomethane and 0.053 M glycine. 1.0 ml of 0.01% bromophenol blue was added to 1000 ml of the cathode buffer to mark the front. The runs were

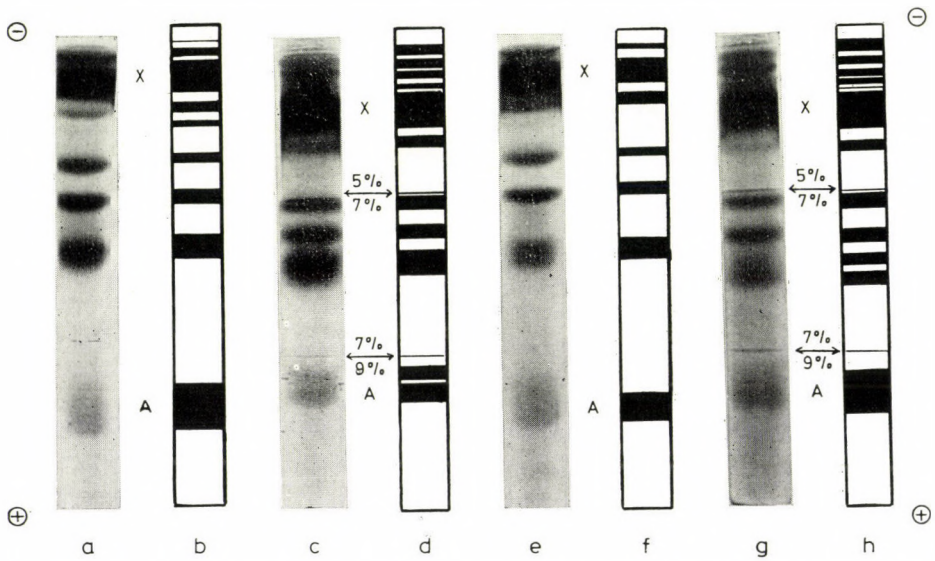

Fig. 1. Polyacrylamide gel ectrophoretic patterns of ChE isozymes in the sera of two healthy children (20 μl of serum per gel column). Columns *a* and *e*: electrophoretograms stained by dithio-oxamide of 9% homogeneous gels; *c* and *g*: gradient gels of the same sera. The hatched areas in figures *b*, *d*, and *h* correspond to the location of the peaks in gels *a*, *c*, and *g* as revealed by densitometry. The migration rate of ChE fraction marked "A" is greater than that of albumin. Component "X" corresponds to isozyme ChE, as denoted by Juul (1968)

carried out at 4C; for 190–200 minutes at a stabilized voltage of 245–250 V. When 12 tubes were run simultaneously, the initial current intensity was 34–47 mA.

In the case of separations on homogeneous polyacrylamide gel columns the method uf Juul (1968) was modified so that the volume of the small pore gel column was increased from 1 to 2 ml. These separations lasted for 240–250 minutes with an initial current intensity of 30 mA when 12 columns 9% gel were run simultaneously.

The detection of ChE isozymes was based on the cleavage of butyrylthiocholine (Koelle, Friedenwald, 1949). The liberated thiocholine was precipitated by

cupric sulphate and the white precipitate was stained by dithio-oxamide (Juul, 1968). The distribution of fractions was recorded by a KIPPZONEN densitometer at 620 nm and a slit of 1 mm.

The present work was not aimed at the analysis of the different ChE isozyme variants, only the possibilities of their separation in homogeneous and gradient polyacrylamide gels were compared. As demonstrated by the electrophoretograms in Fig. 1 *a*, *b*, *e* and *f*, ChE isozyme bands, located near the cathode in the homogeneous gel column containing 9% acrylamide, can hardly be distinguished. In the 4–5 mm long part of the gel between the intensively stained fractions (marked "X" in the Figure) and the stacking gel several thin bands are seen. It is evident that only more prolonged electrophoresis could improve the separation of these showly migrating proteins. However, that would lead to the loss of the fast-migrating fraction marked "A". In the literature little importance is attached to this fraction, though it does cleave butyrylthiocholine and according to the densitometric measurements it always contained more than 10% of the total activity. We consider that this fraction is not identical with albumin. Albumin binds a small quantity of bromophenol blue and thus it is readily visible in the gel by the naked eye. However, the migration rate of fraction "A", which cleaves butyrylthiocholine, is somewhat greater than that of the blue albumin band. (It should be noted that during staining for enzyme activity bromophenol blue dissociates from albumin, therefore this fraction can no longer be seen after staining with dithio-oaxamide).

In the case of electrophoresis in gradient gel columns, the main advantage is that in spite of the shorter running time the high molecular weight fractions are well resolved and those of lower molecular weights and thus migrating faster have not left the gel column. Component "A" is always located in the 9% part of the gradient and can readily be evaluated (Fig. 1 *c*, *d*, *g*, *h*). As compared to the 9% gel, the 5% gel constitutes lower resistance to migration of the slow component "X" and at the same time renders the good separation and evaluation of the adjacent thin bands possible. The distortion of the bands has never been observed.

Our knowledge about the origin, properties, role and differential diagnostic importance of plasma ChE isozymes is rather scarce. New and useful information can only be obtained by the application of methods allowing optimal separation and simultaneous evaluation of all the active fractions. In our opinion the various combinations of polyacrylamide pore gradients would constitute an adequate starting point for these efforts.

We thank Mária Zandler for her valuable technical assistance. We are also indebted to REANAL Fine Chemicals Co. for providing us with the analytical polyacrylamide gel, electrophoretic apparatus, type "Modell 69" and the chemicals needed.

References

Clark, C. C., Weis, A. (1968) Biochim. Biophys. Acta *154* 175
Davis, B. J. (1964) Ann. N. Y. Acad. Sci. *121* 404
Grossbach, U., Weinstein, I. B. (1968) Anal. Biochem. *22* 311
Juul, (1968) Clin. Chim. Acta *19* 205
Koelle, G. B., Friedenwald, J. S. (1949) Proc. Soc. Exper. Biol. Med. N. Y. *70* 617
La Motta, R. V., Woronick, C. L. (1971) Clin. Chem. *17* 135
Margolis, J., Kendrick, K. G. (1968) Anal. Biochem. *25* 247
Saeed, S. A., Chadwick, G. R., Mill. P. J. (1971) Biochim. Biophys. Acta *229* 186
Scott, E. M., Weaver, D. D. (1970) Biochem. Med. *4* 349
Slater, G. (1968) Anal. Biochem. *24* 215
Wright, G. L., Mallmann, W. L. (1966) Proc. Soc. Exper. Biol. Med. N. Y. *123* 22

Acta Biochim. et Biophys. Acad. Sci. Hung. Vol. 9 (3), pp. 213–216 (1974)

Phosphopyridoxyl Peptide from Chicken Heart Aspartate Aminotransferase

(Short Communication)

YU. M. TORCHINSKY*, V. M. KOCHKINA*, M SAJGÓ

Enzymology Department, Institute of Biochemistry
Hungarian Academy of Sciences, Budapest, Hungary

(Received December 8, 1973)

In aminotransferases and other pyridoxal-P**-dependent enzymes pyridoxal-P is bound as an aldimine (Schiff's base) to the ε-amino group of a lysine residue of the active site. Reduction of the imine bond with sodium borohydride provides stable covalent attachment of coenzyme to the protein; this renders it possible to isolate the P-Pxy-peptides, which exhibit characteristic blue fluorescence (Fischer et al., 1958). This approach has been successfully applied for the isolation of P-Pxy-peptides from aspartate aminotransferases of pig heart and pigeon breast muscle (Hughes et al., 1962; Polyanovsky, Keil, 1963; Vorotnitzkaya et al., 1968; Morino, Watanabe, 1969).

This communication describes the isolation and elucidation of the structure of P-Pxy-peptide from the chymotryptic digest of aspartate aminotransferase (EC 2.6.1.1) from chicken heart cytosol. A simplified procedure is presented for the purification of P–Pxy-peptides. This procedure is a modification of the one developed by Milstein (1967) and Strausbauch and Fischer (1970); it is based on the altered electrophoretic mobility of the Pxy-peptides after phosphate elimination by alkaline phosphatase.

Aspartate aminotransferase from chicken heart cytosol was purified according to Kochkina and Torchinsky (1974). Reduction of the enzyme with $NaBH_4$ was carried out in 0.15 M phosphate buffer, pH 6.5, in the presence of 0.01 M α-ketoglutarate; 1 mg of $NaBH_4$ was added per 1 ml of enzyme solution containing 2 mg of protein. The reduced protein was dialyzed overnight against distilled water and freeze-dried; it was then dissolved in 0.1 M Tris buffer, pH 8.5, containing 8 M urea, and carboxymethylated with bromacetate under conditions described earlier(Sajgó, 1969). The carboxymethylated enzyme was dialyzed against distilled water and freeze-dried. Digestion with α-chymotrypsin, (Sigma 1 : 3 w/w_4 was carried out in 1 % ammonium bicarbonate (3 hours, 37 °C).

The digest was freeze-dried, dissolved in 0.05 M NH_4OH and subjected to paper electrophoresis at pH 6.5 in pyridine acetate buffer. After electrophoresis

* *Permanent address:* Institute of Molecular Biology, Moscow, USSR.

** *Abbreviations used:* pyridoxal-P, pyridoxal S'-phosphate; Pxy, pyridoxyl; P-Pxy, pyridoxyl 5'-phosphate.

two blue-fluorescent bands were revealed (Fig. 1a). Both bands were cut out, the peptides were eluted and incubated overnight with alkaline phosphatase* in 0.05 M ammonium bicarbonate (0.05 mg of phosphatase was added to the solution of fluorescent peptide isolated from 25 mg aminotransferase). The reaction mixture was freeze-dried and submitted to electrophoresis at pH 6.5. Upon removal of 5'-phosphate from the P-pyridoxyl group the mobility of the fluorescent peptides was drastically changed, and they both shifted to a single position,

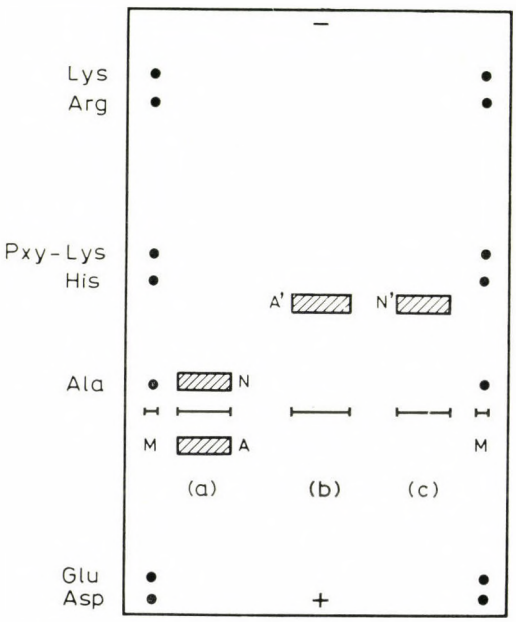

Fig. 1. The electrophoretic mobility of fluorescent chymotryptic peptides before and after phosphatase treatment. Electrophoresis was carried out in a horizontal electrophoretic system at pH 6.5 (pyridine–acetic acid–water, 96 : 4 : 900), 30 V/cm, for two hours, (a) Positions of fluorescent bands of the chymotryptic digest of aspartate aminotransferase; (b) position of peptide A' obtained after treatment of peptide A with phosphatase; (c) position of peptide N' obtained after treatment of peptide N with phosphatase; (M) control amino acid mixture

just behind histidine (Fig. 1, b, c,). Thus peptide A' was immediately obtained in pure form, peptide N' was further purified by paper chromatography in pyridine-isoamyl alcohol–water (7 : 7 : 6) system.

Samples of purified peptides A' and N' were hydrolyzed with 6 N HCl (22 hours, 105°) in sealed evacuated tubes. Amino acid analysis was performed

* We are indebted to Dr R. I. Tatarskaya (Moscow) for providing us with a highly purified preparation of alkaline phosphatase isolated from *E. coli* by the procedure of Abrosimova-Amelyanchik et al. (1967).

by the single-column procedure of Dévényi (1969) in a JEOL JLC-6AH analyzer. Both peptides A' and N' proved to have the same amino acid composition, containing stoichiometric amounts of Ser, (Pxy)Lys, Asp and Phe (assuming the amount of (Pxy)Lys to be equal to the sum of (Pxy)Lys and free Lys) (Table 1); free lysine found in the hydrolysates evidently arose from partial decomposition of ε-(Pxy)Lys. We found that a sample of synthetic ε-(Pxy)Lys underwent partial decomposition during acid hydrolysis with the formation of free lysine and some other products, as observed earlier by Strausbauch and Fischer (1970).

Table 1

Amino acid composition of the Pxy-peptides

Amino acid	Peptide N'	Peptide A'
	(nmoles)	
Asp	4.2	4.1
Ser	4.7	3.1
Phe	4.8	4.0
Lys	1.2	1.8
(Pxy)Lys[a]	3.2	2.3
N-terminal residue	Ser	
C-terminal residue	Phe	
2nd residue[b]	(Pxy)Lys	

[a] (Pxy)Lys emerged from the column between histidine and arginine;
[b] Determined after one step of Edman-degradation.

On the basis of the cationic mobility of the Pxy-peptide (upon treatment with phosphatase) it may be inferred that the peptide contains Asn rather than Asp.

The N-terminal residues and N-terminal sequence were determined by the dansyl-Edman procedure (cf. Hartley, 1970); Ser-(Pxy)Lys proved to be the N-terminal sequence in both peptides.* Phe was identified as the C-terminal residue, on digestion of the peptides with carboxypeptidase A by the micromethod of Sajgó and Dévényi (1972). From these results the amino acid sequence of Pxy-peptide is Ser-(Pxy)Lys-Asn-Phe. The peptide thus proved identical with that previously isolated from aspartate aminotransferase from pig heart cytosol (Morino, Watanabe, 1969).

* Dansyl products of ε-(Pxy)lysine were unambiguously separated from other dansyl amino acids by two-dimensional chromatography on polyamide thin-layer plates (cf. Hartley, 1970).

It is of interest that two fluorescent bands were revealed after the first electrophoretic run and the mobilities of these bands became identical following treatment with phosphatase (Fig. 1). To elucidate this phenomenon the peptides eluted from bands A and N were repeatedly subjected to electrophoresis at pH 6.5 without treatment with phosphatase. We found that in this case band A retained its anionic character whereas band N was separated into fluorescent neutral and anionic bands. It may be inferred that band N contains a dissociable complex of P-Pxy-tetrapeptide with some unidentified compound which masks the charge of the 5'-phosphate group. Removal of the phosphate by phosphatase destroys the complex and imparts cationic mobility to the peptide.

References

Abrosimova-Amelyanchik N. M., Axelrod V. D., Tatarskaya R. I. (1967) Biokhimiya, *32* 240–247
Dévényi, T. (1969) Acta Biochim. Biophys. Acad. Sci. Hung. *4* 297–299
Fischer, E. H., Kent, A. B., Snyder, E. R., Krebs, E. G. (1958) J. Am. Chem. Soc. *80* 2906–2907
Hartley, B. S. (1970) Biochem. J. *119* 805–822
Hughes, E. C., Jenkins, W. T., Fischer, E. H. (1962) Proc. Natl. Acad. Sci. *48* 1615–1618
Kochkina, V. M., Torchinsky, Yu. M. (1974) Biokhimiya, in press
Milstein, C. P. (1967) Nature *215* 1190–1191
Morino, Y., Watanabe, T. (1969) Biochemistry, *8* 3412–3417
Polyanovsky, O. L., Keil, B. A. (1963) Biokhimiya *28* 372–379
Sajgó, M. (1969) Acta Biochim. Biophys. Acad. Sci. Hung. *4* 385–386
Sajgó, M., Dévényi, T. (1972) Acta Biochim. Biophys. Acad. Sci. Hung. *7* 233–236
Strausbauch, P. H., Fischer, E. H. (1970) Biochemistry *9* 233–238
Vorotnitzkaya, N. E., Spyvack, V. A., Polyanovsky, O. L. (1968) Biokhimiya, *33* 375–382

Acta Biochim. et Biophys. Acad. Sci. Hung. Vol. 9 (3), pp. 217–221 (1974)

On the Second Protonation of Adenine and Guanine

(Short Communication)

G. BUDÓ, J. TOMASZ*

Institute of Biochemistry, Biological Research Center, Hungarian Academy of Sciences, Szeged, Hungary

(Received December 6, 1973)

Adenine and guanine have three possible sites of protonation in their predominant tautomeric form: adenine at N1, N3 and N7, and guanine at N3, N7 and O^6. The attachment of the first proton takes place mainly at position N1 of adenine and position N7 of guanine with pK_a values of 4.1 (adenine) and 3.2 (guanine) (Kochetkov, Budovskii, 1971). In the case of adenine the N7 protonated form is present in a small amount at equilibrium with the predominant N1 protonated tautomer, as concluded from kinetic studies (Tomasz et al., 1972) and fluorescence spectra (Börresen, 1967).

The quantitative parameters of the second and third protonations which occur at higher acidities have not yet been determined. The detection and characterization of the multiprotonated species were done on the basis of n.m.r. data obtained in different non-aqueous solvents of high acidities and at low temperatures. Accordingly, both compounds are present as dications in ahydrous trifluoro acetic acid ($H_0 = -4.4$) (Mackor et al., 1957) with the second proton attached to N7 in adenine and to N3 in guanine (Wagner, von Philipsborn, 1971). On the basis of potentiometric (Albert, Brown, 1954) and spectrophotometric studies (Beaven et al., 1955) approximate values were given for the second protonations as $pK_a < 1$ (adenine) and $pK_a < 0$ (guanine).

Our investigations concerning the mechanism of separation of nucleic acid bases and nucleotides on strong cation-exchange thin-layers (Tomasz, 1973) required the determination of pK_a values of the second protonation of the two purines. This was performed by UV spectrophotometry in moderately concentrated aqueous sulphuric acid solutions of known acidities (Flexser et al., 1935), based on the assumption that the overlap between the ranges of the first and second protonations is negligible. The known pK_a value of the first protonation and the very close similarities between the UV spectra of adenine in 0.05 M and 0.005 M sulphuric acid, and between the spectra of guanine in 0.05 M and 0.1 M sulphuric acid supported the validity of this assumption.

Measurements were carried out at $25 \pm 1°C$, by using a Cary recording spectrophotometer, Model 15. Sulphuric acid solutions were prepared by diluting

* To whom all correspondence shcuild be addressed.

reagent grade 95–97% sulphuric acid (VEB Laborchemie, Apolda) with deionized water and their concentrations were determined by titrating aliquots with standard sodium hydroxide. The H_0 values given by Paul and Long (1957) were used to express acidities. Adenine and guanine were commercial products (Sigma) and their purity was checked by paper chromatography (Wyatt, 1955) and by UV absorption (Beaven et al., 1955).

A characteristic bathochromic shift was observed in the UV spectra of both purines with increasing acidity. This was more pronounced with guanine, than with adenine (see Fig. 1). To prove that the spectral changes were due to the second protonation and not to other chemical reactions, solutions of the bases in 95%

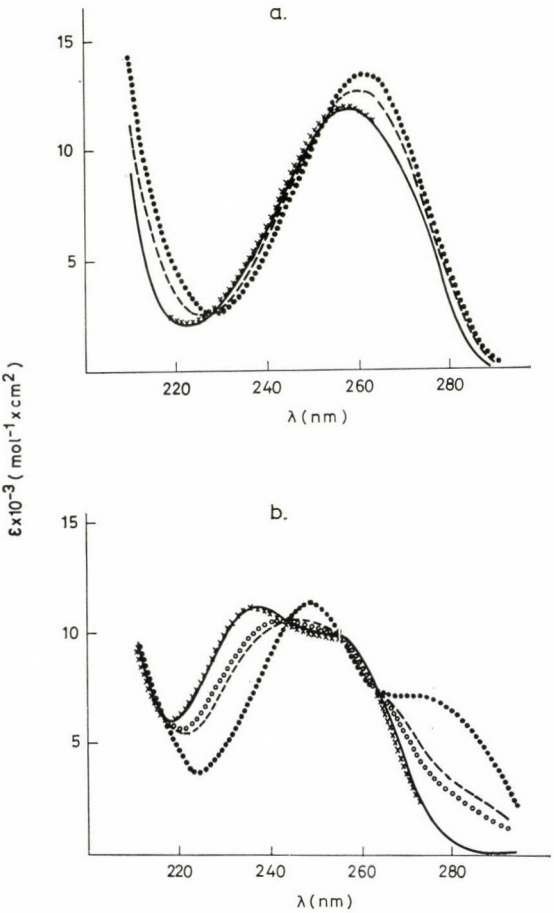

Fig. 1. UV spectra of purines in aqueous sulphuric acid solutions of different molarities a) Adenine in 0.005 M and 0.05 M (. . . .), 0.96 M (----), 3.93 M (——) and 4.87 M (xxxx) sulphuric acid; b) guanine in 0.05 M and 0.1 M (. . . .), 2.52 M (- - - -), 3.02 M (oooo), 5.88 M (——) and 7.39 M (xxxx) sulphuric acid.

Table 1
Spectral data of adenine and guanine

		λ_{max} (nm)	ε_{max} ($mol^{-1} \times cm^2$)	λ_{min} (nm)	ε_{min} ($mol^{-1} \times cm^2$)	ε_{250} ($mol^{-1} \times cm^2$)	$\frac{E_{250}}{E_{260}}$	$\frac{E_{280}}{E_{260}}$	$\frac{E_{290}}{E_{260}}$	$\frac{E_{215}}{E_{240}}$	$\frac{E_{260}}{E_{240}}$	M*
Adenine	Dication	256 – 258.5	11.700	220 – 222	2100	11.600	0.90	0.32	0.008	0.53	1.76	3.93
	Monocation	261 – 263	13.400	227 – 229	2650	13.300	0.76	0.36	0.032	1.43	2.44	0.05
		(262.5)	(13.200)	(229)	(2600)	(13.000)	(0.76)	(0.38)	(0.04)			
										$\frac{E_{230}}{E_{270}}$	$\frac{E_{230}}{E_{275}}$	
Guanine	Dication	237	11.250	218	6000	8700	1.15	0.07	0.03	0.52	6.25	5.88
	Monocation	247.5	11.400	224	3700	8050	1.40	0.80	0.47	0.68	0.69	0.10
		(248.5)	(11.400)	(224)	(3550)	(8000)	(1.37)	(0.84)	(0.50)			

Values in parentheses are those of Beaven et al. (1955)
* The molarity of sulphuric acid solution used for determining the spectrum.

Table 2
Constants of the second protonation of adenine and guanine

	From plots log I *vs.* H_0					From plots (log $I + H_0$) *vs.* ($H_0 + \log [H^+]$)				$\Delta\varepsilon$*
	pK_a	x	σ_y	σ_{sl}	'pK_a'	pK_a	Φ	σ_y	σ_{sl}	
Adenine	– 0.33	1.01	0.016	0.027	– 0.32	– 0.36	– 0.06	0.038	0.072	240 – 215
	– 0.38	1.03	0.024	0.032	– 0.37	– 0.34	0.02	0.042	0.074	240 – 260
Guanine	– 1.04	0.90	0.030	0.022	– 1.15	– 1.03	0.06	0.028	0.031	230 – 275
	– 1.06	0.89	0.021	0.031	– 1.19	– 1.07	0.17	0.030	0.029	230 – 270

x is the slope parameter of equation (1) [see text]. Φ is the slope parameter of equation (2) [see text]. σ_y is the standard deviation of points from the linear regression line in the direction of y. σ_{sl} is the standard deviation of the slope. 'pK_a' is the H_0 value of "half-diprotonation". Eight experimental points were used to calculate pK_a values in each case.
* Values used for calculation according to equation (3) [see text].

sulphuric acid were prepared and diluted with deionized water to an acidity value of pH 1 after standing at room temperature for 1 hour. The UV spectra of these solutions appeared to be identical with those reported in the literature under the same conditions (Beaven et al., 1955). The spectral data of dications compared to those of monocations are summarized in Table 1. It is worth noting that the first protonation or deprotonation causes a hypochromic change in the UV spectra of major nucleic acid bases, whereas the second anionic dissociation of uracil and thymine is connected with a bathochromic spectral shift (Beaven et al., 1955).

Two different methods were used to calculate pK_a values. The first one was deduced by Hammett (1970) who assumed linear relationships between various acidity functions, *viz.*

$$\log I = pK_a - xH_0, \tag{1}$$

where I is the "ionization ratio" defined as [dication]/[monocation] in this case, x is the slope parameter independent of acid concentration, and H_0 is Hammett's acidity function (Hammett, Deyrup, 1932).

The second method was the linear free energy relationship of Bunnett and Olsen (1966). It is a general method for estimating the thermodynamic pK_a of any base undergoing protonation in moderately concentrated aqueous mineral acid solutions with reference to the single acidity function H_0:

$$\log I + H_0 = \Phi(H_0 + \log [H^+]) + pK_a \tag{2}$$

where the slope parameter, Φ, expresses the response of the equilibrium to changing acid concentration.

The log I values were computed from the relationship

$$I = \frac{\Delta\varepsilon_+ - \Delta\varepsilon}{\Delta\varepsilon - \Delta\varepsilon_{++}} \tag{3}$$

by using $\Delta\varepsilon$ values of $\varepsilon_{240} - \varepsilon_{215}$ and $\varepsilon_{240} - \varepsilon_{260}$ for adenine and $\varepsilon_{230} - \varepsilon_{270}$ and $\varepsilon_{230} - \varepsilon_{275}$ for guanine according to Stewart and Granger (1961). The subscripts + and ++ in equation (3) refer to the monocation and dication, respectively. Each set of data was plotted according to equations (1) and (2) and was also subjected to standard linear regression analysis with the aid of a computer (Wang 600).

Results presented in Table 2 clearly delmonstrate that in contrast to the analogous species of guanine, the adenine monocation behaves like a Hammett base, having a Φ value of zero. The pK_a values show that a considerable fraction of adenine and guanine is present as dication already in moderately concentrated aqueous mineral acids (*e.g.* the H_0 value of "half-diprotonation" of guanine roughly corresponds to that of 3.0 N hydrochloric acid). At the same time they corroborate our earlier assumption that the classical separation of nucleic acid bases on cation

exchange resins (Cohn, 1949) is governed by an ion exchange mechanism, since the extent of second protonation of purines is considerable but unequal under the chromatographic circumstances.

The excellent technical assistance of Miss E. Rádi is gratefully acknowledged.

References

Albert, A., Brown, D. J. (1954) J. Chem. Soc. 2060—2071
Beaven, G. H., Holiday, E. R., Johnson, E. A. (1955) In: "Nucleic Acids" (eds) Chargaff, E., Davidson, J. N. Academic Press, New York, Vol. I. pp. 493—553
Börresen, H. C. (1967) Acta Chem. Scand. *215* 2463—2472
Bunnett, J. F., Olsen, F. P. (1966) Can. J. Chem. *44* 1899—1916
Cohn. W. E. (1949) Science *109* 377—378
Flexser, L. A., Hammett, L. P., Dingwall, A. (1935) J. Am. Chem. Soc. *57* 2103—2115
Hammett, L. P. (1970) "Physical Organic Chemistry". McGraw Hill, Co., New York, London, pp. 263—313
Hammett, L. P., Deyrup, A. J. (1932) J. Am. Chem. Soc. *54* 2721—2739
Kochetkov, N. K., Budovskii, E. I. (1971) "The Organic Chemistry of Nucleic Acids". Plenum, New York, Vol. I. pp. 121—182
Mackor, E. I., Smith, P. J., van der Waals, J. H. (1957) Trans. Farad. Soc. *53* 1309—1315
Paul, M. A., Long, F. A. (1957) Chem. Revs. *57* 1—45
Stewart, R., Granger, M. R. (1961) Can. J. Chem. *39* 2508—2515
Tomasz, J. (1973) J. Chromatogr. *84* 208—213
Tomasz, M., Olson, J., Mercado, C. M. (1972) Bicchemistry *11* 1235—1241
Wagner, R., von Philipsborn, W. (1971) Helv. Chim. Acta *54* 1543—1559
Wyatt, G. R. (1955) In: "Nucleid Acids" (eds) Chargaff, E., Davidson J. N. Academic Press, New York, Vol. I. pp 243—265

Acta Biochim. et Biophys. Acad. Sci. Hung. Vol. 9 (3), pp. 223—226 (1974)

Complex Formation between Phosphorylase *b* and Phosphorylase *b* Kinase. A New Evidence for Protein Interactions in the Phosphorylase System

(Short Communication)

P. GERGELY, GY. VEREB, GY. BOT

Institute of Medical Chemistry, University of Medicine, Debrecen, Hungary

(Received May 8, 1974)

The observation that glycogen particles can be isolated from rabbit skeletal muscle is a strong indication that such a complex represents the structural and functional unit existing in the cell (Meyer et al., 1970). Further investigations (Heilmeyer et al., 1970; Haschke et al., 1970) demonstrated that the activation and inactivation processes of phosphorylase occur in the glycogen particles in a similar manner as it is observed *in vivo*. Another important finding was that the modified properties of enzymes in the glycogen particles could probably be attributed to a protein component and not to the presence of glycogen (Haschke et al., 1972).

In the light of the foregoing it seemed to be of interest to examine whether complex formation between these enzymes could be detected under near-physiologic conditions. The possible binding of phosphorylase to phosphorylase *b* kinase and phosphorylase phosphatase was studied because these enzymes catalyze the interconversion of phosphorylase between the *b* and *a* forms.

Frontal analysis gel filtration was chosen as a method for the demonstration of multienzyme complexes (Chiancone et al., 1968; Földi et al., 1973). Crude extracts (which approach the physiological conditions) were used and the elution profiles were determined by measuring the enzymic activities of the components. Crude muscle extract was prepared from fresh minced rabbit skeletal muscle with 1 volume of 100 mM sucrose (adjusted with 0.1 M Tris to pH 6.8) and centrifuged for 20 min at 10 000 × *g*, 4 °C. The supernatant fluid was allowed to stand for 1 hour at 30 °C and recentrifuged for 20 min at 10 000 × *g*, 4 °C. The clear supernatant, referred to as "crude extract", was applied to the column. For the removal of phosphorylase *b* kinase from the "crude extract", the pH was adjusted to 5.8 and it was allowed to stand for 30 min at room-temperature, thereafter the kinase precipitated was collected by centrifugation. The pH of the supernatant was then readjusted to 6.8 and the material obtained was used for gel filtration as "extract without kinase". The absence of phosphorylase *b* kinase was checked by activity assay as reported Brostrom et al. (1971).

Crystalline phosphorylase *b* was prepared from rabbit skeletal muscle according to Fischer and Krebs (1958), its activity was assayed by the procedure of Illingworth and Cori (1953). Phosphorylase *b* kinase was prepared from rabbit skeletal muscle by the method of DeLange et al. (1968). Protein was determined by the biuret-procedure (Lowry et al., 1951) or spectrophotometrically (Sevilla, Fischer, 1969).

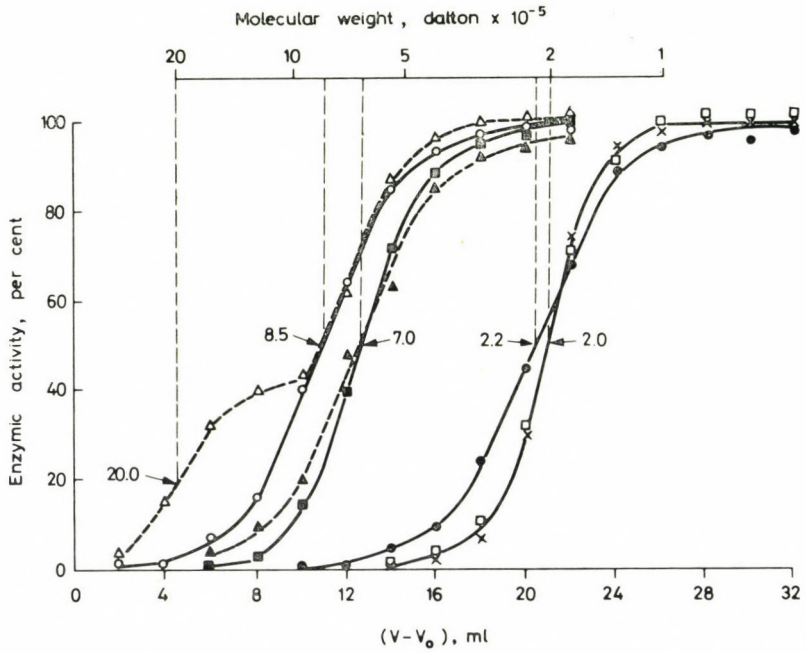

Fig. 1. Elution profiles of muscle extracts, crystalline phosphorylase *b* and purified kinase on Sepharose 4B.

Frontal gel filtration was performed on a column, 1.2 cm × 60 cm (LKB), operated in ascending manner at 23 ± 0.2 °C. The column, equilibrated with 100 mM sucrose (pH 6.8), was calibrated with thyroglobulin (Mw. 670 000), catalase (Mw. 240 000) and phosphorylase *b* (Mw. 190 000). Molecular weights were calculated according to Fischer (1969) from the inflection points of the sigmoidal elution profiles. The void volume (V_0) was determined with Blue Dextran 2000. Enzyme activities are expressed in per cent of activities in the sample applied to the column. Crystalline phosphorylase *b*: □——□, x——x phosphorylase *b* activity (enzyme concentrations 7.5 and 1.0 mg per ml, respectively);
"crude extract": ○——○ phosphorylase *b* and △- - - -△ phosphorylase *b* kinase activity (total protein concentration 37 mg per ml, phosphorylase *b* 1.1 mg per ml, kinase 0.4 mg per ml);
"extract without kinase": ●——● phosphorylase *b* activity (total protein 35 mg per ml, phosphorylase *b* 1.04 mg per ml);
mixture of crystalline phosphorylase *b* and purified kinase: ■——■ phosphorylase *b* and ▲- - - -▲ kinase activity (1.0 and 0.4 mg per ml respectively)

Typical elution profiles of rabbit skeletal muscle extracts, crystalline phosphorylase *b* and purified kinase are presented in Fig. 1, where the per cent of enzymic activities (phosphorylase *b* and kinase) are plotted against the corrected elution volumes ($V-V_0$).

In control experiments solutions of crystalline phosphorylase *b* were used for frontal gel filtration at various concentrations. It is seen from the profiles that crystalline phosphorylase *b* eluted from the column with an apparent molecular weight of about 200 000 daltons, in good agreement with other data in the literature (DeVincenzi, Hedrick, 1967; Seery et al., 1967), and further, the molecular weight is independent of enzyme concentration. In contrast, the apparent molecular weight of phosphorylase *b* in the "crude extract" is much higher than that of the crystalline enzyme, approximately 850 000 daltons. The activity of phosphorylase *b* kinase was simultaneously assayed in the effluent of the "crude extract". Part of this enzyme emerged from the column with a higher molecular weight (about 2 millions) than that of the purified kinase ($1.33 \times \times 10^6$ daltons according to Hayakawa et al., 1973). Thereafter its activity ran parallel with the phosphorylase activity, which indicates the possibility of complex-formation between these enzymes.

When phosphorylase *b* kinase was removed ("extract without kinase"), the apparent molecular weight of phosphorylase *b* decreased to 220 000 daltons. These observations strongly suggest that there are protein–protein interactions between phosphorylase *b* and kinase. This assumption was supported by the frontal gel filtration of a mixture of crystalline phosphorylase *b* and purified kinase, which yielded a complex about 700 000 daltons. However, the molecular weight of the complex does not correspond to the sum of that of the components. This discrepancy can not be interpreted, though it is known that phosphorylase *b* kinase is constituted of subunits (Hayakawa et al., 1973), therefore the dissociation of kinase to lower molecular weight species can not be excluded under these conditions.

Our results demonstrate the protein–protein interaction between phosphorylase *b* and phosphorylase *b* kinase. According to our preliminary investigations the apparent molecular weight of phosphorylase phosphatase is also higher in crude muscle extract than is alone, which indicates a further association in the phosphorylase system. Subsequent studies are required to elucidate the physiological role of these enzyme complexes.

References

Brostrom, C. O., Hunkeler, F. L., Krebs, E. G. (1971) J. Biol. Chem. *246* 1961–1967

Chiancone, E., Gilbert, L. M., Gilbert, G. A., Kellett, G. L. (1968) J. Biol. Chem. *243* 1212–1219

DeLange, R. J., Kemp, R. G., Riley, W. D., Cooper, R. A., Krebs, E. G. (1968) J. Biol. Chem. *243* 2200–2208

DeVincenzi, D. L., Hedrick, J. L. (1967) Biochemistry *6* 3489—3497
Fischer, E. H., Krebs, E. G., (1958) J. Biol. Chem. *231* 65—71
Fischer, L. (1969) in Laboratory Techniques in Biochemistry and Molecular Biology (Work, T. S., Work, E. eds) pp. 157, North-Holland Publishing Company, Amsterdam
Földi, J., Szabolcsi, G., Friedrich, P. (1973) Acta Biochim. Biophys. Acad. Sci. Hung. *8* 263—265
Haschke, R. H., Heilmeyer, L. M. G., Meyer, F., Fischer, E. H. (1970) J. Biol. Chem. *245* 6657—6663
Haschke, R. H., Grätz, K. W., Heilmeyer, L. M. G. (1972) J. Biol. Chem. *247* 5351—5356
Hayakawa, T., Perkins, J. P., Walsh, D. A., Krebs, E. G. (1973) Biochemistry *12* 567—573
Heilmeyer, L. M. G., Meyer, F., Haschke, R. H., Fischer, E. H. (1970) J. Biol. Chem. *245* 6649—6656
Illingworth, B., Cori, G. T. (1953) in Biochemical Preparations (Snell, E. E. ed), Vol. 3, pp. 1—9, John Willey et Sons, Inc., New York
Lowry, O. H., Rosebrough, N. J., Farr, A. L., Randall, R. J. (1951) J. Biol.Chem. *193* 265—273
Meyer, F., Heilmeyer, L. M. G., Haschke, R. H., Fischer, E. H. (1970) J. Biol. Chem. *245* 6642—6648
Seery, V. L., Fischer, E. H., Teller, D. C. (1967) Biochemistry *6* 3315—3327
Sevilla, C. L., Fischer, E. H. (1969) Biochemistry *8* 2161—2171

Acta Biochim. et Biophys. Acad. Sci. Hung. Vol. 9 (3), pp. 227–231 (1974)

Studies on Chlorophyll Accumulation of Maize Leaves Grown under Different Illuminations

B. NÉMET

Institute of Plant Physiology, Biological Research Center, Hungarian Academy of Sciences, Szeged, Hungary*

(Received September 30, 1973)

Chlorophyll (a+b) contents and chlorophyll a/b ratios were compared in post-etiolated maize leaves illuminated intermittently (2 minutes light, 58 minutes dark) or continuously with light of different intensities.

In all cases of intermittent illumination at different intensities the final chlorophyll (a+b) contents were much lower, but the chlorophyll a/b ratios were significantly higher, than in leaves exposed to continuous illumination.

Clorophyll a/b ratios at a given supply of ligth energy were higher in maize leaves illuminated intermittently than in those where illumination was continuous.

Chlorophyll a/b ratios at any given chlorophyll (a+b) content were also higher in leaves grown under intermittent light than in those illuminated continuously.

Introduction

Contrasting data have previously been reported on the effect of light upon the formation of chl-b. According to Shlyk et al. (1963) light has no direct effect on chl-b synthesis. On the other hand it has been demonstrated that chl a/b ratios were permanently high in post-etiolated bean and barley seedlings grown under alternating light–dark conditions (Akoyunoglou, Argyroudi-Akoyunoglou, 1969, Argyroudi–Akoyunoglou, Akoyunoglou, 1970). Recently Thorne and Boardman (1971) reported that chl a/b ratios strongly depended upon the intensity of illumination in greening plants. These data suggest that light may influence the level of chl-b in an indirect manner which can be studied by a systematic combination of intermittent and continuous illuminations of different intensities.

The aim of the present study was to elucidate the effect of periodically intermittent (light–dark) illumination of different intensities compared with continuous illumination of different intensities on the [chl (a + b)] contents and chl a/b ratios of maize leaves.

Abbreviations: (chl-a): chlorophyll-a; (chl-b): chlorophyll-b; (chl a/b): chlorophyll-a/chlorophyll-b; [chl (a+b)]: chlorophyll-a+chlorophyll-b.

* *Present address:* Institute of Experimental Physics, József Attila University, Szeged, Hungary.

Materials and methods

Seedlings of maize (*Zea mays* variety MV 801) were grown in complete darkness on moist filter paper for 7 days. Some of them were illuminated in cycles of 2 min light alternating with 58 min dark periods. The rest of the plants was illuminated with continuous light. In both systems light was provided by tungsten

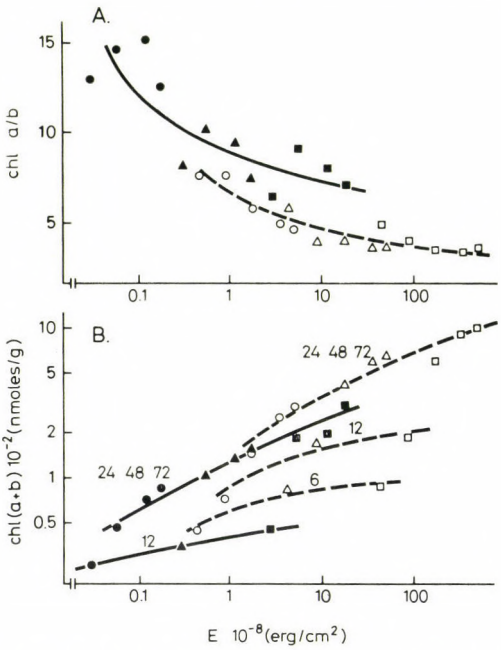

Fig. 1. Chlorophyll a/b ratios (A) and chlorophyll (a+b) contents (nmoles/g fresh weight) (B) of maize leaves versus the integral dose of light energy (E). The maize leaves were grown under intermittent and continuous illumination of different intensities (o, low; △, medium; □, high intensity) to. Solid line, full symbols: intermittent illumination; dashed line, open symbols: continuous illumination. The figures 6, 12, 24 etc. mean that maize leaves were harvested after 6, 12, 24, etc. hours (cycles) of illumination, respectively

lamps and was applied at different intensities corresponding to 2×10^3 (low), 2×10^4 (medium) and 2×10^5 (high) erg/cm^{2}sec at the level of the leaves as measured with a KIPP and ZONEN thermopile. The leaves were harvested 6, 12, 24, 48 and 72 hours after the start of illumination cycles.

The leaf samples (0.5–1 g fresh weight) were ground in acetone and the pigments were transferred to diethyl ether. The amount of chlorophyll was measured by the double wave lengths method (French, 1960) at 662 and 644 nm in a UNICAM SP 1800 spectrophotometer with a zero setting at 700 nm. The data presented were taken from 4–6 measurements performed in 2–3 independent experiments.

Results

Chl (a + b) contents and chl a/b ratios of maize leaves grown under intermittent and continuous illuminations were measured at various times after the beginning of illumination and shown in Fig. 1 as functions of the integral dose of light energy (E) supplied to the leaves; in addition the chl a/b ratios were compared for the same chl (a + b) contents.

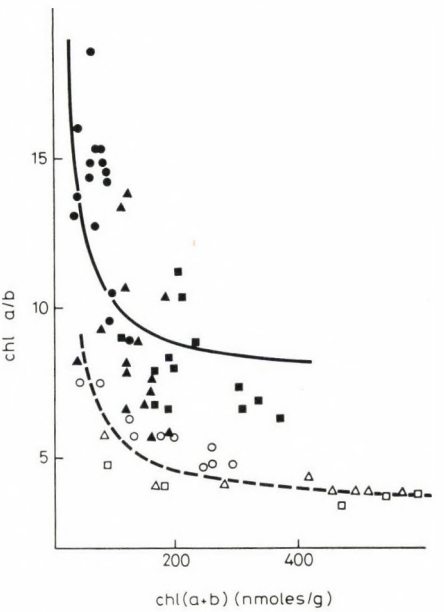

Fig. 2. Chlorophyll a/b ratios versus chlorophyll (a+b) contents (nmoles/g fresh weight) of maize leaves grown under intermittent and continuous illumination of different intensities (symbols as in Fig. 1). Solid line: intermittent illumination, chl a/b = 7.5 + 245.3/ [chl (a+b)]; dashed line: continuous illuminations, chl a/b = 3.47 + 215.5/ [chl (a+b)]

The chlorophyll accumulation of post-etiolated maize leaves subjected to intermittent illumination was less than that of leaves exposed to continuous illumination of the same intensity. The difference was about 3–4 fold. However, in the case of continuous illumination the leaves received 30 times as much light energy per hour as leaves subjected to intermittent illumination. Thus, the utilization of the energy supplied per hour (cycle) for chlorophyll accumulation of maize leaves was 8–10 times as effective under intermittent light as under continuous one of the same intensity. The intermittent illumination resulted in chl a/b ratios about twice as high as those in continuous one. The lower light intensities gave higher chl a/b ratios with both illumination systems. This was particularly striking with the intensity of 2×10^3 erg/cm^{2}sec.

The chl (a + b) contents of the leaves (harvested at the same time) corresponding to a given integral dose of light energy were lower, but the chl a/b ratios were higher, with intermittent illumination than with continuous one (Fig. 1).

Since the decreasing chl a/b ratio is stabilized at about a constant level in the process of greening (Thorne, Boardman, 1971), the relationship between chl a/b ratios and chl (a + b) contents may tentatively be characterized by hyperbolic functions. The two functions calculated by the regression method from the chl (a + b) contents and chl a/b ratios of maize leaves exposed to the two types of illumination are shown in Fig. 2. With the same light intensities and the same chl (a + b) contents intermittent illumination resulted in higher chl a/b ratios than did the continuous one.

Discussion

Different concepts have been developed as to the formation of chlorophyll and chl a/b ratios. Thorne and Boardman (1971) claim that there is an indirect effect of light on the formation of chl-b, however, they do not exclude the possibility that light is directly required for the conversion of chl-a to chl-b. Our data show that the integral dose of light energy supplied to the plant is not the only factor determining transformation of chl-a to chl-b, because the chl a/b ratios of maize leaves grown under intermittent and continuous illuminations plotted against the light energy supplied are different.

According to Veleminsky and Röbbelen (1966) the rate of chl-b accumulation is determined by the rate of chl-a accumulation. Thus the chl a/b ratios are determined by chl (a + b) contents. Our data show that the chl a/b ratios of maize leaves exposed to intermittent and continuous illuminations and normalized to the same chl (a + b) content are also different.

Although the chl-b content was found to be influenced by both the chl (a + b) content and the amount of light energy supplied, the dark periods in the light–dark cycles also seem to be essential. Processes of pigment metabolism (transformation and decomposition) in the dark periods of light–dark alternation have not yet been completely elucidated (Rudoi et al., 1968). The lower amounts of chl-b found upon darkening can be explained by a number of mechanisms. According to Wieckowski and Ficek (1970), in very young leaves the reversion of the chl-a – chl-b reaction may be significant. It is also conceivable that the newly formed molecules of chl-b rapidly decompose under certain conditions (Shlyk et al., 1970).

Another explanation would be that the low chl-b levels result from a lower rate of chl-b synthesis due to a reduced pool of "free" chl-a molecules capable of undergoing transformation to chl-b. The binding sites ensuring the characteristic arrangement of pigment molecules in chloroplast lamellae develop in a light-triggered dark process (Butler, 1961). Thus the chl-a molecules accumulated during the short light periods find the binding sites with a high probability (the

pool of "free" chl-a molecules convertible to chl-b is lowered) and they no longer play a role as chl-b precursors (Shlyk et al., 1963; Shlyk, 1971). This may be an explanation of the relatively low chl-b contents and higher chl a/b ratios obtained with intermittent illumination.

Thanks are due to Drs Ágnes Faludi-Dániel and S. Demeter for their help and encouragement and to Prof. A. A. Shlyk for the valuable discussion while preparing the manuscript.

References

Akoyunoglou, G., Argyroudi-Akoyunoglou, J. H. (1969) Physiol. Plant *22* 288
Argyroudi-Akoyunoglou, J. H., Akoyunoglou, G. (1970) Plant Physiol. *46* 247
Butler, W. L. (1961) Arch. Biochem. Biophys. *92* 287
French, C. S. (1960) In: Encyclopedia of Plant Physiology (ed. Rühland) W.) Springer Verlag Berlin, Göttingen, Heidelberg, Vol. 5/1, pp. 259
Rudoi, A. B., Shlyk, A. A., Vezitsky, A. Y. (1968) Dokl. Akad. Nauk SSSR *183* 215
Shlyk, A. A., Kaler, V. L., Vlasenok, L. I., Gaponenko, V. O. (1963) Photochem. Photobiol. *2* 219
Shlyk, A. A., Rudoi, A. B., Vezitsky, A. Y. (1970) Photosynthetica *4* 68
Shlyk, A. A. (1971) Annual Review of Plant Physiology *22* 169
Thorne, S. W., Boardman, N. K. (1971) Plant. Physiol. *47* 252
Veleminsky, J., Röbbelen, G. (1966) Planta (Berl.) *68* 15
Wieckowski S., Ficek, S. (1970) Bulletin de l'Académie Polonaise des Sciences *18* 47

Acta Biochim. et Biophys. Acad. Sci. Hung. Vol. 9 (3), pp. 233–238 (1974)

Forces Acting between Muscle Filaments

III. A Mathematical Computation of the Resting Elasticity of Bee Wing Muscle

N. GARAMVÖLGYI, G. BICZÓ, A. EŐRY, S. SUHAI

Research Unit, Hungarian College of Physical Education and Central Research Institute for Chemistry, Hungarian Academy of Sciences, Budapest, Hungary

(Received January 28, 1974)

Dedicated to the memory of Professor Jean Hanson F. R. S.
(†August 1973)

In order to check the reality value of our former calculations concerning the resting elasticity of the muscle substance of vertebrate striated muscle we substituted now the exponents of the distance-dependence of the intermolecular adhesive and repulsive forces into the equations of a similar calculation applied to the conditions of bee flight muscle. In this muscle the filament length, relative position of the two kinds of filaments, volume behaviour and length-tension diagram are different from those of vertebrate muscle. *Mutatis mutandis* we obtained with this muscle a good fit of the theoretical and experimental length tension diagrams.

Introduction

In the previous paper of this series (Garamvölgyi et al., 1973) we presented a theoretical computation to explain the resting elasticity of vertebrate muscle in terms of the muscle substance itself. It is an apparent difficulty that the overlap of the two kinds of filaments decreases during passive stretch, while as the length tension diagram exhibits a nearly exponential course (*e.g.* Ernst, 1963). Due to this difficulty the resting muscle is usually regarded as nearly ideally plastic and all the elastic properties are attributed to parallel elements, *i.e.* the sarcolemma, cell membrane and longitudinal sarcoplasmic reticulum (*e.g.* Huxley, 1963). We have shown that by taking the changes of the lateral distance of filaments into account the elastic properties of muscle can be theoretically described in terms of the changing overlap, if the cross-bridges are detached. The best fit of the calculated curve to the experimental length tension diagram of a whole muscle was obtained in the case when the adhesive force was taken to decrease with the seventh, and the repulsive force with the fifteenth, power of the distance. Naturally, when fitting the theoretical curve to an experimental one obtained with a whole muscle we counted with the less favourable case.

It is well known that in the flight muscle of some insects the relative position of the two kinds of filaments differs from that found in vertebrate muscle, inas-

much as instead of being surrounded by three myosin filaments the actin filaments are situated at mid-distance between two myosin filaments. On the other hand, it seems that this muscle does not behave as a body of constant volume. We demonstrated in the first paper of this series that the change of the lateral separation of filaments caused by stretch is much more rapid than required by volume constancy (Garamvölgyi, 1972). It seems therefore impossible to attribute the changes of the lateral separation of the filaments to the constant volume of the whole cell, *i.e.* to a lateral compression caused by a decrease of cell diameter in the case of passive stretch. This observation gave rise to the attempt to explain the regulation of the lateral distance of filaments (*i.e.* of the lattice constant of the hexagonal paracrystalline lattice of filaments) in terms of a changing equilibrium of long-range forces introduced by the changing overlap, instead of a lateral passive compression caused by volume constancy.

Several years ago we performed experiments to establish the mechanical properties of active and inactive bee flight muscle (Garamvölgyi, Belágyi, 1968; Belágyi, Garamvölgyi, 1968). It turned out that in conform with structural observations (*e.g.* Garamvölgyi, 1969), this muscle is highly extensible, in contrast to the fligth muscle of other insects (*e.g.* Hanson, 1956; Pringle, 1967). The length tension diagram of the resting muscle can be divided into two parts, the first of which coincides with the range of the sliding movement of this muscle (Belágyi, Garamvölgyi, 1968).

In this paper we shall deal exclusively with this first range and neglect the second range to be attributed to the elongation of myosin filaments themselves (Garamvölgyi, 1969). The first range of the length tension diagram of resting bee wing muscle is slightly S-shaped. It can be approached by a straigth regression line to a very good approximation (Garamvölgyi, Belágyi, 1968). Since there is no connective tissue in this muscle nor is there a considerable amount of sarcoplasmic reticulum, the nearly linear shape of the length tension diagram has been originally explained (Pringle, 1967; Garamvölgyi, Belágyi, 1969; Garamvölgyi, 1969) by the assumption that the C-filaments anchor myosin filaments to the Z-lines (Auber, Couteaux, 1962, 1963; Garamvölgyi, 1963).

Initial conditions

In the present calculation we generally preserved all conditions postulated in the previous paper of this series (Garamvölgyi et al., 1973). The filaments are regarded as mathematical lines of constant length. Changes of pH and ionic strength have been neglected. On the other hand, some special characteristics of this muscle have been taken into account.

1. Geometry of the hexagonal lattice. Actin filaments are situated between two myosin filaments. The center-to-center distance of myosin filaments (*i.e.* the lattice constant) at the initial length (equilibrium length) was taken to be roughly

500 Å, a value derived from our electronmicrographs of the cross-section of unstretched bee wing muscle myofibrils (Fig. 1).

2. Volume behaviour. This muscle does not follow the principle of volume constancy with respect to sarcomere volume (Garamvölgyi, 1972). For vertebrate muscle we accepted (Garamvölgyi et al., 1973) that the lateral separation of filaments changes with the square root of the sarcomere length, *i.e.*:

$$S_0 d_0^2 = S d^2 = \text{const.}, \tag{1}$$

where S_0 and d_0 stand for the sarcomere length and lattice constant at the equilibrium length, whereas S and d represent actual sarcomere length and lattice constant values, respectively.

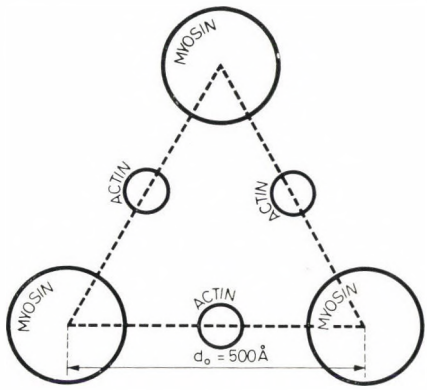

Fig. 1. Geometrical arrangement of three myosin and three actin filaments

We found in bee wing muscle a fourfold decrease of the cross-sectional area accompanied by a twofold increase of sarcomere length (Garamvölgyi, 1972). Since without X-ray diffraction it is impossible to establish the exact course of the change of the lateral distance of filaments, we arbitrarily chose the simplest satisfactory case, *i.e.* a linear relation:

$$S_0 d_0 = S d = \text{const.} \tag{2}$$

3. Sarcomere and filament lengths. The filament lengths were assumed to be 2.7 μ for the myosin filament and 1.3 μ for the actin filament (Garamvölgyi, 1969). Since in the unstretched insect flight muscle there are no well-expressed *I*-bands and the myosin filaments practically reach the *Z*-lines (Hanson, 1956; Auber, Couteaux, 1963), adding the width of a *Z*-line to the length of a myosin filament we obtained 2.8 μ for the equilibrium sarcomere length (S_0), the end of the sliding movements was correspondingly 5.4 μ, *i.e.* roughly equal to the two fold

initial length (Garamvölgyi, Belágyi, 1968; Belágyi, Garamvölgyi, 1968). The calculation was therefore performed in the range of $2.8\ \mu < S < 5.4\ \mu$.

4. The possible role of *C*-filaments has been neglected and we attributed the entire resting elasticity to long-range forces acting between myosin and actin filaments.

Method

The elementary force, dp, acting between the infinitesimal length of the myosin filament (dx_2) and that of the actin filament (dx_1) of the actin filament is given by the following expression:

$$dp = \left(\frac{A_{ab}}{\rho^a} + \frac{B_{ab}}{\rho^b} \right) dx_1\, dx_2 \,. \tag{3}$$

where dp is the distance between elements dx_1 and dx_2 (see Fig. 3 in Garamvölgyi et al., 1973). The constants A_{ab} and B_{ab} were determined previously for different values of the exponents a and b by fitting theoretical curve to the experimental data obtained with frog sartorius muscle (Garamvölgyi et al., 1973). The same procedure was repeated in the present calculation for fixed values of a and b to obtain the values of A_{ab} and B_{ab} which give the best fit to the experimental length-tension curve of bee wing muscle.

The total force acting between the two filaments along the x axis can be obtained as a function of sarcomere length by integrating the elementary force dp over variables x_1 and x_2:

$$P(S) = \int_{(S-S_0)/2}^{S_0/2} dx_2 \int_{(S-S_0)/2}^{S/2} dx_1 \left(\frac{A_{ab}}{\rho^{a+1}} + \frac{B_{ab}}{\rho^{b+1}} \right) (x_2 - x_1) \tag{4}$$

Factor 2 in Eq. (4) reflects the fact that each actin filament interacts simultaneously with two myosin filaments and *vice versa* (Fig. 1). The integrations in Eq. (4) were performed analytically by the use of equations (11) – (12) given in our earlier paper (Garamvölgyi et al., 1973), the modification of geometrical structure was taken into account.

The theoretical length tension curve of bee wing muscle was calculated for exponents a and b with which the best fit was obtained in the case of frog sartorius muscle, *i.e.* $a = 7$, $b = 15$.

Results and discussion

The results of the calculation performed with fixed exponents are shown in Fig. 2, together with the regression line obtained by Garamvölgyi and Belágyi (1968). Up to 5 μ sarcomere length even the slight *S*-shape of the experimental

curve (Fig. 5 in Garamvölgyi, Belágyi, 1968) seems to be reflected in the theoretical curve. The decline of the theoretical curve near the end cannot be interpreted by the sliding mechanism alone. In this muscle the two kinds of filaments do not actually separate from each other at the theoretical no-overlap-point, but at about a sarcomere length of 5 μ the myosin filaments begin to stretch. Even in this

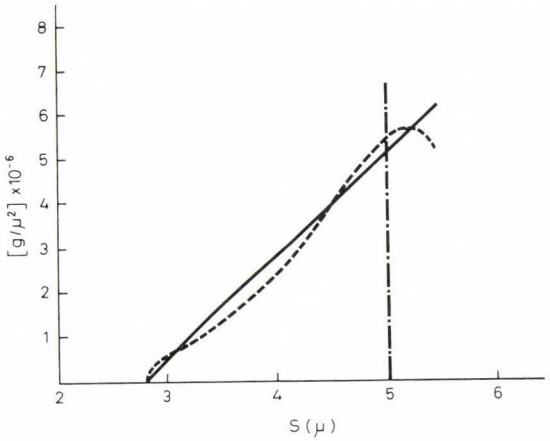

Fig. 2. Theoretical length-tension curve (broken line) and the regression line approximating the experimental length-tension diagram (Garamvölgyi, Belágyi, 1968) (continuous line) at a = 7 and b = 15

case residual zones of overlap of 1000 – 1200 Å length remain (Garamvölgyi, 1969). Thus the decreasing tendency of the theoretical curve observed in the range beyond 5 μ sarcomere length by no means contradicts our assumption, and the fit of the theoretical curve to the regression line approximating the experimental curve may be considered as satisfactory.

It is to be mentioned that with exponents $a = 7$ and $b = 8$ an even better fit to the straight line can be obtained. In our opinion, however, this is of no significance, since even the experimental length tension curve is not perfectly linear. A fit better than that shown in Fig. 2 cannot be expected, since the experimental error in registering the length-tension diagram with a minute specimen, like bee wing muscle, is most probably much greater. At any rate, the theoretical length tension diagram obtained for the structural conditions of the bee flight muscle is sharply different from that obtained with frog muscle, if the same exponents are used (Fig. 4 in Garamvölgyi et al., 1973).

This difference confirms our earlier assumption (Garamvölgyi, 1972) according to which the geometrical arrangement of the hexagonal lattice of filaments may influence the shape of the length tension diagram and, as a consequence the long-range forces maintaining the hexagonal array of the myofilaments may

be made responsible mainly for the elasticity of inactive muscle. At the same time it seems that, contrary to our earlier statement, it is not necessarily the set of *C*-filaments, that is responsible for the practically linear course of the length tension diagram of the resting bee flight muscle (Garamvölgyi, 1969).

References

Auber, J., Couteaux, R. (1962) C. R. Acad. Sci. *254* 3425
Auber, J., Couteaux, R. (1963) J. Microscopie *2* 209
Belágyi, J., Garamvölgyi, N. (1968) Acta Biochim. Biophys. Acad. Sci. Hung. *3* 293
Ernst, E. (1963) Biophysics of Striated Muscle. Akadémiai Kiadó, Budapest.
Garamvölgyi, N. (1963) J. Microscopie *2* 107
Garamvölgyi, N. (1969) J. Ultrastr. Res. *27* 462
Garamvölgyi, N. (1972) Acta Biochim. Biophys. Acad. Sci. Hung. *7* 157
Garamvölgyi, N., Belágyi, J. (1968) Acta Biochim. Biophys. Acad. Sci. Hung. *3* 195
Garamvölgyi, N., Biczó, G. Ladik, J., Előry, A. (1973) Acta Biochim. Biophys. Acad. Sci. Hung. *8* 57
Hanson, J. (1956) J. Biophys. Biochem. Cytol. *2* 691
Huxley, H. E. (1963) In: Muscle. (eds: Paul, W. M., Daniel, E. E., Kay, C. M., Monckton, G.) Pergamon Press, Oxford, p. 3
Pringle, J. W. S. (1967) Progr. Biophys. Mol. Biol. *17* 1

Acta Biochim. et Biophys. Acad. Sci. Hung. Vol. 9 (3) pp. 239–241 (1974)

The Amino Acid Sequence of Rabbit Muscle Aldolase

(Short Communication)

M. SAJGÓ, GYÖNGYI HAJÓS

Enzymology Department, Institute of Biochemistry, Hungarian Academy of Sciences, Budapest, Hungary

(Received March 14, 1974)

The determination of the sequence of rabbit muscle aldolase was based on the analysis of the four fragments obtained by the cyanogen bromide cleavage of the protein, which is built up of four 364-residue subunits (Kawahara, Tanford, 1966; Závodszky, Biszku, 1967; Lai, 1968; Sajgó, 1969).

The alignment of these fragments (Lai, 1968; Sajgó, 1969) and the amino acid sequence of three out of four, i. e. the sequences of fragments CB1 (residues 1–158: Sajgó, Hajós, 1974), CB3 (residues 159–224: Sajgó, 1971; Lai, Oshima, 1971) and CB4 (residues 225–242: Lai, Chen, 1968; Sajgó, 1971), as well as the sequence of the C-terminal 59 amino acids (residues 306–364: Solti et al., 1974), have already been published.

The almost complete sequence of the protein (residues 49–54 and 266–282 in parentheses) has been presented at the 9th International Congress of Biochemistry (Hajós, Sajgó, 1973).

In this paper the complete amino acid sequence of fragment CB2 (residues 243–364) and the total sequence of the protein subunit is described (Fig. 1).

In the total sequence presented there are a few changes relative to our earlier data and some minor discrepancies as compared to the sequence reported by Lai and Oshima (1971).

We could not find any other differences between the subunits than those described earlier (Sajgó, Hajós, 1974; Lai et al., 1970). This means that the subunits are practically identical. This presumable identity of the primary structure of the subunits however, does not exclude conformational dissimilarities, which might be responsible for the non-identical behaviour of subunits towards limited tryptic (Biszku et al., 1973; Solti et al., 1974) or carboxypeptidase (Drechsler et al., 1959; Rutter et al., 1961) attack.

The continuous interest and helpful discussions with Drs G. Szabolcsi and F. B. Straub are gratefully acknowledged. Thanks are due to Mrs Klára Lendvay and Miss Anikó Barabás for the technical assistance and to Mrs Judit Báti for the amino acid analyses.

Acta Biochimica et Biophysica Academiae Scientiarum Hungaricae 9, 1974

```
                5                  10                  15                  20                  25
Pro-His-Ser-His-Pro-Ala-Leu-Thr-Pro-Glu-Gln-Lys-Lys-Glu-Leu-Asp-Ser-Ile-Ala-His-Arg-Ile-Val-Ala-Pro-
               30                  35                  40                  45                  50
Gly-Lys-Gly-Ile-Leu-Ala-Ala-Asp-Glu-Ser-Thr-Gly-Ser-Ile-Ala-Lys-Lys-Leu-Gln-Ser-Ile-Gly-Glx-Thr-Asx-
               55                  60                  65                  70                  75
Thr-Glx-Glx-Asx-Arg-Arg-Phe-Tyr-Arg-Ala-Phe-Pro-Glu-Asp-Asn-Gly-Arg-Pro-Val-Ile-Lys-Gln-Leu-Leu-Leu-
               80                  85                  90                  95                 100
Thr-Ala-Asp-Asp-Arg-Val-Asn-Pro-Cys-Ile-Gly-Gly-Val-Ile-Leu-Phe-His-Glu-Thr-Tyr-Gln-Leu-Lys-Gly-Gly
              105                 110                 115                 120                 125
Val-Val-Gly-Ile-Lys-Val-Asp-Lys-Gly-Val-Pro-Leu-Ala-Gly-Glu-Thr-Thr-Thr-Asx-Glx-Gly-Leu-Asp-Gly-Leu-
              130                 135                 140                 145                 150
Ser-Glu-Arg-Cys-Ala-Gln-Tyr-Lys-Lys-Asn-Gly-Ala-Asp-Phe-Ala-Lys-Trp-Arg-Cys-Val-Leu-Lys-Ile-Gly-Glu-
              155                 160                 165                 170                 175
His-Thr-Pro-Ser-Ala-Leu-Ala-Met-Glu-Asn-Ala-Asn-Val-Leu-Ala-Arg-Tyr-Ala-Ser-Ile-Cys-Gln-Glu-Asn-Gly-
              180                 185                 190                 195                 200
Pro-Ile-Glu-Val-Pro-Glu-Ile-Leu-Pro-Asn-Gly-Asn-His-Asp-Leu-Lys-Arg-Cys-Gln-Tyr-Val-Thr-Glu-Lys-Val-
              205                 210                 215                 220                 225
Leu-Ala-Ala-Val-Tyr-Lys-Ala-Leu-Ser-Asn-His-His-Ile-Tyr-Leu-Gln-Gly-Thr-Leu-Leu-Lys-Pro-Asn-Met-Val-
              230                 235                 240                 245                 250
Thr-Pro-Gly-His-Ala-Cys-Thr-Gln-Lys-Tyr-Ser-His-Glu-Gln-Ile-Ala-Met-Ala-Thr-Val-Thr-Ala-Leu-Arg-Gly-
              255                 260                 265                 270                 275
Arg-Thr-Val-Pro-Pro-Ala-Val-Thr-Gly-Val-Thr-Phe-Leu-Leu-Ser-Gly-Glu-Ser-Glx-Glx-Glx-Glx-Gly-Ala-Ser-
              280                 285                 290                 295                 300
Ser-Val-Thr-Pro-Asx-Ile-Ile-Asn-Leu-Asn-Ala-Ile-Asn-Lys-Cys-Pro-Leu-Leu-Lys-Pro-Trp-Ala-Leu-Thr-Phe-
              305                 310                 315                 320                 325
Gly-Ser-Tyr-Gly-Arg-Ala-Leu-Gln-Ala-Ser-Ala-Leu-Lys-Ala-Trp-Gly-Gly-Lys-Lys-Glu-Asn-Leu-Lys-Ala-Ala-
              330                 335                 340                 345                 350
Gln-Glu-Glu-Tyr-Val-Lys-Arg-Ala-Leu-Ala-Asn-Ser-Leu-Ala-Cys-Gln-Gly-Lys-Tyr-Thr-Pro-Gly-Ala-Ser-Glu-
              355                 360
Ser-Gly-Ala-Ala-Ala-Gln-Leu-Phe-Ile-Ser-Asn-His-Ala-Tyr
```

Fig. 1. The amino acid sequence of rabbit muscle aldolase subunit

References

Biszku, E., Sajgó, M., Solti, M., Szabolcsi, G. (1973) Eur. J. Biochem. *38* 283—292
Dreschler, E. R., Boyer, P. D., Kowalsky, A. G. (1959) J. Biol. Chem. *234* 2627—2634
Hajós, Gy., Sajgó, M. (1973) 9th International Congress of Biochemistry, Stockholm, Abst. nr. 2e17, p. 62
Kawahara, K., Tanford, C. (1966) Biochemistry *5* 1578—1584
Lai, C. Y. (1968) Arch. Biochem. Biophys. *128* 202—211
Lai, C. Y., Chen, C. (1968) Arch. Biochem. Biophys. *128* 212—218
Lai, C. Y., Oshima, T. (1971) Arch. Biochem. Biophys. *144* 363—374
Lai, C. Y., Chen, C., Horecker, B. L. (1970) Biochem. Biophys. Res. Comm. *40* 461—468
Rutter, W. J., Richards, O. C., Woodfin, B. M. (1961) J. Biol. Chem. *236* 3193—3197
Sajgó, M. (1969) Acta Biochim. Biophys. Acad. Sci. Hung. *4* 385—389
Sajgó, M. (1971) FEBS Lett. *12* 349—351
Sajgó, M., Hajós, Gy. (1974) FEBS Lett. *38* 341—344
Solti, M., Biszku, E., Sajgó, M., Szabolcsi, G. (1974) Eur. J. Biochem. submitted for publication
Závodszky, P., Biszku, E. (1967) Acta Biochim. Biophys. Acad. Sci. Hung. *2* 109—112

Acta Biochim. et Biophys. Acad. Sci. Hung. Vol. 9 (3) pp. 243–253 (1974)

Direct Evidence for Connecting C Filaments in Flight Muscle of Honey Bee

K. TROMBITÁS, Anna TIGYI-SEBES

Central Laboratory of Medical University, Pécs

(Received January 26, 1974)

The thin (actin) filaments can be fragmentated during fixing without damaging the thick and *C* filaments. The substance of fragmented filaments is located on the remaining filaments or between them in the form of small granules. This scrap of filaments can be removed from fibrils by intensive homogenization. Afterwards only one continuous set of filaments can be observed in the stretched fibrils. In the *A* band only thick filaments can be observed and, in the *I* band, only thin filaments — *C* filaments — which connect the thick filaments with the *Z* line.

Introduction

A decade ago, Auber and Couteaux (1962, 1963) described — on the basis of examinations of cross-sections — that the myosin filaments of insect flight muscle are connected with the *Z* line by a second kind of thin filaments. Garamvölgyi (1963, 1965, 1969, 1971) corroborated these results with the examination of longitudinal- and cross-sections, and even attributed important mechanical role to these structures. Guba (1968) demonstrated in a filament suspension that the thinned ends of thick filaments continued in thin filaments. Connections between thick filaments and the *Z* line were also assumed by Pringle (1967) who named the filaments connecting them *C* filaments. Many authors are of similar opinion (White, 1966; Rüegg, Tregear, 1966; Chaplain, 1967; 1968a; 1968b; Zebe et al., 1968). At the same time several authors doubt the existence of *C* filaments. For instance Ashhurst (1971) definitely considers the *C* filaments as artefacts produced by the illusion of filaments placed over each other in a thick section (Achátz, 1968). This is an old objection (Huxley, 1957) having a real basis; namely, the filaments belonging together on the *I* — *A* border cannot be determined in a longitudinal section because of the presence of actin filaments. But the problem could be easily decided if we were able to remove actin filaments from fibrils without damaging the other structures. In the present work a method is described with the aid of which actin filaments are fragmented and removed from fibrils. In this way we succeeded in producing isolated *C* filaments in the *I* bands of fibrils.

Material and method

Flight muscle of honey-bee *(Apis mellifica)* was used throughout the experiments. Bees were cooled to 4 °C before preparation. The fresh muscle was fixed – partly by stretching it on glass rods, partly without stretching – after preparation at 0 °C for an hour and a half. Fixation was done with a 1 per cent watery solution of osmium tetroxide. The fixative solution contained

a) 0.14 M of sodium cacodilate or phosphate buffer (pH 7.4) for the control muscle;

b) 0.07 M of sodium cacodilate or phosphate buffer (pH 7.4) and 0.3 M of glucose.

Before applying the latter fixative, the muscle was rinsed in Pringle's solution at 0 °C for one hour. One part of the fixed muscle was embedded into araldite in the usual way, the other part was homogenized in a Potter type homogenizer for 20 min. The homogenate was centrifuged and the pellet embedded in araldite. The thin sections were stained with uranyl acetate and lead citrate. The photographs were taken with a TESLA BS 613type electron microscope at an accelerating voltage of 80 kV.

Results

The two methods of fixing preserved the filaments in different ways.

a) In blocks containing the muscle fixed according to the first method well preserved structures were usually found. Double arrangement of the filaments was seen in the fibrils (Huxley, Hanson, 1955), *i.e.* a regular arrangement of thick and thin filaments could be observed in the longitudinal section of contracted fibrils (Fig. 1a). In cross-sections the thick filaments showed a hexagonal arrangement with a thin filament between two thick filaments (Fig. 1b). In stretched fibrils the *I* bands contained only thin filaments, the *H* zones only thick filaments and, in the overlapping zones, the arrangement of the filaments was identical with that of contracted fibrils (Fig. 2).

b) In the blocks containing muscle fixed according to the second method the extrafibrillar structures were also well preserved and identical with the ones mentioned above. But the structure of the fibrils showed an essential change. In contracted fibrils only thick filaments were found; in the place of thin filaments a finely granulated substance – possibly the fragments of thin filaments – was seen (Fig. 3). In stretched fibrils the number of thin filaments decreased in the *I* band; in the *A* band only thick filaments were found. The fragments of actin filaments produced a background density which marks the borders of *H* zone (Fig. 4). If the muscle which had been treated as before was homogenized after fixation with a Potter type homogenizer for 20 min the filament fragments located between thick filaments could be washed out from the contracted fibrils (Fig. 5a, Fig. 5b). Lack of background density, marking the location of fragmented actin

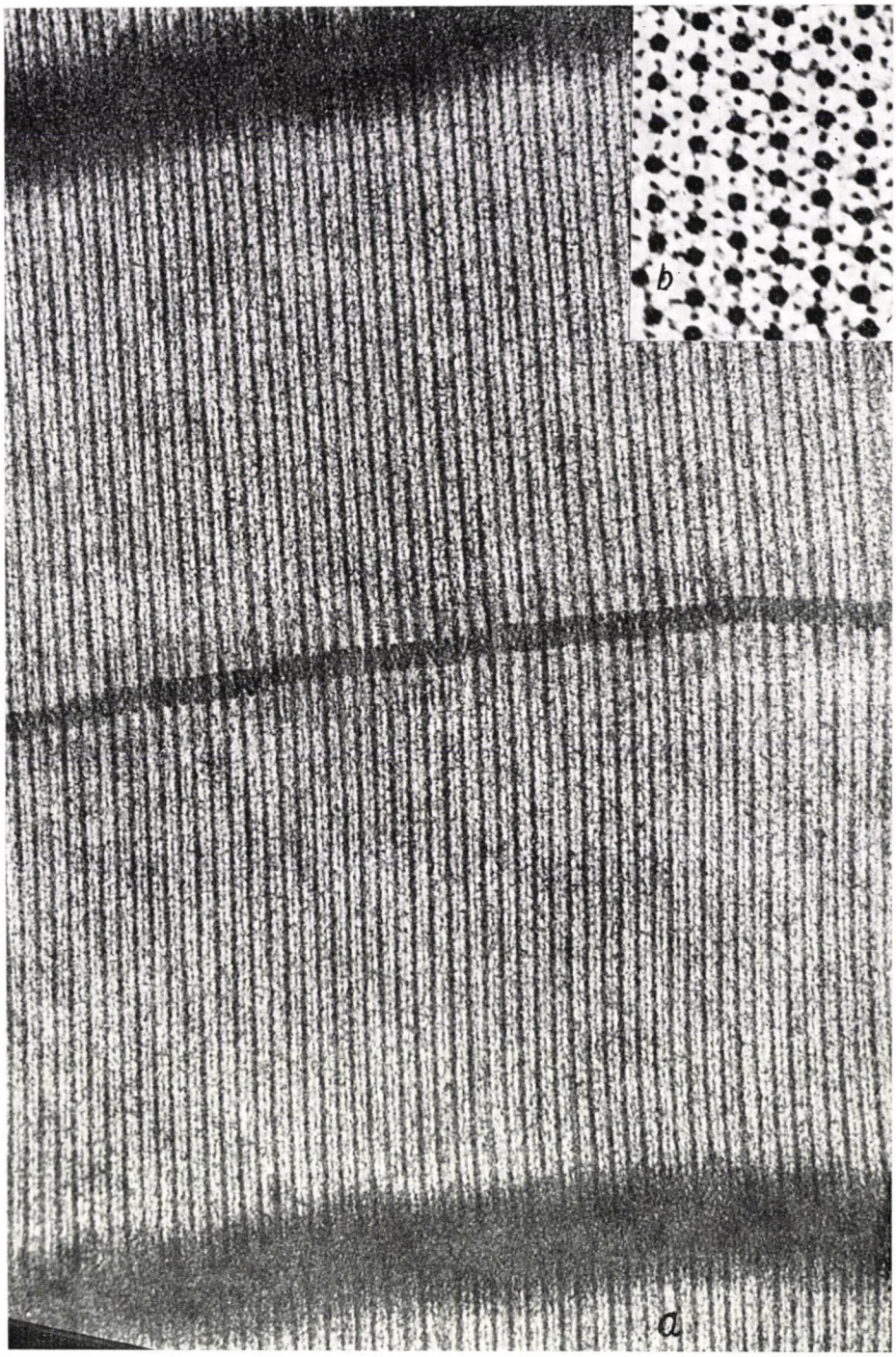

Fig. 1. Contracted flight muscle of bee. a) Regular arrangement of thick and thin filaments can be seen in longitudinal section (59 000×); b) hexagonal arrangement of thick filaments can be seen in cross-section (168 000×)

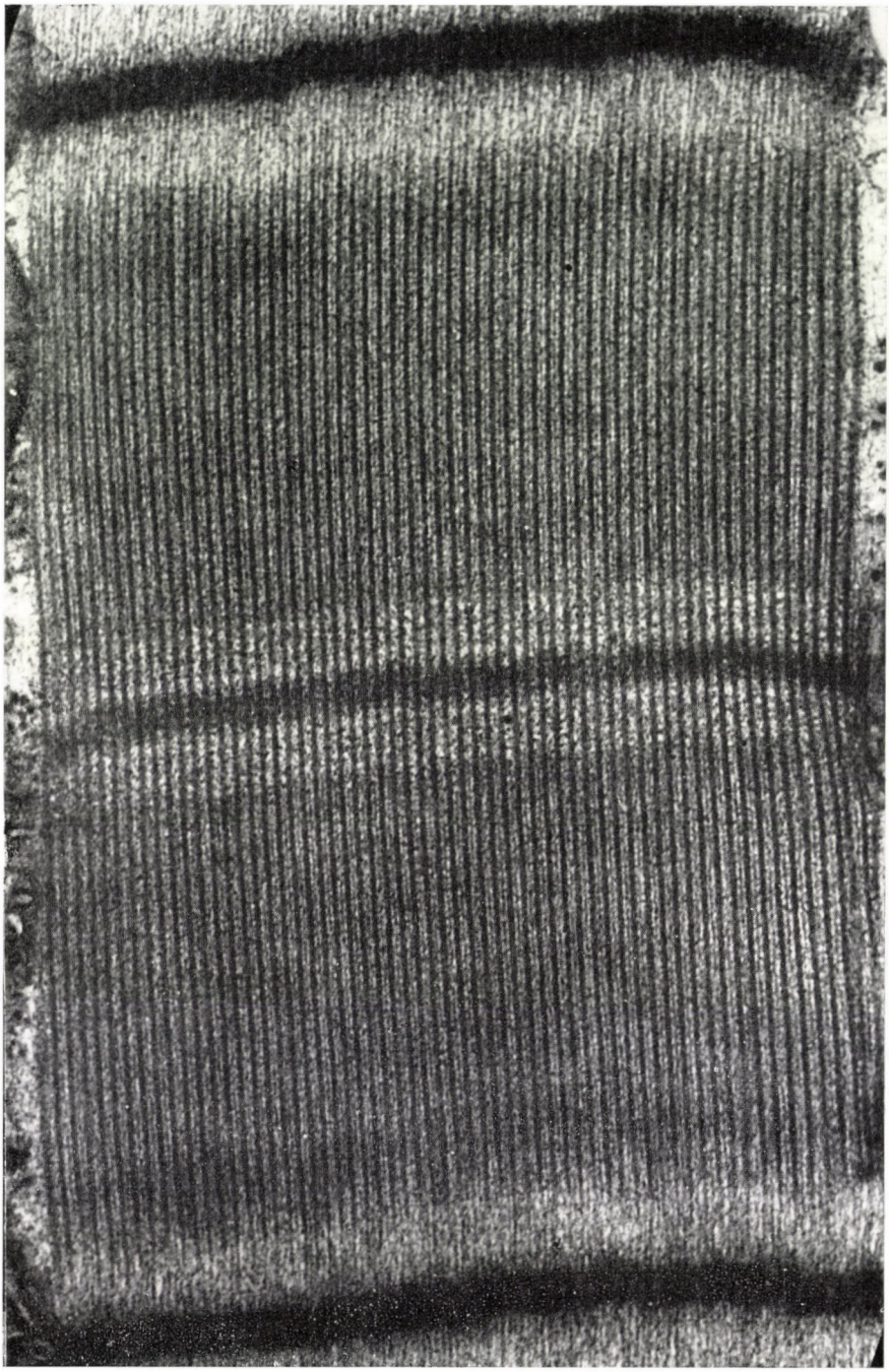

Fig. 2. Stretched flight muscle of bee; thick and thin filaments can be seen in the zone of overlapping (60 000×)

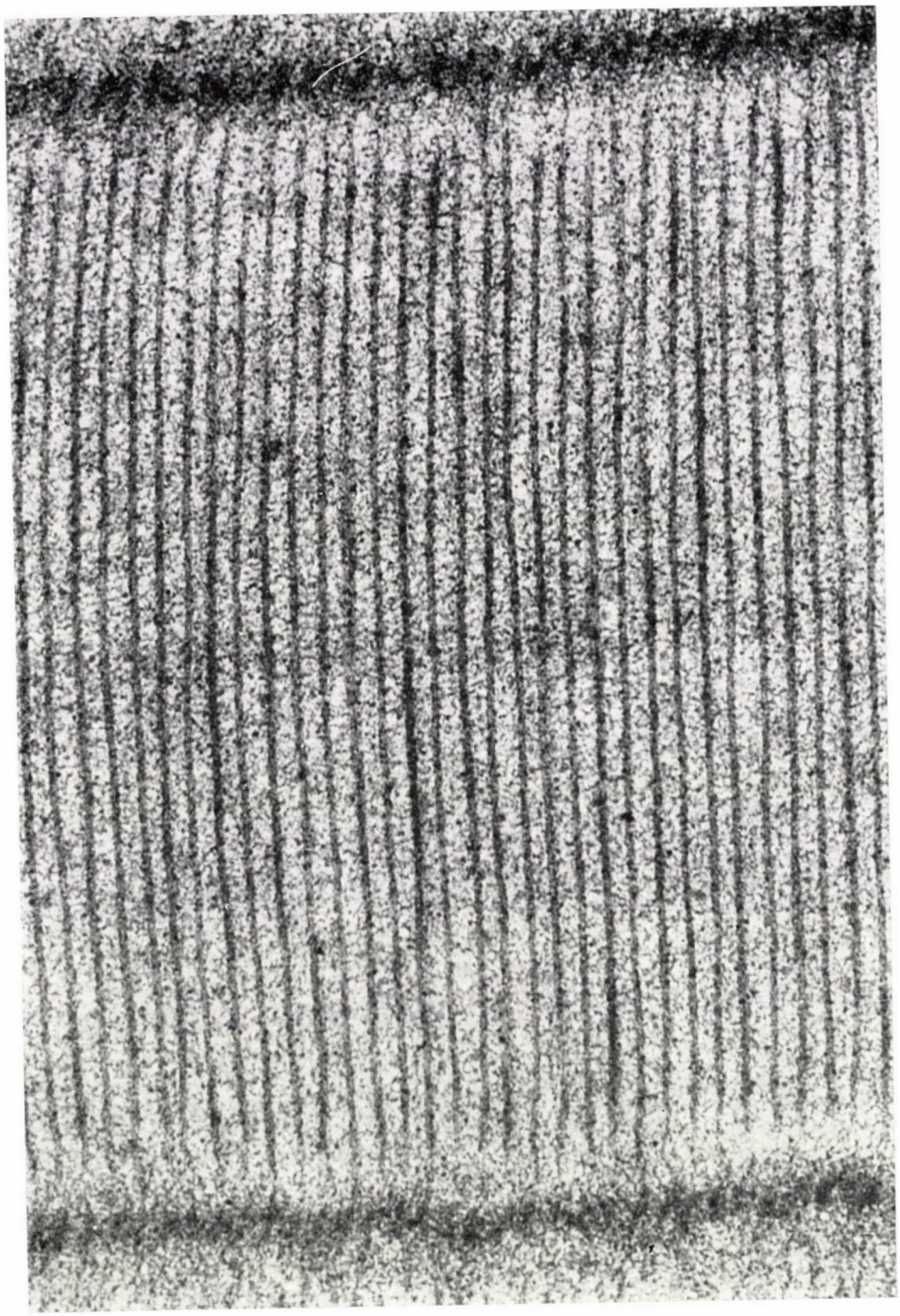

Fig. 3. Contracted flight muscle of bee. The thin filaments are fragmented; among thick filaments granular scraps of filaments can be seen (68 000×)

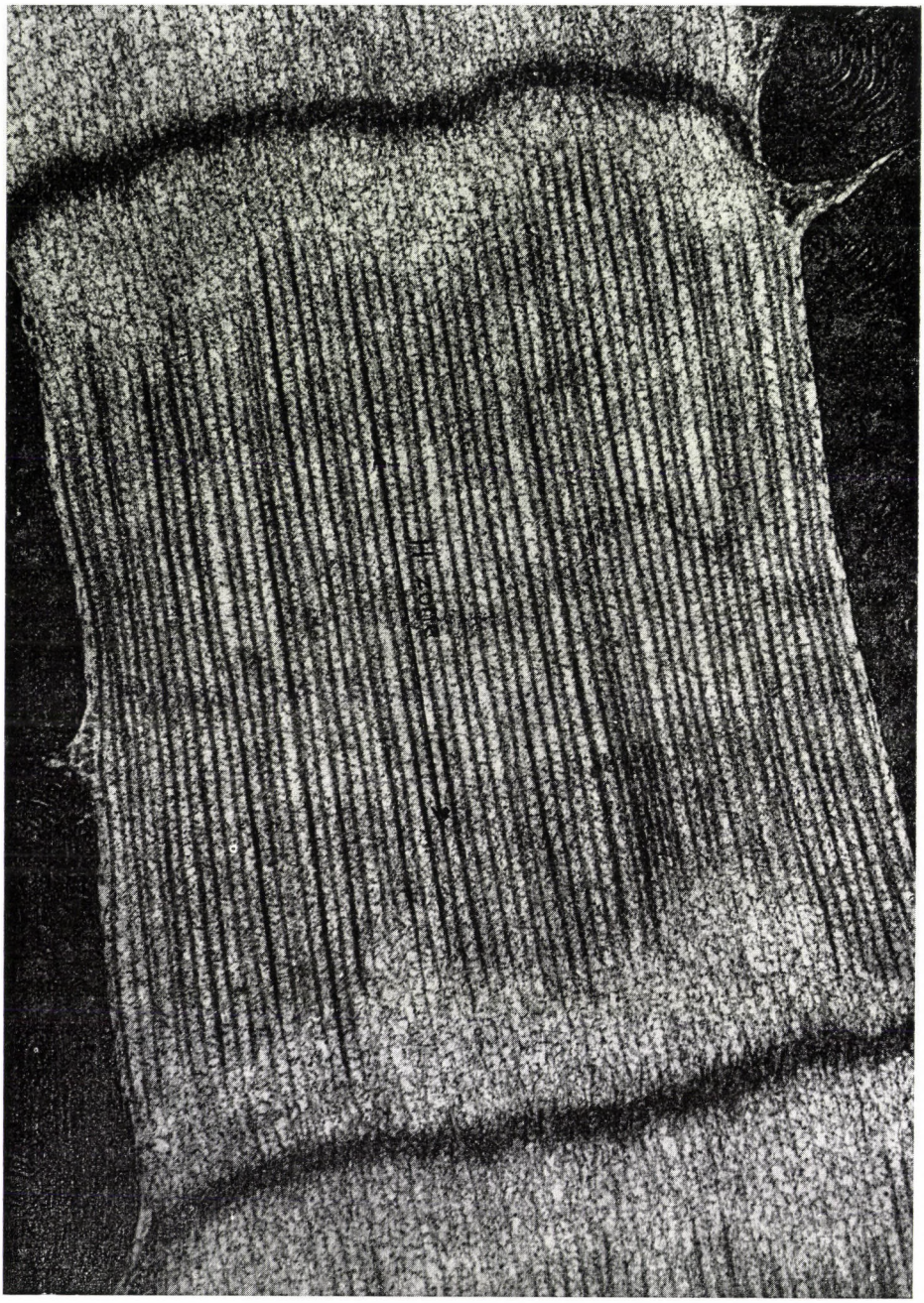

Fig. 4. Stretched flight muscle of bee. The substance of fragmented thin (actin) filaments produced a background density. The number of thin filaments decreased in the I band (48 000×)

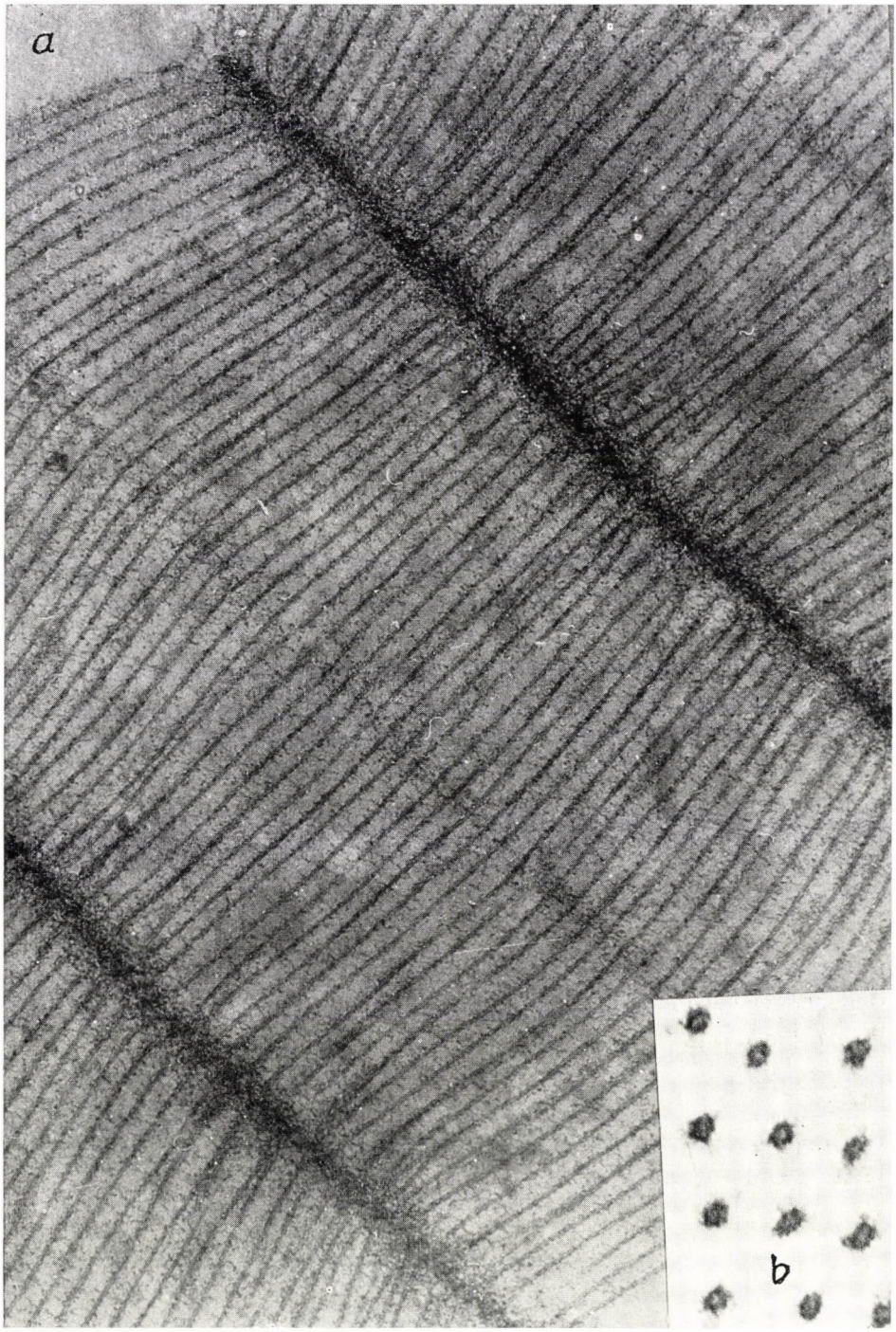

Fig. 5. Contracted flight muscle of bee. The scraps of fragmented thin filaments were washed out of thick filaments by homogenization. a) 45 000×; b) 270 000×

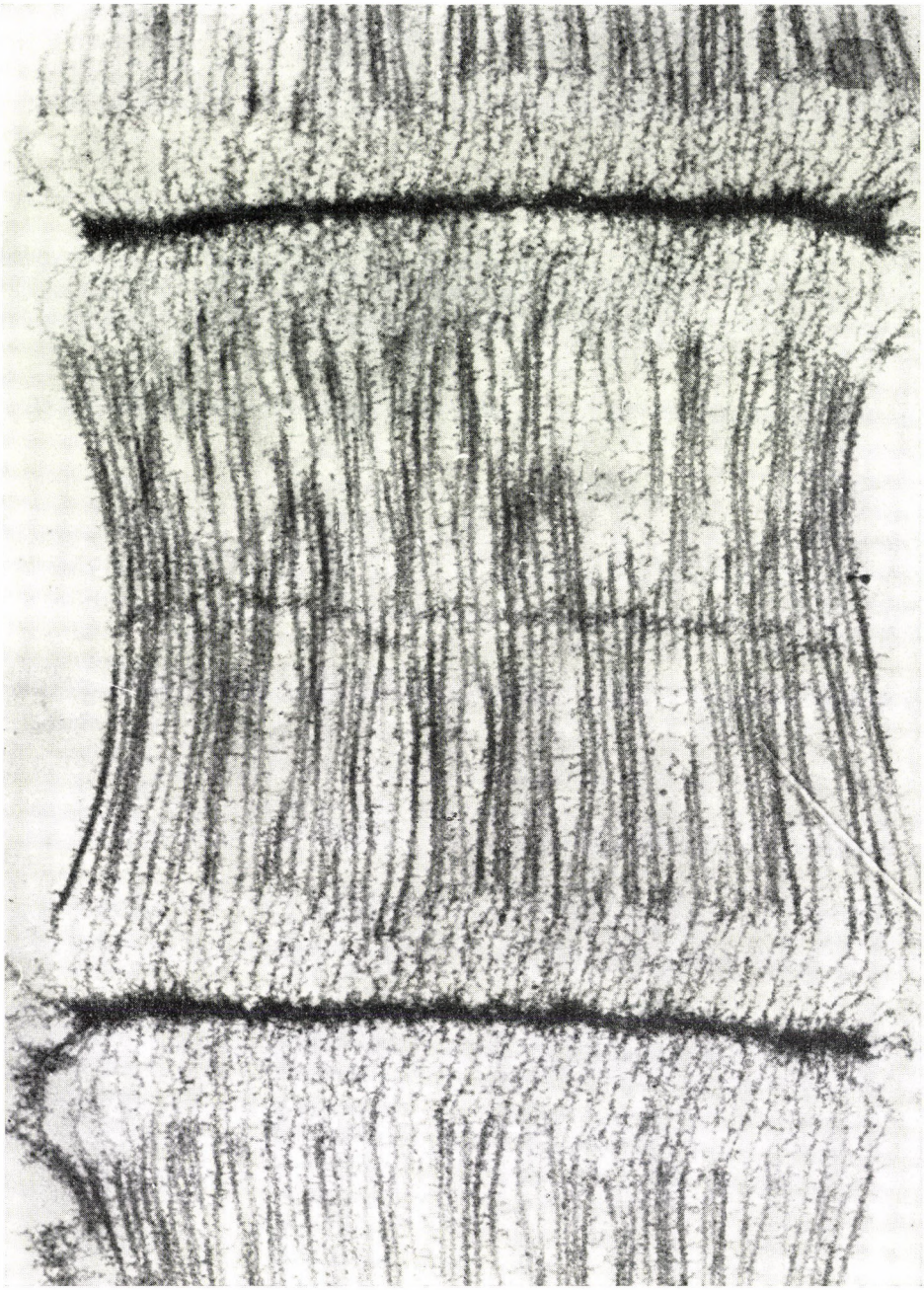

Fig. 6. Stretched flight muscle of bee. The scraps of fragmented thin filaments are washed out by homogenization (40 000×)

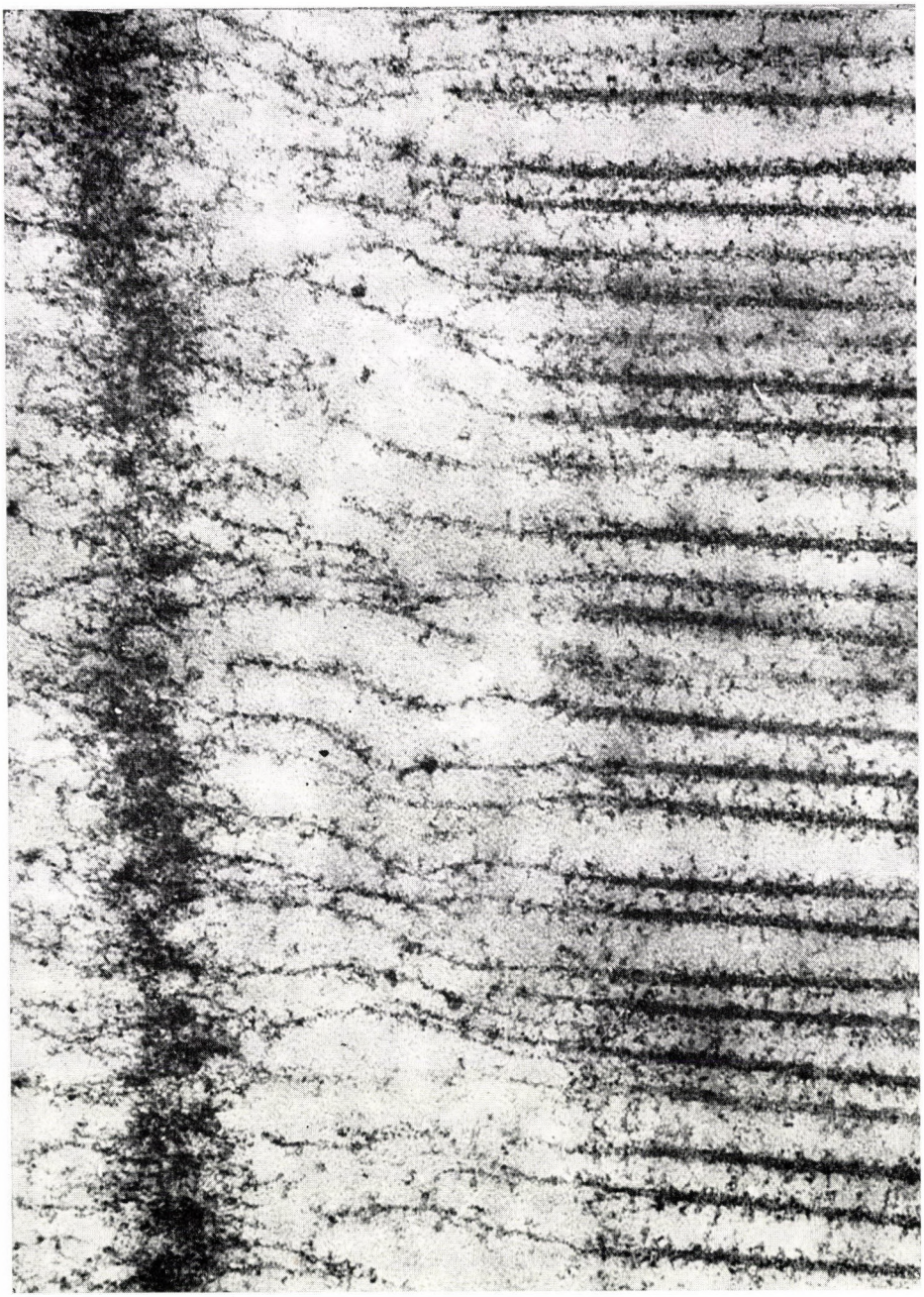

Fig. 7. Flight muscle of bee prepared as the former one. The thick filaments are connected to the *Z* line by thin filaments (100 000×)

filaments, was observed in stretched fibrils after homogenization, and the thin filaments of the *I* band became easily observable (Fig. 6). The *I* filaments remained did not spread into the thick filaments of the *A* band but, starting from the inner core of thick filaments, run through the *I* band to the *Z* line (Fig. 7).

Discussion

It is a well-known fact that the electron microscopic demonstration of the double arrangement of filaments is relatively simple in the case of glycerinized muscles; difficulties can occur, however, with the use of fresh muscles. In connection with this Huxley wrote (1953): ". . .the filaments of the secondary array are only visible where they apparently have become attached to the primary filaments, presumably in those parts of the muscle which have passed into a rigorlike condition during fixation . . ." Also in our experiments the secondary filaments were often badly preserved especially in the case of the application of fixation described in paragraph b. In this case the substance of fragmented actin filaments produced a background density (Figs 3, 4) which was brought about by the fine granules randomly located among preserved filaments. But the *I* band continued to contain thin filaments, though in an essentially smaller amount (Fig. 4). These filaments could be actin filaments surviving fragmentation or *C* filaments; we cannot unambiguously determine it from this picture. But the fact that without exception actin filaments became fragmented in contracted fibrils (though they were bound to the other structures much better in that state), made the latter assumption more probable. This question could be unambiguously answered after homogenizing the fixed muscle, because this procedure removed from the fibrils the fragments of filaments disturbing the judgement. After that only thick filaments could be observed in the contracted fibrils (Fig. 5a, b). In stretched fibrils the continuous system of filaments constituting the fibril consisting of thick filaments in the *A* band and thin ones in the *I* band became visible after the disappearance of the background density. The thin filaments did not spread into the *A* band, they started from the thinning ends of thick filaments and reached as far as the *Z* line. Thus they created a connection between each thick filament and the *Z* line (Figs 6 and 7). On the basis of all what was said above, there is hardly any doubt that we did produce *C* filaments supposed by the authors mentioned above in the *I* band isolately, and presented, thus, a direct evidence of their existence. In spite of this let us examine Fig. 7, whether the apparent continuity of filaments assumed by Huxley (1957) and Ashhurst (1971), mentioned in the introduction, can refer to our case. We are of the opinion that this section of ours contained one layer of filaments. During the intensive homogenization the hexagonal arrangement of thick filaments loosened to a slight degree, the regular arrangement of thin filaments loosened to a great degree. It can hardly be probable that the two accidental changes of

different degrees consistently happened in such a way that the ends of discontinuous thick and thin filaments showed an apparent continuity of filaments by falling consistently into the same plane.

References

Achátz, I. (1968) Acta Biochim. Biophys. Acad. Sci. Hung. *3* 183
Ashhurst, D. E. (1971) J. Mol. Biol. *55* 283
Auber, I., Couteaux, R. (1962) C. R. Acad. Sci. *254* 3425
Auber, J., Couteaux, R. (1963) J. Micr. *2* 309
Chaplain, R. A. (1967) Biochem. Biophys. Acta *131* 385
Chaplain, R. A., Frommelt, B. (1968) Kybernetik *5* 1
Chaplain, R. A., Frommelt, B., Pfister, E. (1968) Kybernetik *5* 61
Garamvölgyi, N. (1963) J. Micr. *2* 107
Garamvölgyi, N. (1965) J. Ultr. Res. *13* 409
Garamvölgyi, N. (1969) J. Ultr. Res. *27* 462
Garamvölgyi, N. (1971) "Contractile Proteins and Muscle" (ed. L. Laki) New York Mercel Dekkor Inc. 1971
Guba, F. (1965) Symp. Muscle, Budapest, Symp. Biol. Hung. Vol. 8, p. 33. Akadémiai Kiadó, Budapest 1968
Huxley, H. E. (1953) Biochem. Biophys. Acta *12* 387
Huxley, H. E., Hanson, J. (1955) Symp. Soc. Exp. Biol. *9* 228
Huxley, H. E. (1957) J. Biophys. Biochim. Cytol. *3* 631
Pringle, I. W. S. (1967) Progr. Biophys. Mol. Biol. *17* 1
Rüegg, I. C., Tregear, R. T. (1966) Proc. Roy. Soc. Ser. B. *165* 497
White, D. C. S. (1966) Ph. D. Thesis (zool.) Oxford University
Zebe, E., Meinrenkev, W., Rüegg, I. C. (1968) Z. Zellforsch. *87* 603

Acta Biochim. et Biophys. Acad. Sci. Hung. Vol. 9 (3), pp. 255—264 (1974)

The Complexity of the Fluorescence of Peroxidase

Z. VÁRKONYI, L. SZALAY

Institute of Biophysics, József Attila University, Szeged

(Received January 18, 1974)

The fluorescence and excitation spectra of tris-buffered (pH 7.0) solutions of peroxidase (1×10^{-5} — $2\times10^{-}$- M) indicate that the bands at 305, 340 and 455 nm in the fluorescence spectra can be ascribed to the fluorescence of tyrosine, tryptophan and tyrosine excimer. In spite of the fact that both tyrosine and tryptophan are present in the molecule, if both amino acids are excited, the intensity of the tyrosine fluorescence is much higher than that of the tryptophan. It can be shown that a contribution is made to the fluorescence of both amino acids by the electronic excitation energy transferred from the histidine.

Introduction

It appears that the fluorescence spectrum of horse-radish peroxidase (HRP) has not yet been studied. In an investigation of the spectrally unresolved fluorescence of the proteins (Weber, Teale, 1959) it was found that, with the exception of peroxidase, the haem-proteins exhibited practically no fluorescence for, as a consequence of inductive resonance interaction, the excitation energy was transmitted almost completely to the haem. For this reason the absolute quantum efficiency of the fluorescence of the haem-proteins is in the order of only 10^{-3}; although that of the peroxidase is markedly higher, it is nevertheless still about 10^{-2} only. The spectral examination of such a weak fluorescence has been rendered possible by utilization of the highly sensitive detection apparatus developed in recent years. The aim of the present work was to determine the fluorescence spectrum of peroxidase. The preliminary examinations showed that the spectrum appreciably differed from that found for proteins in general. Its dependence of various parameters was therefore investigated, in order to establish the molecular groups responsible for the bands in the fluorescence spectrum, and to elucidate the interactions between them by comparison of the absorption and excitation spectra.

Solutions and methods

The HRP used was a lyophilized, trice crystallized product of the Nutritional Biochemical Corporation (Cleveland). The commercial preparation had an activity of 3170 units/mg, and a degree of purity of RZ = 3.0. A tris-buffered

(pH 7.0) 1×10^{-5} M stock solution was prepared from the recrystallized material and diluted to yield 5×10^{-6}, 2×10^{-6}, 1×10^{-6}, 5×10^{-7}, 2×10^{-7}, 1×10^{-7} and 5×10^{-8} M solutions. Prior to measurements the solutions were kept at 0–4 °C for about 24 hours.

Absorption spectra were measured with Optica Milano CF 4DR and Unicam 1800 spectrophotometers.

Fluorescence spectra were taken with a laboratory-built (Várkonyi, Kovács, 1972) and a Perkin–Elmer MPF3 spectrofluorimeter, generally with observation perpendicular to the exciting light. The spectra obtained directly by measurement were corrected for the spectral sensitivity of the photoelectric multiplier. The half-width of the exciting band was 4 nm. The absorbances of the solutions used for the fluorescence measurements lay in the range from 0.1 to 0.8. It was necessary to correct the fluorescence spectra for reabsorption, but the effect of secondary fluorescence was negligible (Várkonyi, 1973). Since the fluorescence spectra were to be taken at different times and different concentrations, and different exciting wavelengths were to be compared, a comparative standard was used in the measurements. A 1 cm thick plate was prepared from a 5×10^{-5} M solid polymethyl methacrylate solution of the standard diaminoacridine; on ultraviolet excitation the fluorescence of this was exhibited everywhere in the range necessary for the examinations, from 300 nm towards longer waves. As Beer's law is not valid for the photoabsorption of peroxidase all of the spectra were given for the same intensity of absorbed light in order to enable the comparison of the fluorescence intensities measured at different concentrations. In the interest of the comparability of the intensities measured at different exciting wavelengths the spectral distribution of the exciting light was taken into account; in the knowledge of this the intensities were given for the same intensity of exciting light. The fluorescence spectra were also corrected for the scattered exciting light, according to Murchio and Allen (1962).

Excitation spectra were recorded with the same instruments as the fluorescence spectra. These spectra were corrected to the same intensity of exciting light by taking into account the spectral distribution of the exciting light. All measurements were made at room temperature (about 20 °C).

Results

The *absorption spectrum* reveals bands at 190, 280 and 405 nm, with a shoulder at about 390 nm (Fig. 1). These originate from the photoabsorption of the peroxidase protein and haem moieties, and peroxidase aggregates (Szalay, Várkonyi, 1974). The diagrams denoted A, B and C give the apparent extinction coefficient in three different steps; the absorption spectrum for the 1×10^{-5} M solution is continued with a continuous line in diagrams B and C in accordance with the step of diagram A, for easier comparison of the photoabsorptions in the various spectral regions.

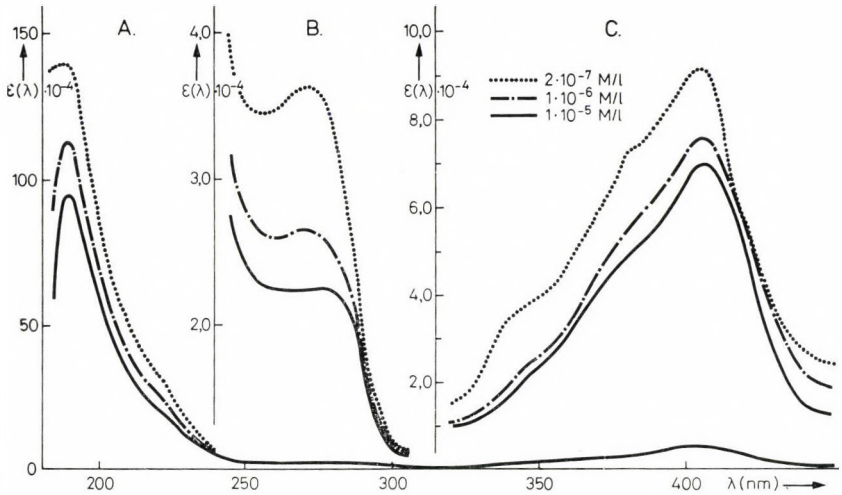

Fig. 1. Absorption spectra of peroxidase at different concentrations. Inserts B and C show the absorption in the regions of 250—300 and 350—450 nm in an enlarged scale of the molar decadic absorption coefficient, $\varepsilon(\lambda)$

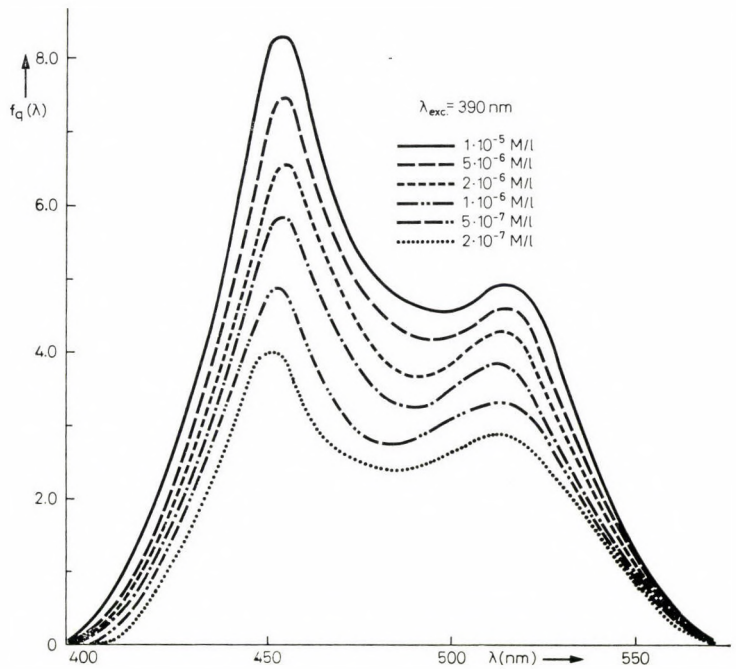

Fig. 2. Fluorescence spectra of peroxidase at different concentrations excited at 390 nm

The *fluorescence spectra* were taken at exciting wavelengths selected from the bands found in the absorption spectrum. Figures 2–4 show the fluorescence spectra as a function of concentration at excitations of 390, 276 and 210 nm. The maxima of the fluorescence spectra are 455 nm on 390 nm excitation and 305 nm on 276 nm excitation. With the decrease of the concentration on excitation at 210 nm besides the 305 nm band another band appears at 350 nm. In

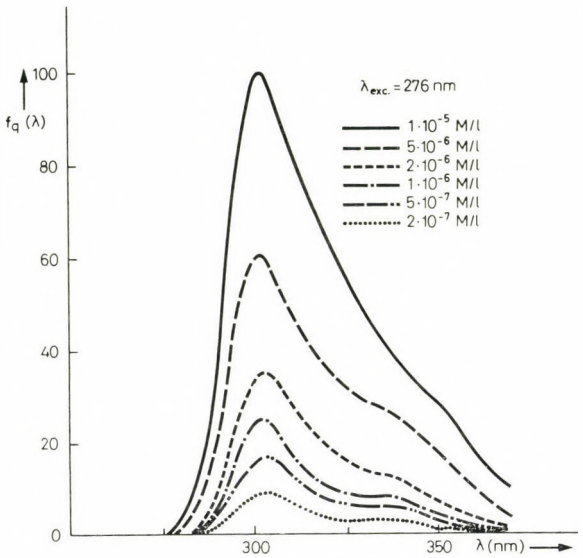

Fig. 3. Fluorescence spectra of peroxidase at different concentrations excited at 276 nm

addition, Fig. 3 reveals a shoulder at about 340 nm in the spectrum obtained on 276 nm excitation, while in Fig. 4 there is a smaller shoulder also at about 455 nm. These spectra show that the fluorescence of peroxidase is fairly complex and presumably arise from a number of components absorbing and emitting somewhat separately from each other. An attempt was made to study the complexity of the fluorescence spectra of peroxidase and the reasons for the complexity in more detail, by comparing the excitation spectra with the absorption spectra. The light of the X_e lamp used to excitation did not give rise to any photochemical change.

The *fluorescence excitation spectra* were taken at observation wavelengths selected from the bands relating to the above described maxima of the fluorescence spectra. With observation at 340 nm (Fig. 5) three maxima are found at about 230–240, 275–280 and 305 nm. If the observation wavelength is 455 nm also another band appears at 390 nm in addition to the first two bands mentioned above, while at 305 nm only the first two bands are seen.

The excitation spectra thus show that the components responsible for the fluorescence of peroxidase absorb not only in the spectral region of the three maxima and the shoulder mentioned in connection with the absorption spectra, but also in another region with a maximum at 305 nm, not directly visible in the absorption spectrum, but showing up in the excitation spectra. The fluorescence spectrum resulting from the component absorbing in this region (Fig. 6) is characterized by a strong band at 340 nm, with another band tending to appear only as a shoulder at about 390 nm. Summing up, the fluorescence of the peroxidase

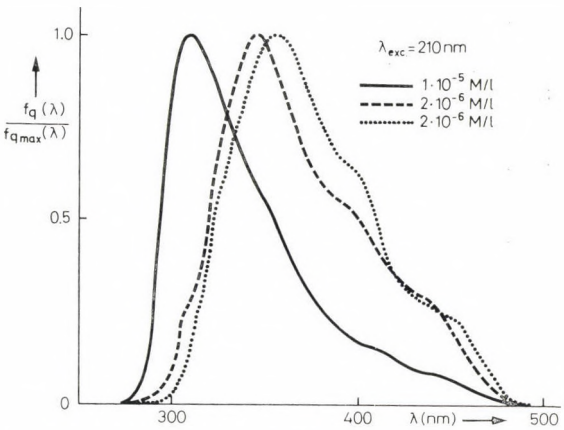

Fig. 4. Relative fluorescence spectra of peroxidase at different concentrations excited at 210 nm

solution is due to three components with fluorescence maxima at 305, 340 and 455 nm, the corresponding absorption bands being at 276, 305 and 390 nm, respectively. With excitation in the absorption bands with a maximum at 210 nm a fluorescence spectrum is obtained (Fig. 4) in which all the fluorescence bands are present to different extents at the various concentrations, appearing separately upon excitation at various positions of the wavelength scale. This can clearly be attributed to the fact that the absorption bands of all components can be found in this spectral region and they overlap one another.

Table 1 lists the positions of the maxima of the fluorescence spectra recorded at the different exciting wavelengths. With excitation at 390 nm also a smaller maximum (not listed in the Table) appears at 515 nm in addition to the 455 nm fluorescence band. In all of the excitation spectra a significant maximum is found at about 230 nm; no conclusion can be drawn as to this band from the absorption spectrum given in Fig. 1. However, if the 200–250 nm region is extended, it emerges that there really is a low-intensity maximum at 230 nm (Fig. 7). With regard to the general presence of the 230 nm band in the excitation spectrum the

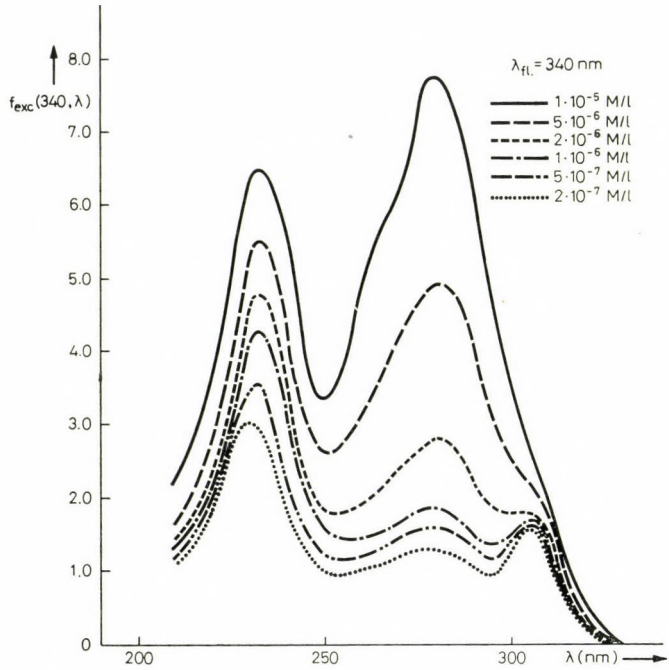

Fig. 5. Fluorescence excitation spectra of peroxidase with observation at 340 nm

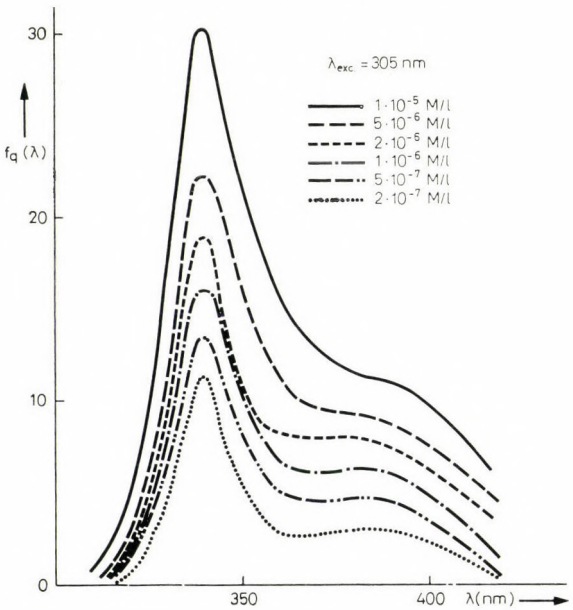

Fig. 6. Fluorescence spectra of peroxidase at different concentrations excited at 305 nm

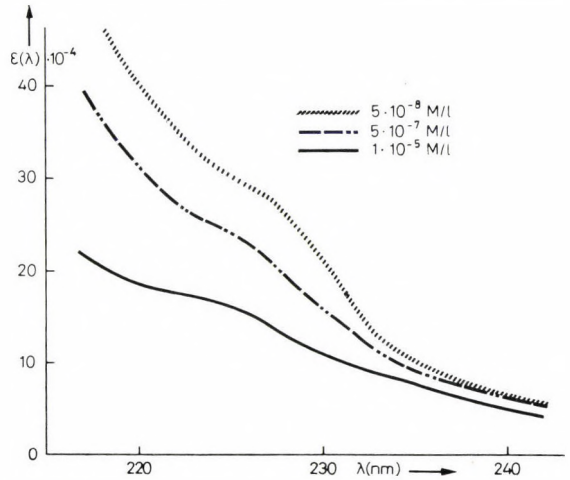

Fig. 7. Absorption spectra of peroxidase at different concentrations in the spectrum region of 200 – 240 nm

related fluorescence spectra were also taken at different concentrations. It turned out that these spectra exhibited bands at about 305 and 340 – 350 nm, just like those produced with 276 nm excitation (Fig. 3).

The data in Table 2 refer to the relative fluorescence intensities.

Table 1

Positions of the fluorescence maxima in tris-buffered neutral solutions of peroxidase at various exciting wavelengths

Exciting wavelength (nm)	Fluorescence spectrum maxima (nm)		
210	305	340	455
276	305	340	
305		340	
390			455

Discussion

The spectral distribution of the fluorescence of the peroxidase solution is complex. As exciting light of various wavelengths gives rise to fluorescence bands at three different wavelengths, the solution contains at least three components which fluoresce more or less independently of each other. The excitation spectra

Table 2

Concentration-dependence of the relative heights of the fluorescence bands obtained at various exciting wavelengths in a tris-buffered neutral solution of peroxidase. The intensity of the 305 nm fluorescence band resulting from 276 nm excitation of the 1×10^{-5} M solution was taken as 100

Exciting wave length (nm)	Fluorescence band (nm)	Concentration (M)		
		2×10^{-7}	2×10^{-6}	1×10^{-5}
210	305	0.01	0.63	8.46
	340	0.87	2.54	4.43
	455	0.22	0.71	0.73
230	305	3.03	4.81	5.90
	340	0.71	1.30	1.50
276	305	9.00	35.00	100.00
	340	2.20	9.80	30.00
305	340	11.37	18.84	30.00
390	460	4.10	6.64	8.33

indicate that the 305 and 340 nm fluorescence bands appearing jointly on short-wave (210 nm) excitation result from the component possessing the highest excitation activity at 276 nm. This is in agreement with the fact that excitation at 276 nm excites both tyrosine and tryptophan in the peroxidase, each of these exhibiting fluorescence; the tyrosine at 305 and the tryptophan at 340 nm. Tyrosine emits at about 305 nm and tryptophan at 332–352 nm also in other proteins (Konev, 1965; pp. 63–78). Unlike in other proteins containing both these amino acids the band belonging to the fluorescence of the tyrosine is much more intense than that of the tryptophan. In order to decide whether it is really the fluorescence of the tryptophan which appears at 340 nm on 276 nm excitation, let us examine the excitation spectra taken at 340 nm (Fig. 5). In these a maximum is found at 305 nm, which means that this region involves the absorption of the component responsible for the fluorescence band at 340 nm. As tyrosine exhibits no absorption at 300 nm and beyond, only the tryptophan can be considered. This finding is supported by Fig. 8. If the fluorescence spectra are recorded with exciting wavelength varied from 280 to 310 nm at 10 nm intervals a transition is seen from the fluorescence of tyrosine, emitting at shorter wavelength, to that of tryptophan, emitting at longer wavelength. With excitation at 300 nm no tyrosine fluorescence can be seen any longer.

The fact that with excitation at 276 nm there is merely a weak tryptophan fluorescence together with intense tyrosine fluorescence can only be interpreted in such a way that the electronic excitation energy in the peroxidase molecules is not transferred from tyrosine to tryptophan, but appears as tyrosine fluorescence.

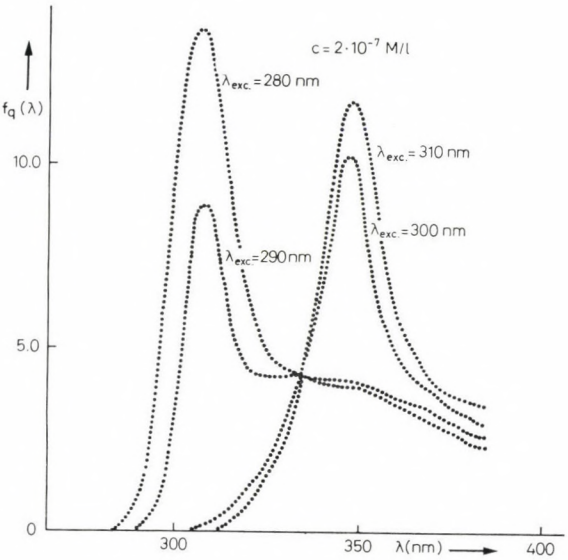

Fig. 8. Fluorescence spectra of peroxidase excited at 280, 290, 300 and 310 nm

This can be understood from the following consideration. With random distribution of the dissolved molecules in the most concentrated solution examined (1×10^{-5} M), the average distance between the molecules is 326 Å. The intermolecular transfer of excitation energy from this distance can be neglected in practice (the critical distance for the tyrosine—tryptophan transfer is 11—14 Å (Konev, 1965)). The dimensions of the peroxidase molecule permit the conclusion that intramolecular energy transfer can also be neglected. Both hydrodynamic measurements and the ultraviolet absorption spectrum indicate that the peroxidase molecule can be approximated to by an ellipsoid with a major axis of 300 Å and an axis ratio of (12—15) : 1 : 1 (Szalay, Várkonyi, 1974). In this the distance of separation of the tyrosine and the tryptophan may easily be more than 11—14 Å. Independently of this, a role may be played in the unusual intensity relations of the tyrosine and tryptophan fluorescence bands by the fact that, in this protein, the absolute quantum efficiency of the tyrosine fluorescence is higher, and that of the tryptophan is lower, than in other proteins.

The frequency band with a maximum at 455 nm is presumably tyrosine excimer fluorescence. According to the partially elucidated amino acid sequence of peroxidase (Welinder et al., 1972) two of the six tyrosines are connected to each other. Keleti (1970) reports that in a 3.3×10^{-2} M solution tyrosine has an excimer band at about 410—420 nm, and it is possible to conclude from its excitation spectrum to an active absorption system with a maximum at about 340 nm. In our case the excimer fluorescence also appears at the lowest concentrations examined, since the "dimer" is present, incorporated in the peroxidase. The shoul-

der at about 340 nm in the absorption spectrum (Fig. 1 C), which is also marked in the excitation spectra (Fig. 5), can presumably be attributed to this dimer. The more significant band at shorter wavelengths in the excitation spectra (Fig. 5) can be ascribed to the fact that the excimer fluorescence arises mainly through energy transfer from tyrosine in the protein and possibly from other amino acids. The shoulder at about 270 nm in the excitation spectrum points to the participation of tyrosine, and the maximum at about 230 nm to that of histidine since, according to Konev (1967; pp. 62) the absorption band of histidine lies in this wavelength region. This is why the band at 230 nm in the excitation spectra takes part generally in the excitation of the fluorescence of both tyrosine and tryptophan, and also of the tyrosine excimer. This conception is supported by the situation of the three histidines between the peptide chains in peroxidase (Welinder et al., 1972).

References

Keleti, T., FEBS Letters (1970) *7* 280—282
Konev, S. V. (1967) Fluorescence and Phosphorescence of Proteins and Nucleic Acids. Plenum Press New York
Murchio, J. C., Allen, M. B. (1962) Photochem. Photobiol. *1* 259—266
Szalay, L., Várkonyi, Z. (1974) Acta Phys. et Chem. Szeged (in press)
Várkonyi, Z. (1973) Magyar Fizikai Folyóirat *21* 311—327
Várkonyi, Z., Kovács, K. (1972) Acta Biochim. Biophys. Acad. Sci. Hung. *7* 89—95
Weber, G., Teale, F. J. W. (1959) Disc. Farad. Soc. *27* 134—141
Welinder, K. G. Smillie, L. B., Schonbaum, G. R. (1972) Canad. J. Biochem. *50* 44—62
Welinder, K. G., Smillie, L. B. (1972) Canad. J. Biochem. *50* 63—90

Acta Biochim. et Biophys. Acad. Sci. Hung. Vol. 9 (3), pp. 265–273 (1974)

Neutron Dose Distribution and Neutron Dose Spectrum Analysis in a Mouse Irradiated in a Modified Fission Spectrum

P. ZARÁND

"Frédéric Joliot-Curie" National Research Institute for Radiobiology and Radiohygiene, Budapest

(Received January 11, 1974)

Average absorbed dose in a mouse phantom (cylinder, various radii) exposed perpendicularly to the longitudinal axis of neutron beam with a modified fission spectrum was calculated by different methods. The average absorbed dose for $r =$ 1.25 cm is 86 per cent of the free in air kerma being in good agreement with published, measured figures. The effect of a tissue-equivalent cage with a wall thickness of 1.5 mm is an additional 2.5 per cent decrease in this ratio. Bilateral irradiation is superior to unilateral and preferable even in animals as small as mice.

Introduction

For biological experiments a class A (ICRU, 1963), homogeneous irradiation is desirable. In case of neutron irradiation "homogeneous" means a practically unchanged neutron spectrum throughout the sample. It is relatively simple to meet this requirement when the energy of the source neutrons is a few MeV and the sample is small. From biological and dosimetrical point of view a volume of about 1 cm^3, filled with tissue-equivalent material, is macroscopically small (Neufeld, 1971). In this case the neutron dose is equal to the free in air kerma and the dose spectrum is the same as the kerma spectrum. Data dealing with dosimetrical conditions in detail and/or measurements in mice exposed to neutrons with a modified fission spectrum are scarce (Goodman, Pearlman, 1965; Auxier, 1967; Davids, et al., 1969). Although an average absorbed dose being by 10–15 per cent less than the free in air kerma means that a mouse is not "macroscopically small" and involves spectrum changes, these latter are not discussed. The problem is of importance as 95 per cent of the kinetic energy of neutrons are imparted to hydrogen and the linear energy transfer (L) of these particles is energy-dependent having a maximum at an energy of about 0.01 MeV (*e.g.* ICRU, 1970). This paper, therefore, analyses the neutron dose spectrum and dose distribution as well as the effect of a plexy cage in a mouse phantom irradiated in the biological channel of a WWR-Sm type thermal reactor.

Experimental

The following simplifications are made during the calculations:

1. The mouse is replaced by a homogeneous mouse-tissue equivalent (Storrer et al., 1957) cylinder having a radius r and a length l.

2. The secondary charged particles lose their energy on the site of their origin. This is only an unimportant restriction as the range of protons with an energy of a few MeV lies within the order of magnitude of 10^{-3} cm (Saigusa, 1970).

Exponential attenuation

For simple estimations of the average absorbed dose it has been assumed that a neutron has not more than one interaction within the phantom.

Neutron and kerma spectra (leakage spectra of a thermal WWR-Sm type reactor, filtered by 10 mm B_4C and 70 mm Bi) of the biological irradiation facility operated at the Central Research Institute for Physics (Zaránd et al., 1971) are the output data of spectrum unfolding code DZBI (Zaránd, 1972).

The average weight of mice used by our team for biological experiments is 20 g. Therefore, for approximate calculations, a length of 8 cm and a diameter of 1.8 cm were used, and this cylinder was replaced by a parallel-epipedon with dimensions of $t \cdot 2r \cdot l$ (t = thickness). The surface $2r \cdot l$ is perpendicular to the beam and $r^2\pi = 2r \cdot t$.

Precise average absorbed dose values, assuming exponential attenuation and using cylinder phantom, were calculated with a PDP-12 computer by using the following expression:

$$D = \frac{1}{r^2\pi} \sum_{i,\,j} K_i \exp(-d_j) r_i \, \Delta r \cdot \Delta\phi \tag{1}$$

where the 2π radians were subdivided in 40 subintervals, while Δr was $r/10$. Free in air kerma, K, was calculated from the neutron spectrum by using group average conversion factors also evaluated by the computer.

Multicollisional model

Unfolded spectrum is used as an input of code MUSPALB (Vértes, 1970) written in FORTRAN language for the ICL-1905 computer of the Central Research Institute for Physics. In its present form the code is suitable to solve one dimensional problems (only slab geometry). The neutron spectrum is calculated in the energy range of 0.215 eV $< E <$ 10.5 MeV in 25 groups. The direction of the source neutrons is left to right, the unit vector in this direction is $\vec{u}$, and $\vec{v}$ is a unit vector in the direction of the velocity of a neutron. In a "transmitted" spectrum as well as in the albedo right (forward-scattered neutrons) the product $v(\vec{} \cdot \vec{u})$ is always positive, while in the dose albedo left (back-scattered neutrons) negative. The neutron spectrum is the sum of albedo left and albedo right.

The tissue-equivalent cylinder phantom is exposed to a neutron beam perpendicular to the longitudinal axis. The spectrum in various points of a chord (parallel with $\vec{u}$) of the cylinder is approximated by the spectrum calculated in a slab infinite in two dimensions with a thickness equal to the length of the chord (h).

With the code MUSPALB it is possible to calculate the neutron spectrum *inside* a slab (thickness = d) at a depth of d_1 from the surface. Neutron spectra are computed with code MUSPALB for, and in, various tissu-equivalent layer thicknesses, in 4 mm steps ($d \leq 28$ mm), while those of transmitted dose and its integral over neutron energy with different codes written in FOCAL language for a PDP-12 computer.

The dose due to forward-scattered neutrons and source neutrons (dose albedo right) in a slab consisting of j 4 mm layers at a depth of the k-th sublayer is indicated by d^r_{jk}, and the dose due to back-scattered neutrons in the same layer by d^l_{jk}.

The dose is in a point P at a distance d_1 from the surface when the chord length through P is h

$$D(h, d_1) = D(h, d_1)\mathrm{l} + D(h, d_1)_r \qquad (2)$$

The quantities on the right hand side are interpolated from the d^l_{jk} and d^r_{jk} elements, respectively.

The dimensions of a mouse are small. Therefore, the dose from captured γ-rays due to $H(n, \gamma)$ reaction can be neglected.

Results

Exponential attenuation

Calculated average absorbed dose value relative to free in air kerma is 81.5 per cent if the mouse (weight 20 g) is replaced by a parallel-epipedon.

Results computed by using expressions (1) are plotted vs. phantom radii in Fig. 1. These results coincide within a curve width with those of "albedo right" (Fig. 1).

Multicollisional models

Neutron dose. Computed d^r_{jk} and d^l_{jk} values are summerized in Table 1 and Fig. 2. Before and behind a slab there is no scattering material. Therefore, the dose matrix elements d^r_{j0} represent the free in air kerma, while the diagonal elements d^l_{jj} are zero. Diagonal elements d^r_{jj} are equal to the transmitted dose. Dose distribution along chords at different distances from the phantom axis for uni- and bilateral irradiations are plotted in Figs 3–4, while Fig. 5 represents the chord average dose values.

Average absorbed dose in the phantom vs. phantom radius is plotted in Fig. 1.

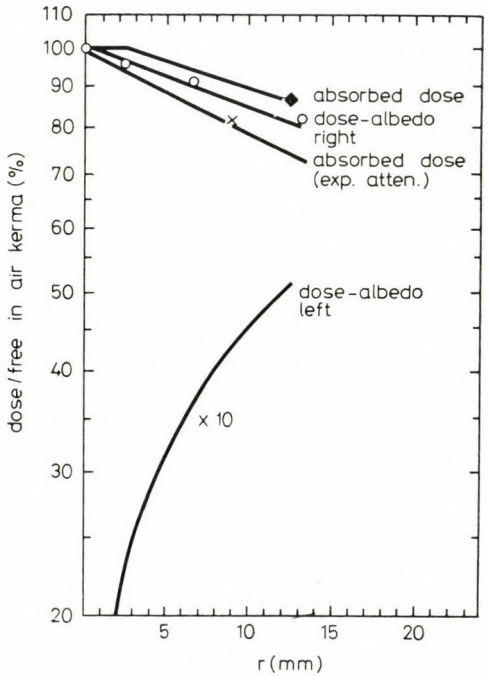

Fig. 1. Calculated (solid lines: present calculations) and measured (○ Davids et al., ◆ Goodman and Pearlman) average absorbed dose to free in air kerma vs. mouse phantom radius. The parallel-epipedon approximation is denoted by *x*

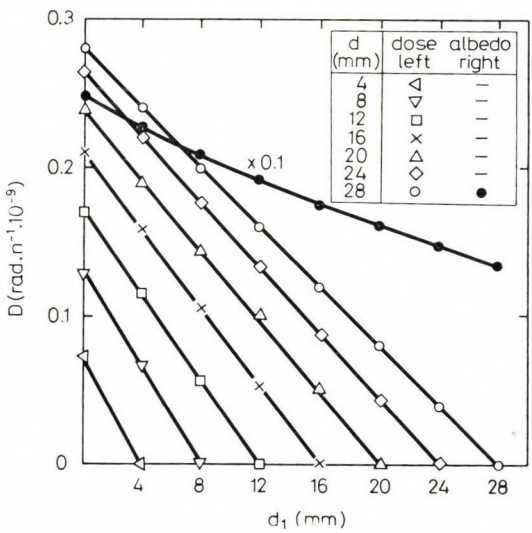

Fig. 2. Dose albedo left and right vs. penetration thickness, d_1 for different slab thicknesses, d

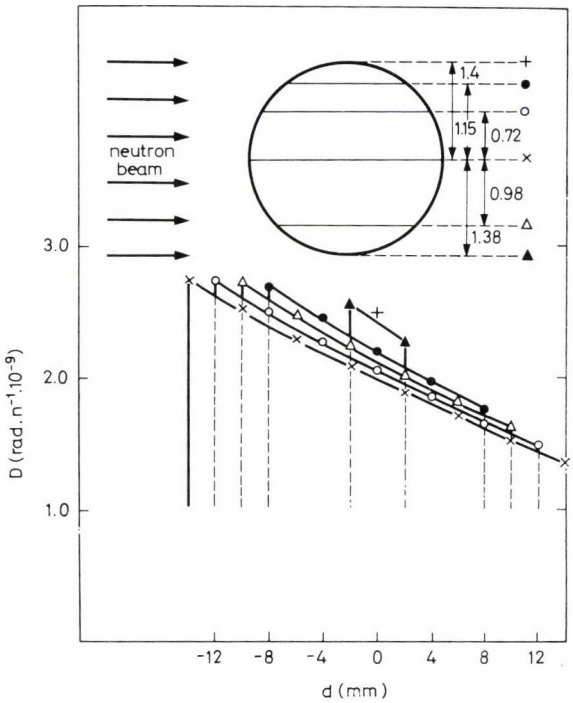

Fig. 3. Dose distribution along different chords in a mouse phantom unilateral irradiation

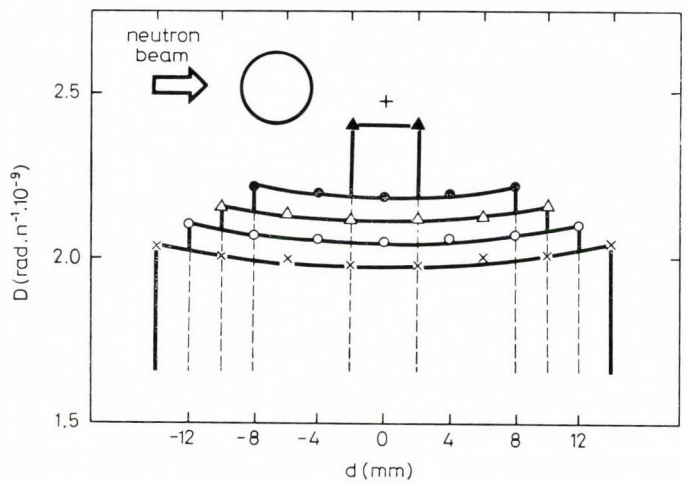

Fig. 4. Dose distribution along different chords in a mouse phantom, bilateral irradiation

Table 1

Dose albedo for different slab thicknesses ($4 \cdot n_1$ mm) and penetration depths ($4 \cdot n_2$ mm). Direction of the neutron beam is left → right

n_1	n_2							
	0	1	2	3	4	5	6	7
Right								
0	2.48							
1	2.48	2.27						
2	2.48	2.27	2.07					
3	2.48	2.28	2.08	1.91				
4	2.48	2.28	2.08	1.91	1.75			
5	2.48	2.28	2.09	1.91	1.75	1.60		
6	2.48	2.28	2.09	1.92	1.76	1.60	1.47	
7	2.48	2.28	2.09	1.92	1.76	1.61	1.47	1.35
Left								
0	0							
1	0.071	0						
2	0.129	0.065	0					
3	0.174	0.114	0.059	0				
4	0.210	0.158	0.105	0.054	0			
5	0.239	0.192	0.145	0.098	0.050	0		
6	0.263	0.220	0.176	0.132	0.088	0.045	0	
7	0.281	0.240	0.200	0.160	0.121	0.082	0.041	0

Neutron dose spectra

In biological experiments the integral quantity, absorbed dose, D and the absorbed dose differential in energy, D_E are of special interest. In Figs 6, 7, therefore, these dose spectra are plotted for uni- and bilateral irradiations, respectively.

Effect of a plexy cage

Animals are irradiated in a plexy glass cage. The wall thickness of this cage was taken to be equivalent to a 1.5 mm tissue-equivalent layer. The average dose relative to the free in air kerma in the phantom was calculated for radii 0.75, 1.00, 1.25 cm and resulted in figures 89.6, 86.6 and 83.5 per cent, respectively.

Discussion and conclusion

A parallel-epipedon is, at least at small dimensions, a good approximation of a cylinder phantom if exponential attenuation is assumed but both are underestimations of the average absorbed dose.

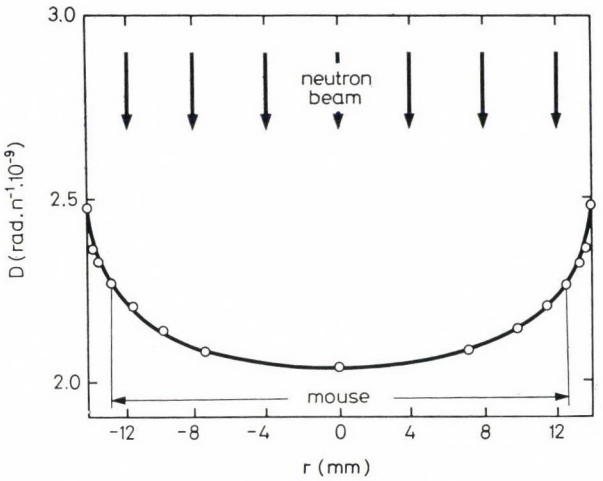

Fig. 5. Average dose along chords parallel with the neutron beam in a cylinder phantom at various distances from the centre line. In the calculations $r = 12.5$ mm and a plexy cage corresponding to a 1.5 mm tissue-equivalent layer were used

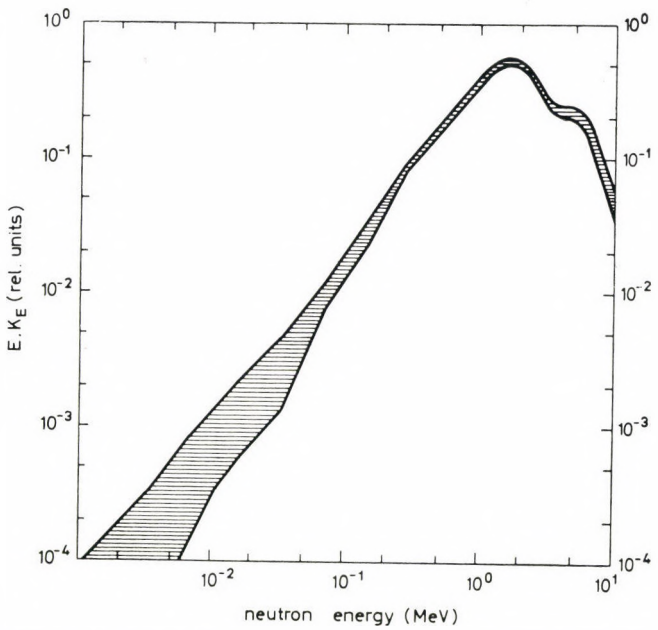

Fig. 6. $E \cdot K_E$ vs. energy in a mouse phantom, unilateral exposure

As the d^r_{jk} and d^l_{jk} elements are both slowly changing functions of thickness, the linear interpolation used in Eq. (2) is justified.

Absorbed dose and dose spectrum in different parts of such a relatively small animal as a mouse may be considerably different. Therefore, a bilateral irradiation is to be preferred. Differences in chord average dose values cannot be

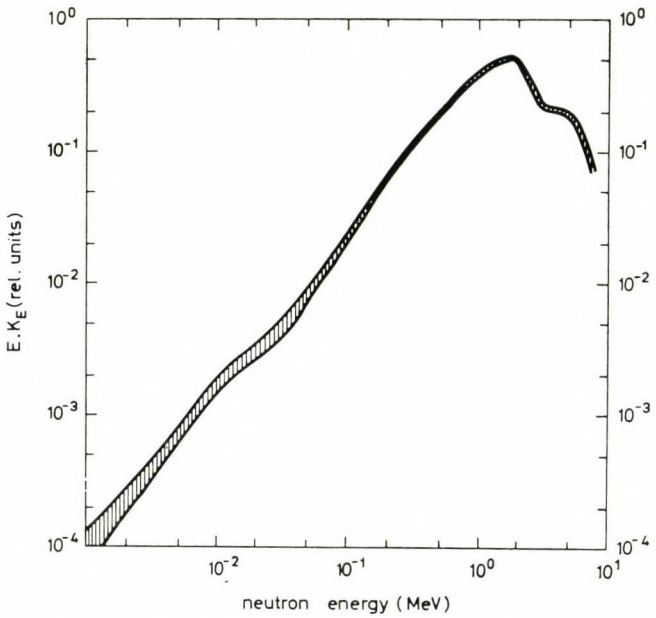

Fig. 7. $E \cdot K_E$ vs. neutron energy in a mouse phantom, bilateral exposure

avoided by this method and necessitate a turning of individual animals around their axis.

Davids et al. (1969) modellized the tissue-equivalent material with nylon layers. These measurements are in good agreement with our calculated transmitted dose and dose albedo right.

Goodman and Pearlman (1965) measured the average absorbed dose in a phantom. Absorbed dose to free in air kerma was 0.90 including a 3 per cent inter-mouse scattering. This latter was subtracted and the result, 0.87, is in excellent agreement with our calculation.

The effect of the plexy cage is rather similar to the effect of a dodger (well-known in radiology) leading to a more homogeneous irradiation. The average absorbed dose is by 2.5 per cent less than the free in air values, as estimated by Davids et al. (1969).

It may be somewhat surprising that the dose albedo left is a linear function of penetration depth. Calculations for thicker slabs (5.2 and 7.2 cm) have shown that this finding only holds for a slab thickness under 3.0 cm.

The author is indebted to Mr. I. Fehér, Head of the Health Physics Department, Central Research Institute for Physics, Budapest, for encouraging this work.

References

Auxier, J. A. (1967) ORNL-4007. ORNL, Oak Ridge, Tenn., U.S.A.
Davids, J. A. G., Mos, A. P. J., De Aude, A. (1969) Phys. Med. Biol. *14* 573
Goodman, L. J., Pearlman, N. (1965) Report Conf. 650616—16 U.S. Dept. of Commerce. Cit. Davids et al., 1969.
ICRU Report (1963) No. 10 e, National Bureau of Standard Handbook 88., U.S. Govt. Printing Office, Washington
ICRU Report (1970) No. 16, International Commission on Radiation Units and Measurements, Washington, U.S.A.
Neufeld, J. (1971) Health Phys. *21* 97
Saigusa, T. (1970) Health Phys. *18* 547
Storrer, J. B., Harris, P. S., Furcher, J. E., Langham, W. H. (1957) Rad. Res. *6* 188
Vértes, P. (1970) KFKI-70-37 RPT, Central Research Institute for Physics, Budapest
Zaránd, P., Makra, S., Sántha, A. (1971) Phys. Med. Biol. *16* 479
Zaránd, P. (1972) KFKI-72-60, Central Res. Inst. for Phys. Budapest

Acta Biochim. et Biophys. Acad. Sci. Hung. Vol. 9 (3), pp. 275–280 (1974)

A Kinetic Model for the Interpretation of UV-Induction of Lysogenic Coli Bacteria

GYÖRGYI RONTÓ, D. NOACK

Institute of Biophysics, Medical University, Budapest and Central Institute of Microbiology and Experimental Therapy, Academy of Sciences of GDR, Jena

(Received January 12, 1974)

The induction of Lambda prophages in lysogenic *E. coli* cells is started after inactivation of repressor molecules coded by the prophage genome itself. All agents known to inhibit bacterial DNA synthesis are capable of initiating a series of processes resulting in the inactivation of these repressors. In the case of UV light as an inducing agent it is suggested that an UV-mediated damage within the bacterial DNA diminishes the replication velocity leading, through several intermediate processes, to the inactivation of phage repressors by accumulation of repressor inactivation precursors of DNA synthesis. The mathematical description of the dose-effect function is the product of the probability P_l of cells with l UV damages multiplied by al after summing up all possible numbers of l. The probability of P_l is calculated on the basis of the radiation kinetic model of Rontó et al. (1967). The theoretical dose-effect curve obtained shows a shoulder with an extrapolation number of 1.3 and a linear part in semilogarithmic plot at high irradiation doses. The experimental data obtained with UV induction of *E. coli* K 12 (λ) are consistent with the model and show that already few UV damages smaller than 10 per bacterial chromosome are sufficient for induction.

Introduction

The lysogenic complex *E. coli* – Phage Lambda contains the genome of the bacteriophage linearly intergrated within the bacterial chromosome as a so-called prophage. The manifestation of genetic information of this prophage is repressed by the action of repressor molecules coded by the CI gene of the prophage. This CI gene is the only one which is not under negative control of repressors. All agents known to inhibit DNA synthesis such as mitomycine C treatment or thymine starvation or UV irradiation lead to the induction of vegetative phage development by lifting the repressor capacity of the phage repressors. Thereafter the prophage is excised and autonomously replicated. The biological effect detectable is the lysis of cells or the formation of infective phage particles, or the loss of colony forming ability (Hershey, 1971). It has been shown by several authors (Noack, Klaus, 1972; Goldthwait, Jacob, 1964; Ruff et al., 1971) that after the stop of DNA synthesis some DNA precursors are accumulated resulting directly or indirectly in the inactivation of phage repressor molecules. In the case of UV irradiation used as inducing agent it should be proved, whether the radiation

kinetic model presented by Rontó et al. (1972) and developed to the special problem of UV mediated inactivation of phage repressors, is consistent with experimental data obtained from *E. coli* bacteria lysogenic with phage Lambda.

Material and methods

Bacterial and phage strains. The wild type strain *Escherichia coli* K 12 (obtained from P. Starlinger, Cologne) has no suppressor and is non-permissive (pm^-) for sus mutants. This strain is lysogenized with the wild type phage λ^+ called λ papa (Dove, 1969).

Cultivation. The lysogenic strain was grown overnight on tryptone (TB) agar plates (8 g Bacto tryptone Difco; 5 g NaCl per litre distilled water). After overnight cultivation at 37 °C for 15 h cells were collected from the surface of TB agar plates and resuspended in phosphate buffer. Samples of appropriate dilutions were transferred into Petri dishes to obtain a suspension layer 1 mm in thickness. After UV irradiation of these samples, the suspensions were plated onto TB agar plates and cultivated in darkness at 37 °C for 15 h. Thereafter the colonies were counted.

UV irradiation. UV irradiation was accomplished at room temperature in darkness, with a high pressure mercury lamp. The distance between the lamp and the bacterial suspension was adjusted to give an incident dose rate of 5 erg/mm^2/sec as measured with a thermoelement of VEB Carl Zeiss, Jena, on the surface of the bacterial suspension layer. The UV light was filtered in order to obtain a wave length range from 240 nm to 320 nm with a maximum at 260 nm.

Results and discussion

I. *The model.* From the point of view of UV-induction four processes must be taken into consideration which are included between UV-irradiation and repressor inactivation:

1. The bacterial DNA is damaged by the UV photons absorbed in the DNA molecule. The number of damages is to be calculated according to the radiation kinetic model (Rontó et al., 1972) developed for the interpretation of UV damaging processes in bacteriophages. As the damage of bacterial DNA – including repair as well – involves the same processes as the damage of phage DNA, we can use the model to estimate the number of damages remaining in the bacterial DNA after irradiation and the following repair processes.

2. The second process, which takes place in the development of inducing effect of UV light, is the diminution of replication velocity as a function of the number of UV damages. Every single damage is known to arrest DNA replication for about 5 seconds. This function can be assumed to be linear because no co-operative effect among the UV damages is to be expected.

3. The concentration of DNA precursors increases as a result of the diminution of DNA replication. As it is suggested both by theoretical and experimental investigations with several mutants of *E. coli* and Lambda phages (Klaus et al., 1972; Noack, Klaus, 1972; Noack, Klaus, 1973), this function can be assumed to be linear, at least in the first part, as shown by the small number of DNA damages remaining within the bacterial chromosome after UV irradiation.

4. The DNA precursors inactivate phage repressor molecules in dependence on the concentration of precursors accumulated. It has been shown in experiments with an *E. coli* mutant sensitive to supplementation of culture medium with DNA precursors, such as adenine, that, in a statistical population, the frequency of induced Lambda lysogenic bacteria is a linear function of the precursor concentration of the medium (Klaus et al., 1972; Ruff et al.,' 1971). At higher precursor concentrations a saturation effect appears.

According to the assumptions mentioned above it can be postulated that the frequency for the induction of prophages in lysogenic bacterial cells with a statistical distribution of cell age increases with the number of UV damages remaining within the bacterial chromosome (Kneser, 1966) after UV irradiation with regard to both the reversion and repair of primarily produced UV damages, because the concentration level of DNA precursors, accumulated due to the inhibition of DNA synthesis, increases with the number of DNA damages. For obtaining the theoretical description of the dose-effect relationship the fact must be considered that a single damage causes induction with a probability of a. A number l of UV damages remaining within the bacterial chromosome provokes induction with a probability of $a \cdot l$. As the probabilityof l damages equals P_l (which depends on the UV-dose), these probabilities must be multiplied and then summed up for all damages to obtain the probability (P) of induction in bacterial population.

$$P = a \sum_{l=0}^{s} l \cdot P_l \tag{1}$$

Here s means the maximal number of DNA sites which can be damaged by UV irradiation, for example thymidine clusters or cytosine clusters. In our previous article (Noack, Rontó, 1974) the coefficient a has been defined as a norming factor in order to obtain P as distribution function, which tends to 1 for high UV doses. According to the interpretation of a mentioned above we can characterize the various mutants having different sensitivities against induction (Klaus et al., 1972). In the sense of this interpretation of a the function P is not a distribution function any more.

The calculation of the frequency P_l is based upon the probability P_{0l} presented in the model of Rontó et al. (1972) containing the production of UV damages within both the bacterial DNA and the phage DNA and their UV mediated reversion. For introducing enzymatic repair processes into the model it is assumed both from experimental and theoretical data that each UV mediated damage in

bacterial and phage DNA is repaired with a probability of β (Rontó, Tarján, 1966; Rontó et al., 1972; Feiner, Hill, 1963). Two damages per DNA molecule were repaired by a probability of β^2 and k damages by a probability of β^k independently from one another. The frequency P_l for the appearance of bacterial cells containing l damages within their DNA molecule is composed of two terms:

$$P_l = P_{0l}\left[1 - \sum_{i=0} \beta^i\right] + \sum_{i=l}^{k} \beta^{i-k} P_{0i} \tag{2}$$

The first term means that the number of cells with l damages in their DNA is diminished as a result of repair by probability β^i. The second term means that the number of cells containing l damages in their DNA is enhanced by repair processes acting on cells with more than l damages within their DNA.

After introducing equation (2) into equation (1) we obtain the dose-effect relationship mentioned above because the probabilities P_{0l} and P_{0i}, respectively, contain the UV dose (mt) as an independent parameter where m means the number of photons absorbed by one DNA molecule in the unit of time, and t is the irradiation time. The other parameters are the following ones: α, β, γ. The numerical values of these are taken on the basis of our previous experiences. Namely, α and γ mean the probabilities of UV-damage and reversion, respectively, by a UV photon of 254 nm (see Rontó et al., 1967). These probabilities must be independent of changing the phage-DNA by bacterial DNA. For the value of β we have taken 0.5 on the basis of our experiences as to the host cell reactivation (dark repair) capacity of the HCR^+ coli cells is to be characterized by the same value. P_{0l} and P_{0i}, respectively, are determined from our radiation kinetic model (Rontó et al., 1972).

II. *The numerical evaluation* of equation (1) carried out on a digital computer yields a theoretical dose-effect curve exhibiting an extended linear initial part. This behaviour results from the existence of a turning point with a dose of $2 \cdot 10^4$ UV photons absorbed by bacterial DNA. The initial slope of 0.0867 per 10^3 UV photons absorbed is reached again with a dose of $4 \cdot 10^4$ UV photons absorbed. The curve shows a maximum value for turning at about $5.8 \cdot 10^4$ UV photons absorbed. The value of the parameter a is calculated from the curve for high UV doses. It is found to be 1/10.515.

The semilogarithmic plot of the surviving fraction $1 - P$ as a function of UV dose yields a dose-effect curve with a small shoulder corresponding to the sigmoidal shape of P as a function of UV dose. The linear part of the curve at high UV doses reveals an extrapolation number of 1.2.

III. *The experimental data* obtained by one of us (D. N.) using the temperature sensitive strain *E. coli* C600 T44 lysogenic with several mutants of the bacteriophage Lambda (Klaus et al., 1972) have shown that the induction effect measured by the lysis of induced lysogenic population increases as a function of UV dose with a slight sigmoidal shape reaching a constant value at high doses

after a relatively drastical turn. Similar results could be obtained with several phage mutants with which the bacterial cells are lysogenized.

This good qualitative agreement with the theoretical results presented above was a stimulus to repeat induction experiments with the wild type *E. coli* K12 lysogenic with the wild type phage Lambda. The biological effect was measured by the loss of colony forming ability due to the inactivation of phage repressors followed by transcription of prophage genes. A comparison of these experimental

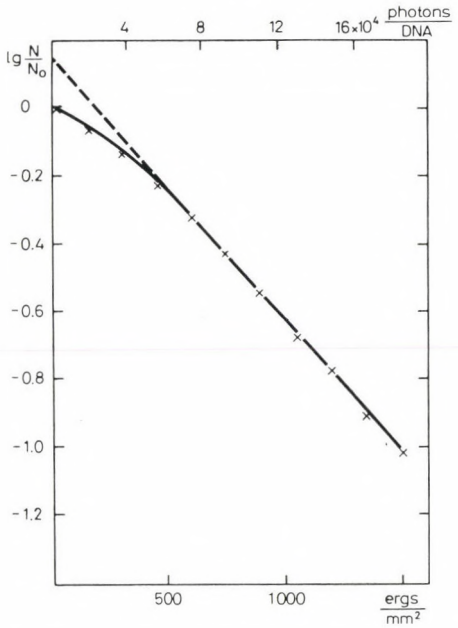

Fig. 1. Comparison of the theoretical and experimental data. The vertical axis shows the logarithm of survival rate (N/N_0), the horizontal one (upper scale) the UV dose as the number of photons absorbed by one single coli chromosome. The lower scale shows the incident UV energy (ergs/mm^2) measured during the irradiation experiment

data and our theoretical results are presented in Fig. 1. The crosses represent the surviving fraction of the irradiated population capable of forming colonies on solid nutrient medium. The mean values of 8 independent experiments are plotted semilogarithmically against the UV dose (bottom scale). The solid line represents the theoretical dose effect curve calculated from the equation (1) using the $\log(1 - P)$ as the function of the UV photons absorbed within the bacterial DNA of an assumed nucleic base pair number of $3 \cdot 10^6$. Calculation from the physico-chemical parameters included in the model of Rontó (Rontó et al., 1972) reveals that the dose of 1 erg/mm^2 corresponds to a number of about $1.4 \cdot 10^4$

photons of the wave length of 254 nm absorbed in one bacterial chromosome. In other words 1500 erg/mm^2 correspond to $2 \cdot 10^7$ photons absorbed per chromosome.

The theoretical dose-effect curve was consistent with the experimental data if the UV dose of 1 *erg/mm*^{2} absorbed by the bacterial chromosome (theoretical dose) corresponded to an UV dose of about 100 *erg/mm*^{2} applied to the surface of the bacterial suspension layer (experimental dose). This discrepancy may be the result of three effects:

a) The wave length interval used for irradiation and measured experimentally contains not only the wave length 254 nm of the maximal emission of the UV lamp but also other ones between 240 nm and 320 nm.

b) The UV photons of the desired wave length interval are absorbed not only by bacterial DNA but also by bacterial RNA which yields a shadow effect.

c) The steepness of the function between precursor concentration and replication velocity.

It can be established from the theoretical dose-effect curve that a number of $9 \cdot 10^4$ photons absorbed by bacterial DNA is needed for the surviving fraction of 37 per cent. This dosis yields a mean number of about 8 UV damages within the *E. coli* chromosome. When also enzymatic repair processes are taken into account about 4 DNA damages remain within the DNA resulting in a survival of 37 per cent. This is in accordance with the data published by Kneser (1966). Finally, the extrapolation number of 1.3 calculated from experimental data is in good agreement with the extrapolation number of 1.2 calculated from the theoretical dose-effect curve (dotted line in Fig. 1).

As a summary it is concluded that the model presented is consistent with experimental data obtained on the bacterial strain *E. coli* K12 lysogenic with the phage Lambda.

References

Dove, W. (1969) Virology *38* 349—351
Feiner, R. R., Hill. K. F. (1953) Nature *200* 291—293
Goldthwait, D. A., Jacob, F. (1964) C. R. Acad. Sci. Paris *259* 661—664
Hershey, A. D. (1971) The Bacteriophage Lambda. Cold Spring Harbor Laboratory 211—238
Klaus, S., Noack, D., Hüller, E. (1972) Z. Allg. Mikrobiol.*12* 403—422
Kneser, H. (1966) Virology *28* 701—706
Noack, D., Klaus, S. (1972) Molec. Gen. Genetics *115* 216—224
Noack, D., Klaus, S. (1973) Acta Phys. Acad. Sci. Hung. *33* 369—374
Noack, D., Rontó Gy. (1974) Z. Allg. Mikrobiol. *14* 73—77
Rontó, Gy., Tarján, I. (1967) Strahlenther. *132* 143—145
Rontó, Gy., Sarkadi, K., Tarján, I. (1967) Strahlenther. *134* 151—157
Rontó, Gy., Karczag, A., Tarján, I. (1972) Studia biophys. *33* 121—130
Ruff, N., Kriby, E. P., Goldthwait, D. A. (1971) J. Bacteriol. *108* 994—998
Scherneck, S., Theile, M. (1969) Beiträge zum Mechanismus der Induktion lysogener Bakterien. Thesis. Rostock

Hoppe-Seyler's Zeitschrift für Physiologische Chemie

Editors in Chief

A. KOSSEL · F. KNOOP · K. THOMAS

Subscription Rate

for one Volume (12 parts) DM 540,—

Vol. 355 No. 1 CONTENTS Januar 1974

Indexed in Current Contents

Walter de Gruyter · Berlin · New York

Hoppe-Seyler's Zeitschrift für
Physiologische Chemie

Editors in Chief

A. KOSSEL · F. KNOOP · K. THOMAS

Subscription Rate

for one Volume (12 parts) DM 540,—

Vol. 355 No. 2 CONTENTS February 1974

Indexed in Current Contents

Walter de Gruyter · Berlin · New York

Printed in Hungary

A kiadásért felel az Akadémiai Kiadó igazgatója. Műszaki szerkesztő: Zacsik Annamária
A kézirat nyomdába érkezett: 1974. III. 26 .Terjedelem: 11,2 (A/5) ív 42 ábra

74.228 Akadémiai Nyomda, Budapest — Felelős vezető: Bernát György

Reviews of the Hungarian Academy of Sciences are obtainable at the following addresses:

ALBANIA

Drejtorija Qändrone e Pärhapjes
dhe Propagandimit tä Librit
Kruga Konferenca e Päzes
Tirana

AUSTRALIA

A. Keesing
Box 4886, GPO
Sydney

AUSTRIA

Globus
Höchstädtplatz 3
A-1200 Wien XX

BELGIUM

Office International de Librairie
30, Avenue Marnix
Bruxelles 5
Du Monde Entier
5, Place St.-Jean
Bruxelles

BULGARIA

Hemus
11 pl Slaveikov
Sofia

CANADA

Pannonia Books
2 Spadina Road
Toronto 4, Ont.

CHINA

Waiwen Shudian
Peking
P. O. B. 88

CZECHOSLOVAKIA

Artia
Ve Směčkách 30
Praha 2
Poštovní Novinová Služba
Dovoz tisku
Vinohradská 46
Praha 2
Mad'arska Kultura
Václavské nám. 2
Praha 1
Slovart A. G.
Gorkého
Bratislava

DENMARK

Ejnar Munksgaard
Nörregade 6
Copenhagen

FINLAND

Akateeminen Kirjakauppa
Keskuskatu 2
Helsinki

FRANCE

Office International de Documentation
et Librairie
48, rue Gay-Lussac
Paris 5

GERMAN DEMOCRATIC REPUBLIC

Deutscher Buch-Export und Import
Leninstraße 16
Leipzig 701
Zeitungsvertriebsamt
Fruchtstraße 3—4
1004 Berlin

GERMAN FEDERAL REPUBLIC

Kunst und Wissen
Erich Bieber
Postfach 46
7 Stuttgart S.

GREAT BRITAIN

Blackwell's Periodicals
Oxenford House
Magdalen Street
Oxford
Collet's Subscription Import
Department
Dennington Estate
Wellingsborough, Northants.
Robert Maxwell and Co. Ltd.
4—5 Fitzroy Square
London W. 1

HOLLAND

Swetz and Zeitlinger
Keizersgracht 471—487
Amsterdam C.
Martinus Nijhof
Lange Voorhout 9
The Hague

INDIA

Hind Book House
66 Babar Road
New Delhi 1

ITALY

Santo Vanasia
Via M. Macchi 71
Milano
Libreria Commissionaria Sansoni
Via La Marmora 45
Firenze
Techna
Via Cesi 16
40135 Bologna

JAPAN

Kinokuniya Book-Store Co. Ltd.
826 Tsunohazu 1-chome
Shinjuku-ku
Tokyo
Maruzen and Co. Lt
P. O. Box 605
Tokyo-Central

KOREA

Chulpanmul
Phenjan

NORWAY

Tanum-Cammermeyer
Karl Johansgt 41—43
Oslo 1

POLAND

Ruch
ul. Wronia 23
Warszawa

ROUMANIA

Cartimex
Str. Aristide Briand 14—18
Bucureşti

SOVIET UNION

Mezhdunarodnaya Kniga
Moscow G—200

SWEDEN

Almquist and Wiksell
Gamla Brogatan 26
S—101 20 Stockholm

USA

F. W. Faxon Co. Inc.
15 Southwest Park
Westwood Mass. 02090
Stechert Hafner Inc.
31 East 10th Street
New York, N. Y. 10003
Dr. Alan Bergelson
Corning Scientific Instruments
Medfield, Massachusetts 02052

VIETNAM

Xunhasaba
19, Tran Quoc Toan
Hanoi

YUGOSLAVIA

Forum
Vojvode Mišića broj 1
Novi Sad
Jugoslovenska Knjiga
Terazije 27
Beograd

Contents

23. VIII. 1974 Index: 26.030

VOLUME 9
NUMBER 4
1974

Acta biochimica et biophysica

ACADEMIAE SCIENTIARUM HUNGARICAE

AKADÉMIAI KIADÓ, BUDAPEST

ABBPAP 9 (4) 281–401 (1974)

Acta Biochimica et Biophysica

Academiae Scientiarum Hungaricae

Szerkeszti:

STRAUB F. BRUNÓ és ERNST JENŐ

Technikai szerkesztők:

SAJGÓ MIHÁLY és NIEDETZKY ANTAL

Szerkesztőség postai címe: 1502 Budapest, Pf. 7 (biokémia)
7643 Pécs, Pf. 99 (biofizika)

Az *Acta Biochimica et Biophysica* a Magyar Tudományos Akadémia idegen nyelvű folyóirata, amely angol nyelven (esetleg német, francia vagy orosz nyelven is) eredeti tanulmányokat közöl a biokémia és a biofizika — fehérjék (struktúra és szintézis), enzimek, nukleinsavak, szabályozó és transzport-folyamatok, bioenergetika, izom-összehúzódás, radiobiológia, biokibernetika, funkcionális és ultrastruktúra stb. — tárgyköréből.

A folyóirat negyedévenként jelenik meg, a négy füzet évente egy kb. 400 oldalas kötetet alkot. Kiadja az Akadémiai Kiadó.

Megrendelhető az Akadémiai Kiadónál (1363 Bp. Pf. 24.), a külföld részére pedig a Kultúra Könyv és Hírlap Külkereskedelmi Vállalatnál (1389 Budapest 62, P.O.B. 149).

The *Acta Biochimica et Biophysica*, a periodical of the Hungarian Academy of Sciences, publishes original papers, in English, on biochemistry and biophysics. Its main topics are: proteins (structure and synthesis), enzymes, nucleic acids, regulatory and transport processes, bioenergetics, excitation, muscular contraction, radiobiology, biocybernetics, functional structure and ultrastructure.

The Acta Biochimica et Biophysica is a quarterly, the four issues make up a volume of some 400 pages per annum. Manuscripts and correspondence with the editors and publishers should be sent to

Akadémiai Kiadó, Budapest 24, P.O.B. 502.

The subscription rate is $ 32.00 per volume. Orders may be placed with *Kultúra* Trading Co. for Books and Newspapers (1389 Budapest 62, P.O.B. 149) or with its representatives abroad, listed on p. 3 of the cover.

Acta Biochimica et Biophysica — журнал Академии Наук Венгрии, публикующий на английском языке (возможно и на немецком, французском и русском языках) оригинальные статьи по проблемам биохимии и биофизики — белков (структура и синтез), энзимов, нуклеиновых кислот, процессов регуляции и транспорта, биоэнергетики, мышечного сокращения, радиобиологии, биокибернетики, функциональной структуры и ультраструктуры и т. д.

Журнал выходит ежеквартально, выпуски каждого года составляют том объемом около 400 страниц. Журнал выпускает Издательство Академии Наук Венгрии.

Рукописи и корреспонденцию просим направлять по следующему адресу:

Akadémiai Kiadó, Budapest 24, P.O.B. 502.

Подписная цена — $ 32.00 за том. Заказы принимает:

Предприятие по внешней торговле книгами и газетами «Kultúra» (1389 Budapest 62, P.O.B. 149) или его заграничные агентства.

Acta Biochim. et Biophys. Acad. Sci. Hung. Vol. 9 (4), pp. 281–294 (1974)

Thermodynamic Analysis of D-glyceraldehyde-3-phosphate Dehydrogenase Action

T. Q. TRO',* T. KELETI

Enzymology Department, Institute of Biochemistry, Hungarian Academy of Sciences, Budapest, Hungary

(Received April 7, 1974)

The changes in enthalpy, entropy and free enthalpy of all elementary steps of the oxidation of the physiological substrate D-glyceraldehyde-3-phosphate and of the substrate analogue D-glyceraldehyde were determined.

The linear Arrhenius and van't Hoff plots indicate that the mechanism of D-glyceraldehyde-3-phosphate dehydrogenase action does not change between 15 and 35°C in either of the two reactions and there is no measurable change in heat capacity.

The thermodynamic parameters of the alternative pathways of D-glyceraldehyde-3-phosphate oxidation confirm the partially random AB mechanism suggested previously from the kinetic analysis. The rate-limiting step is characterized by a change in activation free enthalpy of about +14 000 cal/mole at 25°C. The saturation of the enzyme by all substrates ("infinite" substrate concentrations) would produce a system of enzyme and enzyme-substrate complexes more ordered than at the experimentally attainable "optimum" conditions. Under "optimum" conditions the enzyme is in a partially inhibited form.

The thermodynamic analysis also confirms the previous suggestion that D-glyceraldehyde oxidation can be described by the general mechanism, assuming a rate-limiting step.

Introduction

GAPD** is one of the best known enzymes of the glycolytic pathway. However, very few data are at our disposal concerning the thermodynamic parameters even of the overall reaction. The data so far available are the following:

a) The activation energy of the irreversible oxidation of GAP in the presence of arsenate is +13 to +19 kcal/mole as measured with GAPD isolated from yeast, rabbit muscle and arctic fish (Rapkine et al., 1949; Greene, Feeney, 1970; Cowey, 1967; Low et al., 1973).

* *Permanent address:* Institute of Biochemistry, University of Agriculture, Hanoi, Viet-Nam.

** *Abbreviations:* GA, D-glyceraldehyde; GAP, D-glyceraldehyde-3-phosphate; GAPD, D-glyceraldehyde-3-phosphate: NAD oxidoreductase, phosphorylating (EC 1.2.1.12); GSP, D-glyceric acid-3-phosphate.

b) The activation energies and entropies of the reversible oxidation of both GAP and GA in the presence of phosphate were determined by Keleti et al. (1972) for the pig muscle enzyme. Values of +12 and +7 kcal/mole, respectively, were calculated for the activation energy. The activation entropies were about −12 and −38 cal/degree × mole, respectively.

We do not know of any attempt in the literature concerning the thermodynamic analysis of a multisubstrate enzyme. The purpose of this work was: 1) to give experimental evidence that such an analysis is feasible even in a very complicated system and 2) to test whether the thermodynamic analysis of an enzymic reaction may give further information on the mechanism of action of a multisubstrate enzyme.

Materials and methods

GAPD was isolated from pig skeletal muscle and used after 4 recrystallizations (Elődi, Szörényi, 1956). Before use the crystal suspension was centrifuged, dissolved in 0.1 M glycine buffer, pH 8.5, containing 0.1 M NaCl and gel-filtered on a Sephadex G-50 column equilibrated with the same buffer, in order to remove $(NH_4)_2SO_4$.

Protein concentration was determined by the absorbancy at 280 nm, $E_{lcm}^{lmg/ml} = 1.00$ (Fox, Dandliker, 1956). The molecular weight was taken to be 145 000 (Elődi, 1958).

Enzymic activity was determined spectrophotometrically (Warburg, Christian, 1939) in the direction of NAD reduction, in the presence of P_i. The molar extinction coefficient of NADH at 340 nm was taken to be 6.22×10^3 $M^{-1}cm^{-1}$ (Horecker, Kornberg, 1948). The activity assay mixture and the rapid mixing techniques were described earlier (Keleti, Batke, 1965; Keleti, 1965). Furthermore, an automatic recorder which permitted the determination of reaction rate in the first second after mixing was used. Initial velocity was calculated from the change in absorbancy in the first 5 seconds at 340 nm. The molar activity of enzyme preparations at 20°C and pH 8.5 was 340−470 kat/mole enzyme (cf. Enzyme Nomenclature, Elsevier, 1972. p. 27, i.e. 1 kat = 1 mole/s).

GAP was prepared from fructose-1,6-diphosphate (Reanal) by the method of Szewczuk et al. (1961). Inorganic phosphate was removed as described earlier (Keleti, Batke, 1965).

GA (Fluka) syrup was of 80% purity.

NAD (Reanal and Boehringer), 85−95% pure preparations were used.

All other reagents were commercial preparations of reagent grade.

The temperature of assay mixtures was kept constant (±0.2°C) by using thermostated cuvette holders connected to a KUTESZ Ultrathermostat.

The pH of the reaction mixtures was checked with a RADELKISZ precision pH-meter at the temperature of the experiment.

OPTON PMQ II spectrophotometer and SERVOGOR automatic recorder were used.

The activation enthalpy was calculated from the Arrhenius plot:

$$\ln k = \ln A - E^*/RT$$

where k is the rate constant calculated from the maximum velocity, i.e. $k = V_{max}/E_{total}$. This was determined by extrapolating the concentration of all substrates to the infinite, i.e. from tertiary plots (Keleti, 1965; Keleti, Batke, 1965). A is the pre-exponential factor, E^* is the activation energy: $E^* = \Delta H^* + RT$ (Webb, 1963), where H^* is the activation enthalpy, R the gas constant and T the absolute temperature.

The activation entropy, S^*, was calculated by extrapolating to $1/T = 0$ the plot (Webb, 1963)

$$\log (k/T) = \log (\kappa R/Nh) - \Delta H^*/4.576T + \Delta S^*/4.576$$

where κ is the transmission coefficient assumed to be unity, N is the Avogadro number, and h is the Planck constant. Alternatively, activation entropy was calculated by using the equation:

$$\Delta S^* = \Delta H^*/T - 4.576 [\log (k_B T/h) - \log k] \quad \text{(Dalziel, 1963)}$$

where k_B is the Boltzmann constant.

The activation free enthalpy was calculated from the relation

$$\Delta G^* = \Delta H^* - T\Delta S^*$$

The normal enthalpy, H°, and entropy, S°, were determined from van't Hoff plots:

$$\log K = -\Delta H^\circ/4.576T + \Delta S^\circ/4.576$$

where K is the equilibrium constant defined as the association constant, k_1/k_{-1}, of the elementary step. The normal free enthalpy, G°, was calculated from both equation $\Delta G^\circ = \Delta H^\circ - T\Delta S^\circ$ and $\Delta G^\circ = -RT \ln K$.

Results

a) *D-glyceraldehyde-3-phosphate oxidation*

The kinetic analysis of GAP oxidation was performed between 15 and 35°C at 5°C intervals. At each temperature the experimental data could be well described in terms of the partially random AB mechanism as defined by Dalziel (1969). The kinetic analysis and the determination of the equilibrium constants of the elementary steps were performed as described previously (Keleti, Batke, 1965).

Table 1

Apparent first order rate constant of GAP and GA oxidation at different temperatures

The rate constants were calculated from maximum velocities by extrapolating the concentration of all substrates to infinity (i.e. from tertiary plots)
Maximum velocity was determined in all six possible combinations of the three substrates (GAP, NAD, P_i or GA, NAD, P_i) by keeping the concentration of two of the substrates constant

Reaction	k (sec^{-1})				
	15°C	20°C	25°C	30°C	35°C
GAP oxidation	165 ± 5	180 ± 7	190 ± 4	205 ± 5	220 ± 10
GA oxidation	0.10 ± 0.02	0.12 ± 0.01	0.13 ± 0.01	0.15 ± 0.01	0.17 ± 0.01

Table 1 summarizes the rate constans of the enzyme reaction, as calculated from maximum velocities. The "order" in which the concentration of the substrates was kept constant (i.e. whether NAD, GAP or P_i was the "first", "second" or "third" substrate, cf. Keleti, 1972) did not affect the value of k. The Arrhenius plot of temperature dependence of the rate constant is presented in Fig. 1.

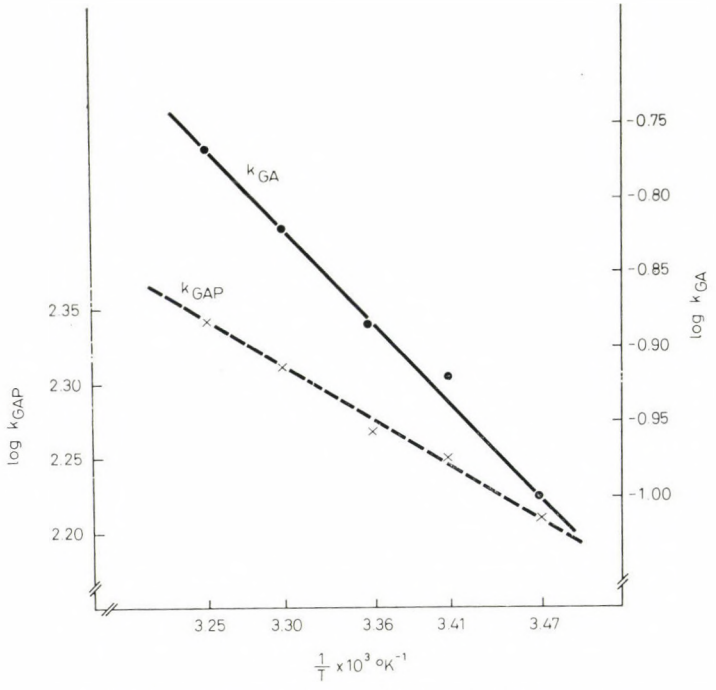

Fig. 1. Arrhenius plots of GAP and GA oxidation

The equilibrium constants of the elementary steps of GAP oxidation at 25°C are summarized in Table 2. Fig. 2 shows that the equilibrium constants of the formation of enzyme–coenzyme and enzyme–substrate complexes (K_1 and K_2) are independent of temperature in the range tested. In contrast to this, the equilibrium constants of the formation of the ternary complex (K_3 and K_4), and that of its intramolecular transformation (K_5), are temperature dependent

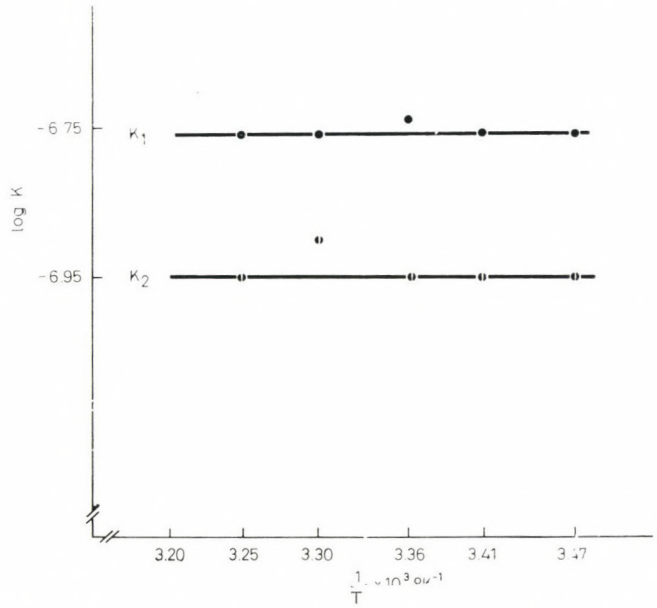

Fig. 2. GAP oxidation. Van't Hoff plots of equilibrium constants K_1 and K_2

with linear van't Hoff plots (Figs 3 and 4). However, the temperature dependence of K_5 shows that in contrast to the elementary steps characterized by K_3 and K_4, the intramolecular transformation of the ternary complex is endothermic.

We should like to mention that the error of determining the absolute value of the equilibrium constants is rather great (cf. the extremes in Table 2). However, the slopes of the van't Hoff plots determined from any single series of experiment agreed with those presented in Fig 2 to 4.

The thermodynamic parameters calculated from the rate constants of GAP oxidation are shown in Table 3. As a comparison we also give the values obtained earlier (Keleti et al., 1972). These latter data were calculated from the rate constant of the highest velocity which could be experimentally determined. (These data will be referred to in the following as determined under "optimum" conditions). It is seen that at 25°C the changes in free enthalpy are approximately the same whether determined under "optimum" conditions or by extrapolating the concentration of all substrates to infinity.

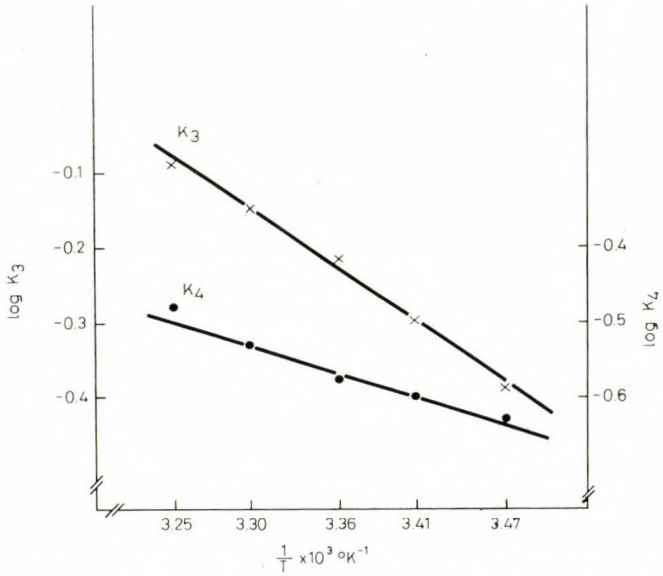

Fig. 3. GAP oxidation. Van't Hoff plots of equilibrium constants K_3 and K_4

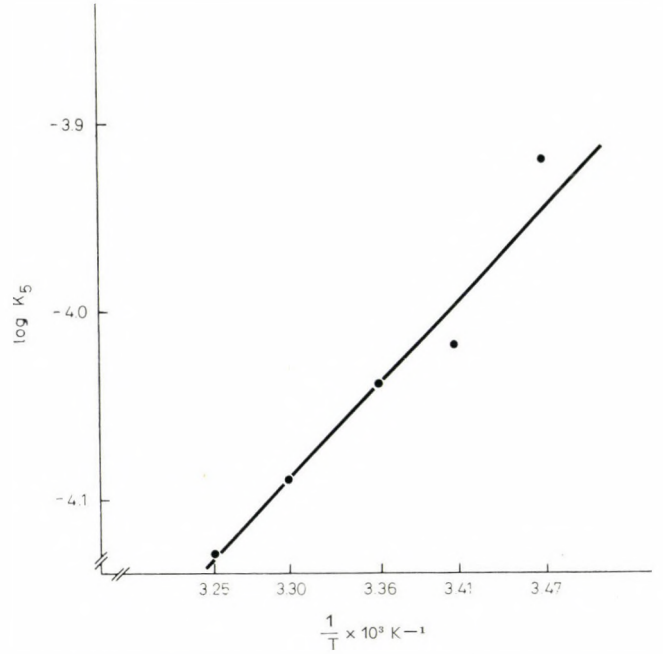

Fig. 4. GAP oxidation. Van't Hoff plot of equilibrium constant K_5

Table 2

Equilibrium constants of the elementary steps of GAP oxidation at 25°C

Each equilibrium constant* was determined in all six possible combinations of the substrates, as described previously (Keleti, Batke, 1965). The ± values are the extremes. The temperature dependence of these constants are presented in Figs 2 to 4 in a typical experiment

$K_1 \times 10^8$, M	18 ± 14
$K_2 \times 10^8$, M	11 ± 7
K_3, M	0.6 ± 0.2
$K_4 \times 10$, M	2.6 ± 2
$K_5 \times 10^5$	9 ± 7

* K_1 = [E] [NAD]/[E-NAD]; K_2 = [E] [GAP]/[E-GAP]; K_3 = [E-NAD] [GAP]/[GAP-E-NAD]; K_4 = [E-GAP] [NAD]/[GAP-E-NAD]; K_5 = [GAP-E-NAD]/[GSP-E-NADH], where E is the enzyme

Table 3

Changes in activation enthalpy, entropy and free enthalpy during GAP oxidation

	ΔH^* kcal/mole	ΔS^* cal/mole × degree	$\Delta G^* \times 10^{-3}$ cal/mole at 25°C
Extrapolating the concentration of all substrates to infinity	+ 1.2	−44	+14
Under "optimum" conditions*	+10.2	−12	+14

* Keleti et al., 1972

Table 4

Thermodynamic parameters calculated from the temperature dependence of equilibrium constants of the elementary steps of GAP oxidation

Equilibrium constant	ΔH° kcal/mole	ΔS° cal/mole × degree	$\Delta G^\circ \times 10^{-3}$ cal/mole at 25°C
K_1	0	+33	−10
K_2	0	+34	−10
K_3	−3.6	−14	~ 0
K_4	−3.2	−14	~ 0
K_5	+3.9	+36	− 7

Table 4 presents normal enthalpy, entropy and free enthalpy changes of the elementary steps, whereas Table 5 gives their sum in the alternative pathways.

Table 5 shows that no appreciable differences can be found whether the thermodynamic parameters are summed up through pathway NAD → GAP → P_i (i.e. by using the values calculated from K_1, K_3 and K_5) or through GAP → → NAD → P_i (i.e. by using the values of K_2, K_4 and K_5).

Table 5

Thermodynamic parameters for the alternative pathways of GAP oxidation

$\Sigma\Delta H^\circ$ of the NAD → GAP → P_i order of binding means the sum of ΔH°-s calculated from K_1, K_3 and K_5. Similar definitions hold for $\Sigma\Delta S^\circ$ and $\Sigma\Delta G^\circ$. $\Sigma\Delta G^\circ + \Delta G^*$, i.e. the total free enthalpy change starting from the free substrates and enzyme to the formation of the activated complex equals −3000 cal/mole at 25°C

Order of substrate binding	$\Sigma\Delta H^\circ$ kcal/mole	$\Sigma\Delta S^\circ$ cal/mole × degree	$\Sigma\Delta G^\circ \times 10^{-3}$ cal/mole at 25°C
NAD, GAP, P_i	+0.3	+55	−17
GAP, NAD, P_i	+0.7	+56	−17

b) *D-glyceraldehyde oxidation*

The kinetic analysis of GA oxidation and the determination of the equilibrium constants of the elementary steps were performed as described previously (Keleti, 1965). The experiments were also carried out between 15 and 35°C, at 5° intervals.

The experimental data could be described in all cases by the "general mechanism", i.e. by assuming that all possible binary, ternary and quaternary complexes are formed and are active, and that the intramolecular transformation of the quaternary complex is the rate-determining step.

The rate constants of enzyme reaction are listed in Table 1. The substrate analogue, of course, is oxidized at a much slower rate than is the physiological substrate. Fig. 1 shows that, similarly to GAP oxidation, the Arrhenius plot is a straight line.

Table 6 summarizes the equilibrium constants of the elementary steps at 25°C. In Figs 5 and 6 are seen the van't Hoff plots of temperature independent and dependent equilibrium constants, respectively. The equilibrium constants of the formation of binary and ternary complexes, except where free P_i is involved, are independent of the temperature.

Tables 7 and 8 contain the thermodynamic parameters of GA oxidation, whereas Table 9 demonstrates the sum of normal enthalpy, entropy and free enthalpy changes in the alternative pathways.

Discussion

It is seen above that ail Arrhenius and van't Hoff plots of GAP and GA oxidation catalyzed by pig muscle GAPD are linear. From these data two conclusions can immediately be drawn:

1. the mechanism of action of the enzyme does not significantly change between 15 and 35°C;

2. the change in apparent heat capacity of the system, enzyme and enzyme-substrate complexes, is nearly zero.

The thermodynamic analysis of coenzyme binding to the rabbit muscle enzyme was performed by Velick et al. (1971) by microcalorimetry. The authors could assign different free enthalpy, normal enthalpy and normal entropy changes to the four coenzyme binding sites which differ in their dissociation constant. The change in apparent heat capacity, when the enzyme was saturated with coenzyme, equalled -220 cal/degree × mole bound NAD (Velick et al., 1971).

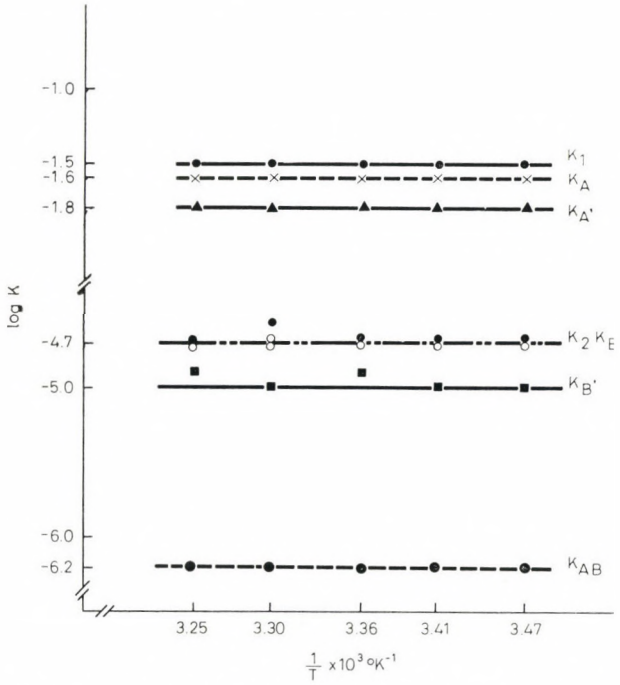

Fig. 5. GA oxidation. Van't Hoff plots of temperature independent equilibrium constants K_1, K_2, K_A, $K_{A'}$, K_B, $K_{B'}$, K_{AB}

The discrepancy between Velick's and our results is only apparent. The thermodynamic analysis based on kinetic measurements provides average values for the thermodynamic parameters and does not permit us to differentiate between the distinct coenzyme binding sites. From the kinetic analysis of enzyme action only an average dissociation constant of the GAPD-NAD complex can be deduced. The different dissociation constants of the individual binding sites can be only determined by special methods (Conway, Koshland, 1968; De Vijlder et al., 1969). We assume that the change in the apparent heat capacity, as determined by microcalorimetry, reflects the changes in steric structure caused by the binding of coenzyme to the apoenzyme (Előd, Szabolcsi, 1959; Listowsky et al., 1965). This phenomenon does not occur during catalysis: the rapid turnover, the enzyme–NAD + NADH ⇌ enzyme–NADH + NAD exchange reaction, does not allow the enzyme to return to the structure characteristic of the apoenzyme.

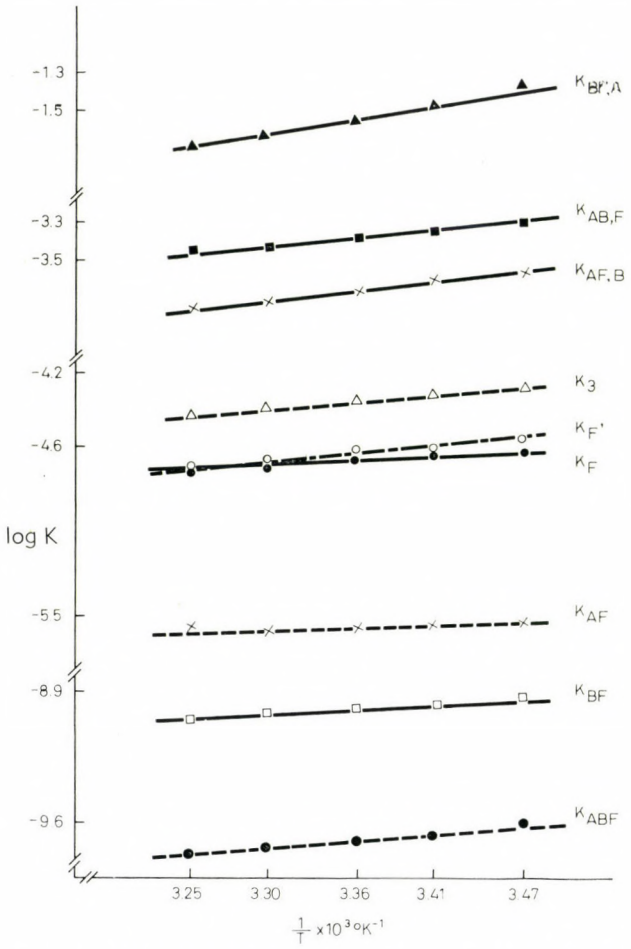

Fig. 6. GA oxidation. Van't Hoff plots of equilibrium constants K_3, K_F, $K_{F'}$, K_{AF}, K_{BF}, $K_{BF,A}$, $K_{AB,F}$, $K_{AF,B}$, K_{ABF}

There are a number of contradictory assumptions in the literature concerning the mechanism of action of GAP oxidation (Furfine, Velick, 1965; Keleti, Batke, 1965; Trentham et al., 1969; Trentham, 1971, 1971a; Orsi, Cleland, 1972; Peczon, Spivey, 1972). The problems of establishing the mechanism of action of a three-substrate enzyme reaction have been discussed in detail (Keleti et al., 1973). The sum of total changes in normal enthalpy, entropy and free enthalpy are equal, if we assume the order of binding NAD → GAP → P_i or GAP → NAD → P_i (cf. Table 5), i.e. the probability of the pathways is equal. This further supports our previous suggestion (Keleti, Batke, 1965) that the mechanism of GAP oxidation can be described by the partially random AB mechanism.

Table 6

Equilibrium constants of the elementary steps of GA oxidation, at 25°C

The equilibrium constants* were determined in all six possible combinations of the substrates, as described previously (Keleti, 1965). The ± values are the extremes. The temperature dependence of these constants is presented in Figs 5 and 6 in a typical experiment

$K_1 \times 10^2$, M	2.8 ± 1.3
$K_2 \times 10^5$, M	1.8 ± 0.2
$K_3 \times 10^5$, M	4.3 ± 0.3
$K_A \times 10^2$, M	2.2 ± 0.3
$K_{A'} \times 10^2$, M	1.4 ± 0.2
$K_B \times 10^5$, M	1.8 ± 0.1
$K_{B'} \times 10^5$, M	1.1 ± 0.1
$K_F \times 10^5$, M	2.1 ± 0.2
$K_{F'} \times 10^5$, M	2.3 ± 0.2
$K_{AB,F} \times 10^4$, M	4.2 ± 0.8
$K_{AF,B} \times 10^4$, M	2.1 ± 0.2
$K_{BF,A} \times 10^2$, M	2.8 ± 0.3
$K_{AB} \times 10^7$, M^2	5.4 ± 0.6
$K_{AF} \times 10^6$, M^2	2.7 ± 0.2
$K_{BF} \times 10^9$, M^2	1.0 ± 0.1
$K_{ABF} \times 10^{10}$, M^3	2.0 ± 0.1

* K_1 = [E] [GA]/[E-GA]; K_2 = [E] [NAD]/[E-NAD];
K_3 = [E] [P_i]/[E-P]; K_A = [E-NAD] [GA]/[GA-E-NAD];
$K_{A'}$ = [E-P] [GA]/[GA-E-P]; K_B = [E-GA] [NAD]/[GA-E-NAD];
$K_{B'}$ = [E-P] [NAD]/[NAD-E-P]; K_F = [E-NAD] [P_i]/[NAD-E-P];
$K_{F'}$ = [E-GA] [P_i]/[GA-E-P]; $K_{AB,F}$ = [GA-E-NAD] [P_i]/[GA-E-NAD-P];
$K_{BF,A}$ = [NAD-E-P] [GA]/[GA-E-NAD-P]; $K_{AF,B}$ = [GA-E-P] [NAD]/[GA-E-NAD-P]
$K_{AB} = K_1K_B = K_2K_A$; $K_{AF} = K_1K_F = K_3K_A$; $K_{BF} = K_2K_F = K_3K_B$;
$K_{ABF} = K_{AB,F}K_{AB} = K_{BF,A}K_{BF} = K_{AF,B}K_{AF}$

Table 7

Changes in activation enthalpy, entropy and free enthalpy during GA oxidation

	ΔH^* kcal/mole	ΔS^* cal/mole × °K	$\Delta G^* \times 10^{-3}$ cal/mole at 25°C
Extrapolating the concentration of all substrates to infinity	+2.6	−54	+19
Under "optimum" conditions*	+5.5	−38	+17

* Keleti et al., 1972

It is known that in GAP oxidation a rate-limiting elementary step can be demonstrated, i.e. phosphorolysis (Velick, 1954; Keleti, Telegdi, 1959a; Keleti, Batke, 1965; 1967). The similarity of activation free enthalpy values determined under "optimum" conditions and by extrapolating the concentration of all substrates to infinity (cf. Table 3) suggests that the rate-limiting step at 25°C requires a change in activation free enthalpy of about +14,000 cal/mole. Table 3 also

Table 8

Thermodynamic parameters calculated from the temperature dependence of equilibrium constants of the elementary steps of GA oxidation

Constant	ΔH° kcal/mole	ΔS° cal/mole × °K	$\Delta G^\circ \times 10^{-3}$ cal/mole at 25°C
K_1	0	+ 7	− 2
K_2	0	+22	− 6.5
K_3	+2.4	+30	− 6.5
K_A	0	+ 8	− 2
$K_{A'}$	0	+ 8	− 2.5
K_B	0	+22	− 6.5
$K_{B'}$	0	+23	− 7
K_F	+2.3	+28	− 6
$K_{F'}$	+3.5	+31	− 6
K_{AB}	0	+29	− 8.5
K_{AF}	+1.8	+27	− 6
K_{BF}	+1.7	+46	−12
$K_{AB,F}$	+3.3	+32	− 6
$K_{AF,B}$	+3.8	+33	− 6
$K_{BF,A}$	+5.7	+24	− 1
K_{ABF}	+3.0	+52	−12.5

Table 9

Thermodynamic parameters for the alternative pathways of GA oxidation

$\Sigma\Delta H^\circ$ for the GA → P_i → NAD order of binding means the sum of normal enthalpies of K_1, K_F, and $K_{AF,B}$. Similar definitions, *mutatis mutandis*, hold for the other thermodynamic parameters and for the different orders of binding. $\Sigma\Delta G^\circ + \Delta G^* \approx +4000$ cal/mole at 25°C

Order of binding	ΔH° kcal/mole	ΔS° cal/mole × °K	$\Delta G^\circ \times 10^{-3}$ cal/mole at 25°C
GA, P_i, NAD	+7	+72	−14
GA, NAD, P_i	+3	+60	−15
P_i, GA, NAD	+6	+71	−15
P_i, NAD, GA	+8	+76	−14.5
NAD, GA, P_i	+3	+61	−15
NAD, P_i, GA	+8	+73	−14

shows that the system, enzyme and enzyme-substrate complexes, is less ordered under "optimum" conditions than if the substrates are at infinite concentration. The activation enthalpy is significantly lower if calculated by extrapolating the concentration of all substrates to infinity than under "optimum" conditions. From these one can infer that under "optimum" conditions the enzyme is in a partially inhibited form. In fact, it was found that excess of NAD and phosphate inhibited GAP oxidation (Nagradova, 1958; Keleti, Telegdi, 1959; Batke, Keleti, 1968; Ovádi et al., 1972; Keleti et al., 1972; Keleti, 1973; Ovádi, 1973). However,

at 25°C the rate of GAP oxidation does not differ appreciably whether or not the enzyme is in a partially inhibited form as indicated by the similarity of activation free enthalpy changes at "optimum" and infinite substrate concentrations. This may occur if the inhibition is mixed or competitive, which is really the case (Batke, Keleti, 1968).

The data presented in this paper also confirm our previous suggestion on the mechanism of action of GA oxidation derived from kinetic analysis (Keleti, 1965). The thermodynamic parameters support the assumption that all possible binary, ternary and quaternary complexes may form and are active, i.e. the "general mechanism" holds (Table 9). Similarly to the mechanism of GAP oxidation the changes in the activation free enthalpy of GA oxidation confirm that, at 25°C, in overall reaction a rate-limiting elementary step may exist, which is characterized by a ΔG^* of about +17 000 cal/mole (Table 7).

In contrast to GAP oxidation, with GA oxidation we have found earlier that excess of NAD or phosphate does not inhibit the oxidation of this substrate analogue (Keleti, 1965; 1965a). Accordingly, the activation enthalpy is not considerably lower at infinite substrate concentrations than at "optimum" concentrations. Moreover, high concentration of substrates does not cause further appreciable changes in the conformation as shown by the small differences in activation entropy (Table 7).

References

Batke, J., Keleti, T. (1968) Acta Biochim. Biophys. Acad. Sci. Hung. *3* 385—395
Conway, A., Koshland, D. E., Jr. (1968) Biochemistry *7* 4011—4023
Cowey, C. B. (1967) Comp. Biochem. Physiol. *23* 969—976
Dalziel, K. (1963) Acta Chem. Scand. *17* Suppl. *1*. 27—33
Dalziel, K. (1969) Biochem. J. *114* 547—556
DeVijlder, J. J. M., Boers, W., Slater, E. C. (1969) Biochim. Biophys. Acta *191* 214—220
Elődi, P. (1958) Acta Physiol. Acad. Sci. Hung. *13* 199—206
Elődi, P., Szabolcsi, G. (1959) Nature *184* 56 (only)
Elődi, P., Szörényi, E. T. (1956) Acta Physiol. Acad. Sci. Hung. *9* 339—350
Fox, J. B., Jr., Dandliker, W. B. (1956) J. Biol. Chem. *221* 1005—1017
Furfine, C. S., Velick, S. F. (1965) J. Biol. Chem. *240* 844—855
Greene, F. C., Feeney, R. E. (1970) Biochim. Biophys. Acta *220* 430—442
Horecker, B. L., Kornberg, A. (1948) J. Biol. Chem. *175* 385—390
Keleti, T. (1965) Acta Physiol. Acad. Sci. Hung. *28* 19—29
Keleti, T. (1965a) Acta Biol. Med. Germ. Suppl. III. 245—249
Keleti, T. (1972) FEBS Letters *28* 287—288
Keleti, T. (1973) in Mechanism and Control Properties of Phosphotransferases. Akademie Verlag Berlin, pp. 253—270
Keleti, T., Batke, J. (1965) Acta Physiol. Acad. Sci. Hung. *28* 195—207
Keleti, T., Batke, J. (1967) Enzymologia *33* 65—79
Keleti, T., Telegdi, M. (1959) Acta Physiol. Acad. Sci. Hung. *16* 235—241
Keleti, T., Telegdi, M. (1959a) Acta Physiol. Acad. Sci. Hung. *16* 243—255
Keleti, T., Földi, J., Erdei, S., Tro', T. Q. (1972) Biochim. Biophys. Acta *268* 285—291
Keleti, T., Batke, J., Tro', T.Q. (1973) Acta Biol. Med. Germ. *31* 175—179
Listowsky, J., Furfine, C. S., Betheil, J. J., Englard, S. (1965) J. Biol. Chem. *240* 4253—4258

Low, P. S., Bada, J. L., Somero, G. N. (1973) Proc. Natl. Acad. Sci. USA *70* 430—432
Nagradova, N. K. (1958) Biokhimiya *23* 511—522
Orsi, B. A., Cleland, W. W. (1972) Biochemistry *11* 102—109
Ovádi, J. (1973) in Mechanism and Control Properties of Phosphotransferases. Akademie Verlag Berlin, pp. 473—478
Ovádi, J., Nuridsány, M., Keleti, T. (1972) Acta Biochim. Biophys. Acad. Sci. Hung. *7* 133—141
Peczon, B. D., Spivey, H. O. (1972) Biochemistry *11* 2209—2217
Rapkine, L., Shugar, D., Siminovitch, L. (1949) Bull. Soc. Chim. Biol. *31* 1201—1210
Szewczuk, A., Wolny, E., Wolny, M., Baranowski, T. (1961) Acta Biochim. Pol. *8* 201—207
Trentham, D. R. (1971) Biochem. J. *122* 59—69
Trentham, D. R. (1971a) Biochem. J. *122* 71—77
Trentham, D. R., McMurray, C. H., Pogson, C. I. (1969) Biochem. J. *114* 19—24
Velick, S. F. (1954) in McElroy, W. D., Glass, B. (eds.) Mechanism of Enzyme Action. Johns Hopkins Press Baltimore, pp. 491—519
Velick, S. F., Baggott, J. P., Sturtewant, J. M. (1971) Biochemistry *10* 779—786
Warburg, O., Christian, W. (1939) Biochem. Z. *303* 40—68
Webb, J. L. (1963) Enzyme and Metabolic Inhibitors. Acad. Press New York, London Vol. 1. pp. 757—758

Acta Biochim. et Biophys. Acad. Sci. Hung. Vol. 9 (4), pp. 295—301 (1974)

The Effect of Quinacrine on the Expression of *lac* Operon in *Escherichia coli* Promoter Mutants

J. SCHLAMMADINGER, G. SZABÓ

Institute of Biology, Medical University of Debrecen, Debrecen (Hungary)

(Received April 2, 1974)

Induced β-galactosidase synthesis displays enhanced sensitivity to quinacrine treatment in wild type *Escherichia coli* cells. Such low doses of this dye which do not affect overall protein synthesis are still able to inhibit β-galactosidase production to a considerable extent. Investigating promoter mutants we succeeded in finding strains which behave like wild type cells and others which do not show enhanced quinacrine sensitivity. We raise the hypothesis that a specific nucleotide sequence exists in the RNA polymerase-binding region of the promoter gene, which is responsible for the apparent quinacrine sensitivity of the *lac* operon.

Introduction

In a previous paper we have already described that an acridine dye, quinacrine* specifically inhibits induced β-galactosidase synthesis in *Escherichia coli* K 12 wild type cells, i.e. doses of QAC which do not influence RNA and protein synthesis inhibited β-galactosidase synthesis to a considerable extent (Schlammadinger, Szabó, 1973). There was no reason to suppose that QAC might act directly upon the *Z* gene. It seemed more probable that the target of this dye in the *lac* operon is one of the control elements. In this respect there are only two candidates, the *P* and *O* genes, because the increased affinity of *I* gene would result in the opposite effect. In preliminary experiments with *E. coli* CA 8050 strain, which bears a UV5 mutation in the promoter region, however, we failed to detect a similar effect of QAC: the overall protein and β-galactosidase syntheses were depressed parallelly. These findings focused our interest to the promoter region of the *lac* operon. Although we have already concluded in the preceding paper (Schlammadinger, Szabó, 1973) that QAC acted on the *P* gene, further investigations on promoter mutant strains were necessary to prove our assumption and exclude a possible effect on the *O* gene. Here we report our results obtained on different *lac* promoter mutant strains and offer some speculations on the base composition of the *P* gene.

* *Abbreviations used:* QAC, quinacrine; TMG, methyl-β-D-thiogalactoside; ONPG, o-nitrophenyl-β-D-galactopyranoside; CRP, cyclic AMP receptor protein; CAP catabolite activator protein; cAMP, cyclic adenosine-3',5'-monophosphate; AD, acrydine orange.

Materials and methods

The experimental procedure was essentially the same as described earlier (Schlammadinger, Szabó, 1973). Log-phase cells were induced with 5×10^{-4} M TMG (SIGMA) in glycerol minimal medium. Protein synthesis was followed by measuring the incorporation of (^{14}C)-L-phenylalanine (0.7 μCi/ml, specific activity 271 mCi/mmole, UVVVR, Prague). Quinacrine HCl was purchased from SIGMA and used in 6.25 – 100.0 μg/ml concentrations. The β-galactosidase activity was determined by the conventional method (Schlammadinger, Szabó, 1973) with ONPG (FLUKA) as substrate.

Results and discussion

Figs 1 and 2 demonstrate our results on different *E. coli* strains showing the rate of induced β-galactosidase synthesis and that of (^{14}C)-L-phenylalanine incorporation into 5% trichloroacetic acid-insoluble fraction at different QAC

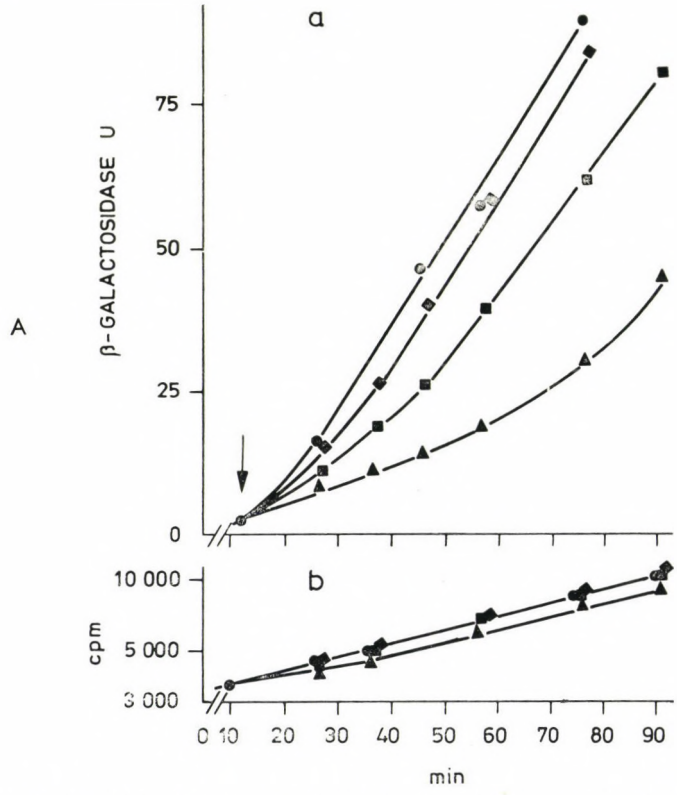

Fig. 1. Effect of quinacrine on the induced β-galactosidase synthesis (a) and (^{14}C)-L-phenylalanine incorporation (b) of *E. coli* K12 (A) and mutant CA 8001 (B). The arrow points to the time of addition of quinacrine. ●—● Control, ♦—♦ 6.25 μg/ml, ■—■ 12.5 μg/ml, ▲—▲ 25.0 μg/ml, □—□ 50.0 μg/ml, ○—○ 100.0 μg/ml quinacrine

concentrations. We consider the different general QAC sensitivities of the strains examined as a consequence of their different permeabilities.

Our results are summarized in Table 1, in which β-galactosidase production is given for different *E. coli* strains in per cent of the controls at the highest QAC concentration that does not affect the overall protein synthesis in that strain. (Data obtained with strain CA 8050 are not listed in Table 1, because in this case the experimental conditions were slightly different.)

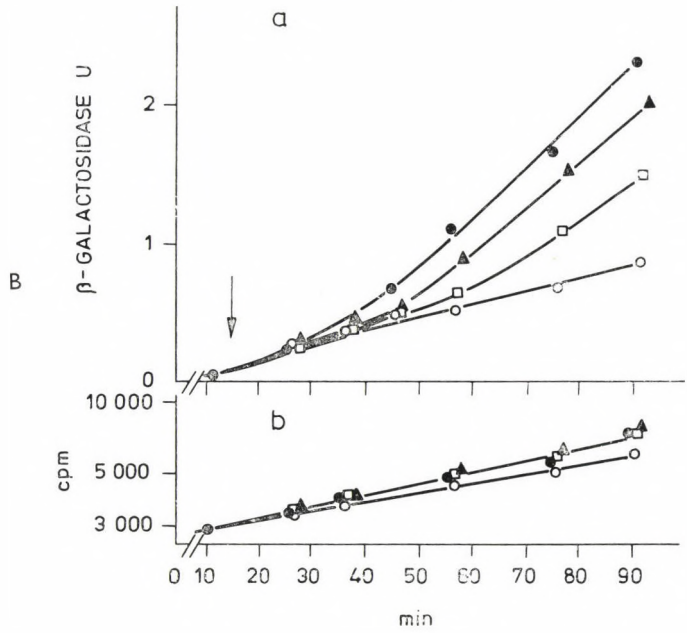

Fig. 1B

On the basis of their behaviour these strains can be divided into two groups: in *E. coli* K12 wild type, CA 8001 and CA 8003 cells the highest QAC concentration, which does not affect overall protein synthesis, significantly inhibits induced β-galactosidase synthesis. In CA 8050, CA 8019 and CA 8224 strains this effect cannot be detected. Looking at the scheme of the *lac* operon in Fig. 3, we can see that the promoter mutations in CA 8001 and CA 8003, which strains behave like K12 wild type, map in the first part, in the regulator proximal half (*Pr*), of the promoter region. In those strains where there is no specific inhibition of β-galactosidase synthesis, in CA 8050, CA 8019 and CA 8224 cells, the mutation is located in the second, operator-proximal part (*Po*), of the *P* gene. The *Pr* region of the promoter is generally considered as a binding site for CRP (also referred to as CAP) + cAMP complex and the *Po* part as a binding and starting point for RNA polymerase (Pastan, DeCrombrugghe, 1972).

Acridine dyes (e.g. proflavine) are known to inhibit transcription (Conde

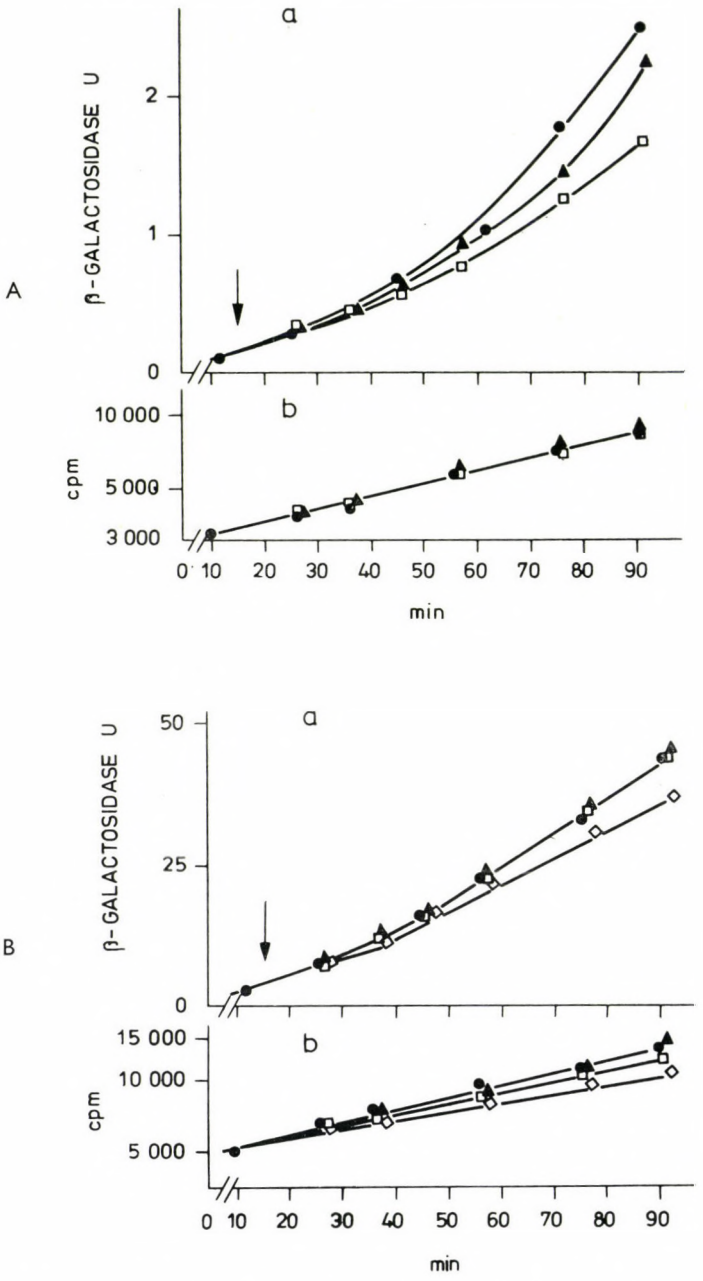

Fig. 2 Effect of quinacrine on the induced β-galactosidase synthesis (a) and (^{14}C)-L-phenylalanine incorporation (b) of *E. coli* mutants CA 8003 (A), CA 8019 (B) and CA 8224 (C). The arrow points to the time of addition of quinacrine. ●—● Control, ▲—▲ 25.0 μg/ml, ◊—◊ 37.5 μg/ml, □—□ 50.0 μg/ml, ○—○ 100.0 μg/ml quinacrine

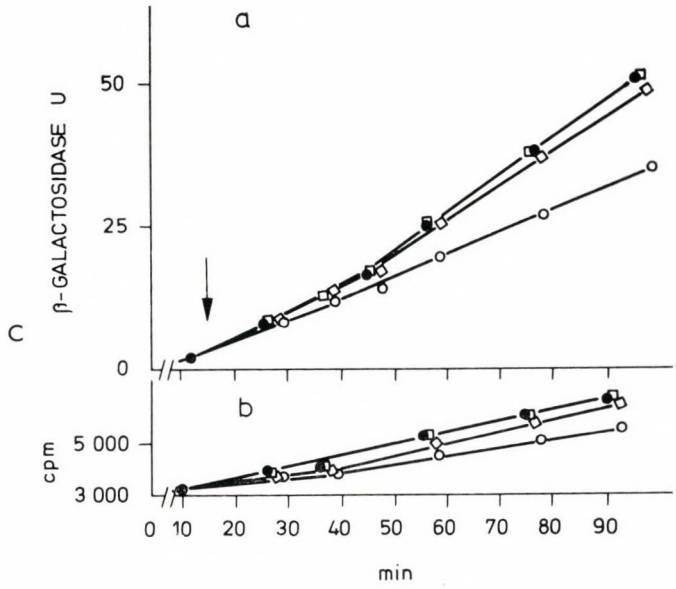

Fig. 2C

et al., 1971). Our interest has been turned to QAC by the publication of Weisblum and de Haseth (1972), who found investigating the mechanism of fluorescent chromosome staining technique, that QAC was specific for AT-rich regions of DNA. Similar results were published by Pachmann and Rigler (1972).

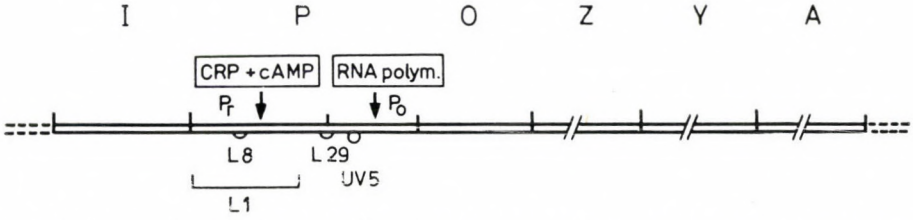

Fig. 3. Scheme of the *lac* operon, based on the results of Yudkin (1970), Pastan and De-Crombrugghe (1972), Arditti et al. (1973) and Sanders and McGeoch (1973)

RNA polymerase binds to specific DNA sequences, to the promoters. This enzyme is considered as a melting protein which, on the basis of thermodynamical calculations, should bind preferentially to dA-dT-rich regions. Regulator proteins are also regarded as factors of changing the melting temperature of DNA (von Hippel, McGhee, 1972). Transcription of the *lac* operon needs CRP + cAMP (Pastan, DeCrombrugghe, 1972).

The data in Table 1 show that mutations in the *Pr* region cause a marked decrease to 2–3% of the wild type level, in the rate of induced β-galactosidase synthesis in otherwise untreated cells. Mutations located in the *Po* part decrease

Table 1

Production of β-galactosidase in different E. coli strains

Strain[a]	Relevant genotype	Rate of induced β-galactosidase synthesis	
		at QAC concentration which did not affect overall protein synthesis, in per cent of the control[b]	in untreated cultures compared to K12 wild type cells[c]
K12	*lac* $I^+P^+O^+Z^+$	57 – 65	100.0
CA 8001	HfrH *lac*$^+P^-_{L1}$	53 – 70	1.9
CA 8003	HfrH *lac*$^+P^-_{L8}$	75 – 76	3.0
CA 8019	HfrH *lac*$^+P^-_{L29}$	95 – 100	49.4
CA 8224	HfrH *lac*$^+P^r_{UV5}$	98 – 105	47.6

[a] The promoter mutant strains were from Professor Jonathan R. Beckwith
[b] The lowest and highest values of three parallel experiments
[c] Averages of three experiments

the expression of the *lac* operon only to about the half of the wild type value. This indicates the importance of binding of the CRP + cAMP complex to its receptor site in determining the rate of transcription.

The results also show that the expression of the *lac* operon displays increased sensitivity to QAC only in wild type and in those promoter mutant strains where the mutation is located at the CRP + cAMP binding site (*Pr*). The enhanced sensitivity is abolished by mutations in the RNA polymerase binding region (*Po*). We can interpret these observations as a consequence of the AT-rich character of, or at least of the presence of AT-rich segment(s) in, the *Po* half of the *P* gene, where the increased affinity and intercalation of QAC to multiple AT base pairs can interfere with the binding (or movement) of the RNA polymerase. Mutations in this region may eliminate or change this sequence, resulting in the loss of increased QAC sensitivity, but also in a decreased rate of β-galactosidase synthesis, as compared to the wild type. An alternative yet very similar explanation of our results is also possible. The binding of CRP + cAMP complex must precede the binding of specific RNA polymerase. We may well suppose that this allosteric protein is able to lower the melting point of the DNA next to its binding site, increasing in this way the frequency of initiation of transcription on the *lac* DNA. This effect would be impaired by QAC, which distorts the secondary structure of DNA in the first part of the RNA polymerase binding site. As for the length of the RNA polymerase binding region there are only indirect evidences indicating 20 – 40 base pairs (Novak, 1969; Damjanovich, personal communication). This length is, however, short enough to permit that mutations located in the *Po* region of the *P* gene might affect the first nucleotides in the RNA polymerase binding site.

During the course of this work very similar results were published by Sankaran and Pogell (1973) with AO as inhibitory agent. Their findings are generally in good agreement with ours although AO is reported to bind equally to AT and GC base pairs (Weisblum, de Haseth, 1972). These authors extended their studies to other operons too, and concluded that intercalating dye sensitivity is a common property of catabolite-sensitive operons. They found cAMP to be effective against AO-specific inhibition. In our preliminary experiments we failed to detect any effect of cAMP upon QAC inhibition. This apparent contradiction may reside in the different characters of the dyes used.

Sankaran and Pogell (1973) came to the conclusion that "the promoter region of catabolite-sensitive operons is peculiarly sensitive to intercalating dyes, possibiy because of a difference in the DNA conformation in these regions resulting from derepression".

Considering our results and the former opinion – and slightly questioning the latter – as well as the main role of binding of the CRP + cAMP complex and its effect upon the expression of the *lac* operon, we regard our results to support the hypothesis that an AT-rich sequence exists in the promoter region, probably in the first part of the RNA polymerase recognition site. This sequence may promote the binding of the enzyme, and its secondary structure and melting ability are affected by binding of the CRP + cAMP complex to the preceding part of the *P* gene, triggering there by the transcription of the induced *lac* operon.

We are indebted to Drs J. R. Beckwith and M. D. Yudkin for bacterial strains, to Dr B. J. Bachmann for her kind assistance in obtaining some of these strains, to Dr J. Janeček for labelled L-phenylalanine, to Dr S. Damjanovich for his interest and for commenting on the manuscript, to Dr J. Csongor for the radioactivity measurement facilities and to Mrs I. Szekeres for skillful technical assistance.

References

Arditti, R., Grodzicker, T., Beckwith, J. (1973) J. Bact. *114* 652
Conde, F., Del Campo, F. F., Ramirez, J. M. (1971) FEBS Lett. *16* 156
von Hippel, P. H., McGhee, J. D. (1972) Ann. Rev. Biochem. *41* 231
Novak, R. L. (1969) Biochim. Biophys. Acta *195* 279
Pachmann, U., Rigler, R. (1972) Expl. Cell. Res. *72* 602
Pastan, I., De Crombrugghe, B. (1972) in Karolinska Symposia on Research Methods in Reproductive Endocrinology, 5th Symposium, Gene Transcription in Reproductive Tissue (ed. by E. Diczfalussy) 298 (Stockholm, Karolinska Institutet)
Sanders, R., McGeoch, D. (1973) Proc. Nat. Acad. Sci. US. *70* 1017
Sankaran, L., Pogell, B. M. (1973) Nature New Biol. *245* 257
Schlammadinger, J., Szabó, G. (1973) Acta Biochim. Biophys. Acad. Sci. Hung. *8* 253
Weisblum, B., de Haseth, P. L. (1972) Proc. Nat. Acad. Sci. US. *69* 629
Yudkin, M. D. (1970) Biochem. J. *118* 741

Acta Biochim. et Biophys. Acad. Sci. Hung. Vol. 9 (4), pp. 303–308 (1974)

Papain Susceptibility and Optical Rotatory Dispersion of Reassociated Autologous H and L Chains of Monotypic IgG2 and IgG4 Proteins

ÉVA RAJNAVÖLGYI, J. GERGELY

Department of Microbiology and Immunology of the Eötvös Loránd University and National Institute of Haematology and Blood Transfusion, Budapest, Hungary

(Received March 29, 1974)

The ORD and papain digestibility of papain-resistant IgG2 and IgG4 myeloma proteins and of their reassociated autologous alkylated or non-alkylated H and L chains were investigated. The Moffitt constants of the native proteins and of the reassociated chains were found to be near zero. The papain digestibilities of reassociated non-alkylated chains and alkylated chains proved to be different. Susceptibility to papain is therefore a sensitive indicator of conformation changes of IgG molecules even if the ORD values do not show any differences.

A number of studies have demonstrated that isolated alkylated chains of IgG molecules associate through non-covalent interactions to form molecules which resemble native IgG. The full recovery of native conformation is, however, questionable.

There are several ways of studying the eventual similarity of recombined chains and native molecules. One can check the restoration of antibody activity, by comparing the antigenic properties of native and reconstituted molecules. The ORD or circular dichroism characterizes the conformation of the proteins (Franek, Nezlin, 1963; Fougereau, Edelman, 1964; Fougereau et al., 1964; Gally, Edelman, 1964; Metzger, Mannik, 1964; Olins, Edelman, 1964; Grey, Mannik, 1965; Gordon, Cohen, 1966; Dorrington et al., 1967; Roholt et al., 1967; Mannik, 1967; Edelman et al., 1967; Björk, Tanford, 1971).

In our previous studies new procedures were applied in the recombination of polypeptide chains and in testing the result of recombination. Beside the recombination of isolated alkylated chains, by reassociation of non-alkylated chains the importance of the restoration of interchain disulphide bonds in the recovery of native conformation could also be examined. Previous investigations proved that the different papain-susceptibility of IgG myeloma proteins reflect the conformation differences of the molecules. The papain-susceptibility of molecules recombined from polypepty chains was therefore studied (Gergely et al., 1967a, b, 1969a, b; Pákh et al., 1971).

In the present work the papain susceptibility and the ORD of IgG molecules obtained by the reassociation of autologous alkylated or non-alkylated H and L chains were compared.

Materials and methods

IgG myeloma proteins

Papain-resistant IgG2 and IgG4 were prepared from sera of myeloma patients by the "DEAE-Sephadex" batch technique (Baumstark et al., 1964).

Isolation of H and L chains

The immunochemically pure IgG preparations were reduced with 0.2 M mercaptoethanol and alkylated with a 50 per cent molar excess of iodoacetamide. The separation of H and L chains was performed on Sephadex G-100 columns with 1 M acetic acid as eluent (Björk, Tanford, 1971).

The preparation, separation and storage of non-alkylated chains were performed in the presence of 0.01 M dithiothreitol (Gergely et al., 1969a, b; Pákh et al., 1971).

Reassociation of chains

Chain association proceeded ove 48 hours by dialysis agains several changes of 0.01 M sodium acetate buffer, pH 5.5. After concentration the recombined product was dialysed against 0.02 M sodium acetate buffer, pH 5.5, containing 0.1 M sodium chloride. The associated molecules were purified by gel filtration on Sephadex G-200 columns (Björk, Tanford, 1971).

Papain-susceptibility

The papain-susceptibility of native IgG and that of the reassociated chains were tested by digestion with twice-crystallized soluble papain (Sigma) enzyme : substrate ratio 1 : 100 at pH 7, for 4 hours at 37°C in the absence of cysteine. Digestion was monitored by gel-filtration of the digests on Sephadex G-100 column and by immunoelectrophoresis (Gergely et al., 1967a, b; Pákh et al., 1971).

ORD studies

ORD was measured with a polarimeter type "Polarmatic 62". Protein was dissolved in saline, 0.1 M sodium chloride to 3–5 mg/ml concentration. From the optical rotation values measured between 600 and 300 the Moffitt equation was calculated:

$$m'(\lambda^2 - \lambda_0^2) = a_0\lambda^2 + \frac{b_0\lambda_0^4}{\lambda^2 - \lambda_0^2}$$

where m' is the reduced mean residue rotation, which depends on the specific rotation at wavelength λ, on the mean residue weight (MRW = 108) (Dorrington et al., 1967), and on the refractive index of the solvent at wavelength λ; $\lambda_0 = 212$ nm. From the plot $m'(\lambda^2 - \lambda_0^2)$ versus $(\lambda^2 - \lambda_0^2)^{-1}$ the values of b_0 and a_0 can be calculated from the slope and intercept, respectively (Fasman, 1963).

Results

Papain susceptibility of the reassociated chains

The papain susceptibilities of molecules obtained by reassociation of autologous alkylated and autologous non-alkylated H and L chains were compared. Figs 1 and 2 show the result of a typical experiment. The molecules obtained by

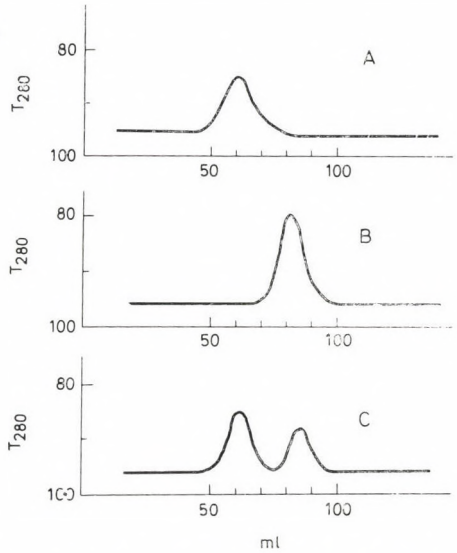

Fig. 1. Gel-filtration of papain digest of the reassociated autologous chains of IgG2 myeloma protein "Wih". The reassociated chains were digested with papain (1 : 100) at pH 7, for 4 hours at 37°C. Gel-filtration was performed on a Sephadex G-100 column (2×55.5 cm), flow rate 5 ml/h, fraction volume 2.5 ml, equilibration and elution with 75 mM phosphate buffer, pH 7.0, containing 75 mM NaCl. *A* undigested protein; *B* reassociated alkylated chains. The reassociated material was completely digested with papain in the absence of cysteine to yield Fab and Fc fragments; *C* reassociated non-alkylated chains. The majority of the reassociated material remained undigested with papain in the absence of cysteine

reassociation of the alkylated chains were completely digestible by papain in the absence of cysteine (Fig. 1*B* and Fig. 2*B*). The majority of reassociated molecules containing non-alkylated chains, like the native IgG2 or IgG4 proteins, were papain-resistant, i.e. undigestible with papain in the absence of cysteine (Fig. 2*A*). This means that the reassociation through non-covalent binding is not sufficient for the recovery of papain-resistant character of the IgG2 and IgG4 proteins.

ORD of the reassociated chains

Fig. 3 shows the linear form of the Moffitt equation calculated from the optical rotation values measured between 600 and 300 nm of a native IgG2 protein, and those of the reassociated alkylated and non-alkylated H and L

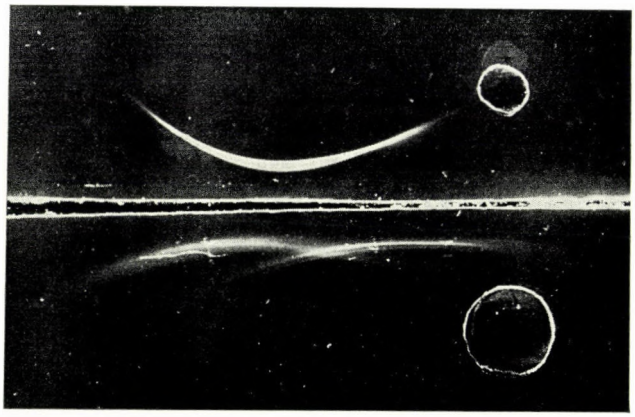

Fig. 2. Immunoelectrophoretic patterns of the papain-digested reassociated autologous chains of IgG2 myeloma protein "Wih". Immune serum: anti-human IgG rabbit serum. *A* reassociated non-alkylated chains (see Figure 1 *C* first fraction); *B* reassociated alkylated chains (see Figure 1 *B*)

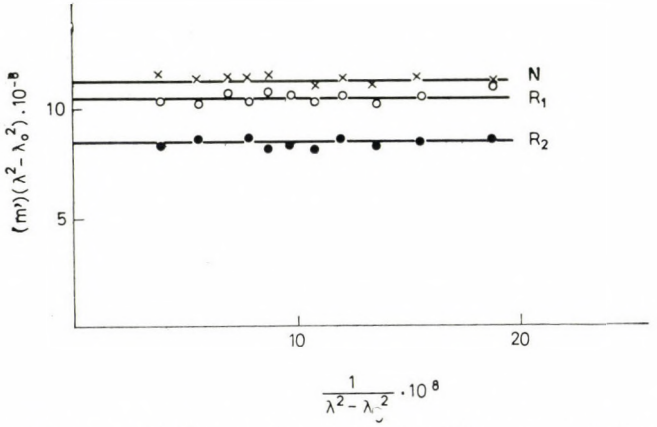

Fig. 3. The linear form of Moffitt equation as calculated from the optical rotation values measured between 600 and 300 nm. *N* native IgG2 myeloma protein "Wih"; R_1 reassociated alkylated chains of IgG2 myeloma protein "Wih"; R_2 reassociated non-alkylated chains of IgG2 myeloma protein "Wih"

chains. The b_0 Moffitt constants that characterize the conformation of proteins were near zero.

Discussion

In recombination experiments on multi-subunit proteins containing S–S bond generally alkylated polypeptide chains are used, which makes it possible to study the role of non-covalent interactions in the association of chains. In pre-

vious experiments (Gergely et al., 1969a; Pákh et al., 1971) beside the recombination of isolated alkylated chains, the reassociation of non-alkylated H and L chains resulted in the restoration of interchain disulphide bonds. Due to the restoration of disulphide bridges between H and L chains the reconstituted molecules eluted from Sephadex G-100 columns in 1 M acetic acid as one symmetrical peak, at the same position as does native IgG (Pákh et al., 1971). Comparative proteolytic studies are very useful in detecting structural differences of protein molecules (Szabolcsi et al., 1959; Szabolcsi, Biszku, 1961). In our previous investigations (Gergely et al., 1967a, b) evidence was presented for the existence of two conformational forms of human IgG, which differ in their papain susceptibilities. Papain-resitance is a very characteristic feature of IgG molecules belonging to the IgG2 and IgG4 sub-classes. Our experiments also proved the importance of inter H–L chain disulphide bonds in developing of conformation characteristic of the papain-resistant subclasses. The reassociation of alkylated H and L chains, obtained from papain resistant IgG2 and IgG4, resulted in papain-sensitive molecules. Reassociated molecules, however, containing non-alkylated chains of the same IgG2 or IgG4 molecules were resistant to papain attack (Pákh et al., 1971). From these data we conclude that the papain-digestibility of reassociated H and L chains prepared from monotypic IgG molecules indicates the degree of recovery of molecular conformation characteristic of papain-resistant IgG2 and IgG4 subclasses.

Björk and Tanford (1971) did not find any differences between native IgG molecules and their reassociated alkylated H and L chains in the antigenic properties, sedimentation constants, circular dichroism and ORD values. Therefore it seemed reasonable to compare the ORD values and papain digestibility of human IgG molecules obtained by the reassociation of autologous alkylated or non-alkylated H and L chains. The Moffitt constants of native IgG2 and IgG4 proteins and those of the reassociated alkylated and non-alkylated chains were found in the present investigations to be near zero. This means that the overall conformation of native IgG2 and IgG4 proteins and that of the reassociated chains do not differ from each other significantly. However, the papain digestibilities of reassociated alkylated chains and of reassociated non-alkylated chains proved to be different when compared with each other and with native IgG molecules. This is in good agreement with our earlier findings and underlines the importance of interchain disulphide bonds in adjusting the conformation responsible for the papain-resistant character of human IgG molecules. The study of papain susceptibility therefore seems to be a very sensitive approach in conformational studies of IgG molecules, even is such cases when the ORD values do not show any differences.

The authors thank Prof. P. Elődi for helpful discussions.

References

Baumstark, J. S., Laffin, R. J., Bardawil, W. A. (1964) Arch. Biochem. Biophys. *108* 514
Björk, I., Tanford, C. (1971) Biochemistry *10* 1289
Dorrington, K. J., Zarlengo, M. H., Tanford, C. (1967) Proc. Nat. Acad. Sci. *51* 996
Edelman, G. M., Olins, D. E., Gally, J. A., Zinder, N. D. (1967) Proc. Nat. Acad. Sci. *50* 753
Fasman, G. D. (1963) Methods in Enzymology *6* 928
Fougereau, M., Edelman, G. M. (1964) Biochemistry *3* 1120
Fougereau, M., Olins, D. E., Edelman, G. M. (1964) J. Exp. Med. *120* 349
Franek, F., Nezlin, R. S. (1963) Biokhimiya *28* 193
Gally, J. A., Edelman, G. M. (1964) *119* 817
Gergely. J., Stanworth, D. R., Jefferis, D., Normansell, E. R., Henney, C. S., Pardoe, G. I. (1967a) Immunochemistry *4* 101
Gergely, J., Medgyesi, G. A., Stanworth, D. R. (1967b) Immunochemistry *4* 369
Gergely, J., Pákh, M. Medgyesi, G. A., Puskás, É. (1969a) Immunochemistry *6* 768
Gergely, J., Medgyesi, Gy., Pákh, M., Puskás, É. (1969b) Orvostudomány *20* 207
Grey, H. M., Mannik, M. (1965) J. exp. Med. *122* 619
Gordon, S., Cohen, S. (1966) Immunology *10* 549
Jirgenson, B. (1965) J. Biol. Chem. *240* 1064
Jirgenson, B. (1966) J. Biol. Chem. *241* 10
Metzger, H., Mannik, M. (1964) J. exp. Med. *120* 765
Mannik, M. (1967) Biochemistry *6* 134
Pákh, M., Boross, L., Medgyesi, G. A., Gergely, J. (1971) Acta Biochim. Biophys. Acad. Sci. Hung. *6* 259
Olins, D. E., Edelman, G. M. (1964) J. exp. Med. *119* 709
Roholt, G. A., Radzimski, G., Pressman, D. (1967) J. exp. Med. *125* 191
Szabolcsi, G., Biszku, E., Szörényi, E. (1959) Biochim. Biophys. Acta *35* 237
Szabolcsi, G., Biszku, E. (1961) Biochim. Biophys. Acta *48* 335

Acta Biochim. et Biophys. Acad. Sci. Hung. Vol. 9 (4), pp. 309—317 (1974)

Studies on the Multiplicity of Polypeptide Hormones

I. Isolation of Human Pituitary Growth Hormone and Characterization of the Aggregates

L. GRÁF, B. SZALONTAI,* ERZSÉBET BARÁT, P. ZÁVODSZKY,*
J. BORVENDÉG, ILONA HERMANN, G. CSEH

Research Institute for Pharmaceutical Chemistry and * Enzymology Department, Institute of Biochemistry, Hungarian Academy of Sciences, Budapest, Hungary

(Received March 27, 1974)

Growth hormone was prepared from acetone-collected human pituitary glands by a simple new procedure. This preparation was resolved into three fractions by gel chromatography. The lowest molecular weight fraction was monomeric human growth hormone. The other two fractions contained different aggregated, biologically inactive forms of the hormone. Ultracentrifugal studies showed that these aggregates underwent dissociation in the precense of sodium dodecyl sulphate. The degree of dissociation was pH dependent.

Introduction

It has been known for some time that HGH preparations (Raben, 1957; Li et al., 1962; Reisfeld et al., 1962; Roos et al., 1963; Fonss-Bech, Schmidt, 1969) contain several protein components. The nature of this heterogeneity has been studied in several laboratories (Ferguson, Wallace, 1961; Lewis, 1962; Hanson et al., 1966; Cheever, Lewis, 1969; Rohde, Dörner, 1969; Schleyer et al., 1970). From these investigations it has become apparent that the heterogeneity of the preparations is mainly due to the multiplicity of different HGH components rather than to the presence of protein impurities.

Evidences have been presented that some multiple forms of HGH ensued as a result of aggregation (Li et al., 1964; Hanson et al., 1966), enzymic cleavage (Lewis, 1962; Lewis et al., 1971), and deamidation (Cheever, Lewis, 1969) of the native hormone during the course of isolation. Consequently, it may depend on the isolation method, which type of secondary changes occur predominantly during the preparation.

We describe below a new isolation method for human growth hormone, which yielded similar amounts of biologically active hormone from pituitary gland as other procedures of the literature. In addition to the active component, however, this preparation also contained an appreciable amount of biologically inactive aggregated growth hormone. The chemical and physico-chemical characterization of these aggregates is also presented in this paper.

Abbreviations: HGH, human pituitary growth hormone; SDS, sodium dodecyl sulphate.

Materials and methods

Preparation procedure of HGH. Human pituitary glands were collected in acetone. The extraction was carried out at 0°C in 65–70% acetone containing 0.35 M HCl. Acetone was added to the extract up to a concentration of 90% and the precipitate was recovered by centrifugation, redissolved in water at about pH 3. Isoelectric precipitation was carried out by adjusting the pH to 5 with 1 M NaOH. The precipitate was separated by centrifugation, redissolved and lyophilized. The method yielded 3–4 g crude hormone per 1000 glands (Gráf et al., 1974). This fraction designated as fraction P was our starting material for further studies.

Fraction P was gel-chromatographed on Sephadex G-75. The biological activity of the fractions was determined by the rat tibia assay (Greenspan et al., 1949). The following homogeneity tests were applied: gel electrophoresis (Davis, 1964), sedimentation analysis in a MOM 3170 analytical ultracentrifuge and N-terminal amino acid analysis (Gray, 1967).

Amino acid analysis was carried out in a JEOL (JLC-5AH) amino acid analyzer. Samples were hydrolyzed in 6 M HCl for 48 hours at 110°C in sealed, evacuated tubes. Half cystine content was determined as cysteic acid from performic acid oxidized samples. *Reduction and alkylation* was carried out as follows: the protein at 4 mg/ml concentration was reduced with a 10-fold molar excess of dithiothreitol over cystine content in 0.1 M tris buffer, pH 8.3, containing 8 M urea, in nitrogen atmosphere for 40 minutes. Then ^{14}C-bromoacetic acid (5.73 mCi/mmol) was added to the solution in 10-fold molar excess to the reducing agent and the mixture was incubated for 10 minutes. The excess of reagent was removed by gel-chromatography on Sephadex G-25 (medium) in 0.05 M NH_4HCO_3, pH 8.3. The protein-containing fractions were pooled and lyophilized.

The reduced and carboxymethylated derivatives of HGH were *digested with trypsin* (Calbiochem, B grade) in 0.05 M ammonium acetate buffer, pH 7.5, with an enzyme to protein ratio of 1 : 50 (w/w) at 37°C for 2 hours. Two mg samples of the hydrolysates were mapped by two-dimensional high voltage paper electrophoresis: first at pH 5.0 (pyridine – acetic acid – water, 10 : 10 : 1000 by volume) and subsequently at pH 2.0 (formic acid – acetic acid – water, 50 : 150 : 800 by volume). Radioautographs were obtained from the peptide maps on Forte X-ray film with an exposition of 60 hours.

Dissociation studies on HGH aggregates were performed by ultracentrifugal molecular weight determinations according to Yphantis (1964) in the presence of guanidine-HCl (Fluka) and SDS (Du Pont Nemours, twice recrystallized from ethanol). In the latter case the fractions were dissolved in 0.01 M phosphate buffer, pH 5.5–8.8, containing 1 mg/ml SDS. No effect of protein concentration on the apparent molecular weight was observed when the protein concentrations varied between 0.2–0.5 mg/ml. The above SDS and protein concentrations correspond to those used by Reynolds and Tanford (1970b).

To determine the binding ratio of SDS to HGH, the same solutions were

centrifuged in a swinging bucket rotor for 20 hours at 132,000 g. The SDS content of the supernatant was determined by titrating its tenfold diluted aliquots with 0.04% methylene blue solution. The SDS-methylene blue complex was shaken out into chloroform until the water phase remained blue indicating the absence of SDS. The difference in the amount of SDS before and after centrifugation was due to the formation of protein-SDS complex, which was pelleted during centrifugation. The binding ratio between SDS and HGH was 1.0 ± 0.1 g SDS/g HGH without any significant changes between pH 5.5 and 8.8. Both the absolute value and pH-independence of the binding ratio are in fair agreement with the data of literature (Pitt-Rivers, Impiombato, 1968; Reynolds, Tanford, 1970a, 1970b; Nelson, 1971).

In order to determine the weight average molecular weight of the HGH–SDS complexes, three parallel high speed equilibrium experiments were performed at each pH value and the average of the individual values was considered. For the calculation of molecular weight, the partial specific volume of native HGH was taken to be $\bar{v} = 0.731$ (Li, Liu, 1964). Since there is probably some difference between the partial specific volume of native HGH and the HGH–SDS complex, the molecular weights obtained for the complexes may differ to some extent from the real values. However, this uncertainty does not influence the molecular weight ratios.

Results and discussion

Isolation and biological, chemical and physico-chemical comparison of the HGH fractions

Fraction P of HGH (see Materials and methods) was resolved into three fractions by gel chromatography on Sephadex G-75 (Fig. 1).* Their electrophoretic patterns show that FI and FIII do not contain identical electrophoretic components (Fig. 2). Biological data on these two fractions are presented in Table 1. Whereas FIII has a high growth-promoting activity, FI proved to be practically inactive by the tibia test. The N-terminal amino acid of all fractions (FI, FII, FIII) were found to be phenylalanine and the amino acid analysis did not reveal any significant difference between their amino acid compositions (Table 2)**. In addition, the tryptic peptide maps of reduced and carboxymethylated FI and FIII appeared to be identical. The autoradiograms of these maps are shown in Figs 3a and 3b. The four radioactive spots in both maps correspond to the four cysteine-containing tryptic peptides of HGH (Li et al., 1969; Li, 1972), as it was also shown by us previously (Gráf et al., 1971).

The results of molecular weight determinations are summarized in Table 3. FIII appeared to be a monodisperse fraction. The estimated molecular weight

* Only 70–80% of fraction P could be dissolved, the precipitate was discarded.

** Further studies are in progress to explain the observation that the values for proline, glycine and alanine are higher and that for phenylalanine is lower than expected from the sequence of HGH (Li, 1972).

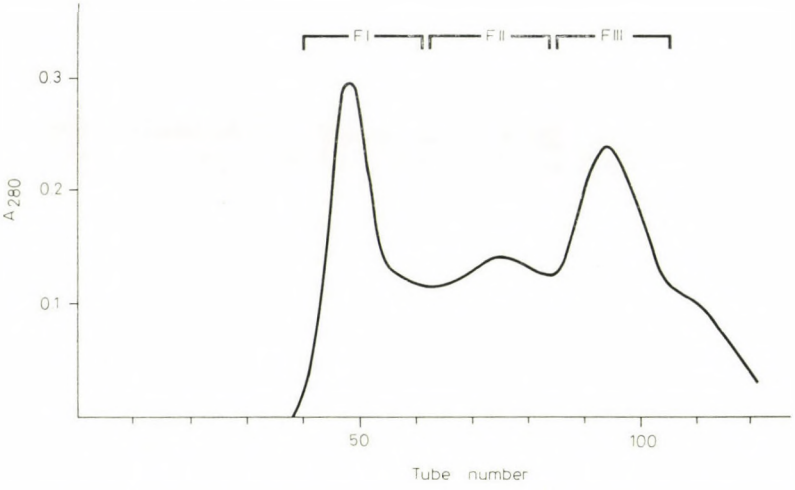

Fig. 1. Gel chromatography of fraction P on Sephadex G-75 column (110×4 cm) in 0.1 M borate buffer, pH 8.5. Flow rate 60 ml/hour, fraction volume 10 ml. The indicated fractions were lyophilized after dialysis against distilled water. Starting material was 500 mg. The yields of FI, FII and FIII were 102 mg, 85 mg and 120 mg, respectively

Table 1

Biological potency of HGH fractions as measured by the rat tibia test

Material	Total dose (μg)	Tibia width (μ)
Saline	0	151 ± 4[a] (25)[b]
FI	50	157 ± 4 (6)
FI	200	176 ± 5 (8)
FIII	50	231 ± 5 (8)
FIII	100	248 ± 6 (6)
FIII	200	275 ± 4 (5)

[a] Means ± standard error of the mean
[b] Number of animals

concurs with those obtained for monomeric HGH from sedimentation equilibrium (Li, Starman, 1964) and sequence data (Li et al., 1969; Li, 1972). The presence of two electrophoretic components in FIII (Fig. 2) is probably due to the partial deamidation of HGH (Cheever, Lewis, 1969). Various HGH preparations (Cheever, Lewis, 1969; Li, Gráf, 1974) show electrophoretic patterns very similar to that of FIII.

The biological test and the chemical and physico-chemical analyses clearly indicate that FIII is identical with monomeric HGH, and FI and FII are composed of aggregated forms of HGH. The same components appear to be present in the

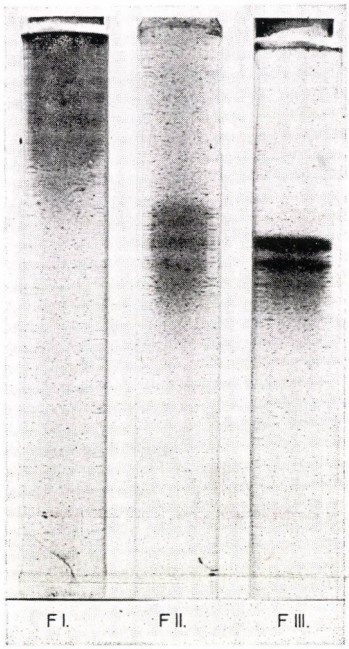

Fig. 2. Gel electrophoresis of FI (200 μg), FII (100 μg) and FIII (100 μg) at pH 9 in 8% polyacrylamide gel. Potential gradient: 30 V/cm, running time: 80 minutes

Table 2

Amino acid composition[a] of HGH fractions

Amino acid	Theoretical[b]	FI	FII	FIII
Lys	9	8.8	9.0	9.1
His	3	2.9	2.9	2.8
Arg	11	10.5	10.3	10.2
1/2 Cys[c]	4	3.9	3.8	3.8
Asp	20	20 0	20.0	20.0
Thr	10	9.8	9.9	10.0
Ser	18	16.7	17.2	17.5
Glu	27	28.5	28.6	28.5
Pro	8	9.4	9.5	9.4
Gly	8	11.2	10.5	10.5
Ala	7	9 4	9.4	9.2
Val	7	7.4	7.3	7.3
Met	3	2 7	2.5	2.4
Ile	8	7.5	7.6	7.6
Leu	26	24.8	24.5	24.7
Tyr	8	6 6	6.7	6.7
Phe	13	10 8	10.7	10.9

[a] Molar ratios based upon 20.0 residues of aspartic acid
[b] Calculated from the sequence proposed by Li (1972)
[c] Determined as cysteic acid

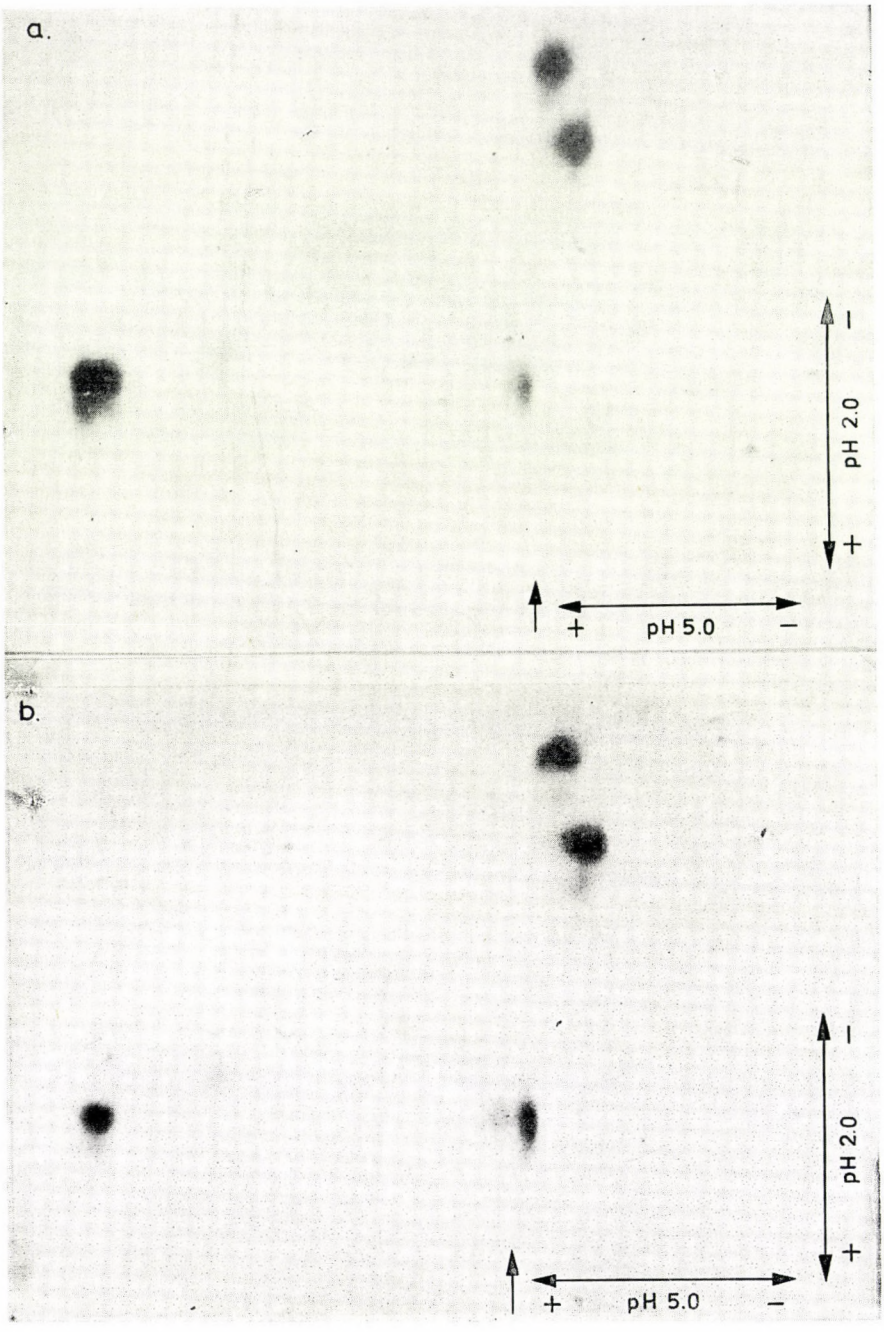

Fig. 3. Radioautographs of the tryptic peptide maps of reduced, carboxymethylated FI (a) and FIII (b). The electrophoresis was made first at pH 5.0 (60 V/cm, 80 min), then at pH 2.0 (50 V/cm, 80 min)

Table 3

Molecular weight of HGH fractions as determined by the high speed sedimentation equilibrium method
(in 0.01 M Na-phosphate buffer, pH 7.5)

	FI*	FII	FIII
Molecular weights	163 000 61 000	47 000 25 000	24 000

* The lowest and highest molecular weights are indicated (see Fig. 4)

electrophoretic pattern of FII as in FIII (Fig. 2). The occurrence of monomeric HGH together with dimeric HGH in FII was indeed demonstrated by sedimentation analysis (Table 3). The gel electrophoretic pattern of FI shows that it is a polydisperse fraction containing several higher molecular weight components (Fig. 2). This is also supported by sedimentation equilibrium experiments. A typical ultracentrifugal analysis of FI is shown in Fig. 4. The shape of the

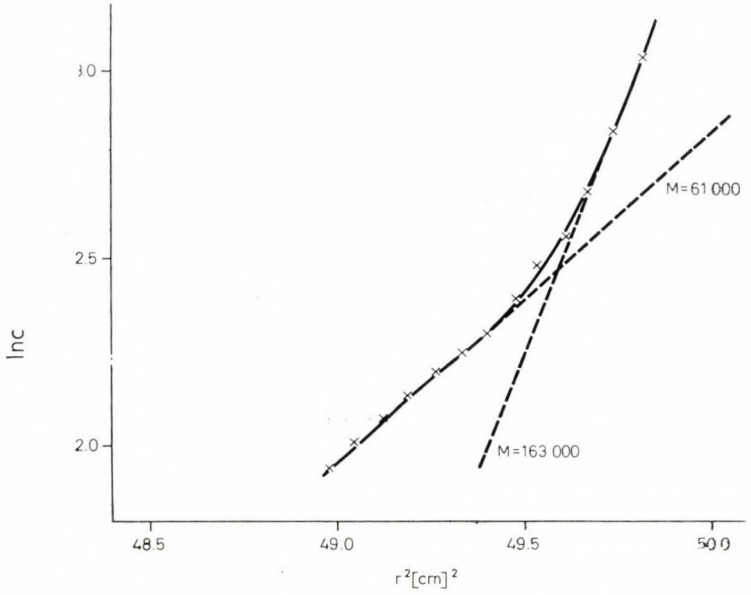

Fig. 4. Determination of the molecular weight of FI by high speed sedimentation equilibrium method.

$$M = \frac{2RT}{(1 - \bar{V}\rho)\omega^2} \cdot \frac{d \ln c}{dr^2},$$

where c is the concentration of protein, r is the distance from the axis of rotation, $\bar{V}$ is the partial specific volume of the protein, ρ is the density of the solution, ω is the angular velocity, R is the universal gas constant, T is the temperature in °K

ln c *vs* r^2 plot clearly indicates that FI consists of a series of aggregated HGH components; the lowest and highest molecular weights for these aggregates were estimated to be 61 000 and 163 000, respectively (Fig. 4 and Table 3). The molecular weight of an HGH aggregate prepared by Li et al. (1964) was also found to be between 50 000 and 150 000.

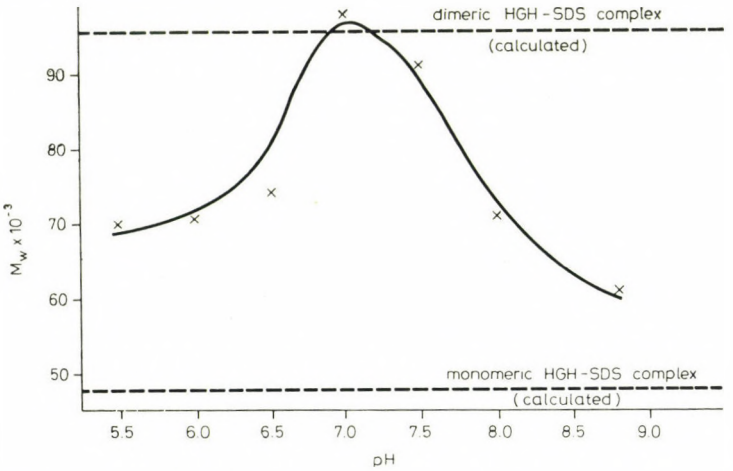

Fig. 5. pH dependence of the weight-average molecular weights of HGH–SDS complexes formed from FI

The dissociation of HGH aggregates

No significant effect of 5 M and 8 M guanidine-HCl was observed on the molecular weight of FI as examined by ultracentrifugation. At the same time SDS dissociated the aggregates of FI. The weight-average molecular weights of FI in the presence of 1 mg/ml SDS at different pH values are shown in Fig. 5, as determined by the high speed sedimentation equilibrium method. These values correspond to the molecular weight of HGH–SDS complexes. Since the pH was found not to affect the binding ratio of SDS to HGH, this pH-dependent variation of the apparent molecular weights may indicate a difference in the degree of aggregation of the HGH molecules. The dotted lines in Fig. 5 show the calculated molecular weight of monomeric HGH–SDS and dimeric HGH–SDS complexes (for binding ratios see Materials and methods). It can be seen that at acidic and alkaline pH predominantly monomeric HGH–SDS complexes are present, while around neutral pH the apparent molecular weight suggests the presence of oligomeric HGH–SDS complexes. These results suggest that beside strong hydrophobic interactions, ionic forces are also involved in holding the HGH molecules together in the aggregates.

Paladini et al. (1970) showed that human growth hormone had a higher sensitivity to unfolding than growth hormones of other species. Such a conformational change in the HGH molecule, in response to different physical and

chemical effects during isolation, may initiate the aggregation of the HGH molecules. However, the question can also be raised to what extent depend the mechanism of such an aggregation and the stability of aggregates formed on the nature of the aggregating effect.

The authors thank Dr Magda Solti for her valuable help in the determination of SDS-hormone binding ratio, Dr A. Patthy for the amino acid analysis and Dr E. Góth for supplying human pituitary glands.

References

Cheever, E. V., Lewis, U. J. (1969) Endocrinology *85* 465
Davis, B. J. (1964) Ann. N. Y. Acad. Sci. *121* 404
Ferguson, K. A., Wallace, A. L. (1961) Nature (London) *190* 632
Fonss-Bech, P., Schmidt, K. D. (1969) Int. J. Prot. Res. *1* 85
Gráf, L., Barát Erzsébet, Borvendég, J., Patthy, A., Cseh, G. (1971) Excerpta Medica Abstr. No. 236 23
Gráf, L., Cseh, G., Borvendég, J., Barát Erzsébet, Székely, J., Kurcz, M. (1974) Hungarian Patent 2251/G0-1194/4.
Gray, W. R. (1967) Methods in Enzymology *11* 469
Greenspan, F. S., Li, C. H., Simpson, M. E., Evans, H. M. (1949) Endocrinology *45* 455
Hanson, L. A., Roos, P., Rymo, L. (1966) Nature *212* 948
Lewis, U. J. (1962) J. Biol. Chem. *237* 3141
Lewis, U. J., Singh, R. N. P., Seavey, B. K. (1971) Biochem. Biophys. Res. Commun. *44* 1169
Li, C. H. (1972) Proc. Am. Phil. Soc. *116* 365
Li, C. H., Gráf, L. (1974) Proc. Nat. Acad. Sci. U. S. *71* 1197
Li, C. H., Liu, W. K. (1964) Experientia *20* 169
Li, C. H., Starman, B. (1964) Biochim. Biophys. Acta *86* 175
Li, C. H., Liu, W. K., Dixon, J. S. (1962) Arch. Biochem. Biophys. Suppl. *1* 327
Li, C. H., Tanaka, A., Pickering, B. T. (1964) Acta Endocr. (Kbh.) Suppl. *90* 155
Li, C. H., Dixon, J. S., Liu, W. K. (1969) Arch. Biochem. Biophys. *133* 70
Nelson, C. A. (1971) J. Biol. Chem. *246* 3895
Paladini, A. C., Dellacha, J. M., Santome, J. A. (1970) Miami Winter Symposia *1* 270 North-Holland Publishing Company, Amsterdam
Pitt-Rivers, R., Impiombato, F. S. A. (1968) Biochem. J. *109* 825
Raben, M. S. (1957) Science *125* 883
Reisfeld, R. A., Lewis, U. J., Brink, N. G., Steelman, S. L. (1962) Endocrinology *71* 559
Reynolds, A., Tanford, C. (1970a) Proc. Nat. Acad. Sci. U. S. *66* 1002
Reynolds, A., Tanford, C. (1970b) J. Biol. Chem. *245* 5161
Rohde, W., Dörner, G. (1969) Acta Endocr. (Kbh.) *60* 101
Roos, P., Fevold, H. R., Gemzell, C. A. (1963) Biochim. Biophys. Acta *74* 525
Schleyer, M., Schröder, K. E., Hinz, A. (1970) Horm. Metab. Res. *2* 174
Yphantis, D. A. (1964) Biochemistry *3* 297

Acta Biochim. et Biophys. Acad. Sci. Hung. Vol. 9 (4), pp. 319–326 (1974)

A Brain-Specific Water-Soluble Antigen in Homogenates of Cat Cerebral Cortex

A. Orosz, A. Falus, Emilia Madarász, J. Gergely, G. Ádám

Department of Comparative Physiology, Eötvös Loránd University and Department of Immunochemistry, National Institute of Haematology and Blood Transfusion, Budapest, Hungary

(Received March 15, 1974)

Rabbits were immunized with the phospholipid-free supernatant of an aqueous homogenate of cat cerebral cortex. From the antiserum obtained, the antibodies produced against the cat serum proteins and the common antigens of other organs, were eliminated. The IgG fraction was isolated from the completely absorbed antiserum. The antibodies prepared gave immunoprecipitation with a water-soluble antigen having electrophoretic mobility similar to the $\beta_1 - \beta_2$ globulins found in human serum. Further purification of the antigen was carried out by means of anion-exchange chromatography and analytical polyacrylamide gel-electrophoresis.

Introduction

Numerous papers have recently been published concerning the application of immunological techniques to the problems of neurobiology. This interdisciplinary approach provides novel possibilities for investigating chemical constituents of highly heterogeneous CNS* structures (Levine, 1967). The advantages of specificity inherent in immuno-identification could facilitate the assigning of functional roles to molecular components of nervous systems.

Clinical studies have suggested that a state of psychosis may be induced by antibodies to CNS proteins (Heath, Krupp, 1967). Specific antibodies against nervous tissue antigens have been identified in the sera of patients suffering from multiple sclerosis (Bornstein, 1969) and myasthenia gravis (Kornguth et al., 1970). Provocation of experimental encephalitis in animals results in the appearance of CNS antibodies in the sera of these animals (Paterson, 1968). Thus an exhaustive study of the antigenic determinants specific for brain tissue may lead to a better understanding of the autoimmune disorders which affect the CNS. Several authors have investigated the antibodies produced against particulate fractions of the brain under in vitro conditions and have studied the water-soluble antigens of the nervous system of different species (Kosinski, Grabar, 1967, Liakopoulou, MacPherson, 1970; Moore, McGregor, 1965; Orosz et al., 1971, 1973, 1974; Warecka et al., 1972). The possibility provided by the simultaneous application of microelectrophysiological and immunological methods was

* *Abbreviations:* CNS, central nervous system.

demonstrated by the experiments performed on different invertebrates analysed the in vivo effect of binding of antibodies (Huneeus-Cox, Fernandez, 1967; Wald et al., 1968).

In the experiments presented here we used an aqueous homogenate of cerebral cortex of cats as the source of antigen. The nuclei, major myelin components and cell debris were eliminated and rabbits were immunized with the fraction obtained. After different absorption procedures the IgG fraction was isolated from the immuno-serum. The antigenic activity of the water-soluble fraction of homogenates of the brain tissue was examined by haemagglutination, immunodiffusion and immunoelectrophoretic methods.

Materials and methods

Brains of anesthetized cats were extensively perfused with cold physiological saline solution. After the perfusion the grey matter of the forebrain of the cats was separated as quickly as possible. From one animal we obtained about 4.0–4.5 g of grey matter. The antigen was isolated according to the procedures of Jankovic et al. (1968). The brain cortical tissue was homogenized in two volumes of physiological saline solution MSE Blendor-homogenizer; 5 min, 1000 rpm. From the supernatant resulting from centrifugation of $2000 \times g$ (Janetzki K 60) the proteins were precipitated by adding two volumes of ethanol (96%) at $-20°C$. After suspending the pellet in distilled water the suspension was freeze-dried. The phospholipids were extracted with cold ethanol : ether (2 : 1) mixture (Schneider, 1945) and the phospholipid-free fraction was dehydrated. All preparative procedures were carried out at 4°C. Similar preparations were obtained from the aqueous extract of cat liver and kidney.

A sample of antigen corresponding to about 20 mg of protein was incorporated in complete Freund-adjuvant. Chinchilla rabbits were immunized with the incorporated antigen subcutaneously at seven sites (hind footpads, either side of the lumbar region, above the scapulae and the cervical fat pads). Three weeks later a similar procedure was carried out with the same amounts of antigen incorporated into incomplete Freund-adjuvant administered intramuscularly. Three subsequent intraperitoneal inoculations without adjuvant were administered with the same amounts of antigen in every 14 days. After 10 days of the last injection the animals were bled from the heart.

For the elimination of non-specific antibodies in the antiserum produced against antigenic compounds derived from cat cerebral cortex the antiserum was absorbed with cat serum and with soluble extracts of cat liver and kidney. One ml of the antiserum was incubated with 0.1 ml of cat serum at 36°C for 1 hr. The procedure was repeated three times. Similarly, 1 ml of antiserum was incubated three times with 0.1 mg each of the soluble extracts of cat liver and kidney. All precipitates were sedimented and discarded. The absorption procedures were checked by means of gel-immunodiffusion analysis. The complement factors were eliminated at 56°C from the completely absorbed antiserum and the IgG fraction was isolated according to the procedure of Baumstark et al. (1964).

The immunodiffusion analysis was carried out according to the method of Ouchterlony (1953); 2% agar-gel was prepared in sodium and potassium phosphate buffered physiological saline solution (pH = 7.2). The immunoelectrophoresis was executed according to the procedures of Grabar and Williams (1953) and Scheidegger (1955) in 1.5% agar-gel in 0.05 M Na-veronal buffer solution (pH 8.2 – 8.3). Electrophoresis was carried out at a constant current of 5 mA/plate. Bromophenol-blue was used as a marker dye. In some cases comparative immunoelectrophoresis was carried out according to the procedure of Osserman (1960). The micropassive haemagglutination assay was performed according to the method of Csizmas (1960) on a microtitration plate.

The soluble fractions were separated from the homogenates of cerebral cortex, liver, kidney, spleen, lung, testis, ovary and thyroid of cats. The tissues were homogenized in a Potter homogenizer with a teflon-pestle for 3 min with two volumes of buffered physiological saline solution (pH = 7.0). The supernatant obtained after centrifugation at $105{,}000 \times g$ (Beckman Spinco L-50) was exhaustively dialysed against (an excess) 0.005 M sodium and potassium phosphate buffer solution (pH = 7.2). A DEAE-cellulose column (1.5 × 20 cm) equilibrated with the same buffer solution was used for the further fractionation of the soluble proteins of cerebral cortex (150 mg of protein was applied to the column). The following solutions were used for the discontinuous gradient: 5 mM phosphate buffer (pH = 7.2) (I), 50 mM phosphate buffer (pH = 7.2) without NaCl (II), and with 0.1 M (III), 0.25 M (IV), 0.5 M (V) and 1.0 M NaCl (VI). Protein content of the fractions (5 – 5 ml) was measured by light absorbance at 280 nm. All separation procedures were carried out at 4°C.

Electrophoresis was performed in 15% polyacrylamide gels (0.6 × 7 cm) according to the procedures of Davies (1964) with slight modifications. The samples subjected to electrophoresis contained 0.4 – 0.7 mg of protein. Electrophoresis was performed for 2 – 3 hr at a constant current of 3 – 4 mA/tube. During the running time the bromophenol-blue marker dye migrated about 65 mm. The gels were stained by immersion in a solution of 1% Amidoblack 10B in 7% acetic acid for 1 hr. The excess of dye was removed by repeated washing of the gels in 7% acetic acid. Gel-electrophoretograms were analyzed densitometrically at 500 nm with a Zeiss chromatogram-densitometer. In certain cases unstained gels were cut in 3 equal parts according to stained marker control gels. The identical parts of the gels were homogenized in sodium and potassium phosphate buffered saline solution (pH = 7.2). The obtained gel-debris was sedimented and the supernatant was retained. These procedures were carried out at 4°C.

Protein was estimated by the method of Lowry et al. (1951). Bovine serum albumin was used for the standard calibration curve. Measurements of DNA and RNA were carried out according to the method of Dische (1955).

Results

The extract of the phospholipid-free homogenate of cat cerebral cortex prepared from 100 g (wet weight) of nervous tissue proved to contain about 1 g of protein. In 100 mg of the antigen we could estimate about 2 – 3 mg of RNA

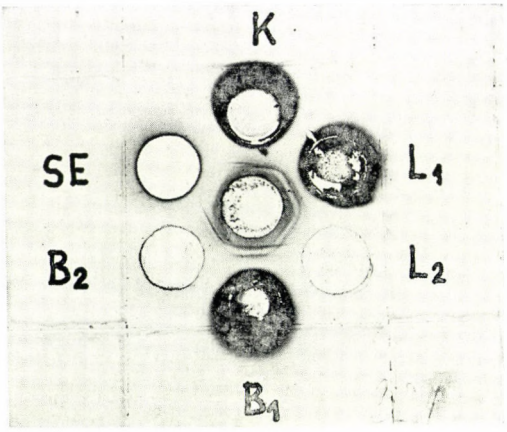

A)

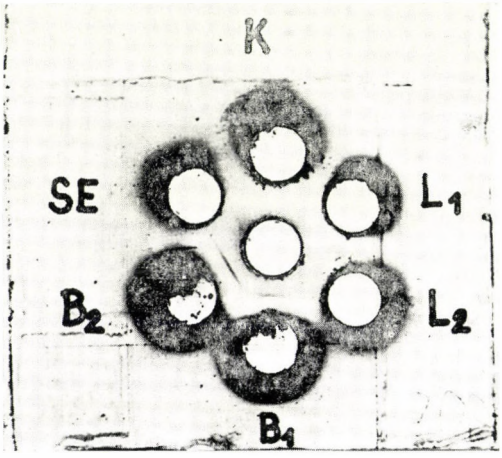

B)

Fig. 1. Immunoprecipitation reactions of antiserum. *A)* Antiserum (central well) reactions with the soluble extracts of kidney (K), liver (L_1) and brain cerebral cortex (B_1); $2000 \times g$ supernatant of the phospholipid-free extract of the liver (L_2) and brain cerebral cortex (B_2); cat serum (SE). *B)* Antiserum absorbed with cat serum, soluble extracts of liver and kidney homogenates (central well) reacted only with the antigenic components of brain fractions (B_1, B_2)

and traces of DNA. From other organs much greater amounts of protein were extracted.

The population of antibodies produced against the antigen mixture gave precipitation lines not only with the cerebral extracts but also with liver and kidney extracts and with serum (Fig. 1*A*). Obviously, there are a great number of common antigen determinants in the antigen preparation (B_2) and the soluble

fraction (B_1) of the cerebral cortex of cats. There were common precipitation lines extending over the extracts of brain, liver and kidney of the cat, and all of the fractions mentioned contained precipitation lines common with the cat serum. Considering Fig. 1*A*, one can establish the presence of a brain-specific antigen-determinant; there is a definite unique precipitation reaction of the antiserum with cerebral extracts which is absent from the other organ fractions examined. The antiserum was absorbed with cat serum, as well as with soluble extracts of liver- and kidney-homogenates. The absorption with cat serum eliminated the precipitating activity of the immune serum with the antigens originat-

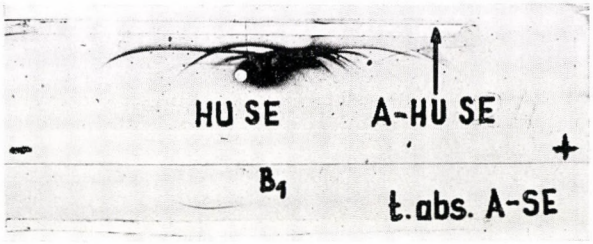

Fig. 2. Immunoelectrophoretic assays for comparing the electrophoretic mobility of antigenic components of water-soluble extracts of brain cerebral cortex and those of the antigens of human serum. Upper: anti-human-serum (A-HUSE) precipitates the antigenic compounds of human serum (HUSE); lower: antiserum absorbed with cat serum, soluble extracts of liver and kidney homogenate (t. abs. A-SE) reacts with soluble extracts of brain cerebral cortex. Note the $\beta_1-\beta_2$-globulin like mobility of the brain-specific antigen

ing from serum contamination of the brain homogenate. When the absorption procedures were accomplished with the liver and kidney extract the antiserum obtained precipitated only with the components of the original antigen preparation, as well as with the appropriate components of the soluble fraction of cat cerebral cortex (Fig. 1*B*), and did not react with the soluble fractions of other cat organs. The completely absorbed immune serum and the isolated IgG-fraction may be considered to have antibodies specific to cerebral cortex. The immunoelectrophoretic investigations of the soluble extract with the completely absorbed immune serum indicated the human serum $\beta_1-\beta_2$ globulin-like mobility of the antigen-determinant molecules examined (Fig. 2).

Further information on the chemical nature of the soluble brain-specific antigen was obtained by anion-exchange chromatography and acrylamide gel-electrophoresis. The results derived from the discontinuous [Cl^-] gradient are summarized in Fig. 3. For the sake of immunological analysis the fractions were subjected to micropassive haemagglutination assay. The results obtained with the completely absorbed antiserum indicated the highest titre in the fifth peak, eluted at 0.5 M NaCl concentration (1 : 256). The fourth, as well as the sixth, peak contained a much lower amount of antigen. Electrophoretic analysis of the com-

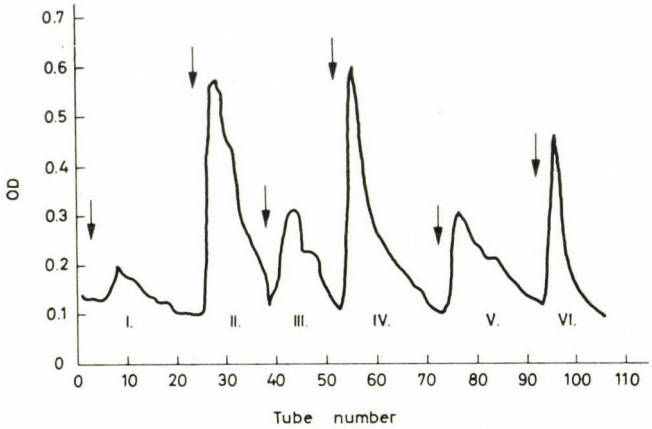

Fig. 3. DEAE-cellulose chromatography of the soluble components of cerebral cortex of cats. I. 5 mM phosphate buffer (pH 7.2); II. 50 mM phosphate buffer (pH 7.2); III. 50 mM phosphate buffer (pH 7.2) + 0.1 M NaCl; IV. 50 mM phosphate buffer (pH 7.2) + 0.25 M NaCl; V. 50 mM phosphate buffer (pH 7.2) + 0.5 M NaCl; VI. 50 mM phosphate buffer (pH 7.2) + 1.0 M NaCl

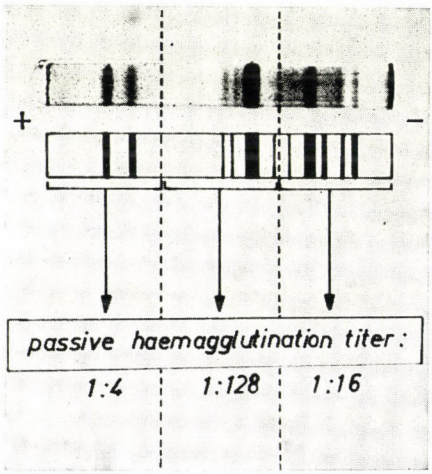

Fig. 4. Microhaemagglutination assay on the gel-electrophoresis column of the fifth peak of DEAE-cellulose chromatography. (The proteins of the three parts of polyacrylamid-gel were extracted, concentrated and adjusted to the same concentration)

ponents of the fifth peak indicated about 10–11 well-defined protein bands. Some of the acrylamide gels, electrophoresed under similar conditions, were unstained and sliced on the basis of stained bands. The same amounts of concentrated samples of the eluted solution of these slices were subjected to micropassive haemagglutination assay. Antigens were found in the middle part of the gel-columns among the proteins of intermediate mobility (Fig. 4).

Discussion

In spite of the highly developed differentiation of the CNS there is a homogeneity in the antigenic composition of the different areas examined. Antigenic preparations of the nervous tissue inevitably contain a significant amount of contamination from strongly antigenic blood proteins, as well as antigenic moieties common to many other organs. Thus, the humoral immune response produced against an immunogenic preparation of nervous tissue generally contains antibodies specific to the antigen determinants of common embryonic origin, in addition to the antibodies reacting only with the antigen components specific to the nervous tissue itself. Thus, without any absorption procedures the presence of the not brain-specific antibodies in the "anti-brain" sera might cause many nonspecific effects in their *in vivo* administration.

In the experiments presented here we absorbed exhaustively the immuno sera with cat serum, liver and kidney extracts. After this procedure we obtained a population of antibody molecules specific to the brain tissue of the cat the level of sensitivity of the immunodiffusion method. The electrophoretic mobility of the water-soluble antigen proved to be similar to the $\beta_1-\beta_2$ globulins of human sera and it could be eluted from a DEAE-cellulose column with 0.5 M NaCl solution in the presence of 0.05 M phosphate buffer (pH = 7.2). A micropassive haemagglutination assay of the disc-electrophoretic bands of the higher antigenically active chromatographic peak indicated that the antigen migrated among the components of the middle range on the acrylamide gels.

Numerous papers have been published on the chemical compartmentation of neurons and glial cells. Nevertheless there are few exact data available on the cellular and subcellular distribution of the CNS-specific components studied. By using different procedures some authors demonstrated the S-100 protein and glial fibrillary acidic protein, among others, to be found mainly in glial cells and the 14−3−2 protein in neurons (Cicero et al., 1970, Sviridov et al., 1972, Dahl, Bignami, 1973).

Further experiments are required to decide whether the water-soluble antigen described by us is located in the neurons or in glial cells or in both.

References

Baumstark, J. S., Laffin, R. J., Bardawil, W. A. (1964) Arch. Biochem. Biophys. *108* 514
Bornstein, M. B. (1969) in: P. A. Mieschner and H. J. Muller-Eberhard (Eds) Textbook of Immunopathology Vol. 2. Grune and Stratton, New York and London, p. 507.
Cicero, T. J., Cowan, W. M., Moore, B. W., Suntzeff, V. (1970) Brain Res., *18* 25
Csizmas, L. (1960) Proc. Soc. Exp. Biol. Med. *103* 157
Dahl, D., Bignami, A. (1973) Brain Res. *57* 343
Davies, B. J. (1964) Ann. N. Y. Acad. Sci. *121* 404
Dische, Z. (1955) in: The Nucleic Acids. Chemistry and Biology. Acad. Press, N. Y., p. 285
Grabar, P., Williams, C. A. (1953) Biochim. Biophys. Acta *10* 193
Heath, R. G., Krupp, I. M. (1967) in: O. Walass (Ed.) Molecular Basis of some Aspects of Mental Activity. Acad. Press London—N. Y., *2* 313

Huneeus-Cox, F. C., Fernandez, H. L. (1967) J. Gen. Physiol. *50* 2407
Jankovic, B. P., Rakic, Lj., Veskov, R., Horvat, J. (1968) Nature (London) *218* 270
Kornguth, S. E., Hanson, J. C., Chun, R. W. M. (1970) Neurology, *20* 749
Kosinski, E., Grabar, P. (1967) J. Neurochem. *14* 273
Levine, L. (1967) in: G. C. Quarton, T. Melnechuk and F. O. Schmitt (Eds) The Neurosciences. A study program. Rockefeller Univ. Press N. Y., p. 220.
Liakopoulou, A., MacPherson, C. F. C. (1970) J. Immunol. *105* 512
Lowry, O. H., Rosenbrough, N. J., Farr, A. L., Randall, R. J. (1951) J. Biol. Chem. *193* 265
Moore, B. W., McGregor, D. (1965) J. Biol. Chem. *240* 1647
Orosz, A., Falus, A., Gergely, J., Madarász, E., Ádám, G. (1971) Proc. Int. Un. of Phys. Sci. XIV. Int. Cong., Munich, Abs., p. 433
Orosz, A., Hámori, J., Falus, A., Madarász, E., Lakos, I., Ádám, G. (1973) Nature New Biol. *245* 18
Orosz, A., Madarász, E., Falus, A., Ádám, G. (1974) Brain Res., *76* 119
Osserman, E. F. (1960) J. Immunol. *84* 93
Ouchterlony, O. (1953) Acta Path. Microbiol. Scand. *32* 231
Paterson, P. Y. (1968) in: P. A. Mieschner and H. J. Muller-Eberhard (Eds) Textbook of Immunopathology. Grune and Stratton, New York and London *1* 132
Scheidegger, J. J. (1955) Intern. Arch. All. Appl. Immunol. *7* 103
Schneider, W. C. (1945) J. Biol. Chem. *161* 293
Sviridov, S. M., Korochkin, L. J., Ivanov, V. N., Maletskaya, E. I., Bakhtina, T. K. (1972) J. Neurochem. *19* 713
Wald, F., Mazzuchelli, A. N., Lapetina, E. G., DeRobertis, E. (1968) Exp. Neurol., *21* 336
Warecka, K., Moller, H. J., Vogel, H. M., Tripatzis, I. (1972) J. Neurochem. *19* 719

Acta Biochim. et Biophys. Acad. Sci. Hung. Vol. 9 (4), pp. 327–338 (1974)

A Protein Factor Inhibiting the G–F Transformation of Actin

I. An Actin Polymerization Inhibitor Present in the Striated Muscle of Vitamin E Deficient Rabbits

MÁRIA B. PÁPAI, GIZELLA JOSEPOVITS

2nd Institute of Biochemistry, Semmelweis University of Medicine, Budapest, Hungary

(Received February 14, 1974)

1. Flow birefringence studies have confirmed the earlier findings that the polymerizing ability of crude actin prepared from the striated muscle of vitamin E deficient rabbits is reduced as compared to that of normal actin.

2. Polymerizing ability of crude actin from vitamin E deficient rabbits can be enhanced by ultracentrifugal purification to values similar to that of normal actin.

3. The supernatant obtained by the ultracentrifugal purification of crude F-actin from the striated muscle of vitamin E deficient rabbits inhibits the G–F transformation of actin. The F-actin supernatant of normal rabbits fails to exert such an effect. The results obtained so far indicate that the inhibitor is a protein.

4. Tropomyosin isolated from the striated muscle of normal rabbits does not affect the polymerization of actin, whereas the tropomyosin from vitamin E deficient animals has an inhibitory effect.

5. Myosin prepared from the striated muscle of vitamin E deficient rabbits contains protein(s) that inhibits the polymerization of actin.

Introduction

Since Szent-Györgyi and his co-workers established that the protein extracted from striated muscle with 0.5 M KCl consists of two major protein components, i.e. actin (Straub, 1943) and myosin, the investigation of these proteins has been in the focus of biochemical research on muscle. This pertains to both normal and pathological muscle function.

One of the main characteristic features of actin is its transformation or polymerization from a globular form (G-actin) to a fibrous form (F-actin) on the addition of salt. Actin can undergo a loss of polymerizability. As it is well known chemical modifications can cause a reduced polymerizing ability. From functional aspect the most important inhibition phenomena are related to the natural components of muscle (Maruyama, 1965).

The detailed investigations on the properties of actin obtained from dystrophic muscle have been performed by Aloisi et al. (1952, 1953). These authors reported a decreased ability of actin to polymerize, and their results were supported by observations with electron microscope. Others have also tackled the problem and contradictory opinions have also been reported (Feuer, Frigyes, 1951).

Studying the muscle proteins of vitamin E deficient rabbits we also observed a reduced ability of actin to polymerize. In this report, results are presented

which show that crude actin preparations obtained from the muscle of dystrophic animals contain a protein factor that inhibits actin polymerization. A part of this work was briefly reported (Székessy-Hermann et al., 1961).

Materials and methods

Rabbits weighing about 600 to 900 g were used. The animals were classified into three groups: the first group that was subjected to E-avitaminosis was given Goettsch-Pappenheimer (1931) diet. The control group was fed the same diet supplemented with 2 mg α-tokopherolacetate per kg body weight per os twice weekly. The third, normal group was nourished with the natural green and grain rabbit fodder. The vitamin E deficient animals were killed in the terminal phase of muscle dystrophy, which was indicated by rapid loss of body weight, increase in the creatin content of urine and by the characteristic behaviour of the animals.

All proteins used in the experiments were stored at 2–3°C not more than five days.

Actin was prepared according to Bárány et al. (1954). From the acetone-dried muscle powder actin was extracted at 0–2°C (Drabikowski, Gergely, 1962) or at room temperature in some experiments. As the amount of acetone-dried muscle powder that can be extracted from the vitamin E deficient animals is much less than that from normal rabbits, in some experiments the muscle powders of several rabbits were pooled. Actin was purified by the ultracentrifugal method of Mommaerts (1952). ATP was removed by Dowex-1 (Cl^-) anion exchange resin suspension according to Asakura (1961). The designation "normal (N) actin" will be used for the protein prepared from the striated muscle of normal rabbits, the term "E-avitaminotic (E) actin" will denote the preparation obtained from the muscle of dystrophic rabbits by the same procedure. The terms "normal (N) supernatant" and "E-avitaminotic (E) supernatant" refer to the supernatants obtained by ultracentrifugal purification of "normal" and "E-avitaminotic" crude F-actin solutions, respectively. Ultracentrifugations were carried out at 105, 000 × g for 2 hours after polymerization of crude G-actin in 0.1 M KCl at pH 8.0.

Myosin was prepared essentially according to the method of Portzehl et al. (1950). The last precipitate was dissolved in 0.5 M KCl and the pH was adjusted to 7 with KOH. The myosin solution was clarified by ultracentrifugation at 100,000 × *g* for one hour. In the course of myosin preparation there are differences depending on whether myosin is extracted from normal or dystrophic muscles. Whereas with "normal" myosin the amount of protein precipitated at 0.28 μ is small, with "dystrophic" myosin the same procedure precipitates the majority of proteins. For this reason in the preparation of myosin from vitamin E deficient rabbits the precipitation of actomyosin at 0.28 μ was omitted. The terms "normal myosin" and "E-avitaminotic myosin" refer to myosins obtained from normal and dystrophic rabbits, respectively.

Tropomyosin was prepared according to Bailey (1948). A 10-min heat treatment at 100°C was also applied as the last purification step. The tropomyosin

thus obtained displayed low viscosity in 0.1 M KCl, and it had the characteristic high viscosity at low ionic strength.

Protein concentration was measured by the micro-Kjeldahl procedure, using a nitrogen factor of 6.25.

The polymerization of G-actin was followed by viscosity and flow birefringence measurements. The viscometric study of actin polymerization was performed in Ostwald-type viscometers at 24°C in a volume of 6 ml. If not stated otherwise, the assay conditions were: 0.1 M KCl, 1 mM $MgSO_4$, 0.05 M Tris-HCl, pH 7.4. The degree of flow birefringence was measured using an Edsall-type apparatus (Rao Company) at a velocity gradient of $200-300$ sec^{-1}.

Actomyosin formation was evaluated by determining the fall in viscosity obtained when ATP was added to a solution containing myosin and F-actin (Bárány et al., 1954). Viscosity determinations were carried out in an Ostwald-type viscometer at 24°C in a volume of 4 ml reaction mixture. The flow times of viscometers were $30-40$ sec at 24°C for 4 ml solvent.

ATP was a product of Reanal, all other chemicals were commercial preparations of analytical reagent grade.

Results

Earlier viscometric data (Székessy-Hermann et al., 1961), which showed a reduced polymerizing ability of crude actin extracted from the striated muscle of vitamin E deficient rabbits have been confirmed by flow birefringence studies. The increase in flow birefringence that accompanies the G–F transformation of actin is considerably diminished in the case of "E-avitaminotic" actin as compared to the "normal" (Fig. 1).

The formation of actomyosin complex from "normal" myosin and unpurified "E-avitaminotic" actin has been studied. In Fig. 2 actomyosin formation of a representative control and of several "E-avitaminotic" actin samples is demonstrated. A close parallelism can be observed between the specific viscosity of F-actins and their ability to complex with myosin. Different F-actin preparations from dystrophic animals varied considerably in specific viscosity, in contrast to the "normal" actins. This might be due to several factors, for example to marked differences in the stage of E-avitaminosis. Seasonal variations may also interfere.

If actin extracted from acetone-dried muscle powder is purified by depolymerization and repolymerization according to the method of Mommaerts (1952), the polymerizing ability of "E-avitaminotic" G-actin will be similar to that of "normal" actin. As a result of purification, the specific viscosity of "normal" F-actin increases by about 1/6 of the viscosity value of crude F-actin, whereas the specific viscosity of "E-avitaminotic" F-actin increases more than twofold. In absolute values, however, the maximal specific viscosity of purified "E-avitaminotic" F-actin is less than the viscosity of "normal" F-actin (Table 1). Accordingly, "E-avitaminotic" F-actin yields G-actin similar to the "normal" regarding both polymerizing ability and combination with myosin (Fig. 3).

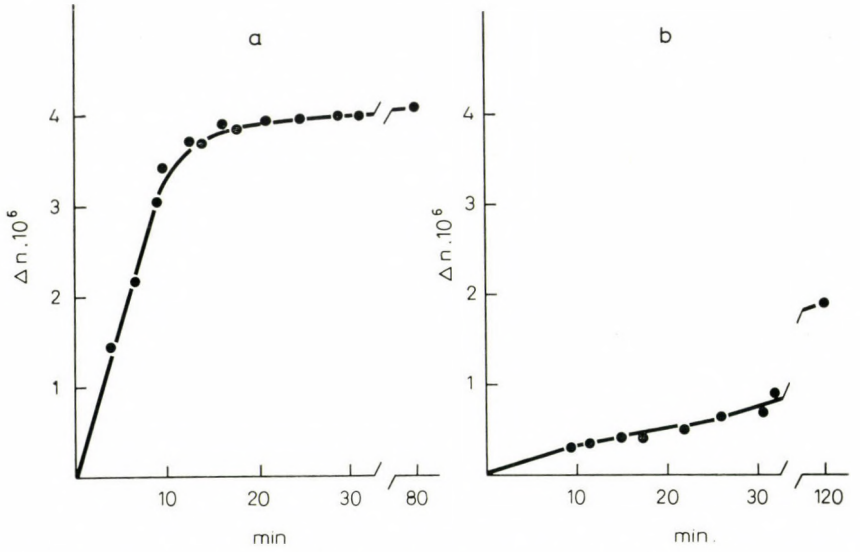

Fig. 1. Time course of flow birefringence during polymerization of crude G-actin extracted from the acetone-dried muscle powder of normal and vitamin E deficient rabbits. Measurements were carried out in 0.1 M KCl, 1 mM $MgSO_4$, 20 mM Tris HCl, pH 7.4, continuously at a constant velocity gradient.

a) "Normal" G-actin, 0.3 mg/ml, velocity gradient 227 sec^{-1}, room temperature (23°C);
b) "E-avitaminotic" G-actin 0.3 mg/ml; velocity gradient 251 sec^{-1}, room temperature (20°C)

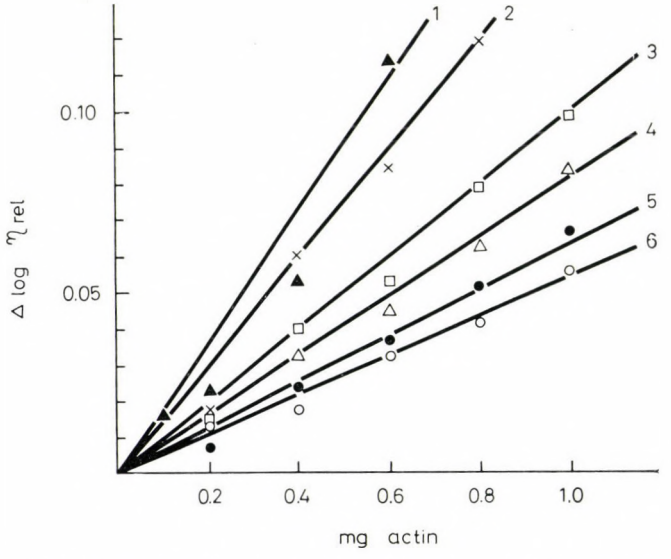

Fig. 2. The ability of crude actin obtained from vitamin E deficient and control rabbits to complex with myosin. Experimental conditions: 0.5 M KCl, 0.5 mM $MgSO_4$, 10 mM phosphate buffer, pH 7.0, volume 4 ml, temperature 24°C. The specific viscosity (η_{sp}) of F-actins

Table 1

Ultracentrifugal purification of actin from normal and vitamin E deficient rabbits

Actin was purified according to Mommaerts (1952). Free ATP was removed by a suspension of Dowex-1 (Cl^-) anion exchange resin. The viscosity of G-actin was measured in H_2O, that of F-actin in 0.1 M KCl, 1 mM $MgSO_4$, 50 mM Tris-HCl, pH 7.4. N: actin prepared from normal rabbit muscle; E: actin prepared from vitamin E deficient rabbit muscle

	Protein (mg/ml)		Viscosity (η_{sp}) G-actin (1 mg/ml)		F-actin (1 mg/ml)	
	N	E	N	E	N	E
Crude actin	2.81*	3.35*	0.025	0.03	0.74	0.28
Supernatant	0.66	2.16	—	—	—	—
F-actin precipitate after depolymerization (homogenized in 0.2 mM ATP, pH 6.3)	3.98	2.07	0.04	0.06	0.96	0.60
Purified actin after dialysis against ATP	3.40	2.05	0.02	0.04	0.95	0.67
Purified actin after removing free ATP	3.21	1.95	0.05	0.09	0.85	0.61

* The data presented here do not provide information as to the extractability of "E-avitaminotic" actin. In E-avitaminosis the amount of protein extracted from the acetone powder is less than that from normal animals (Székessy-Hermann et al., 1961)

Fig. 4 demonstrates the effect of supernatant obtained by ultracentrifugation of crude F-actin on the actin polymerization. The addition of N-supernatant reduces the rate of actin polymerization without affecting the final viscosity values. If G-actin is polymerized in a medium where E-supernatant is present, not only the rate of polymerization decreases substantially, but also the final viscosity values are much less than those of the uninhibited ones.

Different E-supernatant preparations varied in their inhibitory effect. The most active preparations gave about 45% inhibition with the 1 : 1 E-supernatant-to-actin weight ratio (Table 2).

as measured in the above reaction mixture at 1 mg/ml protein concentration were as follows: 1) 0.55 ("control"*); 2) 0.48 ("E-avitaminotic"); 3) 0.39 ("E-avitaminotic"); 4) 0.22 ("E-avitaminotic" 5) 0.18 ("E-avitaminotic"); 6) 0.15 ("E-avitaminotic")
Abscissa: mg actin added to 3 mg of myosin. Ordinate: decrease in the logarithm of relative viscosity on the effect of 0.8 mM ATP

* Actomyosin formation of actin from control animals generally agrees with that of normal animals.

Table 2

Effect of the supernatant obtained by ultracentrifugation of crude F-actin from vitamin E deficient rabbits on the polymerization of actin

The polymerization of G-actin in the presence of "E-avitaminotic" supernatant was followed by viscometry. The percentual inhibition was calculated from the specific viscosity values obtained at 40 min after initiation of polymerization. Experimental conditions: 0.1 M KCl, 1 mM $MgSO_4$, pH 7.4, temperature 24°C. G-actin and E-supernatant concentration as indicated

"E-avitaminotic" supernatant		G-actin		Inhibition of actin polymerization in %
No.	mg protein/ml	No.	mg protein/ml	
$E_{142,143,144,145}$	0.73	K_{39}	0.75	49
$E_{176,177,178,181,182,186}$	0.75	N_{40}	0.67	31
E_{187}	0.56	K_{51}	0.67	12
$E_{199,200}$	0.88	K_{53}	0.67	18
$E_{223,225}$	0.61	N_{46}	0.67	43
E_{257}	0.77	N_{50}	0.67	43
E_{260}	0.62	N_{51}	0.67	25
E_{261}	0.67	N_{65}	0.67	26
$*E_{310,311,313,316}$	0.50	N_{73}	0.51	46

* G-actin was extracted from the acetone powder at 0—2°C

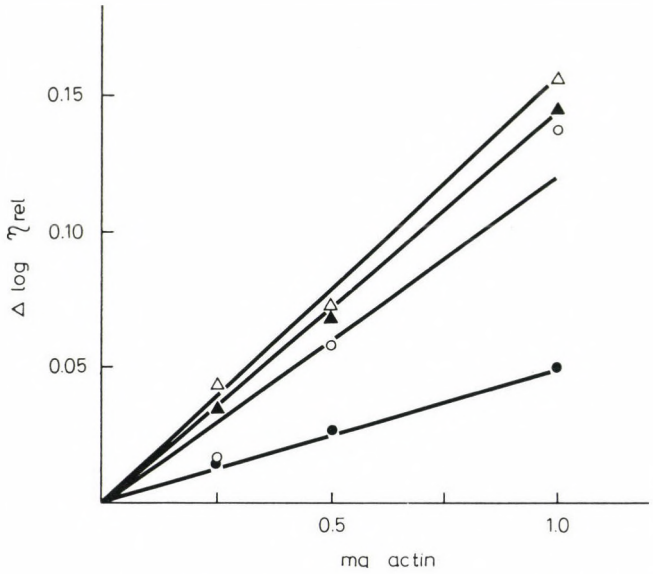

Fig. 3. The ability of "E-avitaminotic" and "normal" actins purified by depolymerization and repolymerization to complex with myosin. Experimental conditions: 0.5 M KCl, 0.5 mM $MgSO_4$, 50 mM Tris-HCl, pH 7.4, temperature 24°C, volume 4 ml. Abscissa: mg actin added to 3 mg of myosin. Ordinate: decrease in the logarithm of relative viscosity on the effect of 0.8 mM ATP. (○) crude "normal" F-actin; (△) the same after purification; (●) crude "E-avitaminotic" F-actin; (▲) the same after purification

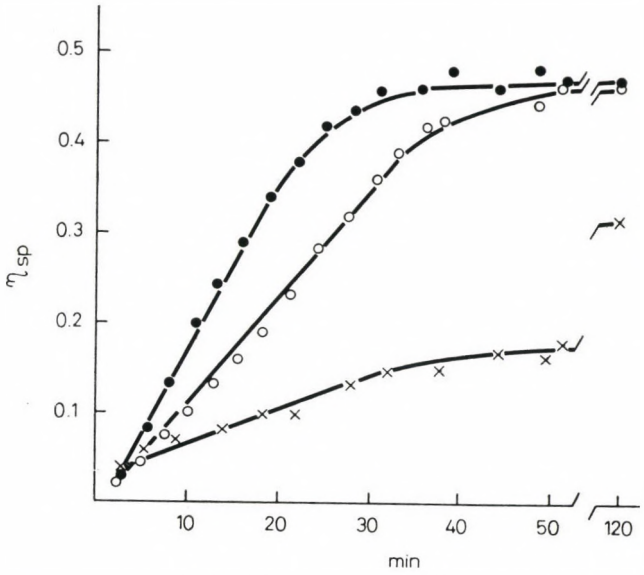

Fig. 4. Effect of supernatant obtained by the ultracentrifugal purification of actins isolated from normal and vitamin E deficient rabbits on the polymerization of G-actin. Experimental conditions: 0.1 M KCl, 1 mM $MgSO_4$, 50 mM Tris-HCl, pH 7.4, temperature 24°C, final volume 6 ml. Polymerization was started at zero time by the addition of 4 mg "normal" G-actin. Polymerization of 4.0 mg G-actin (●) without "normal" supernatant; (○) in the presence of "normal" supernatant (3.8 mg protein); (×) in the presence of "E-avitaminotic" supernatant (3.8 mg protein)

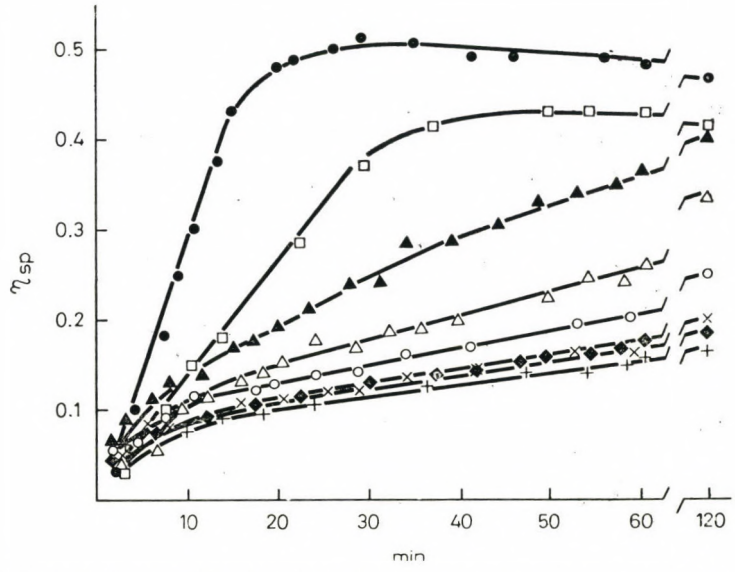

Fig. 5. Effect of different "E-avitaminotic" supernatant concentrations on the polymerization of G-actin. The reaction mixture contained various amounts of "E-avitaminotic" supernatant in 0.1 M KCl, 1 mM $MgSO_4$, 50 mM Tris-HCl, pH 7.4. Final volume 6 ml. Temperature 24°C. At zero time 4 mg "normal" G-actin was added to the reaction mixture. Polymerization of actin (●) without supernatant; with (□) 1 mg, (▲) 2 mg, (△) 3 mg, (○) 5 mg, (×) 7 mg, (♦) 9 mg, and (+) 11 mg of supernatant protein

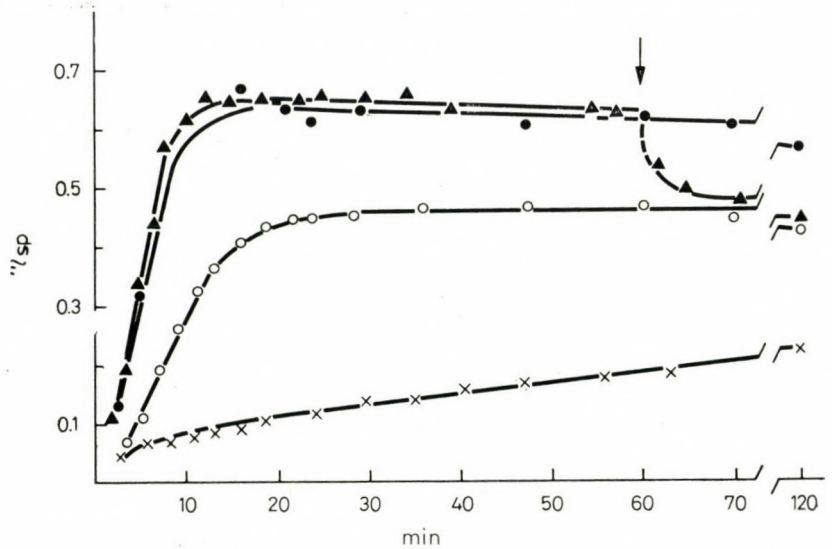

Fig. 6. Effect of "E-avitaminotic" supernatant on G- and F-actin. Conditions: 0.1 M KCl, 1 mM $MgSO_4$, 50 mM Tris-HCl, pH 7.4, temperature 24°C. (●) Polymerization of 4 mg "normal" G-actin in 4 ml volume without "E-avitaminotic" supernatant; (○) polymerization of 4 mg "normal" G-actin in 6 ml volume without "E-avitaminotic" supernatant; (×) polymerization of 4 mg "normal" G-actin in 6 ml volume in the presence of "E-avitaminotic" supernatant (5.8 mg protein); (▲) polymerization of 4 mg "normal" G-actin in 4 ml volume, the arrow indicates the addition of 2 ml of "E-avitaminotic" supernatant (5.8 mg protein) to the reaction mixture

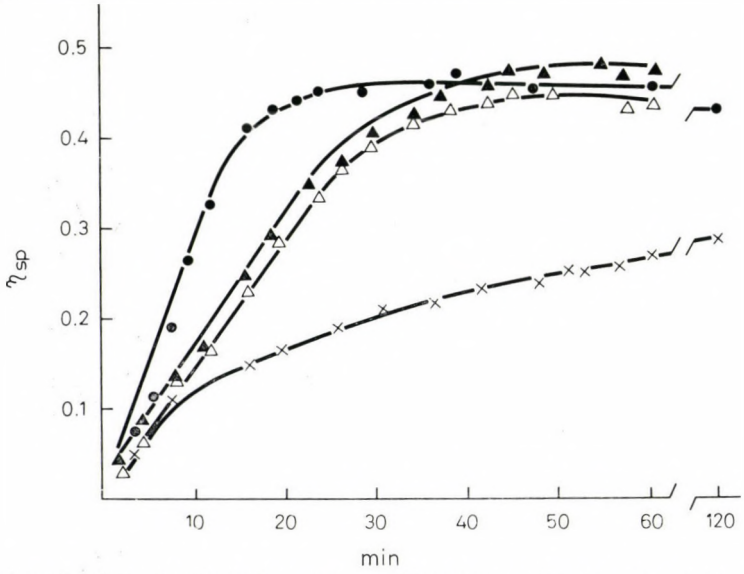

Fig. 7. Polymerization of actin in the presence of heat-treated "E-avitaminotic" supernatant. The reaction mixture contained 5.8 mg "E-avitaminotic" supernatant in 0.1 M KCl, 1 mM $MgSO_4$, 50 mM Tris-HCl, pH 7.4. Final volume 6 ml. Temperature 24°C. At zero time 4 mg "normal" G-actin was added to the mixture. Polymerization of 4 mg actin (●) without supernatant; (×) in the presence of "E-avitaminotic" supernatant (5.8 mg protein); (△) in the presence of "E- avitaminotic" supernatant (5.8 mg protein) incubated at 100°C for 30 min; (▲) in the presence of "E-avitaminotic" supernatant (5.8 mg protein) incubated at 100°C for 60 min

As it can be seen in Fig. 5, inhibition is proportional to the concentration of E-supernatant.

Actin polymerization is diminished when E-supernatant is present during polymerization, but E-supernatant does not act as an inhibitor when actin polymerization is completed. This was proved as follows (Fig. 6). As a control, the polymerization of 4 mg G-actin was measured in 4 and 6 ml volumes. At the same time in

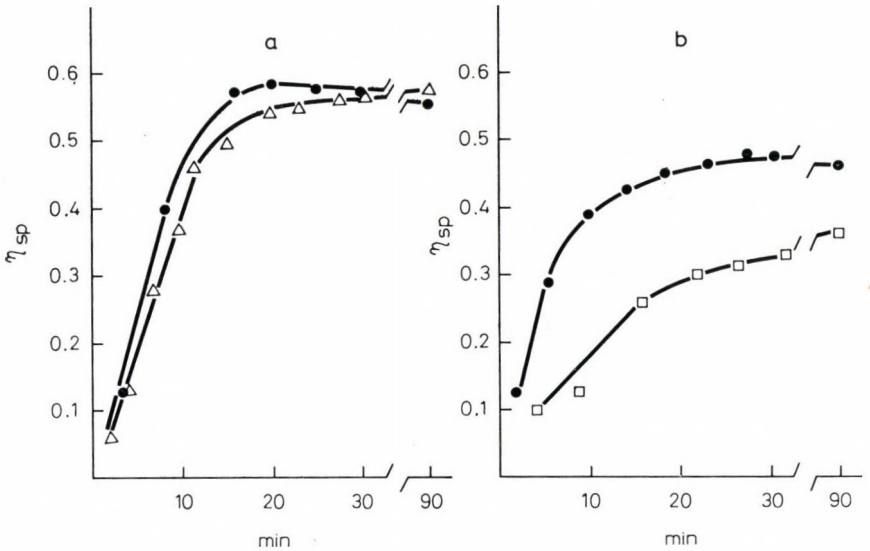

Fig. 8. Polymerization of actin in the presence of "normal" (a) and "E-avitaminotic" (b) tropomyosin. The reaction mixture contained 0.1 M KCl, 1 mM $MgSO_4$, 50 mM Tris-HCl, pH 7.4 and "normal" or "E-avitaminotic" tropomyosin. Final volume 6 ml. Temperature 24°C. (●) Polymerization of 4 mg "normal" G-actin without tropomyosin; (△) with "normal" tropomyosin (4 mg); and (□) with "E-avitaminotic" tropomyosin (5.9 mg protein)

other two viscometers 2 ml (5.8 mg) "E-avitaminotic" supernatant were added to 4 ml G-actin samples; in one of them at the beginning of polymerization (at 0 time), in the other at 60 min, i.e. when the polymerization of actin was completed. In the first case inhibition of polymerization was obtained, in the other case the specific viscosity did not fall below the values corresponding to the dilution in spite of the addition of "E-avitaminotic" supernatant. The fact that addition of E-supernatant to polymerized F-actin did not reduce its viscosity suggests that the inhibitor does not depolymerize F-actin.

Fig. 7 demonstrates that in the presence of heat-treated supernatants the extent of actin polymerization reaches the normal level, only the rate of polymerization is slower. From these findings it can be concluded that heat-treatment abolishes the inhibitory effect of "E-avitaminotic" supernatants.

The protein nature of the inhibitory substance is proved by the following experimental findings. 1. The inhibitory effect of supernatant is preserved even

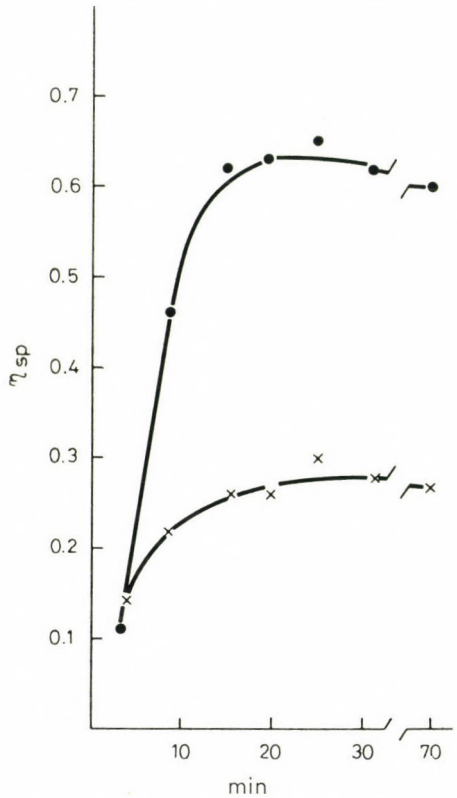

Fig. 9. Actin polymerization in the presence of a protein fraction obtained from "E-avitaminotic" myosin by dialysis. Dialysis was performed against 0.1 M KCl, 10 mM Tris-HCl, pH 7.4, after precipitation the supernatant was applied. Experimental conditions: 0.1 M KCl, 1 mM $MgSO_4$, 50 mM Tris-HCl, pH 7.4, temperature final volume 6 ml, 24°C. (●) Polymerization of 4 mg "normal" G-actin; (×) polymerization of 4 mg "normal" G-actin in the presence of the non-precipitated protein (2.4 mg)

after dialysis, if dialysis is performed under conditions when no precipitate is formed (for example in 0.1 M KCl, above pH 5.5). If precipitate was formed, the precipitate-free supernatant failed to exhibit any inhibitory effect. 2. At 40% ammonium sulphate saturation the majority of supernatant proteins are precipitated and the protein that remained in solution did not affect the polymerization of actin. 3. From the results of heat denaturation experiments it can also be concluded that for the inhibition of actin polymerization the supernatant proteins are responsible.

Actin extracted from acetone-dried muscle powder also contains tropomyosin (Drabikowski, Gergely, 1962; Laki et al., 1962), therefore we examined the polymerization of actin in the presence of tropomyosin prepared according to the method of Bailey (1948). Fig. 8 illustrates that tropomyosin from normal rabbits does not influence the polymerization of actin, whereas tropomyosin isolated from vitamin E deficient rabbits has some inhibitory effect.

Earlier studies in our laboratory (Székessy-Hermann et al., 1958) and investigations of Corsi et al. (1959) have also shown that in muscle dystrophy, induced by vitamin E deficiency, the properties of myosin also change. For this reason it appeared worth-while to examine whether myosin preparations from vitamin E deficient rabbits contained also proteins inhibiting actin polymerization. Myosin extracted from the striated muscle of vitamin E deficient rabbits was dialysed against 0.1 M KCl – 0.01 M Tris-HCl, pH 7.4, and the effect of protein that did not precipitate was examined on the polymerization of actin. As shown in Fig. 9, the inhibition of actin polymerization is nearly 50% even at a dialysed myosin-to-actin ratio of about 1 : 2, which calls the attention to the fact that from dystrophic muscle considerable amount of protein, inhibiting the polymerization of actin, is extracted with myosin.

Discussion

The polymerization of actin extracted from the acetone-dried muscle powder of vitamin E deficient rabbits has two characteristics: first, the final specific viscosity of polymerized actin is markedly diminished, and, second, the rate of polymerization is slower. Essentially the same is observed when the time course of polymerization of "E-avitaminotic" actin is measured by flow birefringence.

Earlier studies (Székessy-Hermann et al., 1961) have also demonstrated that ultracentrifugation of unpurified "E-avitaminotic" F-actin resulted much less sedimented protein than that of "normal" actin. The results presented here also suggest that in experimental muscle dystrophy only a small portion of crude actin can be polymerized, in contrast to that observed with normal muscle. However, this polymerized actin, after reversible depolymerization yields G-actin having essentially the same properties as "normal" actin regarding the polymerizability and to complex with myosin.

The major, non-polymerizable portion of "E-avitaminotic" crude actin is presumably composed of tropomyosin (Laki et al., 1962; Drabikowski, Gergely, 1962), α-actinin (Ebashi, Ebashi, 1965), and among other proteins also contains protein(s) that inhibit(s) the polymerization of actin.

According to our viscometric data tropomyosin isolated from striated muscle of normal rabbits has no inhibitory effect on the polymerization of actin. These results are in accordance with those of Tanaka and Oosawa (1971) obtained by means of flow birefringence. Prágay and Gergely (1968) reported that tropomyosin accelerates the rate of actin polymerization. In our experiments tropomyosin did not exert such an effect.

On the effect of α-actinin F-actin is gelatinized or precipitated. β-actinin (Maruyama, 1965; 1971), inhibits the network formation of F-actin and keeps the lenghth of F-actin around 1 to 2 μ. If G-actin is polymerized in the presence of α-actinin, the specific viscosity of F-actin is greater than without α-actinin (Maruyama, Ebashi, 1965). β-actinin inhibits the polymerization of actin, but according to Maruyama (1965) this protein cannot be isolated from acetone-dried muscle powder.

Our earlier reports were the first to demonstrate that from striated muscle of dystrophic (Székessy-Hermann et al., 1961) and normal (Pápai et al., 1964) rabbits, protein(s) can be extracted that inhibit(s) the polymerization of actin. Further experiments are required to elucidate whether the protein factor, described by us is identical with β-actinin isolated by Maruyama (1965).

The authors express their thanks to Professor Vilma Székessy-Hermann for the continuous help during this work.

References

Aloisi, M., Ascenzi, A., Bonetti, E. (1952) Experientia *8* 266
Aloisi, M., Ascenzi, A., Bonetti, E. (1953) Biochim. Biophys. Acta *10* 70
Asakura, S. (1961) Arch. Biochem. Biophys. *92* 140
Bailey, K. (1948) Biochem. J. *43* 271
Bárány, M., Biró, N. A., Molnár, J., Straub, F. B. (1954) Acta Phys. Acad. Sci. Hung. *5* 369
Corsi, A., Gallucci, V., Bargellini, P. (1959) Brit. Journ. Expt. Path. *15* 375
Drabikowski, W., Gergely, J. (1962) J. Biol. Chem. *237* 3412
Ebashi, S., Ebashi, F. (1965) J. Biochem. *58* 7
Feuer, Gy., Frigyes, Á. (1951) Kísérletes Orvostud. *3* 96
Goettsch, M., Pappenheimer, A. B. (1931) J. Exp. Med. *54* 145
Laki, K., Maruyama, K., Kominz, D. R. (1962) Arch. Biochem. Biophys. *98* 323
Maruyama, K., Ebashi, S. (1965) J. Biochem. *58* 13
Maruyama, K. (1965) Biochim. Biophys. Acta *94* 208
Maruyama, K. (1971) J. Biochem. *69* 369
Mommaerts, W. F. A. M. (1952) J. Biol. Chem. *198* 445
Pápai, M. B., Székessy-Hermann, V., Szőke, K. (1964) Abstr. of the Ist FEBS Meeting, London, 1964, abstract A65
Prágay, D. A., Gergely, J. (1968) Arch. Biochem. Biophys. *125* 727
Portzehl, H., Schramm, C., Weber, H. A. (1950) Z. Naturforsch. *5B* 61
Straub, F. B. (1943) Studies, Inst. Med. Chem. Univ. Szeged *3* 23
Székessy-Hermann, V., Josepovits, G., Vodnyánszky, L., Zsuberács, B. (1958) Acta Phys. Acad. sci. Hung. Suppl. *12* 75
Székessy-Hermann, V., Josepovits, G., Pápai, M. B. (1961) Abstr. of the Vth International Congress of Biochem. Moscow, 1961, abstract 2.148
Tanaka, H., Oosawa, F. (1971) Biochim. Biophys. Acta *253* 274

Acta Biochim. et Biophys. Acad. Sci. Hung. Vol. 9 (4), pp. 339–347 (1974)

Effect of Trypsin on the Ca^{2+} Uptake and the Enzymological Properties of the Sarcoplasmic Reticular Fraction

A. KÖVÉR, M. SZABOLCS, A. CSABAI, ÉVA OLÁH

Institute of Physiology and Central Research Laboratory, University School of Medicine, Debrecen, Hungary

(Received July 28, 1972, and in revised form November 14, 1972)

The Ca^{2+} uptake and enzymological properties of the sarcoplasmic reticular fraction prepared from a homogenate of white skeletal muscle of the catfish *(Amiurus nebulosus)* are considerably changed on tryptic digestion (trypsin : SRF protein = 1 : 5–1 : 62). In the course of tryptic digestion of SRF, cholinesterase activity and ATPase activity (both in the presence and absence of Ca^{2+}) were increased. Activation by Ca^{2+} of the ATPase of SRF was lost after 5 to 10 minutes of tryptic digestion and Ca^{2+} uptake fell nearly to zero. In some SRF preparations, after tryptic digestion for 1–2 minutes, activation of ATPase by Ca^{2+} was increased for a short period whereas Ca^{2+} uptake decreased. The same preparations displayed significantly higher cholinesterase activities measured without previous tryptic digestion, than those preparations which only showed a decrease, without any temporary increase, in the Ca^{2+} activation of ATPase on tryptic digestion.

Introduction

It has been observed that the ATPase and cholinesterase activities of the sarcoplasmic reticular fraction* isolated from the white skeletal muscle of the catfish *(Amiurus nebulosus)* and stored at 0 °C are increased, and its Ca^{2+} uptake is decreased during the course of storage (Szabolcs et al., 1966). Digestion of SRF by phospholipase-C leads to somewhat similar functional changes (Martonosi, 1964).

The structure of muscle SRF is built up beside the phospholipids, mainly of proteins present in a proportion of 50–60% which may play important roles as enzymes and structural elements. There were no literary data available regarding the functional relations of these proteins when these experiments were begun.

In this paper, the effect of tryptic digestion in modification of certain characteristics of SRF will be described.

Materials and methods

SRF was prepared from the homogenized white skeletal muscle of the catfish *(Amiurus nebulosus)* as described previously (Szabolcs et al., 1966). Experiments were carried out with fresh preparations, in spring and in autumn.

* *Abbreviations used:* SRF, sarcoplasmic reticular fraction; ACh, acetylcholine.

Ca^{2+} uptake of SRF was measured by the application of a cellulose column and $^{45}CaCl_2$ (Szabolcs, Kövér, 1966). The values of Ca^{2+} uptake were expressed as μmoles Ca^{2+}/mg protein.

ATPase activity was measured at 23°C in an incubation mixture containing 0.05 M KCl + 0.002 M $MgCl_2$ + 0.002 M ATP + 0.00 or 0.06 mM $^{45}Ca\ Cl_2$ + + 0.01 M Tris-maleate (pH 7.0), also used for measurements of Ca^{2+} uptake. The reaction was stopped by the addition of trichloroacetic acid after 5 minutes of incubation, Inorganic phosphate (P_i) was determined by the method of Taussky and Shorr (1953).

Cholinesterase activity was measured at 23 °C in the above incubation mixture with 0.001 – 0.0015 M acetylcholine instead of ATP. The acetylcholine content of aliquots of the incubation mixture was determined at the zero and 5th minutes according to the method of Hestrin (1949).

SRF was digested by trypsin in the following way: SRF suspensions in the washing solution (0.055 M KCl + 0.005 M $MgCl_2$ + 0.01 M Tris-maleate or histidine buffer, pH 7.0) were digested at different trypsin : protein ratios (1 : 5 – 1 : 62) for different times at 22 – 23°C. Digestion were terminated by the addition of a double amount (calculated for active trypsin) of soybean trypsin inhibitor (3 × crystallized, Sigma).

Crystalline trypsin preparations (Serva, Organon) were dissolved in 0.005 M HCl at a final concentration of 5 mg/ml and were kept at 37°C for 24 hours in order to inactivate possible chymotryptic contaminations. The tryptic activities of the preparations were then measured according to Kunitz (Laskowski et al., 1966). On the ground of these measurements, the amounts of trypsin applied in the experiments were expressed in active trypsin weight units.

Protein determinations were carried out by the micro-Kjeldahl method.

Results

Release of proteins from SRF on tryptic digestion. The amount of solubilized protein was measured as follows. Digestion was stopped after different times of incubation and the digestion mixture was centrifuged at 60 000 × g for 1 hour. The protein content of the supernatant was then determined, the amounts of added trypsin and trypsin inhibitor taken into account. In Fig. 1 is seen the change in the amount of solubilized protein (expressed as percentage of the protein content of untreated SRF) in the supernatant of digestion mixtures digested for different times with trypsin and centrifuged at 60 000 × g for 60 minutes. The rate of protein release from SRF is evidently high in the first 20 minutes of digestion.

Changes of the enzymological properties and Ca^{2+} uptake of SRF on tryptic digestion. The changes occurring in the enzymological characteristics and Ca^{2+} uptake of SRF as a result of tryptic digestion, are demonstrated in Fig. 2. After 7 minutes of digestion cholinesterase activity is 3 – 4 times as high as before digestion. The ATPase activity of SRF in the absence and in the presence of 0.06

mM Ca^{2+} is increased, reaching a maximum in the 7th minute of digestion. Ca^{2+} uptake is decreased and is practically stopped after 7–10 minutes of digestion.

The data obtained in further experiments concerning the enzymological changes that occur on tryptic digestion of SRF are summed up in Table 1.

It is revealed from the data in Table 1 that on tryptic digestion both cholinesterase and ATPase (with and without Ca^{2+}) activities are considerably increased

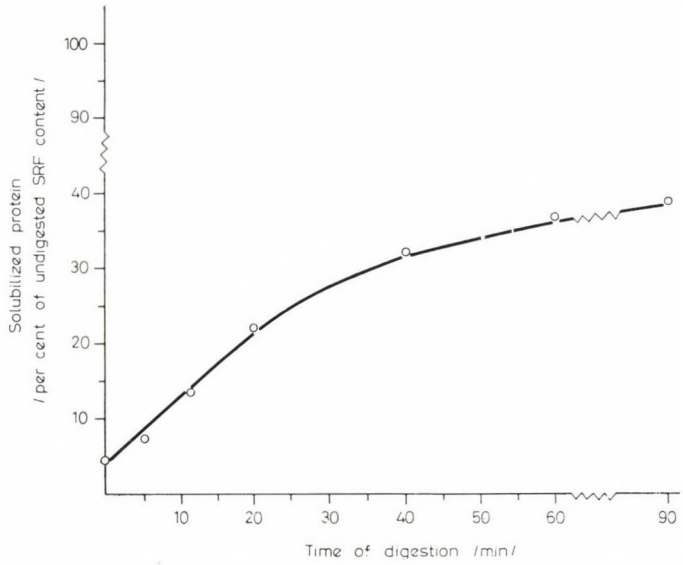

Fig. 1. Protein release from SRF during tryptic digestion. Trypsin : protein = 1 : 14; for other details see the text

in each preparation tested. It must be noted that cholinesterase activity of SRF reaches its maximum usually in the first 40 minutes of incubation with trypsin, while its ATPase activity (in the presence and absence of Ca^{2+}) reaches a maximum in the first 20 minutes of incubation. Cholinesterase activity is increased to a higher extent than ATPase activity.

Fig. 1 shows that in the first 30–40 minutes of tryptic digestion a considerable amount of protein is solubilized from SRF. At the same time, according to the data in Table 1, cholinesterase activity is increased to a higher extent. From these observations the conclusion can be drawn that in the course of tryptic digestion cholinesterase activity is solubilized. For this reason the distribution of the cholinesterase and specific cholinesterase activities between the pellet and the supernatant of a digestion mixture of SRF was examined after 0 and 40 minutes of tryptic digestion.

As shown in Table 2 a significant part of cholinesterase activity is solubilized after 40 minutes of digestion. The specific cholinesterase activity and the protein

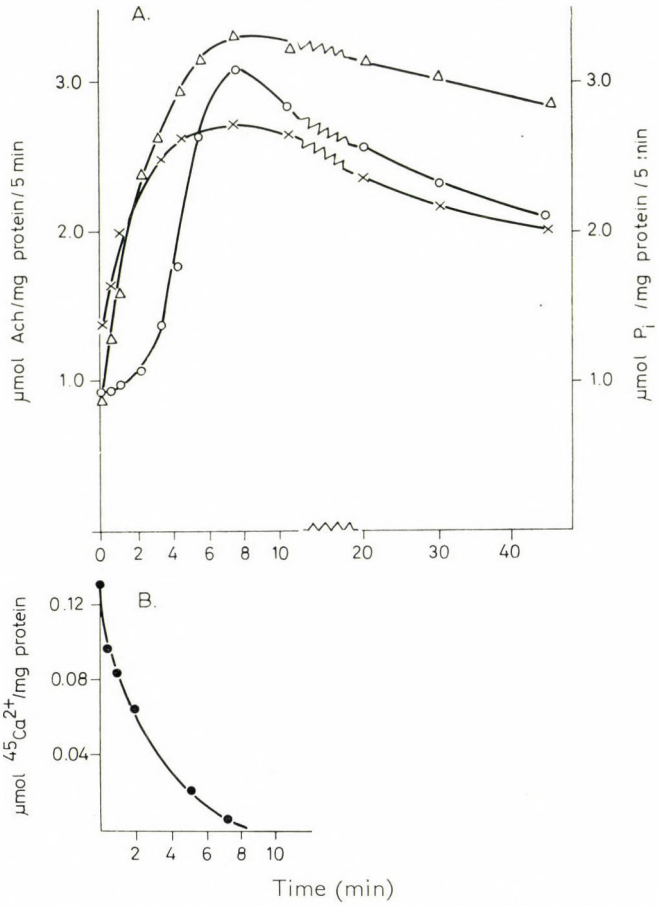

Fig. 2. Effect of trypsin on the functional properties of SRF from fish muscle. Trypsin : protein = 1 : 62. Composition of the incubation mixture for ATPase measurements: 0.05 M KCl + 0.002 M ATP + 0.002 M $MgCl_2$ + 0.00 or 0.06 mM $^{45}CaCl_2$ + 0.01 M Tris-maleate buffer, pH 7.0. For cholinesterase measurements the same incubation mixture was used with 0.0015 M acetylcholine instead of 0.002 M ATP. The experiments were carried out at room temperature: ○——○ ATPase activity in the absence of Ca^{2+}; ×——× ATPase activity in the presence of 0.06 mM Ca^{2+}; △——△ cholinesterase activity; ●——● $^{45}Ca^{2+}$ uptake

content of the supernatant are 40 times and 8 times as high as those of the control supernatant, respectively, which indicates that the increase in cholinesterase activity is not simply a consequence of being released from the structure.

Change in the activation by Ca^{2+} of the ATPase of SRF on tryptic digestion. A further analysis of the data on the tryptic digestion of SRF reveals that there are differences between individual SRF preparations as regards the susceptibility of ATPase to be activated by Ca^{2+}.

The activation of ATPase by Ca^{2+} is presented in Table 3. Here the ratios of ATPase activities in the presence of Ca^{2+} to those in the absence of Ca^{2+} are

Table 1

Maximal increase of enzyme activities (ATPase and cholinesterase) occurring on tryptic digestion of fish muscle SRF

Experimental conditions: SRF from fish muscle was digested by trypsin at the indicated trypsin : protein ratios, under the conditions specified in Materials and methods. ATPase and cholinesterase activities were measured at 23°C as described in Materials and methods

No.	Trypsin : protein ratio	Increase as compared to the control (= 1.00)		
		Cholinesterase	Adenosine triphosphatase	
			in the absence of Ca^{2+}	in the presence* of Ca^{2+}
1	1 : 24	3.04	4.16	2.32
2	1 : 16	7.20	3.85	2.64
3	1 : 14	3.50	3.26	2.30
4	1 : 14	4.95	3.73	1.76
5	1 : 62	3.80	3.46	2.05
6a	1 : 5	4.23	2.92	2.60
6b	1 : 18	4.00	3.55	3.20
7	1 : 15	3.80	1.14	1.98
8a	1 : 14	2.71	1.92	1.75
8b	1 : 50	2.12	2.27	2.08

* 0.06 mM $CaCl_2$

Table 2

Distribution of protein content and cholinesterase activity (Che) in fish muscle SRF before and after tryptic digestion

Cholinesterase activity was measured at 23°C under the conditions specified in Materials and methods. For other details see the text. The experiment was repeated 5 times with similar results. Trypsin : protein ratio = 1 : 14

Preparation	Protein mg/ml	Total Che activity μmole ACh/ml/hour	Specific Che activity μM ACh/mg prot/hour	Che spec. act. (fraction tested) / Che spec. act. (control SRF)
Undigested SRF	10.0	50.00	5.0	1.00
Sediment of undigested SRF	9.4	44.16	4.6	0.92
Supernatant of undigested SRF*	0.5	0.15	0.3	0.06
Digested SRF	9.9	100.00	10.1	2.02
Sediment of digested SRF	5.8	74.24	12.8	2.80
Supernatant of digested SRF	4.0	48.00	12.0	2.40

* After centrifugation at $60\,000 \times g$ the supernatant of undigested SRF contains 5–8% of the total protein content of SRF. After concentration, this protein was studied in the analytical ultracentrifuge (Phywe U-77). On the basis of photographs taken under sedimentation the protein in the supernatant of undigested SRF was found to sediment with 9.2 *S* and to contain no microsomal fractions

Table 3

Change in the activation by Ca^{2+} of ATPase of fish muscle SRF as a function of time of tryptic digestion (0—5 minutes)

The extent of activation by Ca^{2} is expressed as the ratio of activity in the presence of 0.06 mM Ca^{2+} to that in the absence of Ca^{2+}. For experimental conditions see Table 1. The serial numbers indicate the same trypsin : protein ratios as in Table 1

No.	Digestion time, minute					
	0	1	2	3	4	5
1	1.74				1.00	0.85
2	1.92	1.75	1.68	1.69	1.53	1.22
3	1.34	1.97	1.50	1.53	1.06	1.00
4	1.80	1.63	1.60	1.66	1.51	1.30
5	1.54	2.10	2.30	1.80	1.51	0.97
6a	1.12	1.83	1.95	1.35		1.15
6b	1.12	1.68	1.78	1.57		1.61
7	1.98	1.07	1.00	1.00	1.00	
8a	1.07	1.30	1.51	1.49		1.20
8b	1.07	1.15	1.24	1.41		1.20

Table 4

Cholinesterase and ATPase activities of fish muscle SRF before tryptic digestion

ATPase and cholinesterase activities were measured at 23°C under the conditions specified in Materials and methods

No.	Cholinesterase activity	ATPase activity without Ca^{2+}
	μmole ACh/mg protein/5 minutes	μmole P_i/mg protein/5 minutes
1	1.45	1.12
2	0.77	0.80
4	0.74	0.91
7	1.15	1.17
Mean value:	1.03 ± 0.34	1.00 ± 0.17
3	1.20	1.11
5	1.69	0.90
6a		
6b	2.10	1.41
8a		
8b	2.01	0.74
Mean value:	1.75 ± 0.4	1.04 ± 0.29

summed up for different digestion times. If the ratio is 1.0 or lower, no activation by Ca^{2+} takes place. In these ATPase measurements incubation time was 5 minutes in each case.

It is seen in some SRF preparations Ca^{2+} activation of ATPase is maximal without tryptic digestion, i.e. at 0 time of digestion (1, 2, 4, 7), whereas in other preparations activation reaches its maximum after 1 minute (3), 2 minutes (5, 6a, 6b, 8a) or 3 minutes (8b) of tryptic digestion.

These data are not inconsistent with those of Table 1, as in Table 1 the maxima of the increase in ATPase activities measured in the presence of Ca^{2+} are listed and not the extent of activation by Ca^{2+}.

Our SRF preparations could be divided into two groups on the basis of the tryptic modification of ATPase activity, measured in the presence of Ca^{2+}, independent of the fact that our experiments were carried out with fresh preparations and under standard conditions. The differences observed in the behaviour of the individual preparations are probably due to variations in some still unknown environmental factors.

It is seen in Table 4 that there is no difference between the ATPase activities, measured in the absence of Ca^{2+}, of preparations 0, 2, 4, and 7 (first group) and those of preparations 3, 5, 6a, 6b, 8a and 8b (second group). The mean value of ATPase activity is 1.00 ± 0.17 μmoles/mg protein/5′ for the first group, and 1.04 ± 0.29 μmoles/mg protein/5 minutes for the second group.

However, the cholinesterase activities of the two groups are different: 1.03 ± 0.34 μmoles ACh/mg protein/5 minutes for the first group and 1.75 ± 0.4 μmoles ACh/mg protein/5 minutes for the second. The difference between the cholinesterase activities of the two groups is significant.

Comparison of Tables 3 and 4 reveals a correlation between the cholinesterase activity of undigested SRF and the Ca^{2+} activation of its ATPase activity. The cholinesterase activity of undigested SRF is relatively low (1.03 ± 0.34, Table 4) in those preparations which display a decrease in Ca^{2+} activation of ATPase on tryptic digestion (Tables 3 and 4, preparations 1, 2, 4, 7). With preparations in which the Ca^{2+} activation of ATPase is temporarily increased on tryptic digestion (Table 3, preparations 3, 5, 6a, 6b, 8a, 8b), the cholinesterase activities of the undigested SRF are relatively high (1.75 ± 0.4, Table 4).

Discussion

The tryptic digestion of SRF from fish muscle results in the solubilization of 25–30% of the protein content of SRF during the first 20 minutes of digestion (Fig. 1).

The ATPase activity measured in the absence of Ca^{2+} and the cholinesterase activity of SRF from fish muscle are increased and Ca^{2+} uptake is decreased on tryptic digestion (Fig. 2). As regards ATPase activity and Ca^{2+} uptake similar results were published by Martonosi (1968), Ikemoto et al. (1968) and Inesi and Asai (1968) for SRF from rabbit muscle.

We have found earlier (Szabolcs et al., 1965, 1966) that SRF preparations from fish muscle possess a considerable cholinesterase activity. At the same time the cholinesterase activity of SRF from rabbit muscle prepared by differential centrifugation was described by Ulbrecht and Kruckenberg (1965). According to our measurements the cholinesterase activity of rabbit muscle is 0.3–0.4 μmoles ACh/mg protein/hour at 37°C whereas Ulbrecht and Kruckenberg reported an activity of 7–8 μmoles ACh/mg protein/hour at 37°C. The cholinesterase activity of fish muscle SRF is 100–200 times as high as that of rabbit muscle.

It appears from Table 1 that on tryptic digestion of SRF, cholinesterase activity is increased to a higher extent than the ATPase activity. The cholinesterase activity of SRF cannot be removed by washing and on storage at 0°C it is increased parallel with ATPase activity (Szabolcs et al., 1966). This led us to the conclusion that cholinesterase molecules were integral parts of SRF. Our results presented in Table 2 supply further data to support this view. In the supernatant of SRF digest with trypsin for 40 minutes specific cholinesterase activity is 40-fold increased. This may indicate that, released from the structure of SRF, cholinesterase molecules assume a more favourable three-dimensional structure, which results in such an increased cholinesterase activity that is not proportional to, but considerably higher than the amount of protein released. On tryptic digestion of SRF from rabbit muscle, ATPase activity remains associated with the membranes as it can be sedimented by centrifugation at $30\,000 \times g$ for 1 hour (Martonosi, 1968). Part of the cholinesterase activity of SRF from fish muscle, however, is solubilized under similar conditions.

Ikemoto et al. (1968) demonstrated the changes of ATPase activity brought about by tryptic digestion of mouse muscle SRF also by means of a histochemical reaction detected under the electron microscope. These authors assume that in the course of tryptic digestion the ATPase active sites are rearranged, which causes an increase in ATPase activity.

It is apparent from the data of Table 3 that in certain cases (Table 3, preparations 3, 5, 6a, 6b, 8a, 8b), the activation by Ca^{2+} of the ATPase is not decreased but rather increased at the beginning of tryptic digestion. In spite of this, however, the Ca^{2+} uptake of SRF decreased in even case, as shown in Fig. 2. These observations suggest that the structure of SRF is changed by tryptic digestion. This alteration may be submicroscopic, detectable by the electron microscope, or it may be conformational change that cannot be resolved by this technique. It has been shown for rabbit muscle SRF (Inesi, Asai, 1968; Martonosi, 1968) and mouse muscle SRF (Ikemoto et al., 1968) that the functional changes brought about by tryptic digestion are accompanied by morphological changes at the submicroscopic level.

The cholinesterase activities of the undigested preparations are not identical (Table 4): the SRF preparations in which ATPase activity, measured in the presence of Ca^{2+}, does not increase after tryptic digestion, possess a lower cholinesterase activity. It is evident when comparing the data in Tables 3 and 4 that there exists a correlation between the cholinesterase activity and the activation by Ca^{2+} of the ATPase of any given SRF preparation. In our opinion the

ordered structural integrity of SRF can be estimated on the basis of its cholinesterase activity.

The authors wish to thank Prof. Dr Emil Varga for his useful advices and support and Mrs E. Csorba and Mrs K. Móré for the technical assistance.

References

Hestrin, S. (1949) J. Biol. Chem. *180* 249
Ikemoto, N., Sreter, F. A., Nakamura, A., Gergely, J. (1968) J. Ultrastructure Res. *23* 216
Inesi, G., Asai, H. (1968) Arch. Biochem. Biophys. *126* 469
Laskowski, M., Sr., Kassell, B., Peanasky, R. J., Laskowski, M., Jr. (1966) in Handbuch der physiologisch- und pathologisch-chemischen Analyse, Lang, K., Lehnartz, E. (eds) Springer Verlag Berlin *6*, C part, pp. 248—250.
Martonosi, A. (1964) Fed. Proc. *23* 913
Martonosi, A. (1968) J. Biol. Chem. *243* 71
Szabolcs, M., Kövér, A., Kovács, L., Csabai, A. (1965) Magyar Biokémiai Társaság II. Nagygyűlése, Bp. Előadáskivonatok p. 43
Szabolcs, M., Kövér, A., Kovács, L., Rácz, M. (1966) Acta Biochim. Biophys. Acad. Sci. Hung. *1* 233
Szabolcs, M., Kövér, A. (1966) Acta Biochim. Biophys. Acad. Sci. Hung. *1* 159
Taussky, H. H., Shorr, E. (1953) J. Biol. Chem. *202* 675
Ulbrecht, G., Kruckenberg, P. (1965) Nature *206* 305

Acta Biochim. et Biophys. Acad. Sci. Hung. Vol. 9 (4), pp. 349—357 (1974)

The Role of Membrane-Bound Ca^{2+} in the Regulation of Sarcoplasmic Reticulum Function

A. KÖVÉR, M. SZABOLCS, A. CSABAI, Z. NAGY

Institute of Physiology and Central Research Laboratory, University School of Medicine, Debrecen, Hungary

(Received July 8, 1973)

Sarcoplasmic reticular fractions (SRF) were prepared from the white muscle of catfish *(Amiurus nebulosus)*. The functional role of membrane-bound Ca^{2+} and the effect of its removal on the properties of SRF were studied. It was established that on treatment with EGTA at a final concentration of 1 mM at pH = 7.1—8.0, the cholinesterase activity, as well as ATPase activity in the presence and absence of Ca^{2+}, of SRF is manifold increased, whereas Ca^{2+} uptake is practically arrested. The changes in Ca^{2+}, Mg^{2+} and Zn^{2+} contents of the sarcoplasmic reticular fraction were also studied. It was found that, out of the divalent cations tested, it is only the about 70% decrease of Ca^{2+} content that can be correlated with the functional changes observed.

Introduction

It is well-known from the literature that Ca^{2+} plays an important role in the regulation of permeability of surface membranes (Cole, 1941, 1949; Gordon, Welsh, 1948; Hodgkin et al., 1949; Brink, 1954; Shanes, 1958; Tasaki et al., 1967; Watanabe et al., 1967; Bianchi, 1968). Very little is known, however, about the permeabilities of intracellular membranes, the sarcoplasmic reticulum (Hasselbach, 1964; Martonosi, Feretos, 1964; Weber, 1966; Duggan, Martonosi, 1970).

The sarcoplasmic reticulum* (SR) regulates the intracellular Ca^{2+} concentration of muscle cells (Weber, 1966; Bianchi, 1968; Ebashi, Endo, 1968; Sandow, 1970). It can be stated in general that Ca^{2+} accumulation, that depends upon SR ATPase activity, is responsible for the relaxation of striated muscle, while activation of the contractile system is brought about by the mobilization of Ca^{2+} accumulated in the SR. As under physiological conditions the amount of accumulated Ca^{2+} is strictly correlated with the cleavage of ATP used for active transport (Hasselbach, Makinose, 1962, 1963; Weber et al., 1966; Yamada et al., 1970; Kanazawa et al., 1971), from the change in this correlation conclusions can be drawn about the modification of membrane characteristics.

In the present work the role of membrane-bound Ca^{2+} and of other divalent cations in the determination of the functional state of SR membrane was studied.

* *Abbreviations used:* SR, sarcoplasmic reticulum; SRF, sarcoplasmic reticular fraction; ACh, Acetylcholine.

Materials and methods

Sarcoplasmic reticular fraction was prepared from the white skeletal muscle of the catfish *(Amiurus nebulosus)* by the method described earlier (Szabolcs et al., 1966). To remove myofibrillar proteins the fraction was suspended in a solution of 0.6 M KCl + 5 mM histidine, pH 7, and centrifuged at $25,000 \times g$ for 1 hour. The pellet was suspended in 0.1 M KCl and used for the experiments. In each experiment a fresh preparation produced the same day was used.

Determination of protein content was carried out by the micro-Kjeldahl or the biuret method (Layne, 1957).

Suspending *solution:* 0.1 M KCl. Buffered suspending solution: 0.1 M KCl + 5 mM histidine, pH. 7. EGTA stock solution: 10 mM, neutralized with KOH solution. KOH stock solution: 250 mM, from which Ca^{2+} was removed on a Dowex-50 column. ATP containing incubation mixture 0.1 M KCl + 5 mM ATP + 5 mM $MgCl_2$ + 5 mM potassium oxalate + 5 mM histidine + 0.1 mM EGTA + none or 0.15 mM $CaCl_2$, pH 7 (in the measurements of Ca^{2+} uptake the amount of $^{45}Ca^{2+}$ used for labelling was taken into account). Acetylcholine incubation mixture 0.1 M KCl + 5 mM histidine + 1.5 mM acetylcholine chloride, pH 7. All solutions were made in deionized water (resistance: 3×10^6 ohms).

The pH measurements were carried out on a Radiometer PHM 4c type pH-meter.

Ca^{2+} uptake was studied by the use of $^{45}Ca^{2+}$ and the Millipore filter technique. In order to decrease the specific adsorption of $^{45}Ca^{2+}$, filter paper discs were washed with 250 mM KCl and then with deionized water prior to use. Incubation time was 10 minutes. Aliquots of the incubation mixtures containing $^{45}Ca^{2+}$ and SRF were filtered through discs of 9 mm diameter made of HA Millipore filter paper (pore size: 0.45 μ) by a filtering equipment developed specially for this purpose and by vacuum air-pumps. The filtering process took 5 sec. After the filtration of the incubation mixture containing SRF, 3×1 ml of buffered suspending solution were sucked through the filter paper discs. The discs were placed on aluminium planchets, dissolved in glacial acetic acid, dispersed with ethanol, dried under an infrared lamp and their radioactivities were measured in an NK 108 counter. For the preparation of Ca^{2+} standard samples different amounts of the incubation mixture containing $^{45}Ca^{2+}$ were spread on filter paper discs 0.1 mg of SRF placed on aluminium planchets; the further procedures were as described above. Knowing the total Ca^{2+}-content and radioactivity of the incubating solution, we calculated the extent of Ca^{2+}-uptake from the activity of samples as compared to those of the standards.

The ATPase activity of samples was calculated on the ground of the increase in P_i content of the incubation mixtures – with and without SRF – after incubation for 10 minutes, at 23°C. The enzymic reaction was arrested by the addition of 10% trichloroacetic acid. Enzymic activities were measured in Ca^{2+}-free incubation mixtures, as well as in mixtures containing 0.15 mM Ca^{2+}. The difference between ATPase activities measured in Ca^{2+}-free and Ca^{2+} containing

incubation mixtures gives, the extent of activation by Ca^{2+} of the SRF, i.e. the so-called extra ATP splitting. P_i was determined according to Taussky and Shorr (1953).

Cholinesterase activities of the SRF samples were calculated from the decrease in ACh content measured after 10 minutes of incubation at 23°C in incubation mixtures, with and without SRF, containing initially 1.5 mM acetylcholine. ACh content was measured by the method of Hestrin (1949).

The divalent cation content of SRF was determined as follows. Treated and untreated SRF samples were diluted eightfold with buffered suspending solution and centrifuged for 90 minutes at $60{,}000 \times g$. The pellets were dissolved in silica glass flasks in 1 ml of perchloric acid with the stepwise addition 0.5 ml of 30% H_2O_2. The solutions obtained were made to equal volume in calibrated polyethylene tubes with deionized water.

The divalent cation content of the solutions was measured by an atomic absorption spectrophotometer (Unicam SP 90 A) and spectrographically (Zeiss Q 24), by using Sr as an internal standard. At the same time, the nitrogen content of the solutions was measured by the micro-Kjeldahl method and their P_i content according to Taussky and Shorr (1953). Cation content of the samples was expressed per mg nitrogen content.

ATP (Reanal) freed from Ca^{2+} according to Seidel and Gergely (1963); acetylcholine chloride (VEB Berlin-Chemie); EGTA (Fluka); $^{45}CaCl_2$ (OAB Isotope Institute) specific activity 2.68 Ci/g; all other chemicals were analytical grade Reanal preparations.

Results

Effect of EGTA on the properties of SRF at different pH values. To 1 ml of SRF of 4 mg/ml protein concentration suspended in 0.1 M KCl, 0.11 ml of 10 mM EGTA solution was added (final concentration of EGTA 1 mM). To 1 ml of each sample not to be treated with EGTA 0.11 ml of deionized water was added. The pH was then adjusted to the values shown in Fig. 1 by the addition of KOH solution and the samples were kept at 0°C for 5 min. The samples were then diluted to a final volume of 8 ml with the suspending solution. Aliquots of the diluted SRF suspension were the taken for the measurement of ATPase and cholinesterase activities, and of Ca^{2+} uptake 1 min after treatment and dilution. The samples were further diluted with the incubating solutions 20-fold in the case of measurements of ATPase and Ca^{2+} uptake, and 25-fold in the cholinesterase assay, thus the EGTA and pH-treatment practically did not change the EGTA concentration and pH of the incubating solutions.

The adjustment of pH to 6.2, 7.1 and 8.0 (Fig. 1, columns 1, 3 and 5) alone did not markedly influence the functional state of SRF. After treatment with 1 mM of EGTA, however, definite changes were observed when the pH of the samples was adjusted to 7.1 (Fig. 1, column 4) or 8.0 (Fig. 1, column 6). In these cases Ca^{2+} uptake by SRF decreased practically to zero, while its cholinesterase and ATPase activities were considerably increased. It is remarkable

that ATPase activity in the presence of Ca^{2+} (Fig. 1, columns 4 and 6) increased to a much higher extent at pH 7.1 and 8.0, as compared to samples not treated with EGTA (Figs 1, 3, 5) than did control ATPase activity measured tn the absence of Ca^{2+}. As the difference between these two activities given the measure of ATPase activity linked to Ca^{2+} transport (extra ATP splitting), ihis observation may be interpreted so that the decrease or cessation of Ca^{2+}

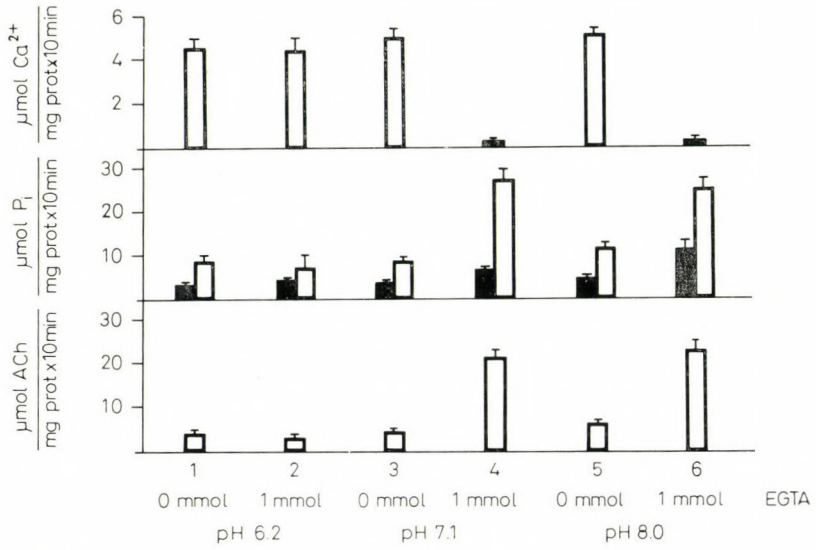

Fig. 1. Effect of EGTA on the properties of SRF at different pH values. In the upper row of columns the Ca^{2+} uptake of SRF, in the middle row control ATPase activities (■) and those measured in the presence of 0.15 mM Ca^{2+} (▁), and in the lower row cholinesterase activities are shown in the units indicated on the ordinates. On the common abscissa the serial numbers of columns corresponding to each other in respect of treatments, and below them the way of treatment of the individual samples are indicated. For other details see Materials and methods and the text. Standard deviation is shown on the columns, n = 9

uptake was brought about parallel with the increase in extra splitting ATP. This means at the same time that the well-known strict correlation between extra ATP splitting and Ca^{2+} uptake has also vanished.

Effect of different concentrations of EGTA on the state of SRF. In another series of experiments, after the addition of EGTA the pH of SRF samples was adjusted to 7.1. In the case of 0.2 mM EGTA (Fig. 2, column 3) the extent of Ca^{2+} uptake decreased by 80%, with a simultaneous 2-fold increase in cholinesterase activity. The ATPase activities are hardly influenced at all by this EGTA concentration. Treatment of SRF samples with 0.4 mM EGTA (Fig. 2, column 4), however, results in a further decrease in Ca^{2+} uptake and, in addition to a further increase in cholinesterase activity, in a 3-fold rise in extra ATP splitting. The

effect of higher concentrations of EGTA during pretreatment (Fig. 2, columns 5, 6, 7) was found to be essentially the same.

Effect of Ca^{2+} on the functional changes of SRF induced by treatment with EGTA. In these experiments we examined whether the functional alterations observed on treatment of SRF with 1 mM EGTA at pH 7, 1, i.e. increase in ATP-ase activity, in extra ATP splitting and cholinesterase activity and decrease in

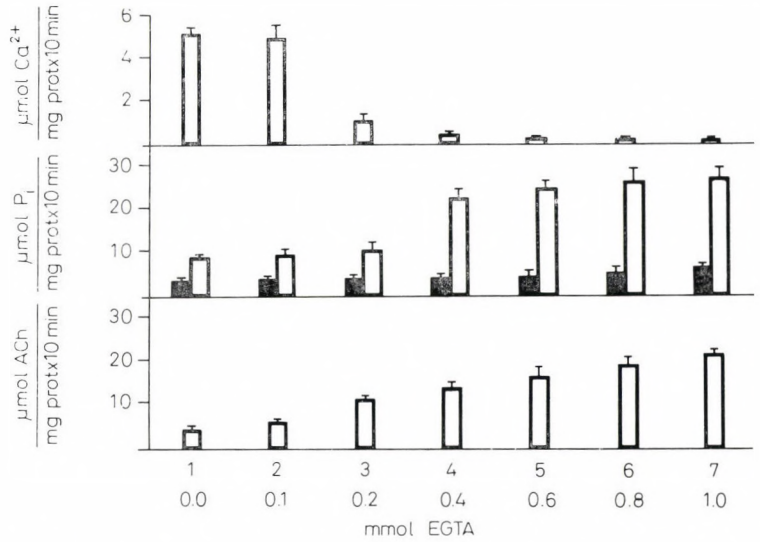

Fig. 2. Effect of various EGTA concentrations on the properties of SFR. The upper row of columns shows the Ca^{2+} uptake of SRF, the middle row represents control ATPase activities (▬) and those measured in the presence of 0.15 mM of Ca^{2+} (▭), and in the lower row cholinesterase activities are shown in the units indicated on the ordinates. On the common abscissa the serial numbers of columns corresponding to each other in respect of treatment and below them, the way of treatment of the individual samples are indicated. For other details see Materials and methods, and the text. Standard deviation is shown on the columns, n = 6

Ca^{2+} uptake can be reversed or prevented by the addition of Ca^{2+} to the SRF samples at a final concentration of 2 mM (Fig. 3). If Ca^{2+} was added after the addition of EGTA (at a final concentration of 1 mM) and the adjustment of pH to 7.1 (Fig. 3, column 3), the effect of EGTA was practically not modified by Ca^{2+}. However, if Ca^{2+} was added after EGTA to the SRF samples but before the adjustment of pH to 7.1 (Fig. 3, column 4), it prevented the effect of EGTA completely. A similar result was obtained if Ca^{2+} was added before EGTA (Fig. 3, column 5). It must be noted that under the above conditions 1 mM Ca^{2+} had only a partial protective effect.

Change in the divalent cation content of SRF on treatment with EGTA. Treatment of SRF samples with EGTA at pH 6.2 and 7.1 was carried out as

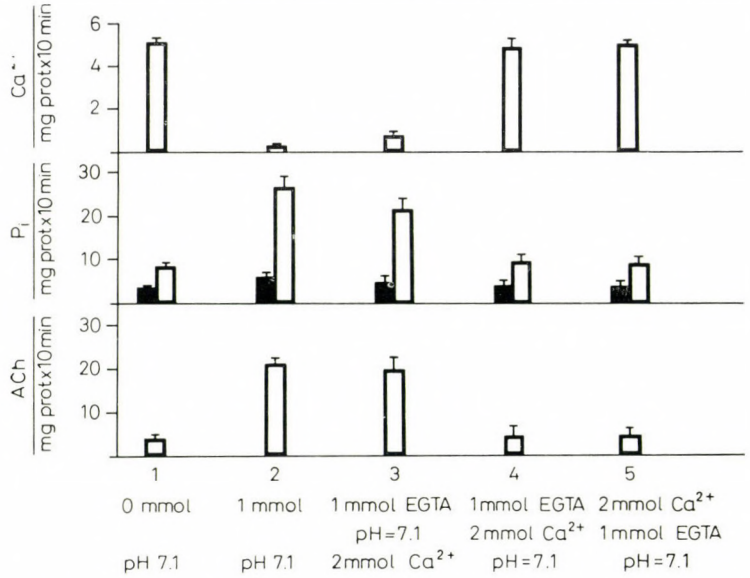

Fig. 3. Effect of Ca^{2+} on the functional changes of SRF induced by treatment with EGTA. The upper row of columns shows the Ca^{2+} uptake of SRF, the middle row represents control ATPase activities (▩) and those measured in the presence of 0.15 mM of Ca^{2+} (□), the lower row shows cholinesterase activities in the units indicated on the ordinates. On the common abscissa the serial numbers of the columns corresponding to each other in respect of treatment, and below them the way of treatment (i.e. the order of addition of chemicals and pH adjustment) are shown. For other details see Materials and methods, and the text. Standard deviation is shown on the columns, n = 6

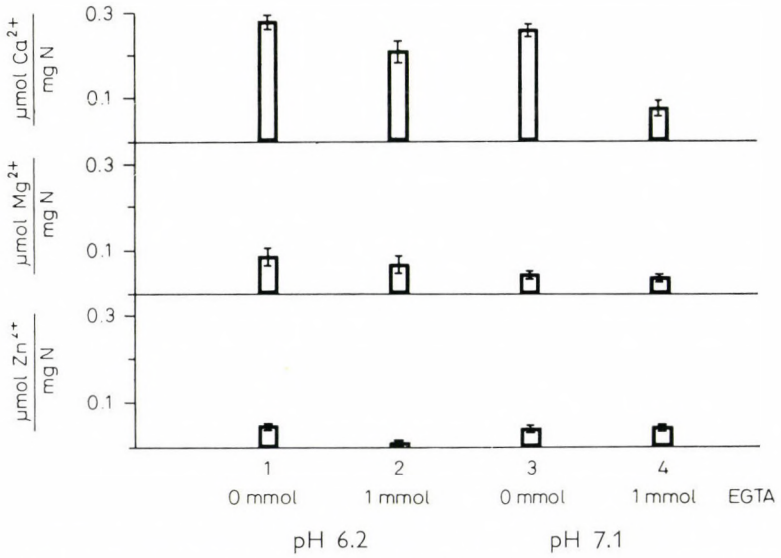

Fig. 4. Changes in the divalent cation content of SRF induced by treatment with EGTA. The upper row of columns represents the Ca^{2+} content, the middle row the Mg^{2+} content

described for the experiments shown in Fig. 1. The samples were then diluted, centrifuged, and the pellet dissolved as described in Materials and methods. The total nitrogen and total P_i contents of the dissolved samples were identical within 5% limits of error independently of the way of treatment, which indicates that the structure of SRF was not solubilized by the procedures used.

As shown by our atomic absorption measurements, the Ca^{2+}, Mg^{2+} and Zn^{2+} contents of the dissolved samples differ according to the way of treatment (Fig. 4). From the elements studied, only the about 70% decrease of Ca^{2+} content of SRF can be correlated to the change of the functional state of SRF (cf. Fig. 1, columns 3, 4 and Fig. 4, columns 3 and 4).

The spectrographic analysis of the dissolved samples shows that the Ca^{2+} and Mg^{2+} contents of SRF were similar to those presented in Fig. 4. At the pH values specified above, the Fe^{3+}, Mn^{2+}, Cu^{2+} and Pb^{2+} contents of SRF were essentially unaffected by treatment with EGTA.

Discussion

Recently more and more data support the assumption that the Ca^{2+} uptake of sarcoplasmic reticulum is strictly correlated to the concomitant ATP cleavage (Ca^{2+}/ATP = 2) (Hasselbach, Makinose, 1962, 1963; Weber et al., 1966; Yamada et al., 1970; Kanazawa et al., 1971). From the change of this correlation one can draw conclusions concerning the modification of membrane permeability (Duggan, Martonosi, 1970; Weber, 1971a).

Our results (Fig. 1) clearly show that the adjustment of pH of SRF suspension to 7.1 or 8.0 alone, i.e. the decrease of relative proton content of the membrane fragments, does not lead to functional changes. However, if the pH of the suspension is adjusted to the above values in the presence of 1 mM of EGTA, both cholinesterase and ATPase (in the presence of Ca^{2+}) activities, as well as the extent of extra ATP cleavage are manifold increased as compared to the control sample, while the Ca^{2+} uptake of the fraction practically ceases. At pH 7.1 EGTA 0.2 mM (Fig. 2) brings about an increase in cholinesterase activity of SRF, also accompanied by the decrease in Ca^{2+}-uptake. In both cases the Ca^{2+}/ATP ratio is altered, the inference being that the permeability of the membrane is increased. Under the experimental conditions applied, the functional changes occurring after treatment with EGTA and the pH adjustment cannot be influenced by the subsequent addition of Ca^{2+} to the suspension (Fig. 3).

According to data in the literature (Hasselbach, Makinose, 1963; Onishi, Ebashi, 1964; Makinose, Hasselbach, 1965; Weber et al., 1966; Harigaya et al.,

---

and the lower row the Zn^{2+} content of SRF in the units indicated on the ordinates. On the common abscissa the serial numbers of the columns corresponding to each other in respect of treatment, and below them the way of treatment of the individual samples are shown. For other details see Materials and methods, and the text. Standard deviation is shown on the columns, n = 8

1968; Weber, 1968; Yamamoto, Tonomura, 1968; Makinose, 1969; Weber, 1971a, 1971b) the immediate external and internal (intravesicular) Ca^{2+} concentrations of SR markedly influence the extent of Ca^{2+} accumulation and the ATPase activity linked to it, as well as the mobilization of Ca^{2+} stored in the SR. It seems probable from the results of Duggan and Martonosi (1970) and Weber (1971a) that ATPase is released from the regulatory effect of intravesicular Ca^{2+} concentration, owing to an increase in membrane permeability which results in a considerable increase in the Ca^{2+}-dependent ATP splitting and in the modification of the Ca^{2+}/ATP ratio.

It has earlier been observed that chelators increase the permeability of membranes depending upon the pH of the medium (Molnár, Loránd, 1962; Abrams, 1965; Settlemire et al., 1968). On the ground of our and other authors' results it can also be supposed that certain chelators exert their effect by removing membrane-bound Ca^{2+} (Fig. 4; Duggan, Martonosi, 1970). In our experiments, too, it is the structural changes induced by the removal of membrane-bound Ca^{2+} that manifest themselves in the increase of cholinesterase activity. This is supported by earlier results from this laboratory (Szabolcs et al., 1966; Kövér, Szabolcs, 1967; Szabolcs, Kövér, 1967) which showed that any kind of structural disorganization of SRF brought about an increase in cholinesterase activity, in addition to arresting Ca^{2+} uptake. At the same time, our experiments on SRF prepared from the muscle of rabbits of different ages indicated that parallel to the progress of structural organization, the increase of the Ca^{2+} uptake of SRF is accompanied by a decrease in cholinesterase activity (Szabolcs et al., 1967).

With the knowledge of literary data, the following conclusion can be drawn from our present results. In SRF prepared from the skeletal muscle of the catfish Ca^{2+} constitutes an integral part of the membrane and the presence or absence of membrane-bound Ca^{2+} fundamentally determines the permeability and other functional properties of the membrane.

The authors are indebted to Prof. Emil Varga for his useful advices and for supporting their work, to Dr Jakab Loch for the atomic absorption measurements, and to Mrs E. Csorba, Miss Florence Jeney and Mrs K. Móré for technical assistance.

References

Abrams, A. (1965) J. Biol. Chem. *240* 3675
Bianchi, C. P. (1968) Cell Calcium. Butterworths
Brink, F. (1954) Pharmacol. Rev. *6* 243
Cole, K. S. (1941) Cold Spring Harbour Symp. Quant. Biol. *8* 110
Cole, K. S. (1949) Arch. Sci. Physiol. *3* 253
Duggan, P. F., Martonosi, A. (1970) J. Gen. Physiol. *56* 147
Ebashi, S., Endo, M. (1968) Progr. Biophys. Mol. Biol. *18* 123
Gordon, H. T., Welsh, J. H. (1948) J. Cell. comp. Physiol. *31* 395
Harigaya, S., Ogawa, Y., Sugita, H. (1968) J. Biochem. *63* 324
Hasselbach, W. (1964) Progr. Biophys. Mol. Biol. *14* 167

Hasselbach, W., Makinose, M. (1962) Biochem. Biophys. Res. Comm. *7* 132
Hasselbach, W., Makinose, M. (1963) Biochem. Z. *339* 94
Hestrin, S. (1949) J. Biol. Chem. *180* 249
Hodgkin, A. L., Huxley, A. F., Katz, B. (1949) Arch. Sci. Physiol. *3* 129
Kanazawa, T., Yamada, S., Yamamoto, T., Tonomura, Y. (1971) J. Biochem. *70* 95
Kövér, A., Szabolcs, M. (1967) Acta Biochim. Biophys. Acad. Sci. Hung. *2* Suppl. 61
Makinose, M. (1969) Eur. J. Biochem. *10* 74
Makinose, M., Hasselbach, W. (1965) Biochem. Z. *343* 360
Martonosi, A., Feretos, R. (1964) J. Biol. Chem. *239* 648
Molnár, J., Loránd, L. (1962) Arch. Biochem. Biophys. *98* 356
Ohnishi, T., Ebashi, S. (1964) J. Biochem. *55* 599
Sandow, A. (1970) Annual Rev. Physiol. *32* 87
Seidel, J. C., Gergely, J. (1963) J. Biol. Chem. *238* 3648
Settlemire, C. T., Hunter, G. R., Brierley, G. P. (1968) Biochim. Biophys. Acta *162* 487
Shanes, A. M. (1958) Pharmacol. Rev. *10* 87
Szabolcs, M., Kövér, A. (1967) Acta Biochim. Biophys. Acad. Sci. Hung. *2* Suppl. 104
Szabolcs, M., Kövér, A., Kovács, L. (1967) Acta Biochim. Biophys. Acad. Sci. Hung. *2* 409
Szabolcs, M., Kövér, A., Kovács, L., Rácz, M. (1966) Acta Biochim. Biophys. Acad. Sci. Hung. *1* 233
Tasaki, I., Watanabe, A., Lerman, L. (1967) Am. J. Physiol. *213* 1465
Taussky, H. H., Shorr, E. (1953) J. Biol. Chem. *202* 675
Watanabe, A., Tasaki, I., Lerman, L. (1967) Proc. Natl. Acad. Sci. U. S. *58* 2246
Weber, A. (1966) Curr. Top. Bioenerg. *1* 203
Weber, A. (1968) J. gen. Physiol. *52* 760
Weber, A. (1971a) J. gen. Physiol. *57* 50
Weber, A. (1971b) J. gen. Physiol. *57* 64
Weber, A., Herz, R., Reiss, I. (1966) Biochem. Z. *345* 329
Yamada, S., Yamato, T., Tonomura, Y. (1970) J. Biochem. *67* 789
Yamamoto, T., Tonomura, Y. (1968) J. Biochem. *64* 137

Acta Biochim. et Biophys. Acad. Sci. Hung. Vol. 9 (4), pp. 359—366 (1974)

Osmosis; Facts and Theories

II. Volume Flow towards Higher Vapour Pressure and Nonlinearity

F. VETŐ

Biophysical Institute, Medical University, Pécs, Hungary

(Received December 20, 1973)

Volume flow of concentrated D_2O of lower vapour pressure into normal watery solutions of higher vapour pressure was demonstrated in osmometers containing $Cu_2Fe(CN)_6$ membrane. Such a volume flow, directed towards a solution of higher vapour pressure, occurred several times also among normal watery solutions containing different solutes. Thus, knowing only the difference of vapour pressure we cannot reliably conclude to the direction and extent of osmotic substance flows on real membranes.

In our osmometer systems the volume flow caused by pressure difference exhibited non-linear characteristic curves in several cases, and even explicitly rectifying characteristics appeared. These findings indicate that linear theories can be applied for describing real transport processes but to a limited degree.

Introduction

In a previous paper (Vető, 1974) we reported osmometric experiments in which an osmosis, volume flow, of pure H_2O took place through a $Cu_2Fe(CN)_6$ membrane into D_2O solution of 99.75 per cent. This happens in some cases even against remarkable pressure (e.g. 1.6 atm) without the presence of dissolved crystalloids or colloids and other forces. It seems that the process can be interpreted in a simple way on the basis of the vapour pressure theory, i.e. H_2O of higher vapour pressure (17.53 mmHg at 20°C) flows into D_2O of lower vapour pressure (14.97 mmHg at 20°C). In connection with this the following questions arise:

If it is only the difference of vapour pressure what really counts one can expect that, if the vapour pressure of pure H_2O is somewhat decreased by dissolved crystalloids, water will flow from this solution still having a higher vapour pressure into heavy water of lower vapour pressure. Is that so? Can every real osmotic volume flow be generally interpreted (at least qualitatively, considering its direction) on the basis of vapour pressure difference of the solvent (water)?

How do experimental data harmonize with the linear nonequilibrium thermodynamical method of description?

What conclusions can be drawn for the role of the structure (complex and interactions, respectively, of membrane – water – solutes)?

It was the aim of the experiments to collect data for answering the above questions.

Methods*

The experiments were performed in osmometers, described previously (Vető, 1974), containing $Cu_2Fe(CN)_6$ membrane (or heat coagulated egg-white) in the wall of the clay cylinder. One cell was constituted by the inner volume (about 80 cm^3) of the cylinder having a surface of 170 to 180 cm^2, while the other one by the volume (about 120 cm^3) surrounding the cylinders from the outside. These cells were filled with the solutions to be examined, and the extent of osmotic volume flow was read off on appropriately divided volume measuring tubes. Either of the cells could be placed under a pressure of maximum 2.00 atm with the aid of a pumpe and aneroid manometer. The experiments were performed at room temperature. For the solutions we used bidistilled water, analytically pure chemicals and heavy water (D_2O) of 99.75 per cent. Vapour pressure values of the solutions were calculated by using appropriate tables (Hodgman, 1953; Roth, Scheel, 1923) or measured with the aid of Hewlett–Packard's vapour pressure osmometer (type 301 A) whenever necessary (e.g. polyethylene glycol, PEG 6000). The amount of transmigrated substance was determined by volume measurement, density measurement with pycnometer and dry substance measurement. In these calculations the porous wall of the cylinder was considered retain about 30 cm^3 of water and solutes (the quantity of which was not exactly determined, but could be judged from the deficiencies). The concentration of solutions containing one dissolved component was continuously checked with a Zeiss's refractometer.

Results

1. Opposing heavy water of 99.75 per cent to watery solution of different crystalloids (urea, saccharose, NaCl) *concentrated heavy water, having lower vapour pressure, flowed into the normal watery solutions having significantly higher vapour pressure, through the membrane in every case* (Table 1*a*). When similar solutions were opposed to normal distilled water in the same apparatuses, the osmosis was normally directed from distilled water of higher vapour pressure towards solutions of lower vapour pressure (Table 1*b*). The time-course of experiments No. 4 of Table 1 is shown in Fig. 1. Thus, just like to H_2O, also D_2O flows towards urea solution, though its vapour pressure is significantly lower. Concentration measurements revealed that, while 7.5 cm^3 net volume flow occurred towards the urea solution placed in the outside cell, significantly more D_2O flowed here and, at the same time, normal watery urea solution flowed from here towards the inner D_2O. The concentration of every component was shifted to equilibrium during the whole process.

2. In the next type of our experiments the common watery solution of substance "a" was used on the one side of the membrane and the common watery

* With the technical assistance of Miss Gabriella Bod.

Table 1

Comparison of vapour pressure and volume flow values in watery solution — D_2O and watery solution — H_2O systems

No.	Quality of membrane	Outside		Inside		Volume flow	
		solution gmol/l water	vapour pressure at 20°C mmHg	solution	vapour pressure at 20C° mmHg	direction s = solution	speed cm^3/ hour
			1a				
1.	$Cu_2Fe(CN)_6$	NaCl 2.0	16.4	cc. D_2O	15.0	s ← D_2O	0.9
2.	$Cu_2Fe(CN)_6$	NaCl 0.5	17.3	cc. D_2O	15.0	s ← D_2O	0.3
3.	$Cu_2Fe(CN)_6$	urea 4.0	16.5	cc. D_2O	15.0	s ← D_2O	0.4
4.	$Cu_2Fe(CN)_6$	urea 4.0	16.5	cc. D_2O	15.0	s ← D_2O	0.3
5.	$Cu_2Fe(CN)_6$	urea 4.0	16.5	cc. D_2O	15.0	s ← D_2O	0.07
6.	$Cu_2Fe(CN)_6$	urea 1.0	17.3	cc. D_2O	15.0	s ← D_2O	0.06
7.	$Cu_2Fe(CN)_6$	urea 1.0	17.3	cc. D_2O	15.0	s ← D_2O	0.05
8.	$Cu_2Fe(CN)_6$	saccharose 1.0	17.3	cc. D_2O	15.0	s ← D_2O	0.14
9.	protein	saccharose 1.0	17.3	cc. D_2O	15.0	s ← D_2O	0.06
			1b				
1.	$Cu_2Fe(CN)_6$	H_2O	17.5	NaCl 1.4	16.8	H_2O → s	1.0
2.	$Cu_2Fe(CN)_6$	H_2O	17.5	NaCl 0.7	17.1	H_2O → s	0.6
3.	$Cu_2Fe(CN)_6$	urea 4.0	16.5	H_2O	17.5	s ← H_2O	0.5
4.	$Cu_2Fe(CN)_6$	urea 4.0	16.5	H_2O	17.5	s ← H_2O	0.5
5.	$Cu_2Fe(CN)_6$	urea 1.0	17.3	H_2O	17.5	s ← H_2O	0.05
6.	$Cu_2Fe(CN)_6$	urea 1.0	17.3	H_2O	17.5	s ← H_2O	0.09
7.	$Cu_2Fe(CN)_6$	urea 1.0	17.3	H_2O	17.5	s ← H_2O	0.10
8.	$Cu_2Fe(CN)_6$	saccharose 1.0	17.3	H_2O	17.5	s ← H_2O	0.22
9.	protein	saccharose 1.0	17.3	H_2O	17.5	s ← H_2O	0.07

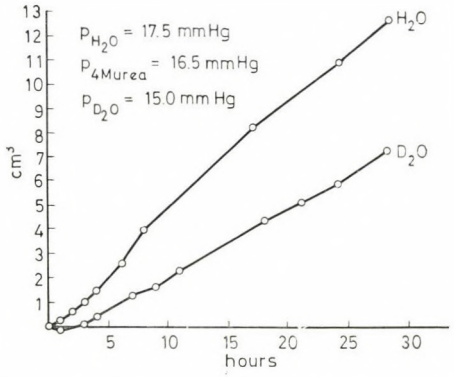

Fig. 1. Osmosis of H_2O and D_2O into urea solution of 4.0 osm/l

solution of substance "b" on the other side. In most of these experiments it was examined what the direction of volume flow was in the case of an osmolal concentration difference, i.e. vapour pressure difference and, in some others, whether the system was in "equilibrium" in the case of an equal osmolality? *When the common watery solution of substance "a" was placed on the one side of the membrane and the common watery solution of substance "b" on the other side in different osmolality, i.e. with different vapour pressure*, a volume flow corresponding to the vapour pressure difference was only obtained in about half of the experiments not treated here in detail. The other half of *the experiments produced a volume flow of opposite direction, i.e. one from a place of lower vapour pressure towards higher vapour pressure.* Table 2 contains the data of the latter experiments. Experiment No. 3 is especially striking here (protein membrane!); in this, a remarkable volume flow was observed from a NaCl solution of 0.5 osm/l higher concentration towards the more dilute saccharose solution.*

Table 2

Comparison of vapour pressure and volume flow values in systems of watery solution "a" and watery solution "b" containing different solutes

No.	Quality of membrane	Outside			Inside			Volume flow	
		solution g/l water	vapour pressure at 20°C mmHg	conc. osm/l	solution g/l water	vapour pressure at 20°C mmHg	conc. osm/l	direction i = inside o = outside	speed cm^3/hour measuring for 1–2 days
1.	$Cu_2Fe(CN)_6$	NaCl 42.80	17.10	1.46	sacchar. 342.30	17.24	1.00	o → i	0.04
2.	$Cu_2Fe(CN)_6$	sacchar. 342.30	17.24	1.00	NaCl 42.80	17.10	1.46	o ← i	0.05
3.	protein	NaCl 42.80	17.10	1.46	sacchar. 342.30	17.24	1.00	o → i	0.14
4.	protein	NaCl 42.80	17.10	1.46	sacchar. 342.30	17.24	1.00	o → i	0.02
5.	protein	NaCl 42.80	17.10	1.46	sacchar. 342.30	17.24	1.00	o → i	0.04
6.	$Cu_2Fe(CN)_6$	NaCl 4.73	17.49	0.15	PEG 133.00	17.51	0.06	o → i	0.04
7.	$Cu_2Fe(CN)_6$	NaCl 3.09	17.50	0.10	PEG 100.00	17.52	0.04	o → i	0.04
8.	$Cu_2Fe(CN)_6$	NaCl 116.91	16.33	3.73	KCl 159.17	16.33	3.73	o → i	0.05
9.	$Cu_2Fe(CN)_6$	NaCl 116.91	16.33	3.73	KCl 159.17	16.33	3.73	o → i	0.40

* We mention it as a rare "anomaly" that, in our practice, there occurred 3 model apparatuses in which volume flow was found from the more concentrate anelectrolyte solution towards the more dilute solution containing the same solute or water, respectively, through a $Cu_2Fe(CN)_6$ membrane, with a decrease of the concentration difference between the two cells.

3. The intensity of volume flow plotted against hydrostatic pressure difference (ΔP) was measured in the following series of experiments with the same distilled water (or 99.75 per cent heavy water) in both cells. Before the measurements the solutes were removed from the wall of the cylinder by repeated rinsing. For cylinders having small "factor of merit" (Vető, 1974), thus being of relatively great permeability, the relationship can be considered linear. But in certain cylinders having greater "factor of merit" *the intensity of volume flow is a non-linear function of the pressure difference according to our experimental data, and even the wall of the cylinder and the membrane, respectively, can have "rectifying characteristics" on water flow (e.g. Fig. 2).*

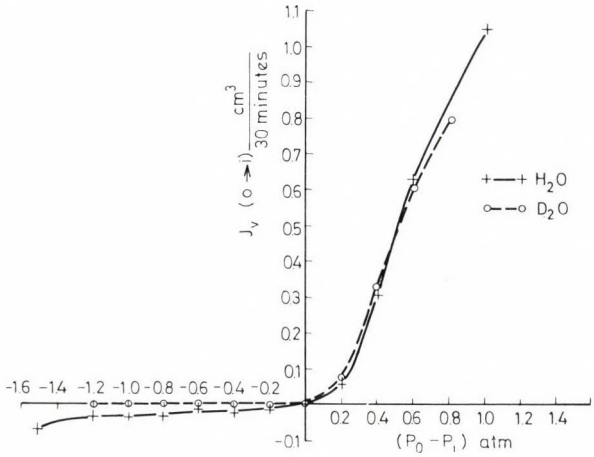

Fig. 2. H_2O and D_2O volume flow plotted against ΔP

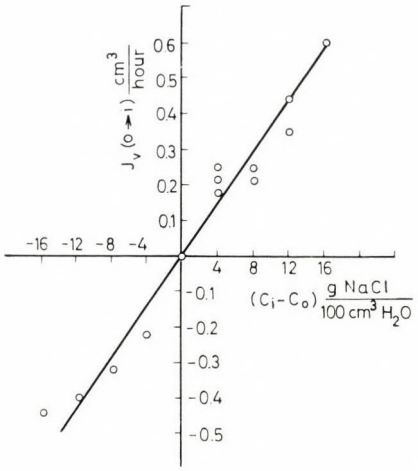

Fig. 3. Volume flow plotted against Δc

This shows different characteristics in each cylinder and also polarity of opposite direction occurs. Measurements performed with H_2O and D_2O gave approximately the same results.

4. Contrasting with this, when the intensity of volume current was measured so that there was NaCl solution of varying concentration in one cell and H_2O in the other, thus volume flow ($\Delta P = 0$) being examined as a function of concentration difference, the change *could be considered as linear* with a rough approximation, at least nonlinearity was less expressed (e.g. Fig. 3).

Discussion

The measured data unambiguously prove that we cannot reliably conclude to the extent of real osmotic substance flows and pressure values, and not even to their direction, if we know only the quantity, composition and vapour pressure (osmolal concentration or decrease of freezing point) of the compounds in question. These data only give information on the maximal working capacity supposed for an ideal case through chemical potential difference, thus only the *energetical possibility* is known. It is the *structural potentialities* and the dynamic interactions of components with each other and the membrane which determine what will really happen in a concrete system. The relationship $\pi = \frac{RT}{v} \ln \frac{p_0}{p_1}$ concerning equilibrium is only valid in an ideal semipermeable case, i.e. in the case of a membrane absolutely impermeable (!?) for every dissolved component, but the *processes* (e.g. the speed of migration of water) are determined by concrete structural–dynamical potentialities also in this case. Our data support the former findings concerning the *simultaneous* importance of energetics and structure, and are essentially in accordance with the experimental data interpreted on non-equilibrium thermodynamical basis with phenomenological and reflection coefficients characteristic of structure and interactions (e.g. Meschia, Setnikar, 1958; Kedem, Katchalsky, 1961; Ginzburg, Katchalsky, 1963; Lifson et al., 1960).

Accordingly, volume flow in systems of several components:

$$J_v = L_p(\Delta P - \sum_{i=1}^{n} \sigma_i \Delta \pi_i),$$

where L_p is the filtration coefficient, ΔP is the hydrostatic pressure difference, σ_i is a reflection coefficient for the individual solutes and $\Delta \pi_i$ is the osmotic pressure difference which, in an ideal case, can be calculated for each single dissolved component (Katchalsky, Curran, 1965). This is why, for instance, in our experiments with urea solution – D_2O ($\Delta P = 0$):

$$J_v = -L_p(\sigma_1 \Delta \pi_1 + \sigma_2 \Delta \pi_2).$$

Let us consider urea as solute 1 and D_2O as solute 2. The reflection coefficient estimable from our measurements (Vető, 1974) is of order of magnitude of

$\sigma_1 \approx 0.1$ for crystalloids and $\sigma_2 \approx 0.001$ for heavy water i.e. $\sigma_1 \gg \sigma_2$; thus it is understandable that the volume flow caused by urea solution of lower mol-concentration is greater than the volume flow caused by heavy water of higher mol-concentration. (The state of affairs is similar also in colloid-osmotic processes.)

Thus a part of our experimental results can be explained on the basis of the linear theory of nonequilibrium thermodynamics even in the case of different dissolved crystalloids, where supposedly $\sigma_a \neq \sigma_b$ because of the different molecule volume; and even the anomal "inverse" osmosis can be understood, if in these cases $\sigma < 0$ (negative), i.e. solute moves quicker than water. (The cause and structural-molecular mechanism of formation of this negative σ value are not known, the question deserves further examination.) With the aid of structural – dynamical parameters we can also explain the "inverse" *thermo-osmotic* experiments (e.g. with urea solution, Vető, 1969), during which volume flow proceeds towards warmer solutions of higher vapour pressure.

With recognition of the role of structure in transport processes importance has to be attached to the model experiments (e.g. on bimolecular lipid membranes, Karvaly, 1973; on liposomes, Haest, 1972) and measurements performed on biological units, which aim at determining these characteristic kinetic parameters and the underlying microphysical background (e.g. Bentzel et al., 1968; Leaf, 1965; Dainty, Ginzburg, 1964; Stadelmann, 1969; Stein, 1967; Bresler, 1973; Rapoport, 1973; Hempling, 1973). The recognition of the complex constituted by membrane-water-solutes and its dynamic characteristics will probably enable us to obtain an explanation of the nonlinear nature of pressure-volume curves experienced. The experienced nonlinearity, the invalidity of the Hagen – Poisseuille law raise the necessity of the study of microviscosity and rheology of this complex, in addition to other examinations aimed at throwing light on the structure anomalies caused by the interactions of solid surface-water-dissolved components (e.g. Weyl, Ormsby, 1960; Dreyer, Kahrig et al., 1969; Drost-Hansen, 1970; Erdey-Grúz, 1971).

As to the surprising water flow-rectifying characteristic, we do not know the cause and mechanism of its formation. This problem also deserves further examination. In any case, the polarity of individual membranes, membrane systems has been known, and debated, in the literature for a long time (e.g. Kamiya, Tazawa, 1956; Kamiya et al., 1962; Dainty, 1963; Van Bruggen, et al., 1973). The consequences of this polarity are far-reaching both from practical and theoretical point of view. Realization e.g. of the analogues of electric phenomena (rectification, amplification, oscillations, etc.) with membrane systems, by means of water and substance flows, can be of an essential possibility for practice. Of the phenomenological theories we only refer to the necessity of developing non-linear thermodynamics (efforts of such direction e.g. Gyarmati, 1961; 1970; Kedem, 1972), since Onsager's phenomenological equations and the above equation suppose linear connections, which restrict the practical applicability of the theory. This is demonstrated by the above nonlinear data which need further corroboration and explanation (Fig. 2).

Relying upon all these findings the author supposes that one can approach to the exact exploration of biological transport processes by phenomenological, and then molecular-microphysical recognition of the processes of relatively simpler physical-chemical models not at all unproblematic nowadays.

References

Bentzel, C. J., Davies, M., Scott, W. N., Zatzman, M., Solomon, A. K. (1968) J. Gen. Physiol. *51* 517–533

Bresler, E. H. (1973) Abstracts Biophys. Soc. Ann. Meeting, Columbus, p. 106a

Dainty, J. (1963) Advan. Botan. Res. *1* 279

Dainty, J., Ginzburg, B. Z. (1964) Biochim. Biophys. Acta *79* 102

Dreyer, G., Kahrig, E., Kirstein, D., Erpenbeck, J., Lange, Fr. (1969) Naturwissenschaften *56* 558–559

Drost-Hansen, W. (1970) in: Physical Principles of Biological Membranes (ed.) Snell, F. et al. Gordon and Breach New York p. 243

Erdey-Grúz, T. (1971) Transport Processes in Watery Solutions (in Hungarian) Akadémiai Kiadó Budapest

Ginzburg, B. Z., Katchalsky, A. (1963) J. Gen. Physiol. *47* 403

Gyarmati, I. (1961) Period. Polytechn. *5* 219, 321

Gyarmati, I. (1970) Nonequilibrium Thermodynamics, Springer Berlin

Haest, C. W. (1972) Biochim. Biophys. Acta *225* 720

Hempling, H. G. (1973) Abstracts Biophys. Soc. Ann. Meeting, Columbus, p. 261a

Hodgman, C. D. (ed.) (1953) Handbook of Chemistry and Physics. Chemical Rubber Publ., Cleveland

Kamiya, N., Tazawa, M (1956) Protoplasma (Wien) *46* 394–422

Kamiya, N., Tazawa, M., Takata, T. (1962) Plant and Cell Physiol. *3* 285–292

Karvaly, B. (1973) Nature *244* 25

Katchalsky, A., Curran, P. F. (1965) Nonequilibrium Thermodynamics in Biophysics Harvard Univ. Press, Cambridge, Mass.

Kedem, O., Katchalsky, A. (1961) J. Gen. Physiol. *45* 143

Kedem, O. (1972) J. Membrane Biology *10* 213

Leaf, A. (1965) Ann. New York Acad. Sci. *125* 559

Lifson, N., Grim, E., Johnson, J. A. (1960) in: Medical Physics III. (ed.) Glasser, O., Year Book Publ., Chicago p. 410–416

Meschia, G., Setnikar, I. (1958) J. Gen. Physiol. *42* 429–444

Rapoport, S. (1973) Abstracts Biophys. Soc. Ann. Meeting, Columbus p. 230a

Roth, W. A., Scheel, K. (1923) Landolt-Börnstein Physikalisch-Chemische Tabellen II. Springer Berlin

Stadelmann, Ed. J. (1969) Ann. Rev. Plant Physiol. *20* 585

Stein, W. D. (1967) The Movement of Molecules across Cell Membranes. Acad. Press New York

Van Bruggen, J. T. et al. (1973) Abstracts Biophys. Soc. Ann. Meeting, Columbus, p. 109a

Vető, F. (1969) Thesis, Pécs

Vető, F. (1974) Acta Biochim. Biophys. Acad. Sci. Hung. *9* 141–149

Weyl, W. A., Ormsby, W. C. (1960) in: Rheology (ed.) Eirich, F. R. Acad. Press New York p. 249

Acta Biochim. et Biophys. Acad. Sci. Hung. Vol. 9 (4), pp. 367–370 (1974)

Effect of Heat Denaturation on Glycerinated Muscle Fibers as Studied by Spin Label Epr

(Short Communication)

J. BELÁGYI, W. DAMERAU

Central Laboratory, Medical University, Pécs, Hungary and Division of Method and Theory, Central Institute of Molecular Biology, Academy of Sciences of GDR, Berlin-Buch, GDR

(Received February 14, 1974)

An interesting problem in protein biochemistry is the action of denaturing agents and the recovery from denaturation. Perrin and Monod (1963) have shown in an earlier work that the activity of the enzyme β-galactosidase can be partly recovered from thermal inactivation by treatment with high concentrations of urea. Similar observations on other enzymes were reported by White (1960) and Takagi (1962). In the present experiments we tried to study whether heat-induced structural changes in muscle could be at least partially restored by urea. The study was carried out with the electron paramagnetic resonance (epr) spin label technique which had proved to be a useful tool in investigation on structural changes of proteins (McConnell, McFarland, 1970; Hamilton, McConnell, 1968).

The fiber bundles isolated from rabbit m. psoas were handled in slightly stretched state according to the method described by Huxley (1963). The fibers were glycerinated over 3 weeks before use. Glycerol was then removed by a solution of 0.1 M KCl, 0.001 M $MgCl_2$ and 0.07 M phosphate buffer at pH 7. The preparations were spin labelled in the same solution by 10^{-4} M 4-maleimido-2,2,6,6-tetramethylpiperidinooxyl (label I) or 3-maleimido-2,2,5,5-tetramethyl-1-pyrrolidinyloxyl (label II, both purchased from Synvar) by incubation at 4°C for 16 hours. I and II are known to be mainly attached to SH groups of proteins (Hamilton, McConnell, 1968). The fiber bundles were repeatedly washed in a large amount of salt solution for 1 hour in order to remove unbound label before recording epr spectra.

The epr spectra were taken at room temperature in a special teflon device using a Zeiss spectrometer ER 9. The long axis of the fiber bundles was perpendicular to the magnetic field. Heat denaturation was carried out in a thermostat at 60°C for 60 min, in the salt solution mentioned above. After epr measurement the preparations were incubated in 8 M urea for 15 min and measured again. The urea was washed out with 250 ml of salt solution two or three times at 4°C for 15 hours.

The epr spectra recorded on the m. psoas fiber bundles labelled with I or II (Fig. 1) have a character similar to that published by Cooke and Morales (1969), and represent the superimposition of two types of spectra due to a strong immobilization (spectral component A, characterized by the hyperfine coupling parameter $2A_{zz}$ measured between the outermost hyperfine extrema) and a weak

Fig. 1. Epr spectra of spin labelled glycerinated muscle fibers (label II). The uppermost curve shows the epr spectrum of the preparation before treatment, the second spectrum was taken after heat denaturation, the third curve shows the epr spectrum after urea-induced denaturation. At the bottom the epr spectrum of the spin labelled fibers is presented after the experimental procedure. The epr spectra were not normalized to the central line

immobilization of the attached label, respectively (spectral component B, characterized by the isotropic hyperfine splitting constant a_{iso} measured as separation between the narrower lines in the spectrum).

The spectral changes induced by heat and urea and the following removal of urea (Fig. 1) are summarized in Table 1, which also shows $\Delta H_{+1}(A)$ and the ratio $I_{+1}(A)/I_{+1}(B)$. $\Delta H_{+1}(A)$ as an empirical parameter, is the separation between the low field line and the central line of the spectrum of the strong immobilized label[1], whereas $I_{+1}(A)$ and $I_{+1}(B)$ are heights of the low field peaks of the spectral components A and B, respectively.

[1] $\Delta H_{+1}(A)$ characterizes the spectrum of the strong immobilized label in a similar way as $2A_{zz}$ but, due to the better resolution of the low field line, $\Delta H_{+1}(A)$ can be measured more precisely than $2A_{zz}$.

Table 1

Spectrum parameters of spin labelled glycerinated muscle fibers

Treatment	a_{iso} (G)	$H_{+1}(A)$ (G)	$2A_{zz}$ (G)	$I_{+1}(A)/I_{+1}(B)$
Label I				
—	16.4 ± 0.2	27.2 ± 0.3	65.5 ± 0.3	2.46
Heat denaturation	16.5 ± 0.2	28.2 ± 0.3	66.5 ± 0.3	0.80
Urea incubation	16.4 ± 0.2	not measurable		0.03
After washing	16.5 ± 0.2	27.8 ± 0.3	65.5 ± 0.3	0.67
Label II				
—	15.7 ± 0.2	28.3 ± 0.3	65.5 ± 0.3	1.75
Heat denaturation	15.0 ± 0.2	26.7 ± 0.3	64.5 ± 0.3	0.81
Urea incubation	15.2 ± 0.2	not measurable		0.03
After washing	15.4 ± 0.2	27.8 ± 0.3	65.2 ± 0.3	0.65

In the case of labelling with spin label I small spectral changes are observable. Heat denaturation leads to a small increase of $\Delta H_{+1}(A)$ and $2A_{zz}$ suggesting an increased immobilization of the strongly immobilized label. a_{iso} remains constant within the experimental error. Incubation of the heat denatured muscle fibers with urea is followed by a strong increase of the more mobile component B at the expense of the strongly immobilized form A due to an unfolding effect of urea. The rotational correlation time τ_c for this weakly immobilized label was calculated to be $\tau_c = (2.4 \pm 0.5)$ nsec according an equation given by Kusnetsov et al. (1971).[2] After removal of urea the strongly immobilized component reappears, but the ratio $I_{+1}(A)/I_{+1}(B)$ remains reduced (0.67) and is not restored to the value of the preparation before heat denaturation (2.46).

Using label II $\Delta H_{+1}(A)$ and $2A_{zz}$ as well as a_{iso} all decrease after heat denaturation. This decrease of $\Delta H_{+1}(A)$ is at first sight surprising because a stronger immobilization has been expected from the findings with label I. A diminution of $\Delta H_{+1}(A)$ (and of $2A_{zz}$), however, can be caused not only by an increased mobility of the label but also by a decreased polarity of the environment of the label (Lassmann et al., 1973). Therefore, it cannot be excluded the possibility that the decrease of $\Delta H_{+1}(A)$ is mainly brought about by an increase of hydrophobic interactions in the environment of the strongly immobilized label. An argument for changes of this type is the decrease of a_{iso} showing a diminished polarity in the environment of the weakly immobilized label II.

During urea incubation of the heat denaturated muscle fibers the broad spectral component A disappears and the spectrum of weakly immobilized label II increases. Its correlation time is $\tau_c = (1.8 \pm 0.5)$ nsec.[3] After removal

[2] See footnote on page 368.

[3] The values τ_c for component B in the spectrum of the untreated or heat-denatured muscle fibers were not determined because of the relatively low concentration of B. However, τ_c can be roughly estimated as being within the range of 1–3 nsec in these cases.

of the urea the values for $\Delta H_{+1}(A)$ and a_{iso} are restored nearly to the values found before heat treatment. On the other hand, the ratio $I_{+1}(A)/I_{+1}(B)$ remains reduced just as after heat treatment.

The findings mentioned above lead to the conclusions as follows:

1. The glycerinated muscle fibers spin labelled with II undergo local structural changes after heating at 60°C which seem to reduce the polarity in the environment of label molecules bound to SH groups.

2. After urea treatment the strong immobilized bound label becomes more mobile due to the unfolding of the denatured glycerinated muscle fibers, in accordance with the data in the literature. Similar results were obtained on heat denatured myosin prepared from rabbit psoas. Details of these experiments will be published in a following paper.

3. As it can be seen from the ratios of $I_{+1}(A)/I_{+1}(B)$ for labels I and II, the treatment with high urea concentrations cannot restore the original conformation of the protein system. The reversible changes in the values $\Delta H_{+1}(A)$ and a_{iso} for the bound label II show that a partial recovery by urea treatment from heat-induced structural changes is not excluded.

References

Cooke, R., Morales, M. F. (1969) Biochemistry *8* 3188

Hamilton, C. L., McConnell, H. M. (1968) Spin Labels in Structural Chemistry and Molecular Biology. (Ed.) A. Rick and M. Davidson, W. H. Freeman and Co., San Francisco p. 115,

Huxley, H. E. (1963) J. Mol. Biol. *7* 281

Kusnetsov, A. N., Wasserman, A. M., Volkov, A. U., Korst, N. N. (1971) Chem. Phys. Letters *12* 103

Lassmann, G., Ebert, B., Kusnetsov, A. N., Damerau, W. (1973) Biochim. Biophys. Acta *310* 298

McConnell, H. M., McFarland, B. G. (1970) Quart. Rev. Biophys. *3* 91

Perrin, D., Monod, J. (1963) Biochem. Biophys. Res. Comm. *12* 425

Takagi, T., Isemura, T. (1962) J. Biochem. *52* 314

White, Jr., F. H. (1960) J. Biol. Chem. *235* 383

Acta Biochim. et Biophys. Acad. Sci. Hung. Vol. 9 (4), pp. 371—381 (1974)

A New Type of Microcalorimeter for Examination of the Heat Production of Muscle

D. LŐRINCZI, Z. FUTÓ

Biophysical Institute, Medical University, Pécs, Hungary

(Received February 14, 1974)

A thermopile heat conduction calorimeter with a sensitivity of $dQ/dt = 10^{-7}$ cal/s and time constant of (τ) 145s was developed for measuring the heat which develops during muscular activity. A power transducer of a sensitivity of (1.49 ± 0.27) pond/mV and a displacement transducer of a sensitivity of (0.02 ± 0.001) mm/mV were built into the system.

Introduction

Microcalorimetrical measurement is a method serving for the high-precision measurement of heat phenomena accompanying the physical-chemical processes going on in living and inanimate nature.

By measuring the different parameters characterizing the process we can calculate important thermodynamic functions such as entropy (S), enthalpy (H) etc., with the aid of which important conclusions can be drawn concerning, for instance the structure of the object under examination.

A very significant development was achieved in the field of methodology in the last 30 years (Swietoslawski, 1946; Sturtevant, 1959; Calvet, Prat, 1963; Benzinger, Kitzinger, 1949; 1963; Benzinger, 1969; Fales, 1967; Wadsö, 1970).

Most calorimeters are usually designed for chemical purposes. The works of Bürker (1911), Hill (1965) and Tigyi (1958, 1959) give a comprehensive methodological survey of the calorimeters made for the examination of muscular activity. The first calorimeter specially made for biological purposes (examination of macromolecules) was constructed by Privalov et al. (1954) and Wadsö (1970).

Methodologically, the examination of the heat production of muscle can be divided into two main parts:

1. microcalorimetric measurements,
2. myothermic measurements.

The two methods of measurement are distinguished from each other by the factor of time. In a microcalorimetric method the measurement can last from a few minutes even to hours, while the time-resolution power of myothermic measurements is in ms order. This is rendered possible by the muscle's direct touching the thermopile. But this means an essential source of error.

In order to avoid this source of error Tigyi, in 1958, developed a microcalorimeter for the investigation of muscular activity in this institute. This is

based on the theory of microcalorimetric method and is appropriate for determining the *exact* value of heat production, not depending either on possible changes in the data of heat conduction, heat radiation, etc., of the muscle, the errors due to displacement caused by mechanical change during activity or the errors of the direct contact with thermoelements, respectively. However, the process of heat production can be followed in time but with a greater inertness.

The sensitivity of the system was $5 \cdot 10^{-4}$ cal. On the basis of the experiences of our institute, as well as the development achieved in microcalorimetrical methods, a new microcalorimeter has been constructed which is appropriate for biophysical purposes.

Methods

Our microcalorimeter was planned by considering the requirements as follows.

1. As it is complicated to ensure adiabatic conditions, our system was constructed for isothermic conditions.

2. In order to reach the smallest possible inertness and maximum thermovoltage our thermopile is a so-called "area thermopile" which surrounds the area to be measured in a netlike fashion (Benzinger, Kitzinger 1963). So the principle of operation of our calorimeter is the principle of the so-called "heat-burst" or thermopile heat conduction calorimetry.

3. Power and displacement transducers were built into our system so that the simultaneous recording of the mechanical parameters of heat production and muscular activity did not disturb each other.

4. Isothermic conditions must be ensured in the range from $-5°C$ to $+30°C$ with an accuracy of $10^{-4}°C$.

The main parts of our system are as follows (see Fig. 1).

1. Thermopile with the muscle holder with stimulating electrodes and calibrating heater.
2. Stabilizing water bath.
3. Vacuum thermoinsulation.
4. Mechanical auxiliary devices.

Thermopile

Our thermopile is a pile containing about 5000 constantan-copper thermoelements. The thermoelements were not made in the traditional way by soldering, but by copper electroplating on the constantan in the following way (see Fig. 2):

Enamelled constantan, 0.14 mm in diameter and enamelled copper separating wire of a diameter of 0.12 mm were wound up together on a plastic tube 3 mm in outer and 1.2 mm in inner diameter. In this, there was a copper core of a diameter of 1.1 mm to prevent the deflection of the tube when the wire is

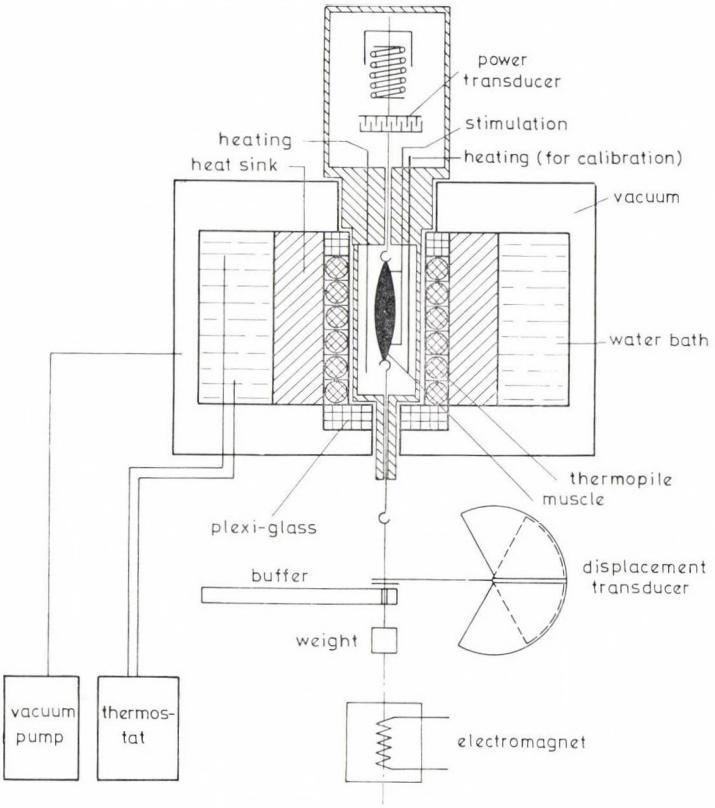

Fig. 1. Scheme of the structure of the microcalorimeter

wound up. This coil was wound up on a reel 15 cm in diameter, and placed in the turns of the reel in such a way that half of it stood out from them.

The enamel insulation was removed from the free half of the wire wound up in this way, and, after careful cleaning and degreasing, the cleaned part of the copper was electroplated in a thickness of about 0.05 mm in a cyan bath containing Cu^{I}. After rinsing, drying an fixing the turns, the copper separator was wound back and the remained constantan and constantan copper surfaces were insulated electrically. After that, the copper core was removed from the plastic tube.

Striving for the best possible covering of the area to be measured we wound up the ready thermoelements on a copper cylinder of a wall thickness of about 0.2 mm and an inner diameter of 20 mm so that the joints of constantan and constantan-copper got at the cylinder. The winding up was done bifilarly in order to eliminate self-induction. After that, with the aid of a cylinder surface cut to three, a slight pressure was exerted on the thermoelements in order to ensure a perfect contact. The whole was surrounded with a tightly fitting copper cylinder of a great mass. This plays the part of the heat sink or point of reference.

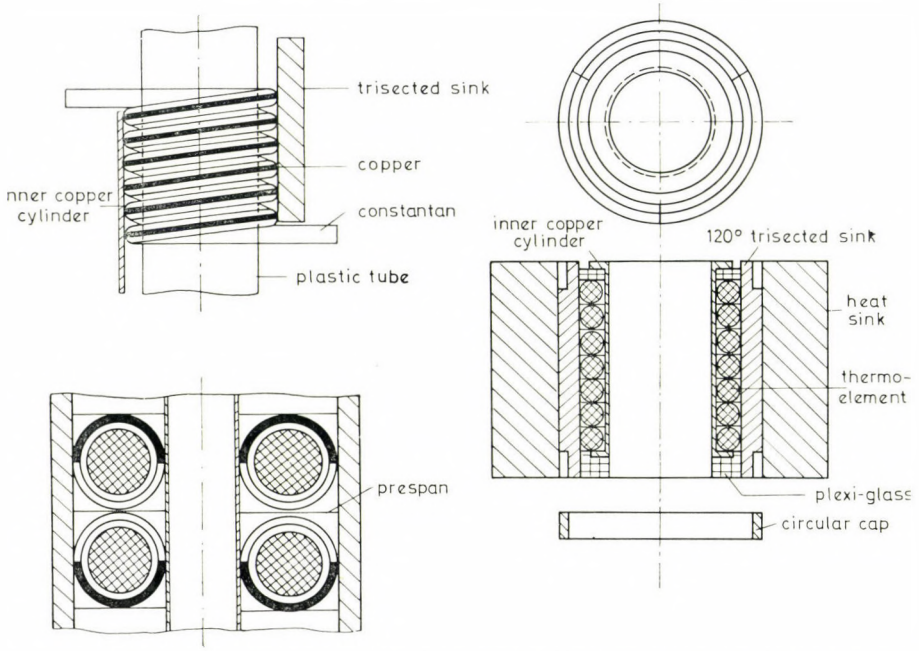

Fig. 2. Chief steps in the construction of the thermopile (for more detailed explanation see the text)

The functioning of the thermopile

With the inner copper cylinder, our aim is to accelerate heat transfer to thermoelements and to make it more steady. So the heat developed in the area of work flows through the thermoelements towards the heat sink, the great mass of which ensures the isothermic conditions, together with the stabilizing water bath.

We consider each thermoelement to be series-connected from an electric point of view and connected in parallel shunt form the point of view of heat conduction.

In each thermoelement the developed thermovoltage v and the heat flux dq/dt are proportional to c, the difference of temperature between the thin copper cylinder surrounding the area of work and the heat sink for which the following formula is valid (Wadsö, 1970):

$$v = c\frac{dq}{dt}. \tag{1}$$

In an ideal case all the heat passes through the thermoelements into the heat sink as follows:

$$v = \sum_{i=1}^{n} v_i = \sum_{i=1}^{n} c\frac{dq_i}{dt}; \tag{2}$$

and

$$V = c\frac{dQ}{dt} \tag{3}$$

where V is the voltage of the thermopile and dQ/dt is the total heat flux passing through the thermopile.

Practically, not the whole heat flux passes through the thermoelements, but a part of it gets into the heat sink through the calibrating heater, the insulation of thermoelements, the plastic tubing, etc.

If the density of thermoelements is great enough and the difference of temperature between the area of work and the heat sink is small (as in the case of microcalorimetry), then this effect is small; so the equation

$$V = c'\frac{dQ}{dt} \tag{4}$$

can be considered as a good approximation, where c' is an effective proportion factor and $dQ = \sum_{i=1}^{n} dqi + dq'_i$, where dq_i is the heat not conducted through the thermoelement.

By integrating equation (4) we obtain

$$Q = \frac{1}{c'} \cdot \int V dt\,. \tag{5}$$

The quantity of the developed heat is proportional to the area under the voltage-time diagram:

$$Q = KA, \tag{6}$$

where the K proportion factor can be determined by calibration.

Because of the construction of the thermopile described above, a signal of steep acceleration and exponential decrease in time will be obtained for an impulse-like heat production.

Calibration

Calibration was done in an electric way. We can calculate the introduced Joule's heat by connecting a voltage generator to a manganine heating resistance of R = 43.4 Ω and operating if for the given period of time. Adopting the $V(t)$ diagram, the area under the curve is proportional to the introduced quantity of heat. With the aid of the proportion factor calculated from this the absolute value of an optional quantity of transmitted heat can be calculated.

Stabilizing water bath

On the one hand, the water bath has the role to permit the measurements to be performed at different temperatures; on the other hand, it increases the mass of the heat sink and promotes thus, a better fulfilment of isothermic conditions. The required temperature of work is ensured by perfusion for which a home-made thermostate stabilizing with an accuracy of 10^{-4}°C is used. When the given temperature is reached (the thermovoltage of the thermopile is nearly zero V) the system will be closed. Once the complete thermic equilibrium is reached the measurement can be started (this happens 1.5 to 2 hours after the beginning of perfusion).

Vacuum thermoinsulation

In order to decrease the outer thermic disturbances, which would break the isothermic condition, the thermostating block was surrounded with a vacuum mantle. The pressure in the mantle is under 10^{-1} torr.

Mechanical auxiliary devices

1. Power transducer:

Our power measurer is a transducer making use of the change of capacity (Machin, 1958; Schilling, 1960). It is a chief requirement of apparatuses of this type that the displacement of the moving armature be a minimum (e.g. isometry must not be damaged by the measurement in isometric contraction), but give the greatest possible signal.

This was achieved in our case in such a way (see Fig. 3) that the surface of the opposite electrodes was greatly increased by applying an air-trimmer system. Thus, in the case of a displacement of about 0.2 mm a signal greater than 500 mV could be obtained.

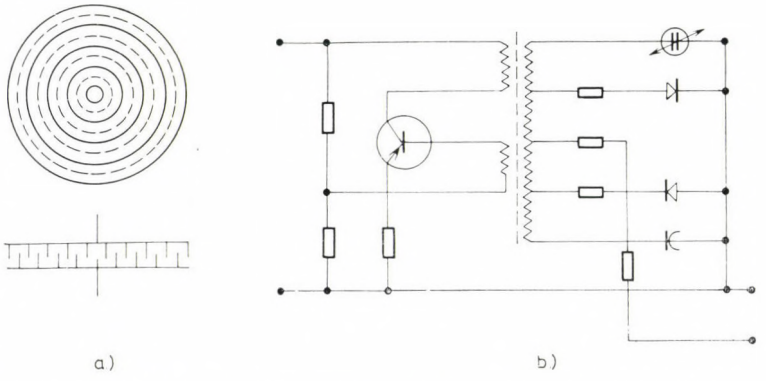

Fig. 3. *a)* Arrangement of the armatures; *b)* electronics of the power transducer

2. Displacement transducer:

This, too, is a capacitive transducer with negligeable inertness. It does not load the object to be measured (muscle), it follows its displacement inertialessly so that it only registers the change falling into the main direction, but not the one perpendicular to it. Thus the "twisting", occurring with the shortening of gastrocnemius muscle was disengaged as regards registration. This was done so

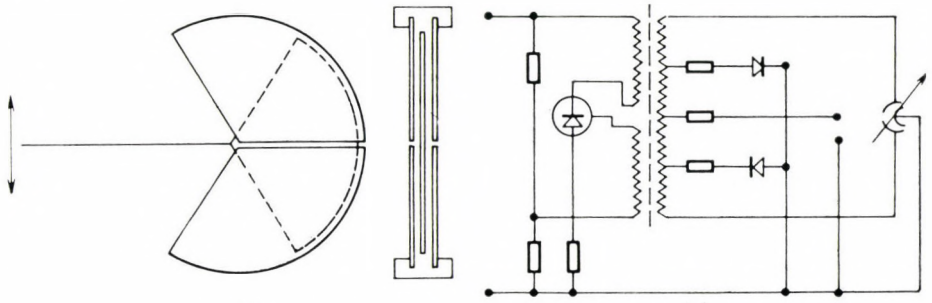

Fig. 4. *a)* Arrangement of the armatures; *b)* electronics of the displacement transducer

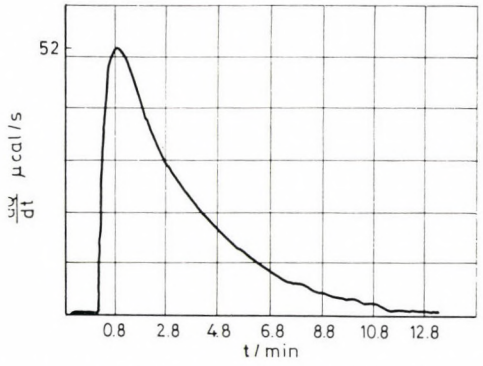

Fig. 5. Calibration of the thermopile with an impulse-like dissipation of heat of $Q = 5.53$ mcal/s

(see Fig. 4) that an armature, which had the form of a sector of 240°, was cut in half, and a similar one was placed parallel with it. The opposite parts were connected. An armature of the form of a sector of 120° and placed on a ruby bearing moved between them. In this way it is only the displacement perpendicular to the axis which causes a change in capacity (which is equal with the main direction of shortening of the muscle). A displacement of 10 mm results in a signal of 500 mV. Both transducers are driven by an oscillating circuit working at 994 KHz.

3. Programmable pulling magnet:

The pulling-in time of the magnet is less than 10 ms. It can work at a distance of 10 mm against a power of 1.2 kp. With the aid of a square-wave generator

its supply unit can be started with different delays, it can be kept in pulling-in state for different periods of time with adjustable frequency, etc. Thus it helps to simulate muscle activities of different types.

Results

Fig. 5 shows a thermovoltage response to an impulse-like dissipation of heat 5.53 mcal was introduced in an electrical way into the system during 1 s.

Fig. 6 shows a thermopile response to a constant heat effect clearly demonstrating the stability of the "steady-state voltage value". The time-constant of the system $\tau = 145$ s (the time after which $U = 0.37\ U_{max}$ at cooling), while the so-called half period $t_{1/2}$, during which the amplitude of the signal decreases from the maximum to its half, is 101 s. The sensitivity of the system, supposing the minimal 2 : 1 signal-noise ratio is 10^{-7} cal/s.

The thermovoltage response of a semimembranous muscle to a single stimulus can be seen in Fig. 7 which, at the same time, proves the suitability of the calorimeter for biological purposes.

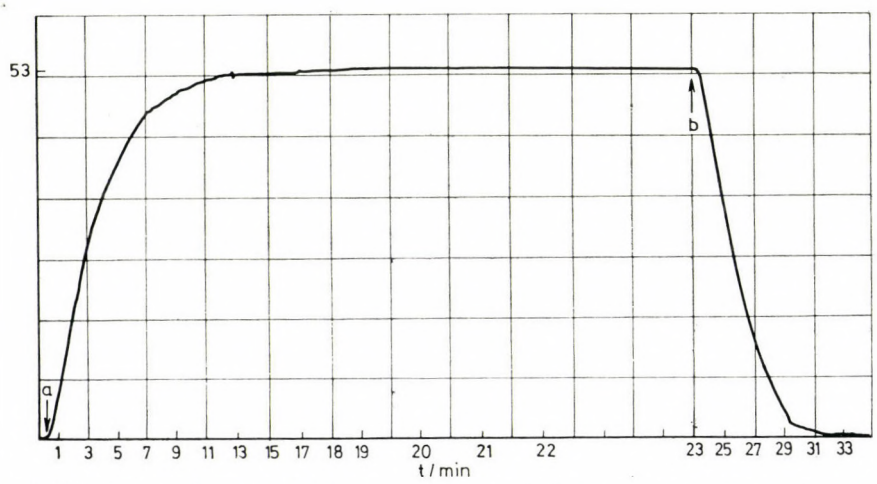

Fig. 6. Calibration of thermopile heat conduction calorimeter with steady electric current *a)* beginning of heating, *b)* switching-off of heating

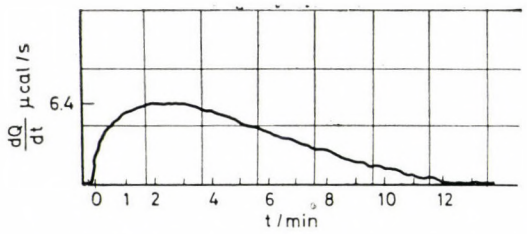

Fig. 7. Heat production of semimembranous muscle during a single isometric twitch at length of rest at room temperature (Q total = 2.75 mcal)

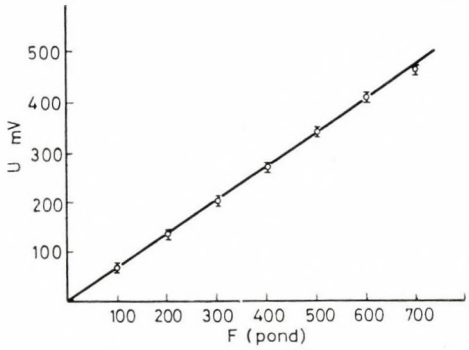

Fig. 8. Calibration diagram of power transducer

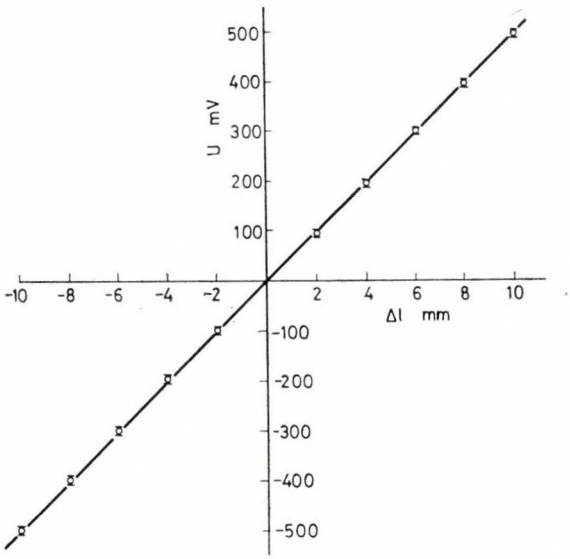

Fig. 9. Calibration diagram of displacement transducer

The calibration diagram of the power transducer can be seen in Fig. 8. The figure proves the linearity of capacity transducer: in a range of 0–600 p the output signal of the transducer changes linearly as a function of loading; the slope of the straight line is (0.67 ± 0.06) mV/pond. The sensitivity of the apparatus is (1.49 ± 0.27) pond/mV.

The calibration diagram of the displacement transducer is shown in Fig. 9. The slope of the straight line is (49.54 ± 0.12) mV/mm, its sensitivity (0.02 ± 0.001) mm/mV.

Discussion

For the working of a calorimeter, as a good analytical instrument, a good resolution time is necessary in addition to high sensitivity. The sensitivity of calorim-

eters made for classic chemical purposes is good, but their rate is low. An objection can be raised against Hill's calorimeter having an extremely good resolution time, because of the effect of the mechanical activity of the muscle on thermoelements.

With the aid of the thermopile heat conduction calorimeter principle (or heatburst microcalorimetry) (Benzinger, Kitzinger, 1963; Fales et al., 1967; Wadsö, 1970), there is a possibility to create a system of great sensitivity (magnitude of $(dQ/dt = 10^{-7}$ cal/s) and good resolution time. For the sake of comparison the most characteristic data of some types of calorimeters are presented in Table 1. Our system, made on the basis of such a principle, follows the change going on in the area of work with an inertness smaller than 100 ms.

Sensitivity can be increased by increasing the number of thermoelements (an upper limit is given by the relation of the inner resistance of the thermopile and the input resistance of the recorder, as well as the so-called heat production of rest). On the other hand, the reaction time of the thermopile can be decreased by interpolating different accelerators (with the decrease of the size of thermo element the $\Delta T/\Delta X$ relation increases and, thus, also increases the velocity of heaconduction; the velocity of heat transfer toward the thermoelements can bd increased by inserting a good heat-conductor "warm point" wall), and thus the resolution time also increases. Thus we have a tool at our disposal, with the aie

Table 1

Calorimeter	τ (s)	$t_{1/2}$ (s)	Sensitivity
Privalov	—	—	10^{-7} cal/s
Benzinger—Kitzinger*	144	100	10^{-7} cal/s
LKB—Flow*	141	98	10^{-7} cal/s
Lőrinczi—Futó	145	101	10^{-7} cal/s

* H. P. Stauffer and C. Jeanneret (1972), Science Tools 19, 17.

of which we can meet the requirements necessary for the examination of muscle activity, and we can further decrease the number of the possible sources of error.

A further great advantage of our apparatus is that the displacement, effort and thus the mechanical work of the muscle can be measured with high accuracy without influencing heat production.

With the aid of other mechanical auxiliary devices belonging to the system (e.g. programmable system of magnets) we were able to construct an apparatus which measures the mechanical parameters and heat production with high accuracy and good resolution and which can be universally used for the purpose of muscle research.

Biochemical reactions can also be examined in our system with very little modification, and thus it can also be used for the examination of the energetics of muscle activity.

The authors express their thanks to prof. J. Tigyi for raising the questions, as well as to J. Örkényi, S. Papp and B. Bakos for their help given in the construction of certain electronic parts of the experimental apparatus.

References

Benzinger, T. H. (1969) Ultrasensitive Reaction Calorimetry (A Laboratory Manual of Analytical Methods of Protein Chemistry. Ed. P. Alexander and H. P. Lundgren. Pergamon Press New York)

Benzinger, T. H., Kitzinger, C. (1949) The Rev. of Sci. Instr. *20* 849

Benzinger, T. H., Kitzinger, C. (1963) Microcalorimetry, New Methods and Objectives. (Temperature — Its Measurement and Control in Science and Industry, Vol. 3. Part 3, Ed. J. Hardy, Reinhold New York)

Bürker, H. (1911) Tiegerstedts. (Handb. d. Physiol. Methoden Leipzig)

Calvet, E., Prat, H. (1963) Recent Progress in Microcalorimetry (Ed. H. A. Skinner, Pergamon Press London)

Fales, J. T., Crawford, W. J., Zierler, K. L. (1967) Am. Journ. Physiol. *213* 1427

Hill, A. V. (1965) Trails and Trials in Physiology (Edward Arnold London)

Machin, K. E. (1958) Transducers (Electronic Apparatus for Biological Research Ed. Donaldson. P. E. K., Butterworts Scient. Publ. London)

Privalov, P. L., Kafiani, K. A., Monaselidze, D. R., (1954) Dokl. A. N. USSR. *156* 951

Schilling, M. O. (1960) Rev. Sci. Instr. *31* 1215

Sturtevant, J. M. (1959) Calorimetry (Techniques of Organic Chemistry Ed. A. Weissberger, John Wiley and Sons New York)

Swietoslawski, W. (1946) Microcalorimetry. Reinhold Publ. Comp. New York

Tigyi, J. (1958) Kísérletes Orvostudomány Vizsgáló Módszerei. Akadémiai Kiadó Budapest, V. 4

Tigyi, J. (1959) Acta Physiol. Acad. Sci. Hung. *16* 129

Wadsö, I. (1970) Quart. Rev. of Biophys. *3* 383

Acta Biochim. et Biophys. Acad. Sci. Hung. Vol. 9 (4), pp. 383—387 (1974)

Heat Production of Muscle in Isotonic and Isometric Circumstances at Length of Rest during One Twitch

D. LŐRINCZI

Biophysical Institute, Medical University, Pécs, Hungary

(Received February 14, 1974)

The heat development during the activity of muscle was examined with a thermopile heat conduction calorimeter having a sensitivity of 10^{-7} cal/s. It was found with muscles of different types that the heat production for one twitch at length of rest was about 1/3 greater in isometric (stretch) than in isotonic (non-stretch) contraction. It is assumed that crystallization of muscle proteins plays a part in the difference.

Introduction

The investigation of heat phenomena accompanying muscular activity is an old problem of muscle-biophysics and physiology which, though having been examined for a long time, is not yet solved even now.

On the basis of the different methods used in such investigations two main trends can be distinguished in this field.

The one is the so-called Hill's school (Fenn, 1923; Hill, 1938, 1950, 1953, 1956) who, working with myothermic method and examining the rate of heat production during the finite phases of muscle contraction, came to the conclusion that heat production is smaller during isometric than during isotonic contraction because, in the latter case, the muscle shortens and so mobilizes extra energy. According to the other view (Tigyi, 1958, 1959; Ernst, 1963) heat production is greater during isometric contraction, because this process goes together with a structural arrangement of the muscle proteins (crystallization). Recently, several papers appeared proving both views: Fales (1967, 1969) corroborated Hill's view with a method of gradient-layer calorimetry, while Mórocz-Juhász (1962) provided data to the Tigyi—Ernst conception; Carlson, Hardy, and Wilkie (1963) repeated Fenn's experiment and, failing to find any heat of shortening during contraction, are of the opinion that Q isomet. $> Q$ isoton. Hill's work tried to answer these questions (1964b). The work of Aubert and Lebacq (1970), which argues in favour of Hill's theory, results also in "negative" heat production for the case of Q isoton. $- Q$ isomet. (Table 6).

On the basis of the contradictory data in the literature we thought it right to re-examine this question.

Methods

Gastrocnemius as well as semimembranosus and sartorius muscles isolated from *Rana esculenta* were used in the experiments. A thermopile heat conduction calorimeter further developed in this institute (Lőrinczi, Futó, 1974) was used which had a sensitivity of 10^{-7} cal/s and a half-time of 101 s.

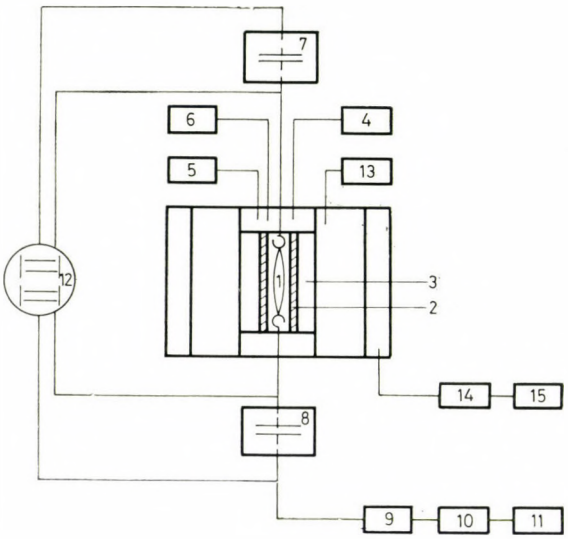

Fig. 1. Scheme of the arrangement of microcalorimetrical experiments: (1) muscle, (2) thermopile, (3) heat sink, (4) KIPP BD-5 micrograph, (5) stimulation, (6) calibrating heating, (7) power transducer, (8) displacement transducer, (9) pulling magnet, (10) supply unit of the magnet, (11) timing circle of the supply unit, (12) two-beam oscilloscope, (13) stabilizing water bath, (14) vacuum pump, (15) vacuum gauge

The schematic arrangement of the experiments can be seen in Fig. 1. The prepared muscle (1) was placed into the area of work of the thermopile (2–3). The thermovoltage obtained for heat effects was recorded with a Kipp BD-5 micrograph (4). The stimulating electrodes (platinum), operated by a square-pulse generator (5), and the calibrating heating apparatus, operated by a supply unit, were built into the muscle holder which could be lifted out. The power transducer (7) and the displacement transducer (8), the signals of which were transmitted to a two-beam cathode-ray oscilloscope, also constituted a part of the muscle holder. Constant temperature was ensured by a stabilizing water bath (13) and vacuum insulation (14–15).

Results

Fig. 2 is actually a calibration pattern which shows the thermo-voltage response obtained for an impulse-like dissipation of heat introduced during 1 s and having a magnitude of 5.53 mcal.

Fig. 3 demonstrates the heat production of the gastrocnemius muscle for a single stimulus at length of rest in an isotonic–isometric–isotonic case.

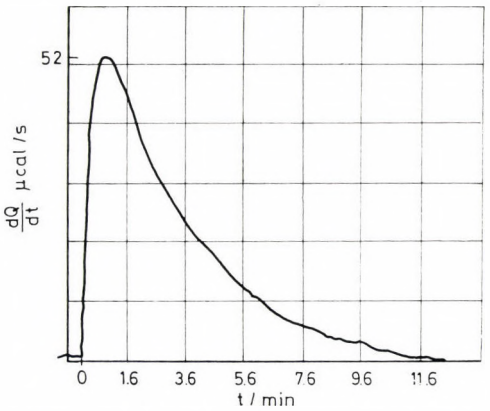

Fig. 2. Calibration diagram obtained for impulse-like dissipation of heat (5.53 mcal/s)

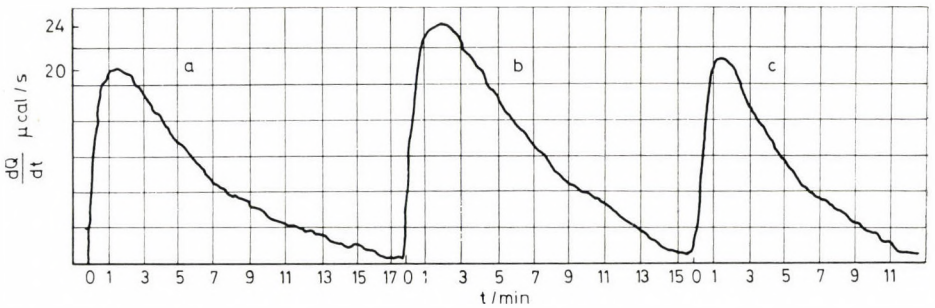

Fig. 3. Heat production of gastrocnemius muscle at length of rest at room temperature during a single twitch in *a)* isotonic, *b)* isometric, *c)* isotonic case

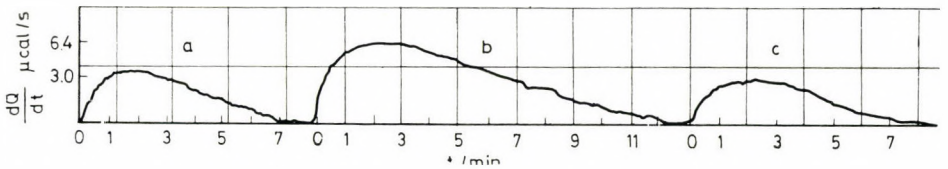

Fig. 4. Heat production of semimembranous muscle in *a)* isotonic, *b)* isometric, *c)* isotonic case

In the isotonic case, the length of rest was reached with a loading of 50 g. Isometric condition was achieved by fixing at length of rest with the aid of an arrester.

Fig. 4 shows the heat production of the semimembranous muscle obtained in similar cases (Loading: 15 g).

Fig. 5 shows the heat production in the case of sartorius muscle (Loading: 5 g).

The above experimental data were obtained on one single muscle in such a way that the muscle rested after isotonic and isometric contractions for about 10 min with this arrangement we tried to ensure equal starting conditions.

The experiments were performed in 8 muscles each, at room temperature, using 10 diagrams for each muscle for evaluation, where the values of heat production refer to units of mass (see Table 1).

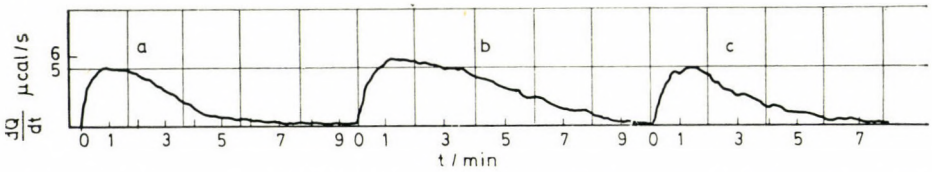

Fig. 5. Heat production of sartorius muscle in *a)* isotonic, *b)* isometric, *c)* isotonic case

Table 1

Magnitude of heat production (mcal/g)

Type of muscle / contraction	Gastrocnemius muscle	Semimembranous muscle	Sartorius muscle
Isotonic	3.38 ± 0.17	3.71 ± 0.48	3.32 ± 0.27
Isometric	4.75 ± 0.15	4.73 ± 0.39	4.82 ± 0.41
Isotonic	3.19 ± 0.14	3.52 ± 0.41	3.08 ± 0.19

Discussion

In 1923, Fenn published two articles, already classic today, on the energy production of contracting (active) muscle. He found the release of energy to be greater in an isotonic than in an isometric case.

By developing the methods further, Hill (1938, 1950, 1953, 1956) found that Q isoton. > Q isomet. Tigyi (1958, 1959) modified the methods, referring to methodological difficulties (the muscle is lying on thermo-elements; during shortening there is a mechanical interaction between it and the thermo-element), and demonstrated the semimembranous muscle to produce about 1/3 greater quantity of heat in isometric than in isotonic tetanus.

He explained this difference by a structural re-arrangement (crystallization) of muscle protein during isometric contraction (Flory, 1956), referring to the

results obtained when examining the volume decrease (Ernst, Tigyi, 1951; Ernst et al., 1951; Ernst, Tigyi, 1951) and the mechanical activity of the muscle.

This was also corroborated by the experiments of Mórocz-Juhász (1962) performed on myosin.

The results obtained with our modified method well agree with the results of this Institute published up to now. We found the difference between the two kinds of muscle activity to be about 1/3 greater in the case of isometry; this difference can be interpreted in terms of a "crystallization" of muscle protein (Flory, 1956; Tigyi, 1959; Mórocz-Juhász, 1962; Ernst, 1963).

The author thanks prof. J. Tigyi for raising the problem and for his useful advices during the experimental work.

References

Aubert, X., Lebacq, J. (1971) J. Physiol. *216* 181
Carlson, F. D., Hardy, D. J., Wilkie, D. R. (1963) J. gen. Physiol. *46* 851
Ernst, E., Tigyi, J. (1951) Acta Physiol. Acad. Sci. Hung. *2* 243
Ernst, E., Balog, J., Tigyi, J., Sebes, A. (1951) Acta Physiol. Acad. Sci. Hung. *2* 253
Ernst, E., Tigyi, J. (1951) Acta Physiol. Acad. Sci. Hung. *2* 261
Ernst, E. (1963) Biophysics of the Striated Muscle Akad. Kiadó Budapest pp. 239—306
Fales, J. T., Crawford, W. J., Zierler, K. L. (1967) Am. Journ. Physiol. *213* 1427
Fales, J. T. (1969) Am. Journ. Physiol. *216* 1184
Fenn, W. O. (1923) J. Physiol. *58* 175
Fenn, W. O. (1923) J. Physiol. *58* 373
Flory, P. J. (1956) Science *124* 53
Hill, A. V. (1938) Proc. Roy. Soc. B. *126* 136
Hill, A. V. (1950) Proc. Roy. Soc. B. *137* 268
Hill, A. V. (1950) Proc. Roy. Soc. B. *137* 40
Hill, A. V. (1953) Proc. Roy. Soc. B. *141* 503
Hill, A. V. (1956) Brit. Med. Bull. *12* 174
Hill, A. V. (1964) Proc. Roy. Soc. B. *159* 596
Lőrinczi, D., Futó, Z. (1974) Acta Biochim. Biophys. Acad. Sci. Hung. *9* 371
Mórocz-Juhász, M. (1962) Acta Physiol. Acad. Sci. Hung. *22* 281
Tigyi, J. (1958) Kísérletes Orvostud. Vizsgáló Módszerei. Ed. Kovách, A. Akad. Kiadó Budapest, p. 4
Tigyi, J. (1959) Acta Physiol. Acad. Sci. Hung. *16* 129

Acta Biochim. et Biophys. Acad. Sci. Hung. Vol. 9 (4), pp. 389—394 (1974)

Subatomic Biology[1]

E. ERNST

Biophysical Institute, Medical University, Pécs, Hungary

(Received May 31, 1974)

I. *Chemical or physical aspect of the phenomena of life*

Due to the results of chemical processing in agriculture, the radiance of biochemistry, the achievements of pharmacochemistry, the chemical character of the phenomena of life has come into prominence in science and public opinion. This chemical aspect has been corroborated by the discovery of hormones and vitamins and formulated as *molecular biology*. Although the ion-conception, according to physical chemistry, and the publications describing the electronic structure of proteins have shown some development in the scientific approach to *electron biology*, the chemical aspect of biophenomena, in our age of quantum or electron chemistry, has not been shaken by it.

I.1. However, it is just the rapid spread of electron biology (Chance, 1972), further the demonstration of the semiconductor-like characteristics of biological growths (Eley et al., 1953; Ernst, 1955—56, 1956, 1963; Tigyi, 1963; Tigyi et al., 1966; Lakatos, 1969) that have clearly signalized that the *leading role of the chemical aspect of molecular biology should be given up* in studying exact biology. The same direction has appeared in the newer biochemical works dealing with bioenergetics (Szent-Györgyi, 1957; Klotz, 1957; Lehninger, 1965; Pullman, Pullman, 1967), in which the mechanism of the *molecular* processes of bioenergetics are treated at *subatomic* level. Briefly: *the physical subatomic aspect is necessary for the elaboration of exact biology.*

I.2. In order to clarify the former train of thoughts more effectively, the question of isotopes in biology should be considered, then the chemical aspect will immediately turn out to be insufficient. Namely, it is *well-known that living systems are able to discriminate between chemically identical isotopes* (Bigeleisen, 1965). Thus H_2O and D_2O are very different for biological systems (Katz, Crespi, 1966; Ernst, 1970); many other experimental data refer to the isotopes $^{12}C-{}^{13}C-{}^{14}C^*$, $^{14}N-{}^{15}N$ and $^{16}O-{}^{18}O$ (Schönheimer et al., 1939; Rittenberg et al., 1939; Rabinowitz et al., 1958, Uphaus et al., 1967; Flaumenhaft et al., 1970);

[1] A study discussed at the session of the Biophysical Committee on March 27 and the first "Proceedings of the Physical and Biophysical Committees" of the Hungarian Academy of Sciences on April 17, 1974.

we have shown that the heart, muscle and spermium of frogs discriminate between ^{39}K and ^{41}K (Ernst, 1970; Ernst, Juricskay, 1971; Niedetzky, Lajtai, 1963). All these data indicate that the *physical subatomic aspect is indispensable* in scientific cognition and description of living systems, because the experimental results just mentioned are in connection with *the supernumerary neutrons of these isotopes* Accordingly, a possible aspect of *neutronbiology* will be discussed in this paper.

II. *Plus neutrons in bioatoms*

The organic compounds serving as basic materials of biological systems are made up of atoms (H, C, N, O) all of which have isotopes containing plus neutrons; their atomic weights and frequencies are shown in Table 1.

II.1. These atoms are known to be contained by proteins, carbohydrates and lipids in different percentage, notwithstanding the error will not be great, if the atomic constitution of a man (60–70 kg, 70–75 per cent water content) is computed as in Table 2. Thus according to the atom-tables the following quantities of isotopes with plus neutrons can be computed in the human organism (Table 3).

II.2. These statements are completed and especially illuminated by those numerous data according to which the isotopes containing plus neutrons generally show a greater relative frequency (e.g. 15_N/all N) in the living unit than computed

Table 1

Weights and frequencies of bioisotopes

Symbols of atoms	Atomic weights, frequencies (per cent)					
H	1	99.98	2	0.02	3	10^{-10}
C	12	99	13	1	14	10^{-12}
N	14	99.6	15	0.4		
O	16	99.8	17	0.04	18	0.2

Table 2

The atomic constitution of man (approximately)

Symbols of atoms	Per cent of the organic material	Weight (g)
H	10	1000
C	50	5000
N	20	2000
O	20	2000
	of the water content	
H	10	4500
O	90	40,000

Table 3

Isotopes with plus neutrons in the human body (approximately)

Symbols of atoms	Weight of isotopes (g)	g atoms
^{2}D	1	0.5
^{13}C	50	4.0
^{15}N	8	0.5
^{17}O	17	1.0
^{18}O	84	4.5

earlier. That is: *living systems are able to accumulate in their substance the isotopes having supernumerary neutrons* (besides the papers quoted above Hübner, 1958; Vedder, 1959). That means that there is *an abundance of isotopes with supernumerary neutrons in the organism.*

Besides that it also should be taken into consideration that most "inorganic" bioatoms: B, Mg, Si, S, Cl, K, (K*), Ca, Fe, Ni, Cu, Zn, Mo have isotopes with supernumerary neutrons.[2]

III. *Instability of the neutron*

According to the universal view, living systems are continuously changing in time in contrast to inorganic materials as salt, water, minerals, the latters being the same immemorially. Biology of today also emphasizes the contrast between inanimate nature and *living systems consisting of the same constituents but continuously undergoing a change.*

III.1. *The neutron is less stable* than the other two constituents (proton, electron) of the atomic world; e.g. according to the doctrine the "free" neutron is radioactive in contrast to the neutron bound in an atom. The more correct and general formulation would read: *the instability of the neutron appears in different forms depending on its actual bond* (see the next two items).

III.2. *The instability of the plus neutron is of a greater degree:* the bond energy of the nucleus of $^{9}_{4}Be$ is 58.0 Mev, i.e. $\sim$6.4 Mev per nucleon, but that of a single neutron (of the plus neutron?) in the same atom is $\sim$1.6. The situation is similar in the case of the bioisotopes with supernumerary neutrons: the bond energies per nucleon are (in Mev) $\sim$1.1 for ^{2}D and $\sim$2.8 for ^{3}T*. Furthermore, although these energies for the atoms ^{12}C and ^{16}O are (in Mev) $\sim$7.7 and $\sim$8.0, respectively, the differences between the bond energies of the nuclei of their isotopes are much less: $^{13}C-^{12}C \sim 4.9$, $^{17}O-^{16}O \sim 4.1$ and $^{18}O-^{16}O \sim 6.1$ Mev. Briefly: *less bond energy belongs to the plus neutrons than the average value per nucleon.*[3]

[2] Na, P, Mn, Co have no natural isotopes.

[3] In the case of the nucleus of ^{14}N the ratio of proton–neutron (7 : 7) is odd : odd, and thus the bond energy, due to the pair energy, is less than that in ^{15}N, where this ratio (7 : 8) is odd : even.

III.3. The instability of the neutron can be demonstrated also by the following: cosmic neutrons and atomspheric N atoms produce, according to the reaction

$$^{14}_{7}\mathrm{N} + {}^{0}_{1}\mathrm{n} = {}^{14}_{6}\mathrm{C}^{*} + {}^{1}_{1}\mathrm{p}\,,$$

radioactive carbon isotopes. This free neutron was β-active with a $t_{1/2} \sim 13$ m and $E_m \sim 0.78$ Mev; in contrast to that the β-activity in the $^{14}C^{*}$ shows the values $t_{1/2} \sim 5700$ a and $E_m \sim 0.16$ Mev. Consequently it can be stated: *the exogenous neutron has become endogenous, and its activity and energy have changed to a high degree in the new atom.*[4]

IV. *Plus neutrons in atoms, molecules and macrosystems*

IV.1. Proton and neutron are known to be different states of the nucleon: $p \rightleftarrows n$; in connection with this the question may arise *what role is played by the supernumerary neutrons in a nucleus.*

IV.2. Atoms with excess neutrons *differ, in many respects*, from their isotopes; so e.g. the nuclei of some rare earth metals containing 88 neutrons are spherical in contrast to the nuclei of the isotopes containing two more neutrons, which are deformed and show therefore a greater quadrupole momentum (Dickman, Dietrich, 1973). Further, the rate of reaction of molecules made up of atoms containing supernumerary neutrons may differ from that of others containing atoms without plus neutrons (Kritchevsky, 1960; Thomson, 1963).

IV.3. The conformation of macromolecules can be changed if an isotope with a plus neutron is substituted for one without supernumerary neutron; e.g. the length of the H-bridge in $H\cdots O-H$ can be changed by substituting isotopes differing in the number of neutrons, and then the strength and energy of this bond simultaneously change (Scheraga, 1960; Tomita et al., 1962).

IV.4. *The energy* accompanying neutron processes can be *degraded:* the formula of the difference of the so-called lethargy (l)

$$\Delta l = \ln \frac{E_0}{E_d}\,,$$

where E_0 = initial energy and E_d = degraded energy, shows the slowing of the neutron, i.e. the energy decrease of the neutron in the atom, e.g. from the value of 2 Mev to 0.03 ev. Among the technical *moderators* used for such a purpose D_2O is 200–300-times more appropriate than H_2O; other moderators as $^{9}_{4}$Be and graphite, containing $^{13}_{6}$C, also have supernumerary neutrons. *The plus neutrons may play an important role in moderation.*

[4] The analogous reaction

$$^{40}_{20}\mathrm{Ca} + {}^{1}_{0}\mathrm{n} = {}^{40}_{20}\mathrm{K}^{*} + {}^{1}_{1}\mathrm{p}$$

is of some interest for biology, because Ca is produced during the decay of the $^{40}K^{*}$ atom (similarly to production of ^{14}N due to the decay of $^{14}C^{*}$).

V. *Plus neutrons and biosystems*

V.1. *The quantities of energy accompanying the neutron processes* surpass the usual "chemical" energies $10^3 - 10^6$-times. Even these smaller chemical energies are known to be produced in the organism by a step-wise dissimilation of organic compounds and accordingly to appear also step by step only. Let us suppose that also the energy accompanying the neutron processes is, similarly, used not as a whole but step-wise in the organism due to a "*biomoderation*" *brought about by the supernumerary neutrons in the bioisotopes.*

V.2. According to some experiences the isotopes having plus neutrons accelerate chemical reactions, furthermore they exert a biopositive effect in certain cases. Generally the question arises: *what a role can be ascribed to the plus neutrons of bioatoms in the mechanisms and energetics of vital processes?*

V.3. It has been stated above that the basic substance of biosystems exclusively consists of atoms having isotopes with supernumerary neutrons. For a semiquantitative valuation let us consider a protein molecule with 10^5 mu and consisting of mere radicals of alanine; such a radical contains 3C + 5H + 1N + + 1O and 71 mu. Thus this protein molecule consist of ~1400 radicals of alanine, i.e. of the atoms

4200 C, 7000 H, 1400 N, 1400 O.

a) Therefore in this protein molecule the numbers of the isotopes having plus neutrons (see Table 1) would be

$$\sim 42\ ^{13}C,\ \sim 1.4\ ^{2}D,\ \sim 5.6\ ^{15}N,\ \sim 0.3\ ^{17}O,\ \sim 2.8\ ^{18}O.$$

b) Further, a protein molecule is hydrated in a biosystem e.g. in the ratio of 1 : 1;[5] water of 10^5 mu means 5500 water molecules containing about 11,000 H atoms and 5500 O atoms. Among these the following numbers of isotopes with plus neutrons can be found:

$$\sim 2.2\ ^{2}D,\quad \sim 2.2\ ^{17}O,\quad \sim 11\ ^{18}O.$$

Accordingly, this hydrated protein molecule would contain the following numbers of isotopes with supernumerary neutrons:

$$\sim 42\ ^{13}C,\ \sim 3.6\ ^{2}D,\ \sim 5.6\ ^{15}N,\ \sim 2.5\ ^{17}O,\ \sim 14\ ^{18}O.$$

c) However, as mentioned above, biosystems are able to accumulate the isotopes with supernumerary neutrons. Consequently, the number of these isotopes can be estimated as being much greater, at least in the order of magnitude of hundred in this hydrated protein molecule.

V.4. On account of all these the second question arises: whether and to what extent *the origin of living matter* can be ascribed to the circumstance that

[5] The actual ratio of protein : water in the cell is 1 : 5—1 : 10.

a) the frequencies of the four elements of small atomic weight (H, C, N, O) are the greatest in the nature,[6] *b)* in consequence of the coincidence of these isotopes having plus neutrons a "*critical collective*" has come into existence, in which instability of a certain degree is combined with relative constancy of the constituents.

References

Bigeleisen, J. (1965) Science *147* 463—471
Chance, B. (1972) FEBS Letters *23* 3
Dickmann, F., Dietrich, K. (1973) Z. Physik *263* 211—225
Eley, D. D., Parfitt, S. D., Perry, M. J., Taysum, D. H. (1953) Trans. Faraday Soc. *49* 79
Ernst, E. (1955—56) Wissenschaftl. Z. der Humboldt Univ. zu Berlin Math. Naturwiss. Reihe *5* 167
Ernst, E. (1956) Бисфизика (Moscow) *1* 296
Ernst, E. (1963) Biophysics of the Striated Muscle, Akadémiai Kiadó Budapest, pp. 226—233
Ernst, E. (1970) Acta Biochem. Biophys. Acad. Sci. Hung. *5* 463
Ernst, E. (1970) ibid. *5* 469
Ernst, E., Juricskay, St. (1971) ibid. *6* 165
Flaumenhaft, K. E., Uphaus, R. A., Katz, J. J. (1970) Biochim. Biophys. Acta *215* 421
Haissinsky, M. (1957) La Chimie nucléaire et ses applications, Masson et C^ie^, Ed. Paris; Hungarian translation, (1963) pp. 292—296
Hübner, G. (1958) Chem. Technik *10* 699
Katz, J. J., Crespi, H. L. (1966) Science *151* 1187—1194
Klotz, I. M. (1957) Some Principles of Energetics in Biochemical Reactions. Acad. Press, Inc., New York
Kritchevsky, D. (1960) Ann. New York Acad. Sci. *84* Art. 16. p. 575
Lakatos, T. (1969) Acta Biochim. Biophys. Acad. Sci. Hung. *4* 429—436
Lehninger, A. L. (1965) Bioenergetics. The Molecular Basis of Biological Energy Transformations. W. A. Benjamin Inc., New York
Niedetzky, A., Lajtai, Cs. (1973) Acta Biochim. Biophys. Acad. Sci. Hung. *8* 412
Pullman, A., Pullman, B. (1967) in: Comprehensive Biochemistry, (Ed.) M. Florkin, Vol. 22. Bioenergetics, Elsevier Publ. Comp. Amsterdam
Rabinowitz, J. I., Lafair, J. S., Strauss, H. D., Allen jr. H. C. (1958) Biochim. Biophys. Acta *27* 544
Rittenberg, D., Schönheimer, R., Keston, A. S. (1939) J. Biol. Chem. *128* 603
Scheraga, H. A. (1960) Ann. New York Acad. Sci. *84* Art. 16. p. 608
Schönheimer, R., Ratner, S., Rittenberg, D. (1939) J. Biol. Chem. *127* 333
Szent-Györgyi, A. (1957) Bioenergetics. Acad. Press. Inc., New York
Thomson, J. F. (1963) Biological Effects of Deuterium, Pergamon Press., Oxford
Tigyi, J. (1963) Acta Physiol. Acad. Sci. Hung. *24* 129
Tigyi, J., Kállay, N., Kutas, L. (1966) Studia Biophys. *1* 77
Tomita, K. T., Rich, A., Lozé, C., Blout, E. R. (1962) J. Mol. Biol. *4* 83
Uphaus, R. A., Flaumenhaft, E., Katz, J. J. (1967) Biochim. Biophys. Acta *141* 635
Vedder, R. (1959) Z. Bergbau, Hüttenw. verwandte Wiss. *11* 173

[6] If the frequency of the atom H is ~ 1000, then that of each of the atoms C,N,O is ~ 1, while those of all others are smaller (Haissinsky, 1963).,

Acta Biochim. et Biophys. Acad. Sci. Hung. Vol. 9 (4), pp. 395–398 (1974)

Determination of "Available" Methionine in Plant Materials

(Preliminary Cummunication)

T. DÉVÉNYI[1], JUDITH BÁTI[1], B. HALLSTRÖM[2], CH. TRAGARDH[2],
P. U. KRALOVÁNSZKY[3], T. MÁTRAI[3]

(Received October 9, 1974)

Methionine is the limiting amino acid in legumes and has similar importance in plant materials of other species. Therefore to measure deficiencies and or availability is of primary interest. Several possibilities of methionine determination has been elaborated, e.g. ion-exchange chromatography (Moore, 1963, Dévényi, 1971) gas-chromatography (Gehrke et al., 1971), and thin layer ion-exchange chromatography (Ferenczi et al., 1971). The most accurate method is based on the determination of methionine sulphone in performic acid treated samples (Moore, 1963).

Certain treatments such as grinding, milling, solvent-extraction, heat-reatments, etc. may partially oxidize the methionine to its sulphoxyde and sulphone. Both are biologically unavailable but these are also measured when methionine is estimated as $MeSO_2$ in the performic acid treated sample. In feeding-experiment such samples will represent an uncorrent, higher methionine-content. It seems to be basically important to differentiate between the "true" or "available"* methionine (present in the sample in thioether form) and its biologically unavailable oxydation products. A method is proposed by using amino acid analyzer technique, based on the determination of the destruction rate of the methionine. The destruction of methionine is depending highly on the individual properties of the sample, partly on the composition of the material (presence of oxidizing substances or antioxidants, carbohydrate content or others) partly on the character and intensity of treatments during processing. Therefore, it seems necessary to determine the destruction rate of methionine in each individual sample. In the present work as test materials leaf protein concentrates (LPC) were used, prepared in Swedish technological experiments through various steps of processing.

20 mg LPC sample was hydrolyzed at 105 °C for 48 hours in 5 ml 6N HCl under N_2 atmosphere. Evaporation was performed in vacuo at 60 °C over solid

* "Available" is used in the chemical sense, not identical with the ratio of the amino acids resorbed and amino acid ingested, i.e. availability in the sense of nutritional science.

[1] Department of Enzymology, Institute of Biochemistry, Hungarican Academy of Sciences, Hungary,
[2] Chemical Center, Food Engineering, Alnarp, Sweden,
[3] State Office of Technical Development, Budapest, Hungary

P_2O_5 and KOH. The dried residue was redissolved in 5 ml of deionized water. 0.5 ml of the solution corresponding to 2 mg of the sample was analyzed.

Beckman Unichrom amino acid analyzer was used in the following experimental conditions:

Resin: 14 cm (Rapidex LA-6 Chinoin – Nagytétény, Budapest)
Buffer flow-rate: 100 ml/hour at 55 °C
Buffer: sodium citrate, 0.2N Na^+, pH = 3.28
Program: 0 – 25 min Buffer
25 – 27 min 0.2N NaOH
27 – 40 min Buffer

The methionine sulphone was determined with a BioCal BC 200 amino acid analyzer, interrupting the chromatography after the elution of glutamic acid.

20 mg sample was treated for 30 minutes with 5 ml freshly prepared performic acid (HCOOH + H_2O_2 9 : 1 by volume) at room temperature. The solution was diluted with 5 ml deionized water and evaporated in vacuo over solid P_2O_5 and KOH. The dried residue was hydrolyzed as described above.

In order to determine the hydrolytic decomposition 20 – 20 mg samples were hydrolyzed in the presence of increasing amounts (1, 2, 3 and 5 μmol) of methionine under the experimental conditions described above. Each sample was analyzed and the degree of the decomposition (D%) was calculated using the following formula:

$$D^{\%} = 100 - \left(\frac{MET^x - MET^s}{MET^a} \right) \times 100$$

MET^x = Met measured in sample in the presence of added Met

MET^s = Met measured in the sample (NO added Met!)

MET^a = Met added to the sample

MET^s value corrected with the decomposition-factor D% can be considered as the amount of "true" or "available" methionine (= MET^c)

$$MET^c = \frac{100 \times MET^s}{100 - D^{\%}}$$

Considering that the quotient of the molecular weights of methionine and methionine sulphone is 0.82, the amount of Met measured as the sulphone, MET^{ox} (in performic acid treated samples) can be calculated by multiplying these figures with 0.82:

$$MET^{ox} = 0.82 \times MeSO_2$$

From these data the "availability" of methionine:

$$\text{"Availability"} \ \% = \frac{MET^c}{MET^{ox}} \cdot 100$$

Table 1

*"Available" methionine content of different leaf protein concentrates***

Sample(+)	D%	MET^{c} g/100g	$MeSO_2$ g/100g	MET^{ox} g/100g	"Availability"
H-0 Freeze-dried ultrafiltrated raw juice	24.6	0,73	1.24	1.02	71
H-1 Spray-dried raw juice	23	0.37	0.65	0.53	70
H-2 Spray-dried ultrafiltrated juice	25	0.84	1.40	1.15	73
H-3 Solvent precipitated raw juice, vacuum dried	26.5	0.71	1.10	0.90	79
H-4 Solvent precipitated ultra-filtrated raw juice, vacuum dried	26.7	1.41	1.65	1.35	104
H-5 Spray dried sludge from non-heated juice	18	0.36	0.53	0.43	84
H-6 Heat-precipitated spray-dried LPC	10	0.90	1.21	1.00	90
H-7 Solvent extracted H-6	25	1.40	1.68	1.37	102
H-8 Spray-dried chloroplastic LPC	20	0.80	0.99	0.81	101
H-9 Spray-dried heat-precipitated cytoplasmatic LPC	10	1.20	1.43	1.17	102
H-10 Spray-dried, acid-precipitated cytoplasmatic LPC	10	0.67	0.84	0.68	98

* The leaf protein concentrates were prepared at the Chemical Center, Food Engineering, Alnarp, Sweden. Details will be published elsewhere.

Table 1 shows "availability" values of LPC samples obtained through various processing. Due to processing alternatives, figures are ranging from 74 to 100%. Values higher than 100% indicate some overoxidation of methionine during the evaporation of the performic acid treated sample. Several samples were tested to determine their protein efficiency ratio (PER) in mice. Table 2 summarizes the PER-values and suggests fairly good parallelism with the "availability" of methionine.

The aim of this study was to find a chemical approach to establish the extent of oxidative destruction of methionine in food or fodder i.e. to measure the "available" methionine content.

Table 2

Correlation between methionine "availability" and the protein efficiency ratio (PER)

Sample	"Availability"	PER(+)	
		Average	Range
H-1	70	ALL ANIMALS DIED	
H-2	73	0.48	0.1—0.8
H-3	79	1.19	0.8—1.6
H-6	90	0.67	0.3—1.2
H-8	101	1.57	1.0—2.2
H-7	102	1.77	1.6—1.9
H- (9+10)	100	1.92	1.3—2.5
H-4	104	2.00	1.7—2.3

* The feeding experiments were carried out at the Swedish Seed Association, Svalöf. Each group consisted of 8 male SPF mice.

The authors wish to thank Professor F. Bruno Straub for his interest, help and advice.

References

Dévényi, T. (1971) Acta Biochim. Biophys. Acad. Sci. Hung. *6*, 129—131
Ferenczi, S., Báti, J., Dévényi, T. (1971) Acta Biochim. Biophys. Acad. Sci. Hung. *6* 123—128
Gehrke, C. W. Kuo, K. C., Zumwalt, R. W. (1971) J. Chromatog. *57* 209—217
Moore, S. (1963) J. Biol. Chem. *238* 235—237

Acta Biochim. et Biophys. Acad. Sci. Hung. Vol. 9 (4), pp. 399—401 (1974)

Book Reviews

Z. Vodrázka: *General and Physical Chemistry for Medical and Biology students* (Obecná a fyzikálni chemie pro lékare a biology). Avicenum, Praha 1972.

During the last decade biology and medicine came into an ever closer connection with physics and chemistry. The book of Z. Vodrázka treats the subject matter of the structure of matter and physical chemistry well-presented for students and workers in the fields of medicine and biology, who generally lack training in higher mathematics. No such textbook has been published in Hungarian during the last years, apart from some university lecture notes covering narrower fields.

The book consists of four parts: the structure of matter, chemical reactions, equilibrium systems, and solutions. The first part is the most extensive, it constitutes more than half of the 500-page book, but this apparent disproportion originates from the weight and importance of the subject. The author divided the material from the atomic structure to the structure of biopolymers into five chapters. The way of treatment is uniform, logical and readily understandable throughout. In contrast to the general practice, the methods of investigation of the physical properties and the physical properties themselves are discussed together with the laws of matter, but this novel treatment is one of the virtues of the book.

The next three parts are practically similar to the textbook of Tibor Erdey-Grúz: "The principles of physical chemistry", which is widely used in Hungary, but is meant for a broader scale of readers. Vodrázka's book omits, or treats only very briefly, those parts which are less important for medical and biology students. Its style is less concise, readily digestible; the involvement of higher mathematics is skillfully avoided.

As compared with the first part, the other three parts are less uniform, but this is no drawback as the author here concentrates on the details essential for medical and biology students.

The book comprises more than 200 excellently constructed figures and tables. These and the already mentioned clear and readable style are real virtues of the book.

It goes without saying that even this valuable book has some mistakes. Part of these come from the omission of higher mathematics. At other points the explanations could have been more thorough, for example in the chapters on the magnetic properties of matter and on the absorption and dispersion properties of optically active compounds. The chapter that deals with the relationship between structure and reactivity seems to be somewhat undersized, considering the importance of these problems.

As a conclusion one can say that the author undoubtedly succeeded in reconciling a high standard with the frame of possibilities in regard of both form and content. This book may considerably promote the strengthening of the connection between these two branches of natural sciences.

Olivér RÁCZ

Joseph Larner: *Intermediary Metabolism and its Regulation.* Prentice Hall, Inc. Englewood Cliff, New Jersey, 1971. 308 pages.

The book "Intermediary Metabolism and its Regulation" by Joseph Larner is part of a four-volume series. Biochemistry is still a common field for biological and physical sciences. Therefore it is a rather difficult and controversial task to write a comprehensive book for students, of all branches of natural sciences, reading biochemistry, which clearly conveys the basic principles of biochemistry to all of them. It was with these thoughts in mind that the "Foundation of Modern Biochemistry" series was initiated.

One of the essential questions of biochemistry: how the molecules and structures of the living cell are synthesized and how they are broken down, — was with problem covers all aspects of intermediary metabolism and metabolic regulation — is dealt with in the book.

Although this volume is an integral part of the series "Foundation of Modern Biochemistry", it can be excellently used separately. The integration of the four parts of the series is achieved by the numerous cross-references between the individual books.

Joseph Larner's book is printed on fine paper with excellent typography. The use of two different colours in the great number of figures adds to the aesthetic appearance, intelligibility and clarity of the book.

The logical construction and the structure of the ten chapters help the reader to understand the material. The first half of the book gives a complete review of metabolism: the energy generation, the breakdown, synthesis and interconversion of carbohydrates, lipids, and N-containing compounds. In the second part the control of these three branches of metabolism are discussed. The approaches used to delineate metabolic pathways can be found in Chapter 2, and Chapter 6 treats the evaluation of the in vivo significance of metabolic reactions.

In such a book written for students, and at the same time at a very highly scientific level, the concise and precise definitions of the "Glossary" and the tables of the "Appendix" are very helpful.

The most outstanding merits of "Intermediary Metabolism and its Regulation" are that it examines the relationship of in vitro observations to in vivo control mechanisms; compares non-hormonal and hormonal controls, and discusses the approaches and techniques used in the study of metabolic pathways and their control mechanisms.

Joseph Larner's book on intermediary metabolism and regulation is written at a high scientific standard and at the same time its clear style meets the requirements of a text-book. Therefore this volume of the "Foundation of Modern Biochemistry" series, can be recommended to both experts and students.

Gyöngyi HAJÓS

T. Dévényi and J. Gergely: *Amino Acids, Peptides and Proteins.* Publishing House of the Hungarian Academy of Sciences, 1974 (in English). 343 pages, 55 + 11 figures, XI + III tables.

The intensive development of protein chemistry, the precise analytical techniques and the new methods applied in biochemical research have set up new claims. The techniques of protein chemistry are important not only for protein chemists proper but they should be in hand in medical routine laboratories, as well as in other branches of research.

T. Dévényi and J. Gergely's book has a beautiful presentation, is excellently understandable and it clearly describes the most common techniques in protein chemistry. An outstanding value of the book is that beside the illuminating and well-chosen figures, photographs also support the applicabilities of the methods described.

The book treats the fundamentals of methodology, general methods, procedures and equipment of protein analysis, gives a detailed practical description of the low, medium and high voltage electrophoretic analysis of proteins.

In the chapters on immunochemical and electrophoretic analysis of proteins, both practical problems and recent results concerning proteins of biological importance are discussed. The most up-to-date techniques of automatic amino acid analysis are critically surveyed. One of the analyser programmes elaborated for routine tests, for instance the determination of tryptophan, is of great importance in the clinical practice.

A comprehensive review of the purification and isolation methods of proteins, peptides and amino acids can be found in the book. Beside the precise description of paper chromatography, ion exchange chromatography, thin-layer chromatography and gel filtration, the book provides detailed instructions about their applicability. The chapter on end-group analysis and stepwise degradation of proteins and peptides deals with the most modern techniques of amino acid sequence determination.

The "Appendix" covers a rather special field: the gas chromatographic analysis of amino acid derivatives, its scope and limitation.

The detailed and very clear description of the modern techniques, completed with the indication of possible sources of error and their elimination, the high quality illustrations and the great number of references will certainly make this book a very useful and valuable aid for experts interested in protein chemistry.

Gyöngyi HAJÓS

Ergebnisse der experimentellen Medizin 13. Diagnostische Enzymologie. Ed. by H. Friedmann and R. Winter. VEB Verlag Volk und Gesundheit. Berlin, 1973. 208 pages, 29 figures.

The book comprises the material of the Congress of the clinical-chemical and laboratory diagnostical society of GDR held in Leipzig 1971.

The small-sized book consists of 208 pages and comprises 29 lectures carefully illustrated with figures, tables and references. The Congress gave a survey of the present state of the applied clinical enzyme diagnostics. It approaches the serum and tissue enzyme diagnostics in the light of the morphological localization of the enzymes; then it deals with the way of modern methodics: catalytic and non-catalytic methods. About half of the further 28 lectures describes the changes of enzyme activity as the symptom of pathological processes or adaptive mechanisms in liver, bile and pancreas diseases, in tumour, in kidney and muscle laesion and in connection with pregnancy.

A smaller number of reports is connected with genetic enzyme defects, also dealing with the practical routine application of modern biochemical methods of separation in connection with G6-PD (Density-gradient Separation of Erythrocytes in Dextran Medium).

Finally, we can read more than 10 lectures on methodics. They deal — among others — with enzyme standardization (LDH), with the normal value of CPK, with the determination of gamma-GT, catalase, aldolase, and they give account of fluorimetric enzyme analysis and ultramicro-method.

The study of the book convinces the reader of the varied work of the clinical-chemical laboratories of GDR, their professional skill and instrumental preparedness, which all support serviceably the diagnostic work of extra- clinicians with the data of enzyme determinations and raise the clinical work to a high level.

K. JOBST

Hoppe-Seyler's Zeitschrift für Physiologische Chemie

Editors in Chief

A. BUTENANDT · F. LYNEN · G. WEITZEL

Subscription Rate

For one volume (12 parts) DM 480,—

Vol. 355 No. 3 March 1974

CONTENTS

Indexed in Current Contents

Walter de Gruyter · Berlin · New York

Hoppe-Seyler's Zeitschrift für Physiologische Chemie

Editors in Chief

A. BUTENANDT · F. LYNEN · G. WEITZEL

Subscription Rate

For one volume (12 parts) DM 480,–

Vol. 355 No. 4 April 1974

CONTENTS

Indexed in Current Contents

Walter de Gruyter · Berlin · New York

Hoppe-Seyler's Zeitschrift für Physiologische Chemie

Editors in Chief

A. BUTENANDT · F. LYNEN · G. WEITZEL

Subscription Rate

For one volume (12 parts) DM 480,—

Vol. 355 No. 5 CONTENTS May 1974

Indexed in Current Contents

Walter de Gruyter · Berlin · New York

Hoppe-Seyler's Zeitschrift für Physiologische Chemie

Editors in Chief

A. BUTENANDT · F. LYNEN · G. WEITZEL

Subscription Rate

For one volume (12 parts) DM 480,–

Vol. 355 No 6. June 1974

CONTENTS

Indexed in Current Contents

Walter de Gruyter · Berlin · New York

Hoppe-Seyler's Zeitschrift für Physiologische Chemie

Editors in chief

A. BUTENANDT · F. LYEN · G. WEITZEL

Subscription Rate

For one volume (12 parts) DM 480,–

Vol. 355 No. 7 July 1974

CONTENTS

Indexed in Current Contents

Hoppe-Seyler's Zeitschrift für Physiologische Chemie

Editors in Chief

A. BUTENANDT · F. LYNEN · G. WEITZEL

Subscription Rate

For one volume (12 parts) DM 480,–

Vol. 355 No. 8 CONTENTS August 1974

Indexed in Current Contents

W DE G

Walter de Gruyter · Berlin · New York

INTERNATIONAL BIOMATERIALS SYMPOSIUM

April 26—30, 1975

First Meeting of the Society of Biomaterials at Clemson University
and
Seventh Symposium at Clemson University

With the advent of the Society of Biomaterials the Symposium is broadening its horizons to include a wider range of materials and medical applications than ever before. As in past years, our aim will be to provide a forum for the leading investigators in clinical and basic research to present recent findings, to promote the transfer of research developments into clinical practice and to seek new directions and approaches in the development of all biomaterials. In addition, the keynote addresses and invited presentations will be of a tutorial character in keeping with the expanded mission of the Symposium.

– SESSIONS –

I – cranio-facial materials
II – oral-dental materials
III – recent advances in research & applications
IV – cardiovascular materials
V – orthopedic materials

Symposium with International Participation on

PREVENTION IN GERIATRICS

Bratislava, May 21—23, 1975

Topics

a) Clinical Aspects of Primary and Secondary Prevention in Geriatrics
b) Health and Social Problems in Preventive Geriatrics
c) Early Aging and Basic Research

Languages

Russian, English, German, Czech and Slovak

Chairman of the Symposium
Dr. E. GRESSNER
Chairman of the Czechoslovak
Society of Gerontology

Secretary General of the Symposium
Dr. S. LITOMERICKÝ
Geriatric Unit
834 31 Bratislava — POD. Biskupice

Printed in Hungary

A kiadásért felel az Akadémiai Kiadó igazgatója — Műszaki szerkesztő: Zacsik Annamária

A kézirat nyomdába érkezett: 1974. VI. 23. — Terjedelem: 11,9 (A/5) ív 58 ábra

74.701 Akadémiai Nyomda, Budapest — Felelős vezető: Bernát György

Reviews of the Hungarian Academy of Sciences are obtainable at the following addresses:

ALBANIA

Drejtorija Qëndrore e Përhapjes dhe Propagandimit të Librit
Kruga Konferenca e Pazes
Tirana

AUSTRALIA

A. Keesing
Box 4886, GPO
Sydney

AUSTRIA

GLOBUS
Höchstädtplatz 3
A — 1200 Wien XX

BELGIUM

Office International de Librairie
30, Avenue Marnix
1005 Bruxelles
Du Monde Entier
162, Rue du Midi
1000 Bruxelles

BULGARIA

HEMUS
11 pl Slaveikov
Sofia

CANADA

Pannonia Books
2, Spadina Road
Toronto 4, Ont.

CHINA

Waiwen Shudian
Peking
P. O. B. 88

CZECHOSLOVAKIA

Artia
Ve Směčkách 30
Praha 2
Poštovní Novinová Služba
Dovoz tisku
Vinohradská 46
Praha 2
Mad'arská Kultura
Václavské nám. 2
Praha 1
SLOVART A. G.
Gorkého
Bratislava

DENMARK

Ejnar Munksgaard
Nörregade 6
Copenhagen

FINLAND

Akateeminen Kirjakauppa
Keskuskatu 2
Helsinki

FRANCE

Office International de Documentation de Librairie
48 rue Gay-Lussac
Paris 5

GERMAN DEMOCRATIC REPUBLIC

Deutscher Buch-Export und Import
Leninstraße 16
Leipzig 701
Zeitungsvertriebsamt
Fruchstraße 3—4
1004 Berlin

GERMAN FEDERAL REPUBLIC

Kunst und Wissen
Erich Bieber
Postfach 46
7 Stuttgart 1.

GREAT BRITAIN

Blackwell's Periodicals
Oxenford House
Magdalen Street
Oxford
Collet's Subscription Import Department
Dennington Estate
Wellingborough, Northants.
Robert Maxwell and Co. Ltd.
4 — 5 Fitzroy Square
London W. 1

HOLLAND

Swets and Zeitlinger
Keizersgracht 471—487
Amsterdam C.
Martinus Nijhof
Lange Voorhout 9
The Hague

INDIA

Hind Book House
66 Babar Road
New Delhi 1

ITALY

Santo Vanasia
Via M. Macchi 71
Milano
Libreria Commissionaria Sansoni
Via La Marmora 45
Firenze
Techna
Via Cesi 16.
40135 Bologna

JAPAN

Kinokuniya Book-Store Co. Ltd.
826 Tsunohazu 1-chome
Shinjuku-ku
Tokyo
Maruzen and Co. Ltd
P. O. Box 605
Tokyo-Central

KOREA

Chulpanmul
Phenjan

NORWAY

Tanum-Cammermeyer
Karl Johansgt 41 — 43
Oslo 1

POLAND

RUCH
ul. Wronia 23
Warszawa

ROUMANIA

Cartimex
Str. Aristide Briand 14—18
Bucureşti

SOVIET UNION

Mezhdunarodnaya Kniga
Moscow G—200

SWEDEN

Almquist and Wiksell
Gamla Brogatan 26
S—101 20 Stockholm

USA

F. W. Faxon Co. Inc.
15 Southwest Park
Westwood Mass. 02090
Stechert Hafner Inc.
31. East 10th Street
New York, N. Y. 10003

VIETNAM

Xunhasaba
19, Tran Quoc Toan
Hanoi

YUGOSLAVIA

Forum
Vojvode Mišića broj 1
Novi Sad
Jugoslovenska Knjiga
Terazije 27
Beograd

Contents

30. XII. 1974 Index: 26.030